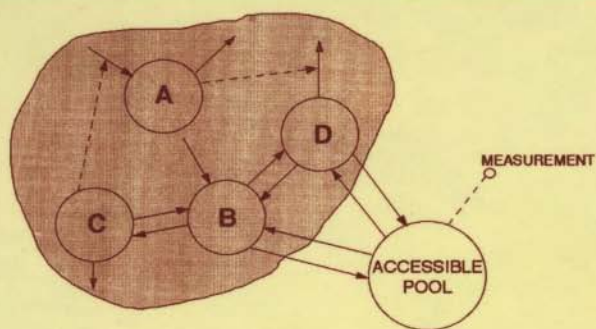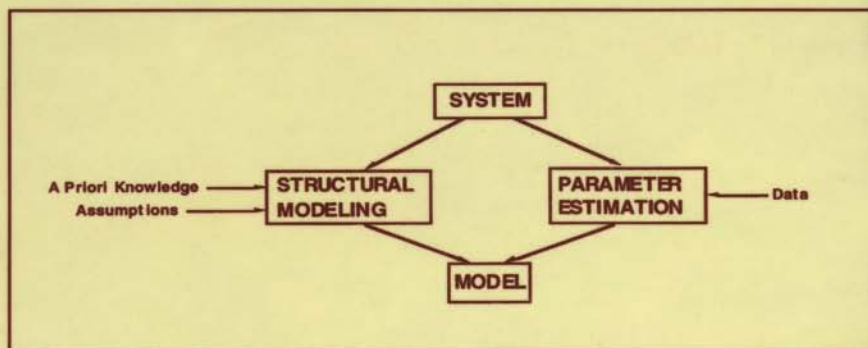# Tracer Kinetics in Biomedical Research

From Data to Model

Claudio Cobelli, David Foster, and Gianna Toffolo

Tracer Kinetics in Biomedical Research

This page intentionally left blank.

Tracer Kinetics in Biomedical Research

From Data to Model

Claudio Cobelli
University of Padova
Padova, Italy

David Foster
University of Washington
Seattle, Washington

and

Gianna Toffolo
University of Padova
Padova, Italy

Created in the United States of America

Visit Kluwer Online at: http://www.kluweronline.com
and Kluwer's eBookstore at: http://www.ebooks.kluweronline.com

Preface

    The use of mathematical modeling techniques in biomedical research is playing an increasingly important role as one seeks to understand the physiopathology of disease processes. This includes not only understanding mechanisms of physiological processes, but diagnosis and treatment. In addition, its introduction in the study of genomics and proteomics is key in understanding the functional characteristics of gene expression and protein assembly and secretion. Finally, with the increasing complexity and associated cost of drug development, modeling techniques are being used to streamline the process.

    We have worked in close collaboration with colleagues in biomedical and pharmaceutical research for a number of years applying and refining mathematical modeling techniques to a variety of problems. In addition, we have worked in collaboration with colleagues in applied mathematics and statistics to develop new algorithms to solve new sets of problems as they emerge in our research efforts. Finally, we have worked with colleagues in computer science to develop new software tools that bring the power of mathematical modeling to a broad research community. This books brings together much of what we have learned over the years, and presents the material in a format that should be accessible both to the novice reader and those desiring more detailed information about specific techniques.

    We are indebted to many of our colleagues who were extremely patient and helpful during the preparation of the book for publication. We are encouraged by the support we have received from our respective institutions and also review panels for several of the research grants we have obtained during the work on the book.

    There are many research programs that have led directly to material presented in the text. Special mention must be given to the Biomedical Technology Program in the National Center for Research Resources at

the National Institutes of Health (USA) whose resource facility grant Resource Facility for Kinetic Analysis (RFKA) supported all authors during the development of the SAAM II software system. There is a tight link between the material developed in this text and SAAM II; SAAM II was used to develop all examples in the text.

The preparation of the book would not have been possible without regular travel between Seattle and Padova. Funding for the travel was provided by RFKA and the Ministero della Università e Ricerca Scientifica e Tecnologica of Italy. We are most grateful for this support.

Finally, we would like to thank Agnes Sieger and Mike Macaulay for the final preparation of the text.

CLAUDIO CODELLI, PADOVA, ITALY
DAVID FOSTER, SEATTLE, WASHINGTON, USA
GIANNA TOFFOLO, PADOVA, ITALY

Contents

This page intentionally left blank.

Chapter 1

INTRODUCTION

1.1   WHY MODELING?

The use of tracers to study metabolic systems is becoming increasingly important in biomedical research. The fundamental reason is that while the tools of molecular biology have provided much new information about the structure of different components of metabolic systems, information is also needed about the function of these components. This information can come from a knowledge of the systems kinetics, that is, the temporal and spatial distribution of the components comprising the system. Tracers are used as a tool to obtain the kinetic information. One reason why tracer kinetics is enjoying a resurgence is that significant improvements have been made in both the quality and quantity of data that are available from a tracer experiment. This is due both to new instruments to measure data previously not available and new instruments, especially for stable isotopes, to measure kinetic information in increasingly small samples. For example, PET and NMR studies using radioactive and stable isotopes are revealing details of metabolic events heretofore unavailable.

In general, tracer kinetic studies are undertaken to understand the physiology and pathophysiology of the metabolism of substances that already exist in the body. Such substances include glucose, insulin, vitamins, minerals, amino acids and proteins, or aggregates of material such as the plasma lipoproteins. While studies are most commonly conducted at the "whole body" level, new techniques are permitting studies at the organ, cellular and subcellular levels.

In order to interpret kinetic data from an experiment, one requires a mathematical model of the system under study. A model is a construct

invented by a researcher to summarize what is known and hypothesized about a system under study. It breaks the system down to a level of detail required into component parts indicating the relationship among these parts. A mathematical model is simply a model that can be described by a set of mathematical equations.

Why is mathematical modeling necessary? It is necessary because researchers desire quantitative information on the system under study. Models provide a means by which to calculate parameters characterizing these nonaccessible parts of the system from information available only from those parts of the system that are accessible for measurement. The situation can be schematized in Figure 1.1.1.
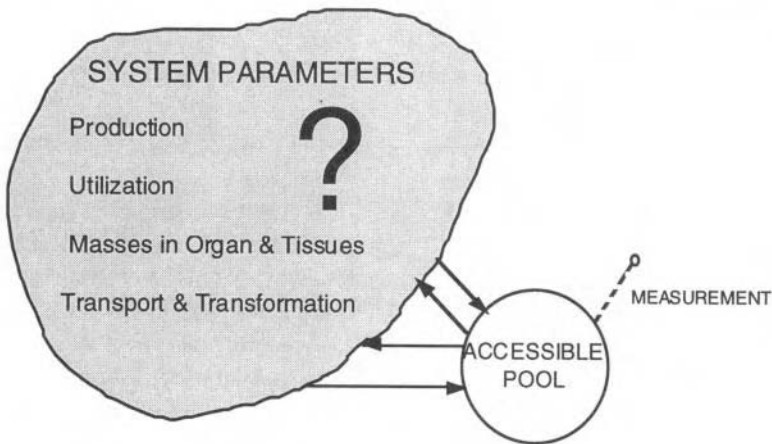
Figure 1.1.1. A schematic of a system characterized by unknown parameters. A portion of the system called the accessible pool is available for measurements.

Thus to estimate these kinetic parameters, one has to link the information available from the accessible pool measurements with the events occurring in both in the accessible and nonaccessible portions of the system. This requires making some assumptions about how the system functions. In short, one has to postulate a model of the system based upon known physiology and biochemistry, and assumptions about how the system is interconnected. Once this is done, the model must be described mathematically. The situation is illustrated in Figure 1.1.2.
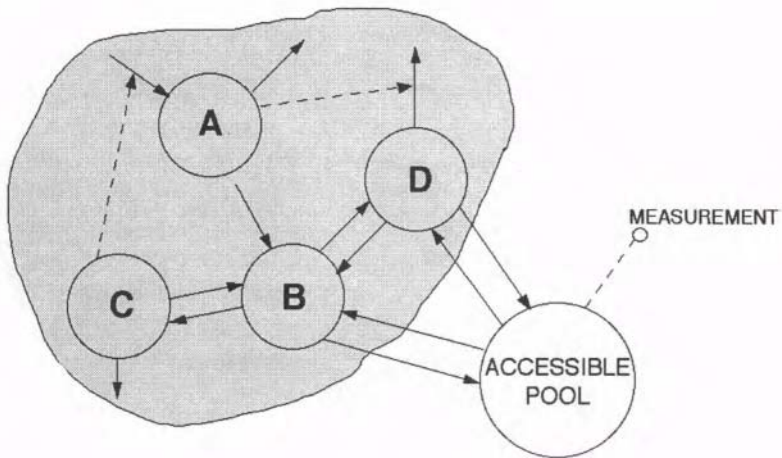
Figure 1.1.2. A schematic of a structural model of the system. Different components are illustrated by the circles labeled A, B, C and D. Arrows connecting the circles represent biochemical transformation and/or transport. Arrows leaving the circles represent utilization. Arrows entering the circles represent production. Each circle has associated with it a mass. The accessible pool relationships with the nonaccessible pools is also shown.

1.2   HOW MODELING?

How are these models constructed? As indicated in Figure 1.2.1, there are basically two steps involved: structural modeling and parameter estimation. As mentioned previously, structural modeling is the process by which ones knowledge and assumptions about the system are formalized first as a schematic and then mathematically. As will be seen in this text, the model will always contain hypotheses and simplifications for a variety of reasons: parts of the system are unknown, or only some features are relevant for the study. However, the model must be parsimonious and usable. Parameter estimation is the process by which the parameters characterizing the model are adjusted so as to obtain a best fit of the available data. For any hypothesized structural model, parameter estimation provides information to assess the adequacy of the model. Criteria based upon goodness-of-fit, precision of the parameter

estimates, parsimony, and plausibility permit an investigator to judge the quality of the model.
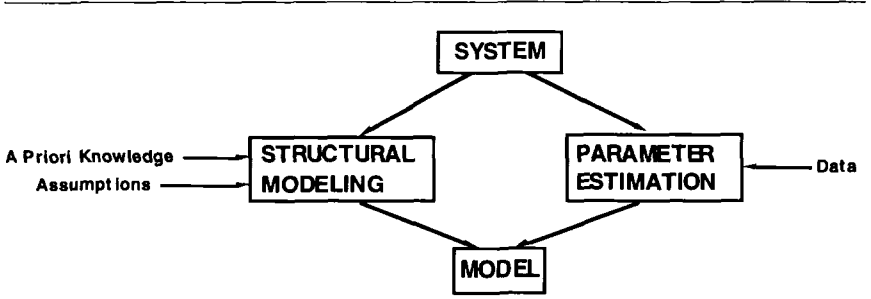
Figure 1.2.1.   A schematic of the steps involved in constructing a mathematical model of a system.

The best one can hope for is a model to be compatible with the data and be physiologically plausible. While never the truly "correct" model of the system, it can be used for predictive purposes, e.g. estimating the system parameters and simulating future experiments. However, one must have confidence in the results and predictions of the model. This confidence can be obtained through the process of validating the model. Validation criteria and strategies are available which take into account the models complexity and available data. The model is also dynamic in the following sense. The hypotheses that are incorporated in the models structure can be tested through new experiments. The model will either correctly predict the results of these experiments or not. If it does not, then the model structure will have to be changed, and the process of compatibility with previous data and physiological plausibility reexamined.

There are many types of mathematical models that can be used to interpret tracer kinetic data. All have assumptions associated with them that need to be understood in order to apply them correctly. In addition, what type of model is chosen for a particular situation can depend upon the information that is needed. Thus while a particular set of data could be very rich in information content, a simple method of analysis could be used to estimate a limited set of parameters.

1.3   AIM OF THE BOOK

The aim of this book is to explain how mathematical models can be used as a powerful research tool in the design and analysis of experiments in which tracer kinetic data are generated. Starting with a description of radioactive and stable isotopes, it will give a detailed description of the steps involved in developing and using mathematical models.

The focus will be on systems that are studied in the steady state, since most of the metabolic systems are non-linear, and this makes them difficult to study since the mathematical equations describing them are also non-linear, and the nature of the non-linearities is difficult to describe mathematically. To overcome this problem, many tracer kinetic studies are conducted in the steady state, i.e. under conditions where the masses and fluxes of material in the system are maintained in near constant conditions. This assumption results in mathematical models that are linear and, with the numerical techniques now available in many software programs, easy to solve.

Two common types of linear models will be presented: noncompartmental and (linear) compartmental models. The underlying assumptions of each will be explained in detail. The underlying mathematics and statistics will also be explained, but at a level that is transparent to the novice reader. They will be explained in terms that are easy to understand. This is especially true in the areas of parameter estimation and model identifiability, two areas that are critical in the process but a poorly understood because most material in these areas is given in full generality with little intuition as to the "what", "how" and "why". Here the concepts will be explained in understandable terms; the concepts will be carefully illustrated using several examples. The goal is that the reader, upon completing the book, will be able to use mathematical models and software programs necessary to solve them and use them as powerful research tools. Since the modeling machinery is transparent, it is also useful in other contexts. For example, it should be noted that much of the material in the book is relevant to study pharmacokinetic/pharmacodynamic systems, nonsteady state systems and physiological control system.

1.4   WHO SHOULD READ THE BOOK?

Mathematical modeling has received considerable attention both in the past and present kinetic studies. Many books and papers have been written on the subject. The most frequently cited text include Anderson [1983], Atkins [1969], Atkinson [1999], Carson et al. [1983], Gibaldi and Perrier [1982], Godfrey [1983], Gurpide [1975], Jacquez [1996], Lassen

and Perl [1979], Norwich [1977], Rescigno and Segre [1966], Riggs [1975], Rowland and Tozer [1995], Shipley and Clark [1972], and Wolfe [1992]. In addition, there are several seminal articles including Carson and Jones [1979], Cobelli and Caumo [1998], DiStefano and Landaw [1984], and Landaw and DiStefano [1984].

Many of the texts listed above focus only on limited aspects of the modeling process. Others go into mathematical and/or statistical depth that is beyond the ability of the beginning modeler. In this book, emphasis is placed on aspects of analyzing tracer kinetic data obtained from increasingly complex systems using increasingly sophisticated experimental designs. The mathematics involved will illustrate the key points, especially in parameter estimation and model identifiability. However, intuitive arguments will be given in many places so the reader will understand the assumptions and limitations of the various methodologies discussed. When more detail is required, the reader will be pointed to specific texts or the appendices.

With this in mind, who should read this book? The book is intended for those individuals who are using or planning to use tracer kinetic techniques to probe different metabolic systems. In addition, it can be used as an introductory text in tracer kinetic analysis and mathematical modeling of biological systems. Finally, it can be used by researchers in pharmacokinetics who are interested in information in a more global setting than that normally found in many pharmacokinetic text books.

Fortunately there are a number of software systems that are available to aid the research in the model development and data analysis process. Some users take advantage of mathematically oriented scientific software packages; these require the user to write the models equations directly and often require, in addition, programming skills. This level of usage is beyond the scope of the present text so these packages will not be listed.

1.5   ORGANIZATION OF THE BOOK

This book provides a description of the processes involved in designing and analyzing tracer kinetic studies starting from the steps involved in choosing an isotope, or isotopes, for a tracer, or tracers, through formulating models to analyze the kinetic data resulting from an experiment. It begins with a description of the fundamentals of tracer kinetics focusing on the measurement variables, discusses two broadly used modeling techniques including the underlying mathematics and statistics, and discusses how to assess how "good" a model is. It also points out how models can be used to test hypotheses both after an experiment is completed, and before during which time experimental protocols can be simulated before actually performing an experiment. Taken together,

the goal is to obtain information rich data and then to apply modeling techniques to extract the information.

When needed, specific references to more detailed information will be given at the end of each chapter. These bibliographies are not meant to be exhaustive nor historic. They are meant to provide specific supplemental information for those readers wanting more details about specific material presented in the chapter.

Several examples are provided to illustrate key points. Two Case Studies are discussed which permit a comparison of the different methodologies that are provided. A floppy disk with the data files used in the examples and Case Studies is provided so that the reader can recreate them. In this book the SAAM II software was used to generate all examples and Case Studies.

Chapter 2 discusses the fundamentals of tracer kinetics first in general terms, and then specifically related to radioactive and stable isotopic tracers. Careful attention is paid to the measurement variables. Important comparisons between the measurement variables for the two kinds of tracers are made. In addition, a rigorous discussion concerning the various measurement variables for stable isotopic tracers is given. For the readers convenience, a table is included that can help convert the usual measurement variables for stable isotopic tracers into the measurement variable that is needed for data analysis.

Chapters 3 and 4 describe the basics of the noncompartmental and compartmental models of multipool systems. The former, often referred to as the integral equation approach and claimed to be model independent, is shown to be based upon many assumptions that are actually shared, in part, by certain types of multicompartmental models. For noncompartmental models, the standard formulas for the parameters are derived for the different protocols using radioactive and stable isotopic tracers. For compartmental systems, the basic definitions are given. In both cases, it is assumed that the experiment is conducted in the steady state. This will be seen to have a dramatic impact on multicompartmental models since the underlying differential equations have special properties.

Chapter 5 focuses on the a priori identifiability of multicompartmental models. This addresses the following question: given a specific model structure and input-output protocol, will the data (in the ideal sense, i.e. assuming the model structure is correct and the data are error free) permit the estimation of the model parameters? Several examples will be given to show how this crucial step fits into the modeling process. It will be shown that new technologies are being developed which can help to answer this question in the general case.

Chapter 6 will show how to recover kinetic parameters from multi-compartmental models, and in Chapter 7a comparison between these parameters and those generated from noncompartmental models will be given. The reader will see when the two agree, and under which circumstances they do not agree. It will be easy to understand how the imposition of a structure in a multicompartmental model increases the models predictive capability.

Chapter 8 discusses parameter estimation. This crucial chapter discusses unweighted and weighted linear and nonlinear regression. It will be seen that while linear regression is exact, nonlinear regression is an approximation. It describes in detail the error structure in the data, and why it is essential that one appreciate this error in the modeling process. It then goes on to discuss regression, and show why the error structure is necessary if one desires statistical information about the fitting process. The notions of standard and fractional standard deviations, variance-covariance and correlations are also introduced. Chapter 8 ends with a discussion of tests for goodness-of-fit and model order. To provide insights into the regression process, simple examples are given.

Chapter 9 shows how to use sums of exponentials to estimate the parameters of the noncompartmental model. Several examples are given. An appendix is provided which shows the reader how to obtain initial estimates for the coefficients and exponentials in the exponential function.

Chapter 10 does the same for multicompartmental models. Again, an appendix is provided to illustrate how to obtain initial parameter estimates. This will again illustrate the critical link between the coefficients and exponentials in the exponential function, and the rate constants of a multicompartmental model. In both chapters, case studies will serve as examples.

Chapter 11 describes a special application often found in tracer kinetic analysis, precursor-product relationships. Here the equations are derived with the assumptions specifically given allowing the reader to understand fully the results from this type of analysis.

References

Anderson, D.H.: *Compartmental Modeling and Tracer Kinetics.* Springer-Verlag, Berlin, 1983.

Atkins G.L.: *Multicompartment Models for Biological Systems.* Methuen, London,1969.

Atkinson, Art. http://www.cc.nih.gov/ccc/principles/, 1999.

Carson E.R.: Jones E.A.: The use of kinetic analysis and mathematical modeling in the quantitation of metabolic pathways in vivo: Applica-

tion to hepatic anion metabolism. *N. Engl. J. Med. 300*:1016–1027, 1078–1086, 1979.

Carson E.R., Cobelli C., Finkelstein L.: *The Mathematical Modelling of Metabolic and Endocrine Systems*. Wiley, New York, NY, 1983.

Cobelli C., Caumo A.: Using what is accessible to measure that which is not: necessity of model of system. *Metabolism 47*:1009–1035, 1998.

DiStefano, J. III, Landaw E.M.: Multiexponential multicompartmental, and noncompartmental modeling. I. Methodological limitations and physiological interpretations. *Am. J. Physiol. 246:*R651–R664, 1984.

Gibaldi M., Perrier D.: *Pharmacokinetics,* 2nd ed. Marcel Dekker, New York, NY, 1982.

Godfrey K.: *Compartmental Models and Their Application.*

Gurpide E.: *Tracer Methods in Hormone Research.* Springer-Verlag, Berlin, 1975.

Jacquez J.A.: *Compartmental Analysis in Biology and Medicine,* 3rd ed. BioMedware, Ann Arbor,MI, 1996.

Landaw E.M., DiStefano J.J. III: Multiexponential, multicompartmental and noncompartmental modeling. II. Data analysis and statistical considerations. *Am. J. Physiol. 246*:R665-R677, 1984.

Lassen N.A., Perl W.: *Tracer Kinetic Methods in Medical Physiology.* Raven Press, New York, NY, 1979.

Norwich K.H.: *Molecular Dynamics in Biosystems: The Kinetics of Tracers in Intact Organisms.* Pergamon Press, Oxford, 1977.

Rescigno A., Segre G.: *Drug and Tracer Kinetics.* Blaisdell, Waltham, MA, 1966.

Riggs D.S.: *The Mathematical Approach to Physiological Problems.* Williams & Wilkins, Baltimore, MD, 1963 (available edition, MIT Press, Cambridge, MA, 1975).

Rowland M., Tozer T.: *Clinical Pharmacokinetics: Concepts and Applications*, 3rd ed. Williams & Wilkins, Baltimore, MD, 1995.

Shipley R.A., Clark R.E.: *Tracer Methods for in Vivo Kinetics*. Academic Press, New York, NY, 1972.

Wolfe R.R.: *Radioactive and Stable Isotope Tracers in Medicine.* Wiley-Liss, New York, NY, 1992.

This page intentionally left blank.

Chapter 2

FUNDAMENTALS OF TRACER KINETICS

2.1   INTRODUCTION

As defined in Chapter 1, the kinetics of a substance in a biological system are its spatial and temporal distribution in that system. The kinetics are the result of several complex events including circulatory dynamics, transport into cells, and utilization. Utilization usually requires biochemical transformations which are characteristics of the substance. The substance can be an element such as calcium or zinc, or a compound such as amino acids, proteins or sugars. All exist normally in the body, and can be of endogenous or exogenous sources, or both. The primary goal of the kinetic events characterizing the metabolism of a substance is to maintain specific levels of the substance in the various components of its systems. The maintenance of these levels is achieved by internal control mechanisms, and involves input into the system to balance the loss which occurs through utilization and excretion.

One wishes to understand the kinetics of a substance under normal circumstances in order to better understand pathophysiological conditions since these may be a result of abnormal kinetics. A fundamental problem in biology and medicine, therefore, is to describe quantitatively the kinetics of substances existing in the body. Among the tools that are available, tracers have been extensively used. Tracers are substances introduced externally into the system to provide data from which quantitative estimates of events characterizing the kinetics of the substance can be made. Tracers can be substances such as dyes or, as described in more detail below, substances labeled with radioactive or stable isotopes.

In this text, the focus will be on characterizing the kinetics of substances already present in the body by using isotopic tracers as probes.

A naturally occurring substance is called a **tracee.** The tracers will be assumed to be ideal where an **ideal tracer** is a substance with the following characteristics:

    a. it is detectable by an observer,

    b. its introduction into a system does not perturb the system being studied, and

    c. it is indistinguishable with respect to the properties of the tracee system being studied.

The first requirement, that of detectability, means that there must be some method by which the amount of tracer in a sample can be quantified. The second requirement means that the introduction of a tracer into the system has no effect on the ongoing metabolic processes which characterize the system under study. This requirement is usually met by introducing an extremely small amount of tracer compared with the amount of tracee already existing, and arguing this small perturbation does not disturb the system. The third requirement means that the system being studied is not able to distinguish between the tracer and tracee, i.e. both follow the same processes with equal probabilities. These requirements are usually met, but the investigator should be aware that problems associated with them can arise.

By definition, the tracer has its own kinetics. The goal of a tracer kinetic study is to infer from the tracer kinetics information on the tracee kinetics. If the three requirements are met, this goal can be attained.

2.2   THE TRACER-TRACEE SYSTEM

2.2.1   Concepts and Definitions

A convenient scheme to illustrate the kinetics of a substance is shown in Figure 2.2.1. In this figure, the circles represent the masses of two interacting substances in specific forms at specific locations, and the arrows represent the transport or flux of material and/or biochemical transformations. This figure shows two specific substances, A and B, to make the point that kinetics includes both transport between different locations, and biochemical transformation. The goal of the tracer study is to determine the masses and fluxes, i.e. transport and biochemical transformation, in this system.

A fundamental assumption in using tracers is that there is at least one component in the system under study which is accessible for tracer administration, and tracer and tracee sampling. This special component is called the **accessible pool.** Examples of accessible pools are a sub-
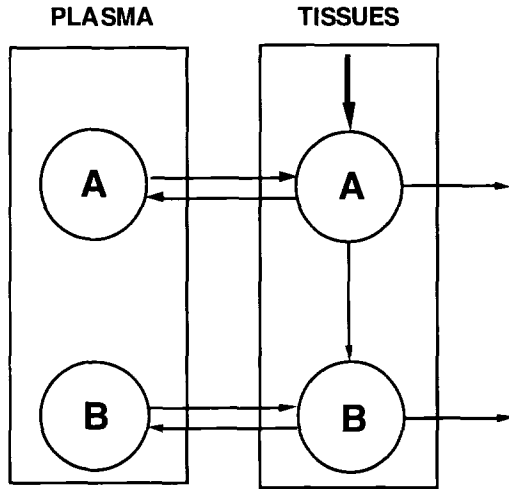
Figure 2.2.1. A schematic of the kinetics of a substance. The circles represent masses and the arrows the fluxes of the substance. The bold arrow into circle A in the tissue represents de novo synthesis. From this pool, it can (i) be irreversibly removed, (ii) exchange with a plasma pool, or (iii) be transformed into form B. In turn, B can exchange with a plasma pool, or irreversibly removed.

stance in physiological spaces such as plasma or a tissue, or a substance in expired air.

Suppose in the system shown in Figure 2.2.1, the plasma component for A is accessible. This means measurements of A can be obtained from plasma. One can redraw this system to emphasize the accessibility of this component for tracee measurement; this is shown in Figure 2.2.2. Notice that while B also exists in plasma, it may not be possible to sample and measure it. Thus plasma B is not accessible, even though it is in plasma. If B could be measured, then this system would have two accessible pools, one for A and one for B. This simple observation will have profound consequences when multiple input-multiple output experimental designs are discussed later.

Suppose the kinetics of the tracee substance described in Figure 2.2.2 is to be studied. The characterization of the system by identifying the components and interconnections, and the availability of at least one accessible pool, set the stage for using a tracer to characterize these
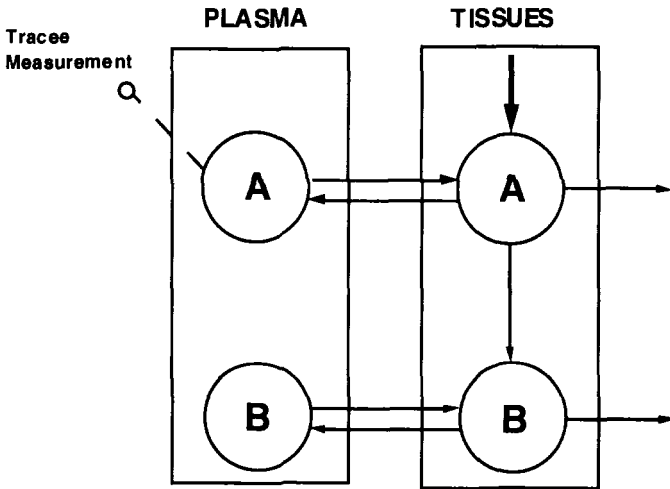
Figure 2.2.2.   The system depicted in Figure 2.2.1 with an accessible pool identified and highlighted by the dotted line with the bullet which indicates tracee measurement. The bold arrow into tissue pool A represents de novo entry of material into the system.

kinetics. By appealing to the definition of an ideal tracer, one can assume that the system described in Figure 2.2.2 for the tracee is the same as that for the tracer. Therefore, superimposing the tracer system on that shown in Figure 2.2.2, one has the system shown in Figure 2.2.3.

These two figures emphasize that the two systems for the tracee and tracer are structurally identical, and demonstrate the need for an accessible pool into which tracer can be introduced and from which measurements of tracer and tracee can be made. The main difference between the two is in the inputs. In the tracee system shown in Figure 2.2.2, the input is endogenous into a nonaccessible component of the system. In the tracer system shown above, the input is exogenous, and is into the accessible pool.

Using these figures as representative of tracee and tracer systems, the following will be discussed: (i) the tracee system, (ii) the tracer experiment and the tracer system, (iii) the relationship between the tracee and tracer systems, and (iv) the quantitation of the tracee system from the tracer data. Following a general discussion, the notions will then be applied to radioactive and stable isotopic tracers where, to pass from
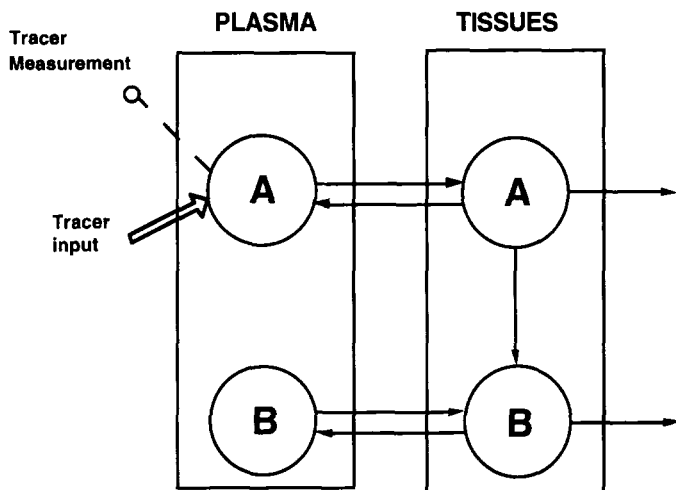
Figure 2.2.3. The tracer system which corresponds to the tracee system depicted in Figure 2.2.2. The administration of the tracer into and sampling from the accessible pool is indicated by the tracer input arrow and tracer measurement sample respectively. The figure implies that once in the system, the tracer is assumed to follow the same pathways the tracee follows.

theory to practice, the measurement of the tracer will be discussed in detail. This strategy will serve to emphasize similarities and differences between using radioactive and stable isotopic tracers, and will form the basis for the analysis of the tracer data with the concomitant inferences about the metabolism of the tracee.

In this Chapter, only the single pool steady-state system will be discussed as a vehicle to introduce the necessary terminology. The precise analyses and the extension to multipool systems will be discussed in subsequent chapters.

2.2.2 The Tracee System

The tracee system to be discussed in this section is given in Figure 2.2.4. The system described in Figure 2.2.4 is a single pool system which is accessible for measurement and in which it is further assumed that the tracee is uniformly distributed. The accessible pool and the system coincide in this particular situation.
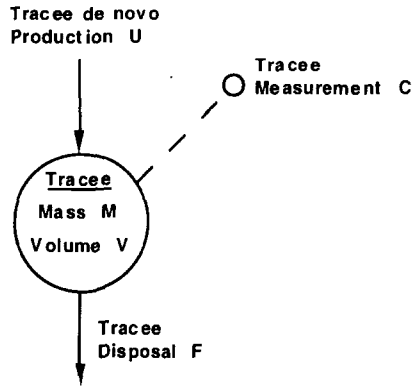
Figure 2.2.4. The tracee system, depicted as a circle, consists of a single pool of volume V containing tracee mass M. Tracee de novo production, U, and disposal F occurs from this pool; they are indicated by the arrows into and leaving the system respectively. The dotted line with the bullet indicates tracee measurement. The symbols given in this figure are summarized in Table 2.2.1

The notation introduced in Figure 2.2.4 which will be used for the tracee system is given in Table 2.2.1. U is sometimes called de novo synthesis, and F utilization, elimination or excretion. Concentration C is defined below in (2.2.3).

Table 2.2.1.   Notation for tracee variables

Symbol	Definition and Units
V	volume
M	mass
C	concentration (mass/volume)
U	de novo production (mass/time)
F	disposal (mass/time)

Assume the tracee system is in the steady-state case. A **steady state** is an experimental situation where de novo production U and disposal F are equal and constant. This means that the tracee mass M remains constant. To formalize this assumption in mathematical terms, one applies the mass balance principal to the tracee system, i.e. at any point in time the rate at which the tracee mass changes is the difference between

de novo production and disposal. Remembering that U and F are equal, the desired formalism can be expressed in the following equation:

$$\frac{dM(t)}{dt} = U - F = 0 \qquad (2.2.1)$$

where t denotes time. In other words, as a result of $U = F$, the rate of change of the tracee mass as a function of time, $\frac{dM(t)}{dt}$, is equal to zero. This means $M(t)$ does not change with time, hence

$$M(t) = M = \text{constant} \qquad (2.2.2)$$

For the tracee, the measured value is usually concentration C where

$$C = \frac{M}{V} \qquad (2.2.3)$$

In the steady state, C, as a result of the balance between U and F, is a constant. However, from a knowledge of C alone, it is not possible to estimate the fluxes U and F; to do this, a tracer must be used.

2.2.3   The Tracer System

The tracer system to be discussed in this section is given in Figure 2.2.5. As in the previous case, this is single pool system which is accessible for measurement and in which the tracer is assumed to distribute uniformly. Because of tracer-tracee indistinguishability, the volume V is equal to the volume of distribution of the tracee. The notation used in this figure is summarized in Table 2.2.2 below. Note in this table, unlike Table 2.2.1, the dependence of some variables such as mass on time t is explicitly noted, i.e. $m(t)$.

Table 2.2.2.   Notation for tracer variables

Symbol	Definition and Units
V	volume
$m(t)$	mass
$u(t)$	rate of input (mass/time)
$f(t)$	disposal (mass/time)
d	total input (mass)

The analogue for (2.2.1) for the tracer can be written by again appealing to the mass balance principal, i.e. the rate of change of tracer mass is the difference between the rate of tracer input $u(t)$ and tracer disposal $f(t)$:
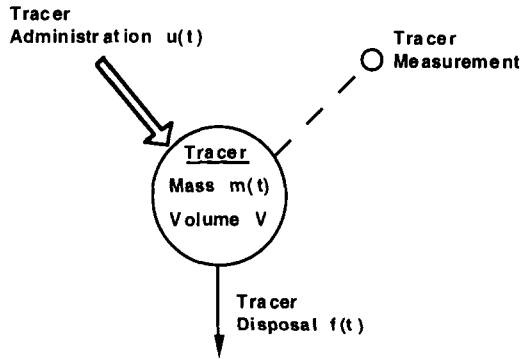
Figure 2.2.5. The tracer system, depicted as a circle, is a single pool of volume V containing tracer mass $m(t)$. Tracer is introduced into the system at a rate $u(t)$; the rate of disposal from this pool is given by $f(t)$. The dotted line with the bullet indicates tracer measurement.

$$\frac{dm(t)}{dt} = u(t) - f(t) \qquad m(0) = 0 \qquad (2.2.4)$$

In (2.2.4), $m(0) = 0$ means that when the experiment starts at $t = 0$, there is no tracer mass in the system. (In mathematical terms, $m(0)$ is called the initial condition). In this situation, unlike the previous case where M is constant, $m(t)$ changes with time and hence $\frac{dm(t)}{dt}$ is no longer equal to zero.

While (2.2.4) is written in terms of tracer mass $m(t)$, the manner in which the amount of tracer is actually quantified depends upon the tracer chosen. As discussed in §2.4, the radioactive tracer is usually quantified in terms of tracer concentration $c(t)$, i.e. tracer mass per unit volume:

$$c(t) = \frac{m(t)}{V} \qquad (2.2.5)$$

In contrast, the most convenient way to express stable isotope measurements as discussed in §2.5 is the tracer mass per unit tracee mass:

$$z(t) = \frac{m(t)}{M} \qquad (2.2.6)$$

Since the volume V is the same for both the tracee and tracer, $z(t)$ also represents the ratio between tracer and tracee concentrations:

$$z(t) = \frac{m(t)}{M} \simeq \frac{c(t)}{C} \tag{2.2.7}$$

2.2.4   The Tracer-Tracee System

The link between the tracer and tracee system comes from the tracer-tracee indistinguishability assumption. This assumption implies that the probability that the tracer leaves the pool is equal to the probability that a particle in the pool is a tracer. This can be written as

$$\frac{f(t)}{F + f(t)} = \frac{m(t)}{M + m(t)} \tag{2.2.8}$$

This equation can be reorganized:

$$\frac{\frac{f(t)}{F}}{1 + \frac{f(t)}{F}} = \frac{\frac{m(t)}{M}}{1 + \frac{m(t)}{M}} \tag{2.2.9}$$

from which one obtains

$$f(t) = \frac{F}{M} m(t) \tag{2.2.10}$$

which, when this expression for $f(t)$ is substituted into (2.2.4), gives

$$\frac{dm(t)}{dt} = u(t) - f(t) = u(t) - \frac{F}{M} m(t) = u(t) - km(t) \tag{2.2.11}$$

where $k = \frac{F}{M}$. This equation is a linear, constant coefficient differential equation which provides the link between the tracer and tracee systems since the tracer parameter k reflects tracee events, $k = \frac{F}{M}$.

2.2.5   System Parameters from Tracer and Tracee Measurements

In the single pool system under consideration, the unknown parameters of interest are F and M. It is the purpose of the tracer experiment to generate the tracer and tracee data from which these parameters can be estimated. One possible method is based on the solution of the tracer model given by (2.2.11). Here $m(t)$ is expressed as a function of the unknown tracer parameter, k, (and thus of the tracee parameters since $k = F/M$) and the known tracer input $u(t)$. For instance, if the tracer

experiment consists of injecting the tracer as a bolus of dose d at time zero, then the solution of (2.2.11) is

$$m(t) = de^{-kt} \qquad (2.2.12)$$

Hence the tracer measurement can be related to the model parameters. In particular, if a radioactive tracer is used and its concentration c(t) is measured, then

$$c(t) = \frac{m(t)}{V} = \frac{d}{V}e^{-kt} \qquad (2.2.13)$$

where the unknown parameters are the volume V and the exponential k. Both parameters can be estimated from the tracer data: the ratio $\frac{d}{V}$ equals the tracer concentration at time zero whence

$$V = \frac{d}{c(0)} \qquad (2.2.14)$$

while k can be estimated from the rate of decay of the tracer. From the estimates of k and V, and knowing the tracee concentration C, the system tracee mass and fluxes can be quantified since, from the definition of C and k,

$$M = C \cdot V \qquad (2.2.15)$$

$$U = F = kM$$

The same procedure applies if a stable isotope is used. In this case, the tracer measurement is the tracer to tracee ratio $z(t)$. The counterpart of (2.2.13) become

$$z(t) = \frac{m(t)}{M} = \frac{d}{M}e^{-kt} \qquad (2.2.16)$$

Here M plays the role that V played in (2.2.13). The parameters k and M can be estimated from the tracer data as before, whence $U = F = kM$.

The rationale applied above serves as the basis for the compartmental modeling analysis which will be expanded in Chapters 4–6. Alternatively, the flux F can be quantified from the tracer and tracee data by using the noncompartmental analysis approach discussed in Chapter 3. Briefly, the conservation of mass principal applied to the tracer (i.e., the amount of tracer introduced into the system equals the amount leaving the system), can be written

$$d = \int_0^\infty u(t)dt = \int_0^\infty f(t)dt \qquad (2.2.17)$$

since d, the total amount of tracer introduced into the system, is equal to $\int_0^\infty u(t)dt$. Substituting the expression for $f(t)$ given in (2.2.10) into this equation, one obtains

$$d = \int_0^\infty \frac{F}{M}m(t)dt \qquad (2.2.18)$$

which, when solved for F, gives

$$F = \frac{d}{\int_0^\infty \frac{m(t)}{M}dt} = U \qquad (2.2.19)$$

From (2.2.19), F can be expressed as a function of tracer and tracee measurements. If the tracer is quantitated in terms of the tracer to tracee ratio $z(t)$, it follows immediately from the definition that

$$F = \frac{d}{\int_0^\infty z(t)dt} = U \qquad (2.2.20)$$

If the tracer measurement is concentration $c(t)$, then the expression for F as a function of $c(t)$ can be derived from the equality $\frac{m(t)}{M} = \frac{c(t)}{C}$, hence

$$F = \frac{d}{\int_0^\infty \frac{c(t)}{C}dt} = \frac{d \cdot C}{\int_0^\infty c(t)dt} = U \qquad (2.2.21)$$

2.3   THE TRACER-TRACEE SYSTEM WITH ISOTOPIC TRACERS

2.3.1   Concepts and Definitions

The preceding section describes the underlying theory for a generic tracer in a steady-state tracee system. In this section, the notation given in Table 2.2.1 and Table 2.2.2 will be expanded to accommodate the theory underlying the use of radioactive and stable isotopic tracers.

While it is assumed that the reader is familiar with the general concepts of isotopes [Sorenson and Phelps, 1987; Watson, 1987; Wolfe, 1992], it is useful to summarize the basics required for the present discussion. Each element is characterized by the number of protons in its nucleus; this determines its atomic number. The nucleus also contains a number of neutrons. This number can vary within limits for each element. The sum of the number of neutrons and protons is the mass number. Atoms of the same clement which have the same number of protons but a different number of neutrons are called isotopes. They have the same atomic number, and thus similar chemical properties, but

a different mass number. Isotopes can either be stable (called **stable isotopes)** or unstable. In the latter case, they spontaneously undergo nuclear transition with the emission of energy, and are called **radioactive isotopes.**

For example, the hydrogen element (symbol H) has one proton and thus its atomic number is equal to 1. In nature, there exist three hydrogen isotopes with the number of neutrons equal to 0, 1 or 2. These isotopes have different mass numbers of 1, 2 or 3, and are denoted ^1H, ^2H or ^3H where the superscript is equal to the mass number of the isotope. Two of the isotopes are stable, ^1H and ^2H while the third, ^3H, is an unstable β^- emitter.

Carbon (symbol C), on the other hand, is characterized by 6 protons. Since the number of neutrons for carbon can range from 4 to 10, seven carbon isotopes exist in nature. Only two, ^{12}C and ^{13}C having 6 and 7 neutrons respectively are stable. Among the unstable isotopes, ^{14}C and ^{11}C are often employed in tracer studies in biology and medicine. The isotope ^{14}C is a β^--emitting isotope and is often used to create a radioactive tracer while ^{11}C, a β^+-emitting isotope, is used in positron emission tomography (PET) studies.

For any given element, the natural abundance of its stable isotopes is remarkably constant, and in a number of cases, one stable isotope is much more abundant than others; this is called the most abundant isotope. For example for hydrogen, the relative abundance of the stable isotopes ^1H and ^2H is respectively 99.985% and 0.015%. For carbon, the relative abundance of ^{12}C and ^{13}C is respectively 98.89% and 1.11%.

By comparison, zinc (symbol Zn) has five stable isotopes existing in nature: ^{64}Zn, ^{66}Zn, ^{67}Zn, ^{68}Zn and ^{70}Zn. The natural abundance of each is respectively 48.89%, 27.81%, 4.11%, 18.57% and 0.62%.

For radioactive isotopes that are used in biology and medicine, their mass in nature is negligible compared with the stable isotopes. For instance in nature, the order of magnitude is one atom of ^{14}C to 10^{12} atoms of ^{12}C

Radioactive and stable isotope tracers are used as isotopic tracers of an element. For instance, the artificially produced radioactive isotope ^{69m}Zn of zinc can be used to study zinc kinetics. As an alternative, a stable isotope of zinc can also be used by producing an elevation of the abundance of, for example, ^{70}Zn, from 0.62% up to 95%.

Isotopes are more commonly used to create tracers for complex molecules. Glucose, for example, consists of carbon, hydrogen and oxygen atoms. Considering the carbon atoms of natural glucose, a typical glucose molecule will essentially contain ^{12}C and ^{13}C isotopes since the relative proportion of unstable isotopes is negligible. To produce an isotopic

glucose tracer, the amount of ^{13}C or ^{14}C is artificially elevated at one or more specific carbon atom positions in the glucose molecule. Hence the isotopic species of the molecule being studied can be defined with reference to one specific element in one or more specific positions. The enriched isotope is frequently called a label while the molecule is said to be labeled by this atom. For example, the carbon isotope ^{14}C can be used to label glucose in the number one position; the labeled species is written [1-^{14}C]-glucose. Similarly, the carbon isotope ^{13}C can be used to label glucose in two positions producing, for example, [1,2-^{13}C$_2$]-glucose. The corresponding unlabeled species are [1-^{12}C]-glucose and [1,2-^{12}C$_2$]-glucose respectively. As will be seen in this Chapter, the problem is how to quantitate the amount of tracer and tracee in a sample.

The following table, which gives a more precise formulation than Table 2.2.2, summarizes the notation to be used for the tracer variables. In addition to the most abundant species ^{a}, one less abundant stable ^{s} and radioactive ^{r} species are considered.

Table 2.3.1.   Expanded notation for tracer variables.

Symbol	Definition and Units
V	volume
$m^a(t),\ m^s(t),\ m^r(t)$	mass of species ^{a}, ^{s} and ^{r}
$u^a(t), u^s(t), u^r(t)$	rate of input (mass/time) of species ^{a}, ^{s} and ^{r}
$f^a(t),\ f^s(t),\ f^r(t)$	disposal (mass/time) of species ^{a}, ^{s} and ^{r}

Paralleling the above notation for the tracer, the notation to be used for the tracee is summarized in Table 2.3.2.

Table 2.3.2.   Expanded notation for tracee variables.

Symbol	Definition and Units
V	volume
M^a, M^s	mass of species ^{a} and ^{s}
C^a, C^s	concentration (mass/volume) of species ^{a} and ^{s}
U^a, U^s	*de novo* production (mass/time) of species ^{a} and ^{s}
F^a, F^s	disposal (mass/time) of species ^{a} and ^{s}

Figure 2.3.1 summarizes the above definitions and notation. It will help to elucidate the basic ideas discussed in §2.4 and §2.5 related to the measurement of radioactive and stable isotope tracers.
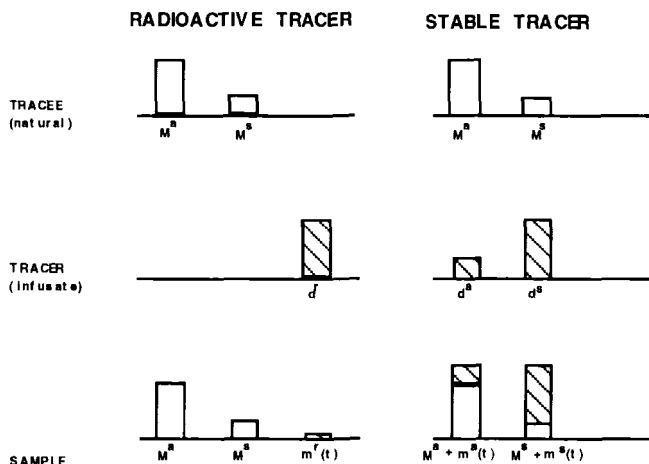
Figure 2.3.1.   Bar chart showing the relative contributions of ^{a}, ^{s} and ^{r} respectively to the tracee and the tracer in a sample taken during either a radioactive or stable isotope tracer experiment. The symbols used are those used in Table 2.3.1 and Table 2.3.2.

2.3.2   Relationships Among Isotopic Variables

Having split the tracer and tracee masses into a number of compo-
nents related to the different isotopic species in the compound, one must
now extend the relationships given in the previous section to each iso-
tope. Considering the tracee first, one can write the indistinguishability
principal for the three isotopic species as

$$\frac{F^a}{M^a} = \frac{F^s}{M^s} = \frac{F}{M} \tag{2.3.1}$$

This is the counterpart to (2.2.10). From the steady-state mass balance
equations for the tracee, one has the counterpart of the general equation

$$0 = U - F \tag{2.3.2}$$

written as follows for the three isotopic species

$$U^a - F^a = U^s - F^s = 0 \tag{2.3.3}$$

from which

$$\frac{U^a}{M^a} = \frac{U^s}{M^s} = \frac{U}{M}$$

(2.3.4)

follows.

This equation states that, for the tracee under steady state conditions, the ratio between the input rate and mass is the same for all isotopic species, and is equal to the ratio between total input U and total mass M. It should be noted that a similar relationship also holds when the above tracee fluxes and masses are time varying, provided that the isotopic composition of the input doesn't change with time:

$$\frac{U^a(t)}{M^a(t)} = \frac{U^s(t)}{M^s(t)} = \frac{U(t)}{M(t)}$$

(2.3.5)

and for the tracer species provided that the isotope composition of the input is constant:

$$\frac{u^a(t)}{m^a(t)} = \frac{u^s(t)}{m^s(t)} = \frac{u^r(t)}{m^r(t)} = \frac{u(t)}{m(t)}$$

(2.3.6)

A formal proof of the above relationships can be found in Appendix A.

2.4   THE RADIOACTIVE TRACER VARIABLES

2.4.1   Measurements

To apply the general theory of isotopic tracers to the particular case where radioactive isotopic tracers are used, it is important to discuss in more detail how the input d and the tracer mass $m(t)$ are quantitated. Usually the measured variable is the tracer concentration $c(t) = \frac{m(t)}{V}$, but its quantitation is in terms of radioactivity in order to take advantage of the fact that radioactive isotopic tracers, being unstable, emit energy as they undergo nuclear change. The measurement of the tracer input $u(t)$ is related to this energy emission as well. Some background information on units and measurement techniques is necessary in order to describe the quantitation of a radioactive isotopic tracer sample.

The recommended standard SI unit of radioactivity is disintegration per second (dps) or bequerel. The practical units of activity used in biomedical research are disintegrations per minute, dpm, or the curie which equals 3.7×10^{10} disintegrations per second. One usually deals with microcuries, μCi, which is equal to 1/1,000,000 of a curie. One μCi equals: 3.7×10^4 disintegrations per second, or 2.2×10^6 disintegrations per minute (dpm).

One cannot, however, measure radioactivity directly in terms of dpm. For instance, when an investigator uses a beta or gamma counter, a measure of the radioactivity in the sample of interest in terms of counts per minute, cpm, instead of dpm, is obtained. The cpm data are a function of the counter and the isotope being analyzed, and include background activity from, for example, electronic noise, detection of cosmic rays, natural radioactivity. For each counter and isotope, there are rules the investigator must follow to convert from cpm to dpm. It will be assumed in this text that the investigator is familiar with these concepts, and if using a radioactive isotopic tracer, can correctly calculate the dpm for each sample.

How does the emission of energy by a radioactive isotope help in the quantification of the tracer concentration $c(t)$? For each radioactive isotope of an element, there is a proportional relationship between the mass of the isotope and the dpm emitted by that mass. This can be written

$$\text{dpm of } m^r(t) = \nu m^r(t) \tag{2.4.1}$$

where ν is the proportionality constant. If $c(t)$ denotes the measurement of tracer concentration, in terms of dpm per unit volume, one obtains

$$c(t) = \frac{\nu m^r(t)}{V} \tag{2.4.2}$$

This provides a measure of the tracer mass since when the tracer is carrier free, i.e. $m^a(t) = m^s(t) = 0$ whence $m(t) = m^r(t)$ so that

$$c(t) = \frac{\nu m(t)}{V} \tag{2.4.3}$$

However, as shown in the next section, even if the tracer is introduced with a carrier which is the most common situation in practice, i.e. $m^a(t) \neq 0$ and $m^s(t) \neq 0$, the tracer quantified in terms of dpm can still be used.

Note that the mass $m^r(t)$ introduced with the tracer is negligible since a negligible amount of tracer produces a detectable signal which can be quantitated in terms of dpm. Mass introduced with a carrier, $m^a(t) + m^s(t)$, is also negligible since it is usually of the order of magnitude of $m^r(t)$. This is why in Figure 2.3.1 only the radioactive bar is shown for the tracer (in contrast the most abundant and the stable bar are absent). A mass perturbation is thus normally not an issue with radioactive tracers.

Another measure of radioactivity that is frequently used is the radioactivity per unit mass. This is the quotient of $\nu m(t)$ to $M + m(t)$. This quotient is called **specific activity**, denoted *sa*. It is defined

$$sa(t) = \frac{\nu m(t)}{M + m(t)} \tag{2.4.4}$$

The units are dpm/mass. One usually calculates the specific activity as the quotient of the tracer and tracee concentrations since $m(t) << M$:

$$sa(t) \approx \frac{\nu m(t)}{M} = \frac{c(t)}{C} = z(t) \tag{2.4.5}$$

where $z(t)$ was defined in (2.2.6).

2.4.2   Kinetic Variables

While the variables for the general isotopic tracer are given in units of mass, the measurements of radioactive tracers are not in terms of mass, but energy. In order to rewrite the equations for F given in §2.2 using variables in these units, one must use v to convert d and $m(t)$ from units of mass to units of energy. Consider first the simplest situation where the tracer is carrier free so that $\nu m^r(t)$ provides an indirect measurement of the mass $m(t)$; similarly for u. One can rewrite the mass balance equation (2.2.11) by multiplying both sides by the proportionality constant v to obtain

$$\nu \frac{dm(t)}{dt} = \frac{d(\nu m(t))}{dt} = -k\nu m(t) + \nu u(t) \tag{2.4.6}$$

Therefore the same equation holds for the tracer whether the units are mass as in (2.2.11) or in dpm as in (2.4.6). Paralleling the discussion in §2.2, if one regards (2.2.11) or (2.4.6) as the compartmental model equation, the system is completely specified by coupling the state equation (2.4.6) to the measurement equation (2.4.3). Similarly for the noncompartmental expression given in §2.2 for F, since the tracer is carrier free $d^r = d$, and (2.2.11) can be written in terms of the measured dpms, by multiplying the numerator and denominator of this expression by the proportionality constant v,

$$F = \frac{\nu \cdot d \cdot C}{\int_0^\infty \frac{\nu m(t)}{V} dt} = \frac{\nu \cdot d \cdot C}{\int_0^\infty c(t) dt} = U \tag{2.4.7}$$

In summary for the carrier free case, all of the formulas given in §2.2 are valid whether the radioactive tracer is quantified in terms of mass or dpm. The reason is that the mass and dpm are proportional:

$$\text{dpm of } m^r(t) = \nu m^r(t) = \nu m(t) \qquad (2.4.8)$$

$$\text{dpm of } d^r = \nu d^r = \nu d \qquad \text{dpm of } u^r(t) = \nu u^r(t) = \nu u(t)$$

The crucial observation is that these relations arc still valid even if the tracer is not carrier free. Since the relative composition of species ^{r} in the tracer input, written $\omega^r = \frac{d^r}{d} = \frac{u^r(t)}{u(t)}$ and described in detail in Appendix A, is constant, one has

$$u^r(t) = \omega^r u(t) \qquad (2.4.9)$$

From (2.3.6)

$$m^r(t) = \omega^r m(t) \qquad (2.4.10)$$

The measurements of $u^r(t)$ and $m^r(t)$ in terms of dpm are still proportional to their corresponding masses:

$$\text{dpm of } m^r(t) = \nu m^r(t) = \omega^r \nu m(t) \qquad (2.4.11)$$

$$\text{dpm of } u^r(t) = \nu u^r(t) = \omega^r \nu u(t)$$

These proportionalities guarantee the equivalence of the formalism whether the radioactive tracer introduced on a carrier is quantified in terms of mass or dpm, as it can easily be shown by following the same logic as that used in the carrier free case with $\omega^r \nu$ replacing ν,

In this section, care has been taken to separate the notions of the tracer quantified in terms of mass and dpm. As seen, all formulas listed in §2.2 and §2.3 are valid whether the radioactive tracer is quantified in terms of mass or dpm. For the reason, in the remainder of the text the notation given in §2.2 for the general tracer will be adopted for the radioactive tracer case. This also points out the similarity with other tracers whose mass can be quantified by a measurement proportional to the mass.

2.5   THE STABLE ISOTOPE TRACER VARIABLES

2.5.1   Measurements

As shown in Figure 2.3.1, the situation with stable isotope tracers is different from the radioactive case since (i) the stable isotope tracer introduced into a system usually has nonnegligible mass unlike the radioactive case where the mass can be assumed to be negligible; (ii) there is always some labelled species existing at a natural level in the tracee, (iii) there is some of the naturally most abundant species in the tracer

input; and (iv) the measurement of the stable isotope tracer can be expressed in a variety of ways related to ratios of isotopic species.

The fact that the tracer may have nonnegligible mass is necessary in order to have enough tracer mass in a sample to be quantitated. Therefore, the assumption that the endogenous constant steady-state is not perturbed by the administration of the stable isotope tracer needs to be explicitly taken into account. Usually the tracer perturbation is often confined within a few percent, and hence this assumption is likely to be satisfied. Therefore in the following, the stable isotope measurement and kinetic variables will be discussed assuming that the endogenous steady state is not perturbed by the input of tracer. Later the non-perturbation assumption will be examined, and a method will be outlined to test it.

To apply the general theory of isotopic tracers to the particular case where stable isotopic tracers are used, one must be able to quantitate the tracer input d and mass in a sample. The notation given in Table 2.3.1 and Table 2.3.2 will be used.

The quantification in a sample of the amount of stable isotopes of an element, i.e. the most and least abundant species relies on the ability of the mass spectrometer instrument to distinguish among isotopic species based on differences in their mass number. The output is given in terms of peaks associated with each species along a mass scale; the intensities of the peaks are proportional to the abundances of the isotope combinations in the molecule having a given mass number. In order to derive from the peak intensities the measurements in terms of relative composition in the sample of labelled and unlabelled species, transformations have to be made between the peak intensities and masses. It is assumed that the investigator is familiar with these techniques.

The final measurements can be expressed in a variety of ways [Cobelli et al., 1992]. One is the quotient of the amount of species ^{s} and ^{a} in the sample; this is called the **isotope ratio,** $r(t)$, defined by

$$r(t) = \frac{M^s + m^s(t)}{M^a + m^a(t)} \tag{2.5.1}$$

For convenience, the naturally occurring isotope ratio is denoted r_N:

$$r_N = \frac{M^s}{M^a} \tag{2.5.2}$$

and the isotope ratio of the tracer (before administered into the system) by r_I:

$$r_I = \frac{d^s}{d^a} \tag{2.5.3}$$

As an example of $r(t)$, consider as a tracer glucose molecules enriched by ^{13}C in position 3. In this case, in each sample $m^a(t)$ and $m^s(t)$ will represent the amount of ^{12}C and ^{13}C at position 3 contributed by the tracer while $.M^a$ and M^s is the amount of ^{12}C and ^{13}C at position 3 naturally present in the system. The expression for $r(t)$ is then

$$r(t) = \frac{[3 - {}^{13}\text{C}] - \text{glucose}}{[3 - {}^{12}\text{C}] - \text{glucose}} \qquad (2.5.4)$$

The **isotope abundance,** $a(t)$, is defined as the quotient of the mass of the labeled species and the total mass (the sum of the labeled plus unlabeled species):

$$a(t) = \frac{M^s + m^s(t)}{M + m(t)} = \frac{M^s + m^s(t)}{M^a + m^a(t) + M^s + m^s(t)} \qquad (2.5.5)$$

Isotope abundance $a(t)$ can be expressed in terms of the isotope ratio $r(t)$:

$$a(t) = \frac{r(t)}{1 + r(t)} \qquad (2.5.6)$$

It is convenient to define the natural isotope abundance and the abundance for the tracer (prior to administrating it into the system) by:

$$a_N = \frac{M^s}{M^a + M^s} = \frac{r_N}{1 + r_N} \qquad (2.5.7)$$

and

$$a_I = \frac{d^s}{d^a + d^s} = \frac{r_I}{1 + r_I} \qquad (2.5.8)$$

respectively

The **enrichment,** $e(t)$, is defined as the abundance of the labeled species above its natural level. Unlike $r(t)$ and $a(t)$ which have specific expressions, there are two commonly used ways of expressing $e(t)$ in terms of $r(t)$. These are given below:

$$e_1(t) = a(t) - a_N = \frac{r(t)}{1 + r(t)} - \frac{r_N}{1 + r_N} \qquad (2.5.9a)$$

$$e_2(t) = \frac{r(t) - r_N}{1 + r(t) - r_N} \qquad (2.5.9b)$$

The enrichment $e(t)$ is the most commonly used way of expressing stable isotope data. When multiplied by 100, it is expressed as a percent called atom percent excess. As in the previous cases, it is convenient to define enrichment for the tracer (prior to administering it into the system):

$$e_{1I} = a_I - a_N = \frac{r_I}{1 + r_I} - \frac{r_N}{1 + r_N} \qquad (2.5.10\text{a})$$

$$e_{2I} = \frac{r_I - r_N}{1 + r_I + r_N} \qquad (2.5.10\text{b})$$

Finally, the measurement can also be expressed as **tracer to tracee ratio** directly:

$$z(t) = \frac{m(t)}{M} = \frac{m^a(t) + m^s(t)}{M^a + M^s} \qquad (2.5.11)$$

Two other variables which can be measured are the pre-test tracee concentration and the total concentration during the experiment, respectively

$$C = \frac{M}{V} \qquad (2.5.12)$$

$$C_{tot}(t) = C + c(t) \qquad (2.5.13)$$

2.5.2 Kinetic Variables

It follows from the definitions in the previous sections that the tracer to tracee ratio $z(t)$ is the only measurement variable which is related directly to the tracer mass. If the stable isotope data are expressed in terms of $z(t)$, the output equation for the data is

$$z(t) = \frac{m(t)}{M} \qquad (2.5.14)$$

which is similar to the output equation (2.4.2) for the radioactive tracer; the difference is that the volume V in (2.4.2) is replaced by tracee mass M.

As anticipated in §2.2, the compartmental model parameters k and M can be estimated from the data, and the system fluxes can be evaluated. Similarly an expression for F using the noncompartmental approach can be given in terms of $z(t)$ using (2.2.20).

Neither the compartmental parameters k and M nor the noncompartmental expression for the system fluxes can be written in terms of stable isotope measurements such as $r(t)$, $a(t)$, $e(t)$ or $e_2(t)$ defined above since none of them are directly related to the tracer mass. The tracer to tracee ratio $z(t)$ is thus the most convenient way to express stable isotope data since it also permits a formalism similar to that of radioactive tracer data. Comparing (2.5.14) to (2.4.5), the analogy between $z(t)$ and specific activity is clear.

Often in the literature, enrichment is used as the analogue of specific activity. Why? The reason probably is because the definition of enrichment is very similar to that of specific activity, i.e. it is a measure of the relative amount of the labeled species above the natural level. As a consequence, it has been used instead of the correct variable $z(t)$ in kinetic formulas to estimate, for example, production rates or fractional synthetic rates (FSR). Appendix B is devoted to clarifying the relationship between $z(t)$ and $e(t)$, and to showing that $e(t)$ can be used to estimate the system fluxes from steady state tracer data only in special cases which require modifications to the usual formulas. In addition, it is shown that these formulas cannot be extended to the case where the tracer is time varying with one exception where a very specific assumption on the tracee system is satisfied.

In the general case, it is best to deal with the data in terms of $z(t)$. Thus one must be able to express $z(t)$ in terms of the other commonly used measurement variables. An expression for $z(t)$ in terms of $r(t)$ will be derived; the expression for $z(t)$ in terms of the other measured variables follows from (2.5.6) and (2.5.9).

To begin, one can rewrite the expression for $z(t)$ given in (2.5.11)

$$z(t) = \frac{m^a(t)(1 + \frac{m^s(t)}{m^a(t)})}{M^a(1 + \frac{M^s}{M^a})} \qquad (2.5.15)$$

Using the results in Appendix A, one obtains

$$\frac{m^s(t)}{m^a(t)} = \frac{u^s(t)}{u^a(t)} = \frac{d^s}{d^a} = r_I \qquad (2.5.16)$$

Using (2.5.16) and remembering $\frac{M^s}{M^a}$ is defined as r_N in (2.5.2), the variable $z(t)$ can now be written

$$z(t) = \frac{m^a(t)}{M^a} \frac{(1 + r_I)}{(1 + r_N)} \qquad (2.5.17)$$

Similarly, using (2.5.2) and (2.5.16), $r(t)$ can be expressed in terms of the ratio $\frac{m^a(t)}{M^a}$ by

$$r(t) = \frac{r_N M^a + r_I m^a(t)}{M^a + m^a(t)} = \frac{r_N + r_I \frac{m^a(t)}{M^a}}{1 + \frac{m^a(t)}{M^a}} \qquad (2.5.18)$$

Solving (2.5.18) for $\frac{m^a(t)}{M^a}$ one obtains

$$\frac{m^a(t)}{M^a} = \frac{r(t) - r_N}{r_I - r(t)} \qquad (2.5.19)$$

Substituting this into (2.5.17),

$$z(t) = \frac{r(t) - r_N}{r_I - r(t)} \cdot \frac{1 + r_I}{1 + r_N} \qquad (2.5.20)$$

The expression of $z(t)$ in terms of the variables given in §2.5.1 is summarized in Table 2.5.1. Using these formulas, it is possible to derive $z(t)$ in terms of the stable isotope measurement variables $a(t)$, $e_1(t)$ or $e_2(t)$ The variable $z(t)$ will be used in describing both noncompartmental and compartmental models applied to stable isotope data.

Table 2.5.1. Relation of Measurement Variables to z(t).

Measurement Variable	$z(t)$
$r(t) = \frac{M^s + m^s(t)}{M^a + m^a(t)}$	$z(t) = \frac{r(t) - r_N}{r_I - r(t)} \cdot \frac{1 + r_I}{1 + r_N}$
$a(t) = \frac{r(t)}{1 + r(t)}$	$z(t) = \frac{a(t) - a_N}{a_I - a(t)}$
$e_1(t) = \frac{r(t)}{1 + r(t)} - \frac{r_N}{1 + r_N}$	$z(t) = \frac{e_1(t)}{e_{1I} - e_1(t)}$
$e_2(t) = \frac{r(t) - r_N}{1 + r(t) - r_N}$	$z(t) = \frac{e_2(t)}{e_{2I} - e_2(t)} \cdot \left(1 - e_{2I} \frac{r_N}{1 + r_N}\right)$

The various measurement variables for stable isotopes can in fact have different shapes. Figure 2.5.1 provides an example of these differences.

2.5.3 The Multiple Species Case

Up to this point, only the case where there are two stable isotopic species has been considered. However, it may happen that more than two isotopic species need to be accounted for, either because the element has more than two stable isotopes (e.g. zinc), or because the tracer molecule is labelled in more than one position. For instance, for the $[6, 6, -^2H_2]$-glucose tracer case where two hydrogen atoms in position 6 of a glucose molecule are labelled with deuterium, three species arise: the unlabelled species having two hydrogen atoms in position six, the labelled species having two deuterium isotopes in position 6, and a
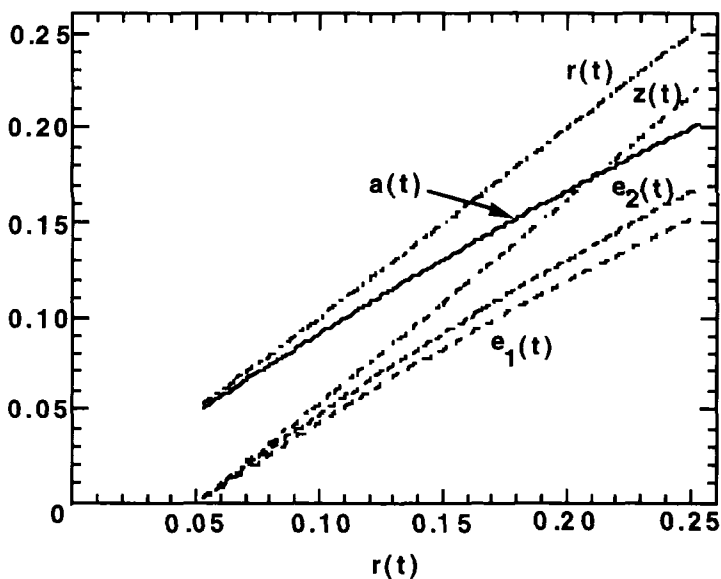
Figure 2.5.1.   The relationship among the variables r, a, e_1 and e_2 and z (for $r_N = 0.05$ and $r_I = 9$) for different values of $r(t)$ between 0.05 and 0.25.

partially labelled species having only one hydrogen atom in position 6 replaced with deuterium.

   The measurement variables such as the isotope ratio, enrichment or abundance refers only to labelled and unlabelled species. However, the tracer and tracee masses appear in the equation for $z(t)$, and by definition, comprise all isotopic species. The link between the isotope ratio r and the tracer to tracee ratio z must be modified:

$$z(t) = \frac{r(t) - r_N}{r_I - r(t)} \frac{1 + r_I + r_I' + r'' + \cdots}{1 + r_N + r_N' + r_N'' + \cdots} \qquad (2.5.21)$$

where $r(t)$, r_I, and r_N indicate as before the ratios between the labelled and unlabelled species, while $r_I', r_I'', \cdots$ and $r_N', r_N'', \cdots$ refer to all the remaining species, and indicate the ratio between each of them and the unlabelled species, in the infusate (subscript I) and the natural material (subscript N) respectively.

2.5.4 A Test of the Endogenous Constant Steady-State Assumption

The assumption that the endogenous constant steady-state is not perturbed by the administration of the stable isotope tracer is not critical; it is only necessary that the tracee fluxes U and F, and thus the tracee mass M are constant and equal to the pre-test level during the study. This condition is met during the tracer perturbation if U is constant and equal to the pre-test level, and the system kinetics are linear in the range of values during the experiment.

In order to prove this, consider the general case where the tracee is perturbed by the experiment. In this case, the tracee mass and fluxes are time varying functions denoted $M(t)$, $F(t)$ and $U(t)$. The mass balance equation for the tracee becomes

$$\frac{dM(t)}{dt} = U(t) - F(t) \tag{2.5.22}$$

The tracer-tracee indistinguishability principle still holds, and the counterpart of (2.2.8) for a time varying tracee becomes

$$\frac{f(t)}{F(t) + f(t)} = \frac{m(t)}{M(t) + m(t)} \tag{2.5.23}$$

or equivalently

$$F(t) = \frac{F(t) + f(t)}{M(t) + m(t)} M(t) \tag{2.5.24}$$

Define $\Delta M(t)$ for the tracee mass perturbation from the steady state level:

$$\Delta M(t) = M(t) - M \tag{2.5.25}$$

From (2.5.22) and (2.5.24), one can write

$$\frac{d\Delta M(t)}{dt} = \frac{dM(t)}{dt} = U(t) - \frac{F(t) + f(t)}{M(t) + m(t)}(M + \Delta M(t))$$
$$\Delta M(0) = 0 \tag{2.5.26}$$

If the system is intrinsically linear, i.e.

$$\frac{F(t) + f(t)}{M(t) + m(t)} = \frac{F}{M} = k \tag{2.5.27}$$

and the endogenous production is not perturbed:

$$U(t) = U = kM \qquad (2.5.28)$$

then (2.5.26) becomes

$$\frac{d\Delta M(t)}{dt} = U - k(M + \Delta M(t)) = k\Delta M(t) \qquad \Delta M(0) = 0 \quad (2.5.29)$$

The solution of (2.5.29) is $\Delta M(t) = 0$ indicating there is no perturbation of the endogenous steady state.

In most cases, the tracer perturbation is confined within a few percent; this range is usually small and the above conditions are likely to be satisfied. However, it is possible to test the steady-state assumption in each experimental situation by a method which relies on measurements only, i.e. no assumptions about the system structure are required.

Briefly, the test that M equals a constant is based on the following. If the tracee constant steady-state has been perturbed, then M becomes a function of time $M(t)$. The measured concentration of the substance of interest in the accessible pool, C_{tot} is thus

$$C_{tot}(t) = C(t) + c(t) = \frac{M(t)}{V} + \frac{m(t)}{V} \qquad (2.5.30)$$

where V is the volume. One can rewrite (2.5.30):

$$C_{tot}(t) = \frac{M(t)}{V}(1 + \frac{m(t)}{M(t)}) = C(t)(1 + z(t)) \qquad (2.5.31)$$

The tracee concentration is thus

$$C(t) = \frac{C_{tot}(t)}{1 + z(t)} \qquad (2.5.32)$$

Since $C_{tot}(t)$ and $z(t)$ are known, (2.5.32) can be used to obtain a plot of $C(t)$. Assuming V is constant during the study, any change in $C(t)$ would reflect a change in $M(t)$. Thus a measure as to how much the tracee concentration $C(t)$ is perturbed from its pro-test constant steady-state value C can be obtained. The test may be a confirmatory one. Alternatively, it may suggest how to improve either the experimental design (e.g. a reduction of tracer dose, a more gentle input format) or the model (e.g. a structural description of feedback mechanisms or of nonlinear kinetics).

2.6   MULTIPLE TRACER EXPERIMENTS

In previous sections of this Chapter, only the case where a single tracer experiment is performed has been considered. That is, each element or compound is labeled with only one stable or radioactive isotopic species to create a tracer. However, more informative experiments can be performed when different tracer inputs are used. For instance, to characterize the absorption of an element, one isotopic species can be injected into plasma and a second given orally. Such a study will result in two tracer curves. Another common example is the study of two interacting substrates. Here each substrate can be labeled, the tracer injected, and four output curves generated: the disappearance of each label for the tracer and the appearance of that label in the other substrate. In all cases it is important that the various tracer inputs are administered simultaneously to assure that the system is in the same condition for each. This implies that all tracers are simultaneously present in the samples taken during the experiment, and that the measurement procedures must be able to quantitate them separately.

When dealing with multiple tracers, several possibilities exist. If radioactive isotopes are to be used, it is possible to distinguish the contributions of different tracers in a sample only if different radioactive isotopes are used as labels. The reason is that the measurement instruments can detect the different levels of energy emitted by the different isotopes. However, since the energy windows of the various isotopes usually overlap, care must be taken in quantitating the contribution of each isotope. It is assumed that the reader using multiple radioactive isotopic tracers is familiar with these problems, and how to deal with them.

If on the other hand stable isotopes are used, several possibilities exist. First, paralleling the above situation, different isotopes can be used. As noted previously, zinc has 5 stable isotopes having masses 64, 65, 66, 67, 68 and 70; ^{65}Zn is the most abundant species. Any two of the less abundant species can be chosen for intravenous and oral administration if absorption is being studied.

Second, the same stable isotope can be used in a different number of positions because the mass spectrometer permits one to quantitate them separately. As example, consider an experiment to characterize the kinetics between acetoacetate (AcAc) and β-hydroxybutyrate (βOHB) in which ^{13}C is the isotopic species used to label the substrates. AcAc can be labeled in two positions to create $[1,2-^{13}C_2]$-AcAc and the latter in four positions to create $[1,2,3,4-^{13}C_4]\beta$OHB. These two tracers can be coinjected, and the mass spectrometer can differentiate in a sample between $[1,2-^{13}C_2]$-AcAc coming from the first tracer and $[1,2,3,4-^{13}$

C_4]-AcAc derived from the conversion of $[1, 2, 3, 4 - {}^{13}C_4]\beta$OHB to AcAc. Similarly for βOHB

Finally, in multiple tracer studies, because of the ethical concern over the total amount of radioactivity that can be administered, many researchers are turning to stable isotopes as described above, or a combination of stable and radioactive isotopes. For instance, glucose turnover during a meal can be studied by administering simultaneously $[6 - {}^3$H]-glucose and $[6, 6, - {}^2H_2]$-glucose intravenously and orally respectively.

The ideas discussed in §2.4 and §2.5 for the single tracer case in terms of the kinetic variables can be extended to the multiple tracer case. In particular, the kinetic variables for radioactive tracers are individual tracer concentrations, or specific activities, while for stable isotopes they are the tracer to tracee ratios. Paralleling the single isotope case, expressions for the tracer to tracee ratios in terms of isotope ratio measurements for a dual stable isotope study are derived in Appendix C. The whole data base consisting of individual tracer and tracee measurements in the accessible pools is analyzed simultaneously to estimate tracee masses and fluxes in the system. The compartmental analysis approach will be discussed in Chapters 4-6 for a generic input-output configuration while the noncompartmental analysis approach will be discussed in Chapter 3 for the two input-four output configuration.

References

Cobelli C., Toffolo G., Foster D.M.: Tracer-to-tracee ratio for analysis of stable isotope tracer data: link with radioactive kinetic formalism. *Am. J. Physiol. 262*:*E968*– E975, 1992.

Sorenson J.A., Phelps M.E.: *Physics in Nuclear Medicine.* Grune & Stratton, Orlando, FL, 1987.

Watson J.T.: *Introduction to Mass Spectrometry.* Raven Press, New York, NY, 1987.

Wolfe R.R.: *Radioactive and Stable Isotope Tracers in Medicine.* Wiley-Liss, New York, NY, 1992.

Chapter 3

THE NONCOMPARTMENTAL MODEL OF MULTIPOOL SYSTEMS: ACCESSIBLE POOL AND SYSTEM PARAMETERS

3.1   FROM SINGLE TO MULTIPOOL SYSTEMS

In Chapter 2, it was seen that in the single pool system, assuming indistinguishability of tracer and tracee and conservation of mass, an estimate of the tracee kinetic parameters de novo production and disposal could be obtained. The purpose of Chapters 3 and 4 is to develop the theory for more complex systems in which the accessible pool is part of a larger system containing non-accessible pools.

There are two classes of models frequently used to study such multipool systems: noncompartmental and compartmental models. This chapter deals with noncompartmental models while Chapter 4 will deal with compartmental models. In particular, in this chapter, parameters characterizing the multipool system using the noncompartmental model will be defined, and formulas to estimate them from a tracer study given.

The transition from the single to multipool system can be described using Figure 3.1.1. In panel (A), the single pool system described in Chapter 2 is given. From the tracer experiment on this system together with tracee measurements, de novo production and disposal together with the mass M and volume V could be calculated. When this pool is embedded in a system consisting of transport among the accessible and nonaccessible pools and biochemical interactions with other substances, the situation becomes more complex. An example which highlights both the accessible pool and the fact this pool is embedded as a component of a larger system is provided in panel (B). As will be seen in this Chapter, while the accessible pool's mass M and volume V can still be measured,
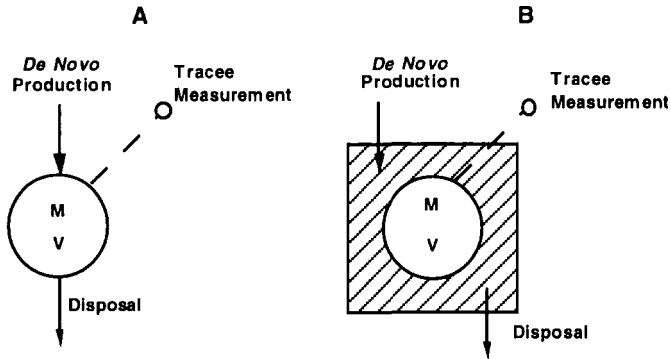
Figure 3.1.1.   Panel (A): The single pool system described in Chapter 2. Panel (B): The single accessible pool with mass M and volume V embedded in a more complex system into which there is *de novo* production and disposal; tracee measurements can be made in the accessible pool.

de novo production and disposal can take place anywhere in the system making its quantitation difficult.

For a more specific example, consider the system illustrated in Figure 3.1.2 which consists of an accessible and a non-accessible pool. The problem is to define and quantitate kinetic parameters which describe the "accessible pool" on the one hand and the "system" (accessible plus non-accessible pools) on the other. In particular, one would like to quantitate the masses and volumes of the pools, estimate production and disposal, and measure the transformation/exchanges processes. One sees in this example immediately a problem: some tracee can enter and leave the system from the non-accessible pool without even passing through the accessible pool. How can this affect parameter definitions and attempts to quantitate them?

The noncompartmental model of multipool systems formalized by Rescigno and Gurpide [1973] is schematized in Figure 3.1.3. The accessible pool is available for measurement. The complexity of the system, *i.e.* transport among system components and biochemical transformations, are "lumped" into the tracee recirculation/exchange arrow.

The important point to note in this figure is that the input and output are no longer called de novo production and disposal, but tracee rate of appearance into and disappearance from the accessible pool. This distinction foreshadows some of the limitations of this method of analysis.
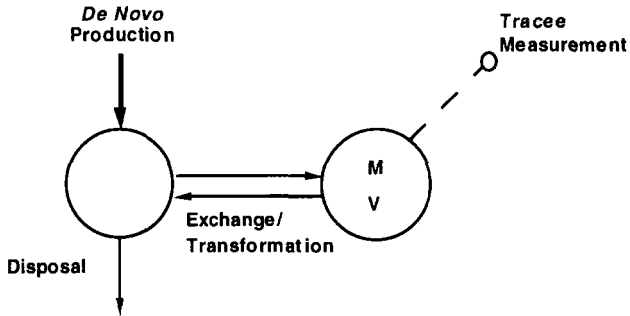
Figure 3.1.2. A system in which tracee is measured in an accessible pool which undergoes transformation and exchange with a non-accessible pool; *de novo* production and disposal occurs from this pool.
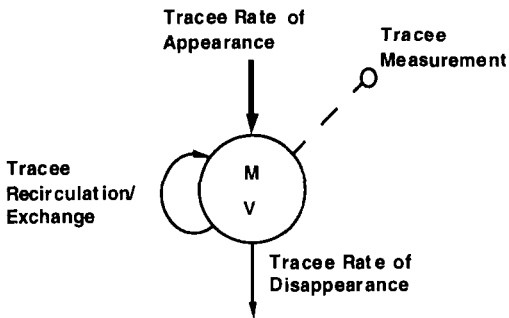
Figure 3.1.3. The noncompartmental model of the multipool system. See text for explanation.

Consider again the system described by the two-pool model illustrated in Figure 3.1.2. Here one sees that de novo production and disposal occur from the non-accessible pool. In addition, there are exchanges between the accessible and non-accessible pool; this exchange is what permits newly synthesized tracee to enter and leave the accessible pool. As noted previously, some tracee material entering the system in the non-accessible pool can be irreversibly lost without even entering the accessible pool. Measurements made in the accessible pool will reflect the kinetics only of that fraction of the tracee which passes through

this pool before being irreversible lost from the system; the accessible pool will "see" only a portion of the total tracee mass. Hence, because some tracee can be irreversibly lost without ever passing through the accessible pool, only a fraction of de novo production, called the tracee rate of appearance and denoted by R_a, can be estimated. With this example in mind, the question becomes: what kinetic parameters can be estimated at the "accessible pool" level, and what can one estimate at the "system" level?

For the noncompartmental model, the accessible pool parameters quantitate characteristics unique to the accessible pool such as mass, volume and residence time. The system parameters characterize "events" in the system occurring outside of the accessible pool but "seen" by that pool. This anticipates the fact that some of the parameters will be correct while others are estimates that are correct only under special circumstances.

In §3.2, the general definitions of the kinetic parameters for the accessible pool in a multipool system will be given, and formulas to estimate them from kinetic data listed. In §3.3, the general definition of the "system" kinetic parameters for the multipool system will be given together with formulas to estimate them from kinetic data. Each section will present the formulas for the bolus, constant infusion, primed infusion, and a generic input of the tracer. All formulas will be derived in Appendix D.

From the formulas given in §3.2 and §3.3, it will be seen that in order to estimate the kinetic parameters, a functional description of the data is required. That is, a mathematical function which "describes" the data must be postulated. This function not only describes the data over the time interval of the experiment, but extrapolates or "predicts" the data for times outside the data collection period. The reason this extrapolation is necessary is that tracer studies have a first and last sample time, but the formulas require a functional expression which can be integrated from time zero to infinity. It is the mathematical function describing the data that is used to evaluate the formulas. The problem of finding a mathematical description of the data is not simple; it is the subject of Chapter 8. Examples are provided in Chapter 9.

The Chapter will close in §3.4 with an extension of single accessible pool model to the situation where there are two accessible pools embedded in a larger, multipool system. This can address a number of situations including: (i) two substances in one "physiological space", (ii) one substance in two "physiological spaces", and (iii) two substances in two "physiological spaces".

3.2   KINETIC PARAMETERS OF THE ACCESSIBLE POOL

3.2.1   Definitions

In this section, the kinetic parameters characterizing the accessible pool will be defined and the formulas used to calculate them given. These are the parameters that quantitate characteristics unique to this pool.

The kinetic parameters for the accessible pool in the multipool system can be introduced using Figure 3.1.3. The notation to be used in this text for the kinetic parameters for the accessible pool are summarized in Table 3.2.1.

Table 3.2.1.   Notation for the Accessible Pool Kinetic Parameters

Notation	*Units*	*Definition*
M	mass	Mass
V	volume	Volume of distribution
CR	vol time^{-1}	Clearance rate
FCR	time^{-1}	Fractional clearance rate
Θ	time	Mean residence time
R_a	mass time^{-1}	Rate of appearance
R_d	mass time^{-1}	Rate of disappearance

The definition of these parameters is given below.

Mass M (units: mass): This is the mass of material in the accessible pool, i.e. the pool in which the tracer is introduced and from which samples measuring its amount will be taken.

Volume of distribution V (units: volume): This is the volume of the accessible pool. It is a volume in which the tracee is uniformly distributed and in which the tracer, once introduced into the system, intermixes uniformly and instantaneously.

Clearance rate CR (units: vol time^{-1}): This is the rate at which the accessible pool is irreversibly cleared of material per unit time.

Fractional clearance rate FCR (units: time^{-1}): This is the fraction of material that is irreversibly lost from the accessible pool per unit time. (The FCR is sometimes called the fractional catabolic rate.)

Mean residence time Θ (units: time): This is the average time a particle spends in the accessible pool during all passages through it before leaving it for the last time.

Rate of appearance R_a (units: mass time^{-1}): This is the rate at which the material enters the accessible pool for the first time.

Rate of disappearance R_d (units: mass time^{-1}): This is the rate at which the material is irreversibly lost from the accessible pool.

The relationship among these parameters is summarized in Table 3.2.2 below where C indicates the measured value of the tracee concentration in the accessible pool.

Table 3.2.2.   Relationships Among the Accessible Pool Parameters

$M = C \cdot V$	(3.2.1)
$FCR = \frac{CR}{V}$	(3.2.2)
$\Theta = \frac{1}{FCR}$	(3.2.3)
$R_a = R_d = FCR \cdot M = CR \cdot C$	(3.2.4)

3.2.2   Formulas

The two experimental situations, i.e. stable and radioactive isotopic tracer, for which the kinetic parameters will be given are shown in Figures 3.2.1 and 3.2.2.
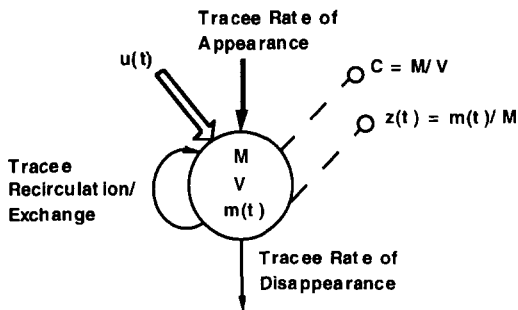
Figure 3.2.1.   The accessible pool in the noncompartmental model for the stable isotope tracer experiment. The tracer input is denoted by $u(t)$. The measured variables are the tracee concentration C and the tracer to tracee ratio $z(t)$ where $z(t)$ can either be measured or calculated from one of the other measurement variables (see Table 2.5.3). The tracee concentration C is constant because it is assumed that the system is in the steady state while $z(t)$ changes as a function of time.
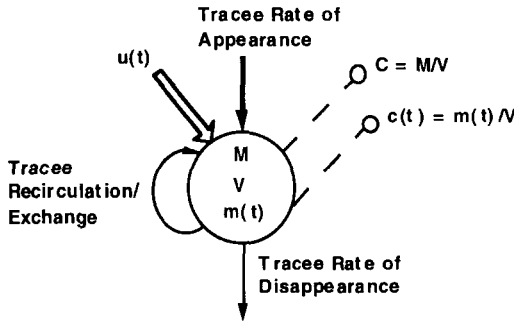
Figure 3.2.2. The accessible pool in the noncompartmental model for the radioactive isotope tracer experiment. Tracer input u is consistent with the notation introduced in Table 2.3.1. The measured tracee and tracer concentration variables are denoted C and $c(t)$. The tracee concentration C is constant because it is assumed that the system is in the steady state while $c(t)$ changes as a function of time.

As indicated in these figures, for stable isotopes, the measurements involve masses of the isotopic species, and $z(t)$ must be measured or derived from other measures. For radioactive tracer experiments, the measurements arc usually $c(t)$ and C separately; as described in Chapter 2, the specific activity is the quotient of these two variables, and can be regarded as a measure of $z(t)$ for the radioactive tracer.

The following two tables give the formulas to estimate the accessible pool parameters. Table 3.2.3 gives the formulas for the generic tracer case when the data are quantified in terms of the measured tracer to tracee ratio $z(t)$. Following the logic given in Chapter 2, these formulas apply to the stable isotope experiment, and to the radioactive isotope experiment when the data are expressed as specific activity. Similarly, Table 3.2.4 gives the formulas for the radioactive isotope case when the data are quantified in terms of the tracer concentration $c(t)$. The notation used here is the same as that used in Tables 2.2.1 and 2.2.2.

In these tables, the four different formats for tracer inputs are explicitly considered: the bolus injection, the constant infusion, the primed constant infusion, and finally the case where a finite dose of tracer is administered with a generic input profile $u(t)$. In Table 3.2.3, z represents the plateau value for the constant or primed, constant infusion experiment, and $\dot{z}(0)$ is the derivative of $z(t)$ evaluated at $t = 0$ (i.e. $\frac{dz(t)}{dt}|_{t=0}$). In Table 3.2.4, c represents the plateau value for the constant

Table 3.2.3.   Formulas for the Accessible Pool Kinetic Parameters

	Bolus Injection d	Constant Infusion u	Primed Infusion u, d	Generic Input $u(t)$
		Using $z(t)$		
M	$\frac{d}{z(0)}$	$\frac{u}{z(0)}$	$\frac{d}{z(0)}$	$\frac{u(0)}{z(0)}$
R_a	$\dfrac{d}{\int_0^\infty z(t)dt}$	$\frac{u}{z}$	$\frac{u}{z}$	$\dfrac{\int_0^\infty u(t)dt}{\int_0^\infty z(t)dt}$
V		$V = \frac{M}{C}$		
CR		$CR = \frac{R_a}{C}$		
FCR		$FCR = \frac{R_a}{M}$		
Θ		$\Theta = \frac{1}{FCR}$		

Table 3.2.4.   Formulas for the Accessible Pool Kinetic Parameters

	Bolus Injection d	Constant Infusion u	Primed Infusion u, d	Generic Input $u(t)$
		Using $c(t)$		
V	$\frac{d}{c(0)}$	$\frac{u}{c(0)}$	$\frac{d}{c(0)}$	$\frac{u(0)}{\dot{c}(0)}$
CR	$\dfrac{d}{\int_0^\infty c(t)dt}$	$\frac{u}{c}$	$\frac{u}{c}$	$\dfrac{\int_0^\infty u(t)dt}{\int_0^\infty c(t)dt}$
M		$M = C \cdot V$		
R_a		$R_a = CR \cdot C$		
FCR		$FCR = \frac{CR}{V}$		
Θ		$\Theta = \frac{1}{FCR}$		

or primed, constant infusion experiment, and $\dot{c}(0)$ is the derivative of $c(t)$ evaluated at $t = 0$ (i.e. $\frac{dc(t)}{dt}|_{t=0}$)

When the measurement is $z(t)$, the physiological reference is mass; thus M appears as the first parameter estimated in Table 3.2.3. When the measurement is tracer concentration $c(t)$, the physiological reference is volume; thus V appears as the first parameter estimated in Table 3.2.4. These "physiological references" dictate the order in which the formulas are presented. Again, it reflects that in the radioactive isotope experiment, the natural starting point is volume since the measurement is usually concentration while in the stable isotope experiment as well as the radioactive isotope experiment where specific activity is adopted, the natural starting point is mass.

The formulas given in Tables 3.2.3 and 3.2.4 are derived in Appendix D. Some comments will be made below on these formulas.

The bolus injection

A typical decay curve following a bolus injection of a tracer into an accessible pool is given in Figure 3.2.3.

Time
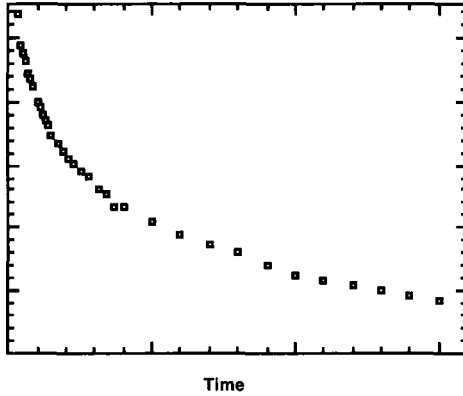
Figure 3.2.3. A typical decay curve following a bolus injection of a tracer into plasma as an accessible pool. The units of the data depend upon the tracer.

In the case where the data are expressed as $z(t)$ ratio, the mass M is calculated as the quotient of the dose d and $z(0)$. Since data are usually never available when $t = 0$, it is necessary to extrapolate from the data an estimate of $z(0)$. Similarly for the radioactive tracer, when the data are expressed as concentration $c(t)$, it is the volume V which is calculated as the quotient of the dose d and $c(0)$; hence a value must be estimated for $c(0)$.

In both cases, it is also necessary to evaluate an integral from $t = 0$ to $t = \infty$. When the data are expressed in terms of $z(t)$, the parameter estimated from the integral is the rate of appearance R_a; when expressed in terms of concentration $c(t)$, it is the clearance rate CR.

This extrapolation to $t = 0$ to $t = \infty$ and the evaluation of the integral is usually accomplished by providing a functional description of the data. Frequently sums of exponentials are used. This is discussed in Chapters 8 and 9.

The constant infusion of tracer

Many experiments are designed where the tracer is infused for a given, finite period of time with serial samples taken from the accessible pool for quantitation of tracer. The "goal" of these experiments is to infuse the tracer for a period of time sufficient to reach a plateau. If, from previous experiments, the time at which a plateau is achieved is known, the first sample may start at this time. When this design is adopted, how the tracer arrives at the plateau is not known. As will be seen, this can create problems in estimating the noncompartmental parameters. An example of tracer data when a constant infusion of tracer is given is illustrated in Figure 3.2.4.

Time
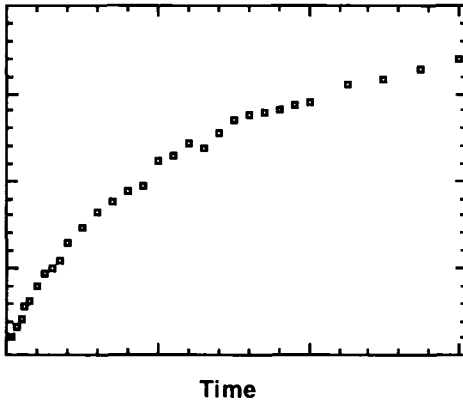
Figure 3.2.4.   A set of data following a constant infusion of tracer. The units of the data depend upon the tracer.

In the case where the data are expressed as $z(t)$ ratio, the mass M is calculated as the quotient of the dose d and $\dot{z}(0)$. That is, one must estimate the derivative of $z(t)$ evaluated at time zero. This requires an extrapolation of the data to $t = 0$ so that the derivative, the initial slope of the data, can be evaluated. In addition, a true plateau must be reached so that the R_a can be estimated.

Similarly for the radioactive tracer, when the data are expressed as concentration $c(t)$. Here it is in the formula for V that an estimated

value for $\dot{c}(0)$ is required. Also, the data must reach a plateau so that *CR* can be calculated.

In terms of what extrapolations are required, the difference between the bolus and constant infusion experiment is that in the former integrals need to be evaluated while; in the latter derivatives at time zero are needed. The rising portion of the curve in the constant infusion experiment is usually that most prone to error, and often a sufficient number of samples are not taken. Knowing this information can help in designing constant infusion experiments which will ensure that the early portion of the rise can be characterized.

The previous point needs to be emphasized. While it is clear that the same kinetic information is, in theory, available from the bolus and constant infusion experiment, the constant infusion protocol is frequently designed in such a way that not all kinetic parameters can be estimated. Without data describing the rising portion of the tracer curve one can only estimate the R_a and *CR* as $R_a = u/z$ and $CR = R_a/C$, or $CR = u/c$ and $R_a = CR \cdot C$ respectively for the cases when the data are expressed in terms of $z(t)$ or $f{:}(t)$. This protocol is very common in stable isotope tracer studies where the most widely used formula to quantify R_a is expressed as a function of enrichment:

$$R_a = u\left(\frac{e_I}{e} - 1\right) \qquad (3.2.5)$$

where $\dot{e}$ is the plateau enrichment value and e/ is the enrichment of the tracer. The equivalence of this formula with the expression for R_a in terms of z which, from Tables 3.2.3 and 3.3.3 can be written

$$R_a = FCR \cdot M = \frac{u}{z} \qquad (3.2.6)$$

has been derived in Appendix B.

The primed, constant infusion of tracer

Experiments can be done in which the tracer is injected as a bolus followed by a constant infusion for a finite period of time. This is the so-called primed, constant infusion method. The reason this protocol is often used is that if properly designed, the priming dose will speed the achievement of a plateau for the tracer concentration. An example of tracer data when a primed, constant infusion of tracer is given is illustrated in Figure 3.2.5.

Estimating the kinetic parameters when this protocol is adopted requires a combination of the formulas given in the tables. The application of the formulas can best be understood by following their derivation given in Appendix D.
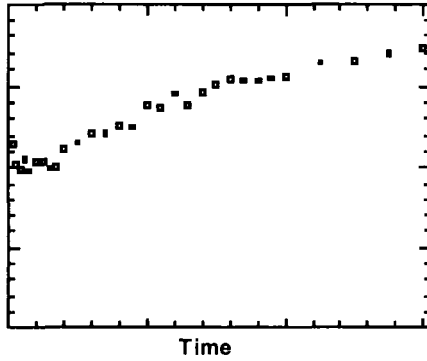
Figure 3.2.5.   A set of data following a primed constant infusion of tracer. The units of the data depend upon the tracer.

The generic tracer input

Kinetic parameters can be calculated from tracer data even if the tracer input is not a bolus, a continuous infusion, or a primed constant infusion, i.e. the input is a generic input. An example of such a situation is given in Figure 3.2.6.
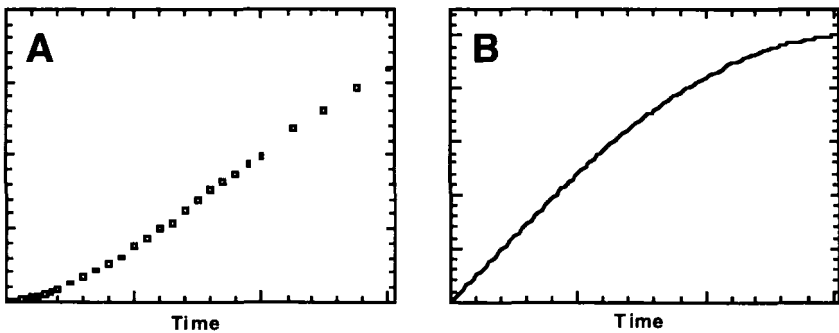
Figure 3.2.6.   A generic input of tracer is administered into a system, and data are collected. Panel (A) shows the data; panel (B) the input function $u(t)$. The units of the data depend upon the tracer.

The situation here is complicated by the fact that the input function $u(t)$ must be known precisely. Whether the data are collected in terms of $z(t)$ or $c(t)$, an extrapolation to time zero and the evaluation of an integral from $t = 0$ to $t = \infty$ is required. One must also know $\int_0^\infty u(t)dt$, the total dose administered.

3.3 KINETIC PARAMETERS OF THE SYSTEM

3.3.1 Definitions

The noncompartmental system parameters characterize events occurring inside and outside the accessible pool. The notation used for these parameters in this text are given below in Table 3.3.1 for the system diagrammed in Figure 3.1.2.

Table 3.3.1.   Notation for the System Kinetic Parameters

Notation	Units	Definition
M_{tot}^{NC}	mass	Whole body mass
V_{tot}^{NC}	volume	Total volume of distribution
MRT^{NC}	time	Mean residence time in the system
Θ_W	time	Mean residence time outside the accessible pool

The definition of these parameters are:

Total mass M_{tot}^{NC} (units: mass): This is the total mass of material contained in the system as "seen" by the accessible pool.

Total volume of distribution V_{tot}^{NC} (units: volume): This is the total volume of the system seen from the accessible pool, i.e. it is the volume in which the total mass would be distributed assuming the concentration of material throughout the system is uniform and equal to the concentration of the accessible pool.

Mean residence time MRT^{NC} (units: time): This is the average time a particle introduced into the accessible pool spends in the system before leaving the accessible pool for the last time.

Mean residence time outside the accessible pool Θ_W (units: time): This is the average time a particle introduced into the accessible pool spends outside the accessible pool before leaving the accessible pool for the last time.

The relationships among the parameters are given in Table 3.3.2.

Table 3.3.2.   Relationships Among the System Kinetic Parameters

$$V_{tot}^{NC} = MRT^{NC} \cdot CR \qquad (3.3.1)$$

$$M_{tot}^{NC} = V_{tot}^{NC} \cdot C = MRT^{NC} \cdot R_a \qquad (3.3.2)$$

$$\Theta_W = MRT^{NC} - \Theta \qquad (3.3.3)$$

The parameter M_{tot}^{NC} is also called exchangeable mass. The parameter V_{tot}^{NC} is sometimes called recirculation, exchangeable or steady state volume. It is important to note that the physical interpretation of V_{tot}^{NC} requires care. In fact, it is an operational volume the knowledge of which permits one to compute a whole body mass M_{tot}^{NC} by multiplying it by the measured tracee concentration C.

Note that the system kinetic parameters do not include any measure of de novo tracee production in the system. In fact, only the rate R_a at which newly synthesized material enters the accessible pool can be estimated in the noncompartmental model. Some comments on the relationship between R_a and de novo tracee production will be given in §3.3.3.

3.3.2   Formulas

Paralleling the development in §3.2, the formulas the kinetic parameters of the system following a bolus injection of tracer, the constant infusion of tracer, the primed infusion of tracer and the generic tracer input are given in Tables 3.3.3 and 3.3.4 as functions of $z(t)$ and $c(t)$ respectively. The formulas are derived in Appendix D. In Table 3.3.3, z represents the plateau value for the constant or primed, constant infusion experiment, and for the washout experiment, T is the time at which the washout phase starts. In Table 3.3.4, c represents the plateau value for the constant or primed, constant infusion experiment, and for the washout experiment, T is the time at which the washout phase starts.

The same comments made in the previous section related to the above formulas also hold. However, for each mode of introducing the tracer, some additional information is possible. This is discussed below.

Table 3.3.3. Formulas for the System Kinetic Parameters

	Bolus Injection d	Constant Infusion u	Using $z(t)$ Primed Infusion u, d	Generic Input $u(t)$	Washout $-$
MRT^{NC}	$\dfrac{\int_0^\infty tz(t)dt}{\int_0^\infty z(t)dt}$	$\dfrac{\int_0^\infty [z-z(t)]dt}{z}$	$\dfrac{\int_0^\infty [z-\frac{u}{d}\int_0^t z(t-\tau)e^{-\frac{u}{d}\tau}d\tau]dt}{z}$	$\dfrac{\int_0^\infty tz(t)dt}{\int_0^\infty z(t)dt} - \dfrac{\int_0^\infty tu(t)dt}{\int_0^\infty u(t)dt}$	$\dfrac{\int_T^\infty z(t)dt}{z}$
M_{tot}^{NC}		$M_{tot}^{NC} = MRT^{NC}\cdot R_a$		$M_{tot}^{NC} = MRT^{NC}\cdot R_a$	
Θ_W		$\Theta_W = MRT^{NC}-\Theta$		$\Theta_W = MRT^{NC}-\Theta$	
V_{tot}^{NC}		$V_{tot}^{NC} = M_{tot}^{NC}/C$		$V_{tot}^{NC} = M_{tot}^{NC}/C$	

Table 3.3.4. Formulas for the System Kinetic Parameters

	Bolus Injection d	Constant Infusion u	Using $c(t)$ Primed Infusion u, d	Generic Input $u(t)$	Washout -
MRT^{NC}	$\dfrac{\int_0^\infty tc(t)dt}{\int_0^\infty c(t)dt}$	$\dfrac{\int_0^\infty [c-c(t)]dt}{c}$	$\dfrac{\int_0^\infty [c-\frac{u}{d}\int_0^t c(t-\tau)e^{-\frac{u}{d}\tau}d\tau]dt}{c}$	$\dfrac{\int_0^\infty tc(t)dt}{\int_0^\infty c(t)dt} - \dfrac{\int_0^\infty tu(t)dt}{\int_0^\infty u(t)dt}$	$\dfrac{\int_T^\infty c(t)dt}{c}$
V_{tot}^{NC}		$V_{tot}^{NC} = MRT^{NC} \cdot CR$		$V_{tot}^{NC} = MRT^{NC} \cdot CR$	
Θ_W		$\Theta_W = MRT^{NC} - \Theta$		$\Theta_W = MRT^{NC} - \Theta$	
M_{tot}^{NC}		$M_{tot}^{NC} = V_{tot}^{NC} \cdot C$		$M_{tot}^{NC} = V_{tot}^{NC} \cdot C$	

The bolus injection of tracer

In addition to the parameters listed in Tables 3.3.3 and 3.3.4 for the bolus injection experiment, it is possible to quantitate the "recirculation-exchange" arrow shown in Figure 3.2.1. Specifically, the recirculation of the tracee, R_W (units: mass per unit time), can be described for $z(t)$ or $c(t)$ using

$$R_W = -\frac{\dot{z}(0)}{z(0)} M - R_d \qquad (3.3.4)$$

or

$$R_W = -\frac{\dot{c}(0)}{c(0)} M - R_d \qquad (3.3.5)$$

where $\dot{z}(0)$ and $\dot{c}(0)$ denote the derivatives of $z(t)$ and $c(t)$ evaluated at time zero respectively.

The first term on the right hand side of (3.3.4) or (3.3.5) is the total output from the accessible pool derived by writing the mass balance equation for $z(t)$ or $c(t)$ at time zero. Considering that the total rate of exit from the accessible pool is made up of the rate of disappearance and the rate of recycling, (3.3.4) and (3.3.5) follow.

The constant infusion of tracer

For the constant infusion experiment, the parameter R_W can be estimated from data collected during the rising portion of the tracer curve. However, it requires the evaluation of the first and second derivatives of the tracer measurements at time zero:

$$R_W = -\frac{\ddot{z}(0)}{\dot{z}(0)} M - R_d \qquad (3.3.6)$$

$$R_W = -\frac{\ddot{c}(0)}{\dot{c}(0)} M - R_d \qquad (3.3.7)$$

where $\dot{z}(0)$, $\dot{c}(0)$, $\ddot{z}(0)$ and $\ddot{c}(t)$ denote the first and second derivatives of $z(t)$ and $c(t)$ evaluated at time zero respectively (e.g. $\ddot{z}(0) = \frac{d^2 z(t)}{dt^2}|_{t=0}$).

If the experiment permits only the estimation of the plateau value, no system parameters can be estimated.

The primed, constant infusion of tracer

In this situation, the system mean residence time requires the evaluation of a double integral which in turn requires a knowledge of a functional description of the data.

The generic input of tracer

The system mean residence time requires the evaluation of several integrals which require a knowledge of both the functional description of the data and the input. There is a special case, however. Consider the situation where the tracer is administered at a constant rate u up to time T and then stopped. The system mean residence time MRT^{NC} is given by

$$MRT^{NC} = \frac{\int_0^\infty tz(t)dt}{\int_0^\infty z(t)dt} - \frac{T}{2} \qquad (3.3.8)$$

The washout experiment

This situation refers to the experimental design when data are collected after the infusion of tracer has stopped in the constant, primed, constant infusion, or generic input experiment. One assumes that a plateau has been reached before the infusion stops. The system mean residence time MRT^{NC} can be estimated by measurements taken only from the plateau and the washout phase as

$$MRT^{NC} = \frac{\int_T^\infty z(t)dt}{z} \qquad (3.3.9)$$

$$MRT^{NC} = \frac{\int_T^\infty c(t)dt}{c} \qquad (3.3.10)$$

where z and c are the plateau values, and T represents the beginning of the washout period.

3.3.3   Limitations of Noncompartmental Models

In the general case, the noncompartmental modeling analysis does not permit one to estimate de novo tracee production in the system since R_a only measures the rate at which endogenous particles enter the accessible pool. It provides a measure of de novo production in the system only if all newly synthesized particles enter the accessible pool, i.e. either they enter directly into the accessible pool or there is no loss in the pathways between the pool into which synthesis takes place and the accessible pool. When this condition is not satisfied, R_a underestimates the true production.

In addition, MRT^{NC}, M_{tot}^{NC} and V_{tot} given by the above formulas provide estimates of the "true" system kinetic parameters, MRT, M_{tot} and V_{tot} only if disposal and de novo production of tracee particles take place

in the accessible pool. If these constraints are not satisfied, MRT^{NC}, M_{tot}^{NC} and V_{tot} will underestimate the true system parameters [DiStefano, 1982; DiStefano and Landaw, 1984]. While a formal proof of these properties will be given in Chapter 7, the tracee system schematizations shown in Figure 3.3.1 illustrate the main points: R_a recovers U in situation (c) and (d) where production takes place in the accessible pool but also in situation (b) since production in a nonaccessible compartment but all tracee particles reach the accessible pool. The parameters MRT^{NC}, M_{tot}^{NC} and V_{tot} are correct measures for these parameters for situation (c) only since in the other cases either de novo production or disposal, or both, take place from the nonaccessible pool.
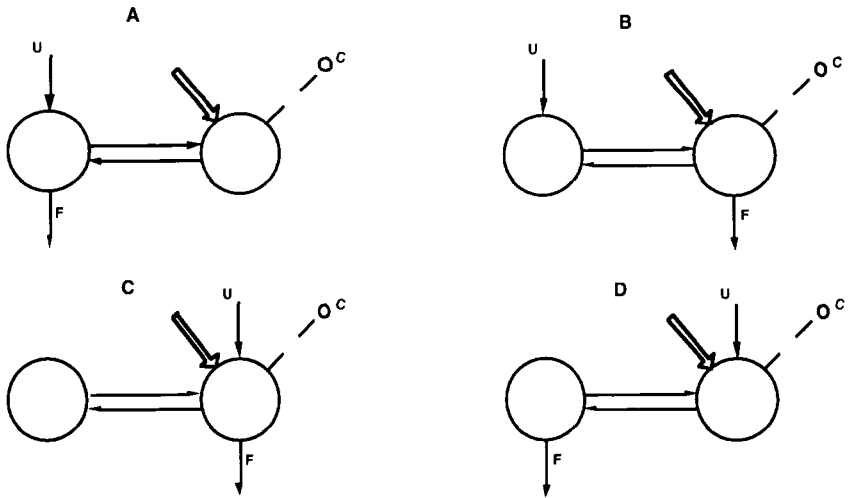
Figure 3.3.1. A two pool schematization of the tracee system. The situations are: in (a) de novo production and disposal occurs in the non-accessible pool; (b) de novo production occurs in the non-accessible pool and disposal occurs from the accessible pool; (c) both de novo production and disposal occur in the accessible pool; and (d) de novo production occurs in the accessible pool and disposal from the non-accessible pool.

3.3.4   Parameters From Total Body Tracer Measurements

Some limitations of the noncompartmental model can be overcome by a different formulation of the system kinetic parameters which requires that time dependent measurements of the total tracer mass in the system are available. In practice, the application of this method is difficult. However, it has been used in some tracer studies such as the glucose turnover studies of Katz [1989] where the tracer was tritiated glucose. The total tracer mass was measured indirectly by sampling the labelled catabolic end product pool, tritiated body water. The amount of tracer in this pool was quantified and subtracted from the administered tracer dose to evaluate the total tracer mass in the system at specific sampling times.

Denote by $m_{tot}(t)$ the time course of the total amount of tracer in the system. For a bolus injection of a tracer dose d, the mean residence time in the system of tracer particles from total body (TB) measurement equals [Bergner, 1964]

$$\text{MRT}^{TB} = \frac{\int_0^\infty m_{tot}(t)dt}{d} \qquad (3.3.11)$$

As will be shown in Chapter 7, MRT^{TB} is the residence time in the system of particles which enter the system in the accessible pool but leaves the system by any route. Thus it provides the correct estimate of the "true" residence time in the system of endogenous particles if de novo production takes place in the accessible pool.

By multiplying MRT^{TB} by R_a, an estimate of the total tracee mass in the system can be derived:

$$M_{tot}^{TB} = R_a \cdot \text{MRT}^{TB} \qquad (3.3.12)$$

Since R_a correctly measures de novo production when it takes place in the accessible pool, M_{tot}^{TB} correctly measures the total mass in the system only if this condition holds. In the general case, it underestimates the true total mass in the system:

$$M_{tot}^{TB} \leq M_{tot} \qquad (3.3.13)$$

In summary, this method correctly estimates the mean residence time in the system of tracer material. It provides a correct estimate of the mean residence time of the tracee if tracee production is only into the accessible pool. Under these circumstances, the total tracee mass can also be correctly quantified. It should be remembered that its application

is restricted to very specific circumstances since the measurement of total system tracer mass is feasible only in a few cases.

3.4 THE TWO ACCESSIBLE POOL NONCOMPARTMENTAL MODEL: ACCESSIBLE POOL AND SYSTEM KINETIC PARAMETERS

3.4.1 Introduction

In the §3.2 and §3.3, only the case where one tracer and one accessible pool are available to probe the system has been considered. As already discussed in §2.6, a more informative experimental protocol is often needed. This includes the situation where two or more pools are accessible for test inputs and measurements.

A multipool system and its two accessible pool noncompartmental model are shown in Figures 3.4.1 and 3.4.2 respectively.

As a step towards understanding how the two accessible pool noncompartmental model yields much more information than the one accessible pool noncompartmental model, the reader should compare the above figures with Figures 3.2.1 and 3.2.2. In the former figures, only one "recirculation-exchange" arrow was defined; in the latter, two such arrows were defined together with two "transport-chemical transformation arrows" to take into account the interconversion of material between the two accessible pools. These model parameters are in general different
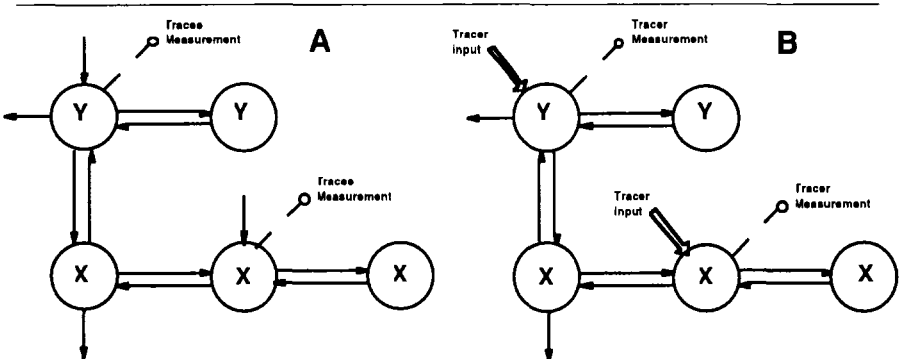
Figure 3.4.1. A multipool system showing the metabolic relationship between substances X and Y. The model for substance X is that shown in Figures 2.2.2 and 2.2.3. A shows the tracee system while B shows the tracer system.
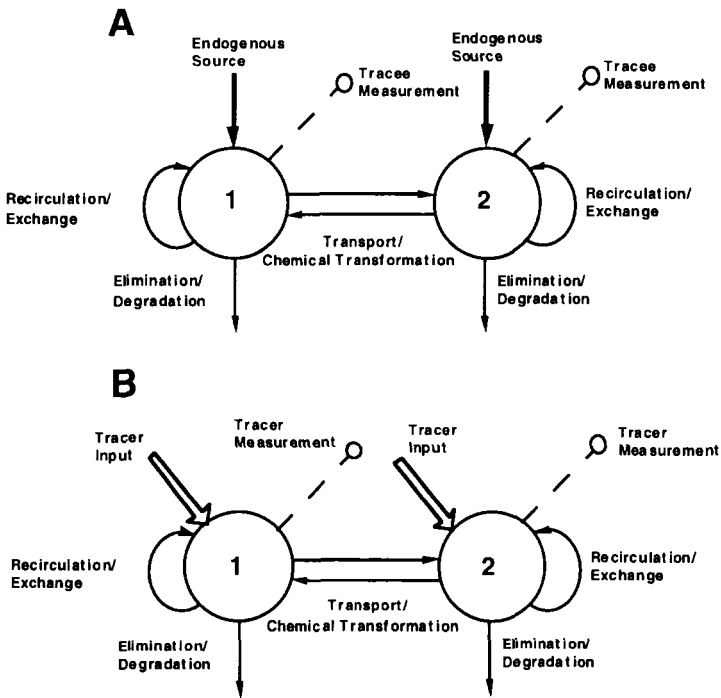
Figure 3.4.2.   **A.** The two accessible pool noncompartmental model of the tracee system shown in Figure 3.4.1. The nonaccessible pools are taken into account by the "recirculation-exchange" and "transport-chemical transformation" arrows. The recirculation-exchange arrows represent kinetic events that occur without passing through the other accessible pool while the transport-chemical transformation arrows represent a series of kinetic events that occurs in order for a substance to appear in one pool from the other. Tracee fluxes and measurements are indicated. **B.** The two accessible pool noncompartmental model of the tracer system in the tracee system illustrated above. Tracer fluxes, inputs and measurements are indicated.

from those one could obtain by applying the one accessible pool noncompartmental analysis to the two pools separately. In this latter case, the recirculation-exchange arrow of each accessible pool model would include both transport-chemical transformation arrows and the recirculation-exchange arrows of the other accessible pool. A second point must be emphasized. Both the recirculation-exchange and transport-chemical

transformation arrows represent sequences of metabolic events and not necessarily a "direct", one event pathway. This point is made for those readers familiar with compartmental models; the arrows here have a different meaning from the arrows linking compartments in a compartmental model.

The most typical situation that can be discussed in this context is the study of the kinetics of two interacting substrates such as acetoacetate and 3-hydroxybutyrate, leucine and α-ketoisocaproate, or hormones such as T_3 and T_4 from measurements in one physical space such as plasma. A protocol would be to label two substances with different isotopes, inject them as, for example, a bolus, and take serial samples. Each sample could then have the amounts of each isotope quantitated in the two substances. This protocol will produce 4 tracer curves (see, for example, Figure 3.4.5). Each of the two tracers will produce a disappearance curve, and, in the other substance, a curve detailing the appearance of label.

A specific example would be an experiment in which leucine labeled with ^{3}H and α-ketoisocaproate labeled with ^{14}C were coinjected into plasma and the amount of ^{3}H and ^{14}C are measured in both substances to produce the four tracer curves. In this example, the reader should not confuse the physical space of plasma with an accessible pool. The two accessible pools are plasma leucine and plasma α-ketoisocaproate.

It is possible to have situation where the two accessible pools are actually different physiological spaces. In this case, it is the location and not the chemical state which identifies the two accessible pools. A specific example can be taken from zinc metabolism where, if ^{69m}Zn free from any carrier and ^{65}Zn labeled red blood cells are coinjected into plasma and serial plasma and red blood cell samples are taken, the amount of both labels in plasma and red blood cells can be followed. Here the two accessible pools are plasma zinc and red blood cell zinc.

In this section, it will be seen that to determine completely the two accessible pool noncompartmerital model, a protocol calling for four tracer curves is necessary, i.e. it is not sufficient to introduce tracer into only one pool even if that tracer can be quantified in the other pool. More specifically, if one obtains only two tracer curves from the injection of only one tracer, one will not be able to apply all of the formulas introduced below. Thus the possible information about the system under study when there are two accessible pools will not be complete. Some kinds of information that are available in the precursor-product setting will be discussed in Chapter 10.

Only the experiment in which the tracer is introduced as a bolus or a constant infusion will be discussed. In this way, it can clearly be seen

how the two accessible pool model is an extension of the one accessible pool model. As with the one accessible pool situation, both pool and system parameters will be described. While the noncompartmental model correctly estimates the accessible pool parameters, the equivalent sink and source constraint discussed in §3.3.5 for the one accessible pool noncompartmental model must apply in order for the system parameters to be correctly estimated. That is, the system parameters are correct only if disposal and de novo production take place in the accessible pools.

3.4.2   The Two Input - Four Output Experiment for Radioactive and Stable Isotope Tracers

The experimental configuration for the two input - four output stable or radioactive isotope tracer experiment is shown in Figure 3.4.3 and Figure 3.4.4 respectively.
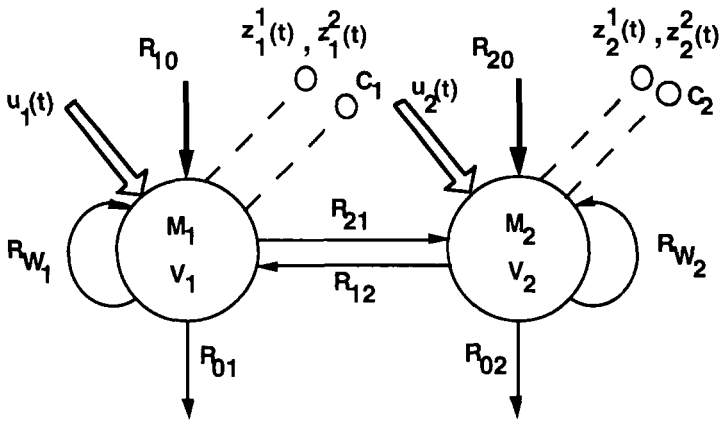
Figure 3.4.3.   The two accessible pool noncompartmental model for the stable isotope experiment showing both pool 1 and pool 2 can be sampled; tracee concentration in each is denoted C_1 and C_2 respectively. Two distinct stable isotope tracers can be administered, one into pool 1 (denoted $u_1(t)$) and the other into pool 2 (denoted $u_2(t)$). The two tracers can be measured in both pools. This is indicated by the $z_i^j(t)$ where the subscript i refers to the substance in accessible pool i and the superscript j refers to tracer 1 or 2. The lines connecting pools 1 and 2, denoted R_{12} and R_{21}, represent transport-chemical transformation kinetic events. Recirculation-exchange from the two accessible pools is denoted R_{W_1} and R_{W_2} respectively.
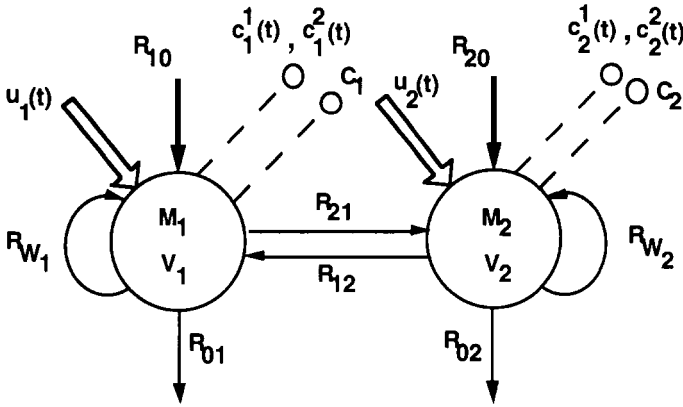
Figure 3.4.4. The two accessible pool noncompartmental model for the radioactive isotope experiment showing both pool 1 and pool 2 can be sampled; tracee concentration in each is denoted C_1 and C_2 respectively. Two distinct radioactive tracers are administered, one into pool 1 (denoted $u_1(t)$) and the other into pool 2 (denoted $u_2(t)$). Both tracers can be measured in both pools. This is indicated by the $c_i^j(t)$ where the subscript i refers to the substance in accessible pool i and the superscript j refers to tracer 1 or 2. The lines connecting pools 1 and 2, denoted R_{12} and R_{21}, represent transport-chemical transformation kinetic events. Recirculation-exchange from the two accessible pools is denoted R_{W_1} and R_{W_2} respectively.

As was the case for the single accessible pool noncompartmental model, tracer measurements can be expressed either as tracer to tracee ratios or as tracer concentrations. For the radioactive isotope experiment, as discussed in Chapter 2, measurements are usually the four tracer concentrations c_i^j and the two tracee concentrations C_1 and C_2. The tracer to tracee ratios, or equivalently the specific activities, can be calculated from

$$z_i^j(t) = \frac{c_i^j(t)}{C_i} \qquad i = 1, 2, \qquad j = 1, 2 \qquad (3.4.1)$$

As discussed in Chapter 2, for the stable isotope experiment, the tracer to tracee ratio can be either measured directly or derived from other mass spectrometry variables such as isotope ratio or enrichment. In particular, z_1^1 and z_1^2, and then z_2^1 and z_2^2, can be derived by applying (C.15) and   in Appendix C. In both cases as defined in Appendix C, r_I and r_I' equal the isotope ratios of tracer input u_1, and

r_J and r'_J are the isotope ratios for tracer input u_2. In the next section, formulas for the kinetic parameters will be given as a function either of z_i^j or c_i^j.

3.4.3   Accessible Pool Parameters: Definitions and Formulas

The notation used for the two accessible pool noncompartmental model is summarized in Table 3.4.1.The relationships among the parameters are given in Table 3.4.2.

Table 3.4.1.   Notation for the Two Accessible Pool Kinetic Parameters

Notation		Units	Definition
M_i	$i = 1, 2$	mass	Mass of the accessible pool i
V_i	$i = 1, 2$	volume	Initial volume of distribution of pool i
R_{i0}	$i = 1, 2$	mass time^{-1}	Rate of appearance "per se" into pool i
R_{0i}	$i = 1, 2$	mass time^{-1}	Rate of disappearance "per se" from pool i
R_{ij}	$i = 1, 2$	mass time^{-1}	Rate of interconversion from pool j to pool i
v_{0i}	i=1,2	vol time^{-1}	Rate of disappearance "per se" from pool i per unit of concentration in pool i.
v_{ij}	$i = 1, 2$	vol time^{-1}	Rate of interconversion from pool j to pool i per unit of concentration in pool j.

The accessible pool masses and volumes are the same as those of the one accessible pool model, applied separately to the two substances. All of the remaining parameters listed above are unique to the two accessible pool noncompartmental model. R_{21} and R_{22} are kinetic parameters describing transport and/or chemical exchange processes as material passes between accessible pools through an indeterminate number of pools. Similarly, R_{01} and R_{02} are introduced. As will be discussed in §3.4.5, these are different from the rates of disappearance of substances

1 and 2 as defined in §3.3. Consider, for example, substance 1. R_{01} differs from the rate of disappearance of substance 1, R_d . The reason is that the rate of disappearance of substance 1 includes that leaving the system via R_{01} plus that which leaves the system as substance 2 after being converted to substance 2. Thus R_{01} is less than or equal to the rate of disappearance of substance 1.

Similar considerations apply to R_{10} and R_{20} as compared to the rates of appearance of substance 1 or 2 defined in §3.3. R_{10} is lower than the rate of appearance of substance 1 into the system since it doesn't include material coming from de novo synthesis which first enters pool 2 before being converted to pool 1.

Remember that this model permits the existence of intermediate pools between accessible pools 1 and 2; for instance, the arrows between pools 1 and 2 include all intermediate steps in the interconversion between substances 1 and 2 so that R_{21} represents the rate of transfer from pool 1 to pool 2 by all pathways in the system. The relationships among the two accessible pool parameters are summarzied in Table 3.4.2, where C_1, C_2 indicate the measured values of tracee concentration in the accessible pools.

Table 3.4.2. Relationships Among the Two Accessible Pools Kinetic Parameters

$M_i = V_i C_i$	$i = 1, 2$	(3.4.2)
$R_{0i} = v_{0i} C_i$	$i = 1, 2$	(3.4.3)
$R_{ij} = v_{ij} C_j$	$i, j = 1, 2, \quad i \neq j$	(3.4.4)
$R_{10} = R_{01} + R_{21} - R_{12}$		(3.4.5)
$R_{20} = R_{02} + R_{12} - R_{21}$		(3.4.6)

As given in Appendix D, the relationships (3.4.5) and (3.4.6) can be derived by balancing the fluxes in the accessible pools; the sum of the input and output fluxes must be equal.

The formulas for these parameters listed in Table 3.4.1 for the bolus injection and continuous infusion experiments are given in Tables 3.4.3 and 3.4.4 for the cases where the tracer measurements are $z(t)$ and $c(t)$ respectively. They parallel Tables 3.2.3 and 3.2.4 for the one accessible pool case.

Table 3.4.3.   Formulas for the Two Accessible Pool Kinetic Parameters

	Using $z(t)$		
	Bolus Injection d_1, d_2		Continuous Infusion u_1, u_2
M_1	$\frac{d_1}{z_1^1(0)}$		$\frac{u_1}{\dot{z}_1^1(0)}$
M_2	$\frac{d_2}{z_2^2(0)}$		$\frac{u_2}{\dot{z}_2^2(0)}$
R_{21}	$\frac{d_2 \cdot Az_2^1}{\Delta Az}$		$\frac{u_2 \cdot z_2^1}{\Delta z}$
R_{12}	$\frac{d_1 \cdot Az_1^2}{\Delta Az}$		$\frac{u_1 \cdot z_1^2}{\Delta z}$
R_{01}	$\frac{d_1 \cdot Az_2^2 - d_2\, Az_2^1}{\Delta Az}$		$\frac{u_1\, z_2^2 - u_2 \cdot z_2^1}{\Delta z}$
R_{02}	$\frac{d_2\, Az_1^1 - d_1 \cdot Az_1^2}{\Delta Az}$		$\frac{u_2 \cdot z_1^1 - u_1 \cdot z_1^2}{\Delta z}$
V_1		$\frac{M_1}{C_1}$	
V_2		$\frac{M_2}{C_2}$	
v_{01}		$\frac{R_{01}}{C_1}$	
v_{02}		$\frac{R_{02}}{C_2}$	
v_{21}		$\frac{R_{21}}{C_1}$	
v_{12}		$\frac{R_{12}}{C_2}$	

A typical set of data for a simultaneous bolus injection into two accessible pools is given in Figure 3.4.5. For the bolus injection experiment, all of the kinetic parameters of the accessible pool can be expressed as functions of four areas under the four tracer curves (such as those given in Figure 3.4.5):

$$Az_i^j = \int_0^\infty z_i^j(t)dt \qquad i, j = 1, 2 \qquad (3.4.7)$$

or

$$Ac_i^j = \int_0^\infty c_i^j(t)dt \qquad i, j = 1, 2 \qquad (3.4.8)$$

In addition to these, the rates of recycling around pool 1, Rw_1 and pool 2, Rw_2, without passing through the other accessible pool are:

Table 3.4.4.   Formulas for the Two Accessible Pool Kinetic Parameters

	Using $c(t)$	
	Bolus Injection d_1, d_2	Continuous Infusion u_1, u_2
V_1	$\frac{d_1}{c_1^1(0)}$	$\frac{u_1}{c_1^1(0)}$
V_2	$\frac{d_2}{c_2^2(0)}$	$\frac{u_2}{c_2^2(0)}$
v_{21}	$\frac{d_2 \cdot Ac_2^1}{\Delta Ac}$	$\frac{u_2 \cdot c_2^1}{\Delta c}$
v_{12}	$\frac{d_1 \cdot Ac_1^2}{\Delta Ac}$	$\frac{u_1 \cdot c_1^2}{\Delta c}$
v_{01}	$\frac{d_1 \cdot Ac_2^2 - d_2 \cdot Ac_2^1}{\Delta Ac}$	$\frac{u_1 \cdot c_2^2 - u_2 \cdot c_2^1}{\Delta c}$
v_{02}	$\frac{d_2 \cdot Ac_1^1 - d_1 \cdot Ac_1^2}{\Delta Ac}$	$\frac{u_2 \cdot c_1^1 - u_1 \cdot c_1^2}{\Delta c}$
M_1	$V_1 \cdot C_1$	
M_2	$V_2 \cdot C_2$	
R_{01}	$v_{01} \cdot C_1$	
R_{02}	$v_{02} \cdot C_2$	
R_{21}	$v_{21} \cdot C_1$	
R_{12}	$v_{12} \cdot C_2$	

$$R_{W_1} = -\frac{\dot{z}_1^1(0)}{z_1^1(0)} M_1 - R_{01} - R_{21} \tag{3.4.9}$$

$$R_{W_2} = -\frac{\dot{z}_2^2(0)}{z_2^2(0)} M_2 - R_{02} - R_{12} \tag{3.4.10}$$

$$R_{W_1} = -\frac{\dot{c}_1^1(0)}{c_1^1(0)} M_1 - R_{01} - R_{21} \tag{3.4.11}$$

$$R_{W_2} = -\frac{\dot{c}_2^2(0)}{c_2^2(0)} M_2 - R_{02} - R_{12} \tag{3.4.12}$$
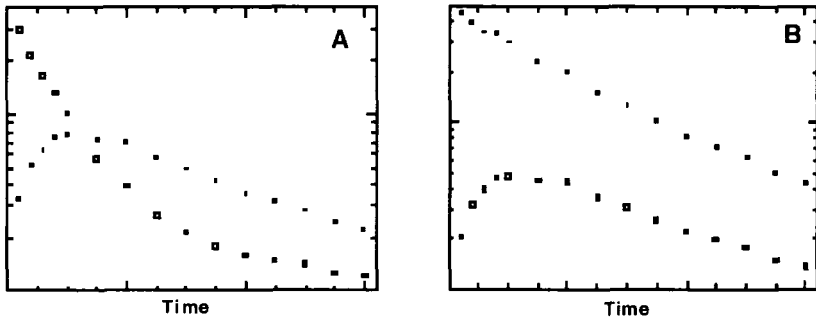
Figure 3.4.5.   An example of the four sets of data obtained from a simultaneous bolus injection of two tracers into two accessible pools. Panels A and B are respectively the results the injecting labeled substance 1 and 2. In both figures, the triangles and squares are respectively substance 1 and 2. Thus in the left hand panel, the triangle represent the decay of substance 1 while in the right hand panel, it represents the appearance of substance 1 following the bolus injection of labeled substance 2.

where $\dot{z}_i^j(0)$ and $\dot{c}_i^j(0)$ are the derivatives of $z_i^j(t)$ and $c_i^j(t)$ respectively evaluated at $t = 0$.

For the constant infusion experiment, the plateau value of substance i in pool j, z_i^j or c_i^j is required. The substitutions used in passing from the bolus to the constant infusion experiment in the formulas given in Tables 3.4.3 and 3.4.4 are

$$d_1 \rightarrow u_1 \quad d_2 \rightarrow u_2$$

$$Az_1^1 \rightarrow z_1^1 \quad Az_2^1 \rightarrow z_2^1 \quad Az_1^2 \rightarrow z_1^2 \quad Az_2^2 \rightarrow z_2^2$$

$$Ac_1^1 \rightarrow c_1^1 \quad Ac_2^1 \rightarrow c_2^1 \quad Ac_1^2 \rightarrow c_1^2 \quad Ac_2^2 \rightarrow c_2^2$$

In Table 3.4.3, $\Delta Az = Az_1^1 \cdot Az_2^2 - Az_2^1 \cdot Az_1^2$ in the case of the bolus injection; $\Delta z = z_1^1 \cdot z_2^2 - z_1^2 \cdot z_2^1$ and $\dot{z}_i^i(0)$ is the derivative of z_i^i at $t = 0$ in the case of the constant infusion. The parameters R_{10} and R_{20} are calculated using (3.4.5) and (3.4.6) respectively. In Table 3.4.4, $\Delta Ac = Ac_1^1 \cdot Ac_2^2 - Ac_2^1 \cdot Ac_1^2$ in the case of the bolus injection; $\Delta c = c_1^1 \cdot c_2^2 - c_1^2 \cdot c_2^1$ and $\dot{c}_i^i(0)$ is the derivative of c_i^i at $t = 0$ in the case of the constant infusion. The parameters R_{10} and R_{20} are calculated using (3.4.5) and (3.4.6) respectively.

While the above tables and formulas apply only to the bolus injection and continuous infusion experiment, formulas can be derived for the primed, constant infusion in a manner similar to that indicated in §3.2.

3.4.4 System Parameters: Definitions and Formulas

The kinetic parameters of a multipool system which can be estimated from a two-input four-output experimental protocol using the two accessible pool noncompartmental model are given in Table 3.4.5.

Table 3.4.5. Notation for the System Kinetic Parameters of the Two Accessible Pool Model

Notation		Units	Definition
M_{tot}^{NC}		mass	Whole body mass
V_{tot}^{NC}		volume	Total volume of distribution
MRT_i^{NC}	i=1,2	time	Mean residence times in the system

These parameters are essentially the same as those defined for the one accessible pool model, and their definitions are similar.

Total mass M_{tot}^{NC} (units: mass): This is the total mass of material contained in the system as "seen" by the accessible pools.

Total volume of distribution V_{tot}^{NC} (units: volume): This is the total volume of the system seen from the accessible pools, i.e. it is either the volume in which the total mass would be distributed assuming that the concentration throughout the system is uniform and equal to the sum of the concentrations of the accessible pools, or the sum of the volumes where substances 1 and 2 distribute throughout the system assuming the same concentrations as in the accessible pools.

Mean residence time MRT_i^{NC} (units: time), $i = 1,2$: These are the average times a particle introduced into the system in accessible pool i spends in the system before leaving the accessible pools for the last time. Notice that formulas (3.4.14) and (3.4.15) give two values for V_{tot}^{NC} described in Table 3.4.6.

In order to express MRT_1^{NC} and MRT_2^{NC} as a function of the measurement variables, it is necessary first to define 4 mean total residence times MRT_i^j, $i, j = 1, 2$; these represent the expected time particle introduced into pool j spends in the system before leaving accessible pool i for the last time. Their expressions as a function of $z_i^j(t)$ or $c_i^j(t)$ as measured for the bolus injection experiment respectively are

Table 3.4.6. Relationships Among the System Kinetic Parameters of the Two Accessible Pool Model.

$$M_{tot}^{NC} = MRT_1^{NC} R_{10} + MRT_2^{NC} R_{20} \qquad (3.4.13)$$

$$V_{tot}^{NC} = \frac{M_{tot}^{NC}}{C_1 + C_2} \qquad (3.4.14)$$

$$V_{tot}^{NC} = \frac{MRT_1^{NC} R_{10}}{C_1} + \frac{MRT_2^{NC} R_{20}}{C_2} \qquad (3.4.15)$$

$$MRT_i^j = \frac{\int_0^\infty t z_i^j(t) dt}{A z_i^j} \qquad (3.4.16)$$

$$MRT_i^j = \frac{\int_0^\infty t c_i^j(t) dt}{A c_i^j} \qquad (3.4.17)$$

where Az_i^j and Ac_i^j are defined in (3.4.7) and (3.4.8).

The mean residence time MRT_1^{NC} can be expressed by weighting MRT_1^1 and MRT_1^2 according to the probability that a particle having been introduced into pool 1 irreversibly leaves the system from pool 1 and 2 respectively; similarly with MRT_2^{NC}:

$$MRT_1^{NC} = MRT_1^1 \frac{R_{01}}{R_{d_1}} + MRT_2^1 (1 - \frac{R_{01}}{R_{d_1}}) \qquad (3.4.18)$$

$$MRT_2^{NC} = MRT_2^2 \frac{R_{02}}{R_{d_2}} + MRT_1^2 (1 - \frac{R_{02}}{R_{d_2}}) \qquad (3.4.19)$$

where R_{d_1} and R_{d_2} are the disappearance rates from pool 1 and 2 as evaluated from the one accessible pool model applied to pool 1 and pool 2 separately.

Equations (3.4.18) and (3.4.19) apply to situations where data are expressed as the tracer to tracee ratios, and the physiological references are masses. When the measurements are tracer concentrations and the physiological references are volumes, the equations can be conveniently expressed as

$$MRT_1^{NC} = MRT_1^1 \frac{v_{01}}{CR_1} + MRT_2^1 (1 - \frac{v_{01}}{CR_1}) \qquad (3.4.20)$$

$$MRT_2^{NC} = MRT_2^2 \frac{v_{02}}{CR_2} + MRT_1^2 (1 - \frac{v_{02}}{CR_2}) \qquad (3.4.21)$$

where CR_1 and CR_2 are the clearance rates from pool 1 and 2 as evaluated from the one accessible pool model applied to pool 1 and pool 2 separately.

The relationships given in Table 3.4.6 permit one to calculate M_{tot}^{NC} and V_{tot}^{NC}, Different definitions for V_{tot}^{NC} are given depending upon the situation. For instance, if the two accessible pools represent two interacting substances in plasma, the use of $C_1 + C_2$ as a reference concentration (eg. in (3.4.14)) is appropriate. On the contrary, if the two accessible pools represent two different locations of a substance, V_{tot}^{NC} can be evaluated by summing up the volumes where substance 1 and 2 distribute, using respectively C_1 and C_2 as the reference (3.4.15).

3.4.5 Relationship Between One and Two Accessible Pool Noncompartmental Models

The definitions of the two accessible pool noncompartmental model parameters given in this section delineate the interactions between the two pools, and require data from a two input-four output experiment. In addition to this analysis, one could apply the one accessible pool noncompartmental model separately to each of the two experimental curves describing the disappearance of the two tracers.

To derive the relationships between the two sets of parameters, consider a double bolus injection experiment where the measurements are expressed in terms of the tracer to tracee ratios $z(t)$. By adopting the notation of the multiple tracer experiment for the formulas given in Table 3.3.2, the rates of appearance and disappearance into accessible pools 1 and 2, now indicated as R_{a_1} R_{d_1} R_{a_2} and R_{d_2} are:

$$R_{d_1} = \frac{d_1}{\int_0^\infty z_1^1(t)dt} = R_{a_1} \qquad R_{d_2} = \frac{d_2}{\int_0^\infty z_2^2(t)dt} = R_{a_2} \qquad (3.4.22)$$

These fluxes are related to the two accessible pool model fluxes R_{ij}, and from their expressions given in Table 3.4.3, it is easy to verify the following equalities:

$$R_{a_1} = R_{10} + R_{20}\frac{R_{12}}{R_{12} + R_{02}} \qquad R_{a_2} = R_{20} + R_{10}\frac{R_{21}}{R_{21} + R_{01}} \quad (3.4.23)$$

$$R_{d_1} = R_{01} + R_{21}\frac{R_{02}}{R_{12} + R_{02}} \qquad R_{d_2} = R_{02} + R_{12}\frac{R_{01}}{R_{21} + R_{01}} \quad (3.4.24)$$

It is evident from these relationships that the two accessible pool schematization is able to isolate de novo appearance and disappearance

fluxes per se from the contribution of the interconversion from the other pool. Consider as an example the first equality. R_{a_1} can be subdivided into de novo appearance into pool 1, R_{10}, plus the fraction of de novo appearance into pool 2, R_{20} which appears in pool 1 after interconversion. Similarly, R_{d_1} is the sum of irreversible removal of material from pool 1 per se, R_{01}, plus the flux of material which leaves the system after being converted to pool 2.

The same considerations also apply to parameters v_{ij} as compared to the clearance rates from accessible pools 1 and 2:

$$CR_1 = v_{01} + v_{21}\frac{v_{02}}{v_{12} + v_{02}} \qquad CR_2 = v_{02} + v_{12}\frac{v_{01}}{v_{21} + v_{01}} \qquad (3.4.25)$$

These equations suggest an interpretation of v_{01} and v_{02} as clearance rates per se which can be compared to CR_1 and CR_2, parameters which measure the clearance in toto from the accessible pools including the effect of interconversion.

3.4.6   Limitations of Two Accessible Pool Noncompartmental Models

To interpret correctly the two accessible pool noncompartmental parameters, one must expand to these models the concepts introduced in §3.3.3 [Cobelli and Toffolo, 1984]. Formal proofs of what follows will be given in Chapter 7. Consider first the conditions on the model structure which permits one to interpret $R_{10} + R_{20}$ as the true de novo production rate in the system. Since R_{10} and R_{20} are the rates at which endogenous particles enter the accessible pools, their sum correctly measures the total production in the system only if all newly synthesized particles enter the accessible pool, i.e. there is no loss of material via the pathways between the pools into which synthesis occurs and the accessible pools. When this condition is not satisfied, $R_{10} + R_{20}$ will underestimate the true production.

Concerning the mean residence time, neither MRT_1^{NC} nor MRT_2^{NC} will in general measure the mean residence time in the system for endogenous particles. An estimate for this parameter can be obtained by weighting MRT_1^{NC} and MRT_2^{NC} according to the probability that an endogenous particle enters the system from accessible pool 1 and 2:

$$MRT^{NC} = MRT_1^{NC}\frac{R_{10}}{R_{10} + R_{20}} + MRT_2^{NC}\frac{R_{20}}{R_{10} + R_{20}} \qquad (3.4.26)$$

It will be shown in Chapter 7 that MRT^{NC} correctly recovers the mean residence time in the system of endogenous particles if productions as

well as irreversible losses take place in the accessible pools only. The same conditions must be satisfied in order for M_{tot}^{NC} to be a correct measure of the total mass in the system.

As already discussed in §3.3.3, the validity of these conditions must be verified in order to interpret correctly the noncompartmental parameters. For instance, with reference to the tracee system schematizations shown in Figure 3.4.6, $R_{10} + R_{20}$ recovers U in situations (b); $R_{10} + R_{20}$ recovers $U_1 + U_2$ in situations (c) and (d) while MRT^{NC} recovers the mean residence time of endogenous particles only in situation (c). This is the only case where M_{tot}^{NC} correctly measures the total mass in the system.
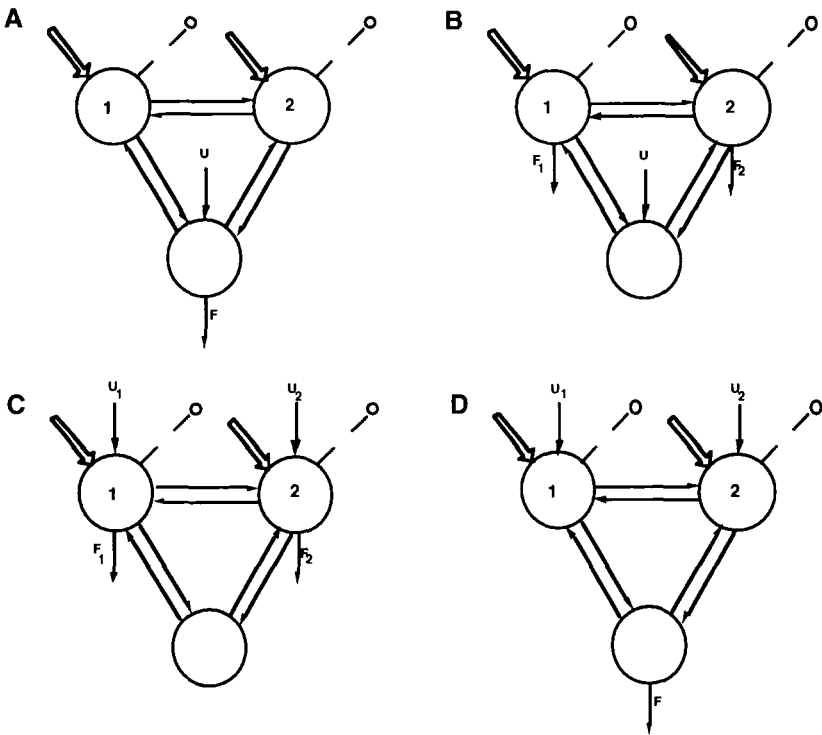
Figure 3.4.6. A three pool schematization of the tracee system. The situations are: in (a) de novo production and disposal occurs in the non-accessible pool; (b) de novo production occurs in the non-accessible pool and disposal occurs from the accessible pools; (c) both de novo production and disposal occur in the accessible pools; and (d) de novo production occurs in the accessible pools and disposal from the non-accessible pool.

Note that in no case does the one accessible pool analysis applied to either pool 1 and 2 give a correct estimate for de novo production and then for M_{tot} since R_{01} and R_{02} of the noncompartmental model are both different from zero and thus

$$R_{a_i} < R_{10} + R_{20} \leq U \qquad i = 1, 2 \qquad (3.4.27)$$

References

Bergner P.E.E.: Tracer dynamics and the determination of pool sizes and turnover factors in metabolic systems. *J. Theor. Biol. 6:*137–158, 1964.

Cobelli C., Toffolo G.: Compartmental vs noncompartmental modeling for two accessible pools. *Am. J. Physiol. 24*7:R488–R496, 1984.

DiStefano III J.J.: Noncompartmental vs compartmental analysis: some basis for choice. *Am. J. Physiol. 12:R1–R6,* 1982.

DiStefano J.J., Landaw E.M.: Multiexponential, multicompartmental and noncompartmental modeling. I. Methodological limitations and physiological interpretation. *Am. J. Physiol. 246*:R651–R664, 1984.

Katz J.: The determination of mass of metabolites with tracers. *Metabolism. 38*:728–733, 1989.

Rescigno A., Gurpide E.: Estimation of average times of residence, recycle, and interconversion of blood-borne compounds using tracer methods. *J. Clin. Endocrinol. Metab. 36*:263–276, 1973.

Chapter 4

THE COMPARTMENTAL MODEL

4.1   INTRODUCTION

In the previous chapter, specific kinetic parameters of the system were defined and their estimation using the noncompartmental model discussed. It was seen, however, that a model of the nonaccessible portion of the system was necessary. The model is shown in Figure 4.1.1 A where the nonaccessible portion of the system is described by the recirculation/exchange arrow.

An alternative to this model is to "compartmentalize" the system, i.e. to postulate a structure for the nonaccessible portion of the system consisting of distinct "compartments" which are interconnected by pathways representing fluxes of material and/or biochemical conversions. An example is illustrated in Figure 4.1.1B where the compartments are represented by circles and the interconnections by arrows. Note that the substances can also enter some of the nonaccessible compartments de novo (arrows entering a compartment not origination from another compartment) and irreversibly leave others (arrows leaving compartments and nor ending at another compartment). This approach gives rise to a compartmental structure that is unique for each system studied since it incorporates known and hypothesized physiology and biochemistry; this is in direct contrast to the noncompartmental approach where the schema is the same for all systems. In the compartmentalization of Figure 4.1.1A given in Figure 4.1.1B, the circles representing compartments and the arrows representing transfers have special meanings which will be defined precisely in this Chapter.

In the noncompartmental approach, one can estimate specific kinetic parameters but obtain no insight into the detailed structure of the sys-
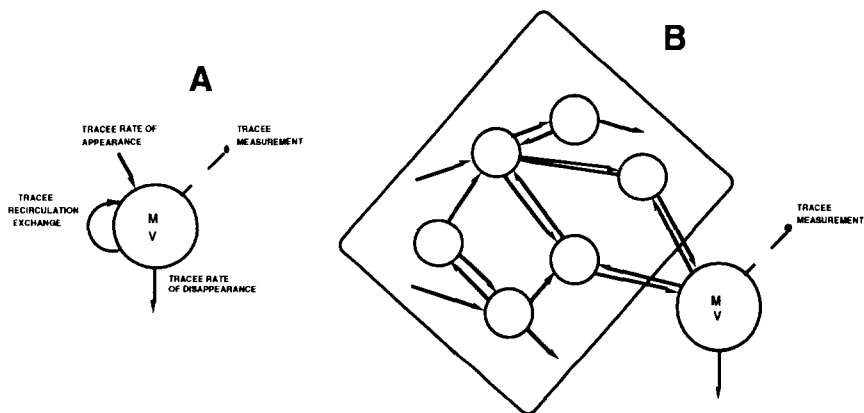
Figure 4.1.1.   A. The noncompartmental representation of a system. B. A compartmental representation of the system. The recirculation/exchange arrow is described by a set of nonaccessible compartments some of which exchange with the accessible compartment. See text for additional explanation.

tern outside of the accessible pool. For this technique, the domain of validity and the limits of the approach are known. The compartmental method relaxes the limits imposed by the noncompartmental model. It will provide the investigator with insights into the system structure, permitting predictions about components of the system not accessible for measurement. However, it is only as good as the assumptions that are incorporated in this structure. This step forward in complexity will reward the investigator with a much richer interpretation of tracer kinetic data.

Both the noncompartmental and compartmental models, however, require the existence of at least one accessible pool into which test substances can be administered and from which measurements can be made. Thus the philosophic difference between them lies in the way the nonaccessible portion of the system is modeled. In the former, the investigator chooses an equivalent type of structure, the recirculation/exchange arrow, with the assumption of no sources or sinks along the arrow since the noncompartmental parameters describing tracee rate of appearance and disappearance R_a and R_d refer to the accessible pool only. In the latter, the investigator postulates a definite structure for the system where de novo production (as illustrated by the arrows into the nonaccessible

pools from "outside" the system shown in Figure 4.1.1B) and disposal can occur from accessible and nonaccessible compartments (as indicated in the same figure by the arrows towards the "outside" of the system, both from the accessible and two of the nonaccessible pools).

4.2   CONCEPTS AND DEFINITIONS

The compartmental system diagrammed in Figure 4.1.1B consists of an accessible compartment and a structure representing the nonaccessible portion of the system consisting of 6 interconnected compartments. The implication is that the nonaccessible portion of the system contains six discrete entities. However, most biological systems are far more complicated than this simple representation.

In fact, it is not possible to track the behavior of every molecule in a biological system at every point in time. Hence it is useful to consider collections of specific molecules at specific sites or in specific forms, i.e. collections of molecules having similar characteristics but existing in the system at different locations, or collections that exist at a given site or location in the system but have different characteristics. As an example of the former, zinc exists in the body in, among other locations, plasma, red cells, muscle and bone. As an example of the latter, consider glucose. Once glucose is transported from plasma to muscle cells, it can be phosphorylated to glucose-6-phosphate. Thus muscle cells are a location in the glucose system where glucose molecules are present in two different forms, glucose and glucose-6-phosphate. One can see that thinking of the system in these terms, i.e. collecting molecules at specific sites or in specific forms, permits a "lumping" of the system into discrete groups, and that arrows can be used to represent the movement from one site or one form to another.

Examples of lumping into a discrete group could be calcium in plasma, zinc in bone, or tri-iodothyrouine in thyroid cells. In some experiments, however, the lumping can exist in the same physical space such as plasma. For example, one could follow the kinetics of glucose, lactate and alanine in plasma; the lumping here is glucose, lactate and alanine as separate group of molecules in the physical space of plasma.

The basis of a compartment in a system is one of lumping material with similar characteristics into discrete collections that are homogeneous and behave identically. The notions of "homogeneous" and "behave identically", however, require precise definitions for it is through the definitions that the link to mathematics is made. The basis of the compartmental system, or model, are the arrows which are used to indicate the interconnections among the various compartments. As will be seen, the interconnections represent a flux of material (mass time^{-1})

which, physiologically, represents transport or a chemical transformation, or both.

The formal definitions or a compartment and compartmental model are:

1. a **compartment** is an amount of material that acts as though it is well-mixed and kinetically homogeneous; and

2. a **compartmental model** is a model consisting of a finite number of compartments with specified interconnections among them.

What exactly is well-mixed and kinetic homogeneity? These notions are illustrated in the Figure 4.2.1 below.
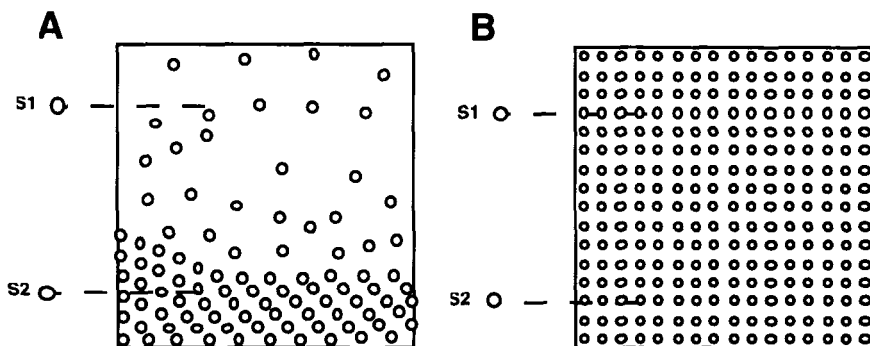
Figure 4.2.1.   A. A mass of substance (denoted by circles) is nonuniformly distributed in a system (represented by the box), i.e. the concentration of substance depends upon where the sample is taken. Thus the two samples illustrated by S1 and S2 would have different concentrations. B. A mass of substance is uniformly distributed in a system. The two samples S1 and S2 taken at two different sites in the system would have the same concentration.

Well-mixed can be described in the context of Figure 4.2.1. In Figure 4.2.1 A and B, consider the system as a single compartment. What well-mixed means is that any two samples taken from the compartment at the same time would have the same concentration of the substance being studied and therefore be equally representative. This is not the case in Figure 4.2.1 A while it is the case in Figure 4.2.1 B. Thus the concept of well-mixed relates to uniformity of information contained in a single compartment. It is worth noting that a single compartment may also

represent amounts of material at two different locations. This lumping of material at two different locations can occur because its actual mixing between these two locations cannot be described within the time frame of a particular experiment. For instance, plasma and red blood cell glucose equilibrate rapidly in humans so the two distinct anatomical locations can be considered a single compartment.

Kinetic homogeneity means the following: every particle in a compartment has the same probability of taking the pathways leaving the compartment. This is illustrated in the following figure. There are several pathways by which material can leave. Each pathway may and probably will have a different probability; the sum of all of the probabilities is, of course, equal to 1. This will be explained in detail below in Figure 4.2.2.
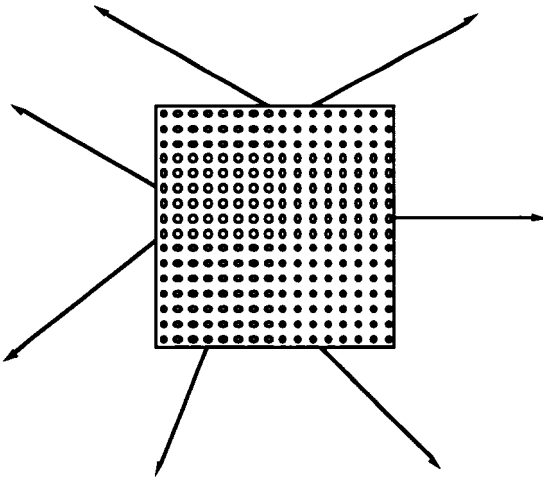
Figure 4.2.2. A compartment showing the pathways by which material can leave the compartment (see text for additional information).

Every compartment is characterized both by an amount of material and what can happen to that material. Basically, material flows into and out from the compartment, and the balance between the two determines the amount of material in the compartment at any point in time. For example, referring to Figure 4.2.1B, if the accessible compartment is plasma, then as material is carried in the circulation, it can exchange

with the various tissues in the body. Depending upon the substance being considered, material will leave the plasma and enter the tissues with different rates. Thus when material leaves a compartment, it does so because of metabolic event related to transport and utilization. For a given compartment, there may be several such events possible. It is the totality of such events that characterize the behavior of material in a compartment. Kinetic homogeneity means that each particle of the material in the compartment have the same probability of leaving due to one of these events.

A compartment, therefore, is a discrete amount of material that behaves identically. The discrete nature of a compartment is what allows one to reduce a complex biological system into a finite number of discrete compartments and pathways. The subject of this and subsequent chapters is how to use tracer kinetic studies to characterize these pathways in the context of a compartmental model. As will be seen, the number of compartments required largely depends both on the system being studied and the specific experimental design chosen to probe it.

In addition, one must distinguish between compartments that are accessible and nonaccessible for measurement. The accessible compartments will play the same role as the accessible pools in noncompartmental models. The accessible compartment has the same problems as the accessible pool in terms of identifying a physical space. Researchers often try to assign physical spaces to the nonaccessible compartments. This is a very difficult problem which is best addressed once one realizes that the definition of a compartment is actually a theoretical construct which may in fact lump material from several different physical spaces in a system; to equate a compartment with a physical space depends upon the system under study and assumptions about the model.

4.3   THE COMPARTMENTAL MODEL OF A TRACER-TRACEE SYSTEM

4.3.1 Introduction

The notation for the tracee and tracer systems to be used in this text are summarized below in Table 4.3.1 and Table 4.3.2. All tracee variables are constant since the tracee system is assumed to be in a steady state. Conversely, all tracer variables, except the compartment volumes, vary in time to indicate that the tracer system is studied dynamically.

The link between the tracee and tracer system comes from the indistinguishability principle of tracer and tracee discussed in Chapter 2:

$$\frac{F_{ij}}{M_j} = \frac{f_{ij}(t)}{m_j(t)} = k_{ij} \qquad i = 1, \cdots, n, \ \ j = 1, \cdots, n, \ \ i \neq j \qquad (4.3.1)$$

Table 4.3.1. Notation for Tracee Variables

Symbol	Definition and Units
n	number of compartments
V_i	volume of compartment i, $i = 1, \cdots, n$
M_i	mass in compartment i, $i = 1, \cdots, n$
C_i	concentration (mass/volume) in compartment i, $i = 1, \cdots, n$
Ui	de novo production (mass/time) into compartment i, $i = 1, \cdots, n$
F_{ij}	transport (mass/time) from compartment j to compartment i, $i = 1, \cdots, n; j = 1, \cdots, n; j \neq i$
F_{0i}	disposal (mass/time) from compartment i, $i = 1, \cdots, n$

Note k_{ij} is constant since F_{ij} and M_j are constant. One then can write for the tracer and tracee the following:

$$F_{ij} = k_{ij} M_j \qquad i = 1, \cdots, n, \quad j = 1, \cdots, n, \quad i \neq j \qquad (4.3.2)$$
$$F_{0i} = k_{0i} M_i \qquad 1 = 1, \cdots, n$$
$$f_{ij}(t) = k_{ij} m_j(t) \qquad i = 1, \cdots, n, \quad j = 1, \cdots, n, \quad i \neq j \qquad (4.3.3)$$
$$f_{0i}(t) = k_{0i} m_i(t) \qquad 1 = 1, \cdots, n$$

The constants k_{ij} defined in (4.3.1) are called **rate constants** or **fractional transfer coefficients.** They have units time^{-1}, and represent the fractional transfer of material between compartments or the fractional losses from compartments. As will be seen below, it is these constants that are estimated from tracer kinetic data. To do so, one must link the equations describing the model with the measurement variables of the tracer experiment.

Table 4.3.2.   Notation for tracer variables

Symbol	Definition and Units
n	number of compartments
V_i	volume of compartment i, $i = 1, \cdots, n$
m_i	mass in compartment i, $i = 1, \cdots, n$
u_i	rate of input (mass/time) into compartment i, $i = 1, \cdots, n$
d_i	total tracer input (mass) into compartment i, $i = 1, \cdots, n$
f_{ij}	transport (mass/time) from compartment j to compartment i, $i = 1, \cdots, n; j = 1, \cdots, n; i \neq j$
f_{0i}	disposal (mass/time) from compartment i, $i = 1, \cdots, n$
c_i	tracer concentration in compartment i, $i = 1, \cdots, n$
z_i	tracer to tracee ratio in compartment i, $i = 1, \cdots, n$

4.3.2   The One Compartment Model

Suppose one is investigating the kinetics of a substance in the steady state, and knows that this substance is uniformly distributed in a single compartment into which de novo production and from which disposal occur. This is the one compartment model, and is identical to the situation described in Chapter 2. Is is diagrammed below in Figure 4.3.1 A; note these figures are identical to Figures 2.2.4 and 2.2.5.

As written in (2.2.1), the mass balance equation for the tracee system is

$$\frac{dM_1}{dt} = -F_{01} + U_1 = 0 \qquad (4.3.4)$$

whence $U_1 = F_{01}$. From the tracee measurements, normally the tracee concentration, one cannot estimate U_1 or F_{01} without more information. A tracer experiment, as diagrammed in Figure 4.3.1B, is designed for these purposes. As written in (2.2.4), the mass balance equation for the
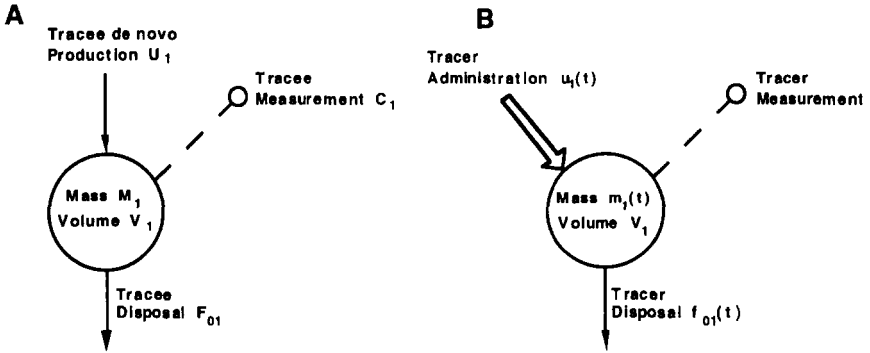
Figure 4.3.1. **A.** The one compartment tracee system. **B.** The one compartment tracer system. See text for additional information.

tracer is

$$\frac{dm_1(t)}{dt} = -f_{01}(t) + u_1(t) \quad m_1(0) = 0 \qquad (4.3.5)$$

Again, as indicated before, the link between the tracee and tracer system comes from tracer-tracee indistinguishability leading to the definition of the rate constant $k_{01} = \frac{F_{01}}{M_1} = \frac{f_{01}(t)}{m_1(t)}$.

In terms of the rate constant k_{01}, (4.3.4) and (4.3.5) can be rewritten:

$$\frac{dM_1}{dt} = -k_{01}M_1 + U_1 = 0 \qquad (4.3.6)$$

$$\frac{dm_1(t)}{dt} = -k_{01}m_1(t) + u_1(t) \quad m_1(0) = 0 \qquad (4.3.7)$$

While these equations describe the mass balance of tracee and tracer, no link has been made to the measurement variable for either. This link comes either via the concentration of tracer $c_1(t) = m_1(t)/V_1$ or the tracer to tracee ratio $z_1(t) = m_1(t)/M_1$. Hence from the tracer data, besides estimating the rate constant k_{01}, one will also have to estimate V_1 or M_1. Knowing the rate constant k_{01} and V_1 or M_1, F_{01} and hence U_1 can be estimated either from $F_{01} = U_1 = k_{01}V_1C_1$ since the tracee concentration $C_1 = M_1/V_1$ is normally measured, or from $F_{01} = U_1 = k_{01}M_1$.

4.3.3   The Two Compartment Model

Suppose one is investigating the kinetics of a substance in the steady state, and postulates the system can be described by a two compartment model. The most general two compartment model is shown in Figure 4.3.2.
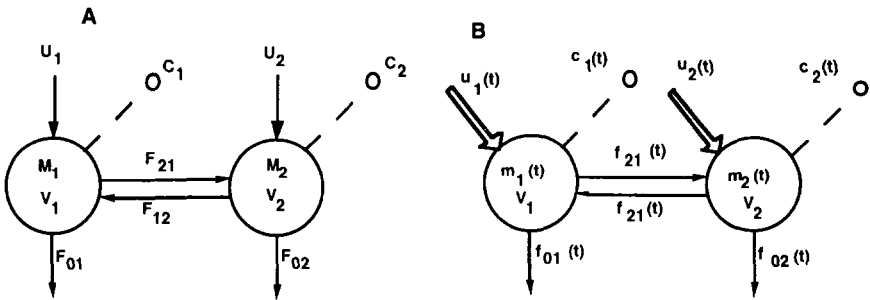
Figure 4.3.2. **A.** The two compartment tracee system; the dotted line with bullets represents **B.** The two compartment tracer system; the dotted lines with bullets represents sampling sites. This can be either the tracer concentration $c_i(t)$ shown here, or tracer to tracee ratio $z_i(t)$. In this most general case, there are tracer inputs $u_1(t)$ and $u_2(t)$ into both compartments. See text for additional explanation.

Extending the ideas of the previous section, the mass balance equations for the tracee system are

$$\frac{dM_1}{dt} = -F_{01} - F_{21} + F_{12} + U_1 = -(k_{01} + k_{21})M_1 + k_{12}M_2 + U_1 = 0 \quad (4.3.8)$$

$$\frac{dM_2}{dt} = F_{21} - F_{02} - F_{12} + U_2 = k_{21}M_1 - (k_{02} + (k_{12})M_2 + U_2 = 0$$

while those for the tracer are

$$
\begin{aligned}
\frac{dm_1(t)}{dt} &= -f_{01}(t) - f_{21}(t) + f_{12}(t) + u_1(t) \quad\quad\quad (4.3.9)\\
&= -(k_{01} + k_{21})m_1(t) + k_{12}m_2(t) + u_1(t) \quad m_1(0) = 0
\end{aligned}
$$

$$
\begin{aligned}
\frac{dm_2(t)}{dt} &= f_{21}(t) - f_{02}(t) - f_{12}(t) + u_2(t) \\
&= k_{21}m_1(t) - k_{02} + (k_{12})m_2(t) + u_2(t) \quad m_2(0) = 0
\end{aligned}
$$

These equations have been written purposely in terms of both the tracee and tracer fluxes and the rate constants k_{ij} to remind the reader of the relationship between the two, and to emphasize the following point: it is the masses and the fluxes that are of interest in the tracee system, while in the tracer system it is the rate constants. In fact, one goal of the tracer experiment is to estimate the rate constants which can then be used to calculate the masses and fluxes in the tracee system. Thus in the remainder of this text, figures and diagrams of the tracee system will be written in terms of these fluxes, U_i and F_{ij}, while those for the tracer will be written in terms of the k_{ij}.

To further illustrate the link between rate constants and tracee fluxes, and to foreshadow the material to be presented in subsequent chapters, consider the special case of the two compartment model shown in Figure 4.3.3.
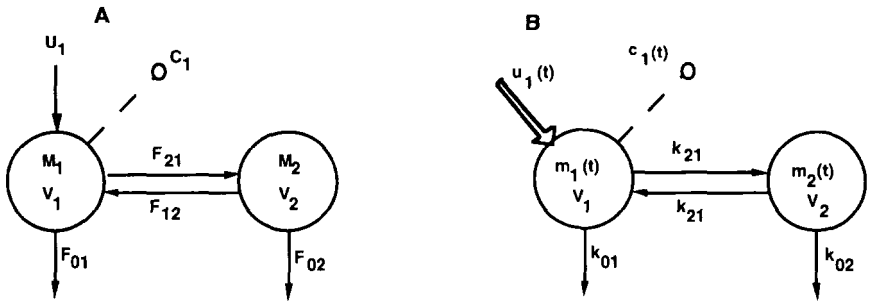
Figure 4.3.3. **A.** A two compartment tracee system in which compartment 1 is the accessible pool as indicated by the dotted line with the bullet. The loss of material occurs from both compartment 1 and 2; material enters the system de novo into compartment 1. **B.** The corresponding two compartment tracer system. Here the tracer is introduced into compartment 1 as indicated by $u_1(t)$. See text for additional information.

The equations for the tracee and tracer are identical to the general equations given in (4.3.8) and (4.3.9) with $U_2 = u_2(t) = 0$. In this example, the tracer is introduced into compartment 1. The tracer concentration $c_1(t) = m_1(t)/V_1$ is measured in this compartment at specified times during the experiment; the tracee concentration $C_1 = M_1/V_1$ is also measured in this compartment. From the resulting data, one wishes to estimate the individual k_{ij} and the tracee fluxes U_i and F_{ij}. The first

question that arises is the following: can one estimate a unique set of rate constants k_{ij} from the data? The implication of this question is that some compartmental structures may be too complicated in terms of the information content in the data, i.e. a unique set of the k_{ij} characterizing them cannot be estimated. On the other hand, it may be possible that more than one set of k_{ij} can be estimated meaning there is not a unique set. These questions relate to the a priori identifiability of the tracer model addressed in Chapter 5.

4.3.4   The N-Compartment Model

As one might anticipate, the description of a general the n-compartment system is more complex. The mass balance equations, however, are obvious extensions of those given for the two compartment system. Given in terms of the rate constants k_{ij}, they are respectively for the tracee and tracer:

$$\frac{dM_i}{dt} = -\sum_{\substack{j=0 \\ j\neq i}}^{n} F_{ji} + \sum_{\substack{j=1 \\ j\neq i}}^{n} F_{ij} + U_i \qquad (4.3.10)$$

$$= -\sum_{\substack{j=0 \\ j\neq i}}^{n} k_{ji}M_i + \sum_{\substack{j=1 \\ j\neq i}}^{n} k_{ij}M_j + U_i = 0 \qquad i = 1,\cdots,n$$

and

$$\frac{dm_i(t)}{dt} = -\sum_{\substack{j=0 \\ j\neq i}}^{n} k_{ji}m_i(t) + \sum_{\substack{j=1 \\ j\neq i}}^{n} k_{ij}m_j(t) + u_i(t) \quad m_i(0) = 0 \quad i = 1,\cdots,n$$

$$(4.3.11)$$

Note $U_i \neq 0$ only when there is de novo entry of material into compartment i, and $u_i(t)$ can be nonzero only for accessible pools.

For a large model, it is common to represent this set of differential equations using matrix notation. It is convenient first to define

$$k_{ii} = -\sum_{\substack{j=0 \\ j\neq i}}^{n} k_{ji} \qquad (4.3.12)$$

which is the sum of all outgoing rate constants from a given compartment, i.e. all rate constants from this to other compartments plus that to the outside environment.

In the general case, let

$$\mathbf{K} = \begin{pmatrix} k_{11} & k_{12} & \cdots & k_{1n} \\ k_{21} & k_{22} & \cdots & k_{2n} \\ \vdots & \vdots & \ddots & \vdots \\ k_{n1} & k_{n2} & \cdots & k_{nn} \end{pmatrix} \qquad (4.3.13)$$

be the matrix of rate constants k_{ij}. The matrix $\mathbf{K}$ is called the compartmental matrix. For the tracee system, let $\mathbf{M}$ be the column vector of steady state masses in compartments $i = 1, \cdots, n$

$$\mathbf{M} = \begin{pmatrix} M_1 \\ M_2 \\ \vdots \\ M_n \end{pmatrix} \qquad (4.3.14)$$

and $\mathbf{U}$ be the column vector of inputs into compartments $i = 1, \bullet \bullet \bullet, n$

$$\mathbf{U} = \begin{pmatrix} U_1 \\ U_2 \\ \vdots \\ U_n \end{pmatrix} \qquad (4.3.15)$$

Remember that some of the U_i may be zero. Then the system of equations describing the tracee system can be written

$$\frac{d\mathbf{M}}{dt} = \mathbf{KM} + \mathbf{U} = 0 \qquad (4.3.16)$$

For the tracer system, let $\mathbf{m}(t)$ be the column vector of tracer masses in compartments $1, \ldots, n$

$$\mathbf{m}(t) = \begin{pmatrix} m_1(t) \\ m_2(t) \\ \vdots \\ m_n(t) \end{pmatrix} \qquad (4.3.17)$$

$\mathbf{u}(t)$ the column vector of tracer inputs into compartments $1, \ldots, n$

$$\mathbf{u}(t) = \begin{pmatrix} u_1(t) \\ u_2(t) \\ \vdots \\ u_n(t) \end{pmatrix} \qquad (4.3.18)$$

and $\frac{d\mathbf{m}(t)}{dt}$ the column vector

$$\frac{d\mathbf{m}(t)}{dt} = \begin{pmatrix} \frac{dm_1(t)}{dt} \\ \frac{dm_2(t)}{dt} \\ \vdots \\ \frac{dm_n(t)}{dt} \end{pmatrix} \tag{4.3.19}$$

Then the system of n differential equations describing the n compartment model can be written

$$\frac{d\mathbf{m}(t)}{dt} = \mathbf{K}\mathbf{m}(t) + \mathbf{u}(t) \quad \mathbf{m}(0) = 0 \tag{4.3.20}$$

For the measurement equations, suppose there are l compartments which are accessible for measurement. Let $\mathbf{y}(t)$ be the column vector of the measurements in terms of tracer concentration or tracer to tracee ratio in the accessible compartments, and let $\mathbf{C}$ be the column vector of tracee concentration in these compartments. Both $\mathbf{y}(t)$ and $\mathbf{C}$ are l-dimensional vectors.

If $V_{i_1}, \cdots, V_{i_l}$ are the volumes of the accessible compartments where $1 \le i_1 \le \cdots \le i_l \le n$, define the lxn matrix V;

$$\mathbf{V} = \begin{pmatrix} \cdots & \frac{1}{V_{i_1}} & \cdots & 0 & \cdots \\ \cdots & \vdots & \ddots & \vdots & \cdots \\ \cdots & 0 & \cdots & \frac{1}{V_{i_l}} & \cdots \end{pmatrix} \tag{4.3.21}$$

All elements in the first row of this matrix are 0 except for the i_1^{th} column where $\frac{1}{V_{i_1}}$ is entered. Similarly for the second row; all entries are zero except for the i_2^{th} column. The measurement equations for the tracee is

$$\mathbf{C} = \mathbf{V} \cdot \mathbf{M} \tag{4.3.22}$$

A similar equations holds for the tracer, where the measurements are expressed in tracer concentration:

$$\mathbf{y}(t) = \mathbf{V}\mathbf{m}(t) \tag{4.3.23}$$

For the case when the tracer-tracee ratios are the measurement variables, the tracer measurement equation becomes

$$\mathbf{y}(t) = \mathbf{D}\mathbf{m}(t) \tag{4.3.24}$$

where the entries of the $\mathbf{D}$-matrix are the reciprocals of the masses $M_{i_1}, \ldots, M_{i_l}$ of the accessible compartments.

$$D = \begin{pmatrix} \cdots & \frac{1}{M_{i_1}} & \cdots & 0 & \cdots \\ \cdots & \vdots & \ddots & \vdots & \cdots \\ \cdots & 0 & \cdots & \frac{1}{M_{i_l}} & \cdots \end{pmatrix} \qquad (4.3.25)$$

For example, if tracee and tracer concentrations are measured in the accessible compartments 2, 4 and 5 of a 6 compartment system, the matrix V is the $3 \ x \ 6$ matrix

$$V = \begin{pmatrix} 0 & \frac{1}{V_2} & 0 & 0 & 0 & 0 \\ 0 & 0 & 0 & \frac{1}{V_4} & 0 & 0 \\ 0 & 0 & 0 & 0 & \frac{1}{V_5} & 0 \end{pmatrix}$$

For the tracee, the vector C can thus be written

$$C = \begin{pmatrix} C_2 \\ C_3 \\ C_5 \end{pmatrix} = V \cdot M = \begin{pmatrix} \frac{M_2}{V_2} \\ \frac{M_4}{V_4} \\ \frac{M_5}{V_5} \end{pmatrix} \qquad (4.3.26a)$$

Similarly for the tracee, the vector $y(t)$ can be written

$$y(t) = \begin{pmatrix} c_2(t) \\ c_4(t) \\ c_5(t) \end{pmatrix} = V \cdot m(t) = \begin{pmatrix} \frac{m_2(t)}{V_2} \\ \frac{m_4(t)}{V_4} \\ \frac{m_5(t)}{V_5} \end{pmatrix} \qquad (4.3.26b)$$

Example

As an example of the matrix formalism for compartmental model equations, consider the two compartment model shown in Figure 4.3.3. The equations equations describing the tracee system in matrix notation can be derived by first writing the counterparts of (4.3.13), (4.3.14), and (4.3.15):

$$K = \begin{pmatrix} -(k_{21} + k_{01}) & k_{12} \\ k_{21} & -(k_{12} + k_{02}) \end{pmatrix} \qquad (4.3.27)$$

$$M = \begin{pmatrix} M_1 \\ M_2 \end{pmatrix} \qquad (4.3.28)$$

$$U = \begin{pmatrix} U_1 \\ 0 \end{pmatrix} \qquad (4.3.29)$$

Then from (4.3.16):

$$\mathbf{KM + U} = \begin{pmatrix} -(k_{21} + k_{01}) & k_{12} \\ k_{21} & -(k_{12} + k_{02}) \end{pmatrix} \begin{pmatrix} M_1 \\ M_2 \end{pmatrix} + \begin{pmatrix} U_1 \\ 0 \end{pmatrix}$$

(4.3.30)

$$= \begin{pmatrix} -(k_{21} + k_{01})M_1 + k_{12}M_2 + U_1 \\ k_{21}M_1 - (k_{12} + k_{02})M_2 \end{pmatrix} = \begin{pmatrix} 0 \\ 0 \end{pmatrix}$$

The equivalence of the notation defined in (4.3.8) and (4.3.30) is seen by comparing (4.3.8) with the last column vector on (4.3.30).

For the tracer system, one has for the above example

$$\mathbf{m}(t) = \begin{pmatrix} m_1(t) \\ m_2(t) \end{pmatrix}$$

(4.3.31)

$$\mathbf{u}(t) = \begin{pmatrix} u_1(t) \\ 0 \end{pmatrix}$$

(4.3.32)

and

$$\frac{d\mathbf{m}(t)}{dt} = \begin{pmatrix} \frac{dm_1(t)}{dt} \\ \frac{dm_2(t)}{dt} \end{pmatrix}$$

(4.3.33)

Then (4.3.20) in this case becomes

$$\frac{d\mathbf{m}(t)}{dt} = \mathbf{Km}(t) + \mathbf{u}(t)$$

$$= \begin{pmatrix} -(k_{21} + k_{01}) & k_{12} \\ k_{21} & -(k_{12} + k_{02}) \end{pmatrix} r$$

(4.3.34)

$$\times \begin{pmatrix} m_1(t) \\ m_2(t) \end{pmatrix} + \begin{pmatrix} u_1(t) \\ 0 \end{pmatrix}$$

Since compartment 1 is the only accessible compartment, the measurement equations for the tracee and tracer concentrations are

$$\mathbf{C} = (C_1) = \mathbf{V} \cdot \mathbf{M} = \begin{pmatrix} \frac{1}{V_1} & 0 \end{pmatrix} \begin{pmatrix} M_1 \\ M_2 \end{pmatrix}$$

(4.3.35)

$$\mathbf{y}(t) = (c_1(t)) = \mathbf{V} \cdot \mathbf{m}(t) = \begin{pmatrix} \frac{1}{V_1} & 0 \end{pmatrix} \begin{pmatrix} m_1(t) \\ m_2(t) \end{pmatrix}$$

(4.3.36)

The equivalence of the notation defined in (4.3.9) and (4.3.34) is seen in a fashion analogous to that of the tracee system.

In this text, most theory will be illustrated by writing the individual equations for the two compartment model in the notation of (4.3.8) and (4.3.9) while for compartmental systems of more than two compartments, the matrix notation will be used.

4.4   STRUCTURAL PROPERTIES

4.4.1   Introduction

In §4.3, the differential equations describing the mass balance of a tracer in a general n-compartmental model were given. Mathematically, since the k_{ij} are constant, this is known as a system of linear, first order, constant coefficient differential equations. A number of results are available from which the structural properties of compartmental models can be obtained [Anderson, 1982; Covell et al., 1984; Eisenfeld, 1979; Eisenfeld, 1981; Hearon, 1963; Matis et al., 1983]. Here structural properties refer only to the structure of the system, i.e. they do not depend upon the nature of the tracer input.

In this section, the properties of the compartmental matrix **K** which appears in the differential equations of a general n-compartment model (see (4.3.20)) will be discussed first. From **K**, the mean residence time matrix $\mathbf{\Theta} = -\mathbf{K}^{-1}$ will be defined, and its properties discussed. Next, it will be seen that the solution of the differential equations given by (4.3.30) are sums of exponentials. Lastly, the properties of this solution and the properties of the **K** matrix will be reviewed.

4.4.2   The Compartmental Matrix

The matrix **K** of rate constants defined in (4.3.13) relates the tracer and tracee masses of an n-compartment model to the tracer input rate as defined in (4.3.20) and de novo tracee input as defined in (4.3.16) respectively. It is usually called the compartmental matrix since it completely specifies the structure of the model.

The matrix has the following properties.

1. The off diagonal elements are non-negative

$$k_{ij} \geq 0 \qquad i \neq j \qquad i,j = 1, \cdots, n \qquad (4.4.1)$$

2. The diagonal elements are non-positive

$$k_{ii} = - \sum_{\substack{j=0 \\ j \neq i}}^{n} k_{ji} \leq 0 \qquad i = 1, \cdots, n \qquad (4.4.2)$$

3. The absolute value of each diagonal element $|k_{ii}|$ is not less than the sum of the other elements in its column:

$$|k_{ii}| \geq \sum_{\substack{j=1 \\ j \neq i}}^{n} k_{ji} \qquad (4.4.3)$$

These properties follow directly from the definition and physical meaning of the rate constants. In particular, property (3) follows because $k_{0i} \geq 0$.

There are two properties that the $\mathbf{K}$ matrix often has. One is that it is invertible, i.e. $\det(\mathbf{K}) \neq 0$. The other is that it is reducible, i.e. there exists a permutation of the indices ij so that the matrix can be written

$$\mathbf{K} = \begin{pmatrix} K_{11} & 0 \\ K_{21} & K_{22} \end{pmatrix}$$

where K_{11} and K_{22} are themselves square matrices of dimension less than n. The matrix written in the above form is called block triangular.

The matrix $\mathbf{K}$ is invertible if two conditions hold.

1. The system is open. That is, there is at least one compartment with loss to the external environment.

2. The system contains no closed subsystems, or traps. That is, there is no subsystem of compartments which can only receive material from other compartments with no losses either to the external environment or to other compartments outside of the subsystem.

Thus $\mathbf{K}$ is invertible if all particles entering the system from any compartment will eventually leave the system.

The matrix $\mathbf{K}$ is reducible if the compartmental model contains a subsystem of compartments which cannot transfer material to any of the remaining compartments, but particles in this subsystem will eventually leave the system. The matrix $\mathbf{K}$ is not reducible, or irreducible, if the compartmental model is strongly connected, that is, a particle in one compartment can reach any other compartment in the model.

Example

Consider the general two compartment model shown in Figure 4.3.3. The $\mathbf{K}$ matrix for this model is

$$\mathbf{K} = \begin{pmatrix} -(k_{21} + k_{01}) & k_{12} \\ k_{21} & -(k_{12} + k_{02}) \end{pmatrix} \tag{4.4.4}$$

Clearly since the rate constants k_{ij} are all non-negative, the diagonal elements are non-positive, and the off-diagonal elements are non-negative. Thus

$$|k_{11}| = k_{21} + k_{01} \geq k_{21} \tag{4.4.5}$$

$$|k_{22}| = k_{12} + k_{02} \geq k_{12} \tag{4.4.6}$$

Assuming k_{12}, k_{21} and one or both of k_{01} and k_{02} arc non-zero, the $\mathbf{K}$ matrix is invertible, or equivalently its determinant is non-zero, since the system is open and it does not contain any closed subsystems. That is,

$$\det(\mathbf{K}) = (k_{21} + k_{01})(k_{12} + k_{02}) - k_{12}k_{21} \neq 0 \qquad (4.4.7)$$

The matrix $\mathbf{K}$ is also irreducible since the model is strongly connected.

The matrix $\mathbf{K}$ becomes non-invertible in the two situations depicted in Figure 4.4.1. In case A, the system is closed since k_{21} and k_{12} are nonzero, but $k_{01} = k_{02} = 0$. From (4.4.7),
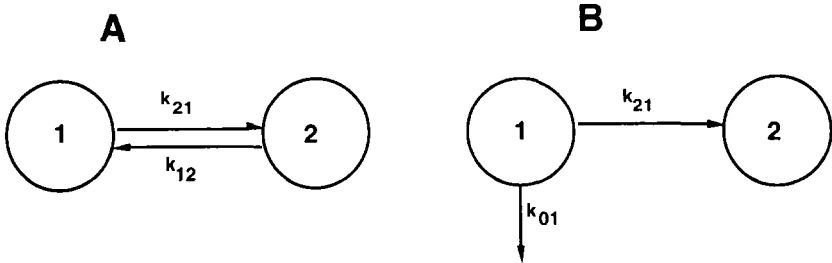
Figure 4.4.1. A. A closed, two compartment system. B. An open two compartment system with a closed subsystem. See text for additional information.

$$\det(\mathbf{K}) = k_{21}k_{12} - k_{21}k_{12} = 0$$

In case B, the system is open since $k_{01} \neq 0$, but it has a closed subsystem, namely compartment 2 since $k_{02} = 0$ and $k_{12} = 0$. From (4.4.7)

$$\det(\mathbf{K}) = (k_{21} + k_{01}) \cdot 0 - 0 \cdot k_{12} = 0$$

In addition, in this case, the matrix $\mathbf{K}$ is reducible since the model is no longer strongly connected, i.e. material cannot move from compartment 2 to compartment 1. The matrix in block triangular form is

$$\mathbf{K} = \begin{pmatrix} -(k_{21} + k_{01}) & 0 \\ k_{21} & 0 \end{pmatrix}$$

4.4.3   The Mean Residence Time Matrix

The concept mean residence time in the accessible pool has already been introduced in the context of noncompartmental analysis in Chapter 4 as the average time a single particle spends in the accessible pool during all passages through it before irreversibly leaving the system. The definition can be extended to any compartment, accessible or not, of an n-compartment system.

From the stochastic interpretation of compartmental models, the n x n matrix Θ defined

$$\Theta = -\mathbf{K}^{-1} \qquad (4.4.8)$$

where $\mathbf{K}$ is the compartmental matrix has significant meaning since the generic element $\theta_{ij}, i, j = 1, \cdots, n$ represents the average time a particle entering the system in compartment j spends in compartment i before irreversibly leaving the system. For this reason, Θ is referred to as the **mean residence time matrix.** This matrix also has an important interpretation in probabilistic terms since the ratio $\frac{\theta_{ij}}{\theta_{ii}}, i \neq j$ equals the probability that a particle in compartment j will reach compartment i, that is

$$0 \leq \mathrm{Prob}[j \rightarrow i] = \frac{\theta_{ij}}{\theta_{ii}} \leq 1 \qquad (4.4.9)$$

Clearly to calculate the mean residence time matrix, the compartmental matrix $\mathbf{K}$ must be invertible; this is why the issue of invertibility was raised in the previous section. As already discussed, this assumes that a particle in a given compartment, no matter how it arrived in that compartment, will eventually leave the system. This means all residence times θ_{ij} are finite.

The mean residence time matrix Θ has the following properties.

1. The elements of the main diagonal of Θ are strictly positive:

$$\theta_{ii} > 0 \qquad i = 1, \cdots, n \qquad (4.4.10)$$

   since they represent the nonzero mean residence time in compartment i for particles entering the system the same compartment.

2. The off-diagonal elements are non-negative.

$$\theta_{ij} \geq 0 \qquad i \neq j \qquad (4.4.11)$$

In particular, $\theta_{ij} = 0$ if and only if the probability of reaching compartment i from compartment j is zero, i.e. there is no pathway connecting compartment j to compartment i [Anderson, 1982].

3. For each column, the main diagonal element is greater than or equal to all other elements in the column.

$$\theta_{ii} \geq \theta_{ij} \qquad j = 1, \cdots, n \qquad (4.4.12)$$

This result follows from (4.4.9), and indicates that the time spent in compartment i is maximum if the particle enters the system in i rather than in some other compartment. One can see that $\theta_{ii} = \theta_{ij}, i \neq j$ if and only if all particles from compartment j will reach compartment i, or equivalently if there is no loss in the pathways connecting j to i.

4. For a compartmental system with a single irreversible loss, say from compartment i, since all particles must pass through i before they can exit the system, one has

$$\text{Prob}[j \rightarrow i] = \frac{\theta_{ij}}{\theta_{ii}} = 1 \qquad (4.4.13)$$

indicating that all elements of the ith row of Θ have the same value. In addition, it can be shown that the mean residence time θ_{ii} is the reciprocal of the rate k_{0i} at which they leave the system. That is, $\theta_{ii} = \frac{1}{k_{0i}}$, and thus from (4.4.13),

$$\theta_{i1} = \cdots = \theta_{in} = \frac{1}{k_{0i}} \qquad (4.4.14)$$

Example

As an example of the mean residence time matrix calculation consider the general two compartment model below; this was originally discussed in Figure 4.3.3.

The compartmental matrix $\mathbf{K}$ is written

$$\mathbf{K} = \begin{pmatrix} -(k_{01} + k_{21}) & k_{12} \\ k_{21} & -(k_{02} + k_{12}) \end{pmatrix} \qquad (4.4.15)$$

and thus

$$\Theta = \begin{pmatrix} \theta_{11} & \theta_{12} \\ \theta_{21} & \theta_{22} \end{pmatrix} = -K^{-1} = \tag{4.4.16}$$

$$\begin{pmatrix} \dfrac{k_{02}+k_{12}}{k_{21}k_{02}+k_{01}k_{02}+k_{01}k_{12}} & \dfrac{k_{12}}{k_{21}k_{02}+k_{01}k_{02}+k_{01}k_{12}} \\ \dfrac{k_{21}}{k_{21}k_{02}+k_{01}k_{02}+k_{01}k_{12}} & \dfrac{k_{01}+k_{21}}{k_{21}k_{02}+k_{01}k_{02}+k_{01}k_{12}} \end{pmatrix}$$

Note that, as expected, all the elements of Θ are strictly positive since compartments 1 and 2 are interconnected, and that $\theta_{11} > \theta_{12}$ and $\theta_{22} > \theta_{21}$.

Next, consider the same model shown in Figure 4.4.2, but now assume k_{02} is zero, i.e. a two compartment model where the only loss is from compartment 1. The matrix Θ is now

$$\Theta = \begin{pmatrix} \theta_{11} & \theta_{12} \\ \theta_{21} & \theta_{22} \end{pmatrix} = \begin{pmatrix} \dfrac{1}{k_{01}} & \dfrac{1}{k_{01}} \\ \dfrac{k_{21}}{k_{01}k_{12}} & \dfrac{k_{01}+k_{21}}{k_{01}k_{12}} \end{pmatrix} \tag{4.4.17}$$

showing that, as expected, all the element of the first row are equal, and equal to $\frac{1}{k_{01}}$.
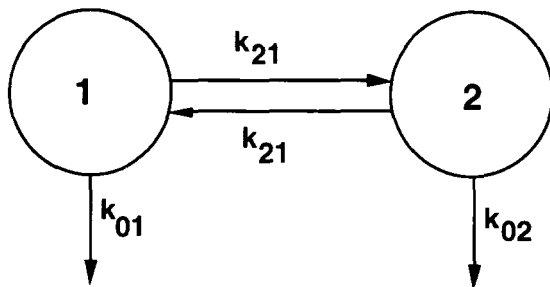
Figure 4.4.2.   A two compartment tracer system used to illustrate the Θ calculations. The tracer and tracee inputs are not shown since Θ depends only upon the **K** matrix.

It is clear that the above ideas can be extended to the n compartment model, i.e. explicit formulas relating the θ_{ij} with the k_{ij} can be formulated. However, they become very complicated as soon as n exceeds 3, and one normally uses numerical techniques to invert the compartmental matrix **K** to obtain the mean residence time matrix.

4.4.4   Sums of Exponentials and the Compartmental Model

From the theory of linear differential equations, the solution of the Compartmental model equations when the k_{ij} are all constant (which is the situation discussed in this text) and the input into the system is a single bolus injection into an arbitrary compartment is a sum of exponentials.

For a one compartment system such as that diagrammed in Figure 4.3.1 in which a bolus of tracer is injected, this can easily be seen by writing (4.3.7)

$$\frac{dm_1(t)}{dt} = -k_{01}m_1(t) \qquad m_1(0) = d \qquad (4.4.18)$$

In this case, since a bolus has been injected, $u_1(t)$ can be written in terms of $m_1(0) = d$ where d is the dose of tracer. The solution of this equation is the decaying monoexponential function

$$m_1(t) = de^{-k_{01}t} \qquad (4.4.19)$$

In a similar fashion, one can show for a constant infusion or a primed, constant infusion that the solution still depends upon the exponential term $e^{-k_{01}t}$. For the constant infusion, the solution is

$$m_1(t) = A(1 - e^{-k_{01}t}) \qquad (4.4.20)$$

and for the primed, constant infusion, the solution is

$$m_1(t) = A_1 - A_2 e^{-k_{01}t} \qquad (4.4.21)$$

In general, for an n-compartment model, the solution of the system of differential equations when the input is a single bolus into a specific compartment is given by a sum of n decaying exponentials. For example, the solution of (4.3.20) for such a bolus input is $\mathbf{m}(t)$ defined in (4.3.17) where the individual components of the vector are of the form

$$m_i(t) = \sum_{j=1}^{n} A_{ij} e^{-\lambda_j t} \qquad (4.4.22)$$

Thus the tracer mass in each compartment is a linear combination of the n decaying exponential functions $e^{-\lambda_i t}$; these exponential functions are called the modes of the system. Remember the notation adopted in this text is that the λ_i are positive whence $-\lambda_i$ are negative. The λ_i depend upon the Compartmental matrix $\mathbf{K}$ since they are the solution of the equation

$$\det|\mathbf{K} + \lambda\mathbf{I}| = 0 \tag{4.4.23}$$

where $\mathbf{I}$ is the $n \times n$ identity matrix.

Finally, the solution for a n-compartmental model for a generic input $u(t)$ is still a function of the modes since, as already discussed in Appendix D, the response of a linear system to a generic input can be derived by combining, via the convolution operator, $u(t)$ with the sum of exponential solutions to a bolus input. The following example will illustrate this situation.

Example

For the two compartment example given in Figure 4.3.2, if compartment 1 is accessible, $u_1(t)$ is a unit bolus injection at time zero, and $u_2(t) = 0$, then

$$m_1(t) = A_{11}e^{-\lambda_1 t} + A_{12}e^{-\lambda_2 t} \tag{4.4.24}$$

$$m_2(t) = A_{21}e^{-\lambda_1 t} + A_{22}e^{-\lambda_2 t} \quad A_{21} + A_{22} = 0$$

with $A_{11} + A_{12} = 1$.
The λ_1 and λ_2 are the solution of the algebraic equation

$$\det(\mathbf{K} + \lambda\mathbf{I}) = (k_{11} + \lambda)(k_{22} + \lambda) - k_{12}k_{21} = 0 \tag{4.4.25}$$

or equivalently

$$\lambda^2 + (k_{11} + k_{22})\lambda + k_{11}k_{22} - k_{12}k_{21} = 0 \tag{4.4.26}$$

Equation (4.4.24) can be used to describe the response of the system to any tracer input $u_1(t)$ into compartment 1. Now let $m_1(t)$ and $m_2(t)$ denote the response of the system to a generic input $u_1(t)$. The relationship between these and the exponential expressions given in (4.4.24), i.e. the response of the system to the unit input, are

$$m_1(t) = \int_0^t u_1(t - \tau)[A_{11}e^{-\lambda_1 \tau} + A_{12}e^{-\lambda_2 \tau}]d\tau$$

$$\tag{4.4.27}$$

$$m_2(t) = \int_0^t u_1(t - \tau)[A_{21}e^{-\lambda_1 \tau} + A_{22}e^{-\lambda_2 \tau}]d\tau$$

The above equations are known as the convolution of $u_1(t)$ and the response of the system to the unit input.

Some properties of the model solution for a generic tracer input can be derived from the properties of the compartmental **K** matrix. These will be discussed in the next section.

As a final remark, it is worth noting that some results given in this section can serve to partially link compartmental and noncompartmental models from a practical point of view. In particular, two points can be made. First, since the parameters for the noncompartmental model are given for systems in a constant steady state, and since such systems can be described by linear, constant coefficient differential equations, sums of exponentials can be used to provide the functional description of a set of tracer data from which the noncompartmental parameters can be estimated. Second, if one first fits a sum of exponentials to a set of tracer data from a single input-single output experiment, and finds that n is the number of exponentials which will provide the best fit, then in general a compartmental model containing of at least n compartments will be required. However, the structure of the n-compartment model needs to be specified. This is simple when $n = 2$ since only the location of the irreversible losses must be specified. It is much more complex when $n > 2$ since the number of possible models becomes very large. For example, when $n = 3$, the number of possible 3 compartment models is 126.

4.4.5 Non-negativity and Stability Properties of Compartmental Model Equations

In this section, some of the more relevant structural properties of the differential equations represented by multicompartmental models will be discussed.

Non-negativity of the compartmental model solution

From an intuitive sense, it is obvious that the model solution for the tracer masses in the compartments of a compartmental model must be non-negative. After all, the models must obey conservation of mass. But this fact can also be shown mathematically. That is, it can be proven that

$$m_i(t) \geq 0 \qquad 0 \leq t \leq \infty \qquad i = 1, \cdots, n \qquad (4.4.28)$$

for an arbitrary, n-compartment model where the input into the system is a unit bolus injection into an arbitrary compartment. Using the idea illustrated by (4.4.27), it can be shown that for an arbitrary

n-compartment model, (4.4.28) holds for an arbitrary, non-negative tracer input. Obviously one cannot have a negative input.

Stability properties

The term stability refers to the property that the response an arbitrary n-compartment model to an experimental tracer input, which is finite or bounded as opposed to an infinite amount, does not grow indefinitely with time. That is, for an arbitrary compartment i in the n-compartmental model, $0 \le m_i(t) \le M$ where M is finite for $0 \le t \le \infty$. This property is related to the properties of the system modes $e^{-\lambda_i t}$ defined in the previous section.

More precisely, suppose that the **K** matrix is irreducible and invertible, i.e. the compartmental model is strongly connected with at least one irreducible loss to the environment. Under these circumstances, the exponentials $\lambda_1, \cdots, \lambda_n$ are either real and positive (corresponding to the λ_i of (4.4.22)), or complex conjugates with positive real parts. The latter situation, which will be illustrated below, arises when the system has damped oscillations; the complex conjugate means that a pair of exponentials, say λ_1 and λ_2, can be written $\lambda_1 = \alpha_1 + \beta_1 i$ and $\lambda_2 = \alpha_1 - \beta_1 i$ where $\alpha_1 > 0$ and $i = \sqrt{-1}$.

The model solution to a bolus input into any compartment is a combination of decaying exponentials and damped oscillations, and decays to zero as t increases:

$$\lim_{t \to \infty} m_i(t) = 0 \qquad (4.4.29)$$

This condition assures that the response of the system to any bounded input also decays to zero with time. In system theory, this property is referred to as bounded input-bounded output stability.

The following two examples will illustrate the stability properties.

Example 1

Consider the two compartment model show in Figure 4.4.2. The exponentials λ_1 and λ_2 are the solutions of the quadratic equation (4.4.26):

$$\lambda_1, \lambda_2 = \frac{-(k_{11} + k_{22}) \pm \sqrt{(k_{11} + k_{22})^2 - 4(k_{11}k_{22} - k_{12}k_{21})}}{2} \qquad (4.4.30)$$

They are real numbers since $(k_{11} + k_{22})^2 - 4(k_{11}k_{22} - k_{12}k_{21}) = (k_{11} - k_{22})^2 + 4k_{12}k_{21} \ge 0$, $k_{11} + k_{22} < 0$ and

$$|k_{11} + k_{22}| > \sqrt{(k_{11} + k_{22})^2 - 4(k_{11}k_{22} - k_{12}k_{21})}$$

Thus the model is stable.

Of course stability could have been observed directly from the fact that the model is strongly connected and has irreversible losses.

Example 2

Consider next the four compartment model shown in Figure 4.4.3.
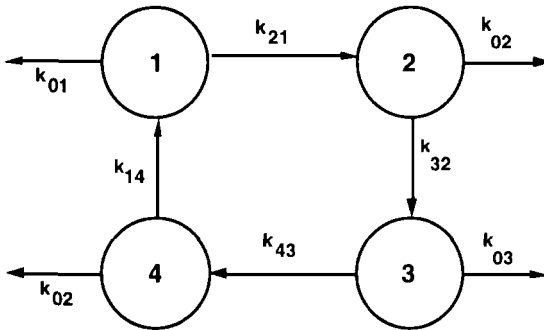
Figure 4.4.3.   A four compartment tracer system. See text for additional information.

As with the previous example, it is clear that the system is stable since it is strongly connected and has irreversible losses. In this example, however, not all λ_i are real. Write the **K** matrix:

$$\mathbf{K} = \begin{pmatrix} k_{11} & 0 & 0 & k_{14} \\ k_{21} & k_{22} & 0 & 0 \\ 0 & k_{32} & k_{33} & 0 \\ 0 & 0 & k_{43} & k_{44} \end{pmatrix} \qquad (4.4.31)$$

For the sake of simplicity, assume the k_{ij} are selected so that $k_{11} = k_{22} = k_{33} = k_{44} = \alpha$ and $k_{21}k_{32}k_{43}k_{14} = \beta$. Then (4.4.23) becomes

$$\det|\mathbf{K} + \lambda\mathbf{I}| = (\alpha + \lambda)^4 - \beta = 0 \qquad (4.4.32)$$

This equation has two real, positive solution λ_1 and λ_2, and two complex conjugate solutions $\lambda_3 = a + bi$ and $\lambda_4 = a - bi$ where a and b are positive real numbers. The model response to a bolus input can be written

$$m_i(t) = A_{i1}e^{-\lambda_1 t} + A_{i2}e^{-\lambda_2 t} + A_{i3}e^{-at}\cos(bt) + A_{i4}e^{-at}\sin(bt) \quad (4.4.33)$$

The terms $A_{i1}e^{-\lambda_1 t}$ and $A_{i2}e^{-\lambda_1 t}$ are two exponentially decaying modes. The other two terms are damped, in terms of e^{-at}, oscillations (in terms of $\cos(bt)$ and $\sin(bt)$). As in the previous example, all $m_i(t)$ decay towards zero as time t increases.

In the discussion and examples so far, it has been assumed that the **K** matrix is irreducible and invertible. What happens for a general n-compartmental model if the **K** matrix is either reducible or singular (noninvertible). Then it can be shown that among the real exponentials λ_i one or more may assume a value equal to zero. This results in a constant mode since $e^{0 \cdot t} = 1$ meaning there is a constant component to the system's response to a bolus input. This means that the model's stability can no longer be proven, and that the response to some bounded input may increase indefinitely with time.

Example 3

Consider the two compartment model given in Figure 4.4.1 A. This is a closed system since there are no irreversible losses. The model solution to a bolus input into compartment 1 is given by (4.4.24) where λ_1 and λ_2 are the solutions of (4.4.23) which is written

$$\lambda^2 - (k_{12} + k_{21})\lambda = 0$$

The two solutions are $\lambda_1 = 0$ and $\lambda_2 = k_{12} + k_{21}$. The masses $m_i(t)$ can be written using (4.4.24):

$$m_1(t) = A_{11} + A_{12}e^{-(k_{12}+k_{21})t}$$

$$m_2(t) = A_{21} + A_{22}e^{-(k_{12}+k_{21})t}$$

where $A_{11} + A_{12}$ equals the amount of the bolus input, and $A_{21} + A_{22} = 0$.

It is clear that for the bolus input into compartment 1, as time t increases towards infinity, $m_1(t)$ approaches A_{11} and $m_2(t)$ approaches A_{21}.

However, the model is not stable. For instance, consider a constant infusion into compartment 1, e.g. $u(t) = u$ for $0 \le t \le \infty$.

$$m_1(t) = B_{11} + B_{12}t + B_{13}e^{-(k_{12}+k_{21})t}$$

$$m_2(t) = B_{21} + B_{22}t + B_{23}e^{-(k_{12}+k_{21})t}$$

Clearly $m_1(t)$ and $m_2(t)$ increase with t, thus the response to a bounded input is unbounded.

Oscillations

As indicated above, oscillations may be present in the solution of a compartmental model. These occur when the exponential λ_i is a complex number. For irreducible systems, a topological condition may exist in the system which will exclude the presence of oscillations.

Define a cycle of length k as a path for which the product $k_{i1,i2}k_{i2,i3} \cdots k_{ik-1,ik}k_{ik,i1}$ is nonzero. It can be shown that no oscillations are present in an arbitrary *n*-compartment model if there are no cycles of length greater than 2 are present in the model. This condition is obviously satisfied for the two compartment model. It is not satisfied, for example, in the model shown in Figure 4.4.3 since there is a cycle of length 4; $k_{12}k_{23}k_{34}k_{41} \neq 0$.

4.5   KINETIC PARAMETERS

In addition to the primary parameters of the compartmental model given in the past two sections, e.g. tracee masses, production rates into specific compartments, fluxes between compartments, and mean residence times, other kinetic parameters can be defined to characterize the system.

Total mass in the system

The **total mass** in the system equals the sum of the tracee masses in each individual compartment:

$$M_{\text{tot}} = \sum_{i=1}^{n} M_i \qquad (4.5.1)$$

Total equivalent distribution volume in the system

The **total equivalent distribution volume** in the system is equal to the volume the tracee occupies in the system assuming its concentration is uniform and equal to its value C_1 in accessible compartment 1:

$$V_{tot} = \frac{M_{tot}}{C_1} \qquad (4.5.2)$$

If more than one compartment is accessible, for example compartments 1 and 2, different definitions for the equivalent distribution volume can be given. As discussed in Chapter 3 for the two accessible pool noncompartmental model, the definition depends upon which concentration is considered as the reference concentration. The possibilities are:

$$V_{tot} = \frac{M_{tot}}{C_1 + C_2} \qquad V_{tot} = \frac{M_{tot}}{C_1} \qquad V_{tot} = \frac{M_{tot}}{C_2} \qquad (4.5.3)$$

Mean residence time in the system

Recalling the definition of the generic element θ_{ij} of the mean residence time matrix Θ as the average time a particle entering compartment j spends in compartment i before irreversibly leaving the system, the sum of the elements of one column of the Θ matrix, say column j, represents the **mean residence time** MRT_j (unit: time) spent in the whole system by one particle entering the system from compartment j:

$$MRT_j = \sum_{i=1}^{n} \theta_{ij} \qquad (4.5.4)$$

In order to evaluate the kinetic parameters of the compartmental model, it is first necessary to obtain a unique solution for the tracer model parameters, i.e. the rate constants k_{ij} and the volumes or masses of the accessible pool from the tracer data of a given input-output experiment. The a priori identifiability analysis to be discussed in Chapter 5 addresses this question. Once the tracer parameters are available, the tracee parameters, i.e. tracee masses and productions, can be evaluated. This is the subject of Chapter 6. The tracer and tracee kinetic parameters provide a detailed, quantitative description of the system, both for the accessible and nonaccessible pools. Most parameters are unique to the compartmental model approach, for instance masses in individual compartments, production rates, intercompartmental fluxes. Others have already been defined in the noncompartmental model formulas, for instance mass, volume and residence time in the accessible compartment and in the system. Additional accessible pool parameters defined in the noncompartmental model approach such as clearance rate, rate of appearance and disappearance, can also be defined and calculated from the compartmental model of the system by using the relationships given in Chapter 3. However, since the interest in these parameters is rather limited if the more detailed kinetic information from the compartmental model of the system is available, they are not included in this section.

Some comments will be given in Chapter 7 where compartmental and noncompartmental approaches will be compared.

4.6 CATENARY AND MAMILLARY MODELS

Catenary and mammillary models are two classes of compartmental models which are frequently used to interpret tracer kinetic data.

Catenary models are compartment models made up of a chain of compartments with each, except the first and last, exchanging bidirectionally with the two adjacent compartments. If the compartment numbers in the chain are sequential from 1 to n, then the rate constants k_{ij} have the following properties:

$$k_{i,i+1} \neq 0 \quad i = 1, \cdots, n-1 \tag{4.6.1}$$

$$k_{i+1,i} \neq 0 \quad i = 1, \cdots, n-1 \tag{4.6.2}$$

$$k_{ij} = 0 \quad j \neq i \pm 1; \; i \neq 0 \tag{4.6.3}$$

The general catenary structure in which the compartments are numbered sequentially is shown in Figure 4.6.1.
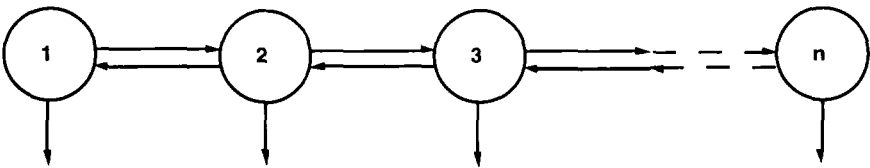
Figure 4.6.1. The n compartment catenary model.

Mammillary models are compartmental models where there is a central compartment which exchanges with the all of the other compartments; there is no exchange between these other compartments. If the numbering of the compartments is as illustrated in Figure 4.6.2, then the rate constants k_{ij} have the following properties:

$$k_{1i} \neq 0 \quad i = 2, \cdots, n \tag{4.6.4}$$

$$k_{i1} \neq 0 \quad i = 2, \cdots, n \tag{4.6.5}$$

$$k_{ij} = 0 \quad i = 2, \cdots, n \quad j = 2, \cdots, n \tag{4.6.6}$$
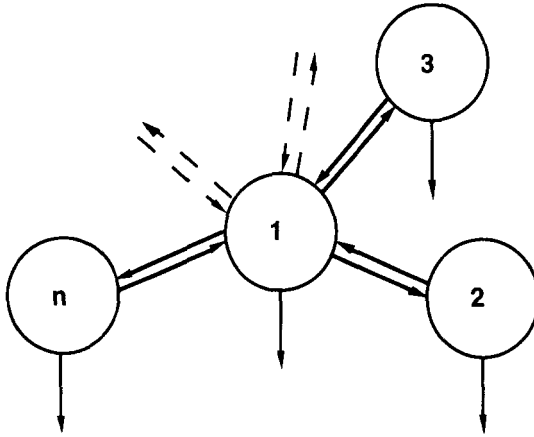
Figure 4.6.2.   The general n compartment mammillary model.

For both the catenary and mammillary model, irreversible losses to the environment are allowed, i.e. $k_{0i} \neq 0$ for some i.

The compartmental $\mathbf{K}$ matrix has the following form for the catenary and mammillary model respectively.

$$\mathbf{K} = \begin{pmatrix} -k_{11} & k_{12} & 0 & \cdots & 0 \\ k_{21} & -k_{22} & k_{23} & \cdots & 0 \\ \vdots & \vdots & \vdots & \vdots & \vdots \\ 0 & 0 & \cdots & k_{n-1,n} & -k_{nn} \end{pmatrix} \qquad (4.6.7)$$

and

$$\mathbf{K} = \begin{pmatrix} -k_{11} & k_{12} & k_{13} & \cdots & k_{1n} \\ k_{21} & -k_{22} & 0 & \cdots & 0 \\ k_{31} & 0 & -k_{33} & \cdots & 0 \\ \vdots & \vdots & \vdots & \vdots & \vdots \\ k_{n1} & 0 & \cdots & 0 & -k_{nn} \end{pmatrix} \qquad (4.6.8)$$

In both cases, $\mathbf{K}$ is irreducible and invertible assuming there is a nonzero loss from at least one compartment, i.e. $k_{0i} \neq 0$ for some i. Under this condition, catenary and mammillary systems are stable. In addition, all λ_i are positive real numbers since both classes of models contain cycles of length 2 or less.

References

Anderson D.H.: Structural properties of compartmental models. *Math. Biosci. 58*:61–81, 1982.

Covell D.G., Herman M., Delisi C.: Mean residence time-theoretical development, experimental determination, and practical use in tracer analysis. *Math. Biosci. 72*:213–244, 1984.

Eisenfeld J.: Relationship between stochastic and differential models of compartmental systems. *Math. Biosci. 43*:289–305, 1979.

Eisenfeld J.: On mean residence times in compartments. *Math. Biosci. 57*:265–278, 1981.

Hearon J.Z.: Theorems on linear systems. *Ann. N. Y. Acad. Sci. 108:*36–78, 1963.

Matis J.H., Wehrly T.E., Metzler C.M.: On some stochastic formulations and related statistical moments of pharmacokinetic models. *J. Pharmacokinet. Biopharm. 11:*77–92, 1983.

This page intentionally left blank.

Chapter 5

IDENTIFIABILITY OF THE TRACER MODEL

5.1   INTRODUCTION

In this Chapter, it will be assumed that a compartmental model structure has been postulated to describe a set of tracer data, i.e. the number of compartments and the connections among them have been specified. This structure reflects known information and assumptions about the system under study. That is, there may be a priori knowledge about the system which can be incorporated in the structure. As described in Chapter 1, one can arrive at a structure by testing via simulation what is needed to fit the data. The result at this stage is a "pencil and paper" model which has as unknowns the rate constants k_{ij} associated with the connections and, assuming a pool is accessible for measurement, either a volume V or a mass M of that pool depending upon whether a radioisotope or stable isotope tracer is used.

Before performing the experiment to collect tracer data to be analyzed using the model or, if the experiment is already completed, before using the model to estimate the unknown parameters from the data, the following questions arises: does the tracer data contain enough information to estimate all of the unknown parameters of the postulated model structure? This question is usually referred to as the **a priori identifiability** problem [Cobelli and DiStefano, 1980; Carson et al., 1983]. It is set in the ideal context of an error-free model structure and noise-free, continuous time measurements, and is an obvious prerequisite for parameter estimation from real data. In particular, if it turns out in such an ideal context that the postulated model structure is too complex for the particular set of ideal tracer data, i.e. some model parameters are not identifiable from the data, there is no way in a real situation

where there is error in the model structure and noise in the data that the parameters can be identified. The a priori identifiability problem is also referred to as the structural identifiability problem because it is set independently of a particular set of values for the parameters. For the sake of simplicity, in what follows, only the words a priori will be used to qualify the problem.

The solution of the identifiability problem in general is a difficult one because it involves the solution of a system of nonlinear algebraic equations which increases in number of terms and nonlinearity degree with the model order, i.e. the number of compartments in the model. These equations become difficult to solve even for compartmental models of relatively few compartments, e.g. 4 or 5. No general solution is available except for the one, two, some three compartment models, and certain catenary and mammillary models. To test a priori identifiability of linear compartmental models of general structure, one can take advantage of methods of computer algebra; this will be illustrated later in this Chapter.

Before discussing the problem in depth and the methods available for its solution, it is useful to illustrate the fundamentals through some simple examples. Then the definitions using these simple examples where the identifiability issue can be addressed can be discussed.

5.2   SOME EXAMPLES

Example 1

Consider a single compartment tracer model shown below in Figure 5.2.1 where the input is a bolus injection of a radioactive tracer given at time zero, and the measured variable is the tracer concentration.

As seen previously in this case, the model and measurement equations are

$$\frac{dm(t)}{dt} = -km(t) \qquad m(0) = d \qquad (5.2.1)$$

$$c(t) = \frac{m(t)}{V} \qquad (5.2.2)$$

The unknown parameters for the model are the rate constant k and the volume V.

Equation (5.2.2) defines the observation on the system, i.e. tracer concentration, in an ideal context of noise-free and continuous-time measurements. In other words, (5.2.2) is the model output describing what is measured continuously and without errors; it is not measurements only at discrete times. The word "output" is used here in the information sense. Specifically, in the context of Figure 5.2.1, $u(t)$ and $c(t)$ define an
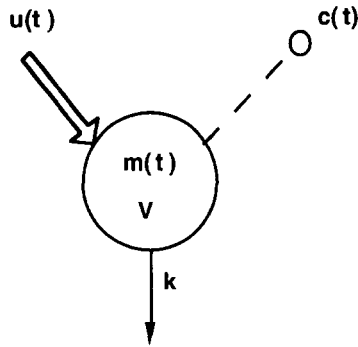
Figure 5.2.1. A single compartment tracer model. The tracer input $u(t)$ is a bolus injection of dose d given at time zero. The pool is characterized by a volume V and tracer mass $m(t)$; the measured variable is the tracer concentration $c(t)$.

input-output experiment, and should not be confused with the material output or outflow from the compartment.

To see how the experiment can be used to obtain estimates of these parameters, note the solution of (5.2.1) is the monoexponential

$$m(t) = de^{-kt} \tag{5.2.3}$$

The model output $c(t)$ can thus be given by

$$c(t) = \frac{d}{V}e^{-kt} \equiv Ae^{-\lambda t} \tag{5.2.4}$$

The model output or ideal data are thus described by a function of the form $Ae^{-\lambda t}$, and the parameters that are determinable by the experiment are A and λ. These parameters are called the observational parameters.

What is the relationship between the unknown model parameters k and V, and the observational parameters A and λ? From (5.2.4) one sees immediately:

$$A = c(0) = \frac{d}{V} \tag{5.2.5}$$

$$\lambda = k \tag{5.2.6}$$

where $c(0)$ represents an extrapolation of the data to time zero.

What happens if instead of a radioisotope tracer a bolus injection of a stable isotope tracer is injected? By expressing the model output in

terms of the tracer to tracee ratio

$$z(t) = \frac{m(t)}{M} \tag{5.2.7}$$

on sees immediately that the above logic can be followed using M instead of V.

In the example above, the unknown parameters k and V (or M) of the model are a priori uniquely or globally identifiable from the designed experiment since they can be evaluated uniquely from the observational parameter A and λ. Since all model parameters are uniquely identifiable, the model is said to be a priori uniquely or globally identifiable from the designed experiment.

This first example was limited to a bolus injection of tracer. The same identifiability results hold for different inputs as well. This is a general result of dealing with linear, time-invariant models such as those describing tracer kinetics in the steady state: the identifiability properties of a model are the same irrespective of the shape of the inputs. This is true for a single input situation, or if there are multiple inputs with different tracers administered simultaneously. The result is no longer true in a multiple input experiment with the same tracer being administered simultaneously.

In the remaining examples, because of the above observation on the identifiability properties of linear, time-invariant systems, only the bolus injection will be considered.

Example 2

Consider next the two compartment tracer model shown in Figure 5.2.2 where a bolus injection of stable isotope tracer is given into compartment 1. The accessible compartment is compartment 2. Assume the measured variable is the tracer to tracee ratio, $z_2(t)$.

The equations describing this model assuming a bolus input are:

$$\frac{dm_1(t)}{dt} = -k_{21}m_1(t) \qquad m_1(0) = d \tag{5.2.8}$$

$$\frac{dm_2(t)}{dt} = k_{21}m_1(t) - k_{02}m_2(t) \qquad m_2(0) = 0 \tag{5.2.9}$$

$$z_2(t) = \frac{m_2(t)}{M_2} \tag{5.2.10}$$

Figure 5.2.2. A two compartment model in which a dose d of a stable isotope tracer is injected into compartment 1 and measurement is in compartment 2. See text for additional explanation.

The unknown model parameters are k_{21}, k_{02} and M_2. To see how the experiment can be used to obtain estimates of these parameters one notes that the solution of (5.2.9) is the following sum of two exponentials:

$$m_2(t) = \frac{d \cdot k_{21}}{(k_{21} - k_{02})}(e^{-k_{21}t} - e^{-k_{02}t}) \qquad (5.2.11)$$

whence the model output or ideal data $z_2(t)$ are given by

$$z_2(t) = \frac{d \cdot k_{21}}{M_2(k_{21} - k_{02})}(e^{-k_{21}t} - e^{-k_{02}t}) \equiv A(e^{-\lambda_1 t} - e^{-\lambda_2 t}) \qquad (5.2.12)$$

where A, λ_1 and λ_2 are the observational parameters.

It is easy to see that k_{21} and k_{02} play an interchangeable role in (5.2.12); in fact, (5.2.12) can rewritten

$$z_2(t) = \frac{d \cdot k_{21}}{M_2(k_{02} - k_{21})}(e^{-k_{02}t} - e^{-k_{21}t}) \equiv A(e^{-\lambda_1 t} - e^{-\lambda_2 t}) \qquad (5.2.13)$$

Notice in (5.2.12) and (5.2.13) that the same sum of exponentials $A(e^{-\lambda_1 t} - e^{-\lambda_2 t})$ describes the data. Thus the link between A, λ_1, and λ_2 and the unknown model parameters k_{21}, k_{02} and M_2 is not unique and two sets of relationships can be formulated:

$$A = \frac{d \cdot k_{21}}{M_2(k_{21} - k_{02})} \qquad \lambda_1 = k_{21} \qquad \lambda_2 = k_{02} \qquad (5.2.14)$$

or

$$A = \frac{d \cdot k_{21}}{M_2(k_{02} - k_{21})} \qquad \lambda_1 = k_{02} \qquad \lambda_2 = k_{21} \qquad (5.2.15)$$

This results in two symmetric solutions for k_{21} and k_{02}; as a consequence, M_2 has two solutions.

If a radioisotope tracer experiment is considered, since the model output would be

$$c_2(t) = \frac{m_2(t)}{V_2} \qquad (5.2.16)$$

one sees immediately that the above derivation remains valid with V_2 replacing M_2.

As discussed here and illustrated by the specific example above, the unknown parameters k_{21}, k_{02} and M_2 (or V_2) of the tracer model cannot be uniquely evaluated from the observational parameters A, λ_1 and λ_2 of the designed experiment. Two solutions are obtained, say k_{21}^I, k_{02}^I and M_2^I (or V_2^I) and k_{21}^{II}, k_{02}^{II} and M_2^{II} (or V_2^{II}) which provide the *same* expression for the model output $z_2(t)$ or $c_2(t)$. When there is a finite number of solutions (more than one; two in this case), the unknown parameters are said to be a priori nonuniquely identifiable or locally identifiable from the designed experiment. When all the model parameters are identifiable (uniquely or nonuniquely) and there is at least one of the model parameters which is nonuniquely identifiable (in this case, all three are), the model is said to be a priori nonuniquely or locally identifiable.

It is worth noting that in this case there are parameters which are a priori uniquely identifiable, but these are not the original parameters of interest. They are combinations of the original parameters. In this particular case, since k_{21} and k_{02} have each two symmetric solutions, their product, $k_{21}k_{02}$, and their sum, $k_{21} + k_{02}$, are uniquely identifiable. In addition, from (5.2.15) and (5.2.16) it is clear that the other uniquely identifiable parameter is $\frac{k_{21}}{M_2}$ (or $\frac{k_{21}}{V_2}$). Thus for the example considered here, the uniquely identifiable parameterization is $k_{21}k_{02}$, $k_{21} + k_{02}$ and $\frac{k_{21}}{M_2}$ (or $\frac{k_{21}}{V_2}$).

To achieve unique identifiability of a nonuniquely identifiable model, additional independent information about the system is necessary. In this particular case, knowledge of M_2 (or V_2), or a qualitative relationship between k_{21} and k_{02}, i.e. k_{21} greater or less than k_{02} (see Figure 5.2.3), allows one to achieve unique identifiability of all model parameters.
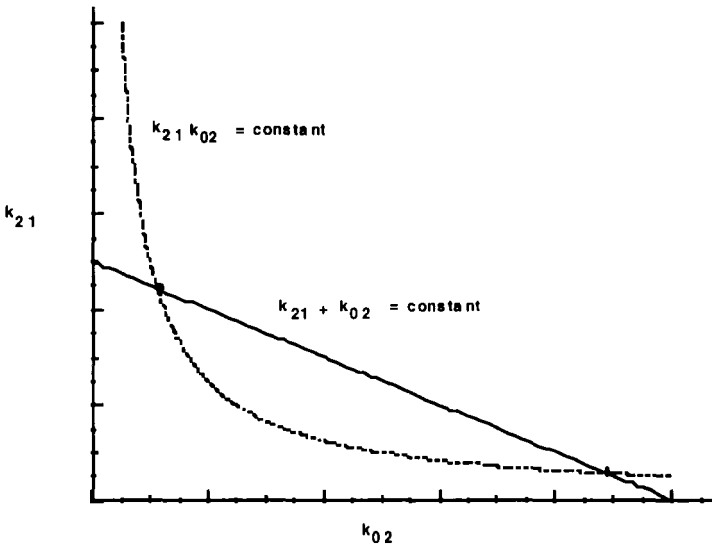
Figure 5.2.3.   A plot of $k_{21}k_{02}$ = constant and $k_{21} + k_{02}$ = constant. The two points where the curves intersect represent the two solutions for k_{21} and k_{02}. See text for additional information.

Example 3

Consider next the two compartment tracer model shown in Figure 5.2.4 where a bolus injection of radioactive tracer is given at time zero and where the measured variable is tracer concentration.

The equations describing this model are

$$\frac{dm_1(t)}{dt} = -(k_{01} + k_{21})m_1(t) \qquad m_1(0) = d \qquad (5.2.17)$$

$$\frac{dm_2(t)}{dt} = k_{21}m_1(t) \qquad m_2(0) = 0 \qquad (5.2.18)$$

$$c_1(t) = \frac{m_1(t)}{V_1} \qquad (5.2.19)$$

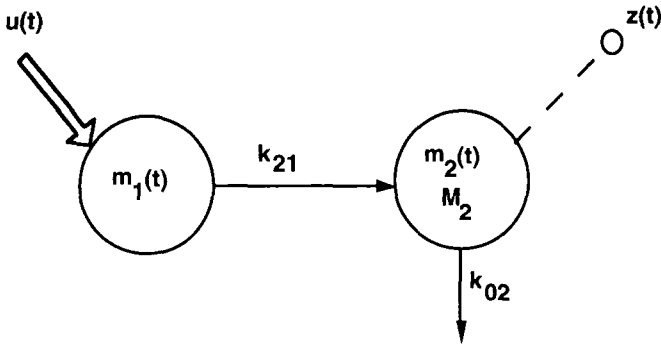The unknown model parameters are k_{21}, k_{01} and V_1.
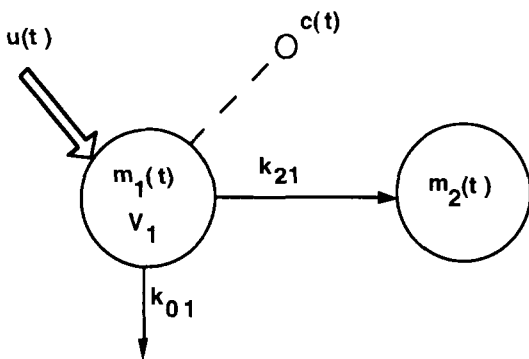
Figure 5.2.4. A two compartment model in which a dose d of radioactive tracer is injected into compartment 1 and measurement is in compartment 1. An irreversible loss occurs from compartment 1 together with an irreversible loss to compartment 2.

To see how the experiment can be used to obtain estimates of these parameters, one notes that the solution of (5.2.17) is

$$m_1(t) = de^{-(k_{01}+k_{21})t} \tag{5.2.20}$$

whence the model output or ideal data $c_1(t)$ are given by

$$c_1(t) = \frac{d}{V_1}e^{-(k_{01}+k_{21})t} \equiv Ae^{-\lambda t} \tag{5.2.21}$$

The model output or ideal data are thus be described by the monoexponential function $Ae^{-\lambda t}$. One can now see immediately the relationship between the unknown model parameters k_{21}, k_{01} and V_1 and the observational parameters of the experiment A and λ:

$$A = \frac{d}{V_1} \tag{5.2.22}$$

$$\lambda = k_{01} + k_{21} \tag{5.2.23}$$

It is easy in this situation to see that while V_1 is uniquely identifiable, k_{01} and k_{21} are not. In fact, as illustrated in Figure 5.2.5, there are an infinite number of solutions lying on the straight line $\lambda = k_{01} + k_{21}$.

When there is an infinite number of solutions for a parameter, one says the parameter is a priori nonidentifiable from the designed experiment. When there is at least one of the model parameters which is
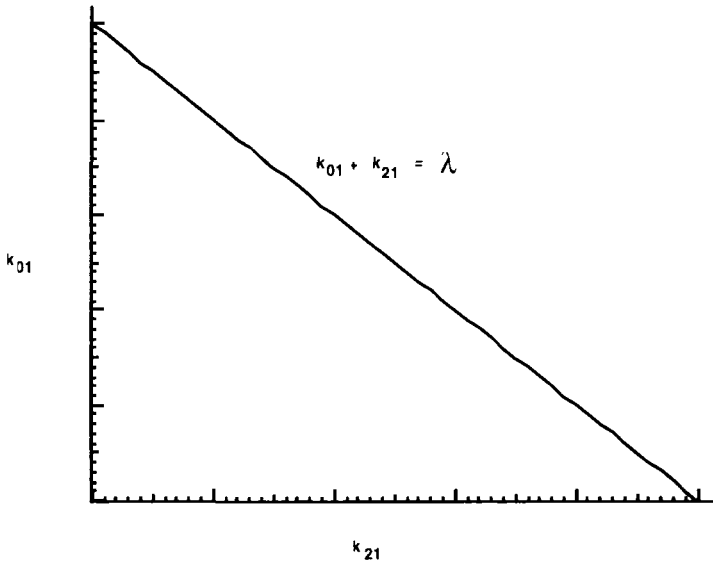
Figure 5.2.5. A plot of $k_{21} + k_{01} = \lambda$. Any point lying on this line will satisfy (5.2.23), and represents a solution for k_{21} and k_{01}. See text for additional information.

nonidentifiable (in this case, there are two), the model is said to be a priori nonidentifiable.

As with the previous example, one can find a uniquely identifiable parameterization, i.e. a set of parameters that can be evaluated uniquely. In this case, the parameter is the sum $k_{01} + k_{12}$ (V_1 has been seen to be uniquely identifiable). Again to achieve unique identifiability of k_{01} and k_{21}, additional information on the system such as a relationship between k_{01} and k_{21} is required.

When a compartmental model is nonidentifiable, however, it is possible to obtain for the nonidentifiable parameters upper and lower bounds for their values, i.e. to identify an interval of values where the parameters may lie. The reasoning is the following. Since by definition k_{01} and k_{21} are greater than zero, one sees immediately from (5.2.23) that the upper bound for each is λ. For instance, for k_{21}, one has

$$k_{21} = \lambda - k_{01} \tag{5.2.24}$$

and thus the upper bound for k_{21}, λ, will be achieved when k_{01} is zero. Similar results hold for k_{01}. The parameter bounds for k_{01} and k_{21} are

$$k_{01}^{\min} = 0 \le k_{01} \le \lambda = k_{01}^{\max} \tag{5.2.25}$$

$$k_{21}^{\min} = 0 \le k_{21} \le \lambda = k_{21}^{\max} \tag{5.2.26}$$

In this example, the intervals are the same; normally, this is not the case.

When there is an upper and lower bound for the values that a non-identifiable parameter can assume, one says the parameter is a priori interval identifiable. When all of the nonidentifiable model parameters are interval identifiable (in this case, all are), the model is said to be a priori interval identifiable.

As with the previous two examples, this discussion holds also for stable isotope tracers by expressing the model output in terms of the tracer to tracee ratio, and by replacing V_1 by M_1.

5.3   DEFINITIONS

The simple examples of the previous section emphasized the importance of understanding the a priori identifiability problem, and provided a means to introduce in an appropriate context some basic definitions [Audoly et al., 1998]. In this section, the definitions will be generalized to the n-compartment model discussed in §4.3.4. It should be noted, however, that the definitions hold for more general model structures such as the nonlinear dynamic models discussed in Cobelli and DiStefano [1980] and Carson et al. [1983]. Both the radioactive and stable isotope tracer models can be written

$$\dot{\mathbf{m}}(\mathbf{p}, t) = \mathbf{K}(\mathbf{p})\mathbf{m}(\mathbf{p}, t) + \mathbf{u}(t) \qquad \mathbf{m}(\mathbf{p}, 0) = 0 \tag{5.3.1}$$

$$\mathbf{y}(\mathbf{p}, t) = \mathbf{V}(\mathbf{p})\mathbf{m}(\mathbf{p}, t) \tag{5.3.2}$$

$$\mathbf{y}(\mathbf{p}, t) = \mathbf{D}(\mathbf{p})\mathbf{m}(\mathbf{p}, t)$$

where the equations in (5.3.2) are the measurement equations for the radioactive and stable isotope models respectively, $\mathbf{p} = [p_1, \cdots, p_p]$ denotes the unknown parameters, i.e. the transfer rate parameters k_{ij}, the volumes V_i or the masses M_i of the accessible pools, and the matrices $\mathbf{K}$, $\mathbf{V}$ and $\mathbf{D}$ are functions of $\mathbf{p}$. The vector $\mathbf{p}$ belongs to the compartmental parameter space $\mathcal{P}$, i.e. the real subspace of the complex space C which satisfies the constraints $k_{ij} \ge 0, V_i \ge 0, M_i \ge 0$, and $k_{ii} = -\sum_{\substack{j=0 \\ j \ne i}}^{n} k_{ij} \le 0, i = 1, \cdots, n$.

Define as ϕ_i, $i = 1, \cdots, R$ the **observational parameter** and as $\mathbf{\Phi} = [\phi_1, \ldots, \phi_R]$ the observational parameter vector. Each particular input-output experiment will provide a particular value $\hat{\mathbf{\Phi}}$ of the parameter vector $\mathbf{\Phi}$, i.e. the components of $\hat{\mathbf{\Phi}}$ can be estimated uniquely from the data by definition. Further, the observational parameters ϕ_i are functions of the basic model parameters p_i which may or may not be identifiable:

$$\mathbf{\Phi} = \mathbf{\Phi}(\mathbf{p}) \qquad (5.3.3)$$

To state the identifiability problem of the basic model parameters p_i, it is convenient to consider the model output $\mathbf{y}(t)$ as a function of time and the observational parameter vector $\mathbf{\Phi}$:

$$\mathbf{y}(t) = \mathbf{y}(\mathbf{\Phi}(\mathbf{p}), t) \qquad (5.3.4)$$

The definitions are given first for a single parameter of the model, and then for the model.

Definitions

For the input class U the single parameter p_i is **a priori**
• **uniquely** or **globally identifiable** if and only if for almost any $\hat{\mathbf{\Phi}} \in \mathcal{R}$ (the real space) the equations

$$\mathbf{y}(\mathbf{\Phi}(\mathbf{p}), t) = \mathbf{y}(\hat{\mathbf{\Phi}}, t) \qquad (5.3.5)$$

have one and only one solution for p_i belonging to C,
• **nonuniquely** or **locally identifiable** if and only if for almost any $\hat{\mathbf{\Phi}} \in \mathcal{R}$ the system of equations (5.3.5) has for p_i more than one but a finite number of solutions in C;
• **nonidentifiable** if and only if for almost any $\hat{\mathbf{\Phi}} \in \mathcal{R}$ the system of equations (5.3.5) has for p_i infinite solutions in C; and
• **interval identifiable** if it is nonidentifiable and has a finite upper and lower bounds that can be calculated from the system of equations (in this case, the parameter interval is defined by the difference between its upper and lower bound).
The model is **a priori**
• **uniquely** or **globally identifiable** if all of its parameters are uniquely identifiable;
• **nonuniquely** or **locally identifiable** if all of its parameters are identifiable, either uniquely or nonuniquely, and at least one is nonuniquely identifiable;
• **nonidentifiable** if at least one of its parameters is nonidentifiable; and

• **interval identifiable** if all its nonidentifiable parameters are interval identifiable.

Thus to investigate the a priori identifiability of model parameters p_i, it is necessary to solve the system of nonlinear algebraic equations in the unknown p_i obtained by setting the polynomials $\mathbf{\Phi}(\mathbf{p})$ equal to the observational parameter vector $\hat{\mathbf{\Phi}}$:

$$\mathbf{\Phi}(\mathbf{p}) = \hat{\mathbf{\Phi}} \qquad (5.3.6)$$

In what follows, these equations will be called the **exhaustive summary** of the model.

Examples have already been provided in §5.2. They are given for the three examples by (5.2.5) and (5.2.6), (5.2.14) and (5.2.15), and (5.2.22) and (5.2.23) respectively.

An additional problem is that the solutions of the set of nonlinear algebraic equations with real coefficients (5.3.6) are in the whole complex space C. Since one is interested only in the solutions belonging to the cornpartmental space $\mathcal{P}$, i.e. real and positive, and not complex or real negative ones, the results on the uniqueness of model solution has to be extended from the complex space to its real and positive subspace $\mathcal{P}$ satisfying the compartmental constraints. This problem can be solved for the global identifiability and nonidentifiability cases but it is an issue for the local identifiability case. Some comments on how to deal with this case will be given in §5.9.5.

5.4   THE TWO COMPARTMENT MODEL

5.4.1   Introduction

The examples of §5.2 introduced the basic ingredients of the a priori identifiability problem. In particular, they dealt with single input-single output tracer experiments only. Against the background provided by §5.2, one can proceed to more complex compartmental models and input-output experiments which will permit a better appreciation of the interplay between the known observational parameters and the desired unknown model parameters.

The general two compartment model with various single or multiple input, single or multiple output tracer experiments serves the purpose. For sake of space only, the radioactive isotope tracer experiment will be described in detail; the extension to the stable isotope tracer experiment is straightforward (see §5.2.1) by expressing the model outputs as the tracer to tracee ratio and by substituting the masses of the accessible pools for the volumes.

5.4.2   Input into a Single Compartment

Tracer input into compartment 1

Consider the general two compartment model shown below in Figure 5.4.1.
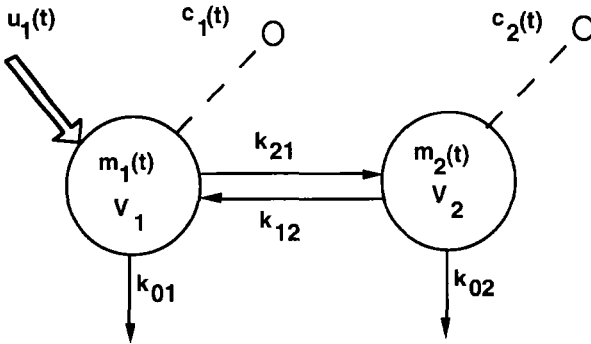
Figure 5.4.1.   A two compartment model where input is into compartment 1. Compartment 1 exchanges with a second compartment, compartment 2. Irreversible loss can occur from both compartments. See text for additional explanation.

Assume that tracer input is into compartment 1 (the case where the input is into compartment 2 is dealt with later in this section) and that the tracer input is a bolus injection. The model equations are

$$\frac{dm_1(t)}{dt} = -(k_{01} + k_{21})m_1(t) + k_{12}m_2(t) \qquad m_1(0) = d_1 \qquad (5.4.1)$$

$$\frac{dm_2(t)}{dt} = k_{21}m_1(t) - (k_{02} + k_{12})m_2(t) \qquad m_2(0) = 0 \qquad (5.4.2)$$

Measurement in compartments 1 and 2

Assume that the measured variables are the tracer concentrations in compartments 1 and 2. The model outputs, or ideal data, are described respectively by

$$c_1(t) = \frac{m_1(t)}{V_1} \qquad (5.4.3)$$

$$c_2(t) = \frac{m_2(t)}{V_2} \tag{5.4.4}$$

The unknown parameters are the rate constants k_{01}, k_{02}, k_{21}, k_{12}, and the volumes V_1 and V_2.

The solution of the system of differential equations (5.4.1) and (5.4.2) for $m_1(t)$ and $m_2(t)$ are biexponential functions (an extension of the single compartment, single exponential case of Example 1 in §5.2) whence the model outputs are given by

$$c_1(t) = A_1 e^{-\lambda_1 t} + A_2 e^{-\lambda_2 t} \tag{5.4.5}$$

$$c_2(t) = -A_3 e^{-\lambda_1 t} + A_3 e^{-\lambda_2 t} \tag{5.4.6}$$

where A_1, A_2, A_3, λ_1 and λ_2 are the observational parameters. They are assumed to be positive with $\lambda_1 > \lambda_2$. Note that $c_1(0) = A_1 + A_2$ while $c_2(0) = 0$.

The functions $c_1(t)$ and $c_2(t)$ provide a description of the ideal tracer data; an example is given in Figure 5.4.2.

Time
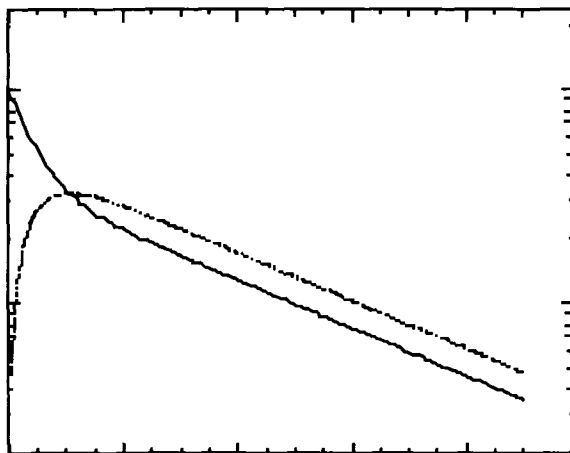
Figure 5.4.2. An example of $c_1(t)$ and $c_2(t)$ when a bolus injection of tracer is introduced into compartment 1, and measurements are taken from compartments 1 and 2. See text for additional explanation.

How are the observational parameters related to the unknown model parameters? In contrast with the situation encountered in Examples 1, 2 and 3 of §5.2, the relation among the observational and the model parameters, i.e. the exhaustive summary, cannot be written in a straightforward manner. One needs to have the analytical expression for $c_1(t)$ and $c_2(t)$ as functions of the model parameters. While this was not difficult to obtain in the single compartment examples of §5.2, it is more difficult here since there is the need to solve a system of two differential equations, (5.4.1) and (5.4.2). If one does this, the exhaustive summary can then be obtained as in the previous examples by equating the observational parameters A_1, A_2, A_3, λ_1 and λ_2 of (5.4.5) and (5.4.6) to their counterparts of the analytical model solutions for $c_1(t)$ and $c_2(t)$ which are functions of the unknown parameters. These equations must then be solved for the unknown model parameters $k_{01}, k_{02}, k_{21}, k_{12}, V_1$ and V_2.

An alternative way to obtain the exhaustive summary which does not require the solution of the system of differential equations and also provides them in a form more easy to handle is the two-step strategy described in Appendix E where all the details of the calculations are given. The exhaustive summary consists of five equations:

$$-A_1 V_1 \lambda_1 = k_{11} V_1 A_1 - k_{12} A_3 V_2 \tag{5.4.7}$$

$$-A_2 V_1 \lambda_2 = k_{11} V_1 A_2 + k_{12} A_3 V_2 \tag{5.4.8}$$

$$A_3 V_2 \lambda_1 = k_{21} A_1 V_1 - k_{22} A_3 V_2 \tag{5.4.9}$$

$$-A_3 V_2 \lambda_2 = k_{21} A_2 V_1 + k_{22} V_2 A_3 \tag{5.4.10}$$

$$d_1 = V_1 (A_1 + A_2) \tag{5.4.11}$$

where k_{11} and k_{22} are given by

$$k_{11} = -(k_{01} + k_{21}) \tag{5.4.12}$$

$$k_{22} = -(k_{12} + k_{02}) \tag{5.4.13}$$

The exhaustive summary can now be solved for the unknown model parameters. By summing (5.4.7) and (5.4.8), one has

$$k_{11} = -\frac{A_1 \lambda_1 + A_2 \lambda_2}{A_1 + A_2} \tag{5.4.14}$$

By subtracting (5.4.8) multiplied by A_1 from (5.4.7) multiplied by A_2 one obtains

$$k_{12} \frac{V_2}{V_1} = \frac{A_1 A_2 (\lambda_1 - \lambda_2)}{A_3 (A_1 + A_2)} \tag{5.4.15}$$

By summing (5.4.9) and (5.4.10), one has

$$k_{21} \frac{V_1}{V_2} = \frac{A_3(\lambda_1 - \lambda_2)}{A_1 + A_2} \qquad (5.4.16)$$

By subtracting (5.4.10) multiplied by A_1 from (5.4.9) multiplied by A_2, one has

$$k_{22} = -\frac{A_2\lambda_1 + A_1\lambda_2}{A_1 + A_2} \qquad (5.4.17)$$

Finally, from (5.4.11), one obtains

$$V_1 = \frac{d_1}{A_1 + A_2} \qquad (5.4.18)$$

Therefore, with a tracer input into compartment 1 and measurements taken in compartments 1 and 2, the model is a priori nonidentifiable since $k_{01}, k_{02}, k_{21}, k_{12}$ and V_2 are nonidentifiable. Only parameter V_1 is uniquely identifiable. The uniquely identifiable parameters are $k_{11}, k_{22}, V_1, k_{12}V_2$ and k_{21}/V_2. In addition, the product $k_{21}k_{12}$ is uniquely identifiable.

How do the various input-output configurations affect the identifiability properties of the model?

Measurement in Compartment 1 Only

In this situation, $c_1(t)$ (cf. (5.4.5)) is the model output, and the observational parameters are A_1, A_2, λ_1 and λ_2 are known while A_3 is unknown. The parameter V_1 is uniquely identifiable from (5.4.18). Next, from (5.4.14) and (5.4.17) it is possible to estimate k_{11} and k_{22} since A_1, A_2, λ_1 and λ_2 are known. As far as k_{12} and k_{21} are concerned, only their product $k_{21}k_{12}$ can be estimated since it is a function of A_1, A_2, λ_1 and λ_2:

$$k_{12}k_{21} = \frac{A_1A_2(\lambda_1 - \lambda_2)^2}{(A_1 + A_2)^2} \qquad (5.4.19)$$

Clearly the model is a priori nonidentifiable since the rate constants k_{01}, k_{02}, k_{21}, and k_{12} are nonidentifiable. The uniquely identifiable parameters are V_1, k_{11}, k_{22}, and $k_{21}k_{12}$

Parameter bounds. It is possible to obtain bounds for the four nonidentifiable parameters. They can be obtained from the observational parameters or from the uniquely identifiable parameters of the model. Suppose that k_{11}, k_{22} and $k_{21}k_{12}$ are known. In addition, since all rate constants k_{01}, k_{02}, k_{21} and k_{12} must be nonnegative,

$$-k_{11} \geq k_{21} \qquad (5.4.20)$$

$$-k_{22} \geq k_{12} \tag{5.4.21}$$

$$k_{21}k_{12} \geq 0 \tag{5.4.22}$$

A lower bound for k_{21} is easily found from

$$k_{21} = \frac{k_{21}k_{12}}{k_{12}} = \frac{k_{21}k_{12}}{-k_{22} - k_{02}} \geq \frac{k_{21}k_{12}}{-k_{22}} = k_{21}^{\min} \tag{5.4.23}$$

Thus by using (5.4.20) the parameter interval for k_{21} can be defined:

$$k_{21}^{\min} = \frac{k_{21}k_{12}}{-k_{22}} \leq k_{21} \leq -k_{11} = k_{21}^{\max} \tag{5.4.24}$$

Using the same logic, the parameter interval for k_{12} can be defined:

$$k_{12}^{\min} = \frac{k_{21}k_{12}}{-k_{11}} \leq k_{12} \leq -k_{22} = k_{12}^{\max} \tag{5.4.25}$$

Further, since

$$k_{01} = -k_{11} - k_{21} \tag{5.4.26}$$

one has the parameter interval for k_{01}:

$$k_{01}^{\min} = 0 \leq k_{01} \leq -k_{11} + \frac{k_{21}k_{12}}{k_{22}} = k_{01}^{\max} \tag{5.4.27}$$

Similarly for k_{02}:

$$k_{02}^{\min} = 0 \leq k_{02} \leq -k_{22} + \frac{k_{21}k_{12}}{k_{22}} = k_{02}^{\max} \tag{5.4.28}$$

Using equations (5.4.24), (5.4.25), (5.4.27) and (5.4.28), the parameter intervals can also be written in terms of the observational parameters; using (5.4.14)–(5.4.17), one has

$$k_{21}^{\min} = \frac{A_1 A_2 (\lambda_1 - \lambda_2)^2}{(A_1 + A_2)(A_1 \lambda_2 + A_2 \lambda_1)} \leq k_{21} \leq \frac{A_1 \lambda_1 + A_2 \lambda_2}{A_1 + A_2} = k_{21}^{\max} \tag{5.4.29}$$

$$k_{12}^{\min} = \frac{A_1 A_2 (\lambda_1 - \lambda_2)^2}{(A_1 + A_2)(A_1 \lambda_1 + A_2 \lambda_2)} \leq k_{12} \leq \frac{A_1 \lambda_2 + A_2 \lambda_1}{A_1 + A_2} = k_{12}^{\max} \tag{5.4.30}$$

$$k_{01}^{\min} = 0 \leq k_{01} \leq \frac{(A_1 + A_2)\lambda_1 \lambda_2}{A_1 \lambda_2 + A_2 \lambda_1} = k_{01}^{\max} \tag{5.4.31}$$

$$k_{02}^{\min} = 0 \leq k_{02} \leq \frac{(A_1 + A_2)\lambda_1 \lambda_2}{A_1 \lambda_1 + A_2 \lambda_2} = k_{02}^{\max} \tag{5.4.32}$$

Role of a priori knowledge. It is of interest to see what happens if one of the irreversible losses k_{01} or k_{02} is equal to zero. Suppose first that k_{02} is equal to zero. Since in this case k_{22} is equal to $-k_{12}$, it is clear that k_{12} is uniquely identifiable. From a knowledge of k_{12} and knowing the product $k_{21}k_{12}$ is uniquely identifiable, one can estimate k_{21}. Finally, since k_{11} is uniquely identifiable, with an estimate of k_{21}, an estimate of k_{01} can be obtained. Thus with the exception of V_2, all other tracer parameters can be estimated.

What happens if k_{01} is equal to zero? Since in this case $k_{11} = -k_{21}$, one can estimate k_{21} uniquely. Again since the product $k_{21}k_{12}$ is uniquely identifiable, one can estimate k_{12}, and as before, k_{02}. Thus once again, all tracer parameters except V_2 can be estimated.

Bound computation from submodels. The two models discussed above represent a situation where one of the irreversible loss parameters is set equal to its lower bound, zero. It is easy to verify that when $k_{02} = 0$, i.e. it reaches its lower bound, k_{12} equals its upper bound (since $k_{12} = -k_{22} - k_{12}$), k_{21} its lower bound (since $k_{21}k_{12}$ is known), and thus k_{01} its upper bound. Conversely, when $k_{01} = 0$, k_{12} equals its lower and k_{21} and k_{02} their upper bounds. In other words, upper and lower bounds k_{ij}^{min} and k_{ij}^{max} for the parameters of the nonindentifiable model can be generated from parameters k_{ij} of two submodels of the original structure (see Figure 5.4.3) obtained by first letting $k_{02} = 0$ and then $k_{01} = 0$.

Measurement in Compartment 2 Only

In this situation, $c_2(t)$ is the model output and thus only A_3, λ_1 and λ_2 are known. It is easy to see from (5.4.14)–(5.4.17) that the uniquely identifiable parameter combinations are

$$k_{11} + k_{22} = -(\lambda_1 + \lambda_2) \tag{5.4.33}$$

$$k_{11}k_{22} - k_{12}k_{21} = \lambda_1\lambda_2 \tag{5.4.34}$$

and

$$\frac{k_{21}}{V_2} = \frac{A_3(\lambda_1 - \lambda_2)}{d_1} \tag{5.4.35}$$

Clearly, the model is a priori nonidentifiable.

Parameter bounds. It is still possible to obtain bounds for the four nonidentifiable parameters. From (5.4.34), one has $k_{11}k_{22} > \lambda_1\lambda_2$. Coupling this with (5.4.33), one can calculate upper and lower bounds, k^{max} and k^{min} for k_{11} and k_{22}:
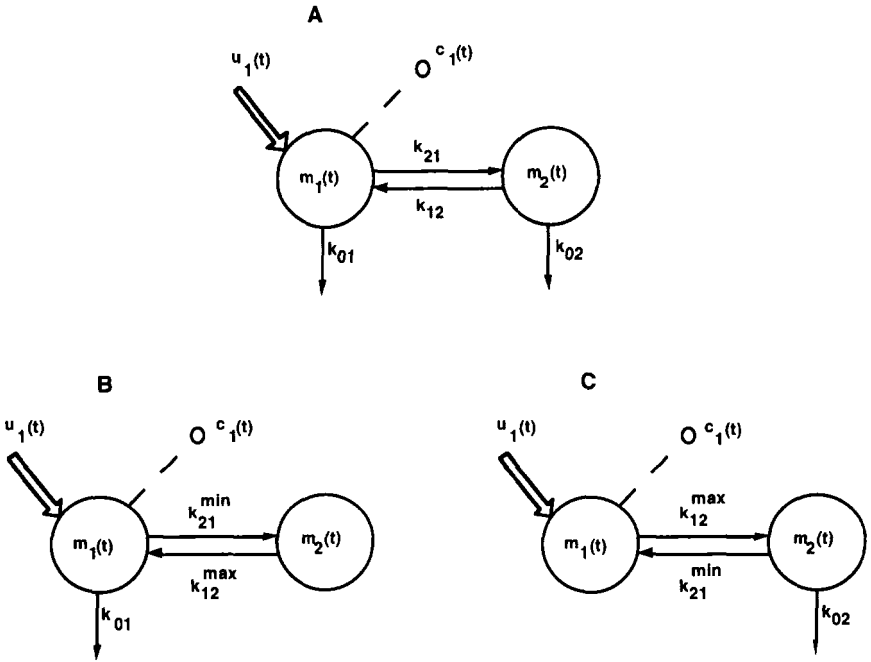
Figure 5.4.3. Panel A. The two compartment model where input and output are in compartment 1. Bounds for the parameters k_{ij} can be interpreted as parameters from the two submodels shown in Panels B and C. Panel B is the submodel where $k_{02} = 0$; Panel C the submodel where $k_{01} = 0$.

$$k^{\max} = \frac{-(\lambda_1 + \lambda_2) + \sqrt{(\lambda_1 + \lambda_2)^2 - 4\lambda_1\lambda_2}}{2} \qquad (5.4.36)$$

$$k^{\min} = \frac{-(\lambda_1 + \lambda_2) - \sqrt{(\lambda_1 + \lambda_2)^2 - 4\lambda_1\lambda_2}}{2} \qquad (5.4.37)$$

Since $k^{\min} \leq k_{11} \leq k^{\max}$ and $k^{\min} \leq k_{22} \leq k^{\max}$ where both $k^{\max}$ and $k^{\min}$ are negative, one can infer $-k^{\min}$ is an upper bound for the four k_{ij} parameters; zero is of course the lower bound. Finally, (5.4.35) provides the bounds for V_2. These are summarized below:

$$k_{01}^{\min} = 0 \leq k_{01} \leq -k^{\min} = k_{01}^{\max} \qquad (5.4.38)$$

$$k_{21}^{\min} = 0 \leq k_{21} \leq -k^{\min} = k_{21}^{\max} \qquad (5.4.39)$$

$$k_{12}^{\min} = 0 \leq k_{12} \leq -k^{\min} = k_{12}^{\max} \qquad (5.4.40)$$

$$k_{02}^{\min} = 0 \leq k_{02} \leq -k^{\min} = k_{02}^{\max} \qquad (5.4.41)$$

$$V_2^{\min} = 0 < V_2 \leq \frac{-k^{\min} d_1}{A_3(\lambda_1 - \lambda_2)} = V_2^{\max} \qquad (5.4.42)$$

Note finally that (5.4.35) excludes the possibility that k_{21} can equal zero since V_2 is different from zero.

Tracer input into compartment 2

In the preceding, only the situation where tracer is introduced into compartment 1 was considered. What happens if the tracer input is into compartment 2, and the parallel cases above are discussed: measurement in compartments 1 and 2, compartment 2 only, and compartment 1 only? Given the symmetry of the model, the solution is straightforward. However, it is useful for what follows in §5.4.3 to go through this case in some detail.

Measurements in Compartments 1 and 2

As before, write the model outputs as

$$c_1(t) = -A_3 e^{-\lambda_1 t} + A_3 e^{-\lambda_2 t} \qquad (5.4.43)$$

$$c_2(t) = A_1 e^{-\lambda_1 t} + A_2 e^{-\lambda_2 t} \qquad (5.4.44)$$

It is easy to see that the analogue of (5.4.14)–(5.4.18) is

$$k_{22} = -\frac{A_1 \lambda_1 + A_2 \lambda_2}{A_1 + A_2} \qquad (5.4.45)$$

$$k_{21}\frac{V_1}{V_2} = \frac{A_1 A_2 (\lambda_1 - \lambda_2)}{A_3 (A_1 + A_2)} \qquad (5.4.46)$$

$$k_{12}\frac{V_2}{V_1} = \frac{A_3 (\lambda_1 - \lambda_2)}{A_1 + A_2} \qquad (5.4.47)$$

$$k_{11} = -\frac{A_1 \lambda_2 + A_2 \lambda_1}{A_1 + A_2} \qquad (5.4.48)$$

$$V_2 = \frac{d_2}{A_1 + A_2} \qquad (5.4.49)$$

where d_2 is the tracer dose administered into compartment 2. It is of interest to note that the identifiability results for this measurement configuration are the same as those obtained for the case of tracer input into compartment 1 if one simply interchanges the suffixes 1 and 2 in

the transfer rate parameters and volumes. Clearly this also applies for other measurement configurations. For instance, if only compartment 2 is observed, V_2 is uniquely identifiable as are the parameter combinations k_{22}, k_{11} and $k_{21}k_{12}$; if only compartment 1 is observed, the combinations $k_{11} + k_{22}$, $k_{11}k_{22} - k_{12}k_{21}$ and $\frac{k_{12}}{V_1}$ are uniquely identifiable.

5.4.3 Input into Both Compartments

Consider again the general two compartment model where now there is tracer input into both compartment 1 and 2; this is illustrated below in Figure 5.4.4. Consider first the situation where two different tracers are administered simultaneously (see Remark for the case where the same tracer is administered). Assume as was done in §5.4.2 that the tracers are administered as a bolus.
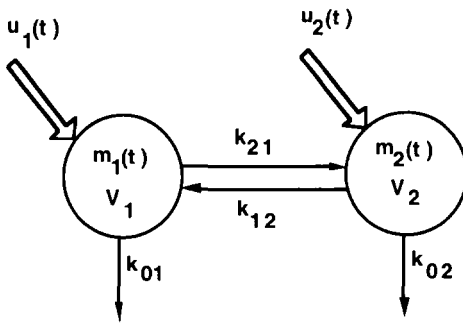
Figure 5.4.4. The general two compartment model where input is into both compartment 1 and 2. See text for additional explanation.

<u>Measurement in Compartment 1 or 2</u>

In this case, there are two model outputs. This situation can be discussed using the results of the previous section. First, with measurement of tracer concentration in compartment 1 following a bolus injection into compartment 1, from (5.4.5) the observational parameters are A_1, A_2, λ_1 and λ_2; thus from (5.4.14)-(5.4.18) one has uniquely V_1, k_{11}, k_{22} and the product $k_{21}k_{12}$. Second, with measurement of tracer concentration in compartment 1 resulting from the bolus injection into compartment 2 the observational parameters are A_3, λ_1 and λ_2 of (5.4.43); thus from (5.4.47) and (5.4.49), one has uniquely k_{12} since V_1 is known from above.

From the knowledge of k_{12} one has uniquely k_{21}, and from k_{11} and k_{22} one has uniquely k_{01} and k_{02} respectively. Hence all parameters except for V_2 are uniquely identifiable. It is essential to note that for each tracer injected, a separate set of A_i first for (5.4.5) and (5.4.6) and then for (5.4.43) and (5.4.44) will be found; the λ_1 and λ_2, however, are the same. Thus the A_3 available from measurements in compartment 1 following the injection into compartment 2 refers to (5.4.44) and not (5.4.6).

If instead of compartment 1, compartment 2 is observed (see (5.4.43) and (5.4.6)), by applying the same reasoning one has uniquely all the parameters except for V_1.

Measurement in Both Compartments 1 and 2

In this case, there are four model outputs corresponding to (5.4.5), (5.4.6), (5.4.43) and (5.4.44). It is easy to see that one needs only three of these in order to obtain unique identifiability of all parameters. In fact, from the previous result, one needs only V_2 or V_1 if measurements were taken in compartment 1 or 2 respectively. One can see that V_2 is uniquely identifiable from either of the two measurements of tracer concentration in compartment 2 due to tracer administered into compartment 2, (5.4.44). or 1, (5.4.46). The first case is straightforward from (5.4.49). For the second situation, (5.4.6), one notes that V_2 can be estimated from (5.4.35) since k_{21} is known.

By a similar reasoning, one can estimate V_1 from the measurement of tracer concentration in compartment 1 due to tracer administered into compartment 1, (5.4.5), or 2, (5.4.43).

A summary of the identifiability results of the two compartment model is given in Table 5.4.1. Given the symmetry of the model, the input-output configurations with the role of compartments 1 and 2 reversed are not given since the results can simply be obtained by reversing 1 and 2.

Remark on Simultaneous Tracer Administration

The above derivation is based on two different tracers being administered simultaneously into compartment 1 and 2. What happens if the same tracer is administered simultaneously into the two compartments? In this case, the measurements in compartments 1 and 2 cannot distinguish between the amount due to each injection; they measure the sum of the two contributions. It can be shown that in this situation, the input waveforms become important. Suppose for instance that the input waveform into compartments 1 and 2 are the same, e.g. bolus injections,

Input	Output	General Structure	Constraints	
			$k_{01} = 0$	$k_{02} = 0$
1	1	$V_1; k_{11} = -(k_{01} + k_{21}); k_{22} = -(k_{02} + k_{12}); k_{12}k_{21}$	$V_1; k_{21}; k_{12}; k_{02}$	$V_1; k_{21}; k_{12}; k_{01}$
1	2	$k_{11} + k_{22}; k_{11}k_{22} - k_{12}k_{21}; k_{21}/V_2$	$k_{22} - k_{21}; k_{21}k_{02}; k_{21}/V_2$	$k_{11} - k_{12}; k_{12}k_{01}; k_{21}/V_2$
1	1,2	$V_1; k_{11}; k_{22}; k_{21}/V_2; k_{12}V_2$	$V_1; V_2; k_{21}; k_{12}; k_{02}$	$V_1; V_2; k_{21}; k_{01}; k_{12}$
$1, 2^a$	1	$V_1; k_{21}; k_{01}; k_{12}; k_{02}$	$V_1; k_{21}; k_{12}; k_{02}$	$V_1; k_{21}; k_{01}; k_{12}$
$1, 2^a$	2	$V_2; k_{21}; k_{01}; k_{12}; k_{02}$	$V_2; k_{21}; k_{12}; k_{02}$	$V_2; k_{21}; k_{01}; k_{12}$
$1, 2^a$	1,2	$V_1; V_2; k_{21}; k_{12}; k_{01}; k_{02}$	$V_1; V_2; k_{21}; k_{12}; k_{02}$	$V_1; V_2; k_{21}; k_{01}; k_{12}$

[a] Different tracers are administered simultaneously

and measurements are taken in compartment 1. At variance with the case where the two tracer inputs were different, k_{22} and k_{11} are no longer uniquely identifiable; only their sum is. If on the other hand the input format is different, for example a bolus injection into compartment 1 and a constant infusion into compartment 2, one has the same identifiability properties as the case where the two tracers were different.

It is worth commenting on the situation where the same tracer is administered at different times; on one occasion, the bolus is administered into compartment 1 and on a second occasion it is administered into compartment 2. If one can assume that the parameters remain the same for both tracer administrations, there are again four model outputs and the same results obtained when two different tracers are administered simultaneously hold.

5.5   THE LAPLACE TRANSFORM METHOD: THE TWO COMPARTMENT MODEL REVISITED

5.5.1   Introduction

Up to this point, the focus has been on the identifiability properties of a model by inspecting the expression of the model output in order to derive the exhaustive summary, i.e. the relationships between the observational parameters and the unknown model parameters. The method is easy to understand since it does not require any particular mathematical skills other than some fundamentals of differential calculus. However, the approach is not practical in general since it works easily only for simple models like the one and the two compartment model. For the three compartment model, the method becomes quite cumbersome, and for more complex models its application is virtually impossible.

A simpler method is available to derive the exhaustive summary. It consists of writing the Laplace transform for the model output. This method is also known as the transfer function method. Fundamentals of the Laplace transform can be found in any textbook on applied mathematics. Briefly, the advantage of the Laplace transform method is that there is no need to use the analytical solution of the system of differential equations. By writing the Laplace transform of the state variables, e.g. masses, and then of the model outputs, e.g. concentrations, one obtains an expression which defines the observational parameters as a function of the unknown model parameters. This gives a set of nonlinear algebraic equations in the original parameters, i.e. the exhaustive summary.

5.5.2 Example of the Laplace Transform Method

To illustrate the Laplace transform method, consider the two compartment model shown in Figure 5.4.1 with a bolus injection into compartment 1 and the tracer concentrations in compartments 1 and 2 as the measured variables. The equations describing the system are (5.4.1)–(5.4.4).

The Laplace transforms of (5.4.1) and (5.4.2) are respectively

$$sL\{m_1\} - d_1 = -(k_{01} + k_{21})L\{m_1\} + k_{12}L\{m_2\} \qquad (5.5.1)$$

$$sL\{m_2\} = k_{21}L\{m_1\} - (k_{02} + k_{12})L\{m_2\} \qquad (5.5.2)$$

where L denotes the Laplace transform, and s is the Laplace variable.

Solving these algebraic equations for $L\{m_1\}$ and $L\{m_2\}$, one has

$$L\{m_1\} = \frac{d_1 s + k_{12} + k_{02}}{s^2 + (k_{12} + k_{21} + k_{01} + k_{02})s + k_{21}k_{02} + k_{12}k_{01} + k_{01}k_{02}}$$
$$(5.5.3)$$

$$L\{m_2\} = \frac{d_1 k_{21}}{s^2 + (k_{12} + k_{21} + k_{01} + k_{02})s + k_{21}k_{02} + k_{12}k_{01} + k_{01}k_{02}}$$
$$(5.5.4)$$

The Laplace transforms for the model outputs are

$$L\{c_1\} = \frac{(d_1 s + k_{12} + k_{02})/V_1}{s^2 + (k_{12} + k_{21} + k_{01} + k_{02})s + k_{21}k_{02} + k_{12}k_{01} + k_{01}k_{02}}$$
$$\equiv \frac{\beta_2 s + \beta_1}{s^2 + \alpha_2 s + \alpha_1} \qquad (5.5.5)$$

$$L\{c_2\} = \frac{d_1 k_{21}/V_2}{s^2 + (k_{12} + k_{21} + k_{01} + k_{02})s + k_{21}k_{02} + k_{12}k_{01} + k_{01}k_{02}}$$
$$\equiv \frac{\gamma_1}{s^2 + \alpha_2 s + \alpha_1} \qquad (5.5.6)$$

Due to the equivalence between the model outputs $c_1(t)$ and $c_2(t)$, and their Laplace transforms, the coefficients α_1, α_2, β_1, β_2 and γ_1 are the observational parameters since they are the parameters which are determinable from the input-output experiment. The exhaustive summary, by defining k_{11} and k_{22} from (5.4.12) and (5.4.13), is

$$k_{21}k_{02} + k_{12}k_{01} + k_{01}k_{02} = k_{11}k_{22} - k_{12}k_{21} = \alpha_1 \qquad (5.5.7)$$

$$k_{12} + k_{21} + k_{01} + k_{02} = -(k_{11} + k_{22}) = \alpha_2 \qquad (5.5.8)$$

$$\frac{k_{12} + k_{02}}{V_1} = -\frac{k_{22}}{V_1} = \beta_1 \qquad (5.5.9)$$

$$\frac{d_1}{V_1} = \beta_2 \qquad (5.5.10)$$

$$\frac{d_1 k_{21}}{V_2} = \gamma_1 \qquad (5.5.11)$$

The identifiability equations can now be solved for the unknown model parameters. One has:

$$V_1 = \frac{d_1}{\beta_2} \qquad (5.5.12)$$

$$k_{22} = -\beta_1 \cdot \frac{d_1}{\beta_2} \qquad (5.5.13)$$

$$k_{11} = -\alpha_2 + \beta_1 \cdot \frac{d_1}{\beta_2} \qquad (5.5.14)$$

$$k_{21} k_{12} = \beta_1 \frac{d_1}{\beta_2}(\alpha_2 - \beta_1 \frac{d_1}{\beta_2}) - \alpha_1 \qquad (5.5.15)$$

$$\frac{k_{21}}{V_2} = \frac{\gamma_1}{d_1} \qquad (5.5.16)$$

The exhaustive summary obtained using the Laplace transform method provides the same information as that obtained with the approach employed previously, i.e. (5.4.14)–(5.4.18). Thus the same conclusions on identifiability can be drawn.

If one applies the Laplace transform method to the three examples given in §5.2, one will clearly arrive at the same conclusions previously reached on a priori model identifiability. It is worth noting that the Laplace transform method gives for examples 1 and 3 of §5.2 the same exhaustive summary obtained in the time domain. In fact, one has for the model outputs of examples 1 and 3 respectively

$$L\{c\} = \frac{d/V}{s + k} \equiv \frac{\beta_1}{s + \alpha_1} \qquad (5.5.17)$$

$$L\{c_1\} = \frac{d/V_1}{s + k_{01} + k_{21}} \equiv \frac{\beta_1}{s + \alpha_1} \qquad (5.5.18)$$

By contrast for the model output of example 2, one has

$$L\{z_2\} = \frac{dk_{21}/M_2}{s^2 + (k_{02} + k_{12})s + k_{02}k_{12}} \equiv \frac{\beta_1}{s^2 + \alpha_2 s + \alpha_1} \qquad (5.5.19)$$

and thus the exhaustive summary is

$$k_{02}k_{12} = \alpha_1 \tag{5.5.20}$$

$$k_{02} + k_{12} = \alpha_2 \tag{5.5.21}$$

$$\frac{d_1 k_{12}}{M_2} = \beta_1 \tag{5.5.22}$$

It is easy to conclude from these equations that there are two solutions for k_{02}, k_{12} and M_2. This observation is somewhat more subtle to recognize in the time domain of (5.2.12)–(5.2.15) where the interchangeable role of k_{21} and k_{02} had to be noticed in the analytical expression for the model output (5.2.12).

5.6   THE DIFFICULTY OF THE IDENTIFIABILITY PROBLEM

The Laplace transform method is simple to use for generating the exhaustive summary of models containing more than two compartments. What becomes more and more difficult is the solution, i.e. to determine which of the original parameters of the model are uniquely determined by the system of nonlinear algebraic equations. In fact, one has to solve a system of nonlinear algebraic equations which is increasing in number of terms and nonlinearity degree with the model order, i.e. the number of compartments in the model. One can easily grasp the nature of the difficulty in moving from two to three compartments. This is illustrated in the following example.

Example

Consider the model shown in Figure 5.6.1 where the input into compartment 1 is a bolus and the two model outputs are the concentrations in compartments 1 and 2.

By using the Laplace transform method, one calculates

$$L\{c_1(t)\} = \frac{\beta_3 s^2 + \beta_2 s + \beta_1}{s^3 + \alpha_3 s^2 + \alpha_2 s + \alpha_1} \tag{5.6.1}$$

$$L\{c_2(t)\} = \frac{\gamma_2 s + \gamma_1}{s^3 + \alpha_3 s^2 + \alpha_2 s + \alpha_1} \tag{5.6.2}$$

The exhaustive summary is

$$k_{32}k_{01}k_{13} + k_{23}k_{12}k_{01} + k_{13}k_{12}k_{01} = \alpha_1 \tag{5.6.3}$$
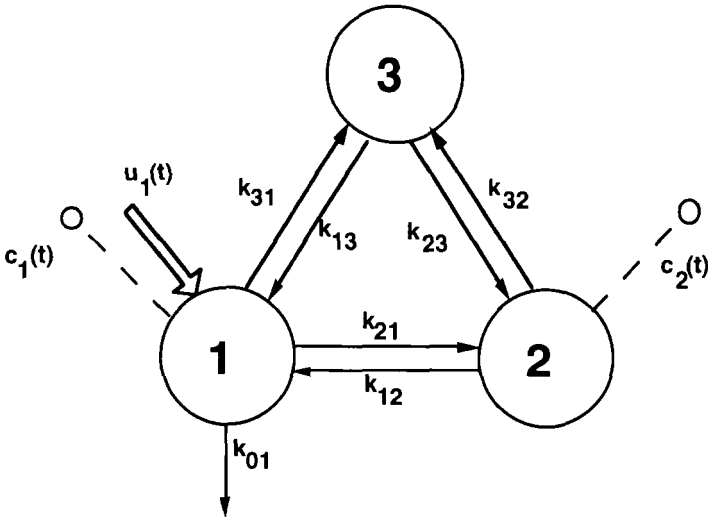
Figure 5.6.1. A three compartment model. The input takes place in compartment 1 and measurements are tracer concentrations in compartments 1 and 2.

$$k_{32}k_{31} + k_{32}k_{21} + k_{32}k_{13} + k_{32}k_{01} + k_{23}k_{21} + k_{23}k_{13} \tag{5.6.4}$$
$$+k_{23}k_{01} + k_{23}k_{31} + k_{13}k_{21} + k_{13}k_{12} + k_{13}k_{01}$$
$$+k_{12}k_{31} + k_{12}k_{01} = \alpha_2$$

$$k_{32} + k_{31} + k_{23} + k_{21} + k_{13} + k_{12} + k_{01} = \alpha_3 \tag{5.6.5}$$

$$\frac{k_{32}k_{13} + k_{23}k_{12} + k_{13}k_{12}}{V_1} = \beta_1 \tag{5.6.6}$$

$$\frac{k_{32} + k_{23} + k_{13} + k_{12}}{V_1} = \beta_2 \tag{5.6.7}$$

$$\frac{1}{V_1} = \beta_3 \tag{5.6.8}$$

$$\frac{k_{31}k_{23} + k_{23}k_{21} + k_{21}k_{13}}{V_2} = \gamma_1 \tag{5.6.9}$$

$$\frac{k_{21}}{V_2} = \gamma_2 \tag{5.6.10}$$

The coefficients α_i, β_i and γ_i are the observational parameters, and the problem is to solve the system of nonlinear equations (5.6.1)–(5.6.10) in the unknowns k_{ij}, V_1 and V_2. Clearly this is very tedious.

It is easy to see that the difficulty of the identifiability problem has increased considerably in moving from the two to the three compartment model. For the two compartment case, the corresponding equations are given by (5.5.7)–(5.5.11). Thus not only are there 8 instead of 5 algebraic equations to solve, but the equations have become more nonlinear, i.e. now there are products of three instead of two k_{ij}; in addition, there are more terms, 13 instead of 3, in the equations containing the product of two k_{ij}
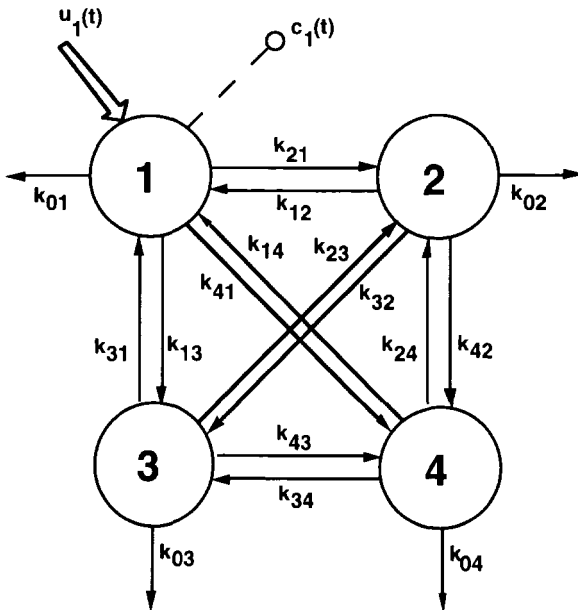
Figure 5.6.2. The general four compartment model. Input and measurement takes place in compartment 1.

To reinforce the fact that the difficulty of the identifiability problem dramatically increases with model order, consider the general four compartment model shown in Figure 5.6.2 with input into and measurement from compartment 1. One can show that the 3rd degree term corresponding to α_1 in (5.6.3) is the sum of 200 terms! This shows clearly that the a priori identifiability test is very difficult, if not impossible, to be performed by hand in the general case.

Some remarks

Previously the difficulty of the identifiability problem has been shown by using the Laplace transform method for its solution. Other methods have been proposed to test a priori identifiability. The three that have received the most attention are the transfer function topological method [Audoly and DAngiò, 1983], the modal matrix method [Norton, 1980], and the similarity transformation method [Walter and Lecourtier, 1981]. The difficulty of the problem remains, however. Each of these methods can be shown to perform better than the others for specific compartmental models, but none of them can be shown to be superior to the others in general. In other words all the methods work well for models of low dimension, e.g. the two and some three compartmental models, but fail when applied to relatively large, general structure models because the system of nonlinear algebraic equations become to difficult to be solved.

Recently, symbolic computer languages such as Reduce [1995] and Maple [1997] have been found to help, but to deal with the problem in general there is the need to resort to computer algebra methods. In particular, a software tool to test a priori identifiability of linear compartmental models of general structure which combines the transfer function topological method with a computer algebra method, the Gröbner basis, is available [Audoly et al., 1998]. Before describing in §5.9 the underlying principals which lead to this tool, in the next two sections, §5.7 and §5.8, some explicit identifiability results which are available on the general three compartment model, and on the mammillary and catenary models will be given. The results given in §5.7 and §5.8, albeit not as complete as those obtained for the two compartment model, provide a catalogue of explicit identifiability results which is extremely useful in practice. Additional explicit identifiability results on some large compartmental models can be found in the literature; these, however, deal with specific compartmental structures.

5.7   THE THREE COMPARTMENT MODEL

In moving from the two to the three compartment model, the number of possible model-experiment combinations becomes very large since one has to consider all the possible variations of the general model shown in Figure 5.7.1 created by allowing some of the k_{ij} to be zero together with all the possible input-output configurations, i.e. now there are three sites for input and output, and input and output can occur at more than one site simultaneously. It has been shown, for example, that even assuming input into one compartment only and permitting observations of one, two or three compartments there are 826 essentially distinct nondegenerate three compartment situations [Norton, 1982]. Thus it is virtually impossible to do, as was done for the two compartment model, an exhaustive identifiability analysis for all the possible three compartment model-experiment configurations.
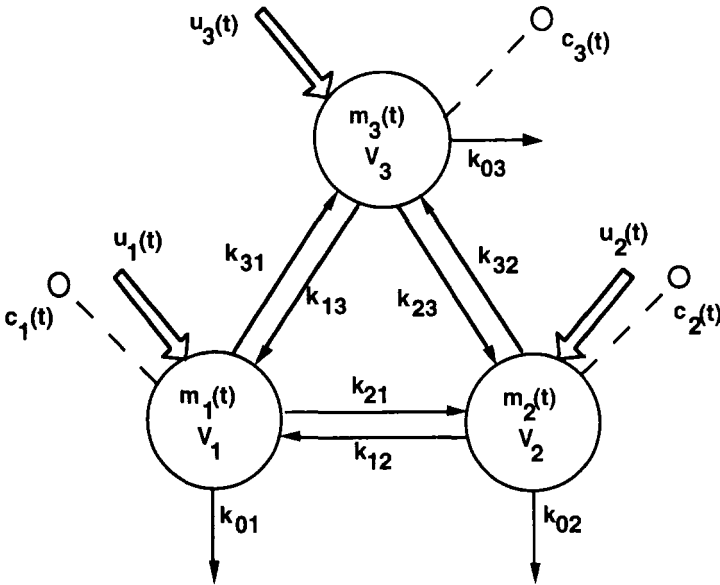
Figure 5.7.1.   The general three compartment model showing all possible rate constants k_{ij}, and possible sites of input and samples. See text for additional explanation.

In what follows, a summary of the catalogue of results obtained in [Norton, 1982] by using the Laplace transform method will be given for the situation mentioned above, i.e. input into a single compartment, say compartment 1, and observations permitted in compartment 1, 2 or 3. It will be assumed that the volumes of the accessible compartments are known, i.e. only the rate constants k_{ij} are unknown. If the volumes are also unknown, apart from the case when compartment 1 is accessible in which case V_1 is uniquely identifiable, a detailed inspection is necessary as far as V_2 and V_3 are concerned. As mentioned previously, there are 826 cases to consider.

The basic 18 model structures are shown in Figure 5.7.2. No losses have been shown in this figure; this will be explained in a moment. In addition, structures for which a reversal of compartments 2 and 3 will result in a model previously considered are excluded. Each compartment in the structures shown will eventually receive material from compartment 1, i.e. input into compartment 1 will eventually reach compartments 2 and 3. For each of the eighteen structures there are seven possible patterns of irreversible loss; there are loss from compartment 1, 2, or 3; compartments 1 and 2, 1 and 3, 2 and 3; and from compartments 1, 2 and 3. Similarly there are seven measurement possibilities. This gives in all 882 combinations. However an examination of the symmetry between compartments 2 and 3 in models 1, 9, 11 and 18 of Figure 5.5.1 results in 14 cases for each model which are not considered. This leaves a total of 826 distinct possibilities. It should be noted that if the measurement configurations are considered in order of increasing complexity, many other cases need not be studied. For instance, if a model is globally identifiable from measurements in compartment 2 only, it is globally identifiable from measurements in compartments 1 and 2, 2 and 3, and 1, 2 and 3. The same comment does not apply generally to the locally identifiable models.

Two catalogues are summarized. Table 5.7.1 gives the minimal set of measured compartments for global identifiability. In Appendix F, Tables F.1 and F.2 list all sets of measured compartments giving local identifiability and the number of solutions.
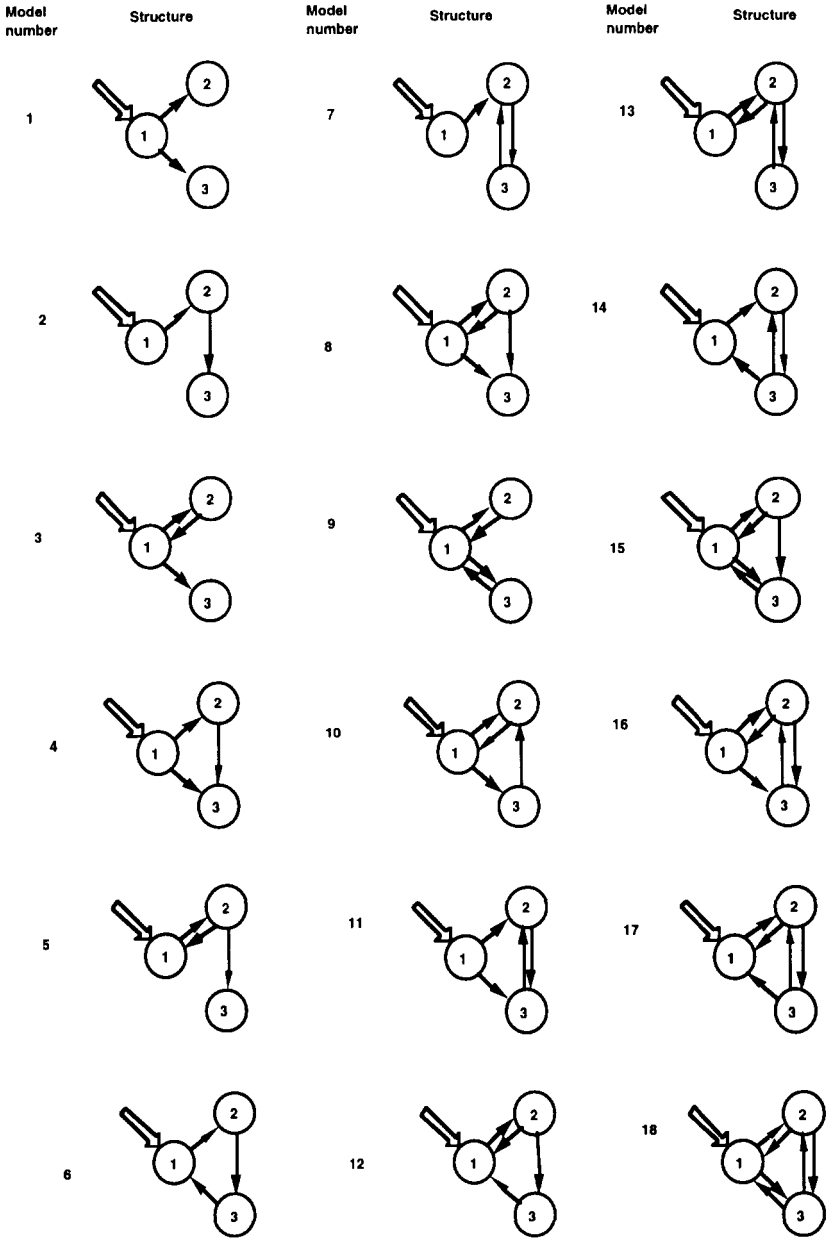
Figure 5.7.2. The basic 18 model structures of a three compartment model; in all cases, tracer input is into compartment 1. See text for additional explanation.

Table 5.7.1. Minimal Sets of Observed Compartments for Global Identifiability

Model Number	Loss from cpt						
	1	2	3	1,2	1,3	2,3	1,2,3
1	2,3	1,2 ; 2,3	a	2,3	a	2,3	2,3
2	1,2 ; 1,3 ; 2,3	1,3 ; 2,3	1,3 ; 2,3	1,2,3	2,3	2,3	1,2,3
3	3	3 ; 1,2	3	2,3	1,3 ; 2,3	1,3 ; 2,3	2,3
4	1,3 ; 2,3	1,3 ; 2,3	1,3 ; 2,3	1,2,3	2,3	2,3	1,2,3
5	1,2 ; 1,3	1,3 ; 2,3	1,3 ; 2,3	1,2,3	1,3	1,3 ; 2,3	1,2,3
6	2 ; 1,3	2 ; 1,3	2 ; 1,3	1,2 ; 2,3	1,2 ; 2,3	2,3	1,2,3
7	1,2 ; 1,3	2	2 ; 1,3	1,2 ; 2,3	1,2 ; 2,3	2,3	1,2,3
8	1,3	1,3 ; 2,3	1,3 ; 2,3	1,2,3	1,3 ; 2,3	1,3 ; 2,3	1,2,3
9	1,2 ; 1,3 ; 2,3	1,2 ; 1,3 ; 2,3	a	1,2 ; 2,3	a	1,2 ; 1,3 ; 2,3	2,3
10	1,2 ; 1,3 ; 2,3	1,2 ; 1,3 ; 2,3	1,2 ; 1,3 ; 2,3	1,3 ; 2,3	1,3	1,3 ; 2,3	1,2,3
11	2,3	1,2 ; 2,3	a	2,3	a	2,3	1,2,3
12	1,2 ; 1,3	2 ; 1,3	2 ; 1,3	1,2	1,2	2,3	1,2,3
13	1 ; 2,3	1 ; 2	1 ; 2	1,2 ; 1,3 ; 2,3	1,2 ; 1,3	1,3 ; 2,3	1,2,3
14	1,2 ; 1,3 ; 2,3	2	2 ; 1,3	1,2	1,2 ; 2,3	2,3	1,2,3
15	1,2 ; 1,3	1,2 ; 1,3 ; 2,3	1,3 ; 2,3	1,2,3	1,2,3	2,3	1,2,3
16	1,2 ; 1,3 ; 2,3	1,2 ; 1,3 ; 2,3	1,3 ; 2,3	1,3 ; 2,3	1,3	1,3 ; 2,3	1,2,3
17	1,2 ; 1,3	1,2 ; 2,3	1,2 ; 1,3 ; 2,3	1,2	1,2	1,2,3	1,2,3
18	1,2 ; 1,3	1,2 ; 2,3	a	1,2,3	a	1,2,3	1,2,3

^{a}Covered by preceding case by symmetry.

5.8   CATENARY AND MAMMILLARY MODELS

Catenary and mammillary models introduced previously in §4.6 are two classes of compartmental models which are frequently used to interpret tracer kinetic data. In this section, some explicit a priori identifiability results which are available for these models for the case of a single input-single output experiment in the same compartment will be reviewed [Cobelli et al., 1979b; DiStefano, 1983]. For convenience, the general catenary and mammillary are reproduced in Figures 5.8.1 and 5.8.2 respectively.
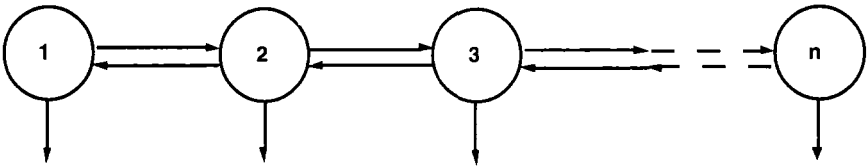
Figure 5.8.1.   The n compartment catenary model.
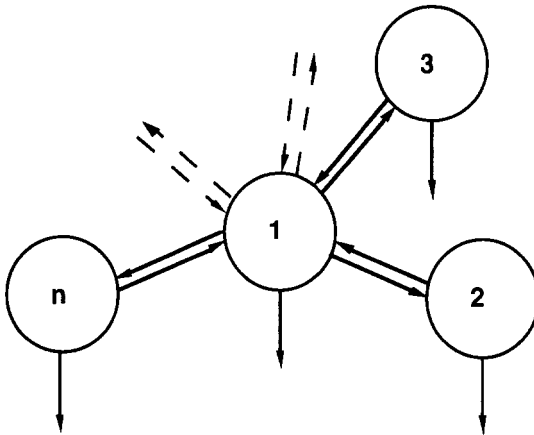
Figure 5.8.2.   The general n compartment mammillary model.

The unknown parameters are the volume or mass of the accessible compartment, and the transfer rate constants k_{ij}. Since the input and observations take place in the same compartment, the volume or mass of that compartment is uniquely identifiable. Thus the unknown parameters are the individual rate constants k_{ij}. The results can be summarized as follows.

Catenary Models

A catenary compartmental model which is either closed (i.e. there is no irreversible loss to the environment so $k_{0i} = 0, i = 1, \cdots, n$) or almost closed (i.e. there is only one non zero k_{0i} which can be from any compartment) is globally identifiable if the accessible compartment (for input and measurement) is an external compartment, i.e. compartment 1 or n in Figure 5.8.1. If the accessible compartment is an intermediate compartment, i.e. $2, 3, \bullet\bullet\bullet$, or $n-1$, the k_{ij} are only nonuniquely identifiable and the number of different solutions increases with the distance of the accessible compartment from either end of the chain. More precisely, if the accessible compartment is j shown in Figure 5.8.3, the number of solutions for the k_{ij} is $\frac{(n-1)!}{(n-j)!(j-1)!}$ where "!" denotes the factorial, i.e. for an arbitrary integer i, $i! = i \cdot (i - 1) \cdots 2 \cdot 1$; if the irreversible loss is from compartment j, then k_{0j} is uniquely identifiable.
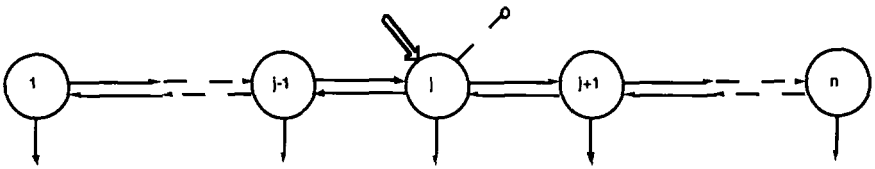
Figure 5.8.3. The general catenary model where compartment j is the accessible compartment. See text for additional explanation.

As an example, consider the model shown below in Figure 5.8.4. In this model, an example of the general case shown above with $j = 2$ and $n = 4$, k_{02} is uniquely identifiable but there are three different solutions for k_{21}, k_{12}, k_{32}, k_{23}, k_{43} and k_{34}.
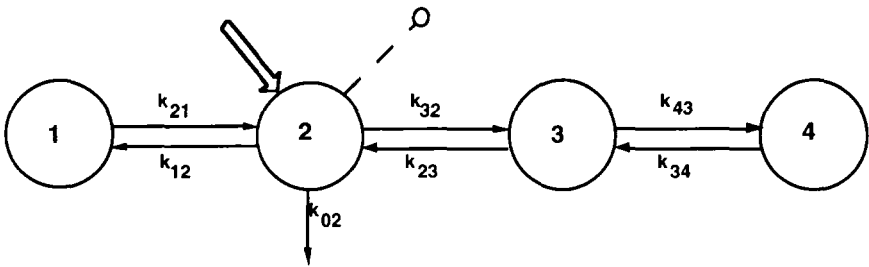
Figure 5.8.4. A four compartment catenary model where compartment 2 is accessible. See text for additional explanation.

A catenary model with more than one irreversible loss is nonidentifiable, but since some combinations of the model parameters are uniquely identifiable, it is still possible to derive upper and lower bounds for the nonidentifiable parameters. If the input-output experiment is in an external compartment (compartment 1 or n of Figure 5.8.1), the uniquely identifiable parameter combinations are the total rate of exit from the compartments, $k_{ii} = -(k_{0i} + k_{i,i-1} + k_{i,i+1}), i = 1, \ldots, n - 1$, and the products $k_{i,i+1}k_{i+1,i}, i = 1, \ldots, n - 1$. An algorithm has been developed for deriving these parameter combinations and the parameter bounds of the k_{ij} from the coefficients of the multi-exponential response to a bolus input introduced into compartment 1 or n [Chao-Min Chen et al., 1985].

Alternatively, the parameter bounds can be computed from the identification of the submodels [Cobelli and Toffolo, 1987] which are defined from the original model structure by setting all of the irreversible losses except one equal to zero. In this case, if the input-output experiment is into an external compartment, the submodels are uniquely identifiable, and their parameters coincide with the upper and lower bounds of the original structure; this is illustrated in Figure 5.8.5.

The above figure addresses the general situation where irreversible losses take place in all compartments. Consider now the case where irreversible losses are only present in some compartments, for example compartment 2 and 3 in Figure 5.8.5. In this case, two submodels have to be considered having respectively $k_{01} = k_{03} = \ldots = k_{0n} = 0$ and
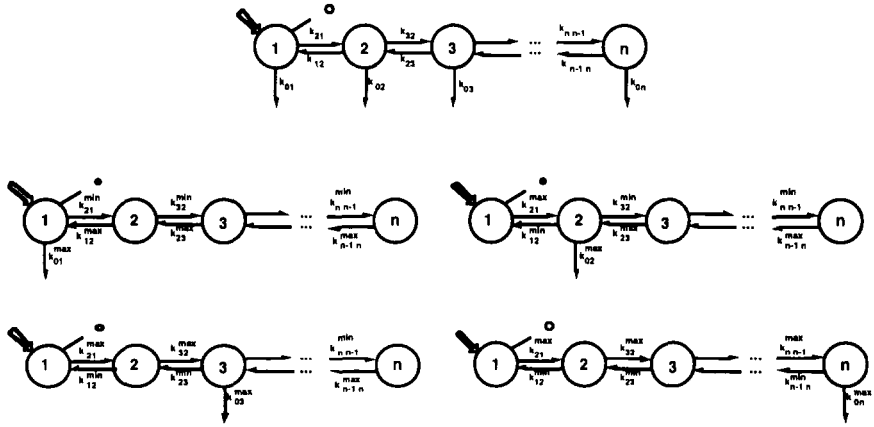
Figure 5.8.5. Top: the general n-compartment catenary model where the input-output is in compartment 1, an external compartment. When more the one irreversible loss are present, the model is nonidentifiable. Bounds for the k_{ij} can be interpreted as parameters of the uniquely identifiable submodels derived from the original one by setting all losses but one equal to their lower bound, zero. These are illustrated in the bottom panels.

$k_{01} = k_{02} = k_{04} = \ldots = k_{0n} = 0$. These two submodels give upper and lower bounds for k_{32}, k_{23}, k_{01} and k_{03}. Values for the remaining parameters from the two submodels coincide since they are uniquely identifiable from the given input-output experiment.

Mammillary Models

A mammillary compartmental model, closed or almost closed, is locally identifiable and the number of different solutions is $(n-1)!$ if the accessible compartment is the central compartment (compartment 1 in Figure 5.8.2). If there is irreversible loss from this central compartment, i.e. $k_{01} \neq 0$, then k_{01} is uniquely identifiable. However, it is sufficient to order the noncentral compartments, e.g. $|k_{22}| > |k_{33}| > \cdots > |k_{nn}|$ where $|k_{ii}| = k_{1i} + k_{0i}$ to render the model uniquely identifiable.

If the accessible compartment is a peripheral compartment, the number of different solutions is $(n-2)!$ but the rate constants k_{ij} connecting

the accessible compartment with the central compartment are uniquely identifiable. Again, if the irreversible loss is from the accessible compartment, this loss is uniquely identifiable. As in the previous case, ordering the central and noncentral nonaccessible compartments is sufficient to solve the ambiguity on model parameters.

A mammillary compartmental model is nonidentifiable when there are more than one irreversible loss. Only some parameter combinations are uniquely identifiable thus making it possible to bound nonidentifiable parameters within finite limits.

The uniquely identifiable parameter combinations when the accessible compartment is the central compartment (compartment 1 in Figure 5.8.2) are the total exits from the compartments. In the case of the model shown in Figure 5.8.2, these would be $k_{11} = -(k_{21}+\cdots+k_{n1}+k_{01})$ and $k_{ii} = -(k_{1i} + k_{0i}), i = 2, \cdots, n$, and the products $k_{i1}k_{1i}, i = 2, \cdots, n$ provided the compartments are ordered as described above. It is immediate to verify that exchange parameters between the central compartment and those compartments where no irreversible loss takes place are uniquely identifiable.

Similar to the case with the catenary model, an algorithm has been developed for computing these parameter combinations and the parameter bounds of the k_{ij} from the coefficients of the multiexponential response to a bolus injection of tracer administered into the central compartment of a generic n-compartment mammillary model [Landaw et al., 1984].

Alternatively, the identification of submodels allows one to derive the bounds of the nonidentifiable parameters. The procedure is similar to that described for catenary models: a number of submodels equal to the number of irreversible losses are defined, each having all the irreversible losses but one set equal to the minimum value, zero. If the non-accessible, non-central compartments are ordered as previously described, the submodels are uniquely identifiable, and their parameters equal the values of the upper and lower bounds of the nonidentifiable parameters of the original model structure, as illustrated below in Figure 5.8.6. Values of the exchanges between the central compartment and those compartments where no irreversible loss takes place are the same for the various submodels since these parameters are uniquely identifiable.
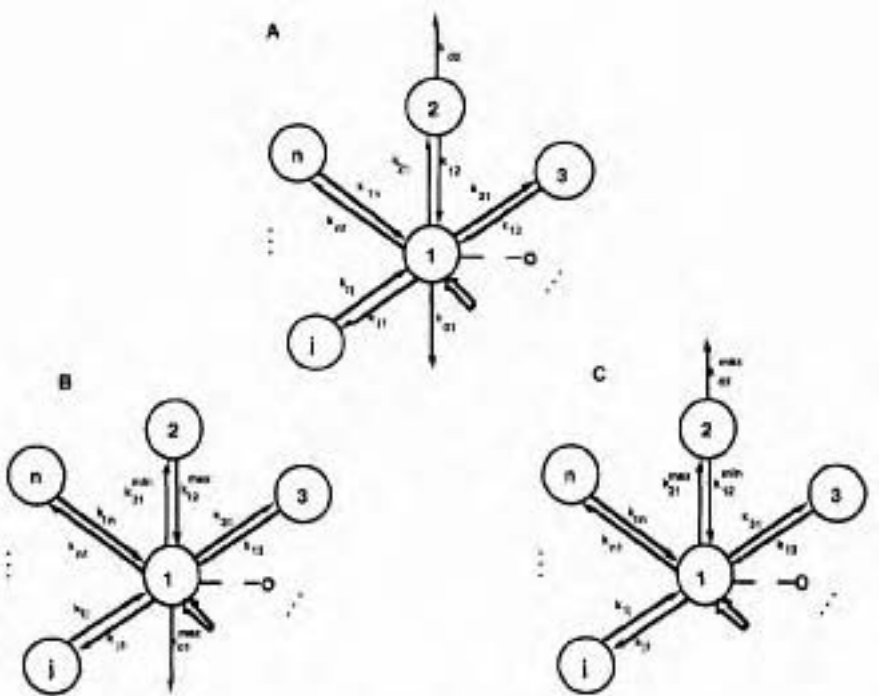
Figure 5.8.6. Panel A. The n-compartment mammillary model where the input-output experiment is in the central compartment. Parameters such as k_{31} and k_{13} are uniquely identifiable while parameters such as k_{01}, k_{12}, k_{21} and k_{02} are nonidentifiable. Panels B and C. The two submodels of the original model structure which permit the quantification of the upper and lower bounds of the nonidentifiable parameters of the original model structure.

5.9   A PRIORI IDENTIFIABILITY OF GENERAL STRUCTURE COMPARTMENTAL MODELS: A COMPUTER ALGEBRA APPROACH

5.9.1   Introduction

The test of a priori identifiability of linear compartmental models of general structure from multiple input-multiple output experiments is a formidable task which, as mentioned previously in §5.6, can take advan-

tage of the tools of computer algebra. However, before describing this approach, it is useful to mention the few available results on identifiability for the general linear compartmental model.

Necessary topological conditions for identifiability are available which can be easily checked on the compartmental diagram [Cobelli et al., 1979a]. This means that nonidentifiability of some models for a given input-output experiment can be easily detected. Among these, it is of interest to discuss input-output connectibility; in order for the model to be identifiable, all of its compartments must be connected to the compartments where the inputs and outputs take place. One can thus eliminate from the model the compartments that are not input and output connected together with the rate constants leaving them. In fact, it is easy to realize that only the input-output connected compartments are reached by the input and reach the outputs, and thus only the k_{ij} parameters not outgoing from compartments which are not input-output connected are possibly identifiable. All of the compartmental model examples discussed so far in this Chapter are input-output connected except the model shown in Figure 5.2.4 where compartment 2 is not output connected. An additional example of a compartmental model which is not input-output connected is given in Figure 5.9.1 A. As a result, the model is nonidentifiable and thus there is a need to arrive at an input-output version of the model. This is shown in Figure 5.9.1 B. This model can now be tested for identifiability. The input-output connectibility as well as the two other necessary topological conditions for identifiability are implemented in the GLOBI (GLOBal Identifiability) software package [Audoly et al., 1998] described later as a preliminary check of nonidentifiability before entering the computer algebra identifiability algorithm.

Another general result that is available is that the rate constants of an input-output connected compartmental model are always interval identifiable. This result has been proven in Cobelli and Toffolo [1984], and stems from the fact that for such a model, one of the observational parameters is always the sum of all the rate constants of the model (e.g. (5.5.8) and (5.6.5) for the models shown in Figures 5.4.1 and 5.6.1 respectively). Thus this gives the upper bound for all the rate constants of the model with the lower bound being zero. While this proves interval identifiability of the input-output connected model, in practice one desires a narrower interval. To achieve this, one can follow the logic
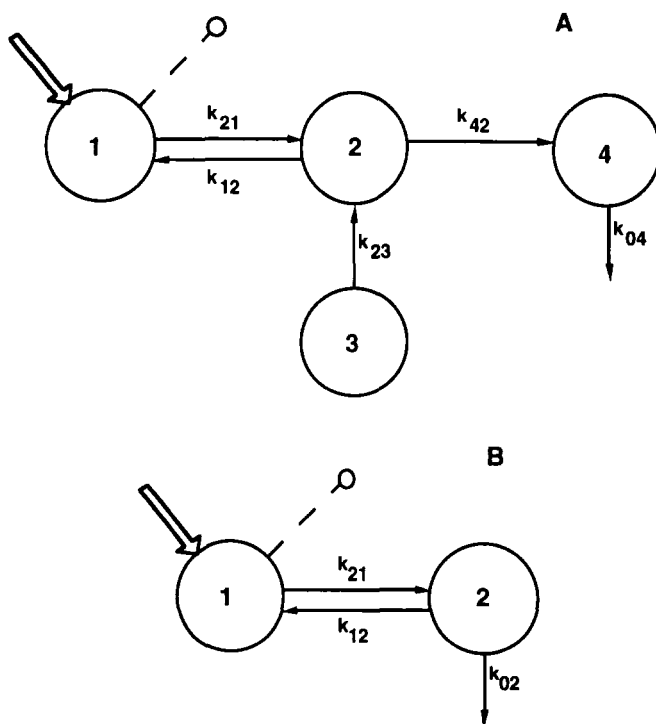
Figure 5.9.1.   A: A four compartment model which is not input-output connected. Compartment 3 is not input-connected while compartment 4 is not output-connected. B: An input-output connected model can be obtained by eliminating compartments 3 and 4 together with their respective loss rate constants k_{04} and k_{23}, and setting k_{42} equal to k_{02}.

used for the two compartment model (§5.4) and for the mammillary and catenary models (§5.8).

While the above refers to the rate constants, it is of interest to note the role played by the volume or mass of the output compartments in an input-output connected model. It is either uniquely identifiable if the input and the output take place in the same compartment, or nonidentifiable if the input and the output take place in different compartments.

5.9.2 Rationale

The idea behind the computer algebra approach is to combine one classical method of a priori identifiability analysis with the Grobner basis, a powerful tool of computer algebra for solving systems of algebraic nonlinear equations such as the . Buchberger [1988] proposed an algorithm for the computation of the Grobner basis which, in some sense, is the analogue of Gaussian elimination for systems of polynomial equations. Details about the definition, the main properties and the many applications of the Gröbner basis and the Buchberger algorithm can be found in Buchberger [1988] and Becker and Weispfenning [1993].

In this section, the main features of a method to solve the exhaustive summary equations which combines the transfer function topological method with the Gröbner basis will be described. The transfer function topological method has been chosen since it is the one which makes, as compared to the other classical methods (e.g. the Laplace transform or transfer function method discussed in earlier in this Chapter, the similarity transformation and the modal matrix), the Buchberger algorithm successful for the largest class of models. Briefly, the method is able to reduce the complexity of the exhaustive summary equations, i.e. the number of equations, the number of terms in each equation, and the degree of nonlinearity, in the most suitable way for the performance of the Buchberger algorithm. The software tool, GLOBI, implements this method to test a priori identifiability of general multicompartmental models from multiple input-multiple output experiments [Audoly et al., 1998].

5.9.3 The Transfer Function Topological Approach

This section provides a brief description of the transfer function topological method showing in particular where it differs from the Laplace transform or transfer function method. The basic idea is to move from the Laplace transform identifiability equations as illustrated in §5.4 where the known coefficients are the observational parameters and the unknowns are the k_{ij} elements to a set of simpler equations, both in the number of terms and nonlinearity degree, where the new unknowns are the cycles and the paths (see below) connecting the input to the output compartments of the compartmental model diagram.

The cycles and paths of an n-compartment model characterized by the K matrix $\mathbf{K} = (k_{ij})$ are defined for $i = 1, \cdots, n$ as

$$c_{i1\ i1} = k_{ii} \qquad i = 1, \cdots, n \tag{5.9.1}$$

$$c_{i1\ i2\ \ldots\ il} = k_{i2\ i1}k_{i3\ i2} \ldots k_{i1\ il} \qquad l = 2, \ldots, n \tag{5.9.2}$$

The paths of length $l, l = 2, \cdots, n$ are

$$p_{i1\ i2\ \ldots\ il} = k_{i2\ i1}k_{i3\ i2} \ldots k_{il\ il} \tag{5.9.3}$$

To provide an example of cycles and paths using these definitions and notation, one can calculate the cycles and paths connecting the input to the output compartments using the model shown in Figure 5.6.1. They are:

$$c_{11} = k_{11} \qquad c_{22} = k_{22} \qquad c_{33} = k_{33}$$

$$c_{12} = k_{12}k_{21} \qquad c_{13} = k_{13}k_{31} \qquad c_{23} = k_{23}k_{32} \tag{5.9.4}$$

$$c_{123} = k_{21}k_{32}k_{13} \qquad c_{321} = k_{23}k_{12}k_{31}$$

$$p_{12} = k_{21} \qquad p_{132} = k_{31}k_{23}$$

The exhaustive summary is greatly simplified by using cycles and paths. For instance, by rewriting the coefficients α_i, β_i and $\gamma_j, i = 1, 2, 3\ j = 1, 2$ of (5.6.3)–(5.6.10) of the two output equations (5.6.1) and (5.6.2) in terms of cycles and paths (5.9.1)–(5.9.3), the equations become

$$c_{32}c_{11}c_{321} - c_{312} + c_{31}c_{22} + c_{33}c_{21} - c_{33}c_{22}c_{11} = \alpha_1 \tag{5.9.5}$$

$$-c_{32} - c_{31} + c_{33}c_{22} + c_{33}c_{11} + c_{21} + c_{22}c_{11} = \alpha_2 \tag{5.9.6}$$

$$-c_{33} - c_{22} - c_{11} = \alpha_3 \tag{5.9.7}$$

$$\frac{-c_{32} + c_{33}c_{22}}{V_1} = \beta_1 \tag{5.9.8}$$

$$\frac{-c_{33} - c_{22}}{V_1} = \beta_2 \tag{5.9.9}$$

$$\frac{1}{V_1} = \beta_3 \tag{5.9.10}$$

$$\frac{-c_{33}p_{12} + p_{132}}{V_2} = \gamma_1 \tag{5.9.11}$$

$$\frac{p_{12}}{V_2} = \gamma_2 \tag{5.9.12}$$

These equations result in a significant decrease in the number of terms of the corresponding equations (5.6.3)–(5.6.10) derived using the classical transfer function approach. For example, (5.9.6) defining α_2 now contains 6 terms instead of 13 corresponding to (5.6.4); equation (5.9.7) defning α_3 now has 3 instead of the 7 terms of (5.6.5).

5.9.4   The Identifiability Algorithm

It is more informative for purposes of this text to go through the main steps of the algorithm by considering three examples and commenting on the results rather than providing a general description.

Example 1

Consider the four compartment model shown in Figure 5.9.2 where input is into compartment 1 and measurements are taken from compartments 1, 2 and 4. Assuming for sake of simplicity that the volumes of the accessible compartments are known, the number of unknowns, the k_{ij}, is 10.
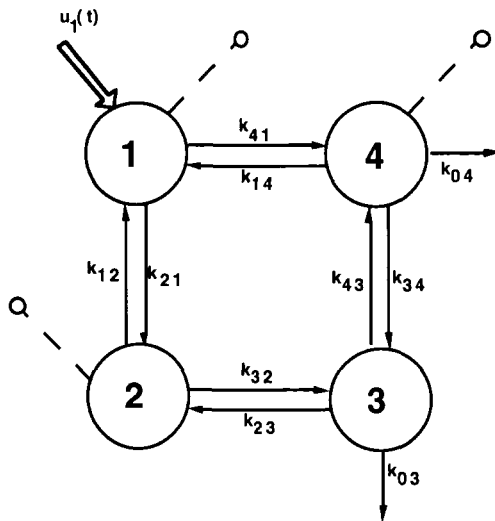
Figure 5.9.2. A four compartment model with input into compartment 1, measurements from compartments 1, 2 and 4, and irreversible losses from compartments 3 and 4.

Step 1: The algorithm calculates the observational parameters from the Laplace transform of the three model outputs. Since the volumes of the accessible compartments are assumed to be known, the model outputs can be considered to be the masses in compartments 1, 2 and 4. Thus one has

$$L\{m_1\} = \frac{s^3 + \beta_3 s^2 + \beta_2 s + \beta_1}{s^4 + \alpha_4 s^3 + \alpha_3 s^2 + \alpha_2 s + \alpha_1} \qquad (5.9.13)$$

$$L\{m_2\} = \frac{\gamma_3 s^2 + \gamma_2 s + \gamma_1}{s^4 + \alpha_4 s^3 + \alpha_3 s^2 + \alpha_2 s + \alpha_1} \qquad (5.9.14)$$

$$L\{m_4\} = \frac{\delta_3 s^2 + \delta_2 s + \delta_1}{s^4 + \alpha_4 s^3 + \alpha_3 s^2 + \alpha_2 s + \alpha_1} \qquad (5.9.15)$$

The three denominators are the same and provide the observational parameters α_1, α_2, α_3 and α_4. The three numerators are different and provide the observational parameters β_1, β_2 and β_3, γ_1, γ_2 and γ_3, and δ_1, δ_2 and δ_3 for the outputs of compartments 1, 2 and 4 respectively.

The algorithm then assumes a numerical value for the observational parameter $\hat{\boldsymbol{\Phi}}$, i.e. $\hat{\alpha}_i$, $\hat{\beta}_i$, $\hat{\gamma}_i$ and $\hat{\delta}_i$, which derives from a particular solution of the parameter vector $\hat{\mathbf{p}}$, i.e. a value $\hat{k}_{ij}$ of the k_{ij} which satisfies the compartmental constraints described in Chapter 4. This particular solution can be generated automatically by a random number generator with subsequent check of the compartmental constraints. Assume the particular solution $\hat{\mathbf{p}}$ is that giving the compartmental matrix $\mathbf{K}$ shown below:

$$\mathbf{K} = \begin{pmatrix} -5 & 2 & 0 & 1 \\ 2 & -3 & 3 & 0 \\ 0 & 1 & -6 & 2 \\ 3 & 0 & 2 & -5 \end{pmatrix} \qquad (5.9.16)$$

The algorithm calculates the corresponding value of the observational parameter $\hat{\boldsymbol{\Phi}}$, i.e. $\hat{\alpha}_i$, $\hat{\beta}_i$, $\hat{\gamma}_i$ and $\hat{\delta}_i$, and the denominator and the three numerator polynomials of (5.9.13)–(5.9.15)

$$s^4 + 19s^3 + 119s^2 + 272s + 126 \qquad (5.9.17)$$

$$s^3 + 14s^2 + 56s + 63 \qquad (5.9.18)$$

$$2s^2 + 22s + 70 \qquad (5.9.19)$$

$$3s^2 + 27s + 49 \qquad (5.9.20)$$

Step 2: The algorithm calculates the observational parameters as functions of the cycles and paths thus the exhaustive summary is given by

$$c_{43}c_{21} - c_{43}c_{22}c_{11} - c_{4321} - c_{2341} + c_{41}c_{32} - c_{41}c_{33}c_{22} \qquad (5.9.21)$$
$$-c_{44}c_{32}c_{11} - c_{44}c_{33}c_{21} + c_{44}c_{33}c_{22}c_{11} = 126$$

$$c_{43}c_{22} \quad + \quad c_{43}c_{11} + c_{41}c_{33} + c_{41}c_{22} + c_{44}c_{32} - c_{44}c_{33}c_{22} \quad (5.9.22)$$
$$- \quad c_{44}c_{33}c_{11} + c_{44}c_{21} - c_{44}c_{22}c_{11}$$
$$+ \quad c_{32}c_{11} + c_{33}c_{21} - c_{33}c_{22}c_{11} = 272$$

$$-c_{43} \quad - \quad c_{41} + c_{44}c_{33} + c_{44}c_{22} + c_{44}c_{11} \qquad (5.9.23)$$
$$- \quad c_{32} + c_{33}c_{22} + c_{33}c_{11} - c_{21} + c_{22}c_{11} = 119$$

$$-c_{44} - c_{33} - c_{22} - c_{11} = 19 \qquad (5.9.24)$$
$$c_{43}c_{22} + c_{44}c_{32} - c_{44}c_{33}c_{22} = 63 \qquad (5.9.25)$$

$$-c_{43} + c_{44}c_{33} + c_{44}c_{22} - c_{32} + c_{33}c_{22} = 56 \qquad (5.9.26)$$
$$-c_{44} - c_{33} - c_{22} = 14 \qquad (5.9.27)$$
$$-c_{43}p_{12} + c_{44}c_{33}p_{12} + p_{1432} = 70 \qquad (5.9.28)$$
$$-c_{44}p_{12} - c_{33}p_{12} = 22 \qquad (5.9.29)$$
$$p_{12} = 2 \qquad (5.9.30)$$
$$-c_{32}p_{14} + c_{33}c_{22}p_{14} + p_{1234} = 49 \qquad (5.9.31)$$
$$-c_{33}p_{14} - c_{22}p_{14} = 27 \qquad (5.9.32)$$
$$p_{14} = 3 \qquad (5.9.33)$$

Step 3: The next step is the application of the Buchberger algorithm to solve these equations. This step may not be successful for computational limits; in this case the problem cannot be solved. If this step is successful, the algorithm returns a new exhaustive summary expressed in terms of the same unknowns, cycles and paths, but now showing a simplified form. For the example under consideration, they are:

$$c_{43} = 4 \qquad (5.9.34)$$
$$c_{4321} + c_{4123} = 40 \qquad (5.9.35)$$

$$c_{41} = 3 \qquad \text{(5.9.36)}$$

$$c_{44} = -5 \qquad \text{(5.9.37)}$$

$$c_{32} = 3 \qquad \text{(5.9.38)}$$

$$c_{33} = -6 \qquad \text{(5.9.39)}$$

$$c_{21} = 4 \qquad \text{(5.9.40)}$$

$$c_{22} = -3 \qquad \text{(5.9.41)}$$

$$c_{11} = -5 \qquad \text{(5.9.42)}$$

$$p_{1234} = 4 \qquad \text{(5.9.43)}$$

$$p_{14} = 3 \qquad \text{(5.9.44)}$$

$$p_{1432} = 18 \qquad \text{(5.9.45)}$$

$$p_{12} = 2 \qquad \text{(5.9.46)}$$

By comparing these equations with the previous ones, one gets the idea of the reduction in both number of terms and nonlinearity degree accomplished by the first application of the Buchberger algorithm. It should be noted that the number of returned independent equations can be less than the number of cycles and paths. This fact does not mean that the basic model parameters, i.e. the k_{ij}, are nonidentifiable since not all cycles and paths are independent functions of the k_{ij}.

Step 4: The algorithm substitutes for the cycles and paths in (5.9.34)–(5.9.46) their expressions in terms of the k_{ij} by applying their definition:

$$k_{43}k_{34} = 4 \qquad \text{(5.9.47)}$$

$$k_{43}k_{32}k_{21}k_{14} + k_{41}k_{34}k_{23}k_{12} = 40 \qquad \text{(5.9.48)}$$

$$k_{41}k_{14} = 3 \qquad \text{(5.9.49)}$$

$$k_{34} + k_{14} + k_{04} = 5 \qquad \text{(5.9.50)}$$

$$k_{32}k_{23} = 3 \qquad \text{(5.9.51)}$$

$$k_{43} + k_{23} + k_{03} = 6 \qquad \text{(5.9.52)}$$

$$k_{21}k_{12} = 4 \qquad \text{(5.9.53)}$$

$$k_{32} + k_{12} = 3 \qquad \text{(5.9.54)}$$

$$k_{41} + k_{21} = 5 \qquad \text{(5.9.55)}$$

$$\kappa_{43}k_{32}k_{21} = 4 \qquad \text{(5.9.56)}$$

$$k_{41} = 3 \tag{5.9.57}$$

$$k_{41}k_{34}k_{23} = 18 \tag{5.9.58}$$

$$k_{21} = 2 \tag{5.9.59}$$

Obviously this set of equations presents a reduction in the number of terms and nonlinearity degree in comparison with the corresponding one in the same unknowns k_{ij} which would have been obtained by applying the transfer function approach directly to the model shown in Figure 5.9.2.

Step 5: By a second application of the Buchberger algorithm, if successful, a new set of equations in the k_{ij} can be found showing a simplified form over those given in Step 4:

$$k_{43} = 2 \tag{5.9.60}$$

$$k_{41} = 3 \tag{5.9.61}$$

$$k_{34} = 2 \tag{5.9.62}$$

$$k_{32} = 1 \tag{5.9.63}$$

$$k_{23} = 3 \tag{5.9.64}$$

$$k_{21} = 2 \tag{5.9.65}$$

$$k_{14} = 1 \tag{5.9.66}$$

$$k_{12} = 2 \tag{5.9.67}$$

$$k_{04} = 2 \tag{5.9.68}$$

$$k_{03} = 1 \tag{5.9.69}$$

This set gives the answer to the identifiability test. In this example, the parameters are uniquely identifiable since the system of equations has one and only one solution.

Example 2

The above example shows the utility of the identifiability algorithm in handling a rather complex model structure and a rich input-output experimental configuration. What happens when one is dealing with a model which is a priori locally identifiable, i.e. all parameters are identifiable but at least one has a finite number $(n > 1)$ of solutions? In other words, how does the final set of equations, the counterparts to those found in Step 5 of the previous case study, look?

Consider, for example, the three compartment model shown in Figure 5.9.3. Here input is into and measurements are taken from compartment 1; the loss is from one of the nonaccessible compartments.
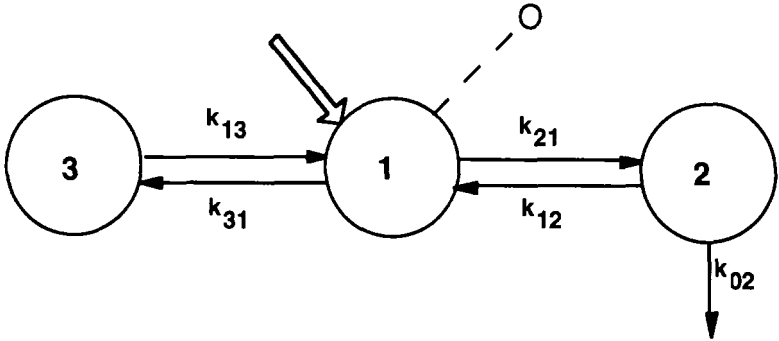
Figure 5.9.3.   The three compartment model used for Example 2.

Assuming that the volume of compartment 1 is unknown, the unknown parameters of interest are thus $k_{31}, k_{13}, k_{21}, k_{12}, k_{02}$ and V_1. By going through the same steps as explained in the previous example, one can generate a particular solution for the parameter vector, i.e. the k_{ij} and V_1, and use this to generate a numerical value for the observational parameters.

Suppose the particular solution is

$$K = \begin{pmatrix} -4 & 3 & 3 \\ 2 & -11 & 0 \\ 2 & 0 & -3 \end{pmatrix} v \qquad (5.9.70)$$

and

$$V_1 = 1 \qquad (5.9.71)$$

The counterpart of Step 5 of the algorithm, i.e. the second application of the Gröbner basis algorithm, for the above example gives the following set of equations:

$$V_1 = 1 \qquad (5.9.72)$$

$$19k_{02}^2 - 176k_{02} = -192 \tag{5.9.73}$$

$$88k_{31} - 19k_{02} = 24 \tag{5.9.74}$$

$$88k_{21} + 19k_{02} = 328 \tag{5.9.75}$$

$$16k_{13} - 19k_{02} = 200 \tag{5.9.76}$$

$$16k_{12} - 3k_{02} = 24 \tag{5.9.77}$$

This set gives the answer to the identifiability test. The system of equations has two solutions for k_{02} and thus for k_{21}, k_{12}, k_{31} and k_{13}. The only globally identifiable parameter is V_1. Thus the model is nonuniquely identifiable.

Example 3

What happens when dealing with an a priori nonidentifiable model? In this example, consider the three compartment model shown in Figure 5.9.3, but suppose the measurement is in compartment 2 instead of compartment 1. Assume in addition that the volume of the accessible compartment 2 is unknown. This situation is illustrated in Figure 5.9.4.
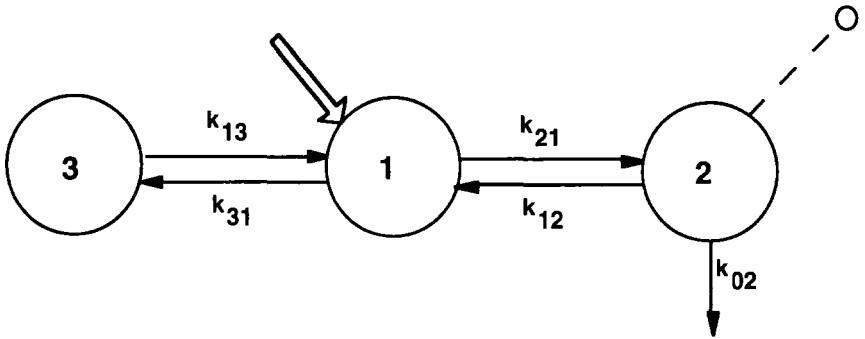
Figure 5.9.4. The three compartment model used in Example 3.

The parameters of interest are $k_{31}, k_{13}, k_{21}, k_{12}, k_{02}$ and V_2. Assume

$$K = \begin{pmatrix} -4 & 3 & 1 \\ 2 & -10 & 0 \\ 2 & 0 & -1 \end{pmatrix} \tag{5.9.78}$$

and

$$V_2 = \frac{1}{2} \tag{5.9.79}$$

is the particular solution of the unknown parameters.

Step 5 of the algorithm returns the following set of equations:

$$k_{31} + k_{12} + k_{02} + V_2 = 14 \tag{5.9.80}$$

$$k_{21} - V_2 = 0 \tag{5.9.81}$$

$$k_{13} = 1 \tag{5.9.82}$$

$$k_{12}^2 + 2k_{12}k_{02} + k_{12}V_2 - 15k_{12} + k_{02}^2 - 15k_{02} - V_2 = -46 \tag{5.9.83}$$

$$k_{12}V_2 = 14 \tag{5.9.84}$$

This system of equations has an infinite number of solutions for k_{31}, k_{02}, k_{21}, k_{12} and V_2, while there is one and only one solution for k_{13}.

Some Remarks

At the end of the identifiability test, two observations are in order:

1. the answer of GLOBI has been obtained by starting from a particular numerical point $\hat{\mathbf{p}}$ of parameter space; and

2. the analysis checks the uniqueness of solutions in the whole complex space C.

Regarding the first point, since the purpose of the algorithm is to provide a technique to check a priori structural identifiability, i.e. holding in the whole parameter space except for points which have probability zero to be considered (this set of points is said to have zero measure), one has to know if the results also hold for all $\hat{\mathbf{p}} \in P$. Note that a priori identifiability is a generic property, that is, if it holds for a generic point in the space it holds for almost all points belonging to that space, i.e. except for a zero measure set. However, the implementation of GLOBI has not been done symbolically, i.e. with a generic point (this would dramatically affect the complexity of the Gröbner basis calculation), but numerically. Thus the answer of GLOBI is true with probability one. Note that the numerical point strategy is a sound alternative to the symbolic one (required to test a structural property) since while

retaining mathematical rigor, it allows to significantly enlarge the class of testable models.

The second point stems from the fact that the algorithm checks a priori identifiability that is the uniqueness of parameter solution in the whole complex space C while we are interested in the solutions belonging to the compartmental space P, i.e. real and positive. If the results is global identifiability, i.e. all the model parameters are uniquely identifiable, this solution, belonging to C, has to coincide with the point $\hat{\mathbf{p}}$ of parameter space which has provided the particular value of the observational parameter vector $\hat{\mathbf{\Phi}}$. However, if the model results locally identifiable or nonidentifiable, to extend the identifiability results obtained in C to the compartmental space P, one must distinguish between two situations:

1. If some model parameters are nonuniquely identifiable, while the test provides the exact number of solutions in the whole complex space C, one cannot know how many of these solutions will be complex, how many will be real but negative and how many will be real and positive when the initial point provided by the experiment will be available. Thus, under these circumstances the number of solutions provided by the algorithm is an upper bound of the number of solutions which fall in P.

2. If some model parameters are nonidentifiable in C this will hold also in all the subspaces of C. Thus one can conclude that the model is nonidentifiable also in the real and positive space P.

The domain of applicability of the algorithm is difficult to establish rigorously in terms of model structure. In fact, this would require to define the limits of applicability of the Buchberger algorithm in solving the exhaustive summary of the model. However, the complexity of the exhaustive summary does not only depend on the model structure but also on the input-output configuration.

The software tool GLOBI which is based upon the algorithm described in this section has been used to test the a priori identifiability of a wide range compartmental models available in the literature. Most of these published models had fewer than 13 compartments with a structure where not all possible connections were present. There were multi input-multi output experiments characterized by "single compartment" and "sum of compartments" measurement configuration, standard inputs, i.e. into a single compartment, and split inputs, i.e. inputs split

between two or more compartments, and by letting unknown parameters be present also in the inputs and in the measurements. Of note is that GLOBI can also handle explicitly constraints, linear or nonlinear, on parameters:

$$\underline{h}(\underline{p}) = 0 \qquad\qquad (5.9.85)$$

where $\underline{h}$ is a vector of polynomial functions describing equality constraints among the components of $\underline{p}$. Examples of (5.9.86) are equalities among some transfer rate constants in a model, or a knowledge of the numerical value for some of the rate constants.

References

Audoly S., DAngiò L.: On the identifiability of linear compartmental systems: A revisited transfer function approach based on topological properties. *Math. Biosci. 66:*201–228, 1983.

Audoly S., DAngiò L., Saccomani M.P., Cobelli C.: Global identifiability of linear compartmental models. A computer algebra algorithm. *IEEE Trans. Biomed. Eng. 45:*36–47, 1998.

Decker T., Weispfenning W.: *Gröbner Bases: A Computational Approach to Commutative Algebra.* Springer-Verlag, New York, NY, 1993.

Buchberger B.: An algorithmical criterion for the solvability of algebraic system of equation. *Aequationes Mathematicae 4*:45–50, 1988.

Carson E.R., Cobelli C., Finkelstein L.: *Modeling and Identification of Metabolic and Endocrine Systems.* Wiley, New York, NY, 1983.

Chao-Min Chen B., Landaw E.M., DiStefano J.J. III: Algorithms for the identifiable parameter combinations and parameter bounds of unidentifiable catenary compartmental models. *Math. Biosci. 76:*59–68, 1985.

Cobelli C., DiStefano J.J. III: Parameter and structural identifiability concepts and ambiguities: A critical review and analysis. *Am. J. Physiol. 239*:R7–R24, 1980.

Cobelli C., Lepschy A., Romanin Jacur G.: Identifiability of compartmental systems and related structural properties. *Math. Biosci. 44:*1–18, 1979a.

Cobelli C., Lepschy A., Romanin Jacur G.: Identifiability results on some constrained compartmental systems. *Math. Biosci. 47*:173–196, 1979b.

Cobelli C., Toffolo G.: Identifiability from parameter bounds. Structural and numerical aspects. *Math. Biosci. 71*:237–243, 1984.

Cobelli C., Toffolo G.: Theoretical aspects and practical strategies for the identification of unidentifiable compartmental systems. Walter E.

(ed.): *Identifiability of Parametric Models.* Pergamon Press, Oxford, 85–91, 1987.

DiStefano J.J. III: Complete parameter bounds and quasiidentifiability conditions for a class of unidentifiable linear systems. *Math. Biosci.* *65*:51–68, 1983.

Landaw E.M., Chao-Min Chen B., DiStefano J.J. III: An algorithm for the identifiable parameter combinations of the general mammillary compartmental model. *Math. Biosci. 72*:199–212, 1984.

Maple V Learning Guide (Version A): Release 5. Springer-Verlag, New York, NY, 1997.

Norton J.P.: An investigation of the sources of non-uniqueness in deterministic identifiability. *Math. Biosci. 60*:89–108, 1982.

Norton J.P.: Normal-mode identifiability analysis of linear compartmental systems in linear stages. , *Math. Biosci. 50*:95–115, 1980.

Reduce Users Manual: Version 3.6. RAND Publication, Santa Monica, CA, 1995.

Walter E., Lecourtier Y.: *Math. Biosci. 56:*1–25, 1981.

This page intentionally left blank.

Chapter 6

USING THE TRACER MODEL
TO ESTIMATE KINETIC PARAMETERS

6.1   INTRODUCTION

As stated previously, the goal of compartmental modeling is to quantify from the tracer model a number of kinetic parameters. Some of them, such as mean residence times, apply both to the tracer and tracee system. Others specifically describe the behavior of the tracee; these include the tracee mass in the nonaccessible compartments, tracee production and intercompartmental fluxes. Parameters that apply both to the tracer and tracee system can be calculated by applying the formulas given in Chapter 4. The evaluation of the parameters that apply to the tracee system only is a more complex task, since it requires solving the tracee steady state system equations. Thus specific conditions must hold on the tracee system to guarantee a unique solution of these equations.

Consider the a priori uniquely identifiable model shown in Figure 6.1.1. What is estimated from the data are the rate constants k_{21}, k_{12} and k_{01}, and the volume V_1 or mass M_1 of the accessible compartment. Thus one has directly an estimate for the fluxes leaving compartment 1:

$$F_{01} = k_{01} M_1 \qquad\qquad (6.1.1)$$

$$F_{21} = k_{21} M_1 \qquad\qquad (6.1.2)$$

In order to evaluate the remaining tracee fluxes, i.e. F_{12} and U_1, and the mass M_2 in the nonaccessible compartment 2, the steady state equations for the tracee system have to be considered. For the model shown in Figure 6.1.1, they can be written:
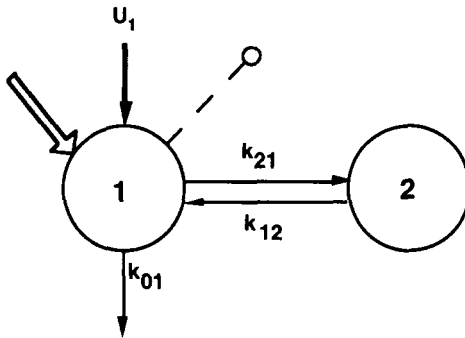
Figure 6.1.1. A two compartment model with tracer and tracee input only into compartment 1, and samples taken from compartment 1. See text for additional explanation.

$$U_1 + k_{12}M_2 - (k_{21} + k_{01})M_1 = 0$$
$$k_{21}M_1 - k_{12}M_2 = 0 \tag{6.1.3}$$

These are two independent equations in two unknowns, U_1 and M_2; the solution is given by

$$M_2 = \frac{k_{21}}{k_{12}}M_1 \qquad U_1 = k_{01}M_1 \tag{6.1.4}$$

It is now possible to evaluate the fluxes leaving the nonaccessible compartment 2, $F_{12} = k_{12}M_2$, and parameters related to the whole system such as the total tracee mass $M_{tot} = M_1 + M_2$.

There are situations, however, where even if the model is a priori uniquely identifiable, it is not possible to evaluate all of the tracee parameters. Consider for instance the same structure as that in Figure 6.1.1, but assume now that tracee production can enter both compartments, i.e. $U_2 \neq 0$ as well as $U_1 \neq 0$. This is shown below in Figure 6.1.2.

In this case, (6.1.1) and (6.1.2) are still valid, the counterpart to (6.1.3) becomes

$$U_1 + k_{12}M_2 - (k_{21} + k_{01})M_1 = 0$$
$$U_2 + k_{21}M_1 - k_{12}M_2 = 0 \tag{6.1.5}$$

This system of two independent equations has three unknowns, U_1, U_2, and M_2, meaning there is no unique solution. Only the sum $U_1 + U_2 =$
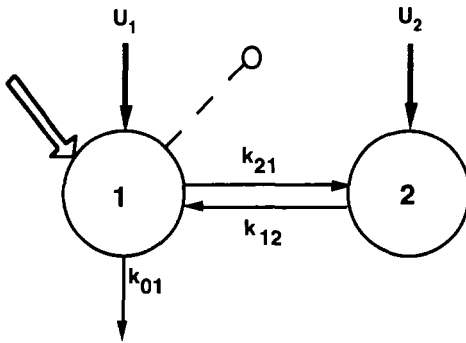
Figure 6.1.2. A two compartment model with tracer input and samples in compartment 1, but tracee input in both compartment 1 and 2. See text for additional explanation.

$k_{01}M_1$ can be evaluated uniquely, while there are an infinite number of solutions for the individual U_1, U_2 and M_2, and thus for the flux F_{12} and the total mass M_{tot}.

Consider now a generic n-compartment model. The evaluation of the tracee variables requires the solution of a system of n algebraic linear equations derived from the tracee steady state equation:

$$\mathbf{KM} + \mathbf{U} = 0 \qquad (6.1.6)$$

If the model is a priori uniquely identifiable, the matrix of rate constants $\mathbf{K}$ and the masses in the accessible pools are known uniquely. The unknowns are the masses in the nonaccessible compartments and the de novo production rates, i.e. those U_i which are not zero. A unique value for these variables can be obtained only if conditions on the tracee system hold which guarantee unique solution of the steady state system (6.1.6).

It is important, therefore, to realize there are two situation that must be satisfied in order to obtain unique estimates of the tracee parameters. One is that the model is uniquely identifiable; the other is that there is unique solution to the steady state equations. For convenience, in what follows, the estimation of kinetic parameters will be discussed first for the case where the tracer model is uniquely identifiable. Then how to deal with a nonidentifiable tracer model will be discussed.

6.2   ESTIMATION FROM A PRIORI UNIQUELY IDENTIFIABLE MODELS

For an a priori uniquely identifiable n-compartment model, the elements of the **K** matrix and the masses in the accessible pools are known from the tracer experiment. As already discussed in §4.4.3, the matrix **K** can be assumed to be invertible. The tracer-tracee kinetic parameters such as the elements of the mean residence time matrix can also be uniquely estimated whereas the estimation of the kinetic parameters which specifically describe the behavior of the tracee requires, as anticipated in §6.1, the solution of the steady state system (6.1.6). It is a system of n linear algebraic equations where the matrix **K** is known uniquely since the tracer model is a priori identifiable. In addition, the invertibility of **K** assures that the system equations are independent. Thus, the only condition for the system to have a unique solution is that the number of unknowns, denoted by N_u, equals n, the number of equations, or equivalently the number of compartments. Usually the unknowns are the masses in all of the nonaccessible compartments and the de novo productions; their number N_u equals n if the number of de novo production fluxes equals the number of accessible compartments. This means that the tracee parameters can be evaluated from an experiment where only one compartment is accessible if the tracee production enters the system in a single compartment. In the case where two compartments are accessible, two entry sites for the tracee are admissible, and so forth. It is worth noting that in those cases where a priori knowledge exists on some of the tracee variables, there will be constraints among them that will affect N_u. For instance, consider a 5 compartment model and suppose a priori knowledge is available on the total tracee mass. If only compartment 1 is accessible, and de novo production enters compartments 1 and 3, N_u is the number of nonaccessible compartments plus the number of tracee entry sites minus the number of constraints; in this case, $N_u = 4 + 2 - 1 = 5$. This number equals the number of compartments, hence the tracee variables are uniquely identifiable from the input-output experiment.

In the following, three different situations will be discussed:

1. If $N_u = n$ there is a unique solution for **U** and the nonaccessible masses M_i;

2. if $N_u > n$, there are an infinite number of solutions for **U** and the nonaccessible masses M_i; and

3. if $N_u < n$, constraints among the k_{ij} arise from the steady state equation (6.1.6).

$N_u = n$: Unique solution for the tracee variables.

If the number of unknowns equals the number of compartments, then the tracee steady state system (6.1.6) can be solved uniquely, and all the tracee variables are uniquely identifiable. In practice, one can solve the system analytically as was done in §6.1 for the two compartment model shown in Figure 6.1.1. If there are known constraints among the tracee variables, they must be explicitly considered in solving the system. This procedure is simple when the number of compartments is small, but may become complex if the number of compartments is large. It is convenient to derive general expressions for the unknown tracee variables in terms of the elements θ_{ij} of the mean residence time matrix Θ

To evaluate the tracee variables, write the solution for the masses M of the tracee steady state system

$$\mathbf{M} = -\mathbf{K}^{-1}\mathbf{U} = \Theta\mathbf{U} \qquad (6.2.1)$$

Consider first the case where only one compartment, say compartment 1 is accessible, and assume that there is de novo production entering compartment h so that the number N_u of unknowns, that is the tracee masses $M_2, \cdots, M_n$ and tracee production U_h equals n. The vector U has only one nonzero element, U_h, thus from (6.2.1) the components of M are

$$M_1 = \theta_{1h}U_h \qquad \cdots \qquad M_n = \theta_{nh}U_h \qquad (6.2.2)$$

The de novo production U_h can be derived by solving the first equation:

$$U_h = \frac{M_1}{\theta_{1h}} \qquad (6.2.3)$$

and the tracee masses in the nonaccessible compartments can be evaluated

$$M_i = \theta_{ih}U_h = \frac{\theta_{ih}}{\theta_{1h}}M_1 \qquad i = 2, \cdots, n \qquad (6.2.4)$$

Equations (6.2.3) and (6.2.4) are general expressions of the unknown tracee variables as a function of M_1 and the θ_{ij}

From the knowledge of the masses in all compartments, all tracee fluxes can be evaluated

$$F_{ij} = k_{ij}M_j \qquad i = 0, \cdots, n, \qquad j = 1, \cdots, n \qquad i \neq j \qquad (6.2.5)$$

The total tracee mass (4.5.1) is then equal to

$$M_{\text{tot}} = \sum_{i=1}^{n} M_i = \sum_{i=1}^{n} \theta_{ih} U_h = MRT_h U_h \qquad (6.2.6)$$

The parameter M_{tot} is the product of the tracee production rate U_h times MRT_h which represents the mean residence time in the system of tracee particles since they enter the system in compartment h.

In addition, one can calculate the total equivalent distribution volume, V_{tot}, using (4.5.2):

$$V_{\text{tot}} = \frac{M_{tot}}{C_1} \qquad (6.2.7)$$

Consider the two compartment model shown in Figure 6.1.1. Equation (6.2.2) becomes

$$M_1 = \theta_{11} U_1$$
$$M_2 = \theta_{21} U_1 \qquad (6.2.8)$$

thus

$$U_1 = \frac{M_1}{\theta_{11}} \qquad (6.2.9)$$

$$M_2 = \frac{\theta_{21}}{\theta_{11}} M_1 \qquad (6.2.10)$$

The total tracee mass in the system M_{tot} is

$$M_{\text{tot}} = M_1 + M_2 = (\theta_{11} + \theta_{21}) U_1 = MRT_1 U_1 \qquad (6.2.11)$$

The parameter MRT_1 measures the mean residence time of tracee particles since they enter the system from compartment 1.

If tracee production is into compartment 2 instead of compartment 1, (6.2.2) becomes

$$M_1 = \theta_{12} U_2$$
$$M_2 = \theta_{22} U_2 \qquad (6.2.12)$$

and then

$$U_2 = \frac{M_1}{\theta_{12}}$$
$$M_2 = \frac{\theta_{22}}{\theta_{12}} M_1 \qquad (6.2.13)$$

$$M_{\text{tot}} = M_1 + M_2 = (\theta_{12} + \theta_{22}) U_2 = MRT_2 U_2$$

The mean residence time in the system of the tracee is now MRT_2 since the tracee particles now enter the system from compartment 2.

Consider now the situation where two compartments, say 1 and 2, of an *a priori* uniquely identifiable n compartment model are accessible, and suppose there is de novo tracee input into two compartments, say h and k. Thus in the vector **U**, there are two nonzero components, U_h and U_k. There are now $n - 2$ unknown tracee masses, $M_3, \cdots, M_n$ Thus the number of unknown parameters is n, the $n - 2$ masses and the two tracee inputs. Since the number of unknowns equals the number of compartments the steady state system can be solved uniquely. From (6.2.2), the components of **M** are:

$$M_1 = \theta_{1h}U_h \quad + \quad \theta_{1k}U_k$$
$$\vdots \qquad\qquad\qquad\qquad (6.2.14)$$
$$M_n = \theta_{nh}U_h \quad + \quad \theta_{nk}U_k$$

Using the first two equations, the productions U_h and U_k can be expressed as functions of M_1 and M_2:

$$U_h = \frac{\theta_{1k}M_2 - \theta_{2k}M_1}{\theta_{2h}\theta_{1k} - \theta_{1h}\theta_{2k}}$$
$$(6.2.15)$$
$$U_k = \frac{\theta_{1h}M_2 - \theta_{2h}M_1}{\theta_{2h}\theta_{1k} - \theta_{1h}\theta_{2k}}$$

Substituting these values into (6.2.14), the tracee masses for the nonaccessible compartment can easily be evaluated.

The total tracee mass in the system can be written

$$M_{\text{tot}} = \sum_{i=1}^{n} M_1 = \sum_{i=1}^{n} \theta_{ih}U_h + \sum_{i=1}^{n} \theta_{ik}U_k = MRT_hU_h + MRT_kU_k \quad (6.2.16)$$

The parameter M_{tot} is thus expressed as a function of tracee production rates into compartments h and k and the mean residence times in the system for tracee particles entering de novo into compartments h and k.

$N_u > n$: Infinite number of solutions for the tracee variables.

What happens in the case where the number of unknown tracee variables N_u exceeds the number of compartments? In this situation, even if the tracer model is a priori identifiable, the unknown tracee variables cannot be solved uniquely since the tracee steady state system has an infinite number of solutions. However, it is possible to obtain upper and lower bounds for their values, i.e. to identify the interval of values in which the parameters must lie.

Consider the model shown in Figure 6.1.2, and express the tracee masses according to (6.2.14):

$$M_1 = \theta_{11}U_1 + \theta_{12}U_2$$
$$M_2 = \theta_{21}U_1 + \theta_{22}U_2$$

(6.2.17)

Since the only loss is from compartment 1, $\theta_{11} = \theta_{12}$. The sum $U_1 + U_2$ can be derived from (6.2.17):

$$U_1 + U_2 = \frac{M_1}{\theta_{11}}$$

(6.2.18)

The sum $U_1 + U_2$ provides the upper bound for the individual U_1 and U_2 while the lower bound is zero:

$$U_1^{\min} = 0 \le U_1 \le \frac{M_1}{\theta_{11}} = U_1^{\max}$$
$$U_2^{\min} = 0 \le U_2 \le \frac{M_1}{\theta_{11}} = U_2^{\max}$$

(6.2.19)

In order to derive upper and lower bounds for M_2, consider from the properties of the Θ matrix the following inequalities hold:

$$\theta_{12} \le \theta_{11} \qquad \theta_{21} \le \theta_{22}$$

(6.2.20)

Then from (6.2.17), for M_2 one has

$$\theta_{21}(U_1 + U_2) \le M_2 \le \theta_{22}(U_1 + U_2)$$

(6.2.21)

Using (6.2.18), the upper and lower bounds for M_2 as a function of M_1 and the θ_{ij} are

$$M_2^{\min} = \frac{\theta_{21}}{\theta_{11}} M_1 \le M_2 \le \frac{\theta_{22}}{\theta_{11}} M_1 = M_2^{\max}$$

(6.2.22)

Concerning the intercompartmental fluxes, $F_{01} = k_{01}M_1$ and $F_{21} = k_{21}M_1$ can be calculated uniquely while F_{12} has an infinite number of values bounded according to the following formula:

$$F_{12}^{\min} = \frac{k_{12}\theta_{21}}{\theta_{11}} M_1 \le F_{12} = k_{12}M_2 \le \frac{k_{12}\theta_{22}}{\theta_{11}} M_1 = F_{12}^{\max}$$

(6.2.23)

It is easy to verify that bounds for U_1, U_2, M_2 and F_{12} can also be calculated by defining the submodels of the original structure in a manner analogous with the procedure outlined in Chapter 5 for deriving bounds for interval identifiable tracer parameters. In fact, when $U_1 =$

0, i.e. it reaches its lower bound, U_2, M_2 and F_{12} reach their upper bounds. Conversely, when $U_2 = 0$, $U_1 = U_1^{\max}$, $M_2 = M_2^{\min}$, and $F_{12} = F_{12}^{\min}$. Therefore, upper and lower bounds for the nonidentifiable tracee variables can be generated from the tracee variables of two submodels of the original structure (see Figure 6.2.1) obtained by first letting $U_1 = 0$ and then $U_2 = 0$.
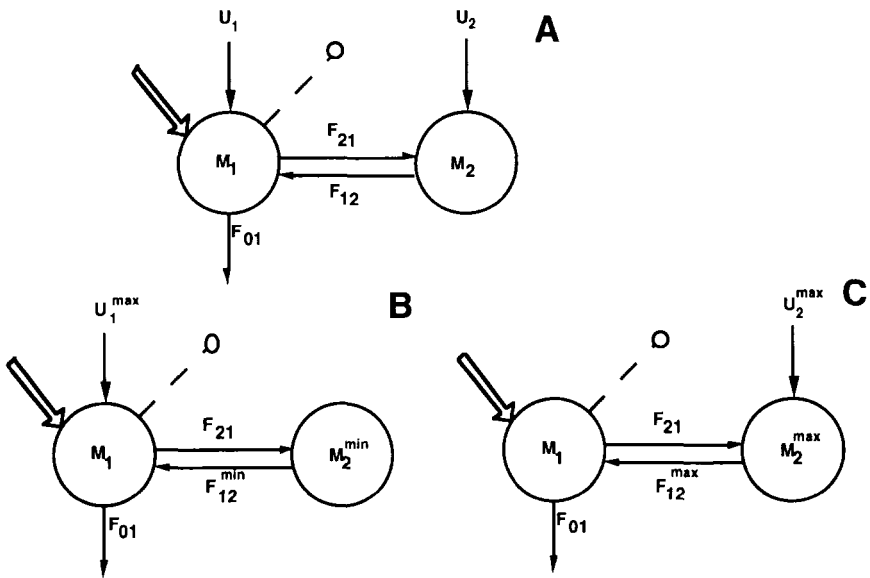
Figure 6.2.1. Panel A: A two compartment model. The tracer model is *a priori* uniquely identifiable but the tracee variables U_1, U_2, M_2 and F_{12} have an infinite number of solutions. Bounds for them can be interpreted as parameters of the two submodels shown in Panels B and C. The tracee variables of these submodels can be solved uniquely.

The concepts presented above can easily be extended to a generic n compartment model. Consider, for instance, the situation where only compartment 1 is accessible, but the tracee de novo production enters into compartments h and k, i.e. U_h and U_k are nonzero. Then there are $n + 1$ tracee unknowns, the masses in the $n - 1$ nonaccessible compartments and the two productions, but only n equations. Thus there are an infinite number of solutions for the tracee parameters. From (6.2.14), the tracee mass in compartment 1 can be expressed

$$M_1 = \theta_{1h}U_h + \theta_{1k}U_k \qquad (6.2.24)$$

A relationship between U_h and U_k can be derived

$$U_h = \frac{M_1 - \theta_{1k}U_k}{\theta_{1h}} \qquad (6.2.25)$$

from which the upper bound for U_h can be obtained when $U_k = 0$, while the lower bound for U_j is zero:

$$U_h^{\min} = 0 \le U_h \le \frac{M_1}{\theta_{1h}} = U_h^{\max} \qquad (6.2.26)$$

Similarly for U_k

$$U_k^{\min} = 0 \le U_k \le \frac{M_1}{\theta_{1k}} = U_k^{\max} \qquad (6.2.27)$$

In order to derive upper and lower bounds for the tracee masses in the nonaccessible compartments, say for example compartment 2, consider the system (6.2.1) and write for M_2

$$M_2 = \theta_{2h}U_h + \theta_{2k}U_k \qquad (6.2.28)$$

By substituting the expression (6.2.25) for U_k, one has

$$M_2 = \frac{\theta_{2h}}{\theta_{1h}}M_1 + (\theta_{2k} - \theta_{1k}\frac{\theta_{2h}}{\theta_{1h}})U_k \qquad (6.2.29)$$

Suppose now that the following inequality hold:

$$\theta_{2k} - \theta_{1k}\frac{\theta_{2h}}{\theta_{1h}} > 0 \qquad (6.2.30)$$

For convenience, this can be rewritten

$$\frac{\theta_{2k}}{\theta_{1k}} > \frac{\theta_{2h}}{\theta_{1h}} \qquad (6.2.31)$$

Then the lower bound for M_2 is reached when U_k reaches is minimum value, i.e. $U_k = 0$, and the upper bound is reached when U_k reaches it maximum value, $U_k = \frac{M_1}{\theta_{1k}}$. Thus

$$M_2^{\min} = \frac{\theta_{2h}}{\theta_{1h}}M_1 \le M_2 \le \frac{\theta_{2k}}{\theta_{1k}}M_1 = M_2^{\max} \qquad (6.2.32)$$

If on the other hand, $\frac{\theta_{2k}}{\theta_{1k}} < \frac{\theta_{2h}}{\theta_{1h}}$, then the upper and lower bounds exchange:

$$M_2^{\min} = \frac{\theta_{2k}}{\theta_{1k}} M_1 \leq M_2 \leq \frac{\theta_{2h}}{\theta_{1h}} M_1 = M_2^{\max} \qquad (6.2.33)$$

As regards the intercompartmental fluxes, only those which leave the accessible compartment can be uniquely evaluated. The remaining fluxes have an infinite number of solutions, but it is easy to evaluate upper and lower bounds from the upper and lower bounds of the tracee masses $M_i, i = 2, \cdots, n$.

$$F_{ij}^{\min} = k_{ij} M_j^{\min} \leq F_{ij} = k_{ij} M_j \leq k_{ij} M_j^{\max} = F_{ij}^{\max} \qquad (6.2.34)$$

As with the two compartment model, the upper and lower bounds for all tracee parameters of a generic n compartment model can be calculated from submodels of the original model structure obtained by letting U_h and U_k equal zero. For example, when U_h equals zero, U_k reaches its upper bound as well as the tracee masses in those compartment l for which $\frac{\theta_{lk}}{\theta_{1k}} < \frac{\theta_{lh}}{\theta_{1h}}$ while the tracee masses in the remaining compartments reach their lower value.

$N_u < n$: Constraints among the parameters.

The last situation to be examined arises when the number of unknown tracee variables is less than the number of equations. This results in constraints among the parameters, as illustrated in the following example.

Consider the model shown in Figure 6.2.2 where two compartments are accessible but there is de novo production only into compartment 1.

In this situation, (6.2.9) becomes

$$\begin{aligned} M_1 &= \theta_{11} U_1 \\ M_2 &= \theta_{21} U_1 \end{aligned} \qquad (6.2.35)$$

where M_1, M_2, θ_{11} and θ_{21} are known from the tracer experiment. This situation where the number of unknowns is less than the number of equations results in a constraint among the parameters:

$$\frac{M_1}{\theta_{11}} = \frac{M_2}{\theta_{21}} \qquad (6.2.36)$$

or, from the expressions for θ_{11} and θ_{21} in terms of the k_{ij}

$$M_1 k_{21} = M_2 (k_{02} + k_{12}) \qquad (6.2.37)$$

This constraint has to be explicitly considered when estimating k_{ij}, M_1 and M_2 from the tracer data in order to make the tracer system compatible with the *a priori* knowledge of a single tracee production. This
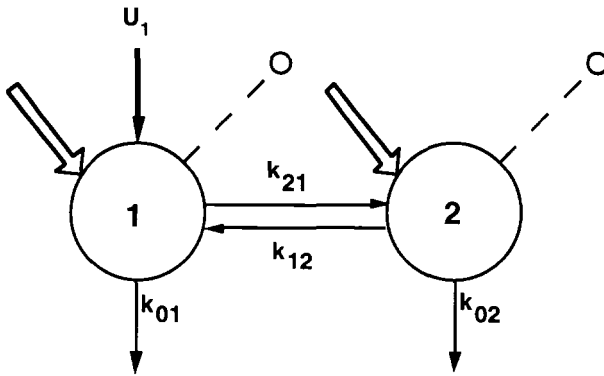
Figure 6.2.2. A multiple input-output experiment on a two compartment model with tracee input only into compartment 1. See text for additional explanation.

can be accomplished if one parameter, for instance k_{21}, is expressed as a function of the others, $k_{21} = \frac{M_2}{M_1}(k_{02} + k_{12})$, and the model equations are parameterized in terms of k_{12}, k_{01}, k_{02}, M_1 and M_2:

$$\frac{dm_1}{dt} = -(k_{01} + \frac{M_2}{M_1}(k_{02} + k_{12}))m_1(t) + k_{12}m_2(t) + u_1(t)$$

$$\frac{dm_2}{dt} = \frac{M_2}{M_1}(k_{02} + k_{12})m_1(t) - (k_{02} + k_{12})m_2(t)$$

The formulas given in this section to calculate the tracee kinetic parameters for a generic, uniquely identifiable n-compartmental model are summarized below in Table 6.2.1 for the one and two accessible compartment model situations. The parameters, and their upper and lower bounds, are expressed in terms of the k_{ij}, the elements θ_{ij} of the mean residence time matrix, and the mass in the accessible compartments, assumed without loss of generality to be M_1 or M_1 and M_2. These formulas are shown in Table 6.2.2 for the two compartment model with an
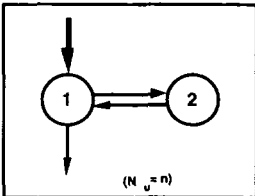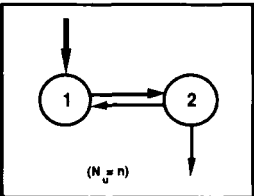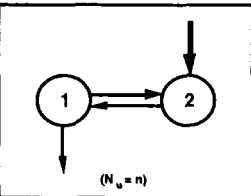
Accessible compartment	*1*	*1*	*1,2*	*1,2*
Tracer input into compartment	h $(N_u = n)$	h, k $(N_u > n)$	h $(N_u < n)$	h, k $(N_u = n)$
U_h	$\frac{1}{\theta_{1h}} M_1$	$U_h^{\min} = 0$ $U_h^{\max} = \frac{1}{\theta_{1h}} M_1$	$\frac{1}{\theta_{1h}} M_1 = \frac{1}{\theta_{2h}} M_2$ *	$\frac{\theta_{1k} M_2 - \theta_{2k} M_1}{\theta_{2h}\theta_{1k} - \theta_{1h}\theta_{2k}}$
U_k	$-$	$U_k^{\min} = 0$ $U_k^{\max} = \frac{1}{\theta_{1k}} M_1$	$--$	$\frac{\theta_{1h} M_2 - \theta_{2h} M_1}{\theta_{2h}\theta_{1k} - \theta_{1h}\theta_{2k}}$
M_1	$\theta_{1h} U_h$ $i = 2, ..., n$	$M_i^{\min} = \min[\theta_{ih} U_h^{\max}, \theta_{ik} U_k^{\max}]$ $M_i^{\max} = \max[\theta_{ih} U_h^{\max}, \theta_{ik} U_k^{\max}]$ $i = 2, ..., n$	$\theta_{ih} U_h$ $i = 3, ..., n$	$\theta_{ih} U_h + \theta_{ik} U_k$ $i = 3, ..., n$
F_{ij}	$k_{ij} M_j$ $i = 0, ..., n$ $j = 1, ..., n$	$k_{i1} M_1 \quad i = 0, ..., n \; ; \; j = 1$ $F_{ij}^{\min} = k_{ij} M_j^{\min} \; ; \; F_{ij}^{\max} = k_{ij} M_j^{\max}$ $i = 0, ..., n \; ; \; j = 2, ..., n$	$k_{ij} M_j$ $i = 0, ..., n$ $j = 1, ..., n$	$k_{ij} M_j$ $i = 0, ..., n$ $j = 1, ..., n$

*This equality results in a constraint among model parameters.
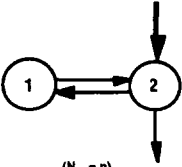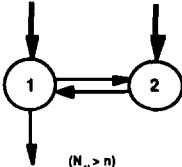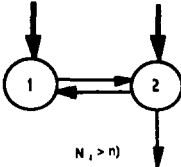
input-output tracer experiment in compartment 1. The tracee kinetic parameters in this table can be expressed as a function of the k_{ij} and the mass in the accessible compartment, M_1

Table 6.2.2.   Formulas for tracee kinetic parameters of uniquely identifiable two compartment models*

	$(N_u = n)$	$(N_u = n)$	$(N_u = n)$
U_1	$k_{01} M_1$	$\dfrac{k_{02}\, k_{21}}{k_{02} + k_{12}} M_1$	0
U_2	0	0	$k_{01} M_1$
M_2	$\dfrac{k_{21}}{k_{12}} M_1$	$\dfrac{k_{21}}{k_{02} + k_{12}} M_1$	$\dfrac{k_{01} + k_{21}}{k_{12}} M_1$
F_{21}	$k_{21} M_1$	$k_{21} M_1$	$k_{21} M_1$
F_{12}	$k_{21} M_1$	$\dfrac{k_{12}\, k_{21}}{k_{02} + k_{12}} M_1$	$(k_{01} + k_{21}) M_1$
F_{01}	$k_{01} M_1$	0	$k_{01} M_1$
F_{02}	0	$\dfrac{k_{02}\, k_{21}}{k_{02} + k_{12}} M_1$	0

*Compartment 1 is accessible, thus M_1 and the k_{ij} are known from the tracer experiment.

Table 6.2.2 (continued).

	$(N_u = n)$	$(N_u > n)$	$(N_i > n)$
U_1	0	$U_1^{min} = 0$ $U_1^{max} = k_{01} M_1$	$U_1^{min} =)$ $U_1^{max} = \frac{k_{02}\,k_{21}}{k_{12} + k_{12}} M_1$
U_2	$\frac{k_{12}\,k_{21}}{k_{12}} M_1$	$J_2^{min} = 0$ $J_2^{max} = k_{01} M_1$	$U_2^{min} =)$ $U_2^{max} = \frac{k_{12}\,k_{21}}{k_{12}} M_1$
M_2	$\frac{k_{21}}{k_{12}} M_1$	$M_2^{min} = \frac{k_{21}}{k_{12}} M_1$ $M_2^{max} = \frac{k_{01} + k_{21}}{k_{12}} M_1$	$M_2^{min} = \frac{k_{21}}{k_{02} + k_{12}} M_1$ $M_2^{max} = \frac{k_{21}}{k_{12}} M_1$
F_{21}	$k_{21} M_1$	$k_{21} M_1$	$k_{21} M_1$
F_{12}	$k_{21} M_1$	$F_{12}^{min} = k_{21} M_1$ $F_{12}^{max} = (k_{01} + k_{21}) M_1$	$F_{12}^{min} = \frac{k_{12}\,k_{21}}{k_{12} + k_{12}} M_1$ $F_{12}^{max} = k_{21} M_1$
F_{01}	)	$k_{01} M_1$	)
F_{02}	$\frac{k_{02}\,k_{21}}{k_{12}} M_1$	0	$F_{02}^{min} = \frac{k_{02}\,k_{21}}{k_{12} + k_{12}} M_1$ $F_{02}^{max} = \frac{k_{02}\,k_{21}}{k_{12}} M_1$

*Compartment 1 is accessible, thus M_1 and the k_{ij} are known from the tracer experiment.

6.3 ESTIMATION FROM INTERVAL IDENTIFIABLE MODELS

Up to this point, only a priori uniquely identifiable tracer models have been considered, i.e. models for which the k_{ij} can be uniquely estimated from the tracer experiment. The two compartment model will be used to illustrate how to deal with nonidentifiable models.

Consider the model shown in Figure 6.3.1.
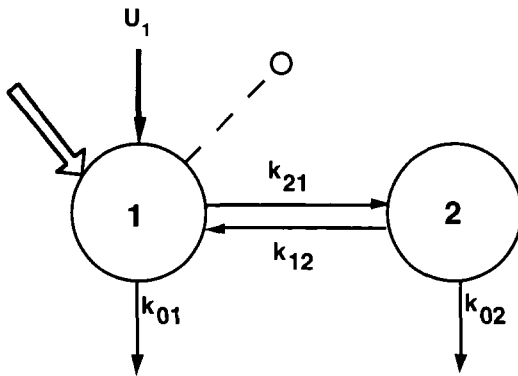
Figure 6.3.1. A two compartment model with tracer and tracee input into compartment 1, and samples from compartment 1. See text for additional explanation.

If compartment 1 is the only accessible compartment, the model is not identifiable, and only some combinations of the rate constants, namely the observational parameters V_1, $k_{11} = -(k_{01} + k_{21})$, $k_{22} = -(k_{02} + k_{12})$ and $k_{12}k_{21}$ are uniquely identifiable. However, as shown in §5.4, it is possible to obtain parameter bounds for all the nonidentifiable parameters. Hence only the kinetic parameters which can be expressed as a function of the observational parameters can be calculated uniquely, while for the others, only the interval of admissible values can be calculated.

Consider first the Θ matrix for the model shown in Figure 6.3.1:

$$\Theta = \begin{pmatrix} \theta_{11} & \theta_{12} \\ \theta_{21} & \theta_{22} \end{pmatrix} = \frac{1}{k_{11}k_{22} - k_{12}k_{21}} \begin{pmatrix} -k_{22} & k_{12} \\ k_{21} & -k_{11} \end{pmatrix} \qquad (6.3.1)$$

The elements θ_{11} and θ_{22} can be calculated even if the model is not uniquely identifiable since they depend only on the observational parameters. For the elements θ_{21} and θ_{12}, it is only possible to obtain upper and lower bounds from bounds on k_{12} and k_{21} respectively:

$$\theta_{21}^{\min} = \frac{k_{12}^{\min}}{k_{11}k_{22} - k_{21}k_{12}} \leq \theta_{21} \leq \frac{k_{12}^{\max}}{k_{11}k_{22} - k_{21}k_{12}} = \theta_{21}^{\max} \qquad (6.3.2)$$

$$\theta_{12}^{\min} = \frac{k_{21}^{\min}}{k_{11}k_{22} - k_{21}k_{12}} \leq \theta_{12} \leq \frac{k_{21}^{\max}}{k_{11}k_{22} - k_{21}k_{12}} = \theta_{12}^{\max} \qquad (6.3.3)$$

From (6.3.2) and (6.3.3), bounds for the mean residence times MRT_1 and MRT_2 can be calculated:

$$MRT_1^{\min} = \theta_{11} + \theta_{21}^{\min} \leq MRT_1 \leq \theta_{11} + \theta_{21}^{\max} = MRT_1^{\max} \qquad (6.3.4)$$

$$MRT_2^{\min} = \theta_{22} + \theta_{12}^{\min} \leq MRT_2 \leq \theta_{22} + \theta_{12}^{\max} = MRT_2^{\max} \qquad (6.3.5)$$

If the tracee de novo production enters compartment 1 only, then the tracee steady state equations are

$$\begin{aligned} M_1 &= \theta_{11} U_1 \\ M_2 &= \theta_{21} U_1 \end{aligned} \qquad (6.3.6)$$

Hence $U_1 = \frac{M_1}{\theta_{11}}$ can be calculated uniquely while $M_2 = \frac{\theta_{21} M_1}{\theta_{11}}$ can assume an infinite number of values which are bounded by

$$M_2^{\min} = \frac{\theta_{21}^{\min} M_1}{\theta_{11}} \leq M_2 \leq \frac{\theta_{21}^{\max} M_1}{\theta_{11}} = M_2^{\max} \qquad (6.3.7)$$

Upper and lower bounds for tracee fluxes F_{21}, F_{01} and F_{02} can then be calculated:

$$F_{21}^{\min} = k_{21}^{\min} M_1 \leq F_{21} = k_{21} M_1 \leq k_{21}^{\max} M_1 = F_{21}^{\max} \qquad (6.3.8)$$

$$F_{01}^{\min} = 0 \leq F_{01} = k_{01} M_1 \leq k_{01}^{\max} M_1 = F_{01}^{\max} \qquad (6.3.9)$$

$$F_{02}^{\min} = 0 \leq F_{02} = k_{02} M_2 \leq k_{02}^{\max} M_2^{\max} = F_{02}^{\max} \qquad (6.3.10)$$

The tracee flux F_{12} can be uniquely calculated since it only depends on the observational parameters and the tracee de novo production:

$$F_{12} = k_{12} M_2 = k_{12} \theta_{21} U_1 = \frac{k_{12} k_{21}}{k_{11} k_{22} - k_{12} k_{21}} U_1 \qquad (6.3.11)$$

These concepts can be extended to a generic n-compartment model; only the kinetic parameters which depend upon the observational parameters can be calculated uniquely while other parameters can assume an infinite number of values, not only because the tracer parameters k_{ij} have an infinite number of solutions between their upper and lower bounds due to the nonidentifiability of the tracer system, but also because the tracee steady state system may have an infinite number of solutions. Calculations are easy for simple models such as the two compartment model of the previous example but become quite cumbersome for more complex models. A different approach to evaluate kinetic parameters of a nonidentifiable model is based on the use of submodels as defined in Chapter 5. They are obtained from the original model structure by setting some k_{ij} parameters equal to zero, and eventually

some production equal to zero so that their tracee parameters, which represent the bounds for tracee parameters of the original structure, can be solved uniquely.

Bounds for the parameters of the nonidentifiable compartmental model shown in Figure 6.3.2A can be generated by using the submodels given in Figure 6.3.2B and C. In fact, when k_{02} reaches its lower bound of zero, k_{01} and k_{12} equal their maximum and k_{21} its minimum. Hence θ_{21}, MRT_1, M_2 and F_{21} reach their lower bounds while θ_{12}, MRT_2 and F_{01} assume their upper bounds. Similarly, when $k_{01} = 0$, θ_{21}, MRT_1, M_2, F_{21} and F_{02} reach their upper bounds while θ_{12} and MRT_2 reach their lower bounds.
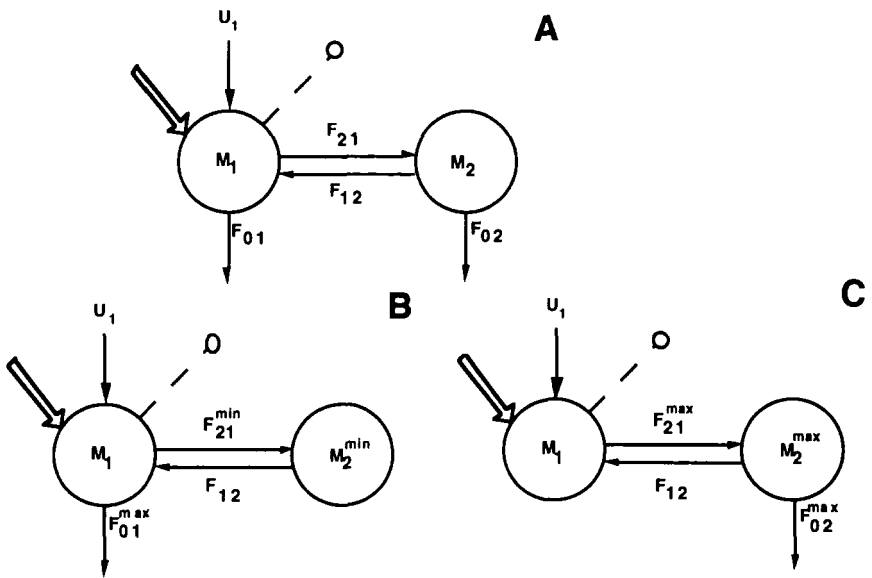
Figure 6.3.2. Panel A: The two compartment model where input and output are in compartment 1. Bounds for the kinetic parameters can be interpreted as the kinetic parameters of the two submodels shown in Panels B and C. See text for additional explanation.

If tracee de novo production enters both compartments 1 and 2 as shown in Figure 6.3.3, bounds on the tracee parameters can still be derived by using the submodels shown in panels B and C of Figure 6.3.3. They combine the unique identifiability of the tracer model with a unique

solution of the tracee steady state equations. The tracee parameters of submodels can be solved uniquely, and they provide bounds for the original structure.
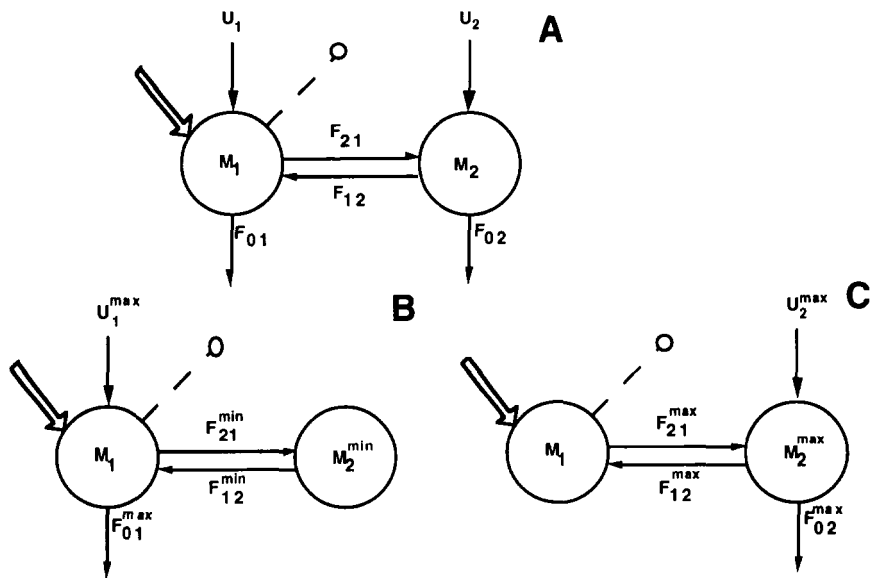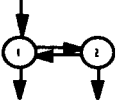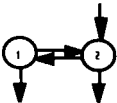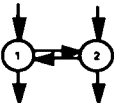
Figure 6.3.3. Panel A: The two compartment model where tracee input is into both compartments 1 and 2. Bounds for the kinetic parameters can be interpreted as the kinetic parameters of the two submodels shown in Panels B and C. See text for additional explanation.

The formulas to derive upper and lower bounds of tracee kinetic parameters for a nonidentifiable two compartment model are given in Table 6.3.1.

In moving from the two compartment model to a generic nonidentifiable n-compartment model, it is impossible to derive general expressions for the bounds of the kinetic parameters. The procedure outlined for the two compartment model can give some guidelines, but each situation must be handled separately. However, some results can be extended to catenary and mammillary models.

Table 6.3.1. Formulas for Tracee Kinetic Parameters of Non-Identifiable Two Compartment Models*

U_1	$(-k_{11} + \frac{\gamma}{k_{22}})M_1$	0	$U_1^{min} = 0 \quad U_1^{max} = (-k_{11} + \frac{\gamma}{k_{22}})M_1$
U_2	0	$U_2^{min} = (-k_{11} + \frac{\gamma}{k_{22}})M_1$ $\quad U_2^{max} = k_{11}(1 - \frac{k_{11}k_{22}}{\gamma})M_1$	$U_2^{min} = 0$ $\quad U_2^{max} = k_{11}(1 - \frac{k_{11}k_{22}}{\gamma})M_1$
M_2	$M_2^{min} = \frac{\gamma}{k_{22}^2}M_1 \quad M_2^{max} = \frac{k_{11}}{k_{22}}M_1$	$M_2^{min} = \frac{k_{11}}{k_{22}}M_1 \quad M_2^{max} = \frac{k_{11}^2}{\gamma}M_1$	$M_2^{min} = \frac{\gamma}{k_{22}^2}M_1 \quad M_2^{max} = \frac{k_{11}^2}{\gamma}M_1$
F_{21}	$F_{21}^{min} = -\frac{\gamma}{k_{22}}M_1 \quad F_{21}^{max} = -k_{11}M_1$	$F_{21}^{min} = -\frac{\gamma}{k_{22}}M_1 \quad F_{21}^{max} = -k_{11}M_1$	$F_{21}^{min} = -\frac{\gamma}{k_{22}}M_1 \quad F_{21}^{max} = -k_{11}M_1$
F_{12}	$F_{12}^{min} = -\frac{\gamma}{k_{22}}M_1 \quad F_{12}^{max} = -k_{11}M_1$	$-k_{11}M_1$	$F_{12}^{min} = -\frac{\gamma}{k_{22}}M_1 \quad F_{12}^{max} = -k_{11}M_1$
F_{01}	$F_{01}^{min} = 0 \quad F_{01}^{max} = (-k_{11} + \frac{\gamma}{k_{22}})M_1$	$F_{01}^{min} = 0 \quad F_{01}^{max} = (-k_{11} + \frac{\gamma}{k_{22}})M_1$	$F_{01}^{min} = 0 \quad F_{01}^{max} = (-k_{11} + \frac{\gamma}{k_{22}})M_1$
F_{02}	$F_{02}^{min} = 0 \quad F_{02}^{max} = (-k_{11} + \frac{\gamma}{k_{22}})M_1$	$F_{02}^{min} = 0 \quad F_{02}^{max} = k_{11}(1 - \frac{k_{11}k_{22}}{\gamma})M_1$	$F_{02}^{min} = 0 \quad F_{02}^{max} = k_{11}(1 - \frac{k_{11}k_{22}}{\gamma})M_1$

*Compartment 1 is the accessible pool; thus k_{11}, k_{22} and $\gamma = k_{21}k_{12}$ are known from the tracer experiment.

Catenary models

For a general *n*-compartment catenary model where the input-output experiment is in the extremal compartment, the mean residence times θ_{ii} can be solved uniquely since $\theta_{ii} = \frac{1}{k_{ii}}$. Upper and lower bounds for the other kinetic parameters can be interpreted as parameters of the uniquely identifiable submodels derived from the original one by setting all losses but one equal to zero. This is shown in Figure 6.3.4.

More precisely, upper and lower bounds for θ_{ij}, $i \neq j$, can be calculated from the mean residence time matrix of the two submodels with tracee production and irreversible loss either in compartment 1 (panel A of Figure 6.3.4) or compartment *n* (panel D of Figure 6.3.4).

$$\theta_{ij} \quad i > j : \quad \theta_{ij}^{\min} \text{ from submodel A}$$
$$\theta_{ij}^{\max} \text{ from submodel D}$$

$$\theta_{ij} \quad i < j : \quad \theta_{ij}^{\min} \text{ from submodel D}$$
$$\theta_{ij}^{\max} \text{ from submodel A}$$

Upper and lower bounds of tracee masses in the nonaccessible compartments, and intercompartmental fluxes can also be calculated from submodels A and D in Figure 6.3.4.

$$M_i \quad i = 2, \cdots, n : \quad M_i^{\min} \text{ from submodel A}$$
$$M_i^{\max} \text{ from submodel D}$$

$$F_{ij} \quad i = 2, \cdots, n-1 : \quad F_{ij}^{\min} \text{ from submodel A}$$
$$j = i \pm 1 \qquad\qquad F_{ij}^{\max} \text{ from submodel D}$$

The lower bound of tracee production and irreversible loss for any compartment is zero. The upper bounds are given by tracee parameters of some specific submodel, e.g. $U_2^{\max}$ and $F_{02}^{\max}$ are the tracee parameters of the submodel with tracee production and irreversible loss into and from compartment 2 (submodel B of Figure 6.3.4). They can be calculated from the kinetic parameters of submodels A and D since, from (6.2.11)
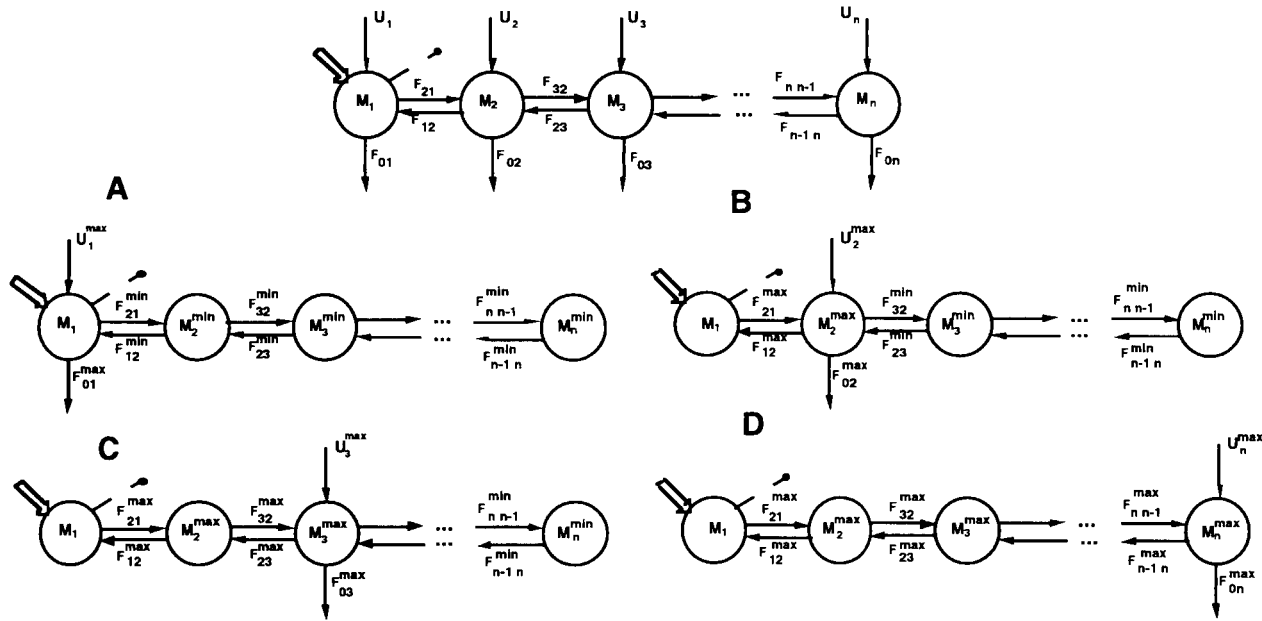
Figure 6.3.4. Top: the general n-compartment catenary model where the input-output is in compartment 1, an extreme compartment. When more the one irreversible loss are present, the model is nonidentifiable. Bounds for the k_{ij} can be interpreted as parameters of the uniquely identifiable submodels derived from the original one by setting all losses but one equal to their lower bound, zero. These are illustrated in the bottom panels, A, B, C and D.

$$U_2^{\max} = \frac{M_1}{\theta_{12}^{\min}}$$

and from the mass balance equation written for the tracee in compartment 2 of submodel B

$$F_{02}^{\max} = F_{21}^{\max} - F_{12}^{\max} + F_{23}^{\min} - F_{32}^{\min} + U_2^{\max}$$

In summary, bounds for all kinetic tracee parameters of the original model can be calculated from the tracee kinetic parameters of submodels A and D of Figure 6.3.4.

Mammillary models
_____

For a general n-compartment mammillary model where the input-output experiment is in the central compartment 1, the mean residence times θ_{ii} are uniquely identifiable since $\theta_{ii} = \frac{1}{k_{ii}}$. Upper and lower bounds for kinetic parameters can be interpreted as parameters of the uniquely identifiable submodel parameters derived from the original model by setting all losses but one equal to zero (see Figure 6.3.5).

The lower bounds of tracee mass in the nonaccessible compartments, and the fluxes between them and the accessible compartment 1 can be calculated from the submodel with tracee production and irreversible loss into and from compartment 1 (submodel A Figure 6.3.5) while the upper and lower bounds for these parameters are the tracee parameters of the submodel having tracee production and irreversible loss in compartment i (Panel C of Figure 6.3.5):

$$M_i \quad i = 2, \cdots, n: \quad M_i^{\min} \text{ from submodel A}$$
$$M_i^{\max} \text{ from submodel C}$$

$$F_{1i} \quad i = 2, \cdots, n: \quad F_{1i}^{\min} \text{ from submodel A}$$
$$F_{1i}^{\max} \text{ from submodel C}$$

$$F_{i1} \quad i = 2, \cdots, n: \quad F_{i1}^{\min} \text{ from submodel A}$$
$$F_{i1}^{\max} \text{ from submodel C}$$

Submodel C also gives the upper bound for tracee production and irreversible loss, the lower bound for both are zero.

$$U_i \quad i = 2, \cdots, n: \quad U_i^{\min} = 0$$
$$U_i^{\max} \text{ from submodel C}$$
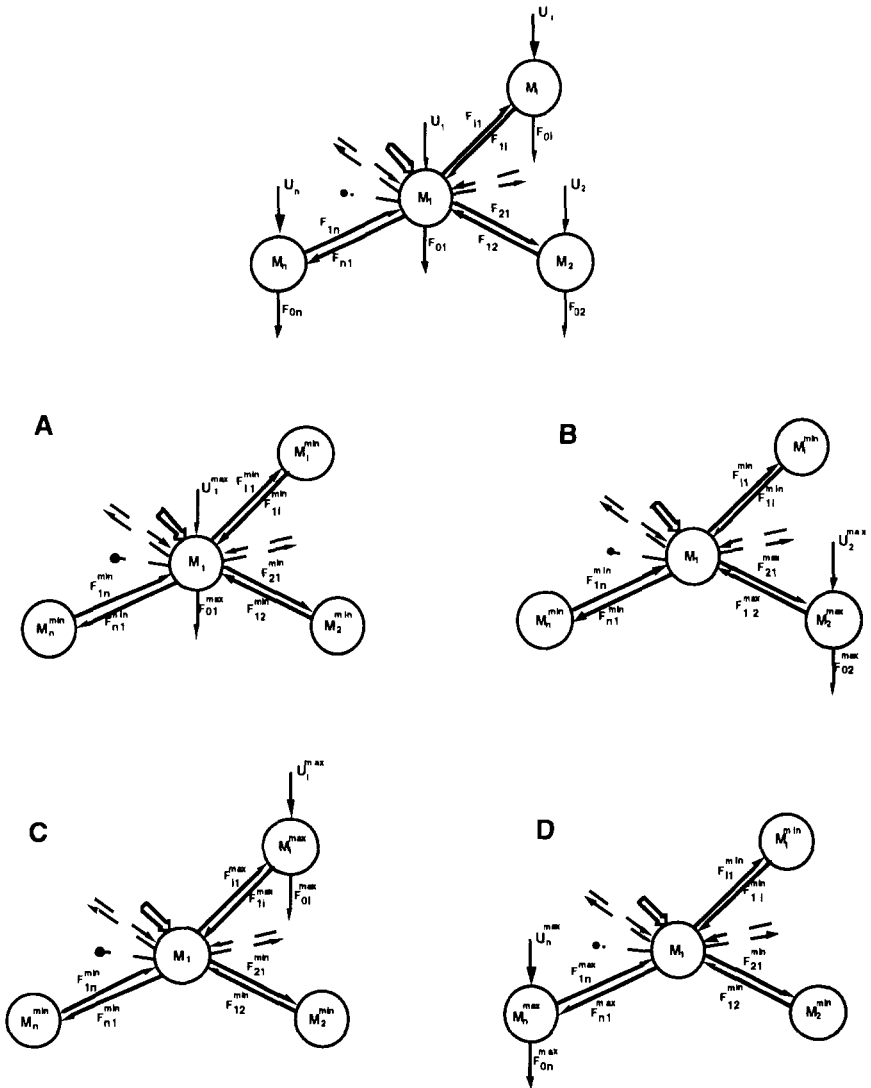
Figure 6.3.5. Top Panel. The n-compartment mammillary model where the input-output experiment is in the central compartment. Parameters such as k_{31} and k_{13} are uniquely identifiable while parameters such as k_{01}, k_{12}, k_{21} and k_{02} are nonidentifiable. Panels A - D: The submodels of the original model structure which permit the quantification of the upper and lower bounds of the nonidentifiable parameters of the original model structure.

$$F_{0i} \quad i = 2, \cdots, n: \quad F_{0i}^{\min} = 0$$
$$F_{0i}^{\max} \text{ from submodel C}$$

Similarly $U_1^{\max}$ and $F_{01}^{\max}$ can be calculated from submodel A. Finally, the submodels also give upper and lower bounds of the θ_{ij} parameters since for Θ of submodel C, the elements of the i-th column assume their lower bounds while those in the i-th row assume their upper bounds.

This page intentionally left blank.

Chapter 7

COMPARTMENTAL VERSUS NONCOMPARTMENTAL KINETIC PARAMETERS

7.1   INTRODUCTION

In the previous chapters, two classes of models, noncompartmental and compartmental, both of which are appropriate to interpret data from tracer experiments in a constant steady state, were examined. Each approach provides a quantitative description of the tracer and tracee system through a number of specific kinetic parameters to be estimated from the tracer and tracee measurements.

As already pointed out previously, the structural difference between the two approaches lies essentially in the way the nonaccessible portion of the system is modeled. For the compartmental model, both the accessible and nonaccessible components of the system need to be specified in terms of the number of compartments, the interconnections among the compartments, and the locations of de novo production and irreversible loss. Kinetic parameters can be estimated for all individual compartments, accessible or not. They are correct if the assumptions about the system that are incorporated into the model structure are correct.

Conversely, the noncompartmental model describes the nonaccessible portion of the system with a recirculation/exchange arrow. Parameters can be derived describing both accessible pool and system events. However, the system parameters are correct only if specific structural conditions in the recirculation/exchange arrow portion of the system hold.

In this Chapter, the relation between the kinetic parameters provided by the two modeling approaches will be analyzed. Both the one and two accessible pool noncompartmental models will be considered. The

accessible pool and the system parameters will be discussed separately to help distinguish the two approaches.

A comparison between the compartmental and noncompartmental model when one pool is accessible for tracer input and measurement will be given first showing the equivalence between the compartmental and noncompartmental definitions of the accessible pool parameters - volume, mass, mean residence time in the accessible pool. Formulas to calculate from the compartmental model other accessible pool noncompartmental parameters such as clearance rate, and rate of appearance and disappearance will also be presented. Then, the compartmental and noncompartmental definitions of kinetic parameters related to the whole system will be discussed, and the domain of validity of the noncompartmental model will be re-examined and formalized. Next, some points will be made related to the parameters of the nonaccessible pools. Noncompartmental models only estimate parameters of the nonaccessible portion of the system as a whole by evaluating the difference between the system and accessible pool parameters. On the other hand, for compartmental models the same parameters as those defined for the accessible pool, e.g. mass and residence time, can also be estimated for any nonaccessible compartment. Finally, kinetic parameters from for compartmental and noncompartmental models will be compared for the case where two pools are accessible to measurement.

7.2   THE MEAN RESIDENCE TIME MATRIX REVISITED

To compare the two modeling methodologies, advantage will be taken of an interpretation of the mean residence time matrix of the compartmental model that is different from that discussed in §4.5. There the i, j^{th} element of the mean residence time matrix $\mathbf{\Theta} = -\mathbf{K}^{-1}$ of a compartmental system was seen as the average time a particle introduced into the system in compartment j spends in compartment i on all its passages through i. In what follows, it will be shown that θ_{ij} is related to the time course of the tracer mass in compartment i resulting from an input into compartment j.

Consider the compartmental model equation (4.3.20) rewritten

$$\frac{d\mathbf{m}(t)}{dt} = \mathbf{K}\mathbf{m}(t) + \mathbf{u}(t) \qquad \mathbf{m}(0) = 0 \qquad (7.2.1)$$

for a generic input of tracer into accessible compartment 1

$$\mathbf{u}(t) = \begin{pmatrix} u_1(t) \\ 0 \\ \vdots \\ 0 \end{pmatrix} \tag{7.2.2}$$

Rearranging (7.2.1), one has

$$\mathbf{m}(t) = \begin{pmatrix} m_1(t) \\ \vdots \\ m_n(t) \end{pmatrix} = \mathbf{K}^{-1} \begin{pmatrix} \frac{dm_1(t)}{dt} \\ \vdots \\ \frac{dm_n(t)}{dt} \end{pmatrix} - \mathbf{K}^{-1} \begin{pmatrix} u_1(t) \\ 0 \\ \vdots \\ 0 \end{pmatrix} \tag{7.2.3}$$

By integrating (7.2.3) from zero to infinity and remembering $\mathbf{\Theta} = -\mathbf{K}^{-1}$

$$\begin{pmatrix} \int_0^\infty m_1(t)dt \\ \vdots \\ \int_0^\infty m_n(t)dt \end{pmatrix} = -\mathbf{\Theta} \begin{pmatrix} m_1(\infty) - m_1(0) \\ \vdots \\ m_n(\infty) - m_n(0) \end{pmatrix} + \mathbf{\Theta} \begin{pmatrix} \int_0^\infty u_1(t)dt \\ 0 \\ \vdots \\ 0 \end{pmatrix}$$
$$\tag{7.2.4}$$

where $m_i(\infty)$ indicates the value of the tracer mass in compartment i as time t tends towards infinity. Since the system is assumed to be open, i.e. there is at least one irreversible loss pathway accessible to any particle in the system, $m_i(\infty) = 0$. In addition, by assumption $m_i(0) = 0$. Thus from (7.2.4)

$$\int_0^\infty m_i(t)dt = \theta_{i1} \int_0^\infty u_1(t)dt \tag{7.2.5}$$

From (7.2.5), θ_{i1} equals the area under the time course of the tracer mass in compartment i resulting from a tracer input into compartment 1 normalized to the tracer dose, i.e.

$$\theta_{i1} = \frac{\int_0^\infty m_i(t)dt}{\int_0^\infty u_1(t)dt} \tag{7.2.6}$$

Equation (7.2.6) holds for any compartment, accessible or not. Consider now a tracer input into a generic compartment, say j. The compartmental equations are the same as before, i.e. (7.2.1), but the tracer input is now

$$\mathbf{u}(t) = \begin{pmatrix} 0 \\ \vdots \\ u_j(t) \\ \vdots \\ 0 \end{pmatrix} \tag{7.2.7}$$

By following the same reasoning as before when (7.2.3) and (7.2.4) were developed, the area under the tracer mass curve in compartment i resulting from an input into compartment j, denoted here by $m_i^j(t)$ is

$$\int_0^\infty m_i^j(t)dt = \theta_{ij} \int_0^\infty u_j(t)dt \qquad (7.2.8)$$

and thus

$$\theta_{ij} = \frac{\int_0^\infty m_i^j(t)dt}{\int_0^\infty u_j(t)dt} \qquad (7.2.9)$$

This equation demonstrates that the ij^{th} element of the mean residence time matrix Θ equals the area under the model-predicted tracer mass in compartment i resulting from an input into compartment j, normalized to the tracer dose.

Recalling that the definition of most noncompartmental parameters is based on evaluating areas under the tracer mass or concentration curves, it is evident that the above interpretation of the elements of the mean residence time matrix will help in the comparison between the compartmental and noncompartmental model parameters.

7.3   EQUIVALENCE OF THE ACCESSIBLE POOL PARAMETERS

The noncompartmental parameters of the accessible pool, defined in §3.2, are the volume of distribution V, tracee mass M, clearance rate CR, fractional clearance rate FCR, and mean residence time in the accessible pool Θ, and the rates of appearance R_a and disappearance R_d. The compartmental model counterparts of V, M, and Θ were defined in §4.4 and §4.5 and can be written, assuming without loss of generality that compartment 1 is the accessible pool, as V_1, M_1, and θ_{11}.

The parameters CR, FCR, R_a and R_d were defined in the noncompartmental framework. The compartmental counterparts of these parameters are, again assuming that compartment 1 is the accessible pool, are CR_1, FCR_1, R_{a1} and R_{d1}. Using the relationships given in Table 3.2.2, they can be also calculated from the compartmental model:

$$FCR_1 = \frac{1}{\theta_{11}} \qquad (7.3.1)$$

$$CR_1 = FCR_1 \cdot V_1 = \frac{V_1}{\theta_{11}} \qquad (7.3.2)$$

$$R_{a1} = R_{d1} = FCR_1 \cdot M_1 = \frac{M_1}{\theta_{11}}v \qquad (7.3.3)$$

First, it will be shown that V, M and θ are equivalent to V_1, M_1 and θ_{11} since the definitions coincide. The equivalence between *FCR, CR, R_a* and R_d and FCR_1, CR_1, R_{a1} and R_{d1} follows.

Volume of distribution and tracee mass

Assume that a dose d of tracer is injected as a bolus into the accessible pool at time zero, and that tracer concentration $c(t)$ is measured. The noncompartmental expression for the volume of distribution of the accessible pool is

$$V = \frac{d}{c(0)} \tag{7.3.4}$$

Suppose now that a compartmental model has be postulated to describe the system and that compartment 1 is the accessible compartment. The measurement equation (4.3.23) is

$$y(t) = c(t) = \frac{1}{V_1} m_1(t) \tag{7.3.5}$$

where $y(t) = c(t)$ denotes the tracer concentration. At time zero,

$$c(0) = \frac{1}{V_1} m_1(0) = \frac{1}{V_1} d \tag{7.3.6}$$

since the value of the tracer mass in the accessible compartment at time zero, $m_1(0)$, equals the injected dose d. Thus

$$V_1 = \frac{d}{c(0)} \tag{7.3.7}$$

Equations (7.3.4) and (7.3.7) prove the equivalence between the noncompartmental and compartmental expressions for the volume of distribution of the accessible pool or compartment for the bolus injection experiment. Similarly, the proof can be extended to any method of introducing the tracer. For instance, if the tracer is infused at a constant rate u, then the noncompartmental expression for the volume of the accessible pool is

$$V = \frac{u}{\dot{c}(0)} \tag{7.3.8}$$

The compartmental model measurement equation remains (7.3.5), but now $c(0) = 0$. Taking the derivative of (7.3.5) and evaluating this at time zero,

$$\dot{c}(0) = \frac{1}{V_1} \dot{m}_1(0) \tag{7.3.9}$$

To evaluate (7.3.9), an expression for $\dot{m}_1(0)$ is required. To do so, evaluate the compartmental model equation (4.3.11) at time zero:

$$\dot{m}_1(0) = -\sum_{\substack{j=0 \\ j \neq 1}}^{n} k_{j1} m_1(0) + \sum_{j=2}^{n} k_{1j} m_j(0) + u_1(t) \qquad (7.3.10)$$

where in this case, $u_1(t) = u$. Since no tracer is present in the system at time zero, $m_i(0) = 0, i = 1, \cdots, n$, and hence $\dot{m}_1(0) = u$. Using this equality in (7.3.9), an expression equivalent to the noncompartmental expression can be obtained:

$$V_1 = \frac{u}{\dot{c}(0)} \qquad (7.3.11)$$

The equivalence of the noncompartmental and compartmental tracee mass of the accessible pool follows immediately since the tracee mass is the volume of distribution multiplied by the tracee concentration measurement.

Suppose now that the tracer measurements are expressed in terms of the tracer to tracee ratio $z(t)$. The equivalence of the noncompartmental and compartmental expressions of tracee mass in the accessible pool or compartment can be proved following the same rationale as above using $z(t)$ in place of $c(t)$, and M and M_1 in place of V and V_1. The equivalence of the expressions for the volumes of distribution follows easily since the volume is the quotient of the tracee mass and concentration.

Mean residence time

From Table 3.2.4, the noncompartmental formula for the mean residence time in the accessible pool Θ for a bolus injection is

$$\Theta = \frac{1}{FCR} = \frac{V}{CR} = \frac{V \int_0^\infty c(t)dt}{d} = \frac{\int_0^\infty V c(t)dt}{d} = \frac{\int_0^\infty m(t)dt}{d} \qquad (7.3.12)$$

where d is the dose and $m(t) = Vc(t)$ is the tracer mass in the accessible pool.

The compartmental model mean residence time in the accessible compartment 1 for particles entering the system into compartment 1 is the $(1,1)^{th}$ element of the Θ matrix (see §7.2):

$$\theta_{11} = \frac{\int_0^\infty m_1(t)dt}{\int_0^\infty u_1(t)dt} = \frac{\int_0^\infty m_1(t)dt}{d} \qquad (7.3.13)$$

since for the bolus injection into compartment 1, $d = \int_0^\infty u_1(t)dt$. Clearly (7.3.12) and (7.3.13) coincide since $m_1(t) = m(t)$. Therefore, when a

single pool is accessible to tracer input and measurement, the definition of the noncompartmental mean residence time in that pool, Θ, coincides with the compartmental model definition of the mean residence time in the accessible compartment for particles entering the system in that accessible compartment.

A parallel argument to that given previously holds for different methods of introducing the tracer, or when the tracer to tracee ratio is the measurement variable.

Fractional clearance rate, clearance rate, and the rates of appearance and disappearance

The equivalence between the compartmental model and noncompartmental estimates of the fractional clearance rate, clearance rate, and the rates of appearance and disappearance follows immediately from their definition, Table 3.2.2 and (7.3.1) - (7.3.3), and from the equivalence between M_1, V_1 and θ_{11} and M, V and θ.

In summary, these results indicate that the accessible pool parameters, estimated using either the compartmental model or noncompartmental modeling methodologies, coincide since their definitions coincide. In practice, the same numerical value will be obtained for them if the same model order is adopted, that is, if the number of exponentials in the sum of exponential model equals the number of compartments in the compartmental model. This guarantees that the same description for the data will be obtained, as illustrated in the following example.

Example 1

Consider the compartmental and noncompartmental model shown in Figure 7.3.1. Assume the tracer is radioactive, and the time units of the experiment are in minutes. The tracer dose, injected as a bolus into the accessible compartment, is $d = 1.4 \cdot 10^7 \mathrm{dpm}$. The model output is tracer concentration $c(t)$ (dpm/ml) in this compartment. Tracee concentration in the same compartment is 100mg/ml. The rate constants for the compartmental model as shown in the figure, in units of min^{-1}, are $k_{21} = 0.0336$, $k_{12} = 0.1011$, and $k_{01} = 0.0134$. The volume of distribution of the accessible pool is 3372 ml. A plot of $c(t)$ is shown in Figure 7.3.1 as the graphic below the two model structures.

The mean residence time in the accessible compartment 1 is

$$\theta_{11} = \frac{1}{k_{01}} = 74.6\mathrm{min}$$
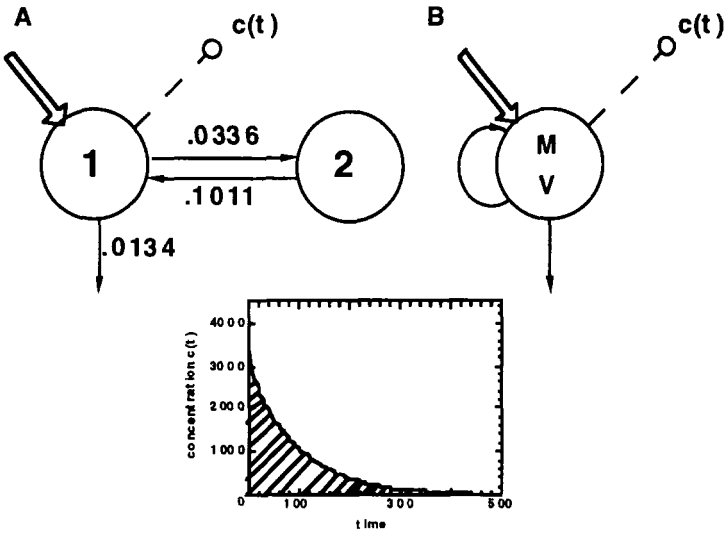
Figure 7.3.1. Comparing the compartmental model (A) and noncompartmental (B) accessible pool parameters estimates. See text for explanation.

Tracee mass $.M_1$ is

$$M_1 = 100 \cdot 3372 = 337200 \text{mg}$$

The accessible pool parameters FCR_1, CR_1, R_{a1} and R_{d1} can be calculated:

$$FCR_1 = \frac{1}{\theta_{11}} = \frac{1}{74.6} = 0.0134 \text{min}^{-1}$$

$$CR_1 = \frac{V_1}{\theta_{11}} = \frac{3372}{74.6} = 45.2 \text{ml/min}$$

$$R_{a1} = R_{d1} = \frac{M_1}{\theta_{11}} = \frac{337200}{74.6} = 4520 \text{mg/min}$$

For the noncompartmental model, $c(t)$ is expressed as the sum of two exponentials

$$c(t) = 1202 e^{-0.1383t} + 2950 e^{-0.0098t}$$

Here $A_1 = 1202$, $A_2 = 2950$, $\lambda_1 = 0.1383$ and $\lambda_2 = 0.0098$. The model predicted tracer concentration at time zero is $c(0) = A_1 + A_2 = 1202 + 2950 = 4152\text{dpm/ml}$. Then the noncompartmental estimates of the accessible pool parameters V, M, θ, FCR, CR, R_a and R_d are:

$$V = \frac{d}{c(0)} = \frac{1.4 \cdot 10^7}{4152} = 3372\text{ml}$$

$$M = C \cdot V = 100 \cdot 3372 = 337200\text{mg}$$

$$\Theta = V \int_0^\infty c(t)dt = \frac{\int_0^\infty c(t)dt}{c(0)} = \frac{\frac{A_1}{\lambda_1} + \frac{A_2}{\lambda_2}}{A_1 + A_2} = \frac{\frac{1202}{0.1383} + \frac{2950}{0.0098}}{1202 + 2950} = 74.6\text{min}$$

$$FCR = \frac{1}{\theta} = \frac{1}{74.6} = 0.0134\text{min}^{-1}$$

$$CR = \frac{V}{\theta} = \frac{3372}{74.6} = 45.2\text{ml/min}$$

$$R_a = R_d = CR \cdot C = 45.2 \cdot 100 = 4520\text{mg/min}$$

In the above example, the numerical equivalence of the accessible pool parameters is clearly seen since in both approaches, the same model order was adopted: a two compartment model and a two exponential noncompartmental model. This guarantees the description of the data provided by both models will be the same since the two exponential model is the solution of the two compartmental model. The equivalence would no longer hold if, for example, a three compartment model were used for the compartmental model and a sum of two exponentials for the noncompartmental model.

Finally, it is worth noting that the accessible pool parameters can be recovered from the compartmental modeling approach even if the model is not a priori uniquely identifiable, since they can be expressed in terms of the observational parameters. The following example illustrates this point.

Example 2

Consider the a priori nonidentifiable model Figure 6.3.1 shown shown again for convenience in Figure 7.3.2. For this model, as already discussed in §6.3, V_1 is uniquely identifiable, M_1 can be uniquely calculated
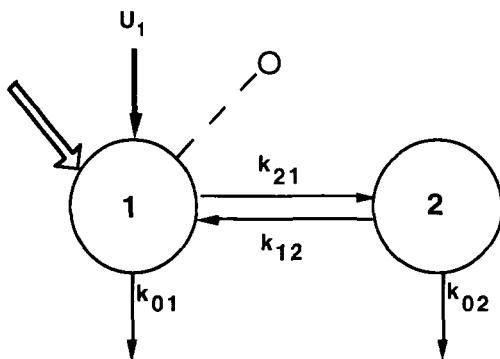
Figure 7.3.2. A two compartment model with tracer and tracee inputs into compartment 1, and samples from compartment 1. See text for explanation.

from the product $C_1 \cdot V_1$ where C_1 is the tracee concentration in compartment 1. The parameter θ_{11} given in (6.3.1) can be uniquely calculated since it only depends upon the observational parameters. Thus FCR_1, CR_1, R_{a1} and R_{d1} can be calculated using (7.3.1) - (7.3.3).

For a general a priori unidentifiable n-compartmental catenary model where the input-output experiment is in the extremal compartment 1, V_1, M_1, and θ_{11} can be solved uniquely, as indicated in §6.3. Hence FCR_1, CR_1, R_{a1} and R_{d1} can be solved uniquely. The same results hold for a general a priori nonidentifiable mammillary model where the input-output experiment is in the central compartment 1.

7.4 NONEQUIVALENCE OF THE SYSTEM PARAMETERS

In addition to the accessible pool parameters, parameters related to the whole system such as total mass, distribution volumes and mean residence time in the system can be estimated using either the noncompartmental or compartmental approach. However, as stated previously in §3.3, the noncompartmental model correctly recovers the true values only if disposal and de novo production take place in the accessible pool. In this section, this observation will be formalized by comparing in more detail the noncompartmental and compartmental estimates of the system parameters.

Mean residence time in the system

Consider first the estimation of the mean residence time in the system of particles entering the accessible compartment in a compartmental model; without loss of generality, assume it is compartment 1. The compartmental parameter is MRT_1, and equals the sum of the residence times in each individual compartment of the system:

$$MRT_1 = \theta_{11} + \theta_{21} + \cdots + \theta_{n1} \tag{7.4.1}$$

For the noncompartmental model the system mean residence time MRT^{NC} were given in Tables 3.3.3 and 3.3.4. For a generic input of tracer, assuming the tracer data are expressed in terms of concentration $c(t)$,

$$MRT^{NC} = \frac{\int_0^\infty t \cdot c(t)dt}{\int_0^\infty c(t)dt} - \frac{\int_0^\infty t \cdot u(t)dt}{\int_0^\infty u(t)dt} \tag{7.4.2}$$

or equivalently, since $Vc(t) = m(t)$ where $m(t)$ is the tracer mass in the accessible pool

$$MRT^{NC} = \frac{\int_0^\infty t \cdot m(t)dt}{\int_0^\infty m(t)dt} - \frac{\int_0^\infty t \cdot u(t)dt}{d} \tag{7.4.3}$$

since $\int_0^\infty u(t) = d$, the total dose of tracer administered.

In order to compare MRT_1 defined in (7.4.1) and MRT^{NC} defined in (7.4.3), one can first use (7.2.5) to relate $\int_0^\infty m_1(t)dt$ to θ_{11}

$$\int_0^\infty m_1(t)dt = \theta_{11} \cdot d \tag{7.4.4}$$

Second, $\int_0^\infty tm_1(t)dt$ can be related to the elements of the compartmental mean residence time matrix Θ. From (7.2.3), by multiplying each term by t and taking the integral from 0 to infinity:

$$\begin{pmatrix} \int_0^\infty t \cdot m_1(t)dt \\ \vdots \\ \int_0^\infty t \cdot m_n(t)dt \end{pmatrix} = -\Theta \begin{pmatrix} \int_0^\infty t \cdot dm_1(t) \\ \vdots \\ \int_0^\infty t \cdot dm_n(t) \end{pmatrix} + \Theta \begin{pmatrix} \int_0^\infty t \cdot u_1(t)dt \\ 0 \\ \vdots \\ 0 \end{pmatrix}$$
$$\tag{7.4.5}$$

The integral $\int_0^\infty t \cdot dm_i(t)$ can be evaluated by integrating by parts

$$\int_0^\infty t \cdot dm_i(t) = t \cdot m_i(t)\big|_0^\infty - \int_0^\infty m_i(t)dt = -\int_0^\infty m_i(t)dt \tag{7.4.6}$$

since $t \cdot m_i(t)\big|_0^\infty = 0$.[1]

---

[1] To see that $t \cdot m_i(t)\big|_0^\infty = 0$, one has $t \cdot m_i(t)\big|_0^\infty = \lim_{t \to \infty} t \cdot m_i(t) = \lim_{t \to \infty} \frac{m_i(t)}{1/t} = 0$ since both terms of the fraction are infinitesimal, that is they tend towards zero as t tends to infinity.

Thus (7.4.5) can be rewritten

$$
\begin{pmatrix} \int_0^\infty t \cdot m_1(t)dt \\ \vdots \\ \int_0^\infty t \cdot m_n(t)dt \end{pmatrix} = \Theta \left[\begin{pmatrix} \int_0^\infty m_1(t)dt \\ \vdots \\ \int_0^\infty m_n(t)dt \end{pmatrix} + \begin{pmatrix} \int_0^\infty t \cdot u_1(t)dt \\ 0 \\ \vdots \\ 0 \end{pmatrix} \right]
$$
$$(7.4.7)$$

whence

$$
\int_0^\infty t \quad \cdot \quad m_1(t)dt = \theta_{11} \int_0^\infty m_1(t)dt + \theta_{12} \int_0^\infty m_2(t)dt \quad (7.4.8)
$$
$$
+ \quad \cdots + \theta_{1n} \int_0^\infty m_n(t)dt + \theta_{11} \int_0^\infty t \cdot u_1(t)dt
$$

Taking advantage of (7.2.5) rewritten here

$$
\int_0^\infty m_i(t)dt = \theta_{i_1} \cdot d \qquad (7.4.9)
$$

(7.4.8) can be rewritten

$$
\int_0^\infty t \cdot m_1(t)dt = d[\theta_{11}^2 + \theta_{12}\theta_{21} + \cdots + \theta_{1n}\theta_{n1}] + \theta_{11} \int_0^\infty t \cdot u_1(t)dt \quad (7.4.10)
$$

By using (7.4.4) and (7.4.10), MRT^{NC} given in (7.4.3) can be expressed as a function of the elements of Θ :

$$
MRT^{NC} = \theta_{11} + \theta_{21}\frac{\theta_{12}}{\theta_{11}} + \cdots + \theta_{n1}\frac{\theta_{1n}}{\theta_{11}} \qquad (7.4.11)
$$

It is now possible to relate the noncompartmental MRT^{NC} given in (7.4.11) to the compartmental MRT_1 given in (7.4.1):

$$
MRT^{NC} = MRT_1 - \theta_{21}\left(1 - \frac{\theta_{12}}{\theta_{11}}\right) - \cdots - \theta_{n1}\left(1 - \frac{\theta_{1n}}{\theta_{11}}\right) \qquad (7.4.12)
$$

Equation (7.4.12) shows that MRT^{NC} provides in general an underestimation of the residence time in the system of particles entering into compartment 1 since from the properties of the mean residence time matrix $\theta_{ij} \leq \theta_{11}$. Moreover, from the probabilistic interpretation of the θ_{ij} elements, $\frac{\theta_{ij}}{\theta_{ii}} = Prob[j \rightarrow i]$, (7.4.12) becomes

---

However, $m_i(t)$ is infinitesimal of higher order since it decays as a sum of exponentials. Thus $m_i(t)$ is an infinitesimal part of the infinitesimal $1/t$. Thus the ratio approaches zero as t approaches infinite.

$$MRT^{NC} = MRT_1 - \theta_{21}(1 - Prob[2 \rightarrow 1])$$
$$- \cdots - \theta_{n1}(1 - Prob[n \rightarrow 1]) \tag{7.4.13}$$

showing that MRT^{NC} underestimates MRT_1 by an amount equal to the time spent in the nonaccessible portion of the system by those particles which will never return to the accessible compartment. .MRT^{NC} equals MRT_1 only when all particles leave the system from the accessible compartment 1. In fact, in this case, $\theta_{11} = \theta_{21} = \cdots = \theta_{n1}$ (see property 4 of the mean residence time matrix, §6.2.2) or equivalently $Prob[2 \rightarrow 1] = \cdots = Prob[n \rightarrow 1] = 1$.

Mean residence time in the system from total body tracer measurements

In Chapter 3, a different noncompartmental expression for the system parameters based on whole body tracer measurements was given. It is now easy to show that the whole body formula for the mean residence time matrix, MRT^{TB}, coincides with the compartmental formula for MRT_1. Using (7.2.5),

$$
\begin{aligned}
MRT^{TB} &= \frac{\int_0^\infty m_{tot}(t)dt}{d} \\
&= \frac{\int_0^\infty m_1(t)dt + \cdots + \int_0^\infty m_n(t)dt}{d} \\
&= \theta_{11} + \cdots + \theta_{n1} = MRT_1
\end{aligned}
\tag{7.4.14}
$$

Total mass

The compartmental total mass in the system is the sum of the masses in all compartments. In Chapter 6, M_{tot} was expressed as the product of the tracee production U_h and the mean residence time in the system of particles entering the system into compartment h:

$$M_{tot} = MRT_h \cdot U_h \tag{7.4.15}$$

The noncompartmental formula was given in Table 3.3.2:

$$M_{tot}^{NC} = MRT^{NC} \cdot R_a \tag{7.4.16}$$

In what follows, first the relationship between R_a and U_h will be derived. The tracee production U_h can be estimated from the compartmental model knowing M_1 and θ_{1h}:

$$U_h = \frac{M_1}{\theta_{1h}} \tag{7.4.17}$$

The rate of appearance in the accessible compartment is given in Table 3.3.2 and 3.2.4 as

$$R_a = M_1 \cdot \frac{d}{\int_0^\infty V \cdot c(t)dt} = M_1 \frac{d}{\int_0^\infty m_1(t)dt} \tag{7.4.18}$$

since following the compartmental nomenclature, $V \cdot c(t) = m_1(t)$ and $M = M_1$. The integral of $m_1(t)$ is related to the compartmental mean residence time θ_{11} (cf (7.4.4)) so that

$$R_a = \frac{M_1}{\theta_{11}} \tag{7.4.19}$$

Comparing the formula (7.4.19) for the rate of appearance with the true rate of production (7.4.17), one can write

$$R_a = U_h \frac{\theta_{1h}}{\theta_{11}} = U_h \cdot Prob[h \to 1] \tag{7.4.20}$$

showing that R_a in general underestimates the true production rate by a factor equal to the probability for de novo synthesized particles entering compartment h reaching compartment 1. The rate of appearance R_a equals U_h either when $h = 1$, or when $h \neq 1$ but $\theta_{1h} = \theta_{11}$, i.e. when the tracee enters the system into the nonaccessible compartment h but reaches compartment 1 with no possibility of being irreversibly lost first.

By using (7.4.20) in (7.4.16),

$$M_{tot}^{NC} = MRT^{NC} \frac{\theta_{1h}}{\theta_{11}} U_h \leq MRT_1 \frac{\theta_{1h}}{\theta_{11}} U_h \tag{7.4.21}$$

since $MRT^{NC} \leq MRT_1$.

In order to compare the compartmental M_{tot}, (7.4.15), and the non-compartmental estimate M_{tot}^{NC}, (7.4.16), one can compare MRT_h with the product $MRT_1 \frac{\theta_{1h}}{\theta_{11}}$. The latter term can also be written

$$MRT_1 \frac{\theta_{1h}}{\theta_{11}} = (\theta_{11} + \cdots + \theta_{n1}) \frac{\theta_{1h}}{\theta_{11}} = \theta_{1h} + \theta_{21} \frac{\theta_{1h}}{\theta_{11}} + \cdots + \theta_{n1} \frac{\theta_{1h}}{\theta_{11}} \tag{7.4.22}$$

Consider the term $\theta_{21} \frac{\theta_{1h}}{\theta_{11}}$ interpreted in terms of probabilities:

$$\begin{aligned} \theta_{21} \frac{\theta_{1h}}{\theta_{11}} &= \frac{\theta_{1h}}{\theta_{11}} \frac{\theta_{21}}{\theta_{22}} \theta_{22} = Prob[h \to 1] \cdot Prob[1 \to 2] \cdot \theta_{22} \tag{7.4.23} \\ &= Prob[h \to 2 \text{ through } 1] \cdot \theta_{22} \leq Prob[h \to 2] \cdot \theta_{22} = \theta_{2h} \end{aligned}$$

Similar interpretations hold for the other terms in (7.4.22) so that

$$MRT_1 \frac{\theta_{1h}}{\theta_{11}} \leq \theta_{1h} + \cdots + \theta_{nh} = MRT_h \tag{7.4.24}$$

Finally, from (7.4.21) and (7.4.24),

$$M_{tot}^{NC} \leq MRT_1 \cdot \frac{\theta_{1h}}{\theta_{11}} U_h \leq MRT_h \cdot U_h = M_{tot} \tag{7.4.25}$$

The noncompartmental estimate of the total mass thus in general underestimates the tracee mass in the system. This estimate is correct only when two conditions hold. First, $MRT^{NC} = MRT_1$ (cf. (7.4.21)), and second, $\theta_{11} \frac{\theta_{1h}}{\theta_{11}} = \theta_{ih}$ (cf. (7.4.23)). The first condition is satisfied when all irreversible loss takes place from the accessible compartment. This implies that all elements in the first row of the mean residence time matrix Θ are equal, $\theta_{11} = \theta_{12} = \cdots = \theta_{1n}$. The second condition becomes $\theta_{i1} = \theta_{ih}$, i.e. a condition of equivalence between the first and h^{th} row of the matrix. This condition can be satisfied only if $h = 1$.

One can conclude that M_{tot}^{NC} provides the correct estimate of the total tracee mass only if all irreversible loss and production occur in compartment 1. This condition assures the correctness of all noncompartmental parameters of the whole system.

These points will be illustrated in the example shown in Figure 7.4.1.
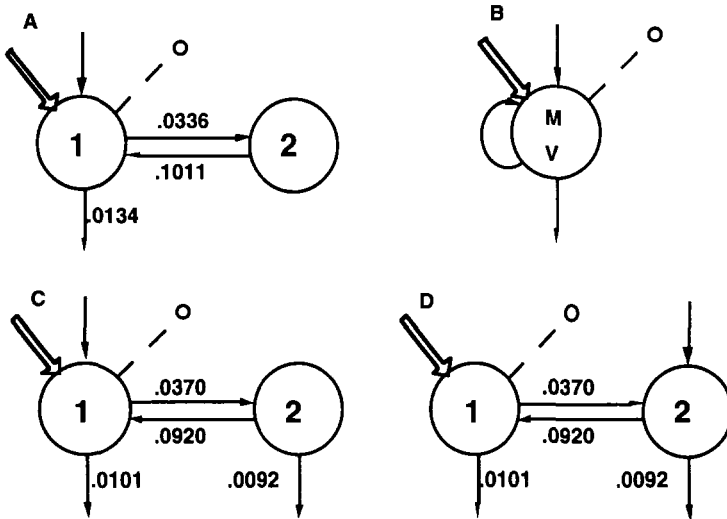
Figure 7.4.1. Comparing the noncompartmental (B) and compartmental model system parameters estimates. Models A and B are those shown in Figure 7.3.1. Models C and D differ from model A in that there is loss from compartment 2, and the site of de novo tracee input differ. See text for explanation.

Example

Consider first the noncompartmental model shown in Panel B. Assuming a bolus injection d equal to $1.4 \cdot 10^7$dpm, the concentration of tracer in the accessible pool was

$$c(t) = 1202e^{-0.1383t} + 2950e^{-0.0098t}$$

From Table 3.3.4 (and the formula written in terms of sums of exponentials as described in Chapter 9 in (9.2.7)), $MRT^{NC} = 99.4$min. The rate of appearance R_a can be calculated using (7.4.18), and equals 4,520mg/min. Finally, the total mass in the system, M_{tot}^{NC}, can be estimated from (7.4.16); it equals 449,288mg.

Consider next model A. This is a situation in which tracer and tracee input and losses are all into the accessible compartment 1. The mean residence time matrix Θ equals

$$\Theta = \begin{pmatrix} 74.6 & 74.6 \\ 24.8 & 34.7 \end{pmatrix}$$

From (7.4.1), $MRT_1 = \theta_{11} + \theta_{21} = 74.6 + 24.8 = 99.4$min which agrees with the noncompartmental estimate MRT^{NC}. The production rate U_1 can be calculated from (7.4.17)

$$U_1 = \frac{M_1}{\theta_{11}} = \frac{337200}{74.6} = 4520\text{mg/min}$$

which again agrees with the noncompartmental estimate for R_a Finally, M_{tot} can be calculated from (7.4.15), and again agrees with the noncompartmental estimates.

For model B, as noted in this section, there is agreement between the two methods of estimating the system parameters since all inputs and losses are from the accessible compartment. What happens with the situations illustrated in models C and D? In model C, all inputs are into the accessible compartment 1, but losses can occur from both compartments 1 and 2. The situation is almost the same in model D except that de novo tracee input occurs in compartment 2, i.e. $U_1 = 0$ while $U_2 \neq 0$.

For both models C and D, the Θ matrix is

$$\Theta = \begin{pmatrix} 74.6 & 67.8 \\ 27.3 & 34.7 \end{pmatrix}$$

From (7.4.1), for both models, $MRT_1 = \theta_{11} + \theta_{21} = 101.9$min; this differs from the estimate $MRT^{NC} = 99.4$min, and shows $MRT^{NC} < MRT_1$.

Next, for model C, $U_1 = \frac{M_1}{\theta_{11}} = 4520\text{mg/min}$; this is equal to the estimate for R_a as the theory predicts. However, from (7.4.19) it is easy to see that the estimates for the total mass in the system will be different because the system mean residence time is different. In this case, $M_{tot} = MRT_1 \cdot U_1 = 460,588\text{mg}$

Finally, for model D where de novo tracee input is into the nonaccessible compartment 2 rather than compartment 1, one has from (7.4.17)

$$U_2 = \frac{M_1}{\theta_{12}} = \frac{337200}{67.8} = 4973\text{mg/min}$$

a number which is considerably different from R_a and U_1 for models B and C. Again since M_{tot} is the product of MRT_1 and U_2, it is clear that for this situation the noncompartmental model will underestimate the total mass in the system.

Model D illustrates another situation which can help explain this difference. It is easy to see in this case with tracee entering the system de novo into compartment 2, that some tracee can be irreversibly lost along the pathway k_{02} without ever appearing in the accessible compartment. Therefore, the tracer will not "see" the kinetics of all tracee particles.

7.5 PARAMETERS OF THE NONACCESSIBLE POOLS

Up to this point, compartmental and noncompartmental models proved to be equivalent in estimating the accessible pool parameters, while they differ in estimating the system parameters. Compartmental models are able to estimate the correct value of the mean total residence time, tracee production and mass while noncompartmental models are only able to provide an underestimate. The two approaches are also substantially different in how the nonaccessible pools of the system are quantitated. Noncompartmental models are only able to estimate the kinetic parameters for the nonaccessible portion of the system as a whole by subtracting from the system parameters the accessible pool parameters. For instance, the noncompartmental estimate for the mean residence time in the nonaccessible portion of the system as denned in Table 3.3.2, denoted Θ_W, is equal to the difference between the total mean residence time in the system MRT^{NC} and the residence time in the accessible pool Θ. Similarly, the difference between the total tracee mass M_{tot}^{NC} and the accessible pool mass M gives an estimate of the tracee mass in the nonaccessible portion of the system.

The compartmental model provides a much more detailed kinetic picture of the system under study since it permits one to estimate kinetic parameters such as masses, productions, residence times and intercompartmental fluxes for any individual compartment. In addition to that, the definition of accessible pool kinetic parameters such as the fractional clearance rate, and the rates of appearance and disappearance can be extended to any nonaccessible compartment since, by writing (7.3.1) and (7.3.2) for a generic compartment i, one has

$$FCR_i = \frac{1}{\theta_{ii}} \qquad (7.5.1)$$

$$R_{ai} = R_{di} = M_i \cdot FCR_i = \frac{M_1}{\theta_{ii}} \qquad (7.5.2)$$

where FCR_i, R_{ai} and R_{di} are the counterparts of FCR_1, R_{a1} and R_{d1}. Note that the evaluation of plasma clearance rate in nonaccessible pools, $CR_i = \frac{V_i}{\theta_{ii}}$ is not feasible unless the tracee concentration C_i is known since $V_i = \frac{M_1}{C_i}$.

Example

Consider the compartmental model shown in Figure 5.4.1B. The kinetic parameters for the nonaccessible compartment 2 are $M_2 = 112.088$mg and $\theta_{22} = 34.7$min from which the fractional clearance rate, and the rates of appearance and disappearance can be evaluated:

$$FCR_2 = \frac{1}{\theta_{22}} = 0.0288 \text{min}^{-1}$$

$$R_{a2} = R_{d2} = M_2 \cdot FCR_2 = 3230 \text{mg/min}$$

7.6   THE TWO ACCESSIBLE POOL MODEL

In this section, a comparison between kinetic parameters of the two accessible pool noncompartmental model discussed in §3.4 and the compartmental model will be discussed.

7.6.1   Accessible Pool Parameters

The noncompartmental two accessible pool parameters are listed in Table 3.4.1. The masses M_1 and M_2 and volumes V_1 and V_2 of the two accessible pools are equivalent to the corresponding compartmental masses and volumes. In fact, as noted in Chapter 3, they are the same

as those for the one accessible pool model applied separately to the two pools; in §7.3 the equivalence between the compartmental model and noncompartmental estimates of masses and volumes of accessible pools was shown. The other accessible pool parameters of Table 3.4.1 such as rates of appearance, disappearance, irreversible removal and interconversion between the accessible pools are unique to the noncompartmental model. That is, they do not have an immediate counterpart in the compartmental model setting. However, they can be recovered from the compartmental model using results given in §7.2.

For instance, the rate of disappearance "per se" from pool 1, R_{01}, was given in Table 3.4.3 for the case of the bolus injection experiment as

$$R_{01} = \frac{d_1 \int_0^\infty z_2^2(t)dt - d_2 \int_0^\infty z_2^1(t)dt}{\int_0^\infty z_1^1(t)dt \int_0^\infty z_2^2(t)dt - \int_0^\infty z_1^2(t)dt \int_0^\infty z_2^1(t)dt} \qquad (7.6.1)$$

Recalling that $z_i^j(t) = \frac{m_i^j(t)}{M_i}$ for $i,j = 1,2$, (7.6.1) can be rewritten

$$R_{01} = \frac{d_1 \frac{\int_0^\infty m_2^2(t)dt}{M_2} - d_2 \frac{\int_0^\infty m_2^1(t)dt}{M_2}}{\frac{\int_0^\infty m_1^1(t)dt}{M_1} \frac{\int_0^\infty m_2^2(t)dt}{M_2} - \frac{\int_0^\infty m_1^2(t)dt}{M_1} \frac{\int_0^\infty m_2^1(t)dt}{M_2}} \qquad (7.6.2)$$

From the equality (7.2.6) between the elements of the mean residence time matrix and the areas under the tracer mass curves, R_{01} can be derived from the compartmental model kinetic parameters as:

$$R_{01} = M_1 \frac{\theta_{22} - \theta_{21}}{\theta_{11}\theta_{22} - \theta_{12}\theta_{21}} \qquad (7.6.3)$$

Similarly,

$$R_{02} = M_2 \frac{\theta_{11} - \theta_{12}}{\theta_{11}\theta_{22} - \theta_{12}\theta_{21}} \qquad (7.6.4)$$

$$R_{21} = M_1 \frac{\theta_{21}}{\theta_{11}\theta_{22} - \theta_{12}\theta_{21}} \qquad (7.6.5)$$

$$R_{12} = M_2 \frac{\theta_{12}}{\theta_{11}\theta_{22} - \theta_{12}\theta_{21}} \qquad (7.6.6)$$

7.6.2 System Parameters

Paralleling the result obtained in §7.4 for the one accessible pool model, one can compare in detail the two accessible pool noncompartmental estimates of the system parameters with the compartmental model ones; this will demonstrate even in this experimental configuration the limitations of the noncompartmental approach.

Mean residence times

The two accessible noncompartmental model permits one to estimate the mean residence times in the system of particles introduced into the system in the accessible pools 1 and 2, MRT_1^{NC} and MRT_2^{NC}, as defined in (3.4.19) and (3.4.20). These were written

$$MRT_1^{NC} = MRT_1^1 \frac{R_{01}}{R_{d1}} + MRT_2^1 (1 - \frac{R_{01}}{R_{d1}}) \qquad (7.6.7)$$

System parameters

$$MRT_2^{NC} = MRT_2^2 \frac{R_{02}}{R_{d2}} + MRT_1^2 (1 - \frac{R_{02}}{R_{d2}}) \qquad (7.6.8)$$

The compartmental model parameters are MRT_1 and MRT_2, and they are equal to the sums of the residence times in each individual compartment of particles entering from compartment 1 and 2:

$$MRT_1 = \theta_{11} + \theta_{21} + \cdots + \theta_{n1} \qquad (7.6.9)$$

$$MRT_2 = \theta_{12} + \theta_{22} + \cdots + \theta_{n2} \qquad (7.6.10)$$

Consider first the link between MRT_1^{NC} and MRT_1, and assume without loss of generality, the bolus injection experiment so that MRT_1^1 and MRT_2^1 are expressed by (3.4.17) and (3.4.18). These equations are written below in terms of the tracer and tracee masses:

$$MRT_1^1 = \frac{\int_0^\infty t \cdot m_1^1(t)dt}{\int_0^\infty m_1^1(t)dt} \qquad (7.6.11)$$

$$MRT_2^1 = \frac{\int_0^\infty t \cdot m_2^1(t)dt}{\int_0^\infty m_2^1(t)dt} \qquad (7.6.12)$$

By following the same reasoning as that given in §7.4 where (7.4.10) was developed, the following equality can be derived:

$$\int_0^\infty t \cdot m_i^j(t)dt = d_j[\theta_{i1}\theta_{1j} + \theta_{i2}\theta_{2j} + \cdots + \theta_{in}\theta_{nj}] \qquad i,j = 1,2 \quad (7.6.13)$$

Using (7.6.13) and (7.2.9), MRT_1^1 and MRT_2^2 can be related with the elements of the mean residence time matrix:

$$MRT_1^1 = \theta_{11} + \theta_{21}\frac{\theta_{12}}{\theta_{11}} + \theta_{31}\frac{\theta_{13}}{\theta_{11}} + \cdots + \theta_{n1}\frac{\theta_{1n}}{\theta_{11}} \qquad (7.6.14)$$

$$MRT_1^2 = \theta_{11} + \theta_{22} + \theta_{23}\frac{\theta_{31}}{\theta_{21}} + \cdots + \theta_{2n}\frac{\theta_{n1}}{\theta_{21}} \qquad (7.6.15)$$

An expression for R_{01} as a function of the elements of the mean residence time matrix has already been derived (7.6.3) as well as for $R_{d1} = R_{a1}$ (7.4.14). By using these equations, and (7.6.7) together with (7.6.14)and (7.6.15), an expression for the noncompartmental parameter MRT_1^{NC} as a function of the compartmental residence times θ_{ij} can be derived:

$$
MRT_1^{NC} = \left[\theta_{11} + \theta_{21}\frac{\theta_{12}}{\theta_{11}} + \theta_{31}\frac{\theta_{13}}{\theta_{11}} + \cdots + \theta_{n1}\frac{\theta_{1n}}{\theta_{11}}\right]\frac{\theta_{11}(\theta_{22} - \theta_{21})}{\theta_{11}\theta_{22} - \theta_{12}\theta_{21}}
$$
$$
+ \left[\theta_{11} + \theta_{22} + \theta_{23}\frac{\theta_{31}}{\theta_{21}} + \cdots + \theta_{2n}\frac{\theta_{n1}}{\theta_{21}}\right]\frac{\theta_{21}(\theta_{11} - \theta_{12})}{\theta_{11}\theta_{22} - \theta_{12}\theta_{21}}
$$

$$(7.6.16)$$

rearranging (7.6.16)

$$
MRT_1^{NC} = \theta_{11} + \theta_{21} + \theta_{31}\left[\frac{\frac{\theta_{13}}{\theta_{11}} - \frac{\theta_{12}\,\theta_{23}}{\theta_{11}\,\theta_{22}}}{1 - \frac{\theta_{12}\,\theta_{21}}{\theta_{11}\,\theta_{22}}} + \frac{\frac{\theta_{23}}{\theta_{22}} - \frac{\theta_{21}\,\theta_{13}}{\theta_{22}\,\theta_{11}}}{1 - \frac{\theta_{12}\,\theta_{21}}{\theta_{11}\,\theta_{22}}}\right] \quad (7.6.17)
$$
$$
+ \cdots + \theta_{n1}\left[\frac{\frac{\theta_{1n}}{\theta_{11}} - \frac{\theta_{12}\,\theta_{2n}}{\theta_{11}\,\theta_{22}}}{1 - \frac{\theta_{12}\,\theta_{21}}{\theta_{11}\,\theta_{22}}} + \frac{\frac{\theta_{2n}}{\theta_{22}} - \frac{\theta_{21}\,\theta_{1n}}{\theta_{22}\,\theta_{11}}}{1 - \frac{\theta_{12}\,\theta_{21}}{\theta_{11}\,\theta_{22}}}\right]
$$

The bracketed terms in (7.6.17) can be given a useful probabilistic interpretation: they represent, respectively, the probability that a particle goes from compartment i to compartment 1 without passing through compartment 2 so that (7.6.17) can be written:

$$
MRT_1^{NC} = \theta_{11} + \theta_{21} \tag{7.6.18}
$$
$$
+ \sum_{i=3}^{n}\theta_{i1}\Big(Prob[i \rightarrow 1 \text{ without passing through 2}]
$$
$$
+ Prob[i \rightarrow 2 \text{ without passing through 1}]\Big)
$$

It is clear that MRT_1^{NC} coincides with MRT_1 if and only if the irreversible losses in the system take place in the accessible pools 1 and 2 only. In fact, under these circumstances, all particles from the generic compartment i will reach either accessible pool 1 or 2 before irreversibly leaving the system, and thus

$$
Prob[i \rightarrow 1 \text{ without passing through 2}] \tag{7.6.19}
$$
$$
+ Prob[i \rightarrow 2 \text{ without passing through 1}] = 1
$$

Similar conclusions can be drawn for MRT_2^{NC}.

Total mass

The compartmental total mass in the system equals the sum of the masses in all compartments. In Chapter 6 for the case where the tracee enters the system in compartment h and k

$$M_{tot} = MRT_h U_h + MRT_k U_k \qquad (7.6.20)$$

while the noncompartment formulas given in Chapter 3 is

$$M_{tot}^{NC} = MRT_1^{NC} R_{10} + MRT_2^{NC} R_{20} \qquad (7.6.21)$$

In order to derive the conditions under which M_{tot} equals M_{tot}^{NC}, relationships among U_h, U_k, R_{10} and R_{20} are needed. The production rates U_h and U_k can be estimated from the masses M_1 and M_2 and the residence times by solving the two steady state equations

$$M_1 = \theta_{1h} U_h + \theta_{1k} U_k \qquad (7.6.22)$$
$$M_2 = \theta_{2h} U_h + \theta_{2k} U_k$$

From (7.6.3) - (7.6.6), R_{10} and R_{20} can be expressed as

$$R_{10} = R_{21} + R_{01} - R_{12} = \frac{M_1 \theta_{22} - M_2 \theta_{12}}{\theta_{11}\theta_{22} - \theta_{12}\theta_{21}} \qquad (7.6.23)$$

$$R_{20} = R_{12} + R_{02} - R_{21} = \frac{M_2 \theta_{11} - M_1 \theta_{21}}{\theta_{11}\theta_{22} - \theta_{12}\theta_{21}}$$

Substituting (7.6.22) into (7.6.23) and rearranging terms, one has

$$R_{10} = U_h \left[\frac{\frac{\theta_{1h}}{\theta_{11}} - \frac{\theta_{12}}{\theta_{11}}\frac{\theta_{2h}}{\theta_{22}}}{1 - \frac{\theta_{12}}{\theta_{11}}\frac{\theta_{21}}{\theta_{22}}} \right] + U_k \left[\frac{\frac{\theta_{1k}}{\theta_{11}} - \frac{\theta_{12}}{\theta_{11}}\frac{\theta_{2k}}{\theta_{22}}}{1 - \frac{\theta_{12}}{\theta_{11}}\frac{\theta_{21}}{\theta_{22}}} \right] \qquad (7.6.24)$$

$$R_{20} = U_h \left[\frac{\frac{\theta_{2h}}{\theta_{22}} - \frac{\theta_{21}}{\theta_{22}}\frac{\theta_{1h}}{\theta_{11}}}{1 - \frac{\theta_{12}}{\theta_{11}}\frac{\theta_{21}}{\theta_{22}}} \right] + U_k \left[\frac{\frac{\theta_{2k}}{\theta_{22}} - \frac{\theta_{21}}{\theta_{22}}\frac{\theta_{1k}}{\theta_{11}}}{1 - \frac{\theta_{12}}{\theta_{11}}\frac{\theta_{21}}{\theta_{22}}} \right]$$

Using the probabilistic interpretation developed in (7.6.18), one can write

$$
\begin{aligned}
R_{10} = \ & U_h Prob[h \to 1 \text{ without passing through 2}] \quad (7.6.25) \\
+ \ & U_k Prob[k \to 1 \text{ without passing through 2}]
\end{aligned}
$$

$$
\begin{aligned}
R_{20} = \ & U_h Prob[h \to 2 \text{ without passing through 1}] \\
+ \ & U_k Prob[k \to 2 \text{ without passing through 1}]
\end{aligned}
$$

The parameters R_{10} and R_{20} correctly recover U_h and U_k if h and k equal 1 and 2, that is, it de novo production takes place in accessible pools 1 and 2. If in addition irreversible loss is only from these pools, then

$$MRT_1^{NC} = MRT_1$$
$$MRT_2^{NC} = MRT_2$$

(7.6.26)

and from (7.6.20) and(7.6.21),

$$MRT_{tot}^{NC} = MRT_1^{NC} R_{10} + MRT_2^{NC} R_{20} = MRT_1 U_1 + MRT_2 U_2 = M_{tot}$$

(7.6.27)

As discussed previously in §3.4, it can be shown that in all other situations, M_{tot}^{NC} underestimates M_{tot}.

This page intentionally left blank.

Chapter 8

PARAMETER ESTIMATION: SOME FUNDAMENTALS OF REGRESSION ANALYSIS

8.1 INTRODUCTION

In the formulas given in Chapter 3 for the noncompartmental parameters, the evaluation of certain integrals is needed. These integrals are evaluated either from some specific time in the time domain of the data to time infinity, or from time zero to infinity. In either case, one must extrapolate beyond the finite time domain of the experimental data. The evaluation of these integrals is best accomplished by providing a functional description of the data. It should be noted that such a function postulates the behavior of the system outside of the time domain of the data.

This Chapter will provide the technical information for the mathematics and statistics of obtaining a generic functional description of a set of data. In the next Chapter, this information will be used to estimate the noncompartmental parameters by using a sum of exponentials as a functional description of the data. Some of the material covered in this Chapter will be used again in Chapter 10 to describe parameter estimation of linear compartmental models.

Parameter estimation is a difficult subject touching various aspects, including statistical and algorithmic ones. Our treatment will try to be comprehensive and in an easy language. For more details on both fundamentals of regression, numerical algorithms statistical tests as well as other techniques like maximum likelihood and Bayesian parameter estimation, the reader can consult Bard [1974], Bates and Watts [1998], Carson et al. [1983], Draper and Smith [1981], Landaw and DiStefano [1994], and Seber and Wild [1989].

8.1.1   The Nature of the Regression Problem

In what follows, denote by $y(t)$ the model output variable. Depending upon the experiment, $y(t)$ can be tracer concentration or the tracer to tracee ratio. For purposes of providing a functional description of the data, the physical meaning of $y(t)$ is not relevant. A function $y(t)$ chosen to describe a set of data is characterized by a set of parameters. For example, the polynomial

$$y(t) = A_0 + A_1t + A_2t^2 \tag{8.1.1}$$

is characterized by the independent variable t which in tracer experiments is usually time, and the coefficients A_0, A_1 and A_2. These coefficients are the parameters for this polynomial. On the other hand, the exponential expression

$$y(t) = A_1e^{-\lambda_1 t} + A_2e^{-\lambda_2 t} \tag{8.1.2}$$

is characterized by the independent variable t, the coefficients A_1 and A_2, and the exponentials λ_1 and λ_2. The parameters here are the coefficients and exponentials. If either of these functions were being used to "describe" a set of data, the parameters characterizing them need to be "adjusted" until a set of values for them is obtained which provides the "best fit" to the data. Regression analysis, which will be defined and described in detail below, is the most widely used method to "adjust" the parameters characterizing a particular function to obtain the "best fit" to a set of data.

It will be seen that there are fundamentally two kinds of regression: linear and nonlinear. The theory of linear regression is mathematically precise with the formulas for the parameters characterizing the function specifically defined. Nonlinear regression is more complex and results only in approximations of the estimates of the parameters. In addition to the parameter estimates, for both linear and nonlinear regression, one usually wants information on the the errors of the parameter estimates. To obtain estimates of these errors, one moves to weighted regression. In weighted regression, a knowledge of the error structure of the data is needed. These errors are used to calculate the weight assigned to a datum during the regression process. The importance of understanding the nature of the error in the data and how this relates to weighted and unweighted regression is an essential ingredient of the regression problem which will be made transparent. Thus there are several ingredients to the regression problem. These will be isolated and explained in detail with examples provided.

With an understanding of the regression problem and an appreciation of the complexities of nonlinear regression in particular, it will become clear that a prerequisite for a successful nonlinear regression is a good software tool, i.e. a computer program which has a robust algorithm for the estimation procedure which also provides statistical information about the fit. This can provide the investigator with an informationally rich output including not only the numerical estimates of the parameters but also a measure of their precision. In addition, a number of diagnostic tests on, for example, the residuals are available to assess the appropriateness of a particular functional description of the data.

How do such software tools work? What does the investigator need to know to use them? The essential ingredients are illustrated in Figure 8.1.1 below:
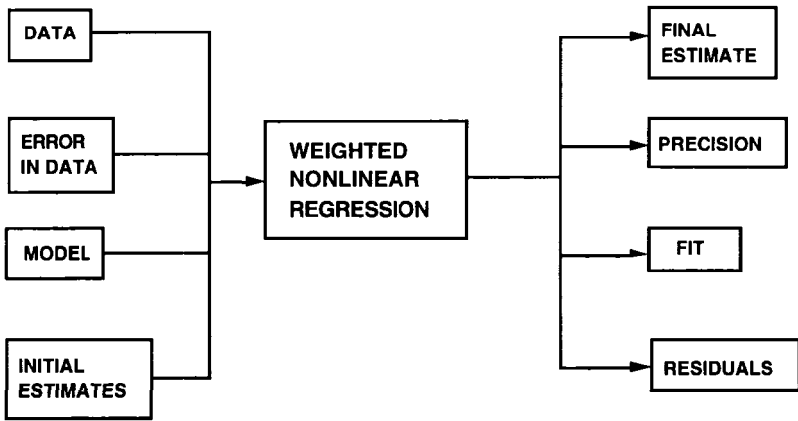
Figure 8.1.1. Schematic for the input into and output from a computer package utilizing weighted non-linear regression.

Here, the box labeled weighted nonlinear regression represents the algorithm the chosen software tool will utilize to perform the weighted nonlinear regression. The investigator must supply certain information, or input, in order to utilize the tool. First, the model must be specified; in the case discussed here, these are the equations that are going to be used to describe the data. These equations are characterized by a set of parameters which are to be estimated from the data. The investigator must supply the data, and an error estimate for each datum; as will be

seen, these errors will be used to assign weights to the data. Finally, initial estimates for each of the parameters must be provided. From the software tool the investigator obtains an output which includes (i) estimated parameter values, (ii) information on the fit (e.g. residuals and sums of squares of residuals), (iii) precision of the individual parameter estimates, and (iv) correlations among the parameters.

Before starting, a very basic point should be made. That is that the first step in the analysis of any set of tracer data should be plotting the data. Whereas this point is so obvious it hardly needs stating, there are many investigators who do not do this, but go directly from the measured sample values to some software tool to process their data.

Why is this step important? The reason is that the investigator should look first for the qualitative characteristics of the data, i.e. features such as the shape of the curve, the times at which "breaks" appear, apparent bumps or humps in the curve, and data that might be spurious. In short, the investigator should become acquainted with the data before proceeding to a quantitative description of them. It is only through this exercise that certain characteristics will be recognized as consistent among various sets while other will be unique to a given set suggesting possible problems with a particular experiment. In addition, by going through the exercise of a careful qualitative evaluation of the data, an investigator can often get a feeling for the parameter estimates or how much information he might actually obtain from the data.

As an example, consider the data given in Figure 8.1.2. These data are from a turnover experiment in which a tracer was injected as a bolus in the system, and serial plasma samples taken for 20 days. On day 9, the subject was given a drug, and the investigator wanted to know whether or not the drug affected the metabolism of the tracee as reflected by changes in the tracer decay curve.

Figure 8.1.2-B shows the best fit obtained from a sum of two exponentials. In Figure 8.1.2-C, a best fit of the data to day nine by a sum of two exponentials is given; the dotted line shows how this functional representation of the data would extrapolate to day 20. The solid line beyond day 9 represents a best fit of those data to a monoexponential. This last curve indicates clearly there is a "break" in the data starting at day 9. Obviously the two curves in Figure 8.1.2-B and Figure 8.1.2-C support markedly different conclusions.

This example should make the reader aware of the amount of information about the system that has been obtained qualitatively from simply plotting the data. One should also be aware of how drawing a curve through the data can bias the interpretation of the data. Figure 8.1.2 illustrates a situation where if one had tried to draw just one
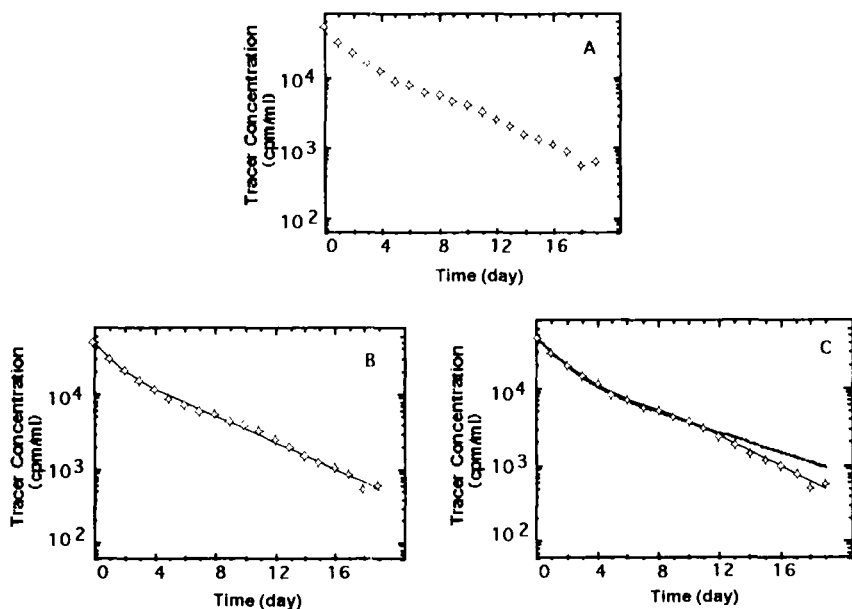
Figure 8.1.2. A. The data from the turnover study described in the text. B. The total data set described by a sum of two exponentials. C. The data to day nine described by a sum of two exponentials, and extrapolated to day 20 (dotted line), and the data fitted first to day nine, and then to day 20 (solid line). See text for additional explanation.

curve through the data, the richness contained therein could have been missed, and possibly an erroneous conclusion reached.

The plots shown in Figure 8.1.2 are semi-logarithmic. For purposes of investigating data "by hand", these are very useful since they indicate how many exponentials may be required to describe the data; this in turn means the number of compartments in a compartmental model. This will also be used in Chapter 9 where a discussion of obtaining initial estimates for the exponentials in a sum of exponentials is given. However, following a fit, the linear plot is more informative. Thus in this Chapter, the plots given after a successful fit will be linear unless otherwise noted.

Once the investigator has thoroughly studied the data through this qualitative graphical analysis, it is time to obtain a functional description of the data in order to subsequently estimate from it the kinetic parameters of interest. This is the subject of the rest of this Chapter.

8.1.2   Linear and Nonlinear Parameters

What constitutes a linear or nonlinear parameter? It is important to understand this since, as seen in the next section, there is an exact solution when the model contains only linear parameters while, as seen in §8.3, the solution is only approximate if the model contains at least one nonlinear parameters. In particular, if $y(t)$ is characterized only by linear parameters, one uses linear regression and can obtain an exact solution. If there is at least one nonlinear parameter in $y(t)$, nonlinear regression must be used, and the parameter estimates, as will be seen, are approximate.

There are many kinds of functions which are linear in their parameters; polynomials such as the following are but one:

$$y(t) = A_0 + A_1 t + A_2 t^2 + \ldots + A_n t^n \qquad (8.1.3)$$

This polynomial $y(t)$ is characterized by the coefficients $A_0, A_1, A_2, \ldots, A_n$ which are the parameters to be estimated in data fitting, and the independent variable is t. Why are polynomials linear? The reason why can be illustrated by using the simple polynomial

$$y(t) = At = y(A, t) \qquad (8.1.4)$$

When $y(t) = y(A, t)$ is written in this manner, it indicates y as a function of the independent variable t and of the value assigned to the parameter A. That is, $y(t)$ will assume different values depending upon a specific value for A. The function $y(t)$ is linear in the parameter A, or equivalently the parameter A *in* (8.1.4) is linear because if the value $. A + A'$ is considered, then

$$y(A + A', t) = (A + A')t = At + A't = y(A, t) + y(A', t) \qquad (8.1.5)$$

For example, doubling the value for the parameter A will double the value for the function $y(t)$.

If $y(t)$ *is* not linear in at least one of its parameters, or equivalently if not all parameters describing $y(t)$ are linear, then $y(t)$ is nonlinear. Nonlinearity is seen when the counterpart of (8.1.5) cannot be written for a particular function. For example, the exponential function $y(t)$ given in (8.1.2) is nonlinear since $y(A_1 + A_1', \lambda_1 + \lambda_1', A_2 + A_2', \lambda_2 + \lambda_2', t)$ is not equal to the sum of $y(A_1, \lambda_1, A_2, \lambda_2, t)$ and $y(A_1', \lambda_1', A_2', \lambda_2', t)$. This function is linear in A_1 and A_2 and nonlinear in λ_1 and λ_2. How to deal with these functions will be discussed in §8.4. One should be aware of the fact that the two types of functions are the basis for the two types of regression discussed in this Chapter. If the function is linear,

one uses linear regression; if the function is nonlinear, one uses non-
linear regression. As will be seen, while the linear regression problem
can be solved "exactly", the nonlinear regression problem involves ap-
proximations based on the linear theory. Thus an understanding of the
linear regression material covered in §8.2 is essential to understand the
nonlinear regression material presented in the following sections.

8.2   BASIC CONCEPTS OF REGRESSION ANALYSIS

8.2.1   The Residual

The basic notions of regression, i.e. finding a set of parameter values
which define a function which will provide the best fit for a set of data,
can be described using the data given in Figure 8.2.1.

t_i	$y_{obs}(t_i)$
10	60
20	70
30	90
40	180
50	230
60	200
70	300
80	290
90	350
100	420
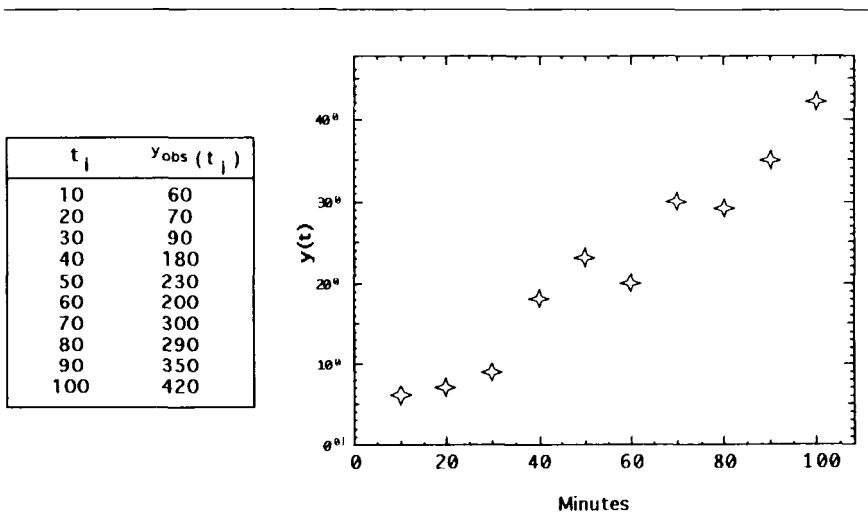
Figure 8.2.1.   Data to be used to illustrate linear regression. See text for explanation.

Suppose an investigator wishes to obtain the best fit of these data to
the straight line

$$y(t) = At \qquad (8.2.1)$$

How can this fit be obtained?

To solve the problem, one sees that, for different values of A, different straight lines will be generated. How does one find the particular value for A which provides the best fit?

Note that for each point in time t_i where there is a datum, denoted $y_{obs}(t_i)$, there is a corresponding value predicted from $y(t)$, $y(t_i)$. Once a value for A is chosen, the difference between the experimentally observed datum and the calculated value, i.e. $y_{obs}(t_i) - y(t_i)$, can be calculated; this is called the **residual.** In general, if $y(t)$ is a function to be fitted to a set of data, and if $y_{obs}(t_i)$ is the ith observation, the residual is written

$$\text{res}(t_i) = y_{obs}(t_i) - y(t_i) \tag{8.2.2}$$

Suppose in (8.2.1), $A = 3.5$. The calculated value and residuals are shown in Table 8.2.1; these are plotted in Figures 8.2.2A and B.

Table 8.2.1.

t_i	$y_{obs}(t_i)$	$y(t_i)$	$\text{res}(t_i)$
10	60	35	25
20	70	70	0
30	90	105	-15
40	180	140	40
50	230	175	55
60	200	210	-10
70	300	245	55
80	290	280	10
90	350	315	35
100	420	350	70

One sees in Figure 8.2.2A that with $A = 3.5$ the fit is not particularly good. This is emphasized by the plot of the residuals in Figure 8.2.2B where clearly there are more residuals that are positive than negative. The best fit with $A = 3.997$ is shown in Figure 8.2.2C along with the residuals in Figure 8.2.2D which now are more randomly scattered about 0. The question is: how was this fit obtained? This question will be dealt with in detail in subsequent sections of this chapter.

8.2.2   Residual Sum of Squares

The expression:

$$\text{RSS} = \sum_{i=1}^{N}(y_{obs}(t_i) - y(t_i))^2 = \sum_{i=1}^{N}\text{res}^2(t_i) \tag{8.2.3}$$

where N is the number of observations ($N = 10$ for the data in Figure 8.2.1) is called the **residual sum of squares,** RSS, since $y_{obs}(t_i) -$
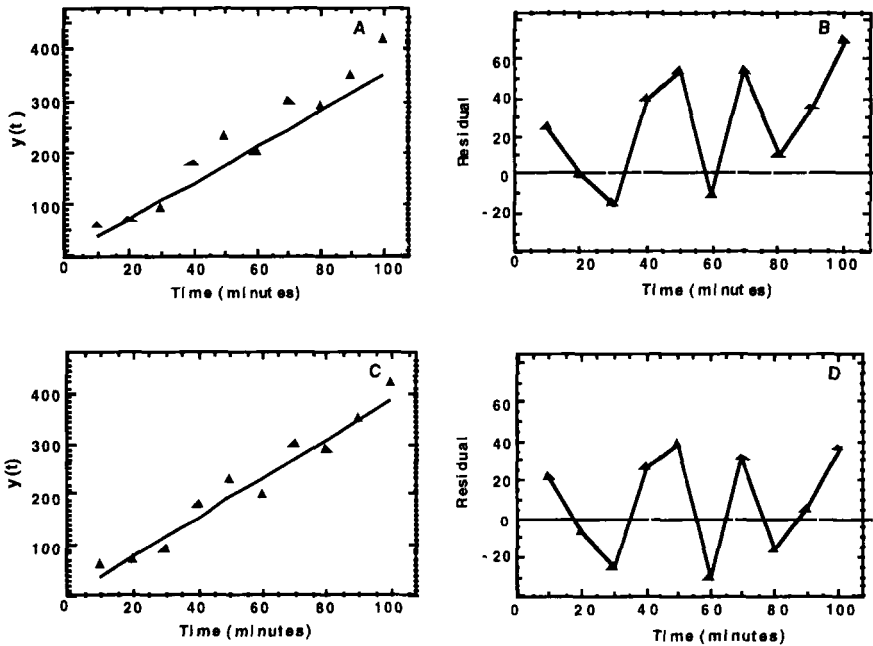
Figure 8.2.2. Panel A. The data given in Figure 8.2.1 are plotted together with a line calculated from the polynomial $y(t) = 3.5t$. Panel B. The plot of the residuals. Panel C. The "best fit" by $y = 3.997t$. Panel D. The plot of the residuals for the best fit. See text for additional explanation.

$y(t_i)$ can be considered as the error between the observed and predicted value for each sample time t_i. For the data given in Figure 8.2.1 and the polynomial $y = 3.5t$, the squares of the residual and RSS are given below in Table 8.2.2.

The residual sum of squares, RSS, can be considered a measure of how good the fit is to the given set of data. For different numerical values of the parameter characterizing (8.2.1), i.e. for different numerical values for *A,* one will obtain a different RSS. Therefore RSS itself can be considered as a function of the parameter characterizing the linear function chosen to describe a set of data. One can write $RSS = RSS(A)$ for (8.2.3) to underline this fact.

The idea behind regression is to minimize RSS with respect to the parameter values characterizing the function to be fitted to the data,

Table 8.2.2.

t_i	$y_{obs}(t_i)$	$y(t_i)$	res(t_i)	res$^2(t)$
10	60	35	25	625
20	70	70	0	0
30	90	105	−15	225
40	180	140	40	1600
50	230	175	55	3025
60	200	210	−10	100
70	300	245	55	3025
80	290	280	10	100
90	350	315	35	1225
100	420	350	70	4900

RSS = 14825

i.e. to find a set of parameter values for $y(t)$ which minimizes RSS. The process is called **least squares.** In the case of the function defined in (8.2.1), the problem would be to find a value for A which minimizes RSS for the set of data given in Figure 8.2.1. Figure 8.2.2-C and D show the results of such a minimization process; how this was reached will be described in detail in §8.4.

Another important ingredient of regression is a number commonly encountered in statistics: degrees of freedom. Suppose a function $y(t)$ described by P parameters is to be fitted to a set of N data points; the **degrees of freedom** is defined as the number N - P. For the example above, y(t) given in (8.2.1) is characterized by the single parameters A, hence P = 1. The number of data given in Figure 8.2.1 is 10, hence N = 10. In this example, the degrees of freedom is 9. The degrees of freedom are important since in order to solve the regression problem, i.e. to find one set of parameter values for which RSS is minimum, it is necessary that the degrees of freedom is one or greater. If the degrees of freedom is less than one, there are an infinite number of parameter values which will minimize RSS.

8.2.3   Weights and Weighted Residual Sum of Squares

As discussed in detail in §8.3, data have errors associated with them. Basically this means that one may have more confidence in some data than in others, i.e. some data may be more "important" than others in the fitting process. One would like some means by which to give greater importance to these data. This is accomplished through assign-

ing weights to each datum; how this is commonly done will be discussed in more detail in §8.3.

The assignment of weights is reflected in the sum of squares. If $y(t)$ is a function to be fitted to a set of data and $y_{obs}(t_i)$ is the ith observation, the expression:

$$\text{WRSS} = \sum_{i=1}^{N} w_i(y_{obs}(t_i) - y(t_i))^2 = \sum_{i=1}^{N} \text{wres}^2(t_i) \qquad (8.2.4)$$

where N is the number of observations is called the sum of **weighted residual sum of squares,** WRSS, since $\sqrt{w_i}(y_{obs}(t_i) - y(t_i))$ can be considered as the weighted error between the observed and predicted value for each sample time t_i. Extending the above, the theory behind minimizing WRSS is called **weighted least squares** (WLS). In this expression w_i is the weight assigned to the ith datum, and the **weighted residual** is written

$$\text{wres}(t_i) = \sqrt{w_i}(y_{obs}(t_i) - y(t_i)) \qquad (8.2.5)$$

RSS and WRSS are functions of the parameters characterizing a function $y(t)$. They are examples of what in the theory of optimization are called an **objective** or **cost function.** While there are other objective functions that can be used, RSS and WRSS are most commonly used in the analysis of tracer data, and will be the focus of this text.

8.3   THE ASSIGNMENT OF WEIGHTS TO DATA

8.3.1   Introduction

In §8.2, RSS and WRSS were defined. The difference between the two is that in the latter case a weight w_i was assigned to each datum. How are these weights obtained? It is natural to link the choice of weights to what is known about the precision of each individual datum. In other words, one seeks to give more credibility, or weight, to those data whose precision is high and less credibility, or weight, to those data whose precision is small. In this section, the following will be discussed: (i) how to obtain an estimate of the error affecting a set of data, and (ii) how to use the errors to assign weights and thus calculate WRSS.

Clearly the sources of error are many and depend upon a given experimental situation as well as the system being studied. While the investigator has some degree of control over some errors such as those involved in the various procedures one must go through in the preparation of samples for measurement of tracer or tracee concentration, other

problems that are unknown or go unnoticed will, in general, produce systematic errors that are often extremely difficult to uncover.

8.3.2   Description of the Error in the Data

Suppose one is fitting a function $y(t)$ to a set of data. In what follows, it will be assumed that the function $y(t)$ is the correct model for the data being considered. As part of the theory to be developed in this Chapter, information is recovered from the fitting process to test if this assumption is in fact "correct".

To start, for each datum $y_{obs}(t_i)$ at sample time t_i, there is a **measurement error** term $e(t_i)$. It is usually assumed that this term is additive, i.e. can be expressed

$$y_{obs}(t_i) = y(t_i) + e(t_i) \tag{8.3.1}$$

In general, one knows little or nothing about $e(t_i)$, and hence assumptions about its characteristics must be made. The most common assumption is that the errors $e(t_i)$ are independent with zero mean and variance either known or known up to a proportionality constant. What this means can be formalized in the statistical setting using the notation E, Var, and Cov to represent respectively mean, variance and covariance. Then:

$$\mathrm{E}(e(t_i)) = 0 \tag{8.3.2}$$

$$\mathrm{Cov}(e(t_i), e(t_j)) = 0 \qquad \text{for } t_i \neq t_j \tag{8.3.3}$$

and

$$\text{Case a}: \mathrm{Var}(e(t_i)) = \sigma^2(t_i) \tag{8.3.4a}$$

or

$$\text{Case b}: \mathrm{Var}(e(t_i)) = v(t_i)\sigma^2 \tag{8.3.4b}$$

Equation (8.3.2) means the errors $e(t_i)$ have zero mean; (8.3.3) means they are independent, and (8.3.4) means the variance is either known (case a) or known up to a proportionality constant (case b). In these equations, $\sigma^2(t_i)$ and $v(t_i)$ are assumed to be known, and σ^2 is the unknown proportionality constant. A standardized measure of the error is case a and b is provided by the **fractional standard deviation** FSD, or the **coefficient of variation** CV:

$$\mathrm{FSD}(e(t_i)) = \mathrm{CV}(e(t_i)) = \frac{\mathrm{SD}(e(t_i))}{y_{obs}(t_i)} \tag{8.3.5}$$

where SD is the standard deviation of the error

$$\text{SD}(e(t_i)) = \sqrt{\text{Var}(e(t_i))} \qquad (8.3.6)$$

The FSD or CV are often expressed as a percent, i.e. the percent fractional standard deviation or percent coefficient of variation, by multiplying $\frac{\text{SD}(e(t_i))}{y_{obs}(t_i)}$ in (8.3.5) by 100.

The difference between case a and b in (8.3.4) is that in case a the precision of the measurements of $y_{obs}(t_i)$ is assumed to be known while in case b only the relative values $v(t_i)$ of the $\text{Var}(e(t_i))$ are known, i.e. σ^2 is unknown. For instance, if $\text{Var}(e(t_i))$ is unknown but constant for all t_i, then clearly from (8.3.4)b, $v(t_i) = 1$, and σ^2 denoted the unknown value of the variance. Similarly if $\text{Var}(e(t_i))$ is unknown but proportional to the square of the measurement, or equivalently $\text{FSD}(e(t_i))$ is unknown but constant, then $v(t_i) = y_{obs}^2(t_i)$, and σ^2 now denotes the unknown value of the square of the fractional standard deviation. It is known that if the errors $e(t_i)$ are Gaussian, (8.3.2)-(8.3.4) specify completely the probability distribution, otherwise they can be seen to provide a description based on the first two moments (mean and variance).

Finally, using the fact that if Y is a random variable, and α and β are constants, $\text{Var}(\alpha + \beta Y) = \beta^2 \text{Var}(Y)$, one has from (8.3.1) that, since $y(t_i)$ is constant, $\text{Var}(y_{obs}(t_i)) = \text{Var}(e(t_i))$, that is, the variance of an individual datum and of its error are equal.

8.3.3   Weights and Error Variances

Knowing the error structure of the data, how are the weights w_i chosen? The natural choice is to weight each datum according to the inverse of the variance. For the two cases introduced above, case a when the variance of the error is known (called **absolute weights**), and case b when it is known up to a proportionality constant (called **relative weights**), the weights are defined as follows:

$$\text{Case a}: w_i \;=\; \frac{1}{\sigma^2(t_i)} \qquad (8.3.7a)$$

$$\text{Case b}: w_i \;=\; \frac{1}{v(t_i)} \qquad (8.3.7b)$$

It can be shown that this natural choice of weights is optimal in the linear regression case, i.e. it produces the minimum variance of the parameter estimates. Therefore, it is very important to have a correct knowledge of the error of the data, and to weight each datum according to this error. Note that only the pattern of weights, i.e. $1/v(t_i)$ or in other words the

relative precision of the data points, needs to be assigned, and even the use of an approximation of this pattern is better than unweighting the data.

   The problem now is how to estimate the error variance. Ideally one would like to have a direct estimate of the variance of all sources of error. This is a difficult problem. For instance, the measurement error is just one component of the error; it can be used as an estimate of the error only if the investigator believes the major source of error is after the sample is taken. To have a more precise estimate of the error, the investigator should have several independent replicates of the measurement $y_{obs}(t_i)$ at each sampling time t_i which can estimate the sample variance $\sigma^2(t_i)$ at t_i. If there is a major error component before the measurement process, for instance an error related to drawing a plasma sample or preparing a plasma sample for measurement, then it is not sufficient to repeat the measurement *per se* on the same sample several times; in theory in this situation it would be necessary to repeat the experiment several times. Such repetition is not often easy to handle in practice. Finally, there is the possibility that the system itself can vary during the different experiments.

   In any case, since the above mentioned approach estimates the variance at each sampling time t_i, it requires several independent replicates of each measurement. A more practical approach will be outlined in the following sections of this Chapter. This consists of postulating a model for the error variance and estimating its unknown parameters from the experimental data.

8.3.4   A Model of the Error Variance

   A flexible model that can be used in tracer studies for the error variance is

$$\sigma^2(t_i) = \alpha + \beta(y(t_i))^\gamma \qquad (8.3.8)$$

to be approximated in practice by

$$\sigma^2(t_i) = \alpha + \beta(y_{obs}(t_i))^\gamma \qquad (8.3.9)$$

where α, β and γ are model parameters relating the variance associated with an observation to the value of the observation itself. As explained below, arbitrary values can be assigned to these parameters, or they can be estimated from the data themselves.

   The three classical applications of the above formula are described below. They are illustrated in Figure 8.3.1 using the function $y(t) = 2625e^{-0.09t} + 3250e^{-0.009t}$.
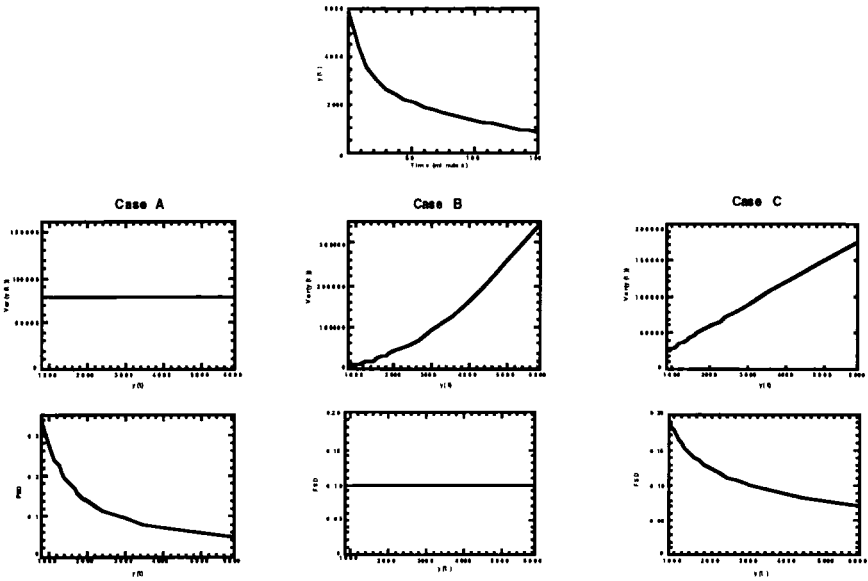
Figure 8.3.1. The top panel shows a graph of $y(t) = 2625e^{-0.09t} + 3250e^{-0.009t}$. This function will be used to illustrate (8.3.9). Cases A, B and C illustrate respectively constant variance, constant FSD, and Poisson statistics (see text for additional explanation). For each case, the top figure is a plot of the variance versus $y(t)$ and the bottom figure is a plot of the FSD versus $y(t)$.

In Case A, one has a constant variance, i.e. $\beta = 0$ whence

$$\sigma^2(t_i) = \alpha \qquad (8.3.10)$$

Thus:

$$\sigma(t_i) = \sqrt{\alpha} \qquad (8.3.11)$$

$$\mathrm{FSD}(e(t_i)) = \frac{\sigma(t_i)}{y_{obs}(t_i)} = \frac{\sqrt{\alpha}}{y_{obs}(t_i)} \qquad (8.3.12)$$

In Case B, one has a constant coefficient of variation or FSD, i.e. $\alpha = 0$ and $\gamma = 2$. In this case:

$$\sigma^2(t_i) = \beta y_{obs}^2(t_i) \qquad (8.3.13)$$

Thus:

$$\sigma(t_i) = \sqrt{\beta} \cdot y_{obs}(t_i) \qquad (8.3.14)$$

$$FSD(e(t_i)) = \sqrt{\beta} \qquad\qquad (8.3.15)$$

For example, if $\beta = 0.01$, FSD $= 0.1$. The error associated with each datum is therefore 10% of the datum. In Case C, one has Poisson (counting) statistics, i.e. $\alpha = 0$ and $\gamma = 1$. Hence:

$$\sigma^2(t_i) = \beta y_{obs}(t_i) \qquad\qquad (8.3.16)$$

Thus

$$\sigma(t_i) = \sqrt{\beta y_{obs}(t_i)} \qquad\qquad (8.3.17)$$

$$FSD(e(t_i)) = \sqrt{\frac{\beta}{y_{obs}(t_i)}} \qquad\qquad (8.3.18)$$

Example

To see the effect that the different choices of α, β and γ have on assigning the weights w_i and ultimately on WRSS, consider the data given in Figure 8.2.1 which are to be fitted by $y(t) = At$. WRSS(A) for this function depends upon these weights. Two separate weighting schemes are illustrated in Table 8.3.1 below, and WRSS(A) is calculated for each case when $A = 3.5$.

Table 8.3.1.

| | | | A $w_i = 1$ | B $\sigma^2(t_i) = 100$ | | C $\sigma^2(t_i) = (0.1 \cdot y_{obs}(t_i))^2$ | |
t_i	$y_{obs}(t_i)$	$y(t_i)$	res$^2(t_i)$	w_i	wres$^2(t_i)$	w_i	wres$^2(t_i)$
10	60	35	625	0.01	6.25	0.028	17.361
20	70	70	0	0.01	0.00	0.020	0.000
30	90	105	225	0.01	2.25	0.012	2.778
40	180	140	1600	0.01	16.00	0.003	4.938
50	230	175	3025	0.01	30.25	0.002	5.718
60	200	210	100	0.01	1.00	0.003	0.250
70	300	245	3025	0.01	30.25	0.001	3.361
80	290	280	100	0.01	1.00	0.001	0.119
90	350	315	1225	0.01	12.25	0.001	1.000
100	420	350	4900	0.01	49.00	0.001	2.778
			RSS $= 14825$	WRSS $= 148.25$		WRSS $= 38.303$	

In Table 8.3.1, the two situations are illustrated in columns B and C labeled $\sigma^2(t_i) = 100$ and $\sigma^2(t_i) = (0.1 y_{obs}(t_i))^2$ respectively; the individual entries in each of these columns are the weights w_i calculated

according to the formula $w_i = \frac{1}{\sigma^2(t_i)}$. Column A is simply the square of the residuals, and RSS(A) equals 14825. As noted above, this corresponds to the case when $w_i = 1$ for all data. Column B illustrates the weights for a constant variance; in this case $\sigma^2(t_i) = 100$ whence $w_i = .01$ for each datum. In this case, WRSS(A) $= 148.25$. Column C illustrates the weights for a constant coefficient of variation; in this case $\sigma^2(t_i) = (0.1 \cdot y_{obs}(t_i))^2$ whence w_i varies for each datum. In this case, WRSS(A) $= 38.3$.

Clearly WRSS(A) varies widely and depends upon how the w_i are selected. How this selection actually affects WLS will be discussed in §8.4 and §8.5.

While using a constant SD or FSD is commonly used to define the error structure in a set of data, there is another alternative. In the next section, how to estimate the parameters α, β and γ of the error model (8.3.9) from experimental data will be discussed. This is important since in most situations no information is available a priori on the error variance.

In closing, it should be noted that only the pattern of weights, i.e. $v(t_i)$, or in other words the relative precision of the data points, needs to be assigned if the variance of each data point is not known or difficult to determine. The previous example illustrates that it is important to know how the assignment of weights to data will affect the sum of squares and ultimately the parameter estimates and their precision.

8.3.5   Estimating the Parameters of the Error Model from Standard Samples

One possible approach to estimate the model parameters α, β and γ of $\sigma^2(t_i) = \alpha + \beta(y_{obs}(t_i))^\gamma$ given in (8.3.9) from experimental data is based on the use of standards. These are samples for which several independent replicates of the measurement process are available. The assumption must be made that all sources of measurement error in the experimental data are present in these standards, and that the standards cover the range of values observed in the experimental data.

Denote by N_r the number of replicates for a generic standard, and by $y_1, \cdots, y_{N_r}$ the values for each of the replicates. The value to be associated with the standard is the mean of the replicates:

$$y_{obs} = \frac{1}{N_r} \sum_{k=1}^{N_r} y_k \qquad (8.3.19)$$

An estimate of the variance of the standard defined in (8.3.19) given by (8.3.20):

$$\hat{\sigma}^2 = \frac{1}{N_r - 1} \sum_{k=1}^{N_r} (y_k - y_{obs})^2 \qquad (8.3.20)$$

For all of the standards, plotting either $\hat{\sigma}^2$ or the ratio $\frac{\hat{\sigma}^2}{y_{obs}}$ versus y_{obs} often suggests the appropriate relation. For instance, if the background variance α is negligible and can be assumed to equal zero, then a plot of $\log(\hat{\sigma}^2)$ versus $\log(y_{obs})$ is a straight line whose slope estimates γ in (8.3.9). A value of 2 for the exponent γ in tracer studies is quite frequent; this situation of course is a constant FSD.

Using the standards to estimate α, β and γ in (8.3.9), one can then apply (8.3.9) to each generic measurement $y_{obs}(t_i)$ to estimate the variance of the error $e(t_i)$. An example is given below.

Example

Suppose one wants to determine the variance associated with mass spectrometry measurements of peak intensity ratios in plasma during a stable isotope glucose tracer experiment in the range of 1-15%. One can prepare, for instance, four standard samples by mixing natural and tracer material in different proportions, and measure ten aliquots of each sample. An example of the kind of results one might expect from such a strategy are summarized below in Table 8.3.2.

Table 8.3.2.

y_{obs}	$\widehat{\sigma^2}$	$\hat{\sigma}$	$\widehat{FSD}$
1.06	0.00238	0.049	4.60%
2.18	0.00297	0.054	2.50%
8.88	0.0133	0.115	1.30%
13.96	0.0236	0.154	1.10%

The results given above suggest that a variance model such as

$$\sigma^2(t_i) = \alpha \qquad (8.3.21)$$

or

$$\sigma^2(t_i) = \beta y_{obs}^2(t_i) \qquad (8.3.22)$$

is not appropriate since neither the variance nor the fractional standard deviation are constant.

An appropriate model for the variance (see Figure 8.3.2) can be obtained by regression analysis (see §8.4) by fitting the function $\sigma^2(t_i) = \alpha + \beta(y_{obs}(t_i))^\gamma$ defined in (8.3.9) to $y_{obs}^2(t_i)$ versus the data listed under $\hat{\sigma}^2$ in Table 8.3.2. The results are

$$\sigma^2(t_i) = 0.0028 + 0.00011 y_{obs}^2(t_i) \qquad (8.3.23)$$
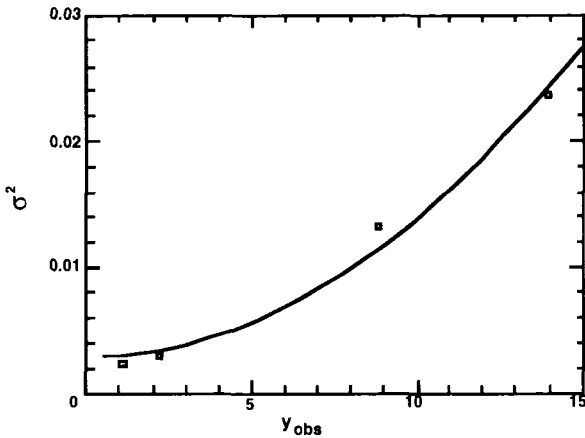
Figure 8.3.2. Plot of the best fit of $\sigma^2(t_i) = \alpha + \beta(y_{obs}(t_i))^\gamma$ to the data given in Table 8.3.2. See text for additional explanation.

8.3.6   Estimating the Parameters of the Error Model from Replicates of the Measurements

Often, to improve the precision of the measurements, samples are measured at least in duplicate or triplicate since the variance of the measurement error is reduced, as compared with the single measurement situation, by a factor equal to the number of replicates. The value of the sample is obtained by averaging the measurements of the two or three replicates (see (8.3.19)). However, since the number of replicates for each sample is small, the sample variance (8.3.20) is only a rough estimate of the true variance.

However, duplicates or triplicates can be used to derive a better estimate of the variance of the measurement error if a large number of

measurements are available. For instance, data from the same experiment performed in a number of different subjects can be pooled. A procedure to do this is illustrated in the following example.

Example

Suppose in a glucose tracer kinetic study, radioactivity is quantitated in each plasma sample in triplicates. Suppose in addition that a total of 100 samples ranging from 20,000 cpm/ml to 400,000 cpm/ml are analyzed from experiments in 4 subjects. Denote by y_1, y_2 and y_3 the three measurements for a generic sample. (In the general situation, one would have N_r samples $y_1, \cdots, y_{N_r}$; here $N_r = 3$). Then the "observed" value, y_{obs} associated with this sample is the mean of the three measurements:

$$y_{obs} = \frac{1}{N_r} \sum_{k=1}^{N_r} y_k = \frac{y_1 + y_2 + y_3}{3} \qquad (8.3.24)$$

The variance of the measurement error is reduced by a factor equal to N_r. Then an estimate of the variance associated with y_{obs} is

$$
\begin{aligned}
\hat{\sigma}^2 &= \frac{1}{N_r - 1} \sum_{k=1}^{N_r} (y_k - y_{obs})^2 = \frac{1}{2} \sum_{k=1}^{3} (y_k - y_{obs})^2 \qquad (8.3.25) \\
&= \frac{1}{2} [(y_1 - y_{obs})^2 + (y_2 - y_{obs})^2 + (y_3 - y_{obs})^2]
\end{aligned}
$$

Due to the low precision of these estimates, the plot of $\hat{\sigma}^2$ versus y_{obs} (Figure 8.3.3) shows a cluster thus making it difficult to derive the model for $\hat{\sigma}^2$.

To facilitate the detection of this relation, it is convenient to split the observation range into a number of intervals, and examine the mean value of $\hat{\sigma}^2$ or equivalently of the ratio $\frac{\hat{\sigma}}{y_{obs}}$ within each interval. The results are summarized in Table 8.3.3 and plotted in Figure 8.3.4. As seen in the Figure, the variance increases with the measurement in a quadratic fashion, or equivalently the fractional standard deviation is approximately constant. The model for the variance is then

$$\sigma^2(t_i) = \beta \cdot y_{obs}^2(t_i) = 0.000225 y_{obs}^2(t_i) \qquad (8.3.26)$$

where the numerical value for β has been evaluated by averaging the square of the fractional standard deviations in Table 8.3.3.
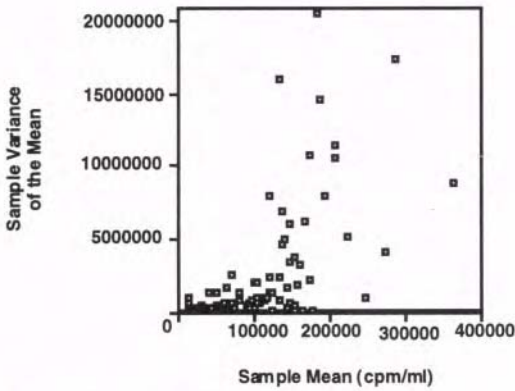
Figure 8.3.3. A plot of the sample variance of the mean versus the mean of each sample. See text for additional explanation.

Table 8.3.3.

Range (cpm/ml)	$\widehat{\sigma^2}$	$\hat{\sigma}$	$\widehat{FSD}$
0–25,000	130,016.16	345.96	0.0222
25,000–50,000	263,953.03	519.04	0.0132
50,000–75,000	506,885.59	738.26	0.0117
75,000–100,000	755,615.63	960.73	0.0109
100,000–125,000	1,629,800	1344.63	0.0118
125,000–150,000	4,286,529	2294.02	0.0165
150,000–175,000	3,136,463	1713.05	0.0105
175,000–200,000	10,818,588	3600.83	0.0193
> 200,000	15,032,556	4063.37	0.0175
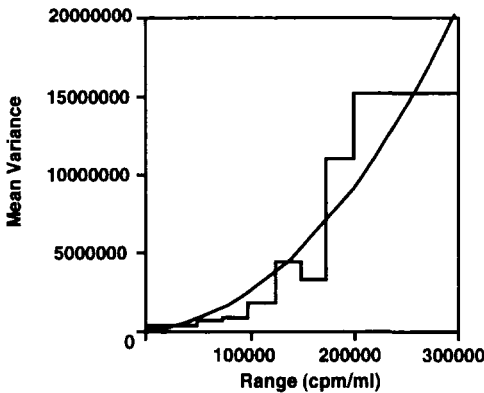
Figure 8.3.4. Bar graph of the mean variance for the ranges given in Table 8.3.3. The continuous line is a plot of $\hat{\sigma}^2(t_i)$ given in (8.3.26). See text for additional explanation.

8.3.7   Propagation of Errors

In some circumstances, the data $y_{obs}(t_i)$ are obtained by combining different primary measurements usually based upon different techniques. For instance, suppose that $y_{obs}(t_i)$ is the concentration in plasma of intact monoiodinated insulin. In order to quantify y_{obs}, one can measure by scintigraphic methods the total concentration of radioactivity in plasma associated not only with intact insulin but also with its degradation fragments, and by liquid gas-chromatography the relative amount of intact material in the sample. Intact radioactive insulin data are thus obtained as the product of two measurements. The problem is how to derive an estimate of the error variance affecting $y_{obs}(t_i)$ from a knowledge of the error variances associated with the two primary measurements. In other words, how do the errors associated with the two primary measurements propagate to the error associated with $y_{obs}(t_i)$ itself?

Suppose, for example, that $y_{obs}(t_i)$ is obtained as a function f of two measurements $m_1(t_i)$ and $m_2(t_i)$:

$$y_{obs}(t_i) = f(m_1(t_i), m_2(t_i)) \qquad (8.3.27)$$

Denote by $e_1(t_i)$ and $e_2(t_i)$ the errors associated with m_1 and m_2. If they are independent, a first order approximation for the variance of the error e affecting y_{obs} is

$$\mathrm{Var}(e(t_i)) \approx (\frac{\partial f}{\partial m_1}|_{t=t_i})^2 \mathrm{Var}(e_1(t_i)) + (\frac{\partial f}{\partial m_2}|_{t=t_i})^2 \mathrm{Var}(e_2(t_i)) \quad (8.3.28)$$

where $\frac{\partial f}{\partial m_1}$ and $\frac{\partial f}{\partial m_2}$ are the partial derivatives of f with respect to m_1 and m_2 evaluated at $t = t_i$.

Example 1

Suppose the m_1 and m_2 are two independent measurements, and that y_{obs} is the difference between the two:

$$y_{obs}(t_i) = m_1(t_i) - m_2(t_i) \qquad (8.3.29)$$

By using (8.3.28), an approximation for the variance of the error e affecting y_{obs} can be computed from the variances of the errors associated with m_1 and m_2:

$$\mathrm{Var}(e(t_i)) \approx \mathrm{Var}(e_1(t_i)) + \mathrm{Var}(e_2(t_i)) \qquad (8.3.30)$$

since $\frac{\partial f}{\partial m_1} = \frac{\partial f}{\partial m_2} = 1$. Therefore the error affecting y_{obs} has variance approximately equal to the sum of the variance of the errors associated with measurements m_1 and m_2.

If on the other hand y_{obs} is obtained as the product of the m_1 and m_2 measurements

$$y_{obs}(t_i) = m_1(t_i) \cdot m_2(t_i) \tag{8.3.31}$$

the variance associated with y_{obs} is given by

$$\text{Var}(e(t_i)) \approx m_2(t_i)^2 \text{Var}(e_1(t_i)) + m_1(t_i)^2 \text{Var}(e_2(t_i)) \tag{8.3.32}$$

or equivalently

$$
\begin{aligned}
\text{FSD}^2(e(t_i)) &= \frac{\text{Var}(e(t_i))}{y_{obs}^2(t_i)} = \frac{\text{Var}(e_1(t_i))}{m_1^2(t_i)} + \frac{\text{Var}(e_2(t_i))}{m_2^2(t_i)} \tag{8.3.33} \\
&= \text{FSD}^2(e_1(t_i)) + \text{FSD}^2(e_2(t_i))
\end{aligned}
$$

That is, the square of the fractional standard deviation of the error of y_{obs} is the sum of the squares of the fractional standard deviations of the errors of m_1 and m_2.

8.3.8 Estimating Error Model Parameters from Extended Least Squares

The procedures discussed so far for estimating the error model parameters require replicates of all, or some at least, measurements. An alternative approach, which does not require replicates, still consists of postulating a model for the error variance such as $\sigma^2(t_i) = \alpha + \beta y_{obs}(t_i)^\gamma$ given in (8.3.9), but its characteristic unknown parameters are estimated simultaneously with the unknown parameters characterizing the model of the system under study. The idea is to use an "extended" form of the weighted residual sum of squares WRSS, *EWRSS* [Peck et al., 1984]:

$$EWRSS = \sum_{i=1}^{N} \left[\frac{1}{\sigma^2(t_i)} (y_{obs}(t_i) - y(t_i))^2 + \ln(\sigma^2(t_i)) \right] \tag{8.3.34}$$

The problem now is to minimize *EWRSS* not only with respect to the unknown parameters characterizing the function $y(t)$ to be fitted to the data, but also to the unknown parameters characterizing the function $\sigma^2(t_i)$, i.e. the parameters α, β and γ in (8.3.9). This requires an extension of the weighted least squares machinery.

8.4   THE FUNDAMENTALS OF LINEAR REGRESSION

8.4.1   Data Fitting and Linear Regression

This section will discuss and illustrate the fundamental ideas of **linear regression** by fitting a straight line through the data given in Table 8.2.1 shown again in Figure 8.4.1. The concepts introduced here, based on least squares theory, carry over to any linear function.
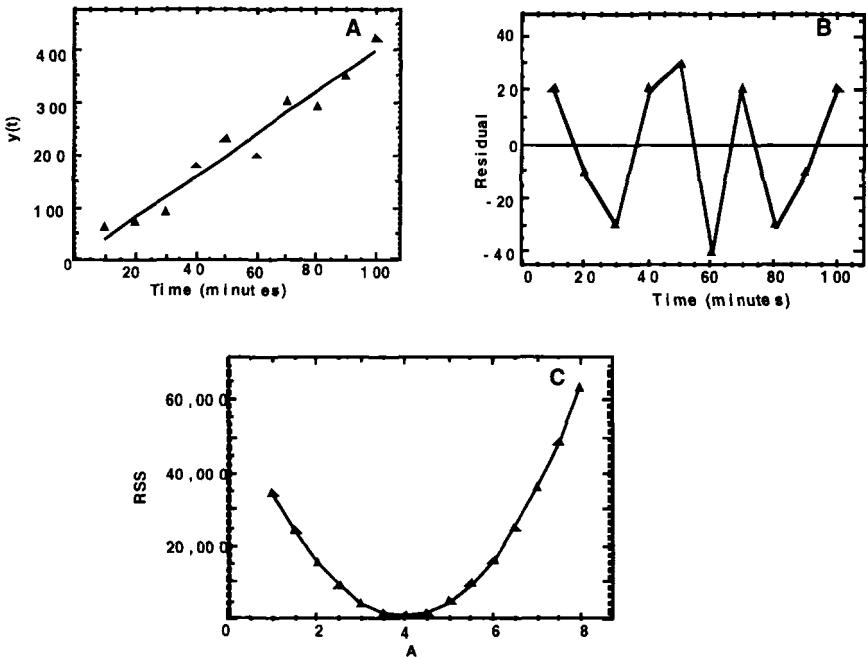
Figure 8.4.1. Panel A shows a set of data with a straight line through them where the line was calculated using linear regression. Panel B is a plot of the residuals illustrating the pattern of "above" or "below" zero. Panel C shows a plot of RSS(A) versus A, and illustrates the main point that there is a unique value of A for which RSS(A) is minimal.

The equation for the straight line used here is

$$y = y(A, t) = At \qquad (8.4.1)$$

where t is the independent variable. The parameter describing this line, A, is linear as described above. Different values for A will produce different lines. Hence, for each value of A there is a different calculated value of RSS, or RSS(A) to denote the functional relationship with A; this is shown in Figure 8.4.1-C. What one seeks is the value of A, $\hat{A}$ which minimizes RSS(A); this point is indicated in Figure 8.4.1-C. As part of the theory of linear regression, it is known that when the degrees of freedom is greater than one, there is a unique value for A which will minimize RSS(A).

In what follows, the theory of least squares and weighted least squares, abbreviated as LS and WLS respectively, will be discussed.

8.4.2   Solving the Linear Regression Problem

How does one find $\hat{A}$? Corresponding to each sample time t_i, which is assumed to be known exactly, there is an experimentally measured datum $y_{obs}(t_i)$, a calculated value $y(t_i) = At_i$, and a residual $\text{res}(t_i) = y_{obs}(t_i) - y(t_i)$. For LS, the sum of squares of the residuals for the example is given:

$$\text{RSS}(A) = \sum_{i=1}^{N} \text{res}^2(t_i) = \sum_{i=1}^{N}(y_{obs}(t_i) - y(t_i))^2 = \sum_{i=1}^{N}(y_{obs}(t_i) - At_i)^2$$

$$(8.4.2)$$

To find the unique value for A which minimizes this sum of squares, one takes the derivative of RSS(A) as given in (8.4.2) with respect to A, sets the resulting expression equal to zero, and solves this equation for A:

$$\frac{d(\text{RSS}(A))}{dA} = -2\sum_{i=1}^{N} t_i(y_{obs}(t_i) - At_i) = 0 \qquad (8.4.3)$$

From differential calculus, it is known that the value for A which is a solution of (8.4.3), $\hat{A}$, will minimize RSS(A). This is given by

$$\hat{A} = \left(\sum_{i=1}^{N} y_{obs}(t_i)t_i\right)\Big/\left(\sum_{i=1}^{N} t_i^2\right) \qquad (8.4.4)$$

One can apply (8.4.4) directly to the data given in Table 8.2.1. The numerator and denominator in (8.4.4) are respectively 153,100 and 38,500; hence $\hat{A} = 3.977$; the plot of $y(t) = 3.997t$ is given in Figure 8.4.1.

It is not enough, however, that one stops here with an estimated value $\hat{A}$. One must also examine the plot of the residuals themselves as has been done in Figure 8.4.1-B. In this situation, there is no apparent correlation in the pattern of the residuals, i.e. a series of positive residuals

followed by a series of negative residuals. Hence it is reasonable to describe these data by a straight line. Formal tests based upon residuals will be discussed in §8.6

What can happen if one takes the estimate of $\hat{A}$ as a blind estimate, i.e. does not examine the residuals as well. One runs the risk of selecting an incorrect functional description of the data. Upon examination of the residuals, nonrandomness of the errors can be discovered by observing a patterning of the residuals. As an example of this situation, consider the data given in Figure 8.4.2.
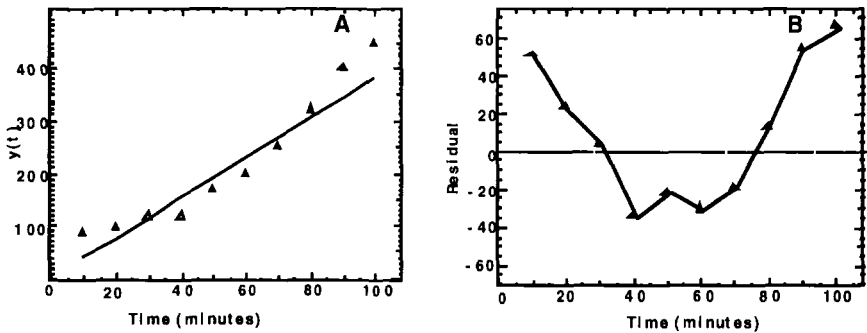
Figure 8.4.2. Plot of a straight line through a set of data (panel A) and the residuals (Panel B). See text for an explanation.

These data are fitted to a straight line in the manner described above. However, a plot of the residuals, shown in Figure 8.4.2-B, clearly indicates systematic deviations between the predicted and the observed values. Thus even though the sum of squares of errors has been minimized, the systematic deviations revealed through plotting the residuals indicates a straight line is probably not an acceptable functional description of these data. Again, this will be discussed in more detail in §8.6.

8.4.3   Weighted Linear Regression

Up to now the focus has been how to obtain an estimate of the parameter A. What confidence can one have in this estimate? In what follows, a detailed description will be given of explicitly how the error in the data affect the precision of the estimated parameter value $\hat{A}$ for the function $y = y(A, t) = At$. In doing this, attention is shifted from least

squares, LS, to weighted least squares, WLS, where errors in the data are explicitly taken into account through weights.

In moving from LS discussed above, which utilizes RSS as the function to be minimized with respect to A, to WLS one assigns weights w_i to each datum. The expression to be minimized is WRSS:

$$\text{WRSS}(A) = \sum_{i=1}^{N} \text{wres}^2(t_i) = \sum_{i=1}^{N} w_i(y_{obs}(t_i) - y(t_i))^2 \quad (8.4.5)$$

$$= \sum_{i=1}^{N} w_i(y_{obs}(t_i) - At_i)^2$$

The problem of minimizing this expression is identical to that discussed previously. One takes the derivative of (8.4.5), set the resulting expression equal to zero, and solves for A to obtain the value $\hat{A}$:

$$\hat{A} = (\sum_{i=1}^{N} w_i y_{obs}(t_i) t_i) / (\sum_{i=1}^{N} w_i t_i^2) \quad (8.4.6)$$

which differs from the previous estimate, (8.4.4), because of the presence of the w_i.

In the WLS situation, it is also possible to obtain an expression for the precision of $\hat{A}$, $\text{Var}(\hat{A})$, which is given for case a (variance known) and case b (variance unknown) in (8.3.7) respectively by:

$$\text{Case a}: \text{Var}(\hat{A}) = 1 \Big/ \sum_{i=1}^{N} (t_i^2 / \sigma^2(t_i)) = 1 \Big/ \sum_{i=1}^{N} w_i t_i^2 \quad (8.4.7a)$$

$$\text{Case b}: \text{Var}(\hat{A}) = \sigma^2 \Big/ \sum_{i=1}^{N} (t_i^2 / v(t_i)) = \sigma^2 \Big/ \sum_{i=1}^{N} w_i t_i^2 \quad (8.4.7b)$$

In Case b, the expression for $\text{Var}(\hat{A})$ involves the unknown proportionality constant σ^2. It is possible to obtain an unbiased estimate for it from

$$\hat{\sigma}^2 = \frac{\text{WRSS}(\hat{A})}{N-1} \quad (8.4.8)$$

where $\text{WRSS}(\hat{A})$ denotes the minimum value of $\text{WRSS}(A)$ obtained with $A = \hat{A}$, N is the number of data, and $N - 1$ is the degrees of freedom.

Remember in this example, A *is* the only parameter being estimated and thus the degrees of freedom is $df = N - 1$, the term in the denominator of (8.4.8). In the general case where P parameters are being estimated, an unbiased estimate of σ^2 can be obtained from

$$\hat{\sigma}^2 = \frac{\text{WRSS}}{df} = \frac{\text{WRSS}}{N - P} \qquad (8.4.9)$$

The precision of the estimate $\hat{A}$ of A is often expressed in terms of standard deviation, i.e. the square root of the variance $\text{Var}(\hat{A})$:

$$\text{SD}(\hat{A}) = \sqrt{\text{Var}(\hat{A})} \qquad (8.4.10)$$

It can also be given in terms of the fractional standard deviation FSD or the coefficient of variation CV, which measures the relative precision of the estimate:

$$\text{FSD}(\hat{A}) = \text{CV}(\hat{A}) = \frac{\text{SD}(\hat{A})}{\hat{A}} \qquad (8.4.11)$$

As noted previously, FSD and CV can be expressed as a percent by multiplying it by 100.

From (8.4.6) and (8.4.7), one sees that both $\hat{A}$ and $\text{VAR}(\hat{A})$ depend upon the w_i. This is why it is essential that the investigator appreciate the nature of the error in his data: weights w_i affect the outcome of both the estimate of $\hat{A}$ and $\text{Var}(\hat{A})$. The link between LS and WLS occurs here as well. Comparing (8.4.6) where the estimate $\hat{A}$ for A was obtained by WLS, with the ordinary LS case, (8.4.4), one sees that the two estimates coincide when in (8.4.6) all $w_i = 1$. This situation, however, is a special case of WLS case b, where $v(t_i) = 1$ for all i indicating that in the case of LS the assumption is made implicitly of a constant but unknown measurement error variance.

8.4.4   The Effect of Weights on Parameter Estimates and Their Precision

How does the assignment of weights affect the estimates of the linear parameters and their precision? Consider again the data shown in Figure 8.2.1 where two different weighting structures were considered.

In the first weighting scheme for case a, σ^2 was constant and equal to 100 hence the weights w_i were constant and equal to 0.01. Evaluating (8.4.6), one finds the numerator and denominator are respectively 1531 and 385, hence $\hat{A} = 3.977$. Notice this estimate is identical to the estimate obtained for LS as expected since (8.4.6) coincides with (8.4.4) when the w_i are equal. In the second weighting scheme, $\sigma^2(t_i) = (0.1 y_{obs}(t_i))^2$. In this case, the numerator and denominator of

(8.4.6) are 252.98 and 66.053 respectively, whence $\hat{A} = 3.830$. Model fits for the two weighting schemes are shown in Figure 8.4.3.
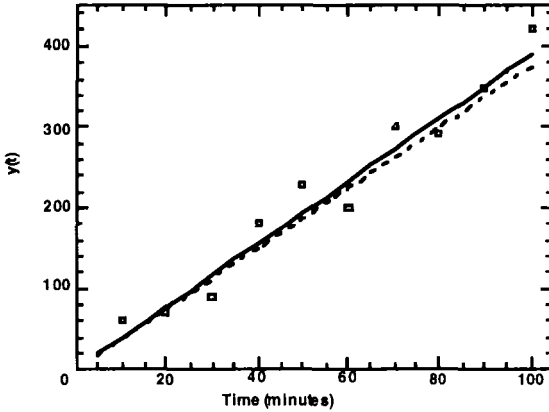
Figure 8.4.3. Plot of the data given in Table 8.2.1 with different fits reflecting the two different weighting schemes. The solid line is a plot of $y(t) = 3.89t$ and the dotted line is $y(t) = 3.75t$. See text for additional explanation.

The assignment of weights has a substantial effect upon the estimate $\hat{A}$ and its estimated standard deviation. Consider first the case where the variance is known. The effect of the two weighting schemes can be evaluated by using (8.4.6) and (8.4.7)a. The results are summarized below in Table 8.4.1.

Table 8.4.1.

	Constant Variance $\text{Var}(e(t_i)) = 100$ $w_i = 1/100$	Constant FSD $\text{Var}(e(t_i)) = y_{obs}^2(t_i) \cdot 0.01$ $w_i = 1/(y_{obs}^2(t_i) \cdot 0.01)$
$\hat{A}$	3.89	3.75
$\text{Var}(\hat{A})$	0.011	0.0246
$\text{SD}(\hat{A})$	0.105	0.157
$\text{FSD}(\hat{A})$	3%	4%
WRSS	41.9	28.58

Consider now the situation where the variance is known up to a proportionality constant, case b, and assume first that the variance is con-

stant but unknown, that is $\text{Var}(e(t_i)) = \sigma^2$ and then that the fractional standard deviation is constant but unknown, that is $\text{FSD}(e(t_i)) = \sigma$ or $\text{Var}(e(t_i)) = y_{obs}^2(t_i) \cdot \sigma^2$. From (8.3.4b), $w_i = 1$ in the former case, and $w_i = \frac{1}{y_{obs}^2(t_i)}$ in the latter. The results are summarized below in Table 8.4.2.

Table 8.4.2.

	Constant Variance, Unknown $\text{Var}(e(t_i)) = \sigma^2$ $w_i = 1$	Constant FSD, Unknown $\text{Var}(e(t_i)) = y_{obs}^2(t_i) \cdot \sigma^2$ $w_i = 1/y_{obs}^2(t_i)$
$\hat{A}$	3.89	3.75
$\text{Var}(\hat{A})$	0.0515	0.0784
$\text{SD}(\hat{A})$	0.227	0.280
$\text{FSD}(\hat{A})$	6%	7%
WRSS	4190	0.2858
σ^2	465	0.0318

The estimates of $\hat{A}$ are the same as for case a, Table 8.4.1. In fact from (8.4.6), it is immediate to verify that, if all the weights are multiplied by a constant factor, the estimate doesn't change. As a consequence, $\hat{A}$ depends on the structure of the variance, and thus it is the same when the measurement error is constant, either known (case a where $\text{Var}(e(t_i)) = 100$, $w_1 = 1/100$) or unknown (case b where $\text{Var}(e(t_i)) = \sigma^2$, $w_i = 1$) since in the two situations the weights differ by a constant factor equal to 100.

Similarly the same estimate for $\hat{A}$ is obtained when the fractional standard deviation of the measurement error is constant, either known (case a where $\text{FSD}(t_i) = 10\%$, $w_i = 1/(y_{obs}^2(t_i) \cdot 0.01)$), or unknown (case b where $\text{FSD}(t_i) = \sigma$, $w_i = 1/y_{obs}^2(t_i)$).

On the other hand, the variance of the estimates in case a and b is different. From (8.4.7), one can predict the link which involves the unknown proportionality constant σ^2 appearing in the measurement error variance of case b. In the constant variance case, σ^2 represents the unknown variance and, for this example, a value equal to 465 is estimated a posteriori. The ratio between $\text{Var}(\hat{A})$ in case a when $\text{Var}(e(t_i)) = 100$ and in case b where the estimated $\text{Var}(e(t_i))$ is 465 is equal to the ratio 100/465. Similarly if the fractional standard deviation of the measurement error is assumed constant but unknown, σ^2 represents the square of the unknown fractional standard deviation. In this example, a value equal to 0.0318 is estimated a posteriori for σ^2, corresponding to a fractional standard deviation equal to 17%. The ratio between $\text{Var}(\hat{A})$ in

case a when $\text{Var}(e(t_i)) = y^2_{obs}(t_i) \cdot 0.01$ and in case b when $\text{Var}(e(t_i))$ is estimated equal to $y^2_{obs}(t_i) \cdot 0.0318$ is equal to the ratio 0.01/0.0318.

8.5   THE FUNDAMENTALS OF NONLINEAR REGRESSION

8.5.1   Introduction

What happens in case $y(t)$, instead of being described by a set of linear parameters, has nonlinear parameters as well? The problem of how to estimate the parameters becomes more complex.

In the previous section, the major points were illustrated using the function $y(A, t) = At$. In this section, the major points will be illustrated using the monoexponential function $y(\lambda, t) = e^{-\lambda t}$ where λ is the nonlinear parameter to be estimated. Later in this section, the function $y(A, \lambda, t) = Ae^{-\lambda t}$ will be used to introduce the covariance (variance-covariance) matrix and the matrix of correlation coefficients.

This section will concentrate on WLS which is available in many popular computer programs. It is essential that the investigator utilizing such programs has some knowledge of what and why certain information is required, and how to interpret the results such programs yield. The intent is to describe the general concepts involved in **nonlinear regression,** present some of the technical difficulties in the context of the monoexponential function defined above, and refer the reader to the literature for more details. In this way, it is hoped the investigator will be able to utilize nonlinear regression wisely and efficiently to extract the desired information from the data.

How is the nonlinear case handled? The problem is solved through a number of iterations that draws on the linear theory to obtain a set of parameter values describing $y(t)$ that minimizes the weighted sum of squares of the residuals WRSS.

Some intuition into these concepts will be given; it will be clear what is similar and different between this and linear regression. The iterative linearization mentioned above can be described using the data given in Table 8.5.1 (shown in Figure 8.5.1).

One starts with a set of data such as those in Table 8.5.1, error estimates of the data, and a function to be used to describe the data. The function is characterized by a set of parameters to be estimated. The function used in this example is $y = e^{-\lambda t}$; the parameter is λ. One starts by choosing a value for λ, say λ^0, and $\text{WRSS}(\lambda^0)$ is calculated as in (8.5.1). How the initials estimate can be obtained is discussed in Appendix G. Then an algorithm is used to try to produce a new estimate of λ, say λ^1, which improves upon λ^0 because $\text{WRSS}(\lambda^1) < \text{WRSS}(\lambda^0)$.

Table 8.5.1.

t_i	$y_{obs}(t_i)$
15	0.856
30	0.797
60	0.538
120	0.318
240	0.133
360	0.069
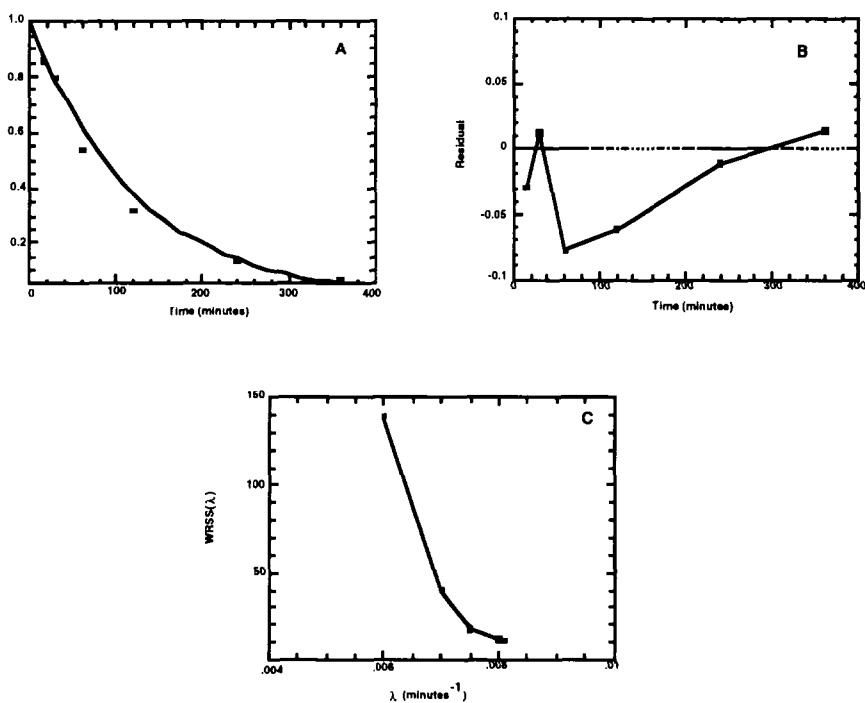
Figure 8.5.1. Panel A: The plot of the data given in Table 8.5.1 together with the values calculated from $y(\lambda, t) = e^{-0.0081t}$. Panel B: The residuals from this plot (see Table 8.5.1). Panel C: A plot of WRSS as a function of different λ. For example, if the error structure in the data assumes a known constant fractional standard deviation of 10%, if the initial estimate of λ is 0.006, WRSS(λ) = 138.9. As successive iterations occurs, a minimum value of WRSS(λ) of 11.0 occurs when $\lambda = 0.0081$. If the initial estimate of λ is greater than 0.0081, successive values of λ will generally occur on other other side of the parabola. See text for additional explanation.

The process of passing from $\text{WRSS}(\lambda^0)$ to $\text{WRSS}(\lambda^1)$ is called an iteration. The algorithm provides a means by which a linear approximation of the nonlinear function can be substituted so that linear regression can be used to produce λ^1. The development of such algorithms is the subject of a branch of applied mathematics called optimization. The algorithm works in such a way that for each iteration, $\text{WRSS}(\lambda)$ becomes smaller until a minimum is reached. In Figure 8.5.1C, the improvement in WRSS is obtained through a number of iterations until a minimum is achieved.

With this example illustrating "iterations" and a knowledge of the principals of linear regression, one can now proceed to the steps involved in nonlinear regression.

8.5.2 The Steps Involved in Nonlinear Regression

STEP 1: DEFINING WRSS IN THE NONLINEAR CASE

In what follows, the same notation from the previous section will be used where w_i is the weight assigned to each datum $y_{obs}(t_i)$, and the expression to minimize is

$$\text{WRSS}(\lambda) = \sum_{i=1}^{N} w_i \big(y_{obs}(t_i) - y(t_i)\big)^2 = \sum_{i=1}^{N} w_i \big(y_{obs}(t_i) - e^{-\lambda t_i}\big)^2 \quad (8.5.1)$$

As noted previously, $y(\lambda, t)$ is a nonlinear function of the parameter λ so an explicit analytical solution for λ analogous to (8.4.4) is not possible. In fact if one takes the derivative of WRSS with respect to λ and sets it equal to zero:

$$\frac{d(\text{WRSS}(\lambda))}{d\lambda} = \frac{d\left(\sum_{i=1}^{N} (w_i(y_{obs}(t_i) - e^{-\lambda t_i})^2)\right)}{d\lambda} = 0 \quad (8.5.2)$$

one obtains:

$$+2\sum_{i=1}^{N} w_i t_i e^{-\lambda t_i} \big(y_{obs}(t_i) - e^{-\lambda t_i}\big) = 0 \quad (8.5.3)$$

which does not yield an explicit expression for λ as a function of the known quantities $y_{obs}(t_i)$, t_i, and w_i.

STEP 2: FINDING MINIMUM VALUES FOR WRSS - CONCEPTS

The problem of finding a minimum for WRSS in the nonlinear case can be explained in the context of Figure 8.5.2. An arbitrary function $y(t)$ is defined by a set of parameters. For example, the function can be written $y(p_1, \ldots, p_n, t)$ indicating the parameters p_i and the independent variable t. WRSS is a function of these parameters. Depending upon the number of p_i that characterize $y(t)$, WRSS can be a line (the one parameter case shown in Figure 8.5.1) or a surface (the case with more than one parameter). In the example given in Figure 8.5.2, there is more than one "minimum" for WRSS. This is distinctly different from the linear regression case where there is only one (unique) minimum. The minima shown in Figure 8.5.2 in mathematical parlance are called local minima. The difference, then, between linear and nonlinear regression is
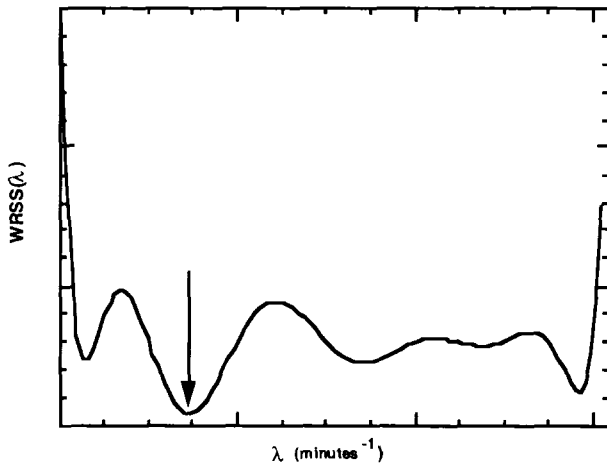
Figure 8.5.2.   A plot of WRSS(λ) as a function of λ illustrating several local minima but only one global minimum over the domain of the function. Notice also that some of the minima are quite well-defined, or sharp, while others are much more gradual.

that in linear regression these is a "unique" minimum for WRSS while in the nonlinear case there may be several local minima for WRSS. Among the local minima, the smallest is called the global minimum. Hence while in the linear case, the mathematical theory to locate the unique minimum is well-defined, in this case, one must propose a scheme to locate these minima, and even when such a minimum is found, one is

not sure it is the smallest of these local minima, i.e. the global minimum. The situation is illustrated in Figure 8.5.2.

Finally, there can be different characteristics of the neighborhoods of the local minima that can affect the iterative process. For example, if the minimum is shallow, the iterative process can be slow or unsuccessful since the changes in WRSS resulting from new estimates of the parameters describing $y(t)$ may be very small.

STEP 3: PARAMETER ESTIMATION BY ITERATIVE LINEARIZATIONS

How is the function

$$y = y(\lambda, t) = e^{-\lambda t} \qquad (8.5.4)$$

fitted to the data in Figure 8.5.1 by iterative linearizations of WRSS? That is, how is an estimate $\hat{\lambda}$ of λ found which results in a "satisfactory" description of the data?

As mentioned at the beginning of this section, one seeks a means by which to transform the problem from one of estimating a nonlinear parameter to one of estimating a linear parameter. How can this be accomplished? One must resort to calculus where it is known that the function $y(\lambda, t)$ can be expressed as an infinite series called a Taylor series around a specific value of λ, say λ^0:

$$y(\lambda, t) = y(\lambda^0, t) + \frac{\partial y(\lambda, t)}{\partial \lambda}\bigg|_{\lambda=\lambda^0} (\lambda - \lambda^0) + \frac{1}{2} \frac{\partial^2 y(\lambda, t)}{\partial \lambda^2}\bigg|_{\lambda=\lambda^0} (\lambda - \lambda^0)^2 + \cdots$$

$$(8.5.5)$$

where ∂ denotes the partial derivative, and $|_{\lambda=\lambda^0}$ means evaluated at $\lambda = \lambda^0$. In writing the Taylor series expansion for $y(\lambda, t)$, one must use the partial derivative since $y(\lambda, t)$ is a function both of λ and t; the Taylor series in (8.5.5) is written for an arbitrary time t. The Taylor series is an infinite series, i.e. the expression on the right hand side of (8.5.5) contains an infinite number of terms. Normally, however, one uses a truncated version of this expression, i.e. a finite number of terms of the series given on the right hand side of (8.5.5). When this is done, the right hand side of (8.5.5) no longer equals $y(\lambda, t)$ exactly, but approximates it with the approximation generally being better as more terms of the series are retained.

Now assume an initial estimate λ^0 of λ is available. The idea behind linearizing the problem is to assume that the terms in (8.5.5) which contain derivatives of second order and higher are small and can be

neglected. This means (8.5.5) can be rewritten:

$$y(\lambda, t) \approx y(\lambda^0, t) + \frac{\partial y(\lambda, t)}{\partial \lambda}\bigg|_{\lambda = \lambda^0} (\lambda - \lambda^0) = e^{-\lambda^0 t} - te^{-\lambda^0 t}(\lambda - \lambda^0) \quad (8.5.6)$$

Notice this equation is now linear in λ since λ^0 is known as the assumed initial estimate of λ. Define:

$$\Delta\lambda = \lambda - \lambda^0 \quad (8.5.7)$$

Equation (8.5.6) can be rewritten:

$$y(\lambda, t) \approx y(\lambda^0, t) + \frac{\partial y(\lambda, t)}{\partial \lambda}\bigg|_{\lambda = \lambda^0} \Delta\lambda = e^{-\lambda^0 t} - te^{-\lambda^0 t}\Delta\lambda \quad (8.5.8)$$

which is an equation linear in $\Delta\lambda$. Assuming the weights w_i for the data $y_{obs}(t_i)$ are known, one can write the following expression for $\text{WRSS}(\lambda)$:

$$\text{WRSS}(\lambda) = \sum_{i=1}^{N} w_i (y_{obs}(t_i) - y(t_i))^2 \quad (8.5.9)$$

$$\approx \sum_{i=1}^{N} w_i (y_{obs}(t_i) - y(\lambda^0, t)|_{t=t_i} - \frac{\partial y(\lambda, t)}{\partial \lambda}\bigg|_{\substack{\lambda = \lambda^0 \\ t = t_i}} \Delta\lambda)^2$$

$$= \sum_{i=1}^{N} w_i (y_{obs}(t_i) - e^{-\lambda^0 t_i} + t_i e^{-\lambda^0 t_i}\Delta\lambda)^2$$

For convenience, define a new term:

$$\Delta y_{obs}(t_i) = y_{obs}(t_i) - y(\lambda^0, t_i) = y_{obs}(t_i) - e^{-\lambda_0 t_i} \quad (8.5.10)$$

Equation (8.5.9) can be rewritten:

$$\text{WRSS}(\lambda) = \sum_{i=1}^{N} w_i (\Delta y_{obs}(t_i) - \frac{\partial y(\lambda, t)}{\partial \lambda}\bigg|_{\substack{\lambda = \lambda^0 \\ t = t_i}} \Delta\lambda)^2 \quad (8.5.11)$$

$$= \sum_{i=1}^{N} w_i (\Delta y_{obs}(t_i) + t_i e^{-\lambda^0 t_i}\Delta\lambda)^2$$

WRSS can now be considered as a sum of squares of linear functions of $\Delta\lambda$, and hence $\Delta\lambda$ can be estimated using the linear regression machinery. Briefly, in (8.4.6), $\Delta y_{obs}(t_i)$ is substituted for $y_{obs}(t_i)$, and $\frac{dy(\lambda, t)}{d\lambda}|_{\substack{\lambda = \lambda^0 \\ t = t_i}}$ for t_i. One obtains:

$$\widehat{\Delta\lambda} = \frac{\displaystyle\sum_{i=1}^{N} w_i \Delta y_{obs}(t_i)\frac{\partial y(\lambda, t)}{\partial \lambda}\bigg|_{\substack{\lambda = \lambda^0 \\ t = t_i}}}{\displaystyle\sum_{i=1}^{N} w_i (\frac{\partial y(\lambda, t)}{\partial \lambda}\bigg|_{\substack{\lambda = \lambda^0 \\ t = t_i}})^2} \quad (8.5.12)$$

$$= \frac{-\sum_{i=1}^{N} w_i \Delta y_{obs}(t_i) t_i e^{-\lambda^0 t_i}}{\sum_{i=1}^{N} w_i t_i^2 e^{-2\lambda^0 t_i}}$$

At this stage, a new estimate for λ can be obtained:

$$\lambda^1 = \lambda^0 + \widehat{\Delta\lambda} \tag{8.5.13}$$

and the process repeated using λ^1 instead of λ^0 in the above formulas. $\text{WRSS}(\lambda^1)$ is obviously smaller than $\text{WRSS}(\lambda^0)$ since $\Delta\lambda$ was chosen to minimize WRSS in the neighborhood of λ^0. At each iteration, both the model function $y(\lambda, t)$ and its derivative with respect to the parameter λ need to be evaluated at the sample times.

The iterative process, which technically could go on forever, usually stops when some preset criterion, for example comparing two consecutive values of WRSS, is satisfied.

STEP 4: PRECISION OF PARAMETER ESTIMATES

The linear regression machinery used to obtain an estimate for λ can also be used to obtain an estimate of the precision of this estimate. Again assume the weights of the data are described using either:

$$\text{Case a}: w_i = \frac{1}{\sigma^2(t_i)} \tag{8.5.14a}$$

$$\text{Case b}: w_i = \frac{1}{v(t_i)} \tag{8.5.14b}$$

Assume in addition that a WLS estimate $\hat{\lambda}$ of λ has been obtained. The straightforward extension of the linear WLS equation, (8.4.7), for $\text{Var}(\hat{\lambda})$ to the nonlinear case provides (using the rationale behind (8.5.12)) an estimate of $\text{Var}(\hat{\lambda})$ denoted $\frac{1}{m(\hat{\lambda})}$ for the two choices of w_i respectively:

$$\text{Case a}: \text{Var}(\hat{\lambda}) \approx \frac{1}{\sum_{i=1}^{N} \frac{1}{\sigma^2(t_i)} \left(\frac{\partial y(\lambda, t)}{\partial \lambda} \big|_{\substack{\lambda=\hat{\lambda} \\ t=t_i}} \right)^2} = \frac{1}{m(\hat{\lambda})} \tag{8.5.15a}$$

or

$$\text{Case b}: \text{Var}(\hat{\lambda}) \approx \frac{\sigma^2}{\sum_{i=1}^{N} \frac{1}{v(t_i)} \left(\frac{\partial y(\lambda, t)}{\partial \lambda} \big|_{\substack{\lambda=\hat{\lambda} \\ t=t_i}} \right)^2} = \frac{1}{m(\hat{\lambda})} \tag{8.5.15b}$$

The derivative term is known:

$$\left.\frac{\partial y(\lambda, t)}{\partial \lambda}\right|_{\substack{\lambda=\hat{\lambda}\\t=t_i}} = -t_i e^{-\hat{\lambda}t_i} \qquad (8.5.16)$$

Therefore, one has respectively

$$\text{Case a}: \text{Var}(\hat{\lambda}) \approx \frac{1}{\sum_{i=1}^{N} \frac{t_i^2}{\sigma^2(.1t_i)} e^{-2\hat{\lambda}t_i}} = \frac{1}{m(\hat{\lambda})} \qquad (8.5.17a)$$

$$\text{Case b}: \text{Var}(\hat{\lambda}) \approx \frac{\sigma^2}{\sum_{i=1}^{N} \frac{t_i^2}{v(t_i)} e^{-2\hat{\lambda}t_i}} = \frac{1}{m(\hat{\lambda})} \qquad (8.5.17b)$$

where the estimate $\hat{\sigma}^2$ for σ^2 is:

$$\hat{\sigma}^2 = \frac{\text{WRSS}(\hat{\lambda})}{df} = \frac{\text{WRSS}(\hat{\lambda})}{N-1} \qquad (8.5.18)$$

where *df*, the degrees of freedom, equals $N - 1$ since there is only one parameter λ to be estimated.

In the case of linear regression, the expressions for $\text{Var}(\hat{\lambda})$ are exact whereas in the case of nonlinear regression, the two expressions given in (8.5.15) provide in general only a lower bound approximation of $\text{Var}(\hat{\lambda})$. More precisely, one has

$$\text{Var}(\hat{\lambda}) \geq m(\hat{\lambda})^{-1} \qquad (8.5.19)$$

An example of (8.5.19) will be given below.

8.5.3   The Covariance and Correlation Matrices

The above is a consequence of dealing with a nonlinear problem in the presence of a limited set of noisy data. Some useful theoretical results are, however, available which hold under certain circumstances. It is more informative to state them in a general context where there is more than one unknown parameter. This will accommodate functions $y(t)$ such as

$$y(t) = A e^{-\lambda t} \qquad (8.5.20)$$

or

$$y(t) = A_1 e^{-\lambda_1 t} + A_2 e^{-\lambda_2 t} \qquad (8.5.21)$$

where in (8.5.20) there are two parameters, A and λ, and in (8.5.21) there are four A_1, A_2, λ_1, and λ_2; the ideas carry over to arbitrary functions

$y(t)$ described by a set of parameters $p_1, \cdots, p_P$. It is convenient to use vector notation to describe the set of parameters. Hence for a set $p_1, \cdots, p_P$, one writes:

$$\mathbf{p} = \begin{pmatrix} p_1 \\ \vdots \\ p_P \end{pmatrix} = (p_1 \cdots p_P)^T \qquad (8.5.22)$$

One says $\mathbf{p}$ is a vector of dimension P; the T is the second expression for $\mathbf{p}$ means the transpose of the vector. The dimensions of the vector of parameters for (8.5.20), $\mathbf{p} = [A \; \lambda]^T$, and (8.5.21), $\mathbf{p} = [A_1 \; A_2 \; \lambda_1 \; \lambda_2]^T$ are 2 and 4 respectively. Parameter space is denoted $\mathcal{P}$.

The problem is now to extend the scalar case approximation for the variance to the P-parameter vector situation; $\mathrm{Var}(\hat{\lambda})$ and $\mathrm{m}(\hat{\lambda})$ become two matrices of dimension PxP, $\mathbf{Cov}(\hat{\mathbf{p}})$ and $\mathbf{M}(\hat{\mathbf{p}})$ respectively, and the inequality given in (8.5.19) becomes:

$$\mathbf{Cov}(\hat{\mathbf{p}}) \geq \mathbf{M}^{-1}(\hat{\mathbf{p}}) \qquad (8.5.23)$$

$\mathbf{Cov}(\hat{\mathbf{p}})$ is the **covariance (variance-covariance) matrix** of dimension PxP. $\mathbf{Cov}(\hat{\mathbf{p}})$ is symmetric. For (8.5.20) this becomes:

$$\mathbf{Cov}(\hat{\mathbf{p}}) = \begin{pmatrix} \mathrm{Var}(\hat{A}) & \mathrm{Cov}(\hat{A}, \hat{\lambda}) \\ \mathrm{Cov}(\hat{\lambda}, \hat{A}) & \mathrm{Var}(\hat{\lambda}) \end{pmatrix} \qquad (8.5.24)$$

where $\mathrm{Cov}(\hat{A}, \hat{\lambda})$ and $\mathrm{Cov}(\hat{\lambda}, \hat{A})$ are equal. The diagonal elements are the variances of the parameter estimates which are positive numbers by definition and the off diagonal elements are the covariances which may be either positive or negative.

A simple relation exists between $\mathrm{Cov}(\hat{A}, \hat{\lambda})$ and the standard deviations of $\hat{A}$ and $\hat{\lambda}$ as expressed by the inequality

$$|\mathrm{Cov}(\hat{A}, \hat{\lambda})| \leq \mathrm{SD}(\hat{A}) \cdot \mathrm{SD}(\hat{\lambda}) \qquad (8.5.25)$$

where $\mathrm{SD}(\hat{A})$ and $\mathrm{SD}(\hat{\lambda})$ are the standard deviations of $\hat{A}$ and $\hat{\lambda}$ respectively (cf (8.4.10)). The matrix of normalized quantities, known as the **correlation matrix**

$$\mathbf{Corr}(\hat{\mathbf{p}}) = \begin{pmatrix} 1 & \frac{\mathrm{Cov}(\hat{A},\hat{\lambda})}{\mathrm{SD}(\hat{A})\mathrm{SD}(\hat{\lambda})} \\ \frac{\mathrm{Cov}(\hat{\lambda},\hat{A})}{\mathrm{SD}(\hat{\lambda})\mathrm{SD}(\hat{A})} & 1 \end{pmatrix} \qquad (8.5.26)$$

is a symmetric matrix since $\mathrm{Cov}(\hat{A}, \hat{\lambda}) = \mathrm{Cov}(\hat{\lambda}, \hat{A})$, having the elements on the main diagonal equal to one. From inequality (8.5.25), all the elements off the main diagonal are in the range between -1 and 1.

The matrix $\mathbf{M}(\hat{\mathbf{p}})$ from the inequality (8.5.23) is the so-called **information matrix.** The generic element of the information matrix $\mathbf{M}(\hat{\mathbf{p}})$, $m_{hl}(\hat{\mathbf{p}})$, is given for the case a and b by

$$\text{Case a}: m_{hl}(\hat{\mathbf{p}}) = \sum_{i=1}^{N} \frac{1}{\sigma^2(t_i)} \frac{\partial y(\mathbf{p}, t)}{\partial p_h}\Big|_{\substack{\mathbf{p}=\hat{\mathbf{p}} \\ t=t_i}} \cdot \frac{\partial y(\mathbf{p}, t)}{\partial p_l}\Big|_{\substack{\mathbf{p}=\hat{\mathbf{p}} \\ t=t_i}} \quad (8.5.27a)$$

$$\text{Case b}: m_{hl}(\hat{\mathbf{p}}) = \frac{1}{\sigma^2} \sum_{i=1}^{N} \frac{1}{v(t_i)} \frac{\partial y(\mathbf{p}, t)}{\partial p_h}\Big|_{\substack{\mathbf{p}=\hat{\mathbf{p}} \\ t=t_i}} \cdot \frac{\partial y(\mathbf{p}, t)}{\partial p_l}\Big|_{\substack{\mathbf{p}=\hat{\mathbf{p}} \\ t=t_i}} \quad (8.5.27b)$$

where an estimate for σ^2 in the above equation is given by:

$$\hat{\sigma}^2 = \frac{\text{WRSS}(\hat{\mathbf{p}})}{df} \quad (8.5.28)$$

For the monoexponential model given by (8.5.20), the matrix M and its inverse $\mathbf{M}^{-1}$ are respectively

$$\mathbf{M}(A, \lambda) = \begin{pmatrix} m_{11}(A, \lambda) & m_{12}(A, \lambda) \\ m_{21}(A, \lambda) & m_{22}(A, \lambda) \end{pmatrix} \quad (8.5.29)$$

$$\mathbf{M}^{-1} = \frac{1}{m_{11}(A, \lambda)m_{22}(A, \lambda) - m_{12}^2(A, \lambda)} \quad (8.5.30)$$
$$\begin{pmatrix} m_{22}(A, \lambda) & -m_{12}(A, \lambda) \\ -m_{21}(A, \lambda) & m_{11}(A, \lambda) \end{pmatrix}$$

Assuming case a, (8.5.27)a applies, and the elements of M are:

$$m_{11}(\hat{A}, \hat{\lambda}) = \sum_{i=1}^{N} \frac{1}{\sigma^2(t_i)} \left(\frac{\partial y(A, \lambda, t)}{\partial A}\Big|_{\substack{A=\hat{A} \\ \lambda=\hat{\lambda} \\ t=t_i}}\right)^2 = \sum_{i=1}^{N} \frac{e^{-2\hat{\lambda}t_i}}{\sigma^2(t_i)} \quad (8.5.31)$$

$$m_{22}(\hat{A}, \hat{\lambda}) = \sum_{i=1}^{N} \frac{1}{\sigma^2(t_i)} \left(\frac{\partial y(A, \lambda, t)}{\partial \lambda}\Big|_{\substack{A=\hat{A} \\ \lambda=\hat{\lambda} \\ t=t_i}}\right)^2 \sum_{i=1}^{N} \frac{\hat{A}^2 t_i^2}{\sigma^2(t_i)} e^{-2\hat{\lambda}t_i} \quad (8.5.32)$$

$$m_{12}(\hat{A}, \hat{\lambda}) = m_{21}(\hat{A}, \hat{\lambda}) \quad (8.5.33)$$

$$= \sum_{i=1}^{N} \frac{1}{\sigma^2(t_i)} \left(\frac{\partial y(A, \lambda, t)}{\partial A}\Big|_{\substack{A=\hat{A} \\ \lambda=\hat{\lambda} \\ t=t_i}}\right)\left(\frac{\partial y(A, \lambda, t)}{\partial \lambda}\Big|_{\substack{A=\hat{A} \\ \lambda=\hat{\lambda} \\ t=t_i}}\right)$$

$$= -\sum_{i=1}^{N} \frac{\hat{A}t_i}{\sigma^2(t_i)} e^{-2\hat{\lambda}t_i}$$

The expressions for case b are derived in a similar fashion.

Prom inequality (8.5.23), the elements of $\mathbf{M}^{-1}$ provide a lower bound for the corresponding elements of the covariance matrix. Therefore, from (8.5.30), in the approximation for the variance of parameter, say A in (8.5.20), given by the information matrix, all the elements of $\mathbf{M}$ play a role:

$$\text{Var}(\hat{A}) \geq \frac{m_{2,2}(\hat{A}, \hat{\lambda})}{m_{11}(\hat{A}, \hat{\lambda})m_{22}(\hat{A}, \hat{\lambda}) - m_{12}^2(\hat{A}, \hat{\lambda})} \tag{8.5.34}$$

Note it is the terms on the right hand side of (8.5.34) that are provided by WLS through (8.5.31), (8.5.32) and (8.5.33). Similarly, for the variance of the parameter λ and for the covariance between A and λ, the following inequalities hold:

$$\text{Var}(\hat{\lambda}) \geq \frac{m_{11}(\hat{A}, \hat{\lambda})}{m_{11}(\hat{A}, \hat{\lambda})m_{22}(\hat{A}, \hat{\lambda}) - m_{12}^2(\hat{A}, \hat{\lambda})} \tag{8.5.35}$$

$$\text{Cov}(\hat{A}, \hat{\lambda}) = \text{Cov}(\hat{\lambda}, \hat{A}) \geq \frac{-m_{12}(\hat{A}, \hat{\lambda})}{m_{11}(\hat{A}, \hat{\lambda})m_{22}(\hat{A}, \hat{\lambda}) - m_{12}^2(\hat{A}, \hat{\lambda})} \tag{8.5.36}$$

In order to evaluate the off diagonal terms of the correlation matrix (8.5.26) from WLS results, note that they are ratio between two terms. Inequality (8.5.36) provides a lower bound for the numerator, and inequalities (8.5.34) and (8.5.35) provide a lower bound for the denominator. Therefore only an approximation can be derived for their ratio:

$$\text{Corr}(\hat{A}, \hat{\lambda}) = \text{Corr}(\hat{\lambda}, \hat{A}) = \frac{\text{Cov}(\hat{A}, \hat{\lambda})}{\text{SD}(\hat{A})\text{SD}(\hat{\lambda})} \tag{8.5.37}$$

$$\approx \frac{-m_{12}(\hat{A}, \hat{\lambda})}{\sqrt{m_{11}(\hat{A}, \hat{\lambda}) \cdot m_{22}(\hat{A}, \hat{\lambda})}}$$

Some results are available on how good the computed approximation of $\mathbf{M}^{-1}(\hat{\mathbf{p}})$ is to $\mathbf{Cov}(\hat{\mathbf{p}})$. The most important ones are the following. The matrix $\mathbf{M}^{-1}(\hat{\mathbf{p}})$, under the assumption of optimally weighted WLS (see (8.3.6)), approaches, for a sufficiently large sample size and/or decreasing variance of the measurement error, $\mathbf{Cov}(\hat{\mathbf{p}})$, and the estimate $\hat{\mathbf{p}}$ approaches a Gaussian distribution. If in addition the measurement errors are Gaussian, then $\mathbf{M}^{-1}(\hat{\mathbf{p}})$ represents the minimum achievable variance-covariance matrix, usually defined as the Cramer-Rao lower bound. Thus $\mathbf{Cov}(\hat{\mathbf{p}})$ of an optimally weighted WLS reaches this lower bound with a sufficiently large sample size. An important result is the equivalence of WLS with maximum likelihood estimation for the case of Gaussian independent measurement errors.

8.5.4   Algorithms and Software for Nonlinear Regression

The steps of nonlinear least squares estimation have been illustrated in §8.5.2 using what is called a Gauss-Newton iterative scheme. This outlines the principles of that class of algorithms which requires the computation of derivatives. These are referred to as **gradient methods.** Numerically efficient algorithms, e.g. the Levenberg-Marquart technique, based on the Gauss-Newton method are available and are implemented in many software tools.

Another category of algorithms for minimizing WRSS which has been applied in compartmental model parameter estimation is one that does not require the computation of the derivatives. These algorithms are known as **direct search methods,** and both deterministic and random search algorithms are available. An efficient deterministic direct search algorithm is the simplex method. Other derivative free algorithms are available. It is worth emphasizing that with a direct search method, the estimation of $\frac{\partial(\mathbf{p},t)}{\partial \mathbf{p}}$ is not required. Albeit a direct comparison of gradient versus direct search methods is difficult and may be problem dependent, available experience in compartmental model parameter estimation tends to favor the gradient type methods.

There are many software tools that both simulate (solve model equations) and optimize the model parameters to obtain a best fit to a set of data. Which tool is best for a given situation can depend upon the nature of the problem being solved.

8.5.5   The Effect of Weights

In §8.4.3, an example of the effect of how weights affect WLS parameter estimates and their precision in the linear regression case were given. In this section, two examples for the nonlinear regression case will be given. The first will examine the monoexponential decay $y(t) = e^{-\lambda t}$; this will focus on estimates of λ and $\mathrm{SD}(\lambda)$. The second will examine the monoexponential decay $y(t) = Ae^{-\lambda t}$. This function is characterized by two parameters, A and λ the former is a linear and the latter a nonlinear parameter. This example will focus both on the parameter estimates and their precision, and on the correlation between them, $\mathrm{Cor}(\hat{A}, \hat{\lambda})$.

Example 1

Consider the data given in Table 8.5.1 shown below in Table 8.5.2A, and assume that the variance is known (case a - absolute weights). Consider two situations. In the first, there is a constant standard deviation of 0.05 assigned to each datum while in the second, a constant fractional

standard deviation equal to 10% is assigned to each datum. The weights are calculated as $w_i = 1/\sigma^2(t_i)$. The two situations are summarized in the table.

Table 8.5.2.A

t_i	$y_{obs}(t_i)$	$\text{Var}(e(t_i)) = 0.0025$ w_i	$\text{Var}(e(t_i)) = (0.1 \cdot y_{obs}(t_i))^2$ w_i
15	0.856	400	136
30	0.797	400	157
60	0.538	400	345
120	0.318	400	989
240	0.133	400	5653
360	0.069	400	21003

When the function $y(t) = e^{-\lambda t}$ is fitted to these data using the two weighting schemes, an estimate of λ and $SD(\lambda)$ is obtained. Table 8.5.2B and Figure 8.5.3 summarize the results. The estimate of λ and its precision clearly depend upon the weighting scheme. This observation underlines the importance of knowing the error structure in the data.

Table 8.5.2.B

	Constant Variance $\text{Var}(e(t_i)) = 0.0025$	Constant FSD $\text{Var}(e(t_i)) = (0.1 \cdot y_{obs}(t_i))^2$
$\hat{\lambda}$	0.00923	0.00808
$\text{Var}(\hat{\lambda})$	0.593×10^{-6}	0.576×10^{-7}
$SD(\hat{\lambda})$	0.77×10^{-3}	0.24×10^{-3}
$FSD(\hat{\lambda})$	8%	3%
WRSS	1.94	11.0

Now consider the situation where the variance associated with $y_{obs}(t_i)$ is known up to a proportionality constant (case b - relative weights) and assume as before two different weighting schemes shown in Table 8.5.3A. According to the first scheme, the variance is known to be constant but its value is unknown so that $v(t_i) = 1$ whence $w_i = 1$. In the second scheme, a constant but unknown fractional standard deviation is assumed, that is $v(t_i) = y_{obs}^2(t_i)$ whence $w_i = \frac{1}{y_{obs}^2(t_i)}$.

When the function $y(t) = e^{-\lambda t}$ is fitted to these data using the two weighting schemes, an estimate of λ and $SD(\lambda)$ is obtained. Table 8.5.3B summarizes the results.

Note that as in the linear regression case, $\hat{\lambda}$ is the same when the structure of the variance is the same, i.e. when a constant value for the

Figure 8.5.3. Left panel: A plot of a function $y(t) = e^{-\lambda t}$ for the case of constant variance (dashed line) and constant FSD (solid line). Right panel: A plot of the weighted residuals for the two cases.

Table 8.5.3.A

t_i	$y_{obs}(t_i)$	$\text{Var}(e(t_i)) = \sigma^2$ w_i	$\text{Var}(e(t_i)) = y_{obs}^2(t_i) \cdot \sigma^2$ w_i
15	0.856	1	1.36
30	0.797	1	1.57
60	0.538	1	3.45
120	0.318	1	9.89
240	0.133	1	56.53
360	0.069	1	210.04

Table 8.5.3.B

	Constant (Unknown) Variance $\text{Var}(e(t_i)) = \sigma^2$	Constant (Unknown) FSD $\text{Var}(e(t_i)) = y_{obs}^2(t_i) \cdot \sigma^2$
$\hat{\lambda}$	0.00923	0.00808
$\text{Var}(\hat{\lambda})$	0.230×10^{-6}	0.130×10^{-6}
$\text{SD}(\hat{\lambda})$	0.48×10^{-3}	0.36×10^{-3}
$\text{FSD}(\hat{\lambda})$	5%	4%
WRSS	0.00486	0.11
$\hat{\sigma}^2$	0.00097	0.0219

variance is assumed, and this is either known or unknown, or similarly when a constant fractional standard deviation is assumed that is either known or unknown. The reason is that $\Delta\lambda$ in (8.5.12) doesn't change if all weights are multiplied by a constant factor. On the other hand, the variance of the estimates is different in case a and b but their relationships, which can be predicted from (8.5.15)a and (8.5.15)b, are the same

as the linear case (see §8.4.3). For instance, for the constant variance case, the proportionality factor between $\text{Var}(\hat{\lambda})$ for case a and b is equal to the ratio between 0.0025 ($\text{Var}(e(t_i))$ for case a) and 0.00097 (estimate $\text{Var}(e(t_i))$ of case b).

Example 2

Consider next the same data and weighting schemes as those used in Example 1, but assume now that the monoexponential function to be fitted to the data is not $y(t) = e^{-\lambda t}$ but $y(t) = Ae^{-\lambda t}$, i.e. both the coefficient A and the exponential λ are parameters to be estimated from the data. The results for cases a and b are summarized below in Tables 8.5.4 and 8.5.5.

Table 8.5.4.

	Constant Variance $\text{Var}(e(t_i)) = 0.0025$	Constant FSD $\text{Var}(e(t_i)) = (0.1 \cdot y_{obs}(t_i))^2$
$\hat{A}$	0.99	0.88
$\hat{\lambda}$	0.0091	0.0075
$\text{FSD}(\hat{A})$	6%	6%
$\text{FSD}(\hat{\lambda})$	12%	5%
WRSS	1.94	6.72

Table 8.5.5.

	Constant Variance $\text{Var}(e(t_i)) = \sigma^2$	Constant FSD $\text{Var}(e(t_i)) = y_{obs}^2(t_i) \cdot \sigma^2$
$\hat{A}$	0.99	0.88
$\hat{\lambda}$	0.0091	0.0075
$\text{FSD}(\hat{A})$	4%	8%
$\text{FSD}(\hat{\lambda})$	9%	6%
WRSS	0.00475	0.0675
$\hat{\sigma}^2$	0.0012	0.0168

The plot of the data versus the fitted values and the weighted residuals are shown in Figure 8.5.4

The fractional standard deviations of the estimates have been calculated from the covariance matrix. For instance, for case a with $\text{Var}(e(t_i))$
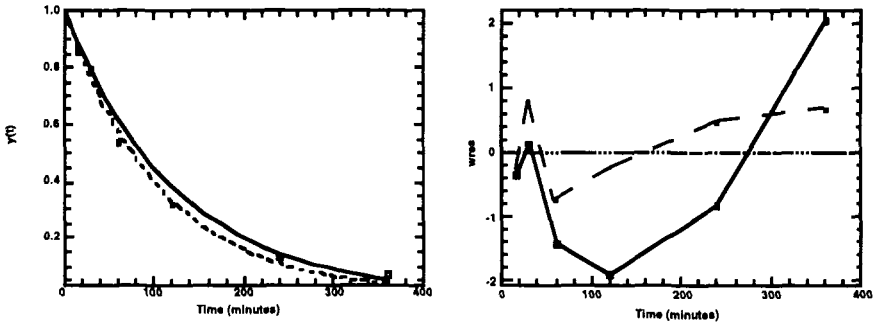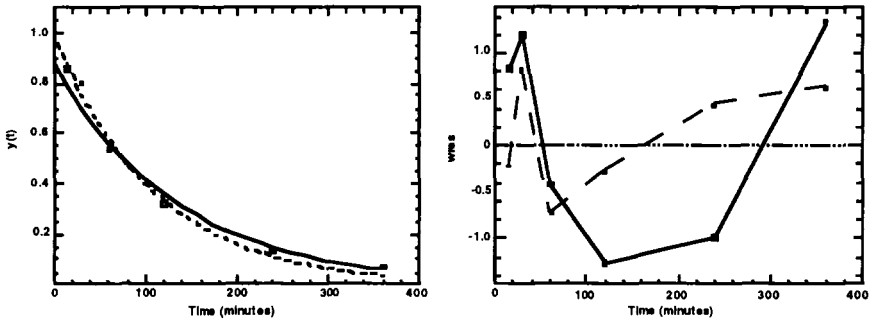
Figure 8.5.4.   Left panel. A plot of a function $y(t) = Ae^{-\lambda t}$ for the case of constant variance (dashed line) and constant FSD (solid line). Panel B. A plot of the weighted residuals.

$= 0.0025$, the matrix is

$$\mathbf{Cov}(\hat{A}, \hat{\lambda}) = \begin{pmatrix} 3.1 \cdot 10^{-3} & 4.6 \cdot 10^{-5} \\ 4.6 \cdot 10^{-5} & 1.3 \cdot 10^{-6} \end{pmatrix}$$

while the correlation matrix is given by

$$\mathbf{Corr}(\hat{A}, \hat{\lambda}) = \begin{pmatrix} 1 & 0.74 \\ 0.74 & 1 \end{pmatrix}$$

For case b with $\mathrm{Var}(e(t_i)) = \sigma^2$ and $\hat{\sigma}^2 = 0.0012$,

$$\mathbf{Cov}(\hat{A}, \hat{\lambda}) = \begin{pmatrix} 1.5 \cdot 10^{-3} & 2.2 \cdot 10^{-5} \\ 2.2 \cdot 10^{-5} & 6.2 \cdot 10^{-7} \end{pmatrix}$$

and

$$\mathbf{Corr}(\hat{A}, \hat{\lambda}) = \begin{pmatrix} 1 & 0.74 \\ 0.74 & 1 \end{pmatrix}$$

Note that as in the previous examples, there is a constant proportionality factor equal to $\frac{0.0025}{0.0012}$ between the covariance matrix of case a and b. As a consequence, the correlation matrix is the same.

8.6   TESTS ON RESIDUALS FOR GOODNESS OF FIT

8.6.1   Introduction

Up to this point, the assumption has been made that the model is correct, i.e. that $y(A, t) = At$ provides the correct functional description of the data given in §8.4, or $y(\lambda, t) = e^{-\lambda t}$ and $y(A, \lambda, t) = Ae^{-\lambda t}$ provide the correct functional description of the data given in §8.5. In this case, from the comparison between the equation describing the data (8.3.1), e.g. for the latter case

$$y_{obs}(t_i) = y(t_i) + e(t_i) = Ae^{-\lambda t_i} + e(t_i) \tag{8.6.1}$$

and the definition of the residuals

$$\text{res}(t_i) = y_{obs}(t_i) - y(t_i) = y_{obs}(t_i) - y(\hat{A}, \hat{\lambda}, t_i) = y_{obs}(t_i) - \hat{A}e^{-\hat{\lambda} t_i} \tag{8.6.2}$$

one can immediately conclude that the residuals $\text{res}(t_i)$ given in (8.6.2) reflect the measurement errors $e(t_i)$ given in (8.6.1). For this in fact to be true, two conditions must hold: (i) the correct model or functional description of the data has been selected, and (ii) the parameter estimation procedure has converged to values (e.g. $\hat{A}$, $\hat{\lambda}$ in (8.6.2)) close to the "true" values. The sequence of residuals can thus be viewed as an approximation of the measurement error sequence.

One can check if the above two conditions hold by testing the assumptions made on the measurement errors on the sequence of residuals. As discussed in previous sections, the measurement error is usually assumed to be a zero mean, independent random process having a known variance, at least up to a proportionality constant. These assumptions can be checked on the residuals by means of statistical tests. This analysis can reveal the presence of errors in the model structure, i.e. in the above example if $y(A, \lambda, t) = Ae^{-\lambda t}$ is not an appropriate model for a given set of data, or the failure of the parameter estimation procedure to converge, i.e. if $\hat{A}$ and $\hat{\lambda}$ are not close to the true values for A and λ. As will be discussed in §8.6.3, the analysis of the residuals can also be used to check and modify the assumptions about the error structure.

8.6.2   Tests for Independence of Residuals

Randomness of the residuals can be tested visually using a plot of the residuals versus time. It is expected that the residuals oscillate around their mean, which should be close to zero, in an unpredictable way. Systematic residuals, i.e. a long run sequence of residuals above or below their mean suggests that the model is an inappropriate description

of the system since it is not able to describe a non-random component of the data. In Figure 8.6.1 a typical plot is shown for a sequence of independent and correlated residuals.
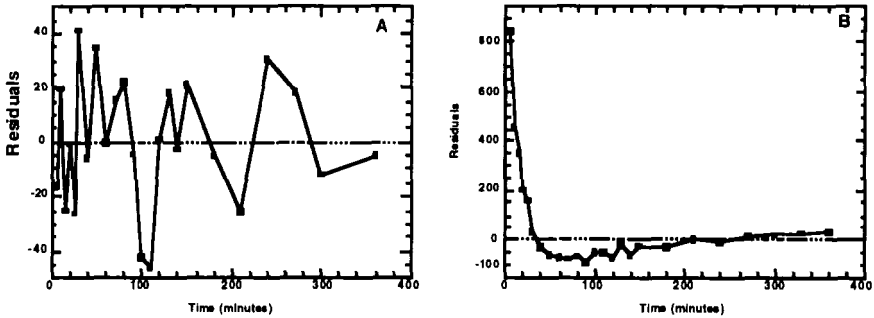
Figure 8.6.1. Plot of residuals versus time. Panel A shows a pattern of independent residuals, Panel B of correlated residuals.

A formal test of nonrandomness of residuals is the **runs test**. A run is defined as a subsequence of residuals having the same sign (assuming the residuals have zero mean); intuitively a very small or very large number of runs in the residual sequence is an indicator of nonrandomness, i.e. of systematic errors in the former and of periodicity in the latter case.

Formally, let R be the number of runs in a sequence of N residuals having n^+ positive and n^- negative values. Clearly $N = n^+ + n^-$. Under the assumption that the elements of the sequence are independent, R is the outcome of a random variable $\mathcal{R}$ having a distribution which tends, as n^+ and n^- become large (the approximation is good when n^+ and n^- are both larger than 10) to the normal distribution $\mathcal{N}(\mu, \sigma^2)$ with mean μ and variance σ^2 equal to:

$$\mu = \frac{2n^+ n^-}{N} + 1 \tag{8.6.3}$$

$$\sigma^2 = \frac{2n^+ n^- (2n^+ n^- - N)}{(N-1)N^2} \tag{8.6.4}$$

For the residuals shown in Figure 8.6.1 A, $N = 24$, $n^+ = 10$ and $n^- = 14$. Using (8.6.3) and (8.6.4), $\mu = 12.67$ and $\sigma^2 = 5.41$ whence, for this situation, $\mathcal{N}(\mu, \sigma^2) = \mathcal{N}(12.67, 5.41)$. The number of runs is

$R = 15$. On the other hand, for the residuals shown in Figure 8.2.1B, $N = 25$, $n^+ = 10$, $n^- = 15$, and $R = 3$. How these values for R can be used to test the independence hypothesis will be described below.

The question is now the following: is the actual value of R consistent with the statistical description of the process? If the answer is yes, it means that the original hypothesis of independence of residuals is correct. If the answer is no, the hypothesis is to be rejected. The question can itself be answered in statistical terms by identifying the region where, with probability $(1 - \alpha)$, the values of the random variable $\mathcal{R}$ falls. Usually α, the level of significance of the test, is small (e.g.. 5%) so that it is very unlikely that $\mathcal{R}$ assumes values out of this region, called the acceptance region of the test. This is illustrated in Figure 8.6.2 for the residuals shown in Figure 8.6.1A.
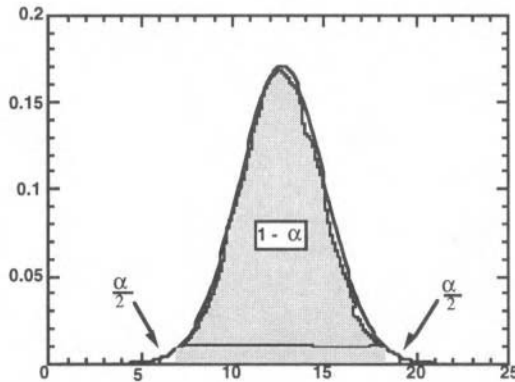
Figure 8.6.2. Plot of $\mathcal{N}(12.67, 5.41)$, the normal density function for the runs test. If α is the level of acceptance, then the shaded area representing $1 - \alpha$, is the range of values of $\mathcal{R}$ for which the hypothesis will be accepted while the two regions denoted by the arrow and $\frac{\alpha}{2}$ are the areas where the hypothesis will be rejected.

If the actual value R falls within the acceptance region, it means that it is compatible with the original hypothesis of independence, and there is no strong reason to question it. On the other hand, a value R outside the range, usually lower than the lower bound of the region thus revealing a systematic error, is unlikely if the original hypothesis was true, therefore the hypothesis of independence is to be rejected. The error associated with this decision, i.e. the error occurring when

the original independence hypothesis is true, but R falls in the region of rejection can be quantified and is in fact equal to α. This possible error is usually called a type I error. Nothing can be said for a type II error, i.e. accepting the hypothesis when in fact it is false.

The upper and lower bounds of the acceptance region satisfy the following equations:

$$\text{Prob}[\mathcal{R} \leq R^{\min}] = \int_{-\infty}^{R^{\min}} p(x)dx = \frac{\alpha}{2} \qquad (8.6.5)$$

$$\text{Prob}[\mathcal{R} \geq R^{\max}] = \int_{R^{\max}}^{\infty} p(x)dx = \frac{\alpha}{2} \qquad (8.6.6)$$

where p is the normal density function of $\mathcal{R}$.

These tests, because each situation requires a knowledge of it own $\mathcal{N}(\mu, \sigma^2)$, are cumbersome. In order to perform the test more easily, it is convenient to standardize $\mathcal{R}$ by means of the transformation

$$\mathcal{Z} = \frac{\mathcal{R} - \mu}{\sigma} \qquad (8.6.7)$$

$\mathcal{Z}$ is a normally distributed random variable $\mathcal{N}(0,1)$ with zero mean and unit variance. The transformed actual value $Z = \frac{R-\mu}{\sigma}$ is to be compared with an acceptance region having $Z^{\min}$ and $Z^{\max}$ as lower and upper bounds respectively which satisfy:

$$\text{Prob}[\mathcal{Z} \leq Z^{\min}] = \int_{-\infty}^{Z^{\min}} \phi(x)dx = \Phi(Z^{\min}) = \frac{\alpha}{2} \qquad (8.6.8)$$

$$\text{Prob}[\mathcal{Z} \geq Z^{\max}] = \int_{Z^{\max}}^{\infty} \phi(x)dx = 1 - \Phi(Z^{\max}) = \frac{\alpha}{2} \qquad (8.6.9)$$

where ϕ and Φ denote the standard normal density and distribution function respectively. These functions are tabulated in many statistics textbooks, and from these tables one can easily evaluate $Z^{\min}$ and $Z^{\max}$ for a given significance level α. For example, with $\alpha = 5\%$, $Z^{\min} = -1.96$ and $Z^{\max} = 1.96$.

For the residuals given in Figure 8.6.1A where $R = 15$, $\mu = 12.67$ and $\sigma = 2.33$, $Z = \frac{15-12.67}{2.33} = 1$. Thus at a significance level of 5%, one can accept the hypothesis on the independence of the residuals. For the residuals given in Figure 8.6.1B. $Z = -4.25$, and the hypothesis on the independence of the residuals should be rejected.

The runs test has been presented in this section as a two-tail test where nonrandomness of the residuals is related to either small or high values of R indicating systematic errors or periodicity respectively. However, the test is often applied as a lower tail test, and in this use, the hypothesis

of no systematic errors in the data is tested by checking whether or not $Z \geq Z^{min}$. For a given level of significance α, Z^{min} now satisifies:

$$\text{Prob}[\mathcal{Z} \leq Z^{min}] = \int_{-\infty}^{Z^{min}} \phi(x)dx = \Phi(Z^{min}) = \alpha \qquad (8.6.10)$$

For example with $\alpha = 5\%$, $Z^{min} = -1.64$.

In the preceding discussion, the procedure of performing the test consists of identifying the acceptable region of $\mathcal{R}$ or equivalently of $\mathcal{Z}$ for a given level of significance α, and checking whether or not the actual value Z falls in this region. An alternative procedure is to calculate the probability that the random variable $\mathcal{Z}$ assumes a value equal to or more extreme than the actual value. This probability is called P value. A small value of P, less than a significance level α, indicates that the test assumption is to be rejected. Therefore, in order to test the hypothesis of no systematic errors in the data, one has to evaluate the probability that $\mathcal{Z}$ assumes a value equal or lower than the actual value:

$$P = \text{Prob}[\mathcal{R} \leq R] = \text{Prob}[\mathcal{Z} \leq Z] = \int_{-\infty}^{Z} \phi(x)ds = \Phi(Z) \qquad (8.6.11)$$

A small P value indicates that the actual number of runs assumes a very unlikely value, much less than expected from the statistical description of the experiment. Therefore the underlying assumption of independence of residuals is to be rejected.

8.6.3   Test on the Variance of the Measurement Error

As has been discussed in previous sections, WLS estimation requires specific assumptions on the variance of the measurement errors which must be known or known up to a proportionality constant. If the model is correct, the residuals must reflect these assumptions.

Consider first case a given by (8.3.4a) where the variance is known, $\text{Var}(e(t_i)) = \sigma^2(t_i)$ and the weights are assigned equal to the inverse of the variance. The weighted residuals are:

$$\text{wres}(t_i) = \sqrt{w_i}\text{res}(t_i) = \frac{\text{res}(t_i)}{\sigma(t_i)} = \frac{\text{res}(t_i)}{\sqrt{\text{Var}(e(t_i))}} \qquad (8.6.12)$$

They are an approximation of the measurement errors normalized to their standard deviations; therefore, they should be a realization of a random process having unit variance.

Similarly in case b given by (8.3.4)b where the variance is known up to a proportionality constant, that is, $\text{Var}(e(t_i)) = v(t_i)\sigma^2$, and the weights

are assigned proportional to the inverse of the variance, the weighted residuals are

$$\text{wres}(t_i) = \sqrt{w_i}\,\text{res}(t_i) = \frac{\text{res}(t_i)}{\sqrt{v(t_i)}} = \sigma \cdot \frac{\text{res}(t_i)}{\sqrt{\text{Var}(e(t_i))}} \qquad (8.6.13)$$

They should be a realization of a random process having a constant variance equal to the unknown factor σ^2.

By plotting the weighted residuals versus time it is thus possible to test visually the assumptions on the variance of the measurement errors. Weighted residuals should lie in a constant wide band symmetrical with respect to the time axis. In case a, the variance of the weighted residuals should equal 1 while in case b the variance is unknown and can only be estimated a posteriori from (8.5.28). A typical plot of weighted residuals are shown in Figure 8.6.3.
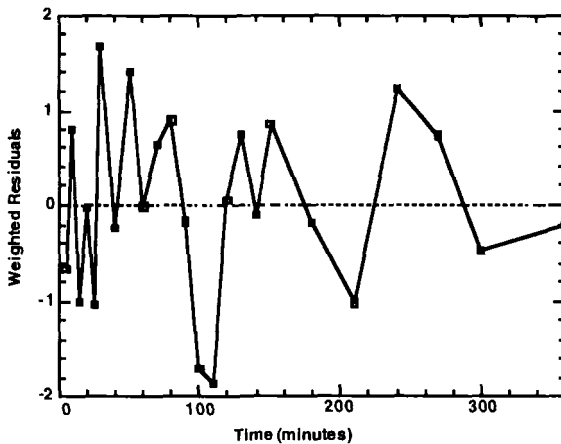
Figure 8.6.3. Plot of weighted residuals versus time. See text for additional explanation.

A pattern of residuals different than expected indicates either the presence of errors in the functional description of the data or that the model is correct but the measurement error model is not appropriate. In this case, it is necessary to modify the assumptions on the measurement error structure. Some suggestions can be derived by examining the plot of the residuals versus either the observed or predicted values.

As an example, consider the case where the variance of the measurement error is assumed to be constant. The residuals are expected to be confined in a constant wide region. If their amplitude tends to increase in absolute value with respect to the observed value, a possible explanation is that the variance of the measurement error is not constant thus suggesting a modification of the assumptions on the measurement error variance.

In case a, a formal test on the variance of weighted residuals can also be applied; this test is exact for linear regression with gaussian measurement errors while it is approximated in the general case. Consider the weighted residual sum of squares WRSS

$$\text{WRSS} = \sum_{i=1}^{N} wres^2(t_i) \qquad (8.6.14)$$

Under the hypothesis that the weighted residuals are independent with unit variance, WRSS is the outcome of a random variable $\mathcal{W}$ distributed approximately as a Chi-square statistic with a number of degrees of freedom equal to $N - P$, the number of data points minus the number of unknown parameters. It is now possible to test the original assumption of unit variance for the weighted residuals by defining, as outlined before for the runs test, the region where, with probability $(1 - \alpha)$, the values of the random variable $\mathcal{W}$ fall. If W^{min} and W^{max} denote the lower and upper bound of the region,

$$
\begin{aligned}
\text{Prob}[\mathcal{W} \leq W^{min}] &= \int_{-\infty}^{W^{min}} \chi^2_{N-P}(x)dx = X^2_{N-P}(W^{min}) \qquad (8.6.15) \\
&= \frac{\alpha}{2}
\end{aligned}
$$

$$
\begin{aligned}
\text{Prob}[\mathcal{W} \geq W^{max}] &= \int_{W^{max}}^{\infty} \chi^2_{N-P}(x)dx = 1 - X^2_{N-P}(W^{max}) \qquad (8.6.16) \\
&= \frac{\alpha}{2}
\end{aligned}
$$

where χ^2_{N-P} and X^2_{N-P} are the Chi-square density and distribution functions respectively having $N - P$ degrees of freedom. These are tabulated in many statistical textbooks. For example, if $N - P = 15$ and $\alpha = 5\%$, $W^{min} = 6.26$ and $W^{max} = 27.49$.

A value of WRSS within the acceptance region indicates that the weighted residuals are likely to have unit variance. Conversely, a value of WRSS outside the acceptance region indicates that the deviations

between the data and model fit are not compatible with the assumptions on the measurement errors due to errors either in the model structure or in the statistical description of the measurement errors.

Since in most cases these errors result in a WRSS value greater than expected, the test is often performed as an upper tail test, the acceptance region has $W^{\max}$ as an upper bound where $W^{\max}$ for a given level of significance α satisfies

$$\begin{aligned} \text{Prob}[\mathcal{W} \geq W^{\max}] &= \int_{W^{\max}}^{\infty} \chi^2_{N-P}(x)dx = 1 - X^2_{N-P}(W^{\max}) \quad (8.6.17) \\ &= \alpha \end{aligned}$$

As for the runs test, one can evaluate the P value which is now equal to the probability that $\mathcal{W}$ assumes a value equal or even larger that the actual value:

$$P = \text{Prob}[\mathcal{W} \geq \text{WRSS}] = 1 - \int_{-\infty}^{\text{WRSS}} \chi^2_{N-P}(x)dx = 1 - X^2_{N-P}(\text{WRSS})$$
$$(8.6.18)$$

A small P value indicates that WRSS assumes a very unlikely value, much larger than expected from the statistical description of the experiment. Therefore, the underlying assumption of unit variance of the residuals is to be rejected.

Example

Consider the plot of the residuals given in Figure 8.6.1 A. They result from fitting the monoexponential function $y(t) = Ae^{-\lambda t}$ to the data in Table 8.6.1 assuming $\text{Var}(e(t_i)) = 2.25 y_{obs}(t_i)$ or equivalently $\text{SD}(t_i) = 1.5\sqrt{y_{obs}(t_i)}$. The estimated parameters are $A = 3234$ and $\hat{\lambda} = 0.00901$. It appears that the residuals are randomly scattered around the origin. The runs test gives $n^- = 11$ and $n^+ = 13$, $N = 24$. The mean and standard deviation of the asymptotic distribution of the number of runs is: $\mu = 12.197$ and $\sigma = 2.378$. The actual number of runs is $R = 13$, and the standardized value $Z = \frac{13 - 12.917}{2.378} = 0.035$. Z is within the region of acceptance when $\alpha = 5\%$, with a P value greater than 50%, therefore the independence assumption can be accepted.

To test visually the assumptions on the variance of the measurement error, consider the plot of the weighted residuals in Figure 8.6.4. Most residuals lie between -1 and 1 indicating that they are consistent with the above assumptions. Apply the χ^2 test. The weighted residual sum of squares is WRSS $= 28.04$, and the degrees of freedom is 22. From the χ^2 distribution, the acceptance region when the level of significance is 5% is bounded by 10.98 and 36.78. WRSS lies in this region with a

Table 8.6.1.

t_i	$y_{obs}(t_i)$	t_i	$y_{obs}(t_i)$
5	3075	100	1272
10	2975	110	1155
15	2800	120	1099
20	2700	130	1022
25	2556	140	914
30	2510	150	860
40	2250	180	635
50	2097	210	462
60	1884	240	403
70	1738	270	303
80	1596	300	205
90	1434	360	121

P value greater than 10%. Therefore the WRSS value is consistent with the test hypothesis of unit variance for the weighted residuals.

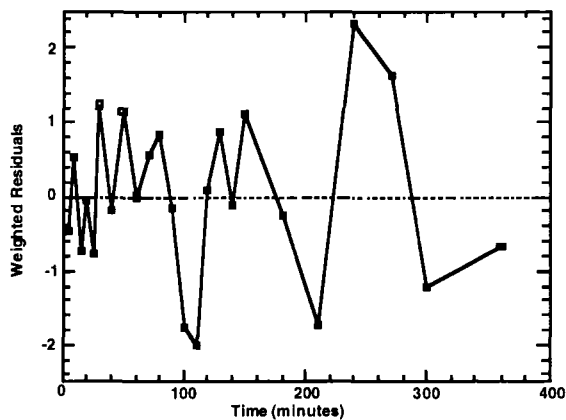*Figure 8.6.4.* Plot of weighted residuals versus time. See text for additional explanation.

8.7   TESTS FOR MODEL ORDER

8.7.1   Introduction

Up to this point, only the problem of testing whether or not a specific model is an appropriate description of a set of data has been examined. Consider now the case where different candidate models are available, and the problem is to select the model which provides the best descrip-

tion of the data. For example, when performing multiexponential modeling of a decay curve

$$y(t) = \sum_{i=1}^{n} A_i e^{-\lambda_i t} \tag{8.7.1}$$

the model order, that is the number n of exponentials, is not known a priori. A mono-, bi- and triexponential model is usually fitted to the data, and the results of the parameter estimation procedure evaluated so as to select the optimum order, i.e. the "best" value for n.

Relying solely upon WRSS and an examination of the weighted residuals to determine the optimum model order is not appropriate since, as the model order increases, WRSS will decrease. For example, in dealing with a tracer decay curve following a bolus injection of material, each additional exponential term to the sum of exponentials will decrease WRSS. Similarly, the pattern of residuals will become more random. However, each time an exponential term is added, two parameters are added (a coefficient and an exponential), and the degrees of freedom are decreased by two. Thus intuitively, while comparing different model structures both WRSS and the degrees of freedom should be evaluated, in order to check whether or not the reduction of WRSS truly reflects a more accurate representation of the data, or is the mere result of the increase in the number of parameters, additional tests are required. Two tests are available that can help in making this decision; they are summarized below. It should be noted that these tests must be viewed as complementary to those described in the previous section.

8.7.2   Three Tests for Model Order

The two tests which are frequently used to compare model structure are the F-test and tests based on the principal of parsimony. It is beyond the scope of this text to go into the details of these tests, but the ideas behind them are illustrated below.

F-test:

The F-test can be used in general to compare two models belonging to the same class, e.g. sums of exponentials describing decaying data, which have a different order, i.e. a different number of parameters. For example, consider two different sums of exponentials models. Denote these two different models by "M_1" and "M_2" respectively. Let P_1 and P_2 be the number of parameters where $P_2 > P_1$ associated with "M_1" and "M_2" respectively.

Suppose WLS has been performed using the models "M_1" and "M_2" with WRSS_1 and WRSS_2 being the value of the residual sum of squares respectively. Define the F ratio:

$$F = \frac{(\mathrm{WRSS}_1 - \mathrm{WRSS}_2)/(P_2 - P_1)}{\mathrm{WRSS}_2/(N - P_2)} \tag{8.7.2}$$

where N is the number of data.

Under the hypothesis that model M_1 is correct, F is the outcome of a random variable $\mathcal{F}$ having an asymptotic Fisher distribution with $(P_2 - P_1, N - P_2)$ degrees of freedom. The hypothesis is to be rejected when model M_2 reduces significantly WRSS, i.e. the actual F is larger than predicted from the statistical description of the process. Therefore, for a given level α of significance of the test, the acceptance region has the lower bound equal to zero, and the upper bound $\mathrm{F}^{\mathrm{max}}$:

$$
\begin{aligned}
\mathrm{Prob}[\mathcal{F} \geq \mathrm{F}^{\mathrm{max}}] &= \int_{\mathrm{Fmax}}^{\infty} f_{(P_2 - P_1, N - P_2)}(x)dx \tag{8.7.3} \\
&= 1 - F_{(P_2 - P_1, N - P_2)}(\mathrm{F}^{\mathrm{max}}) = \alpha
\end{aligned}
$$

where f and F are the F density and distribution functions respectively, having $(P_2 - P_1, N - P_2)$ degrees of freedom. If the actual value of F is greater than $\mathrm{F}^{\mathrm{max}}$, the higher order model M_2 has to be used. For instance, when $\alpha = 5\%$, $P_2 - P_1 = 2$ and $N - P_2 = 15$, $\mathrm{F}^{\mathrm{max}} = 3.68$.

The test can also be formulated by evaluating the P value, that is the probability that the random variable $\mathcal{F}$ assumes values equal to or even larger than the actual value F:

$$
\begin{aligned}
P = \mathrm{Prob}[\mathcal{F} \geq F] &= 1 - \int_{-\infty}^{F} f_{(P_2 - P_1, N - P_2)}(x)dx \tag{8.7.4} \\
&= 1 - F_{(P_2 - P_1, N - P_2)}(F)
\end{aligned}
$$

If P is small, the test hypothesis on the correctness of M_1 is to be rejected.

Tests based on the principle of parsimony:

These tests implement the principle of parsimony, i.e. choose the model which is best able to fit the data with the minimum number of parameters. The Akaike information criterion (AIC) and the Schwarz criterion (SC) are the most commonly used. More than two models can be compared and the model which has the smallest criterion is the best.

If one assumes an optimally WLS has been used and that errors in the data are uncorrelated and gaussian, then the criteria are:

if $w_i = \frac{1}{\sigma^2(t_i)}$,

$$\text{AIC} = \text{WRSS} + 2P \qquad (8.7.5)$$

$$\text{SC} = \text{WRSS} + P\ln N \qquad (8.7.6)$$

or if $w_i = \frac{1}{v(t_i)}$

$$\text{AIC} = N\ln(\text{WRSS}) + 2P \qquad (8.7.7)$$

$$\text{SC} = N\ln(\text{WRSS}) + P\ln N \qquad (8.7.8)$$

where P is the number of parameters in the model and N are the number of data.

While having different derivations, AIC and SC are similar as they are made up of a goodness-of-fit measure plus a penalty function proportional to the number of parameters P in the model. Note that in SC, P is weighted with $\ln(N)$, i.e. with large N, this may become important. Therefore, given the usual small-size data sets encountered in tracer kinetic studies, i.e. $N < 20$ or 30, it is usually good to select the model order by examining the information coming from both tests and from the F-test.

8.7.3   Two Case Studies

While tests for goodness of fit and tests for model order have been discussed separately to illustrate the individual point, they should in fact be conducted simultaneously. The following case studies provides a framework for such a complete model testing process

Case Study 1

Consider the data given in Table 8.7.1; these data are radioactive tracer glucose concentrations measured in plasma following an injection of tracer at time zero. The time measurements are minutes, and the plasma measurements are dpm/ml. The experiment was performed in a normal subject in the basal state [Cobelli et al., 1984]. In order to select the order of the multiexponential model which is best able to describe these data, a one, two and three exponential model can be considered:

$$y(t) = A_1 e^{-\lambda_1 t}$$

$$y(t) = A_1 e^{-\lambda_1 t} + A_2 e^{-\lambda_2 t}$$

$$y(t) = A_1 e^{-\lambda_1 t} + A_2 e^{-\lambda_2 t} + A_3 e^{-\lambda_3 t}$$

The measurement error is assumed to be additive:

Table 8.7.1.

t_i	$y_{obs}(t_i)$	$SD(e(t_i))$	t_i	$y_{obs}(t_i)$	$SD(e(t_i))$
2	3993.50	99.87	28	2252.00	65.04
4	3316.50	86.33	31	2169.50	63.39
5	3409.50	88.19	34	2128.50	62.57
6	3177.50	83.55	37	2085.00	61.70
7	3218.50	84.37	40	2004.00	60.08
8	3145.00	82.90	50	1879.00	57.58
9	3105.00	82.10	60	1670.00	53.40
10	3117.00	82.34	70	1416.50	48.33
11	2984.50	79.69	80	1333.50	46.67
13	2890.00	77.80	90	1152.00	43.04
14	2692.00	73.84	100	1080.50	41.61
15	2603.00	72.06	110	1043.00	40.86
17	2533.50	70.67	120	883.50	37.67
19	2536.00	70.72	130	832.50	36.65
21	2545.50	70.91	140	776.00	35.52
23	2374.00	67.48	150	707.00	34.14
25	2379.00	67.58			

$$y_{obs}(t_i) = y(t_i) + e(t_i)$$

The errors $e(t_i)$ are assumed to be independent Gaussian with zero mean and an experimentally determined standard deviation

$$SD(e(t_i)) = 0.02 \cdot y_{obs}(t_i) + 20$$

These values are shown associated with each datum in Table 8.7.1. The three models are to be fitted to the data by applying weighted nonlinear regression with the weights chosen equal to the inverse of the variance (i.e. case a). The plot of the data and the model predictions with the corresponding weighted residuals are shown in Figure 8.7.1; the model parameters are given in Table 8.7.2.

For the one and two exponential model, all parameters can be estimated with acceptable precision while some parameters of the three exponential model have very high values for the fractional standard deviation. This means that the three exponential model cannot be resolved with precision from the data; in fact, the first exponential is very rapid $(\lambda_1 = 4.6\text{min}^{-1})$, and has practically vanished by the time of the first available datum, $t = 2$ min. The other two exponential terms have values similar to those obtained for the two exponential model. In addition, the final estimates of A_1 and λ_1 are also dependent upon the initial estimates; that is, starting from different initial points in parameter space,
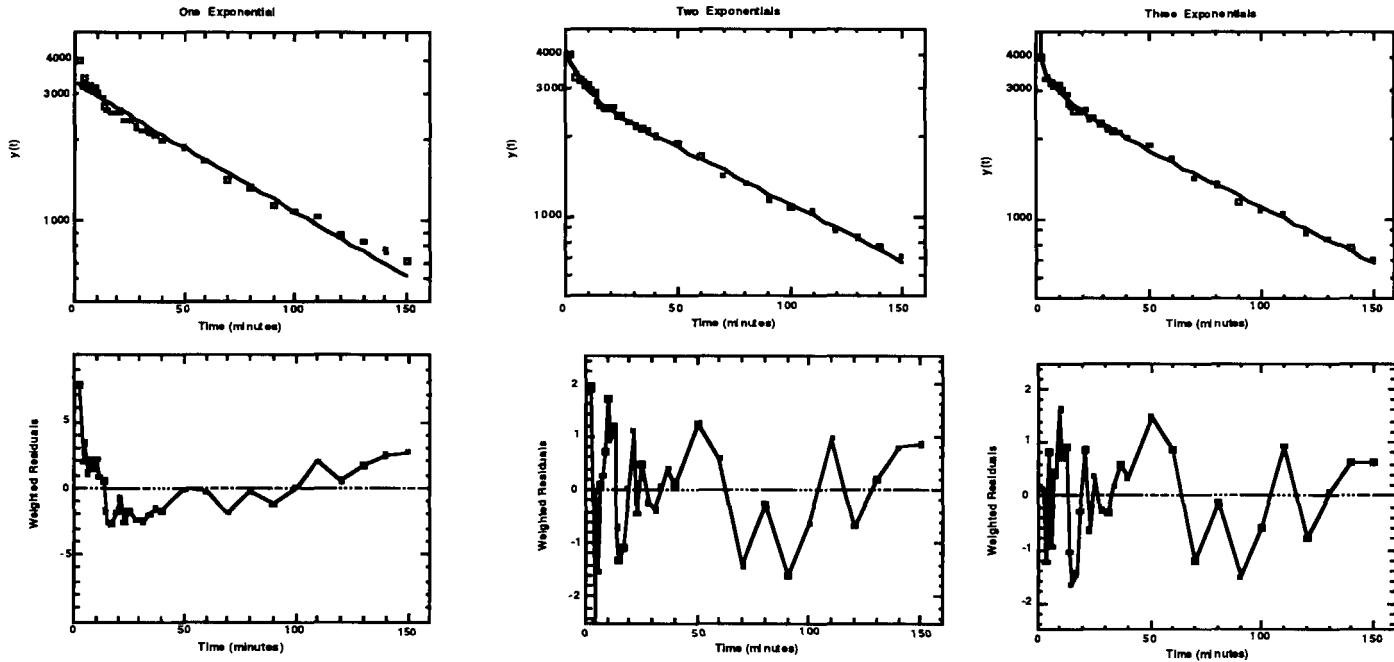
Figure 8.7.1. The best fit of the data given in Table 8.7.1 to a single exponential and a sum of two and three exponentials together with a plot of the weighted residuals for each case. The coefficients and exponentials for each are given in Table 8.7.2.

Table 8.7.2.

		1 Exponential		2 Exponentials	3 Exponentials
A_1		3288 (1%)		1202 (10%)	72486 (535789%)
λ_1		0.0111 (1%)		0.1383 (17%)	4.5540 (7131%)
A_2				2950 (2%)	1195 (14%)
λ_2				0.0098 (3%)	0.1290 (22%)
A_3					2925 (2%)
λ_3					0.0097 (3%)
Runs Test:	Z value	−5.13		−1.51	
	5% region	[−1.96,1.96]		[−1.96,1.96]	
	P value	< 0.5%		> 6%	
χ^2 Test:	WRSS	167.10		32.98	
	5% region	[16.8,47.0]		[16.0,45.7]	
	P value	< 0.5%		> 20%	
F Test:	F ratio	2 vs 1:	29,59		
	5% region		[0,3.33]		
	P value		< 0.5%		
AIC		171.10		40.98	
SC		174.09		46.97	

- Precision of the parameter estimates expressed as percent fractional standard deviation is shown in parentheses.

nonlinear regression yields different final estimates while producing similar values of WRSS. Therefore the three exponential model is not **a posteriori or numerically identifiable,** and can be rejected at this stage. One can now compare the mono- and biexponential fits. Non-randomness of the residuals for the monoexponental model is evident since the plot reveals long runs of consecutive residuals of the same sign. The runs test allows one to check the independence formally, and from the values of Z one can conclude that the residuals of the two exponential model is consistent with the hypothesis of independence since the Z value lies within the 5% region of acceptance [−1.96,1.96], or equivalently the P-value is high. Conversely, for the one exponential model, the Z value indicates that the hypothesis of independence is to be rejected, with a P value less than 0.5%.

Most residuals for the two exponential model lie between −1 and 1 indicating they are compatible with the assumptions on the variance of the measurement error. On the other hand, only a few of the residuals of the one exponential model fall in this range. To test formally if the weighted residuals have unit variance, as expected if the model and/or

assumptions on the variance of the measurement error are correct, the χ^2-test can be applied. For the one exponential model, the degrees of freedom $df = N - P = 31$, and, for the level of significance equal to 5%, the region of acceptance is [16.8,47.0]. Since WRSS is greater than the upper bound 47.0, the assumption of unit variance of the residuals has to be rejected with a P-value less than 0.5%. For the two exponential model, the P-values are higher, and WRSS lies within the 5% region which is equal to [16.05,45.72], indicating that the residuals are consistent with the unit variance assumption. WRSS decreases, as expected, when the number of parameters in the model increases. The F test indicates that the two exponential model reduces WRSS significantly when compared with the one exponential model since the F value is greater than $F^{max} = 3.33$ evaluated for a 5% level of significance from the $F_{(92,29)}$ distribution. Similar conclusions can be derived from AIC and SC which assume their lower values for the two exponential model. The results are summarized below in Table 8.7.3.

Table 8.7.3.

	One Exponential	Two Exponentials
Precision of the estimates	++	+
Randomness of the residuals	–	+
Tests on the variance	–	+
Model fit and number of parameters	–	+

One can conclude that the two exponential model is the most appropriate multiexponential description of the data since it is best able to fit the data with the minimum number of parameters all of which can be estimated with good precision.

Case Study 2

The data shown in Table 8.7.4 are from a tracer glucose kinetic study in sheep in the basal state [Gastaldelli et al., 1997]. As was the situation with the previous case study, radioactive tracer glucose was injected into plasma at time zero, and sequential plasma samples were quantitated for tracer glucose concentrations. In this case, a two, three and four exponential model were fitted to the data; by plotting the data semi-logarithmically, it is clear that the monoexponential cannot fit the data. A measurement error having a constant but unknown fractional standard deviation was assumed. The weights are chosen in this case to be proportional to the inverse of the variance (case b) given by

Table 8.7.4.

t_i	$y_{obs}(t_i)$	t_i	$y_{obs}(t_i)$
2	206701	70	56928
4	171594	80	51757
6	148425	90	47496
8	134377	105	42124
10	123580	120	37425
12	119484	135	32897
14	113790	150	29102
16	109188	165	24598
18	103288	180	21427
20	99108	195	19231
30	87073	210	17596
40	78817	225	15673
50	68707	240	13689
60	64657		

$$\mathrm{Var}(e(t_i)) = y_{obs}^2(t_i) \cdot \sigma^2$$

where σ^2 is unknown and to be estimated from the data, and thus

$$w_i = \frac{1}{y_{obs}^2(t_i)}$$

The plot of the data versus model predictions and the respective weighted residuals are shown in Figure 8.7.2. The results of fitting the data to the two, three and four exponential model are given in Tables 8.7.5 and 8.7.6, where the a posteriori estimate $\hat{\sigma}$ of σ^2 of the square of the unknown fractional standard deviation of the measurement error are also shown.

Briefly, the parameters of the four exponential model cannot be estimated with acceptable precision, indicating that this model is too complex to be resolved from the data. On the other hand, the two exponential model is not able to fit the data since the residuals are nonrandom. The χ^2-test on WRSS cannot be applied here since it requires that the variance of the measurement error is known (case a). The three tests for model order, the F-test, AIC and SC, all indicate that the three exponential model provides the best description of the data. Note that the negative values for AIC and SC arise from the use of (8.7.7) and (8.7.8).
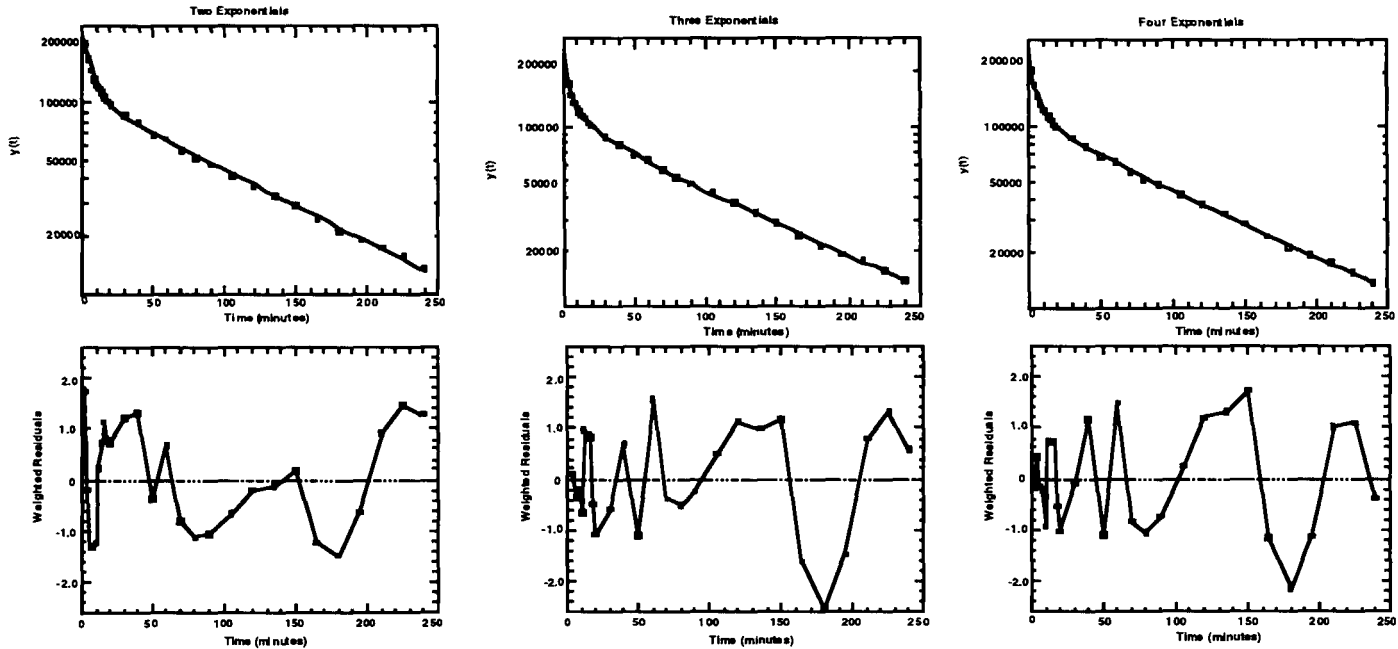
Figure 8.7.2. The best fit of the data given in Table 8.7.2 to a sum of two, three and four exponentials together with a plot of the weighted residuals for each case. The coefficients and exponentials for each are given in Table 8.7.5.

Table 8.7.5.

		2 Exponentials		3 Exponentials	4 Exponentials
A_1		121497 (6%)		126244 (6%)	113032 (23%)
λ_1		0.1412 (7%)		0.2648 (11%)	0.3333 (36%)
A_2		107088 (2%)		38517 (12%)	46838 (55%)
λ_2		0.0087 (1%)		0.0411 (20%)	0.0862 (71%)
A_3				98110 (3%)	64007 (311%)
λ_3				0.0082 (2%)	0.0124 (140%)
A_4					47853 (443%)
λ_4					0.0063 (145%)
$\hat{\sigma}^2$		0.07364		0.02433	
WRSS		15.71		14.60	
Runs Test:	Z value	−2.16		−1.37	
	5% region	[−1.96,1.96]		[−1.96,1.96]	
	P value	< 0.2%		> 8%	
F Test:	F ratio	3 vs 2:	7.03		
	5% region	[0,3.47]			
	P value	< 0.5%			
AIC		−1.15		−1.63	
SC		−1.03		−1.46	

- Precision of the parameter estimates expressed in as percent fractional standard deviation is shown in parentheses.

Table 8.7.6.

	Two Exponentials	Three Exponentials
Precision of the estimates	++	+
Randomness of the residuals	−	+
Model fit and number of parameters	−	+

8.8   **DERIVED STATISTICS**

Up to this point, the focus has been on obtaining a best fit of a function $y(\mathbf{p}, t)$ to a set of data. Suppose a best fit has been obtained with $\hat{\mathbf{p}}$ and that $\mathbf{Cov}(\hat{\mathbf{p}})$ is known. Whereas $\mathbf{p}$ are the primary parameters characterizing the function, often what is wanted, after $\hat{\mathbf{p}}$ and $\mathbf{Cov}(\hat{\mathbf{p}})$ have been estimated, is a parameter which can be calculated from $\mathbf{p}$ through some algebraic manipulation. While it is straightforward to calculate the value of this parameter, the estimation of the error of the derived parameter value resulting from the estimated errors of $\mathbf{p}$ requires some background.

For example, consider the function

$$y = Ae^{-\lambda t} \tag{8.8.1}$$

discussed in §8.5.3. From nonlinear regression analysis, estimates of A, λ, and the variances and covariance of A and λ were obtained. As has been discussed in Chapter 3, to estimate some of the kinetic parameters one needs an estimate of the area under the curve (AUC) of $y = Ae^{-\lambda t}$. It is known that this area is equal to $\frac{A}{\lambda}$. The problem is how can one obtain an error estimate of this derived parameter knowing the estimated errors of the A and λ?

Derived statistics refers to estimating the variances and covariances of functions of the primary parameters characterizing a function. The solution to the problem is nontrivial.

An approximate expression for the variance of the derived parameters is available similar to the one indicated in §8.3.6 for error propagation. The difference here is that primary parameters are usually correlated, therefore not only their variance but also the covariance among them determine the variance of the derived parameters.

Consider the example provided by (8.8.1), and let $\zeta = f(A, \lambda)$ be a generic derived parameter. If $\hat{A}$ and $\hat{\lambda}$ denote the estimated values for A and λ, the derived estimate for ζ is

$$\hat{\zeta} = f(\hat{A}, \hat{\lambda}) \tag{8.8.2}$$

The variance associated with $\hat{\zeta}$ can be approximated by propagating the variances $\mathrm{Var}(\hat{A})$ and $\mathrm{Var}(\hat{\lambda})$ and covariance $\mathbf{Cov}(\hat{A}, \hat{\lambda})$ using the following formula:

$$\mathrm{Var}(\hat{\zeta}) \approx \left(\frac{\partial f}{\partial A}\Big|_{\substack{A=\hat{A}\\ \lambda=\hat{\lambda}}}\right)^2 \mathrm{Var}(\hat{A}) + \left(\frac{\partial f}{\partial \lambda}\Big|_{A=\hat{A},\lambda=\hat{\lambda}}\right)^2 \mathrm{Var}(\hat{\lambda}) \tag{8.8.3}$$

$$+ \left(\frac{\partial f}{\partial A}\Big|_{\substack{A=\hat{A}\\ \lambda=\hat{\lambda}}}\right)\left(\frac{\partial f}{\partial \lambda}\Big|_{\substack{A=\hat{A}\\ \lambda=\hat{\lambda}}}\right)\mathbf{Cov}(\hat{A}, \hat{\lambda})$$

Using (8.8.3) applied to (8.8.1) to estimate the "area under the curve", ζ can be written $\zeta = \text{AUC} = A/\lambda$, and

$$\text{Var}(\hat{\zeta}) = \text{Var}(\text{AUC}) = \frac{1}{\hat{\lambda}^2}\text{Var}(\hat{A}) + \frac{\hat{A}^2}{\hat{\lambda}^4}\text{Var}(\hat{\lambda}) - \frac{\hat{A}}{\hat{\lambda}^3}\text{Cov}(\hat{A}, \hat{\lambda}) \quad (8.8.4)$$

or equivalently

$$\frac{\text{Var}(\text{A}\hat{\text{U}}\text{C})}{\text{A}\hat{\text{U}}\text{C}^2} = \frac{\text{Var}(\hat{A})}{\hat{A}^2} + \frac{\text{Var}(\hat{\lambda})}{\hat{\lambda}^2} - \frac{\text{Cov}(\hat{A}, \hat{\lambda})}{\hat{A} \cdot \hat{\lambda}} \quad (8.8.5)$$

Formula (8.8.3) can be easily extended to the general situation where a derived parameter depends upon more than two primary parameters.

It is important to note that many software tools will automatically generate the derived statistics. Thus the user can specify both the model function $y(\mathbf{p}, t)$ and the derived parameters $\zeta = f(\mathbf{p})$ and, as part of the fitting process, obtain estimates for $\mathbf{p}$ and ζ and errors of these estimates.

References

Bard Y., *Nonlinear Parameter Estimation.* Academic Press, New York, NY, 1974.

Bates D.M., Watts D.G., *Nonlinear Regression Analysis and Its Applications.* Wiley, New York, NY, 1988.

Carson E.R., Cobelli C., Finkelstein L.: *Modeling and Identification of Metabolic and Endocrine Systems.* Wiley, New York, NY, 1983.

Cobelli C., Toffolo G., Ferrannini E.: A model of glucose kinetics and their control by insulin. Compartmental and noncompartmental approaches. *Math. Biosci.* 72:291-315, 1984.

Draper N., Smith H.: *Applied Regression* (2nd ed.). Wiley, New York, NY, 1981.

Gastaldelli A., Schwarz J.M., Caveggion E., Traber L.D., Traber D.L., Rosenblatt J., Toffolo G., Cobelli C., Wolfe R.R.: Glucose kinetics in interstitial fluid can be predicted by compartmental modeling. *Am. J. Physiol.* 272E494-E505, 1997.

Landaw E.M., DiStefano III J.J.: Multiexponential, multicompartmental, and noncompartmental modeling. II. Data analysis and statistical considerations. *Am. J. Physiol. 246*:R665-R677, 1984.

Peck C.C., Beal S.L., Sheiner L.B., Nichols A.I.: Extended least squares nonlinear regression: A possible solution to the choice of weights problem in analysis of individual pharmacokinetic data. *J. Pharmacokin. Biopharm.,* 25:545-558, 1984.

Seber G.A.F., Wild C.J., *Nonlinear Regression.* Wiley, New York, NY, 1989.

This page intentionally left blank.

Chapter 9

PARAMETER ESTIMATION IN NONCOMPARTMENTAL MODELS

9.1   INTRODUCTION

9.1.1   What is Needed?

From the tables listing the formulas for the accessible pool and system kinetic parameters for the one and two accessible pool models given in Chapter 3, one sees that, depending upon how the tracer is introduced into the system, to estimate the parameters certain information is necessary. The best way to obtain this information is through a functional description of the data. Once a particular function such as a sum of exponentials has been chosen, the parameters of the function can be estimated using the techniques described in the previous chapter.

In this Chapter, how to use the information on parameter estimation given in the previous chapter to estimate the noncompartmental parameters will be given. It will be seen that for the canonical inputs of tracer, i.e. the bolus injection, the constant infusion, or primed infusion, sums of exponentials are used. A number of other numerical methods can also be used both for the canonical inputs of tracer as well as generic inputs of tracer such as a staircase infusion where using sums of exponentials can be more difficult. These will be discussed briefly in §9.1.2. The goal in this Chapter is to provide the reader with a means by which the parameters can be estimated with confidence.

9.1.2 Numerical Methods

There are a number of numerical methods that are used to estimate $\int_0^\infty c(t)dt$ or $\int_0^\infty z(t)dt$, hereafter referred to as the area under the curve AUC, and $\int_0^\infty tc(t)dt$ or $\int_0^\infty tz(t)dt$, hereafter referred to as the mean area under the curve (or under the first moment curve) MAUC. To exemplify the nature of the problem, suppose a set of data are collected starting with the first sample at time t_1 and the last sample at time t_n. Noting, for example, that $\text{AUC} = \int_0^\infty y(t)dt$, the question is how to deal with the integral over the interval from time 0 to t_1, and from time t_n to infinity. One can write

$$\int_0^\infty y(t)dt = \int_0^{t_1} y(t)dt + \int_{t_1}^{t_2} y(t)dt + \int_{t_2}^\infty y(t)dt \qquad (9.1.1)$$

To evaluate $\int_{t_1}^{t_2} y(t)dt$, many use "graphical" techniques such as the trapezoidal rule; while this is an easy and convenient method, it can systematically over or underestimate the area for a bolus injection or constant infusion set of data respectively. The real problem to be solved is how to extrapolate to time zero and infinity.

The problems can be illustrated using the data shown in Figure 9.1.1. These data were collected following a bolus injection of $1.8 \cdot 10^7$ dpm of radiolabeled material into a subject; the serial plasma samples are quantitated in concentration units of dpm/ml. In the nomenclature of Chapter 3, the bolus dose d is $1.8 \cdot 10^7$ dpm. A steady state concentration of tracee of l00mg/dl was also measured. In the nomenclature of Chapter 3, this is C, the tracee concentration.

Suppose one wishes to use the trapezoidal rule to estimate AUC and MAUC for the data shown in Figure 9.1.1. Denoting the ith datum $y(t_i)$ and noting $t_1 = 5$ and $t_9 = 150$, then

$$\int_5^{150} y(t)dt = \sum_{i=2}^9 \frac{(c(t_i) + c(t_{i-1}))(t_i - t_{i-1})}{2} \qquad (9.1.2)$$

$$\int_5^{150} ty(t)dt = \sum_{i=2}^9 \frac{(t_i - t_{i-1})}{6}[t_i(c(t_{i-1}) + 2c(t_i)) \qquad (9.1.3)$$
$$+ \quad t_{i-1}(2c(t_{i-1}) + c(t_i))]$$

It is clear what the problems are. First, since these are a decaying set of data, (9.1.2) will overestimate the true AUC. There are more sophisticated methods which solve this problem, e.g. by using an interpolating
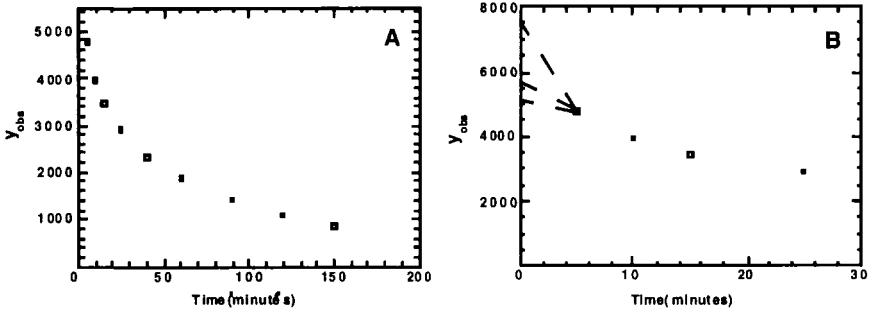
Figure 9.1.1. Panel A. Data shown in a linear plot. Panel B: Data to 30 minutes shown with three possible extrapolations to time zero. The middle extrapolation is a linear interpolation using the first two data. The upper extrapolation indicates that the initial loss may be more rapid. The lower extrapolation represents a slower initial decay as can happen in certain lipoprotein kinetic studies.

polynomial or spline function. Even if this problem is dealt with using these methods, one is left with the problem of estimating $\int_0^5 y(t)dt$ and $\int_{150}^{\infty} y(t)dt$. What zero time value should be chosen? Prom Figure 9.1.1C, it is clear there are many options. One can use linear regression techniques to extrapolate to time zero using the first two or three data; there are no rules. However, AUC between time 0 and 5 can contribute a significant amount to AUC depending upon how "$y(0)$" is estimated. Similarly with $\int_{150}^{\infty} y(t)dt$; there are no set rules on how to extrapolate to infinity.

As seen in the next section and illustrated by the examples in this Chapter, sums of exponentials are very easy to use and appropriate for the canonical input of tracer. As noted there may be instances such as a staircase input of tracer when other numerical techniques are more suitable (e.g. based on interpolating polynomials or spline functions).

9.1.3 Using Sums of Exponentials

The remainder of this chapter will focus on using sums of exponentials to estimate the noncompartmental model parameters. The reasons why exponentials are chosen are twofold. The first reason, as explained in Chapter 4, is that sums of exponentials are the mathematical solution of systems of linear time-invariant differential equations character-

izing compartmental models when a tracer experiment is conducted on a
steady state tracee system, e.g. with the tracer administered as a bolus,
constant infusion or primed constant infusion. The second reason is that
extrapolations are easy using these functions.

For example, if one uses

$$y(t) = A_1 e^{-\lambda_1 t} + \cdots + A_n e^{-\lambda_n t} \tag{9.1.4}$$

to describe a set of tracer data collected either in terms of concentration
$c(t)$ or tracer-tracee ratio $z(t)$ from the accessible pool following a bolus
injection of tracer into that pool, one has

$$y(0) = A_1 + \cdots + A_n \tag{9.1.5}$$

$$\int_0^\infty y(t)dt = \text{AUC} = \frac{A_1}{\lambda_1} + \cdots + \frac{A_n}{\lambda_n} \tag{9.1.6}$$

and

$$\int_0^\infty ty(t)dt = \text{MAUC} = \frac{A_1}{\lambda_1^2} + \cdots + \frac{A_n}{\lambda_n^2} \tag{9.1.7}$$

Equation (9.1.5) provides the required zero time estimate for the concen-
tration $c(0)$ or tracer-tracee ratio $z(0)$. The coefficients A_i and the ex-
ponentials λ_i are estimated from the data using the techniques described
in Chapter 8 and Appendix G. With this information and knowing the
dose d and tracee concentration C, the noncompartmental parameters
can be estimated and, using the techniques given in §8.8, the precision
of these estimates can be obtained.

For the canonical input of tracer, that is the bolus injection, constant
infusion, or primed infusion of tracer, the general expression for $y(t)$ is
given by (9.1.8).

$$y(t) = A_0 + A_1 e^{-\lambda_1 t} + \cdots + A_n e^{-\lambda_n t} \tag{9.1.8}$$

Suppose the data are $(y_{obs}(t_1), \cdots, y_{obs}(t_N))$ obtained at sample times
$t_1, \cdots, t_N$. Once initial estimates of the coefficients A_i and   exponentials
λ_i are determined as explained in Appendix G, one can apply the theory
introduced in Chapter 8 by defining the weighted sum of squares of
residuals

$$WRSS(\mathbf{p}) = \sum_{i=1}^N w_i(y_{obs}(t_i) - y(\mathbf{p}, t_i))^2 \tag{9.1.9}$$

where

$$\mathbf{p} = [A_0, A_1, \cdots, A_n, \lambda_1, \cdots, \lambda_n]^T \tag{9.1.10}$$

is the vector of parameters to be estimated. Applying the theory introduced in Chapter 8, estimates of the parameters and their precision is obtained. An assessment of the goodness of fit can be made. Finally, a selection of how many exponentials are required in order to obtain a best fit can be made by using the tests described in Chapter 8 to compare exponential models.

In summary, obtaining and assessing the "best fit" of an exponential function involves the following:

1. selecting the number of exponential terms n to be used;

2. obtaining initial estimates for the A_i and λ_i;

3. assigning weights to the data;

4. using nonlinear regression to calculate **p** which minimizes WRSS;

5. using tests to assess the goodness of fit; and

6. determining the best value for n.

Once the data have been described by sums of exponentials, one can proceed to estimate the noncompartmental model parameters and their precision. This relies on the theory introduced in §8.8 dealing with derived statistics. Several examples will be given illustrating the points made in this Chapter.

9.2   THE SINGLE ACCESSIBLE POOL MODEL: FORMULAS FOR KINETIC PARAMETERS

9.2.1   Introduction

In this and the following section, how to estimate the accessible pool kinetic parameters given in Tables 3.2.3 and 3.2.4, and the system kinetic parameters given in Tables 3.3.3 and 3.3.4 using sums of exponentials will be discussed for the canonical input of tracer, i.e. the bolus injection, the constant and primed constant infusion. In this section, the formulas will be given using sums of exponentials, and in the next section, several examples will be discussed which illustrate the formulas. These will draw on the material presented in Chapter 8 in terms of evaluating the noncompartmental parameters and estimating their precision.

9.2.2   The Bolus Injection

From Tables 3.2.3 and 3.2.4 for the accessible pool and Table 3.3.2 and 3.3.3 for the system kinetic parameters, what is required is knowing

the initial dose d and tracee concentration C, and obtaining estimates of $z(0)$ or $c(0)$ and the integrals $\int_0^\infty z(t)dt$ or $\int_0^\infty c(t)dt$, and $\int_0^\infty tz(t)dt$ or $\int_0^\infty tc(t)dt$. It is assumed that d and C are known from measurements.

Suppose one has fit the following sum of exponentials to a set of data:

$$y(t) = A_1 e^{-\lambda_1 t} + \cdots + A_n e^{-\lambda_n t} \tag{9.2.1}$$

Then as noted previously,

$$y(0) = A_1 + \cdots + A_n \tag{9.2.2}$$

provides an estimate for the zero time value $z(0)$ or $c(0)$. The integral $\int_0^\infty y(t)dt$ given

$$\text{AUC} = \int_0^\infty y(t)dt = \frac{A_1}{\lambda_1} + \cdots + \frac{A_n}{\lambda_n} \tag{9.2.3}$$

provides an estimate of $\int_0^\infty z(t)dt$ or $\int_0^\infty c(t)dt$. Finally, the integral

$$\text{MAUC} = \int_0^\infty ty(t)dt = \frac{A_1}{\lambda_1^2} + \cdots + \frac{A_n}{\lambda_n^2} \tag{9.2.4}$$

provides an estimate of $\int_0^\infty tz(t)dt$ or $\int_0^\infty tc(t)dt$.

If the data are quantitated in terms of $z(t)$, then using Tables 3.2.3, one has

$$M = \frac{d}{A_1 + \cdots + A_n} \tag{9.2.5}$$

$$\text{FCR} = \frac{d}{M \cdot \text{AUC}} = \frac{A_1 + \cdots + A_n}{\left(\frac{A_1}{\lambda_1} + \cdots + \frac{A_n}{\lambda_n}\right)} \tag{9.2.6}$$

The remaining accessible pool parameters can be calculated from the formulas given in Table 3.2.3. Finally,

$$\text{MRT}^{NC} = \frac{\text{MAUC}}{\text{AUC}} = \frac{\frac{A_1}{\lambda_1^2} + \cdots + \frac{A_n}{\lambda_n^2}}{\frac{A_1}{\lambda_1} + \cdots + \frac{A_n}{\lambda_n}} \tag{9.2.7}$$

The remaining system kinetic parameters can be calculated from the formulas given in Table 3.3.3.

If the data are quantitated in terms of $c(t)$, then using Tables 3.2.3, one has

$$V = \frac{d}{A_1 + \cdots + A_n} \tag{9.2.8}$$

$$\text{CR} = \frac{d}{\text{AUC}} = \frac{d}{\left(\frac{A_1}{\lambda_1} + \cdots + \frac{A_n}{\lambda_n}\right)} \tag{9.2.9}$$

The remaining accessible pool parameters can be calculated from the formulas given in Table 3.2.4. Finally,

$$\mathrm{MRT}^{NC} = \frac{\mathrm{MAUC}}{\mathrm{AUC}} = \frac{\frac{A_1}{\lambda_1^2} + \cdots + \frac{A_n}{\lambda_n^2}}{\frac{A_1}{\lambda_1} + \cdots + \frac{A_n}{\lambda_n}} \tag{9.2.10}$$

The remaining system kinetic parameters can be calculated from the formulas given in Table 3.3.4.

9.2.3 The Constant Infusion

From Tables 3.2.3 and 3.2.4 for the accessible pool and Table 3.3.2 and 3.3.3 for the system kinetic parameters, what is required to estimate the parameters is the plateau value z or c, an estimate of the slope at time zero $\dot{z}(0)$ or $\dot{c}(0)$, and an estimate of the integral $\int_0^\infty [z - z(t)]dt$ or $\int_0^\infty [c - c(t)]dt$. For the constant infusion, suppose the following sum of n exponentials provides a functional representation of the data:

$$y(t) = A_0 + A_1 e^{-\lambda_1 t} + \cdots + A_n e^{-\lambda_n t} \qquad A_0 + A_1 + \cdots + A_n = 0 \tag{9.2.11}$$

The constraint on the coefficients $A_0 + A_1 + \cdots + A_n = 0$ which guarantees that $y(0) = 0$ is formally derived in Appendix H. This constraint must be incorporated in the exponential model which describes data from a constant infusion experiment.

In (9.2.11), A_0 estimates the plateau value z or c. In addition, since

$$\dot{y}(t) = -A_1 \lambda_1 e^{-\lambda_1 t} - \cdots - A_n \lambda_n e^{-\lambda_n t} \tag{9.2.12}$$

one has

$$\dot{y}(0) = -A_1 \lambda_1 - \cdots - A_n \lambda_n \tag{9.2.13}$$

which provides an estimate for $\dot{z}(0)$ or $\dot{c}(0)$. Finally to calculate $[z - z(t)]$ or $[c - c(t)]$ which has to be integrated, one has

$$\begin{aligned} A_0 - y(t) &= A_0 - (A_0 + A_1 e^{-\lambda_1 t} + \cdots + A_n e^{-\lambda_n t}) \tag{9.2.14} \\ &= -A_1 e^{-\lambda_1 t} - \cdots - A_n e^{-\lambda_n t} \end{aligned}$$

whence

$$\int_0^\infty [A_0 - y(t)]dt = -\frac{A_1}{\lambda_1} - \cdots - \frac{A_n}{\lambda_n} \tag{9.2.15}$$

provides an estimate for $\int_0^\infty [z - z(t)]dt$ or $\int_0^\infty [c - c(t)]dt$.

For the case when the data are quantitated in terms of $z(t)$, using Tables 3.2.3 and 3.3.3, one has

$$M = \frac{u}{\dot{z}(0)} = \frac{u}{-A_1 \lambda_1 - \cdots - A_n \lambda_n} \tag{9.2.16}$$

$$\text{FCR} = \frac{u}{M \cdot z} = \frac{u}{M \cdot A_0} = \frac{-A_1\lambda_1 - \cdots - A_n\lambda_n}{A_0} \tag{9.2.17}$$

$$\text{MRT}^{NC} = \frac{\int_0^\infty [z - z(t)]dt}{z} = \frac{-\frac{A_1}{\lambda_1} - \cdots - \frac{A_n}{\lambda_n}}{A_0} \tag{9.2.18}$$

The remaining parameters are calculated from the formulas in Tables 3.2.3 and 3.3.3.

Similarly when the data are quantitated in terms of $c(t)$, using Tables 3.2.4 and 3.3.4, one has

$$V = \frac{u}{\dot{c}(0)} = \frac{u}{-A_1\lambda_1 - \cdots - A_n\lambda_n} \tag{9.2.19}$$

$$\text{CR} = \frac{u}{c} = \frac{u}{A_0} \tag{9.2.20}$$

$$\text{MRT}^{NC} = \frac{\int_0^\infty [c - c(t)]dt}{c} = \frac{-\frac{A_1}{\lambda_1} - \cdots - \frac{A_n}{\lambda_n}}{A_0} \tag{9.2.21}$$

The remaining parameters are calculated from the formulas in Tables 3.2.4 and 3.3.4.

9.2.4   The Primed Constant Infusion

From Tables 3.2.3, 3.2.4, 3.3.3 and 3.3.4, what is required to estimate the kinetic parameters following a primed, constant infusion of tracer is, for data quantitated in terms of $z(t)$, $z(0)$, the plateau value z, and the integral $\int_0^\infty [z - \frac{u}{d}\int_0^t z(t - \tau)e^{-\frac{u}{d}\tau}d\tau]dt$. For data quantitated in terms of $c(t)$, what is required is $c(0)$, the plateau value c, and the integral $\int_0^\infty [c - \frac{u}{d}\int_0^t c(t - \tau)e^{-\frac{u}{d}\tau}d\tau]dt$.

For the primed, constant infusion, suppose the following sum of n exponentials provides a functional representation of the data:

$$y(t) = A_0 + A_1 e^{-\lambda_1 t} + \cdots + A_n e^{-\lambda_n t} \tag{9.2.22}$$

The constraint among the parameters in this situation is more complex than for the constant infusion situation. It is given by

$$A_0 + A_1\left(\frac{\frac{u}{d}}{\frac{u}{d} - \lambda_1}\right) + \cdots + A_n\left(\frac{\frac{u}{d}}{\frac{u}{d} - \lambda_n}\right) = 0 \tag{9.2.23}$$

The derivation of this constraint is given in Appendix H. This constraint must be incorporated in the exponential model which describing data from a primed constant infusion experiment.

Then, as before, $y(0)$ can be used to estimate $z(0)$ or $c(0)$, and A_0 can be used to estimate the plateau z or c. The required integral can be estimated

$$\int_0^\infty [y - \frac{u}{d} \int_0^t y(t-\tau)e^{-\frac{u}{d}\tau}d\tau]dt = \frac{A_1}{\frac{d}{u}\lambda_1^2 - \lambda_1} + \cdots + \frac{A_n}{\frac{d}{u}\lambda_n^2 - \lambda_n} \quad (9.2.24)$$

With this information, all kinetic parameters can be estimated.

Finally, for either the constant or primed, constant infusion, information is available if data are collected during the washout phase. In particular, (3.3.12) and (3.3.13) provide formulas for MRT^{NC} which can be calculated from the washout data assuming that a plateau has been reached at the time T when the infusion stops. What is needed is either $\frac{\int_T^\infty z(t)dt}{z}$ or $\frac{\int_T^\infty c(t)dt}{c}$. These integrals can be estimated as follows. The rising portion of the curve can be described by

$$y_r(t) = A_0 + A_1 e^{-\lambda_1 t} + \cdots + A_n e^{-\lambda_n t} \qquad t \le T \qquad (9.2.25)$$

and the washout by

$$y_w(t) = B_1 e^{-\lambda_1(t-T)} + \cdots + B_n e^{-\lambda_n(t-T)} \qquad t > T \qquad (9.2.26)$$

with

$$B_1 + \cdots + B_n = y_r(T) = A_0 + A_1 e^{-\lambda_1 T} + \cdots + A_n e^{-\lambda_n T}$$

where $y_r(T)$ is the value of the function describing the rise at time T. This constraint guarantees the continuity of the response at time T. Additional constraints exist between the coefficients $A_0, \cdots, A_n$ and $B_1, \cdots, B_n$ of the rising and falling portion of the data; these are derived in Appendix H and must be considered when using this exponential model.

One can easily show that

$$\int_T^\infty y_w(t) = \frac{B_1}{\lambda_1} + \cdots + \frac{B_n}{\lambda_n} \qquad (9.2.27)$$

Equation (9.2.27) can be used to estimate MRT^{NC} using the formulas given in Table 3.3.3 or 3.3.4.

9.3   THE SINGLE ACCESSIBLE POOL MODEL: ESTIMATING THE KINETIC PARAMETERS

9.3.1   Introduction

In this section, a number of examples will be given. For each, it will be assumed that one has determined the model order, i.e. the number of exponentials required to describe each set of data, and assessed

the goodness-of-fit using the techniques discussed in Chapter 8. This information will not be summarized in the table of results.

It should be clear by now that to estimate the noncompartmental parameters, the most time consuming steps deal with the determination of the model order and testing for goodness-of-fit. These were discussed in detail in Chapter 8, and were illustrated in the two case studies in §8.7. In addition, for each model, i.e. for each sum of exponential to be fitted to a set of data, initial estimates for the coefficients and exponentials are required. How to obtain these is discussed in Appendix G.

Once the investigator has selected the appropriate model to describe the data, it is easy to use the formulas given in §9.2 to estimate the noncompartmental parameters.

9.3.2   Example: Bolus Injection

In §8.7, Case Study 1 was a glucose turnover study in a 50.85 kg human in which $4.3037 \cdot 10^7$ dpm of labeled glucose was injected as a bolus, and the measured steady state concentration C was 100 mg/dl. It was found that the two exponential model $y(t) = 1202e^{-0.1387t} + 2950e^{-0.0098t}$ provided the best fit of the data. Here $A_1 = 1202$, $A_2 = 2950$, $\lambda_1 = 0.1387$, and $\lambda_2 = 0.0098$. Knowing these coefficients and exponentials, and the initial dose and steady state concentration, the formulas given in Tables 3.2.4 and 3.3.4 can be used to estimate the noncompartmental accessible pool and system parameters. In addition, knowing the precision of the estimated primary parameters A_1, A_2, λ_1 and λ_2, one can derive, using the approach discussed in §8.8, the precision of the noncompartmental parameter estimates. This is most conveniently done using an appropriate software program. The results are summarized in Table 9.3.1.

Case Study 2 in §8.7 was a glucose turnover study in sheep. Recall that the differences between the two case studies was used to illustrate absolute (Case Study 1) and relative (Case Study 2) weighting. In Case Study 2, the three exponential model $y(t) = 126177e^{-0.2666t} + 38772e^{-0.0417t} + 98287e^{-0.0083t}$ provided the best fit of the data. Hence $A_1 = 126176$, $A_2 = 38772$, $A_3 = 98287$, $\lambda_1 = 0.2666$, $\lambda_2 = 0.0417$ and $\lambda_3 = 0.0083$. Knowing that the initial dose was $4.5 \cdot 10^8$ dpm and the steady state concentration was 80mg/dl, the accessible pool and system parameters can be estimated as illustrated above for Case Study 1. The results are summarized in Table 9.3.2.

The selection of the model order is important. In fact, the question arises as to how the noncompartmental parameter estimates can change as a function of the model order. The interested reader should use the

Table 9.3.1.

Parameter	Estimate with Precision[a]
$c(0)$ (dpm/ml)	4152(3)
AUC (dpm $\cdot$ min/ml)	309663(1)
MAUC (dmp $\cdot$ min^2/ml)	30763100(4)
V (ml)	10363(3)
CR (ml/min)	139(1)
FCR (/min)	0.0134(4)
θ (min)	74.6(4)
M (mg)	10363(3)
MRT^{NC} (min)	99.4(2)
V_{tot}^{NC} (ml)	13809(1)
θ_W (min)	24.8(9)
R_a (mg/min)	139(1)
M_{tot} (mg)	13809(1)

[a] Precision of parameter estimates expressed as a percent fractional standard deviation shown in parentheses.

Table 9.3.2.

Parameter	Estimate with Precision[a]
$c(0)$ (dpm/ml)	263236(4)
AUC (dpm $\cdot$ min/ml)	13312400(1)
MAUC (dmp $\cdot$ min^2/ml)	$1.467 \cdot 10^9$(1)
V (ml)	1709(4)
CR (ml/min)	33.8(1)
FCR (/min)	0.020(4)
θ (min)	50.6(4)
M (mg)	1368(4)
MRT^{NC} (min)	110.2(1)
V_{tot}^{NC} (ml)	3725(1)
θ_W (min)	59.6(3)
R_a (mg/min)	27(1)
M_{tot} (mg)	2980(1)

[a] Precision of parameter estimates expressed as a percent fractional standard deviation shown in parentheses.

data from either case study in §8.7, and evaluate the parameters using the different models tested. For example, for Case Study 2, the estimated volume using the two exponential model is 1963ml. Comparing this

with the estimate of 1709ml, the biexponential model overestimates the volume by 15%. It should also be noted that the precision of both estimates is quite good. For the two exponential model, the fractional standard deviation of 1963ml is 3%. Just because the precision is good does not mean the estimate is the best estimate. The point is that it is absolutely necessary to select the most appropriate model before estimating the noncompartmental parameters.

9.3.3   Example: Constant Infusion

To illustrate how sums of exponentials can be used to estimate the noncompartmental parameters from a constant infusion study, consider the data shown in Figure 9.3.1; these are the data that are discussed in Appendix G in Figure G.16. In this experiment, the infusion rate was 400000dpm/min for 300 minutes; the total amount of tracer administered was $1.2 \cdot 10^8$dpm. The steady state tracee concentration was 50mg/ml.

The two exponential model

$$y(t) = A_0 + A_1 e^{-\lambda_1 t} + A_2 e^{-\lambda_2 t} \qquad (9.3.1)$$

where $A_0 = -(A_1 + A_2)$ provided the best fit of the data assuming a constant coefficient of variation of 10% for the data. Initial estimates for the coefficients and exponentials were obtained as described in Appendix G, and the tests for goodness-of-fit and model order were performed as described in Chapter 8. The best fit of the data is shown in Figure 9.3.1
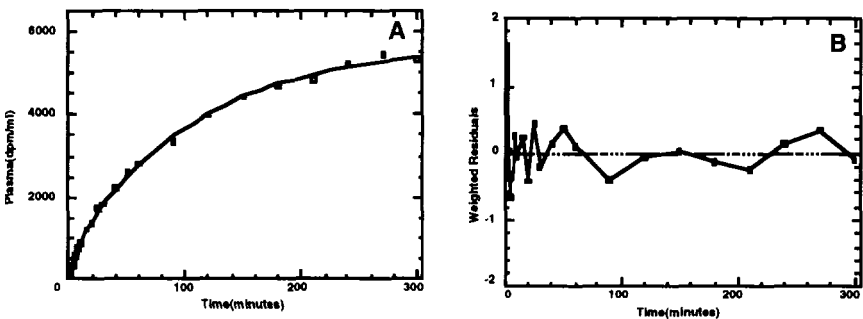

Figure 9.3.1.   A: Plot of the best fit of (9.3.1) to the data. B: Plot of the weighted residuals.

together with the weighted residuals. The results of the parameter estimation are summarized in Table 9.3.3

<div align="center">Table 9.3.3.</div>

Parameter	Estimate with Precision[a]
A_1 (dpm/ml)	$-654.2(55)$
A_2 (dpm/ml)	$-5031(8)$
λ_1 (min^{-1})	$0.1106(45)$
λ_2 (min^{-1})	$0.0093(31)$
A_0 (dpm/ml)	$5685(10)$
$c(0)$ (dpm/ml · min)	$119.0(6)$
INT (dpm · min/ml)[b]	$548969(35)$
V (ml)	$3362(6)$
CR (ml/min)	$70.4(10)$
FCR (/min)	$0.021(13)$
θ (min)	$47.8(13)$
M (mg)	$168085(6)$
MRT^{NC} (min)	$96.6(26)$
V_{tot}^{NC} (ml)	$6794(17)$
θ_W (min)	$48.8(41)$
R_a (mg/min)	$3517(10)$
M_{tot} (mg)	$339700(17)$

[a] Precision of parameter estimates expressed as a percent fractional standard deviation shown in parentheses.
[b] $\text{INT} = \int_0^\infty [c - c(t)]dt$.

As shown in Appendix G, Figure G.18, data were also collected during the washout phase of this experiment. Thus an alternate formula can be used to estimate MRT^{NC} from the washout phase:

$$\text{MRT}^{NC} = \frac{\int_T^\infty c(t)dt}{c} \tag{9.3.2}$$

where $T = 300$ is the time at which the infusion stops. It is assumed that a plateau value has been reached at time T. The washout portion of the curve can be described by

$$y_w(t) = B_1 e^{-\lambda_1(t-300)} + B_2 e^{-\lambda_2(t-300)} \qquad t > T \tag{9.3.3}$$

As described in Appendix H, the constraints between the B_i in (9.3.3) and A_i in (9.3.1) are

$$B_1 = A_1(e^{-\lambda_1 \cdot 300} - 1) \qquad B_2 = A_2(e^{-\lambda_2 \cdot 300} - 1) \tag{9.3.4}$$

The results of fitting the model described by (9.3.1) and (9.3.3) to all of the data from time zero to 500 are summarized in Figure 9.3.2 and Table 9.3.4, where again a constant coefficient of variation of 10% is assumed for the data.
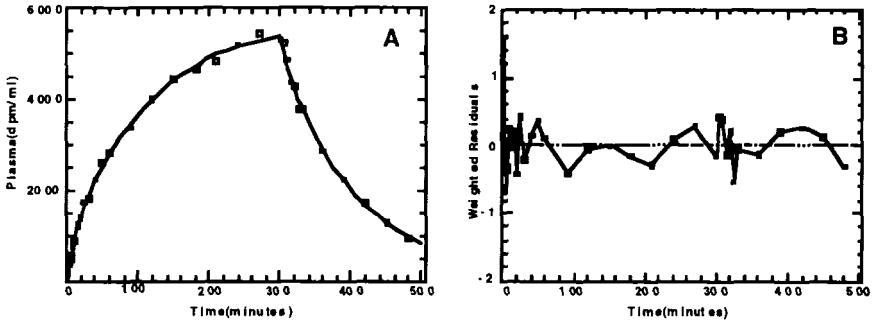

Figure 9.3.2.   A: A plot of the best fit of (9.3.1) and (9.3.3) to the data. B: Plot of the weighted residuals.

Table 9.3.4.

Parameter	Estimate with Precision[a]
A_1 (dpm/ml)	−631(26)
A_2 (dpm/ml)	−5224(4)
λ_1 (min^{-1})	0.115(28)
λ_2 (min^{-1})	0.0089(6)
A_0 (dpm/ml)	5886(2)
B_1 (dpm/ml)	631(26)
B_2 (dpm/ml)	4869(5)

[a] Precision of parameter estimates expressed as a percent fractional standard deviation shown in parentheses.

Notice the estimates for the coefficients A_1 and A_2 and the exponentials λ_1 and λ_2 are slightly different from those given in Table 9.3.3 where only the rising portion of the curve was being fitted. This is because the washout phase has been added to the data set.

More importantly, notice that A_1 and A_2, and B_1 and B_2 will be equal but opposite respectively if a plateau is effectively reached at time T. This is because in the constraints $B_1 = A_1(e^{-\lambda_1 \cdot 300} - 1)$ and $B_2 = A_2(e^{-\lambda_2 \cdot 300} - 1)$, the exponential terms should be zero. However, as can be seen in Figure 9.3.2, a plateau is not reached. The result is that for B_2, $(e^{-\lambda_2 \cdot 300} - 1) = -0.933$ which means $A_2 \neq B_2$. Thus the two integrals required to estimate MRT^{NC} given in Table 3.4.4 will not be equal meaning there will be different estimates for these parameters.

9.3.4 Example: Primed Infusion

To illustrate how to estimate the noncompartmental parameters from an experiment in which the tracer is introduced as a primed constant infusion, consider the data given as Study 2 in Table G.3 in Appendix G.

These data can best be fitted by a monoexponential model

$$y(t) = A_0 + A_1 e^{-\lambda_1 t} \qquad (9.3.5)$$

subject to the constraint, as described in Appendix H, $A_0 = -A_1\left(\frac{u}{u-d\lambda_1}\right)$. The results of the fit, assuming a constant coefficient of variation of 10% for the data, and the parameter estimates are given in Table 9.3.5.

<div align="center">

Table 9.3.5.

</div>

Parameter	Estimate with Precision[a]
A_0 (dpm/ml)	3384(10%)
A_1 (dpm/ml)	15132(2%)
λ_1 (min^{-1})	0.050(7%)
INT (dpm $\cdot$ min/ml)[b]	67484(7%)
V (ml)	3240(7%)
CR (ml/min)	162.5(2%)
FCR (/min)	0.050(7%)
θ (min)	19.9(7%)
M (mg)	162020(7%)
MRT^{NC} (min)	19.9(7%)
V_{tot}^{NC} (ml)	3240(7%)
θ_W (min)	0
R_a (mg/min)	8126(2%)
M_{tot} (mg)	162020(7%)

[a] Precision of parameter estimates expressed as a percent fractional standard deviation shown in parentheses.
[b] $INT = \int_0^\infty [c - \frac{u}{d} \int_0^t c(t - \tau)e^{-\frac{u}{d}\tau} dr] dt$.

The monoexponential model was chosen in this example to illustrate what happens when the accessible pool and system coincide. First, the FCR equals λ_1. Second, Θ and MRT^{NC} coincide. The point is that one can estimate MRT^{NC} using the formula for the required integral given in Table 3.4.4, but this value and Θ are equal meaning that Θ_W is zero. Finally, M_{tot} and M are equal.

For a monoexponential model such as (9.3.5), the system parameters coincide with the accessible pool parameters. Of course, this is no longer true for a multiexponential model.

9.4   THE TWO ACCESSIBLE POOL MODEL: ESTIMATING THE KINETIC PARAMETERS

9.4.1   Introduction

In this section, estimating the two accessible pool noncompartmental model parameters will be discussed for the bolus injection and constant infusion experiments. These experiments are two input-four output studies meaning four sets of data must be described functionally in order to estimate the parameters. Examples will illustrate the main points.

9.4.2   The Bolus Injection

Consider an experiment where there are two accessible pools into which two different tracers have been injected as a bolus. This is a two input-four output study. An example of such a data set is given in Table 9.4.1. In this study, a bolus injection of 200mg and 175mg respectively of tracer 1 and tracer 2 was injected into the accessible pool 1 and 2 respectively; the steady state concentrations of tracee 1 and 2 were respectively 1.43mg/ml and 3.20mg/ml.

These data are expressed in terms of % tracer to tracee ratio $z(t)$. Hence to evaluate the two accessible pool parameters discussed in §3.4, a functional description of these data is required. Following the notation in §3.4, let $z_i^j(t)$ be the tracer to tracee ratio in accessible pool i for tracer j where i and j are 1 or 2. To fit a sum of exponentials to these data, one sees there are two exponential decays $z_1^1(t)$ and $z_2^2(t)$ and two sets of data that rise and fall $z_1^2(t)$ and $z_1^2(t)$, These data can be described by a two exponential model

$$z_i^j(t) = A_i^j e^{-\alpha_i^j t} + B_i^j e^{-\beta_i^j t} \tag{9.4.1}$$

Table 9.4.1.

t	Tracer 1		Tracer 2	
	$z_1^1(t)$	$z_2^1(t)$	$z_1^2(t)$	$z_2^2(t)$
1	3.960	0.075	0.072	1.623
2	3.976	0.138	0.132	1.489
3	3.517	0.185	0.181	1.325
4	3.618	0.235	0.230	1.256
5	3.210	0.292	0.284	1.243
6	3.309	0.335	0.310	1.184
8	2.842	0.384	0.365	1.015
10	2.565	0.452	0.418	0.955
15	2.189	0.507	0.468	0.725
20	1.790	0.512	0.535	0.571
25	1.430	0.497	0.487	0.469
30	1.322	0.476	0.493	0.404
35	1.041	0.437	0.432	0.347
40	0.923	0.440	0.399	0.338
45	0.788	0.388	0.382	0.293
50	0.723	0.373	0.357	0.283
55	0.602	0.352	0.337	0.270
60	0.547	0.324	0.294	0.253
70	0.425	0.276	0.257	0.226
80	0.354	0.240	0.234	0.206
90	0.289	0.229	0.222	0.205
100	0.251	0.198	0.204	0.185
110	0.226	0.185	0.196	0.178
120	0.193	0.175	0.172	0.173
130	0.177	0.174	0.173	0.176
140	0.166	0.170	0.169	0.174
150	0.168	0.159	0.153	0.164
160	0.159	0.163	0.150	0.169
170	0.148	0.153	0.146	0.161
180	0.148	0.159	0.155	0.167

The results of fitting each set of data in Table 9.4.1 to (9.4.1) assuming a constant coefficient of variation of 5% for the data is summarized below in Table 9.4.2 and Figure 9.4.1.

To estimate the parameters, one must convert the data from % tracer to tracee ratio to the actual tracer to tracee ratio. This can be accomplished by multiplying the coefficients A_i^j and B_i^j by 0.01. For example, the functional description of the data in pool 1 for tracer 1, z_1^1, can be written:

$$z_1^1(t) = 0.0369e^{-0.042t} + 0.0029e^{-0.0041t} \qquad (9.4.2)$$

Table 9.4.2. Estimating Noncompartmental Parameters for the Two Accessible Pool Model

| Study | The Bolus Injection Study: Coefficients and Exponentials | | | |
	A_i^j	α_i^j	B_i^j	β_i^j
$z_1^1(t)$	3.69 (2)	0.042 (3)	0.29 (15)	0.0041 (23)
$z_2^1(t)$	−0.57 (2)	0.158 (4)	0.57 (2)	0.0088 (3)
$z_1^2(t)$	−0.54 (2)	0.158 (4)	0.58 (2)	0.0086 (3)
$z_2^2(t)$	1.36 (3)	0.069 (5)	0.26 (6)	0.0028 (15)

Precision of parameter estimates expressed as a percent fractional standard deviation shown in parentheses.
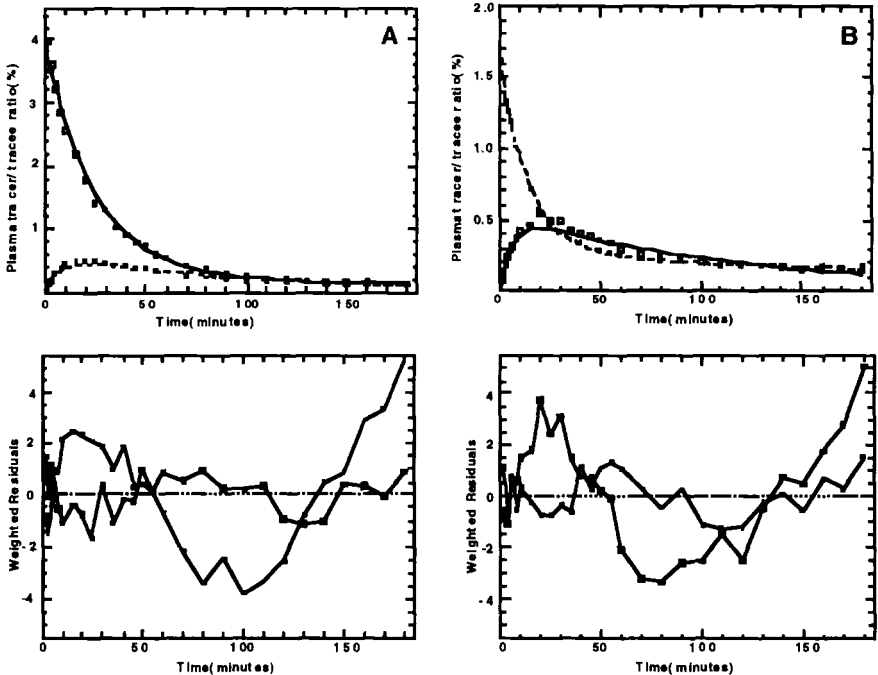
Figure 9.4.1. Plot of the best fit of the model (9.4.1) to the data given in Table 9.4.1. Panel A shows the data for tracer 1 in pool 1 (large squares) and pool 2 (small squares). Panel B shows the data for tracer 2 in pool 1 (large squares) and pool 2 (small squares). The lower figures in Panels A and B are the weighted residuals for both fits respectively.

Table 9.4.3 summarizes the results of the noncompartmental analysis on the set of data presented in Table 9.4.1 using the sum of two exponential model for each data set the parameters of which are given in Table 9.4.2.

Table 9.4.3. Estimating Noncompartmental Parameters for the Two Accessible Pool System

The Bolus Injection Study			
Doses		*Concentrations*	
d_1 (mg)	175	C_1 (mg/ml)	1.43
d_2 (mg)	150	C_2 (mg/ml)	3.20
Areas			
Az_1^1	1.55 (6)	Az_2^1	0.60 (1)
Az_1^2	0.61 (1)	Az_2^2	1.11 (9)
Δz	1.39 (13)		
Parameters			
M_1 (mg)	5024 (2)	V_1 (ml)	3513 (2)
M_2 (mg)	10786 (2)	V_2 (ml)	3371 (2)
R_{21} (mg/min)	76.5 (13)	v_{21} (ml/min)	53.5 (13)
R_{12} (mg/min)	85.7 (13)	v_{12} (ml/min)	26.8 (13)
R_{01} (mg/min)	82.5 (9)	v_{01} (ml/min)	57.7 (9)
R_{02} (mg/min)	152.6 (11)	v_{02} (ml/min)	47.7 (11)
R_{10} (mg/min)	73.4 (11)		
R_{20} (mg/min)	161.7 (26)		
MRT_1^1 (min)	121.8 (23)	MRT_2^1 (min)	122.5 (3)
MRT_1^2 (min)	120.2 (3)	MRT_2^2 (min)	291.9 (16)
MRT_1^{NC} (min)	122.0 (15)	MRT_2^{NC} (min)	156.6 (32)
MRT^{NC} (min)	145.80 (22)		
M_{tot}^{NC} (mg)	34275 (17)	V_{tot}^{NC} (ml)	7403 (17)
R_{a1} (mg/min)	126.1 (6)	R_{a2} (mg/min)	157.9 (9)
CR_1 (ml/min)	92.0 (6)	CR_2 (ml/min)	61.6 (9)

Precision of parameter estimates expressed as a percent fractional standard deviation shown in parentheses.

It is clear from Figure 9.4.1 that when fitting a sum of two exponentials to each data set individually does not yield a "good fit" of the data. One can try adding a third exponential to each, or one at a time, and find that the model is not a posteriori identifiable. Since all one requires is an accurate functional description of the data, is there a resolution to this problem?

Recall from §4.4.4 there is a relationship between sums of exponentials and compartmental models. One can use this information as follows. Since the data in Table 9.4.1 come from the same system, they can be described by the same multicompartmental model where the measurement equation links the solution of the system of differential equations represented by the multicompartmental model and the data. This will be illustrated specifically in the next Chapter.

Here what this means is that each measurement equation, i.e. the measurement equation for $z_i^j(t)$, $i = 1, 2$, $j = 1, 2$, is a sum of exponentials where the corresponding exponentials are equal. That is, one can write

$$z_i^j(t) = A_i^j e^{-\alpha t} + B_i^j e^{-\beta t} + C_i^j e^{-\gamma t} \qquad (9.4.3)$$

for the three exponential model example. It should be noted, again from §4.4.4, that there are also relationships among the A_i^j, B_i^j, and C_i^j, but these are tedious to derive and if all one requires is an accurate representation of the data, not necessary. These relationships, of course, would reduce the degrees of freedom in the fitting process, so the statistical information from the final fitting process could be affected.

The results of fitting the constrained model (9.4.3) to the data in Table 9.4.1 are summarized in Table 9.4.4 and Figure 9.4.2.

What affect does the improved functional description of the data have on the estimates of the noncompartmental parameters? The new estimates are given in Table 9.4.5.

One can easily see that in some cases, there are considerable differences in the estimated parameter values as well as their precision. The differences in the parameter values usually results from the manner in which the data are extrapolated to time zero and infinite while the differences in the error estimates results from the uncertainties of the parameters which are used, as described in §8.8, in the calculation of the derived variables.

Table 9.4.4. Estimating Noncompartmental Parameters for the Two Accessible Pool Model

The Bolus Injection Study: Coefficients and Exponentials of the Constrained Model						
Study	A_i^j	α	B_i^j	β	C_i^j	γ
$z_1^1(t)$	1.48(17)	0.091(3)	2.60(17)	0.032(5)	0.160(12)	0.00091(63)
$z_2^1(t)$	−1.20(6)	=	1.03(6)	=	0.177(10)	=
$z_1^2(t)$	−1.16(6)	=	0.99(6)	=	0.173(10)	=
$z_2^2(t)$	1.07(5)	≈	0.414(10)	=	0.189(9)	=

Precision of parameter estimates expressed as a percent fractional standard deviation shown in parentheses.
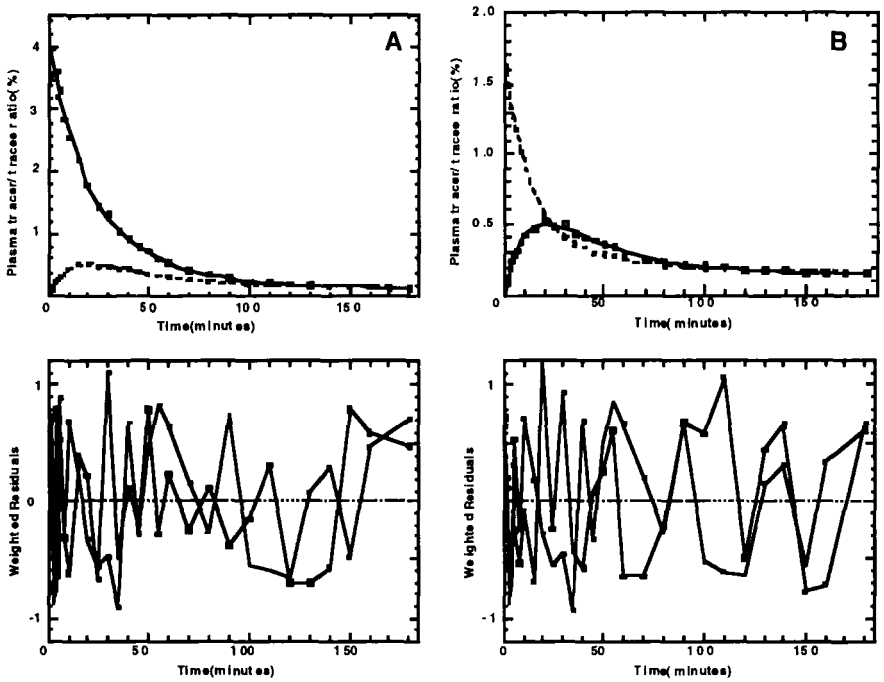
Figure 9.4.2. Plot of the best fit of the model (9.4.3) to the data given in Table 9.4.1. Panel A shows the data for tracer 1 in pool 1 (large squares) and pool 2 (small squares). Panel B shows the data for tracer 2 in pool 1 (large squares) and pool 2 (small squares). The lower figures in Panels A and B are the weighted residuals for both fits respectively.

Table 9.4.5.   Estimating Noncompartmental Parameters for the Two Accessible Pool System

The Bolus Injection Study			
Doses		*Concentrations*	
d_1 (mg)	175	C_1 (mg/ml)	1.43
d_2 (mg)	150	C_2 (mg/ml)	3.20
Areas			
Az_1^1	2.74(34)	Az_2^1	2.09(50)
Az_1^2	2.14(49)	Az_2^2	2.33(49)
Δz	1.94(47)		
Parameters			
M_1 (mg)	4717(3)	V_1 (ml)	3299(3)
M_2 (mg)	10437(2)	V_2 (ml)	3262(3)
R_{21} (mg/min)	193.1(10)	v_{21} (ml/min)	135.0(10)
R_{12} (mg/min)	215(10)	v_{12} (ml/min)	67.3(10)
R_{01} (mg/min)	47.4(7)	v_{01} (ml/min)	33.3(7)
R_{02} (mg/min)	94.7(44)	v_{02} (ml/min)	29.6(44)
R_{10} (mg/min)	25.4(15)		
R_{20} (mg/min)	116.9(35)		
MRT_1^1 (min)	720.9(80)	MRT_2^1 (min)	1011.7(66)
MRT_1^2 (min)	1009.9(67)	MRT_2^2 (min)	988.5(68)
MRT_1^{NC} (min)	821(66)	MRT_2^{NC} (min)	363(139)
MRT^{NC} (min)	455(120)		
M_{tot}^{NC} (mg)	63355(92)	V_{tot}^{NC} (ml)	13684(92)
R_{a1} (ml/min)	72.9(34)	R_{a2} (mg/min)	75.0(49)
CR_1 (ml/min)	74.6(12)	CR_2 (ml/min)	42.9(30)

Precision of parameter estimates expressed as a percent fractional standard deviation shown in parentheses.

9.4.3   The Constant Infusion

Consider next an experiment where there are two accessible pools into which two different tracers have been administered as a constant infusion. Again, this is a two input-four output study. An example of such a data set is given in Table 9.4.6 where, in the nomenclature of Chapter 3, the infusion rates in terms of the tracer to tracee ratio for tracer 1, u_1, and tracer 2, u_2, and 4.0 and 3.8 respectively. Concentrations for tracee 1 and 2 are respectively 0.75mg/ml and 0.50mg/ml. The data are in units %tracer-tracee ratio.

From §3.4, what is needed to estimate the accessible pool and system kinetic parameters is the following. First, each set of data must be described by a sum of exponentials $z_i^j(t)$. These are used to calculate the derivatives of time zero, $\dot{z}_1^1(0)$ and $\dot{z}_2^2(0)$ from which the masses M_1

Table 9.4.6.

| t | Tracer 1 | | Tracer 2 | |
	$z_1^1(t)$	$z_2^1(t)$	$z_1^2(t)$	$z_2^2(t)$
2	0.34	0.00	0.00	0.22
4	0.65	0.02	0.02	0.44
6	0.92	0.05	0.04	0.65
8	1.13	0.09	0.08	0.85
10	1.39	0.12	0.01	1.04
15	1.85	0.24	0.25	1.50
20	2.21	0.38	0.39	1.92
25	2.49	0.54	0.55	2.30
30	2.71	0.70	0.71	2.65
40	3.04	1.03	1.04	3.26
50	3.27	1.34	1.36	3.78
60	3.44	1.64	1.66	4.21
90	3.79	2.38	2.42	5.17
120	4.05	2.96	3.00	5.77
150	4.28	3.41	3.45	6.17
180	4.48	3.78	3.83	6.44
210	4.65	4.09	4.14	6.63
240	4.80	4.36	4.42	6.78
270	4.94	4.60	4.66	6.90
300	5.06	4.81	4.87	7.00

and M_2 can be calculated using the formulas in Table 4.4.3. They are also used to estimate the plateau values z_i^j from which $\Delta z = z_1^1 \cdot z_2^2 - z_1^2 \cdot z_2^1$ is calculated. With Δz, one can calculate R_{21}, R_{12}, R_{01} and R_{02}. These and the remaining accessible pool kinetic parameters can be calculated using the formulas in Table 3.4.3. The system kinetic parameters can then be calculated using the formulas given in §3.4. The interested reader is encouraged to use the data in Table 9.4.4 and estimate the noncompartmental parameters.

This page intentionally left blank.

Chapter 10

PARAMETER ESTIMATION IN COMPARTMENTAL MODELS

10.1   INTRODUCTION

In the previous chapter, how to estimate the parameters defined in Chapter 3 for the noncompartmental model was discussed; this relied on the theory given in Chapter 8. In this chapter, how to estimate the parameters characterizing the multicompartmental model presented in Chapters 4 and 6 will be discussed again using the theory given in Chapter 8 as well as Chapter 5.

It is assumed in this chapter that one is dealing with an a priori globally or locally identifiable model. As discussed in Chapter 6, sometimes this may require the reparameterization of the original model parameterization, or the use of some constraints among parameters. Thus the problem is to estimate the numerical value of the a priori identifiable unknown model parameters and their precision from a real set of data.

Assume for the sake of simplicity the single input-single output case, i.e. a single compartment is accessible for input and measurement; the generalization to the multiple input-multiple output case will be discussed later. Let $y(\mathbf{p}, t)$ denotes the model output, i.e. the tracer concentration or the tracer to tracee ratio in the radioactive and stable isotope case respectively (see §4.3). Recall this is a function of the unknown parameter vector $\mathbf{p}$ which contains the transfer rate constants k_{ij} and the accessible compartment volume V_i or mass M_i. Let $(y_{obs}(t_1), \cdots, y_{obs}(t_N))$ denote the N discrete time noisy measurements (see Chapter 8). The parameter estimation can be formulated as follows using the model (4.3.20) reproduced below in (10.1.1):

$$\frac{d\mathbf{m}(t)}{dt} = \mathbf{K}\mathbf{m}(t) + \mathbf{u}(t) \quad \mathbf{m}(0) = 0 \qquad (10.1.1)$$

307

The measurement equation for the radioactive experiment is (4.3.23) given below in (10.1.2)

$$\mathbf{y}(t) = \mathbf{V}\mathbf{m}(t) \qquad (10.1.2)$$

where V is the matrix

$$\mathbf{V} = \begin{pmatrix} \cdots & \frac{1}{V_{i_1}} & \cdots & 0 & \cdots \\ \cdots & \vdots & \ddots & \vdots & \cdots \\ \cdots & 0 & \cdots & \frac{1}{V_{i_l}} & \cdots \end{pmatrix}$$

given in (4.3.21) where the V_i are the volumes of the accessible compartments.

The measurement equation for the stable isotope experiment is (4.3.24) given below in (10.1.3)

$$\mathbf{y}(t) = \mathbf{D}\mathbf{m}(t) \qquad (10.1.3)$$

where **D** is the matrix

$$\mathbf{D} = \begin{pmatrix} \cdots & \frac{1}{M_{i_1}} & \cdots & 0 & \cdots \\ \cdots & \vdots & \ddots & \vdots & \cdots \\ \cdots & 0 & \cdots & \frac{1}{M_{i_l}} & \cdots \end{pmatrix}$$

given in (4.3.25) where the M_i are the masses of the accessible compartments.

Let **p** be the vector of parameters to be estimated. These include the unknown elements k_{ij} of the **K** matrix, and the unknown volumes V_i of the **V** matrix or masses M_i of the **D** matrix. The measurement equation can then be written for either tracer as $y(\mathbf{p}, t)$. The problem to solve is to estimate the numerical values for **p** from the measurements

$$y_{obs}(t_i) = y(\mathbf{p}, t_i) + e(t_i) \qquad (10.1.4)$$

where $e(t_i)$ is the measurement error first discussed in §8.3.

The model output $y(\mathbf{p}, t)$ is a nonlinear function of the parameter vector **p**. To appreciate this, consider the situation where an analytical solution of the model can be written; in this case the dependency of $y(\mathbf{p}, t)$ on **p** becomes explicit. To illustrate this, consider the single compartment model shown in Figure 10.1.1 where a bolus input of dose d is assumed.

The equations describing the model and the measurement are respectively

$$\frac{dm(\mathbf{p}, t)}{dt} = -km(\mathbf{p}, t) \quad m(0) = d \qquad (10.1.5)$$
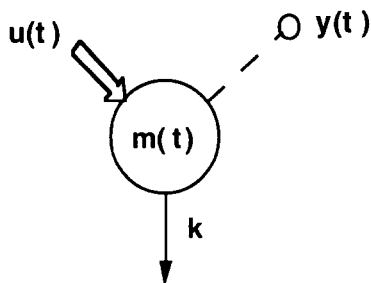
Figure 10.1.1. A single compartment tracer model. The tracer input u is a bolus injection of dose d given at time zero. The pool is characterized by a volume V and tracer mass $m(t)$; the measured variable is the tracer concentration y.

$$y(\mathbf{p}, t) = \frac{1}{V} m(\mathbf{p}, t) \qquad (10.1.6)$$

In this example, $\mathbf{p} = [k, V]^T$. The function $y(\mathbf{p}, t)$ is nonlinear in k and linear in $\frac{1}{V}$ since

$$y(\mathbf{p}, t) = \frac{d}{V} e^{-kt} \qquad (10.1.7)$$

Since the model output $y(\mathbf{p}, t)$ is a nonlinear function of the model parameters, one has to resort to the nonlinear regression theory developed in Chapter 8 to estimate the unknown parameter vector $\mathbf{p}$ by minimizing, in an iterative fashion, the weighted residual sum of squares

$$\mathrm{WRSS}(\mathbf{p}) = \sum_{i=1}^{N} w_i (y_{obs}(t_i) - y(\mathbf{p}, t_i))^2 \qquad (10.1.8)$$

where w_i is the weight assigned to $y_{obs}(t_i)$; the weight is assumed to have been chosen optimally (see §8.3).

It is worth noting that the a priori identifiability analysis described in Chapter 5 has dealt with the ideal situation as defined by (10.1.2). The introduction of (10.1.4) representing real measurements is the new dimension that is added to solve the parameter estimation problem. Thus one moves from the "yes" or "no" a priori identifiability results to quantitative measures of identifiability, i.e. a posteriori or numerical identifiability, which assesses the precision with which the parameters are estimated.

10.2   NONLINEAR LEAST SQUARES ESTIMATION

The parameter estimation problem, i.e. the minimization of WRSS($\mathbf{p}$) is posed similarly to the one discussed in §8.5 with reference to the sum of exponential model. There the unknown parameters were the coefficients and the exponentials of the exponential model while here they are the transfer rate constants appearing in the model differential equations, and the volume or mass characterizing the model output equations. One can thus adopt the same strategy, i.e. obtaining $\hat{\mathbf{p}}$ by minimizing WRSS($\mathbf{p}$) with respect to $\mathbf{p}$ by successive linearizing iterations.

There is, however, an important difference: in general, one does not have the analytical solution of the compartmental model. To understand this difference, recall how model linearization works. Assume an initial estimate $\mathbf{p^0}$ of $\mathbf{p}$ is available. Then $y(\mathbf{p},\,t)$ can be linearized using, as was done in §8.5, a Taylor series expansion about $\mathbf{p^0}$:

$$
\begin{aligned}
y(\mathbf{p}, t) &\approx y(\mathbf{p^0}, t) + \frac{\partial y(\mathbf{p}, t)}{\partial \mathbf{p}}\big|_{\mathbf{p}=\mathbf{p^0}}(\mathbf{p} - \mathbf{p^0}) \qquad (10.2.1) \\
&= y(\mathbf{p^0}, t) + \frac{\partial y(\mathbf{p}, t)}{\partial \mathbf{p}}\big|_{\mathbf{p}=\mathbf{p^0}}\Delta\mathbf{p}
\end{aligned}
$$

where, if $\mathbf{p}$ is a p-dimensional vector, $\Delta\mathbf{p} = \mathbf{p} - \mathbf{p^0}$ is also a p-dimension vector, and $\frac{\partial y(\mathbf{p},t)}{\partial \mathbf{p}}$ is the p-dimensional vector of partial derivatives $\frac{\partial y(\mathbf{p},t)}{\partial \mathbf{p}}\big|_{\mathbf{p}=\mathbf{p^0}} = [\frac{\partial y(\mathbf{p},t)}{\partial p_1}\big|_{\mathbf{p}=\mathbf{p^0}}, \cdots, \frac{\partial y(\mathbf{p},t)}{\partial p_p}\big|_{\mathbf{p}=\mathbf{p^0}}]^T$

Using (10.2.1), WRSS($\mathbf{p}$) becomes linear in $\Delta\mathbf{p}$ whence $\Delta\mathbf{p}$ can be estimated using the linear regression machinery described in Chapter 8. At this stage, a new estimate of $\mathbf{p}$ can be obtained:

$$
\mathbf{p^1} = \mathbf{p^0} + \Delta\mathbf{p} \qquad (10.2.2)
$$

and the process is repeated until some predetermined criterion to stop the iterative process is met.

It is worth noting that the above is exactly the same as that described in §8.5 where the model was $y(\lambda, t) = e^{-\lambda t}$. In the notation used in (10.2.1) and (10.2.2), $\mathbf{p}$, $\mathbf{p^0}$ and $\Delta\mathbf{p}$ play the role of λ, λ^0 and $\Delta\lambda$ respectively. Also of note is that, similarly to what was described in §8.5, one needs for the minimization of WRSS($\mathbf{p}$) the value of the functions $y(\mathbf{p},\,t)$ and $\frac{\partial y(\mathbf{p},t)}{\partial \mathbf{p}}$ only at the sampling times $t_i, i = 1, \cdots, N$

Again, the difference for the multicompartmental model is that in general one does not have the analytical solution of the compartmental model and thus the explicit expression for $y(\mathbf{p},\,t)$ as a function of the unknown parameters k_{ij}, V_i or M_i. Thus in contrast to what was described

in §8.5, one is not able to evaluate $y(\mathbf{p}, t)$ and $\frac{\partial y(\mathbf{p},t)}{\partial \mathbf{p}}$ analytically. One is forced to resort to a different strategy to solve the general problem.

Before describing this strategy, one can ask what happens in the case when an analytical solution is known. For example, for the single compartment model shown in Figure 10.1.1, one has

$$y(\mathbf{p}, t) = \frac{d}{V} e^{-kt} \qquad (10.2.3)$$

In this case, a bolus of dose d was administered and the measurement variable is concentration leaving k and V as the unknown parameters.

It is more instructive for illustrating how parameter estimation works when an analytic solution is known to consider the two compartment model shown in Figure 10.2.1. In this case, assume a unit bolus has been injected into the system at time zero, i.e. $d = 1$
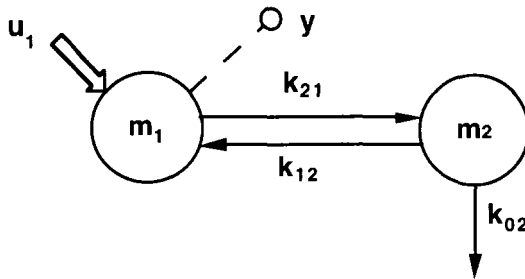
Figure 10.2.1. A two compartment tracer model. The tracer input u_1 is a bolus injection of dose d given at time zero. The measured variable is the tracer concentration y. The unknown parameters are the volume of the accessible pool V_1, and the rate constants k_{21}, k_{12}, and k_{02}.

One knows from §4.5 that $y(\mathbf{p}, t)$ can be written

$$y(\mathbf{p}, t) = A_1 e^{-\lambda_1 t} + A_2 e^{-\lambda_2 t} \qquad (10.2.4)$$

where, in terms of the k_{ij}

$$\lambda_1 = \frac{1}{2}\left((k_{21} + k_{12} + k_{02}) + \sqrt{(k_{21} + k_{12} + k_{02})^2 - 4k_{21}k_{02}}\right) \qquad (10.2.5)$$

$$\lambda_2 = \frac{1}{2}\left((k_{21} + k_{12} + k_{02}) - \sqrt{(k_{21} + k_{12} + k_{02})^2 - 4k_{21}k_{02}}\right) \quad (10.2.6)$$

$$A_1 = \frac{\lambda_1 - (k_{12} + k_{02})}{V_1(\lambda_1 - \lambda_2)} \quad (10.2.7)$$

$$A_2 = \frac{(k_{12} + k_{02}) - \lambda_2}{V_1(\lambda_1 - \lambda_2)} \quad (10.2.8)$$

Thus with (10.2.4) - (10.2.8) known and referring to (10.2.1), one can evaluate $y(\mathbf{p^0}, t)$, $\frac{\partial y(\mathbf{p},t)}{\partial k_{21}}|_{\mathbf{p}=\mathbf{p^0}}$, $\frac{\partial y(\mathbf{p},t)}{\partial k_{12}}|_{\mathbf{p}=\mathbf{p^0}}$, $\frac{\partial y(\mathbf{p},t)}{\partial k_{02}}|_{\mathbf{p}=\mathbf{p^0}}$, $\frac{\partial y(\mathbf{p},t)}{\partial V}|_{\mathbf{p}=\mathbf{p^0}}$ analytically at sampling times t_i where $\mathbf{p}^{0T} = [k_{12}^0, k_{21}^0, k_{02}^0, V^0]^T$ is the initial estimate for the parameter vector $\mathbf{p}^T = [k_{12}, k_{21}, k_{02}, V]^T$. The process of successive iterations proceeds by replacing these initial estimates at each iterative stage with the new estimates calculated using (10.2.2). Of note in this situation is that there are no approximations involved apart from roundoff errors.

Unfortunately the analytical approach becomes impractical for the three compartment model, and virtually impossible as the complexity of the models increase. One has to look at alternative strategies. The problem is not really the evaluation of $y(\mathbf{p}, t)$ at various sample times since one simply needs to solve numerically the model differential equations, and numerical integration algorithms that are both stable and efficient are available. The problem comes in evaluating the partial derivative terms $\frac{\partial y(\mathbf{p},t)}{\partial \mathbf{p}}$ at the various sampling times at each iterative step. The most commonly used methods are explained in Appendix I.

Having solved the problem of calculating $y(\mathbf{p}, t)$ and $\frac{\partial y(\mathbf{p},t)}{\partial \mathbf{p}}$, all of the theory and results described in Chapter 8 can be applied. In particular, one can calculate the lower bound approximation $\mathbf{M}^{-1}(\mathbf{p})$ given in §8.5 of the covariance matrix of the least squares estimate $\hat{\mathbf{p}}$, $\mathbf{Cov}(\hat{\mathbf{p}})$, and the correlation matrix $\mathbf{Corr}(\hat{\mathbf{p}})$. Finally, all the tests of the residuals, measurement error variance and model structure discussed in §8.6 and §8.7 can be applied here.

Needless to say all of the difficulties of nonlinear regression discussed in §8.5, in particular the need for an initial estimate for the parameter vector $\mathbf{p}$ and the presence of local minima, remain. As far as the initial estimates problem is concerned, i.e. initial estimates for the rate constants k_{ij} and volume V or mass M, some help can be provided by preprocessing the data using an exponential model. In Appendix J, how to move from an exponential model where the coefficients A_i and λ_i are estimated (see Appendix G) to an estimate of the k_{ij} and volume V or mass M is discussed.

10.3 THE MULTIPLE OUTPUT CASE

Up until this point, only the single output case has been considered. This accommodates the situation of the single accessible compartment, or the case where several compartments are accessible but the available measurement is a linear combination of them. Suppose now one has multiple outputs denoted $y_j(\mathbf{p}, t), j = 1, \cdots, l$. The observed values will thus consist of l data sets; the j_{th} set contains N_j samples taken at times $t_{1j}, \cdots, t_{N_j j}$. Here the double suffix is needed to allow for different sampling schedules among the l outputs. Denote an observed value by $y_{obs\ j}(t_{ij})$ where $j = 1, \cdots, l$ and $i = 1, \cdots, N_j$

The multiple output case version of WRSS $(\mathbf{p})$ is

$$
\begin{aligned}
\text{WRSS}(\mathbf{p}) &= \sum_{j=1}^{l} \text{WRSS}_j(\mathbf{p}) & (10.3.1) \\
&= \sum_{j=1}^{l} \sum_{i=1}^{N_j} w_{ij}(y_{obs\ j}(t_{ij}) - y_J(\mathbf{p}, t_{ij}))^2
\end{aligned}
$$

The above holds for the case where the weights w_{ij} are known, i.e.

$$
w_{ij} = \frac{1}{var(e(t_{ij}))} = \frac{1}{\sigma^2(t_{ij})} \tag{10.3.2}
$$

The situation is more complicated if the weights are only known up to a proportionality constant, i.e.

$$
w_{ij} = \frac{1}{var(e(t_{ij}))} = \frac{1}{v(t_{ij})\sigma_j^2} \tag{10.3.3}
$$

where σ_j^2 is unknown to be estimated from the data. It has been shown in [Bell et al., 1996] that there is the need to use an "extended" least squares formulation for the counterpart of (10.3.1). This was described in §8.3 and given in (8.3.34). Hence in this case, WRSS$(\mathbf{p})$ becomes

$$
\begin{aligned}
\text{WRSS}(\mathbf{p}) &= \sum_{j=1}^{l} \text{WRSS}_j(\mathbf{p}) & (10.3.4) \\
&= \sum_{j=1}^{l} \left(\sum_{i=1}^{N_j} w_{ij}(y_{obs\ j}(t_{ij}) - y_j(\mathbf{p}, t_{ij}))^2 + \ln(\sigma_j^2) \right)
\end{aligned}
$$

In (10.3.4), it is the presence of the term $\ln(\sigma_j^2)$ which results in the nomenclature of "extended" least squares. The estimate for σ_j^2 is given

by

$$\sigma_j^2 = \frac{1}{N_j} \sum_{i=1}^{N_j} \frac{1}{v(t_{ij})} \left(y_{obs\ j}(t_{ij}) - y_j(\mathbf{p}, t_{ij}) \right)^2 \qquad (10.3.5)$$

In the iterative process, σ_j^2 is recalculated at each iteration.

10.4   THE MULTICOMPARTMENTAL MODEL

In this section, a number of examples of multicompartmental model parameter estimation will be given that parallel those given in Chapter 9. For each, it will be assumed that one has determined the model order, i.e. the number of compartments, or exponentials, required to describe each set of data using the techniques discussed in Chapter 8. The initial estimates for the parameters characterizing the model will be obtained using techniques described in Appendix J.

It is worth noting that the examples given in Chapter 9 focused on determining the best fit and model order in order to estimate the non-compartmental parameters. Attention had to be paid to how the tracer was introduced into the system. That is, the formulas used depended upon whether the tracer was introduced as a bolus, constant infusion, or primed infusion. This is not the case here.

Remember from (4.3.20) the system differential equations for the *n* compartment model are

$$\frac{d\mathbf{m}(t)}{dt} = \mathbf{K}\mathbf{m}(t) + \mathbf{u}(t) \quad \mathbf{m}(0) = 0 \qquad (10.4.1)$$

What one needs to estimate are the entries of the $\mathbf{K}$ matrix, i.e. the individual k_{ij} which are specified by the connectivity of the compartmental model, and the volumes (cf. (4.3.21)) or masses (cf. (4.3.24)). The tracer input is specified by $\mathbf{u}(t)$. Thus, once the initial estimates of the unknown parameters are obtained and the input specified, one is ready to obtain a best fit of the model to the data, and assess this fit using the techniques described in §8.6 and §8.7. Since it is the $\mathbf{K}$ matrix which links the tracer and tracee system, once this and either the volumes or masses are known, all of the desired kinetic parameters of the system can be estimated. Thus except for the techniques used to obtain initial estimates of the unknown parameters, there are no special formulas which depend upon the mode of tracer input.

Example: A two compartment model

In §8.7, Case Study 1 was a glucose turnover study in a 50.85kg human in which $4.3037 \cdot 10^7$ dpm of labeled glucose was injected as a bolus, and the measured steady state plasma glucose concentration C_1 was 100 mg/dl. It was found that the two exponential model $y(t) = 1202e^{-0.1387t} + 2950e^{-0.0098t}$ provided the best fit of the data.

These data will be fitted using the two compartment models shown originally in Figure 5.4.1 modified and reproduced below in Figure 10.4.1. In these models, compartment 1 is assumed to be plasma and compartment 2 is an extravascular compartment which equilibrates with plasma.
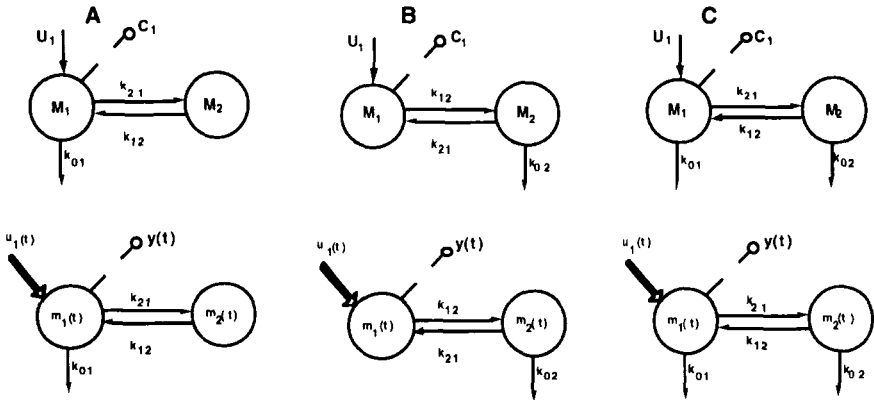
Figure 10.4.1.   Three distinct two compartment models. The upper row shows the tracee models and the lower row the tracer models. Panel A. The two compartment model with no loss from compartment 2. Panel B. The two compartment model with no loss from compartment 1. Panel C. The two compartment model with losses from both compartments 1 and 2. See text for additional explanation.

As noted in Chapter 5, Model A is a priori uniquely identifiable. This model assumes there is no loss from the extravascular compartment. Thus the parameters to estimate are the rate constants k_{21}, k_{12}, and k_{01} and the volume V_1. To obtain initial estimates of these rate constants, one is referred to Appendix J. Briefly, if $y(t) = 1202e^{-0.1387t} + 2950e^{-0.0098t}$ provides a best fit to the data and if one write $A_1 = 1202$, $A_2 = 2950$, $\lambda_1 = 0.1387$ and $\lambda_2 = 0.008$, an initial estimate of V_1 can be found from $\frac{d}{A_1+A_2} = \frac{4.3037 \cdot 10^7}{1202+2950} \approx 10,365$. An initial estimate for k_{11} can

be obtained from (J-3), $k_{11} = \frac{1202 \cdot 0.14 + 2950 \cdot 0.01}{1202 + 2950} \approx 0.048$, and from (J-5), $k_{01} = \frac{1202 + 2950}{\frac{1202}{0.14} + \frac{2950}{0.01}} \approx 0.014$. Knowing k_{11} and k_{01}, k_{21} can be estimated as the difference between 0.048 and 0.014, or 0.034. Finally, $k_{22} = k_{12}$ can be estimated from (J-4) as $\frac{2980 \cdot 0.14 + 1202 \cdot 0.01}{1202 + 2950} \approx 0.1$. The results of these initial estimates are shown in Figure 10.4.2. One should notice this estimate is quite good since the parameters from the best fit by a sum of two exponential were used.

Model B is also a priori uniquely identifiable but, at variance with Model A, all of the loss from the system is assumed to be from the extravascular pool. Again, to obtain initial estimates for the rate constants k_{21}, k_{12}, k_{02} and V_1, the reader is referred to Appendix J. From the knowledge of k_{11}, one has k_{21} since $k_{21} = k_{11} \approx 0.048$. Next, since $k_{21}k_{12} = 0.0034$, k_{12} can be obtained $k_{12} \approx \frac{0.0034}{0.048} = 0.071$. Finally, from $k_{22} = 0.1$, one has $k_{02} = 0.1 - 0.071 = 0.029$. The results of these estimated values are shown in the right hand figure of Figure 10.4.2.
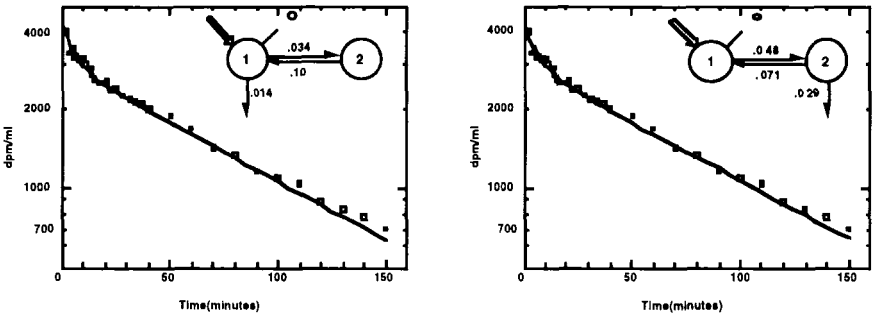
Figure 10.4.2. Left figure: Plot of data (labeled plasma glucose concentration in dpm/ml) and results of model A from Figure 10.4.1 using initial estimates as described in the text. Right figure: Plot of data and results of model B from Figure 10.4.1 using initial estimates as described in the text. The plots are semi-logarithmic to be consistent with the information given in Appendix J.

With these initial parameter estimates, and using the description for the measurement error given in §8.7, Models A and B can be fitted to the data resulting in estimates for V_1 and the k_{ij}. The fit for both models with residuals, shown in Figure 10.4.3, is identical to that shown in Figure 8.7.1 for the two exponential model. Then $M_1 = C_1V_1$ can be calculated, and other kinetic parameters of the tracee system, e.g. tracee mass M_2 in the nonaccessible compartment 2 and tracee production
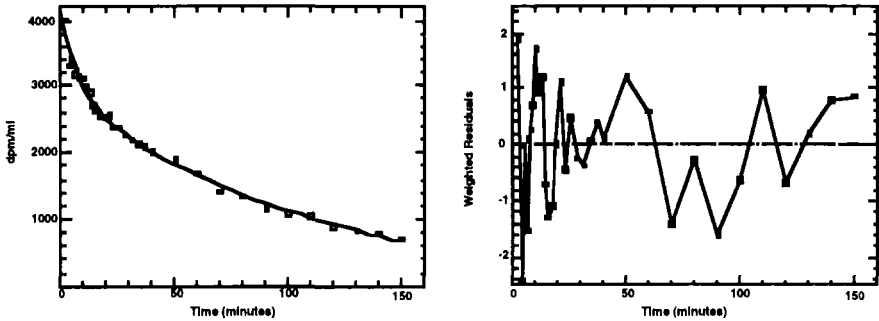
Figure 10.4.3. The fit with residuals of Models A, B, and C of Figure 10.4.1 to the data. All fits are identical, and are identical to that shown in Figure 8.7.1 for a sum of two exponentials.

U_1, can be estimated by solving the tracee steady state system (see Chapter 6) which, in these two cases, have unique solutions since the number of unknowns N_u in the tracee steady state system equals the number n of compartments ($N_u = n = 2$). Note since the elements of the Θ matrix are also known, the noncompartmental clearance rate can be calculated using the formulas given in Chapter 7. The results are summarized in Table 10.4.1 below.

Table 10.4.1.

	Model A	Model B
k_{21} (min^{-1})	0.336(24)	0.0470(18)
k_{12} (min^{-1})	0.1011(16)	0.0723(21)
k_{01} (min^{-1})	0.0134(4)	0
k_{02} (min^{-1})	0	0.0289(7)
V_1 (ml)	10363(3)	10363(3)
CR (ml/min)	139(1)	139(1)
M_1 (mg)	10363(3)	10363(3)
M_2 (mg)	3446(9)	4818(6)
M_{tot} (mg)	13809(1)	15181(2)
U_1 (mg/min)	139(1)	139(2)
θ_{11} (min)	74.6(4)	74.6(4)
θ_{12} (min)	74.6(4)	53.3(3)
θ_{21} (min)	24.8(9)	34.7(7)
θ_{22} (min)	34.7(7)	34.7(7)
MRT$_1$ (min)	99.4(2)	109.3(3)
MRT$_2$ (min)	109.3(3)	88.0(3)

Numbers in parentheses are the precision of the parameter estimates expressed as a percent fractional standard deviation.

It is of interest to compare these parameter values with the noncompartmental estimates given in Table 9.3.1. As expected, the noncompartmental parameters of the accessible pool, V, M and Θ are equal in value to their compartmental counterparts V_1, M_1 and θ_{11} (for both Models A and B). For the system parameters, MRT_{NC} and M_{tot}^{NC} correctly recover the compartmental counterparts MRT_1 and M_{tot} for model A, but underestimate those for model B. In fact, only in the former case is the condition which assures the correctness of all noncompartmental system parameters, i.e. all irreversible loss and production is from and into compartment 1, satisfied. Finally, the noncompartmental parameter R_a equals the production rate U_1 of models A and B since the tracee enters the system in the accessible pool.

While models A and B are both a priori uniquely identifiable, they are, in general, not physiologically plausible. From a physiological point of view, model C with losses from both compartments is more plausible, but it is not a priori identifiable. There are two alternatives in dealing with model C. One is to estimate the bounds of the rate constants. For this example, using models A and B, these are:

$$0 \leq k_{01} \leq 0.0134 \qquad 0 \leq k_{02} \leq 0.0288 \qquad (10.4.2)$$
$$0.0336 \leq k_{21} \leq 0.0470 \qquad 0.0723 \leq k_{12} \leq 0.1011$$

The other alternative is to incorporate a priori knowledge into the model by introducing a constraint among the rate constants k_{ij}. To illustrate this approach, consider the two compartment model shown as Model C in Figure 10.4.1. If the rapidly equilibrating compartment 1 is hypothesized to be responsible for the insulin independent tissues which, in the normal state, utilize about 75% of the total glucose disposal, one can write the following constraint:

$$k_{01}M_1 = 3k_{02}M_2 \qquad (10.4.3)$$

However, since from the tracee steady state $k_{21}M_1 = (k_{12} + k_{02})M_2$, one can rewrite (10.4.3)

$$k_{01}M_1 = 3k_{02}\frac{k_{21}M_1}{k_{12} + k_{02}} \qquad (10.4.4)$$

whence

$$k_{01} = \frac{3k_{02}k_{21}}{k_{12} + k_{02}} \qquad (10.4.5)$$

The constraint (10.4.5) allows Model C to become a priori uniquely identifiable since it provides an additional independent relation among the unknown parameters. The results of fitting this constrained model

are summarized in Table 10.4.2. The fit and weighted residuals are identical to those for Models A and B. One can calculate the system parameters in this case, and compare them with the corresponding parameters from Models A and B shown in Figure 10.4.3. The fact that some are different illustrates a crucial point: if one is using a model to make predictions about nonaccessible compartments in the system, the results are model dependent and it is thus essential that the model structure reflects the physiology of the system.

Table 10.4.2.

	Model C
k_{21} (min^{-1})	0.0370(22)
k_{12} (min^{-1})	0.0920(18)
k_{01} (min^{-1})	0.0101(4)
k_{02} (min^{-1})	0.0092(8)
V_1 (ml)	10363(3)
CR (ml/min)	139(1)
M_1 (mg)	10363(3)
M_2 (mg)	3788(8)
M_{tot} (mg)	14151(2)
U_1 (mg/min)	139(1)
θ_{11} (min)	74.6(4)
θ_{12} (min)	67.8(2)
θ_{21} (min)	27.3(8)
θ_{22} (min)	34.7(7)
MRT$_1$ (min)	101.8(3)
MRT$_2$ (min)	102.5(3)

Numbers in parentheses are the precision of the parameter estimates expressed as a percent fractional standard deviation.

As noted above, it is only the techniques to obtain the initial parameter estimates of the compartmental model that depend upon how the tracer is introduced. The interested reader can follow the example on the constant infusion discussed in Appendix J. Here initial estimates for the two compartment Model A were obtained using the data given originally in Figure H.16. Once the initial estimates are obtained, a best fit can be achieved, and the kinetic parameters can be estimated in exactly the same manner as they were above for the bolus injection.

Example: A three compartment model

Case Study 2 in §8.7 is a glucose turnover study in sheep. In this study, the three exponential model $y(t) = A_1 e^{-\lambda_1 t} + A_2 e^{-\lambda_2 t} + A_3 e^{\lambda_3 t}$ where $y(t) = 126173 e^{-0.2667t} + 38783 e^{-0.0417t} + 98296 e^{-0.0083t}$ provided the best fit of the data. Hence $A_1 = 126173$, $A_2 = 38783$, $A_3 = 98296$, $\lambda_1 = 0.2667$, $\lambda_2 = 0.0417$ and $\lambda_3 = 0.0083$. The initial dose was $4.5 \cdot 10^8$ dpm, and the steady state plasma glucose concentration was 80mg/dl.

These data will be analyzed using the three compartment catenary and mammillary models shown below in Figure 10.4.4. There are several points to be illustrated using these models.
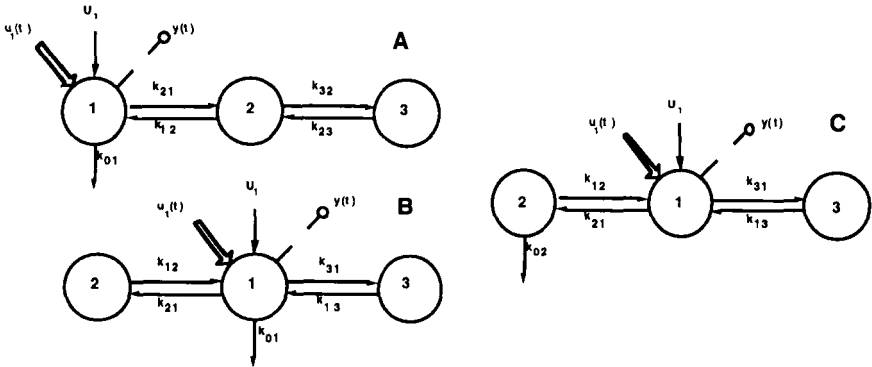
Figure 10.4.4.   Three configurations for the three compartment model discussed in this example. For convenience, the tracee and tracer models are superimposed. Panel A. The three compartment catenary model with input, output and loss from compartment 1. Panel B: The three compartment mammillary model with input, output and loss from central compartment 1. Panel C: The three compartment model with input and output from the central compartment, and loss from a peripheral compartment.

Model A is a priori uniquely identifiable. Both Models B and C are identifiable, but not uniquely since they admit two solutions. For Model B, the solutions are symmetrical, i.e. k_{21} exchanges with k_{31}, and k_{12} exchanges with k_{13}. As discussed in §5.8, this ambiguity can be resolved if compartments 2 and 3 are ordered in terms of "fast" and "slow" compartments, i.e. $|k_{22}| = k_{12} > |k_{33}| = k_{13}$. For Model C, the two solutions are not symmetrical. To resolve this ambiguity, one still could assume

either $|k_{22}| > |k_{33}|$ or $|k_{22}| < |k_{33}|$. Note that, in contrast to Model B, the choice between the two solutions for Model C also involves an assumption on the irreversible loss, which is attributed either to the fast or slow compartment. Thus both Model C solutions will be considered.

Using the same description of the measurement error as that given in §8.7, the results of fitting the models to the data are summarized in Figures 10.4.4 and 10.4.5, and Table 10.4.3. It includes the parameters for Model A, Model B with the assumption that compartments 2 and 3 are the fast and slow compartments as discussed above, and the two solutions for Model C. The tracee parameters, that is the masses and production rates are also given in Table 10.4.3. For each model, unique values can be calculated for them since the number N_u of unknowns in the tracee steady state system equals the number n of compartments $(N_u = n = 3)$. Note that, while the tracee mass in the accessible compartment is the same for all models as in the production rate, the tracee masses in the nonaccessible compartments are different.
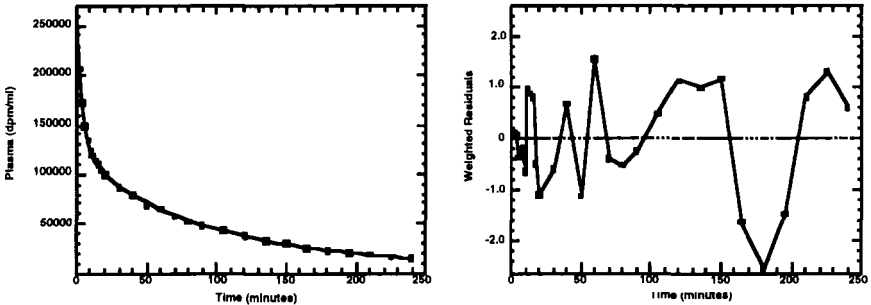
Figure 10.4.5.   The fit with residuals of Models A, B, and C of Figure 10.4.4 to the data. All fits are identical, and are identical to those shown in Figure 8.7.2 for a sum of three exponentials.

The fit and weighted residuals are the same for all models as indicated in Figure 10.4.5. These are also the same as that given in §8.7 for the three exponential model. However, the model predicted tracer masses in the nonaccessible compartments are different as shown in Figure 10.4.6.

For each model, the **K** matrix is

$$\mathbf{K^A} = \begin{pmatrix} -0.137 & 0.133 & 0 \\ 0.117 & -0.145 & 0.035 \\ 0 & 0.012 & -0.035 \end{pmatrix}$$

Table 10.4.3.

	Model A	Model B	Model C-1	Model C-2
k_{21} (min^{-1})	0.117(13)	0.102(12)	0.122(11)	0.034(16)
k_{12} (min^{-1})	0.133(11)	0.148(13)	0.124(4)	0.014(35)
k_{32} (min^{-1})	0.012(33)	–	–	–
k_{23} (min^{-1})	0.035(20)	–	–	–
k_{31} (min^{-1})	–	0.015(33)	0.015(33)	0.102(12)
k_{13} (min^{-1})	–	0.031(17)	0.031(17)	0.148(13)
k_{01} (min^{-1})	0.020(4)	0.020(4)	–	–
k_{02} (min^{-1})	–	–	0.024(10)	0.018(5)
V_1 (ml)	1710(4)	1710(4)	1710(4)	1710(4)
M_1 (mg)	1368(4)	1368(4)	1368(4)	1368(4)
M_2 (mg)	1206(4)	940(10)	1123(10)	941(10)
M_3 (mg)	406(14)	672(15)	672(15)	1537(5)
M_{tot} (mg)	2980(1)	2980(1)	3162(1)	3845(4)
U_1 (mg/min)	27(1)	27(1)	27(1)	27(1)

Numbers in parentheses are the precision of the parameter estimates expressed as a percent fractional standard deviation.
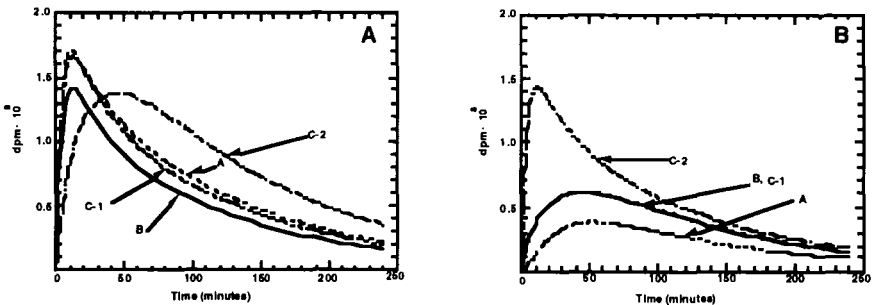
Figure 10.4.6. Model predicted values for the tracer content of the nonaccessible compartments for Models A, B, C-1 and C-2 for compartment 2 (panel A) and compartment 3 (panel B).

$$\mathbf{K^B} = \begin{pmatrix} -0.137 & 0.148 & 0.031 \\ 0.101 & -0.148 & 0 \\ 0.015 & 0 & -0.031 \end{pmatrix}$$

$$\mathbf{K^{C-1}} = \begin{pmatrix} -0.137 & 0.124 & 0.031 \\ 0.122 & -0.148 & 0 \\ 0.015 & 0 & -0.031 \end{pmatrix}$$

$$\mathbf{K^{C-2}} = \begin{pmatrix} -0.137 & 0.014 & 0.148 \\ 0.035 & -0.031 & 0 \\ 0.102 & 0 & -0.148 \end{pmatrix}$$

from which the mean residence time matrices $\mathbf{\Theta} = -\mathbf{K}^{-1}$ can be calculated. They are respectively

$$\mathbf{\Theta^A} = \begin{pmatrix} 50.6 & 50.6 & 50.6 \\ 44.6 & 52.2 & 52.2 \\ 15.0 & 17.5 & 46.2 \end{pmatrix}$$

$$\mathbf{\Theta^B} = \begin{pmatrix} 50.6 & 50.6 & 50.6 \\ 34.8 & 41.5 & 34.8 \\ 24.8 & 24.8 & 56.9 \end{pmatrix}$$

$$\mathbf{\Theta^{C-1}} = \begin{pmatrix} 50.6 & 42.4 & 50.6 \\ 41.5 & 41.5 & 41.5 \\ 24.9 & 20.8 & 56.9 \end{pmatrix}$$

$$\mathbf{\Theta^{C-2}} = \begin{pmatrix} 50.6 & 22.1 & 50.6 \\ 56.9 & 56.9 & 56.9 \\ 34.8 & 15.2 & 41.6 \end{pmatrix}$$

Example: A three compartment model where a flux is the measurement variable

The following example is taken from [Saccomani et al., 1995] where bicarbonate kinetics were being studied in humans. Following an injection of $2.23 \cdot 10^7$ dpm of ^{14}C labeled bicarbonate HCO_3, the ^{14}C loss in expired air (a tracer flux) was measured at specific time points. The data are shown below in Table 10.4.4. The tracee loss, i.e. the CO_2 flux in the expired, was also measured; it was 9 mmol/min.

The model developed to explain the tracer data is shown in Figure 10.4.7. The model parameters to estimate from the data are k_{21}, k_{12}, k_{31}, k_{13}, k_{01}^R and k_{21}^{NR}. The rate constant k_{01}^R represents irreversible loss via expired air and k_{21}^{NR} represents "loss" to other tissues such as bone, urine or sweat. In this experiment, the tracer flux in the expired air is the measured variable. The measurement equation is thus

$$y(t) = k_{01}^R \cdot m_1(t) \tag{10.4.6}$$

Table 10.4.4.

Time (min)	Expired Air (dpm/min)	Time (min)	Expired Air (dpm/min)
1	777000	50	87000
2	641000	55	86900
3	536000	60	76500
4	457000	70	68500
5	369000	80	61100
7	332000	90	55700
9	287000	100	50900
11	259000	120	44000
13	219000	145	35600
15	211000	160	32000
18	213000	180	26400
21	159000	220	19100
24	167000	260	12600
28	124000	300	10100
30	120000	340	8100
35	112000	380	5150
40	99500	420	4080
45	96000		
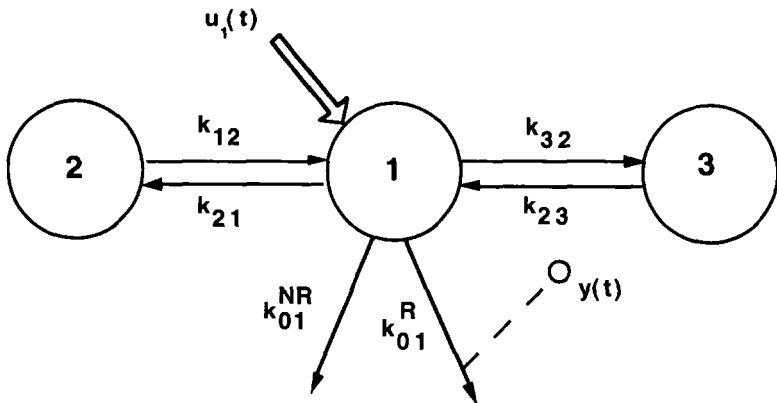
Figure 10.4.7. A three compartment model for bicarbonate metabolism. Labeled material is introduced into compartment 1. The measurement variable is the tracer flux in expired air.

The model parameters k_{01}^R and k_{01}^{NR} are uniquely identifiable, while the parameters k_{21}, k_{12}, k_{31} and k_{13} admit two symmetrical solutions. Assuming $|k_{11}| > |k_{22}|$, the model is a priori uniquely identifiable.

The measurement error in this study was given by

$$var(e(t_i)) = 72900 + 0.006125 y_{obs}(t_i)^2 \qquad (10.4.7)$$

Thus the coefficient of variation ranges from 8% at the higher counts to 11% at the lower counts.

The results of fitting this model to the data are summarized in Table 10.4.5; the fit is shown in Figure 10.4.8.

Table 10.4.5.

Parameter	Estimate
k_{01}^R (min^{-1})	0.046(13)
k_{01}^{NR} (min^{-1})	0.0055(15)
k_{21} (min^{-1})	0.170(40)
k_{12} (min^{-1})	0.224(28)
k_{31} (min^{-1})	0.068(17)
k_{13} (min^{-1})	0.023(8)

Numbers in parentheses are the precision of the parameter estimates expressed as a percent fractional standard deviation.
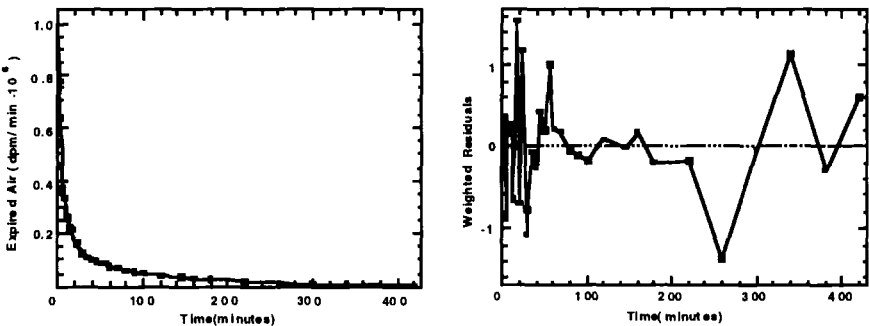
Figure 10.4.8. The best fit of the model shown in Figure 10.4.7 to the data given in Table 10.4.4; the weighted residuals are also shown.

The formulation of the tracee model requires the specification of exact sites of entry of endogenous production of CO_2 into the system. Since a priori knowledge of these sites is not known, a parameter bound approach was taken for quantifying the three possible tracee systems shown in Figure 10.4.9. These three models are distinguished by the site of entry into compartments 1, 2 or 3 respectively, and differ from the tracer model by the addition of a fourth compartment, compartment 4. This new compartment accounts for the exchange of material through a very slowly turning over compartment that is not "seen" by the tracer over the time interval of the experiment. Thus the parameter k_{41} of the tracee model in Figure 10.4.9 coincides with k_{01}^{NR} of the tracer model in Figure 10.4.7.
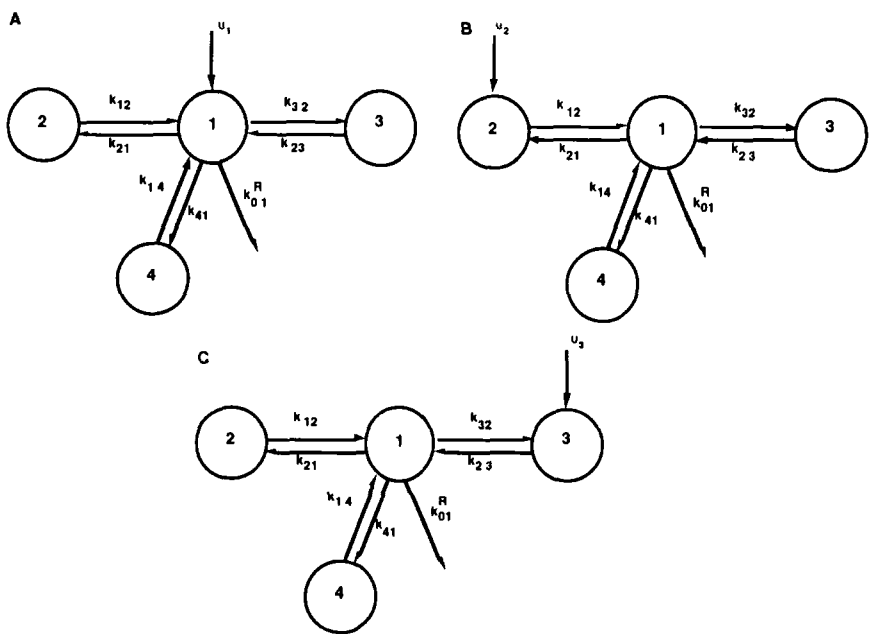
Figure 10.4.9.   Three tracee models corresponding to the tracer model shown in Figure 10.4.7. Models A - C differ in the site of endogenous production.

The uncertainty over the site of entry of de novo CO_2 has no consequence on the estimate of endogenous production itself because the structure of the three models shown in Figure 10.4.7 yields the same

estimate which is identical to the CO_2 loss measured in the expired air: $U_1 = U_2 = U_3 = 9\text{mmol/min}$. Also the mass M_1 of compartment 1 is not affected by the site of entry of CO_2 since for the three tracee models one has

$$M_1 = \frac{9}{k_{01}^R} = 196\text{mmol} \tag{10.4.8}$$

The situation, however, for the masses of compartments 2 - 4, and hence for total CO_2 mass in the system, does depend upon the site of entry of CO_2. First, it should be noted that M_4 cannot be estimated. While the flux from compartment 4 to compartment 1, $k_{14}M_4$, is known since it is equal to the flux from compartment 1 to compartment 4, $k_{41}M_1$, the individual components k_{14} and M_4 are not known. Thus the upper and lower bounds for M_2 and M_3 are

$$M_i^{\min} = M_1 \frac{k_{i1}}{k_{1i}} \leq M_i \leq \frac{k_{i1} + k_{01}^R}{k_{1i}} = M_i^{\max} \qquad i = 2, 3 \tag{10.4.9}$$

The total CO_2 in the system, M_{tot}, can also be calculated for each model where the suffix i represents the site of endogenous production U_i:

$$M_{tot}^1 = M_1 + M_2^{min} + M_3^{min} = 910\text{mmol}$$

$$M_{tot}^2 = M_1 + M_2^{max} + M_3^{min} = 945\text{mmol} \tag{10.4.10}$$

$$M_{tot}^3 = M_1 + M_2^{min} + M_3^{max} = 1295\text{mmol}$$

where $M_1 = 19$. Hence upper and lower bounds for M_{tot} can be evaluated:

$$910\text{mmol} = M_{tot}^{\min} = M_{tot}^1 \leq M_{tot} \leq M_{tot}^3 = M_{tot}^{\max} = 1295\text{mmol} \tag{10.4.11}$$

Example: A three compartment model with a two input-four output experiment

The data given in Table 9.4.1 were used to estimate the noncompartmental parameters for the two accessible pool model. This was a two stable isotope tracer study in which 200 mg of the first label and 175 mg of the second label were injected into the two accessible pools respectively. The tracee concentration in the first and second accessible pool were 1.43 mg/ml and 3.20 mg/ml respectively.

Recall from §9.4.2 that the best fit of the data were obtained using sums of two exponentials when each individual curve was fitted individually. Note here that the exponentials for each sum were different.

As noted in §9.4.2, this raised an important point. While for a single data set, the number of exponentials of the best fit suggests the number of compartment in the system, when dealing with more than one data set, unless all corresponding exponentials in each sums are the same, this is no longer necessarily true. In fact since the data come from the same system, the exponentials for each of the curves must be the same. Additionally, as previously noted, constraints also exist among the co-efficients of the sums of exponentials. These are normally tedious to derive, even for relatively simple models.

In §9.2.4, while the best fit for each data set was obtained using a sum of two exponentials, these fits were not "best" in the sense that the weighted residuals had systematic deviations. Additionally, the sum of three exponential model was not a posteriori identifiable. Recognizing that the data come from the same system, it was seen that sums of three exponentials where corresponding exponentials for all four sums were equal provided a best fit to the data. This suggests that a three compartment model will be required to describe the data.

Recall from Chapter 5 there are many different 3 compartmental structures. Among these, consider the model shown in Figure 10.4.10. The model shown in panel A is the tracee model. This shows material exchanging between the two accessible compartments 1 and 2. Compartment 2 exchanges with an extravascular compartment, compartment 3. De novo input and losses occur in both accessible compartments. The model shown in panel B shows the first tracer being injected into compartment 1; similarly in panel C the second tracer is injected into
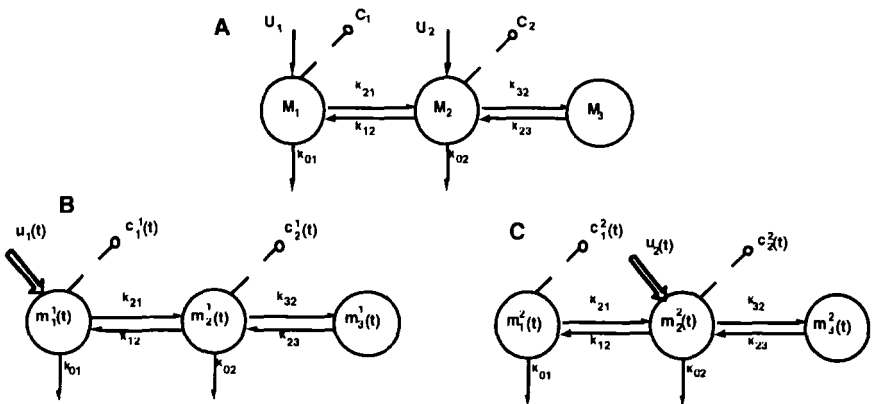
Figure 10.4.10. Models used to describe the data given in Table 9.4.1. See text for additional explanation.

compartment 2. It is assumed that the volumes of the two accessible compartments are the same.

How does this model relate to the sums of exponentials? First, this model represents a system of differential equations the solution of which is a sum of three exponentials. The measurement equations are also sums of three exponentials where the exponentials, the λ_i, are the same for each equation. By analyzing the data simultaneously, instead of individually as was done initially in the example in §9.4.2, the condition that the exponentials λ_i be the same and the constraints among the coefficients are automatically built in.

Following the notation adopted in §3.4, let $m_j^i(t)$ be the mass of tracer i in compartment j, and let M_1 and M_2 be the mass of tracee in compartments 1 and 2 respectively. Then the measurement variables are the four tracer to tracee ratio $z_j^i(t) = \frac{m_j^i(t)}{M_j}$, $i = 1, 2$ $j = 1, 2$. The results of fitting the model to the data, assuming an error structure equal to a constant coefficient of variation and relative weighting, are given in Table 10.4.6 and Figure 10.4.11 The tracee parameters such as the mass of the nonaccessible compartment 3, and the production rates U_1 and U_2 are also shown. They can be calculated uniquely since the number of unknowns N_u equals the number of compartments, $N_u = 3 = n$.

Table 10.4.6.

Parameter	Estimate	Parameter	Estimate
k_{01} (min^{-1})	0.0099(2)	M_1 (mg)	4731(1)
k_{02} (min^{-1})	0.0038(44)	M_2 (mg)	10589(1)
k_{21} (min^{-1})	0.040(1)	M_3 (mg)	58904(10)
k_{12} (min^{-1})	0.020(1)	M_{tot} (mg)	73141(18)
k_{32} (min^{-1})	0.042(3)	U_1 (mg/min)	26.5(5)
k_{23} (min^{-1})	0.0076(8)	U_2 (mg/min)	58.7(28)
vol (ml)	3309(1)		

Numbers in parentheses are the precision of the parameter estimates expressed as a percent fractional standard deviation.

It is clear that the fit shown in Figure 10.4.11 is more in agreement with the constrained sum of exponential model shown in Figure 9.4.2 consistent with the observation made in §9.4 that the data come from the same system, and the fact that a sum of three exponentials where the exponentials are all equal provides a good fit to all data. One can also compare the results given in Table 10.4.6 with those for noncompartmental analysis in Table 9.4.3. In the model shown in Figure 10.4.10 the volumes of the two accessible pools are the same; this differs from
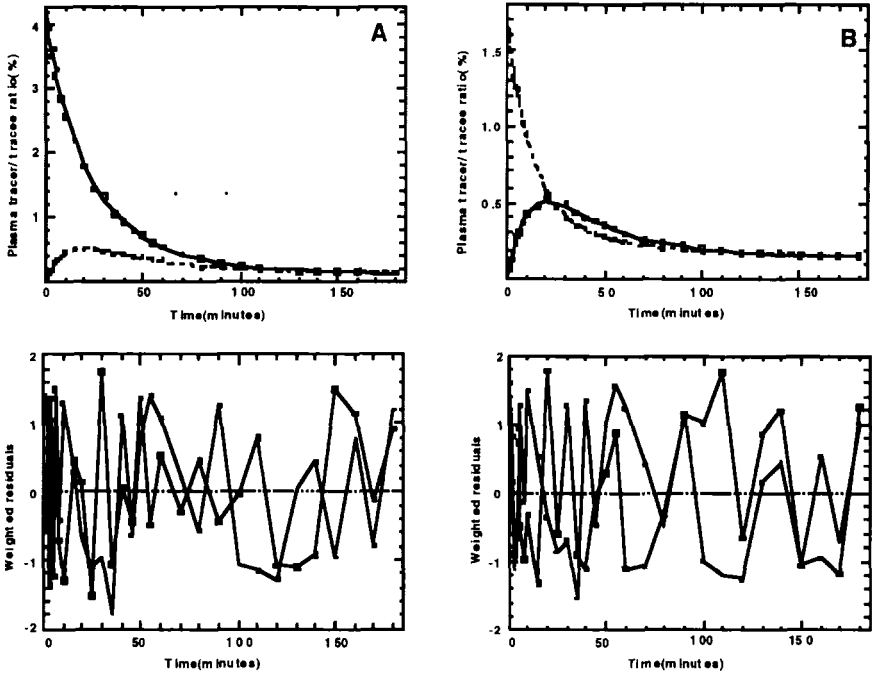
Figure 10.4.11. Plot of the best fit of the model shown in Figure 10.4.7 to the data given in Table 9.4.1. Panel A: Tracer injection into compartment 1. The large squares are the tracer to tracee ratio for tracer 1 in compartment 1; small squares are for tracer 1 in compartment 2. Panel B: Tracer injection into compartment 2. The large squares are the tracer to tracee ratio for tracer 2 in compartment 1; small squares are for tracer 2 in compartment 2. The weighted residuals for each fit are also shown.

the volumes estimated by the noncompartmental approach. However, all estimated volumes are very close. This carries over to the estimates of the masses in the accessible compartments.

For this model, the $\mathbf{K}$ matrix is

$$\mathbf{K} = \begin{pmatrix} -0.0502 & 0.0199 & 0 \\ 0.0403 & -0.0652 & 0.0077 \\ 0 & 0.0415 & -0.0077 \end{pmatrix}$$

The mean residence time matrix $\mathbf{\Theta} = -\mathbf{K}^{-1}$ is thus

$$\Theta = \begin{pmatrix} 61.0 & 51.2 & 51.2 \\ 103.5 & 128.9 & 128.9 \\ 559.9 & 697.8 & 828.4 \end{pmatrix}$$

Example: A four compartment model with constraints

In all the previous examples, the tracee steady state system was uniquely solvable since the number N_μ of unknowns was equal to the number n of compartments. In the next example, a different situation will be illustrated. This was discussed in Chapter 6, and illustrates the situation when N_μ is less than the number of compartments; this results in the need for constraints among the parameters.

The data and the model to be described come from a two input-four output study of ketone body, i.e. acetoacetate (ACAC) and β-hydroxybutyrate (β-OHB), metabolism [Cobelli et al., 1982]. On two different occasions, ^{14}C labeled ACAC $(8.067 \cdot 10^7$ dpm) and β-OHB $(8.894 \cdot 10^7$ dpm) were injected. Because the label is rapidly cleared from the body, the complete study took place in the morning thus assuring that the same tracee steady state was present in the two tracer experiments. The order of the labeled compound that was injected was randomize. A typical data set is given in Table 10.4.7. For this experiment, the concentrations of tracee ACAC and β-OHB were 0.060μmole/ml and 0.107 μmole/ml respectively.

The model used to describe the data is shown in Figure 10.4.12. The model depicts ACAC and β-OHB in blood, compartments 1 and 2 respectively, and assumes the existence of two other compartments, liver (compartment 3) and an extrahepatic compartment (compartment 4), where the two ketones interconvert vary rapidly. Production, denoted in the model by U_3, takes place in the liver. Utilization takes place in the extrahepatic tissues as indicated by the loss k_{04}.

The model is a priori uniquely identifiable where the unknown parameters are the rate constants k_{ij} and the volumes of the accessible compartments V_1 and V_2. However, the tracee steady state system provides a constraint among them since the number N_μ of tracee unknowns is 3 (M_3, M_4 and U_3) which is less than the number of compartments in the model, 4.

To derive the constraint, first write the tracee steady state equations:

$$-(k_{31} + k_{41})M_1 + k_{13}M_3 + k_{14}M_4 = 0$$

Table 10.4.7. Time Course of Both Labeled ACAC and β-OHB Measured After the Two Bolus Injections

Time	Tracer 1		Tracer 2	
	$c_1^1(t)$	$c_2^1(t)$	$c_1^2(t)$	$c_2^2(t)$
2	4751		163	
3	4001		757	5011
4	2225	197	990	3800
5	1710	225	920	3411
6	1199	193	895	2110
8	1050	190	642	1333
10	710	180	535	881
12.5	402	152	389	717
15	217	115	275	602
20	169	59	185	251
25	120	42	110	223
30	63		120	199
40	42		70	210
50			69	115
60			62	74

Data are in units of dpm/ml.

$$-(k_{32} + k_{42})M_2 + k_{23}M_3 + k_{24}M_4 = 0 \qquad (10.4.12)$$

$$-(k_{13} + k_{23})M_3 + k_{31}M_1 + k_{32}M_2 + U_3 = 0$$

$$-(k_{14} + k_{24} + k_{04})M_4 + k_{41}M_1 + k_{42}M_2 = 0$$

From the first two equations, one can write

$$\frac{k_{13}}{k_{23}} = \frac{(k_{31} + k_{41})M_1 - k_{14}M_4}{(k_{32} + k_{42})M_2 - k_{24}M_4} \qquad (10.4.13)$$

and from the last equation, one can write:

$$M_4 = \frac{k_{41}M_1 + k_{42}M_2}{k_{14} + k_{24} + k_{04}} \qquad (10.4.14)$$

Substituting (10.4.14) into (10.4.13), and noting that $M_1 = C_1 \cdot V_1$ and $M_2 = C_2 \cdot V_2$, the ratio $\frac{k_{13}}{k_{23}}$ can be written in terms of the unknown parameters and volumes:
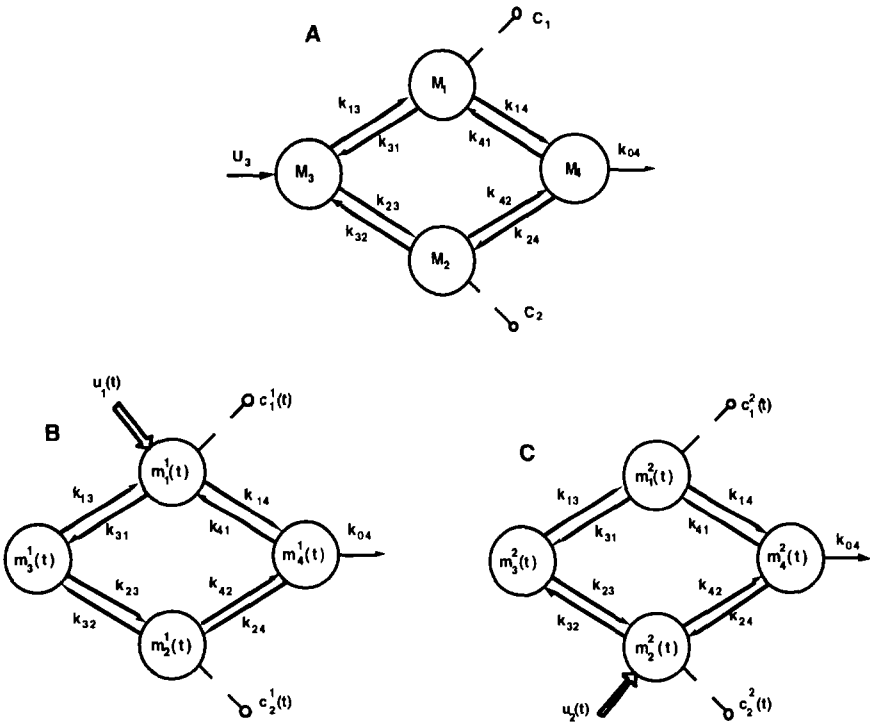
Figure 10.4.12. Models used to describe the data given in Table 10.4.7. A. The tracee model. B. Tracer 1 model with input into compartment 1 and measurements from compartments 1 and 2. C. Tracer 2 model, with input into compartment 2 and measurements from compartments 1 and 2.

$$\frac{k_{13}}{k_{23}} = \frac{C_1 V_1 [k_{31}(k_{14} + k_{24} + k_{04}) + k_{41}(k_{24} + k_{04})] - C_2 V_2 k_{14} k_{42}}{C_2 V_2 [k_{32}(k_{14} + k_{24} + k_{04}) + k_{42}(k_{14} + k_{04})] - C_1 V_1 k_{24} k_{41}}$$

$$(10.4.15)$$

This constraint, which reduces the degrees of freedom by one since k_{13} can be written as a function of the other parameters and measured variables, is to be explicitly considered when fitting the tracer model to the data since it assures a unique solution of the tracee steady state system. The measurement error was assumed to increase linearly with the tracer concentration; the variance was written

$$var(e(t_i)) = 4 y_{obs}(t_i) \qquad (10.4.16)$$

Thus the coefficient of variation ranges from 3% at the higher counts to 28% at the lower. The results are summarized in Table 10.4.8 and Figure 10.4.13.

For this model, the $\mathbf{K}$ matrix is

$$\mathbf{K} = \begin{pmatrix} -0.5772 & 0 & 0.0085 & 0.1168 \\ 0 & -0.2963 & 0.0199 & 0.0176 \\ 0.0173 & 0.0879 & -0.0284 & 0 \\ 0.5600 & 0.2084 & 0 & -0.3797 \end{pmatrix}$$

The mean residence time matrix $\mathbf{\Theta} = -\mathbf{K}^{-1}$ is thus

$$\mathbf{\Theta} = \begin{pmatrix} 1.75 & 0.196 & 0.662 & 5.48 \cdot 10^{-5} \\ .091 & 4.27 & 3.02 & 2.26 \cdot 10^{-5} \\ 1.35 & 13.34 & 44.96 & 0.0001 \\ 0.0003 & 0.0003 & 0.0003 & 0.0003 \end{pmatrix}$$

Besides illustrating some of the theoretical points addressed, this example illustrates two practical points. One is that is a multiple input-multiple output study such as this, it is not necessary that data from each accessible pool be collected at each time point. There are several reasons why this can be the case. Here it is a question of detectability of the tracer. While the experiment ran for 60 minutes, the last sample time for $c_1^1(t)$ was 40 minutes while that for $c_2^1(t)$ was 25 minutes.

The second point is that while the model is compatible with known physiology, there are small portions of the data where the model's description is not entirely adequate. For example, there is a rapid rise in $c_2^2(t)$ that could be better described. However, there is not enough information in the data to support a change in the model structure. In this

Table 10.4.8.

Parameter	Estimate	Parameter	Estimate
k_{04} (min^{-1})	0.245(7)	vol$_1$ (ml/kg bw)	95.1(7)
k_{41} (min^{-1})	0.560(6)	vol$_2$ (ml/kg bw)	118.5(5)
k_{14} (min^{-1})	0.117(9)	M_1 (μmole)	354(7)
k_{13} (min^{-1})	0.0085(21)	M_2 (μmole)	788(5)
k_{31} (min^{-1})	0.017(35)	M_3 (μmole)	10903(18)
k_{32} (min^{-1})	0.088(8)	M_4 (μmole)	954(7)
k_{23} (min^{-1})	0.020(19)	U_3 (μmole/min)	234(3)
k_{24} (min^{-1})	0.018(9)		
k_{42} (min^{-1})	0.209(5)		

Numbers in parentheses are the precision of the parameter estimates expressed as a percent fractional standard deviation.
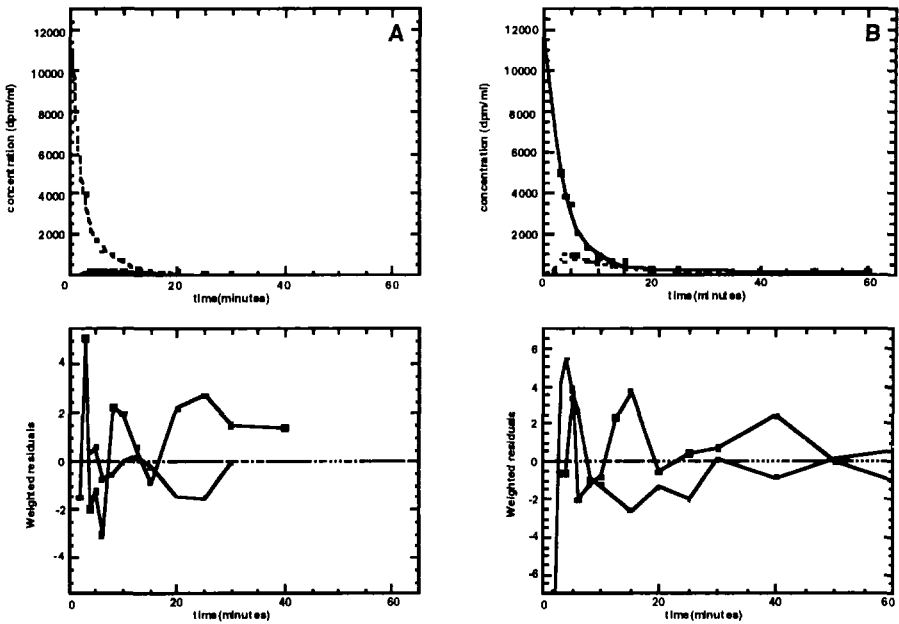
Figure 10.4.13. Plot of the best fit of the model shown in Figure 10.4.9 to the data given in Table 10.4.7. Panel A: Tracer injection into compartment 1. The large squares are the concentration of tracer 1 in compartment 1; small squares are for tracer 1 in compartment 2. Panel B: Tracer injection into compartment 2. The large squares are the tracer to concentration of tracer 2 in compartment 1; small squares are for tracer 2 in compartment 2. See text for additional explanation.

case, the problem goes unresolved until further experiments will yield a richer data set.

References

Bell B.M., Burke J., Shumitzsky A.: A relative weighting method for estimating parameters and variances in multiple data sets. *Comp. Stat. Data Anal. 22:* 119–135, 1996.

Cobelli C., Nosadini R., Toffolo G., McCulloch A., Avogaro A., Tiengo A., Alberti K.G.M.M.: Model of the kinetics of ketone bodies in humans. *Am. J. Physiol. 243:* R7–R17, 1982.

Saccomani M.P., Bonadonna R., Caveggion E., DeFronzo R.A., Cobelli C.: [14C]bicarbonate kinetics in humans: identification and validation of a three-compartment model. *Am. J. Physiol 269*: E183–E192, 1995.

This page intentionally left blank.

Chapter 11

PRECURSOR-PRODUCT MODELS

11.1 INTRODUCTION

A number of investigators use what are termed **precursor-product** models to estimate, for example, the fraction of a precursor that is converted to a product. Some of the commonly used methods will be discussed in this chapter. They will be seen to be special cases either of the two accessible pool noncompartmental model, §11.2, or multicompartmental model, §11.3 and §11.4.

The structure of the general precursor-product model is shown in Figure 11.1.1. In the general precursor-product model shown above, pools 1 and 2 are the accessible precursor and product pools. In the precursor system, this pool can exchange with other pools in the system. Both de novo production and loss can take place from the accessible pool or elsewhere in the system. Similarly for the product system. The box labeled conversion indicates that there may be a number of steps in the conversion of precursor measured in the accessible pool with the product measured in its accessible pool. In addition, losses can occur along with conversion pathways.

In the study of precursor-product systems, one seeks to quantitate characteristics of the conversion of precursor to product by performing a tracer experiment; these are described in the following sections.
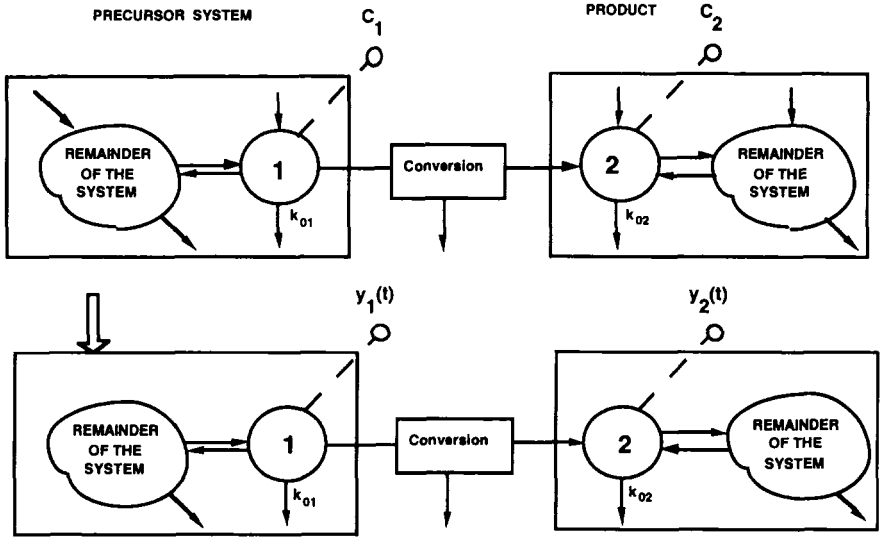
Figure 11.1.1. The general precursor-product model for the tracee (top panel) and tracer (bottom panel). For the tracee system, C_1 and C_2 are respectively the concentration of precursor and product in their respective accessible pools. The tracer input enters the precursor system, and $y_1(t)$ and $y_2(t)$ are the measurement variables, either the tracer to tracee ratio or specific activity, of the precursor and product in their respective accessible pools. The arrows between pools 1 and 2 and the "remainder of the system" describe the exchange processes in this part of the system; the arrows into and out from these respective components represent de novo production and irreversible loss. Tracer labeled precursor is introduced into the system as indicated by the open arrow into the precursor system. Measurements of tracee and tracer are denoted by C_i and $y_i(t)$ respectively.

11.2   ESTIMATING THE FRACTION OF PRODUCT ORIGINATING FROM THE PRECURSOR: THE NONCOMPARTMENTAL MODEL APPROACH

The approach taken to estimate the fraction of product originating from the tracer is usually set in a noncompartmental framework. To do this, one can reformulate the model shown in Figure 11.1.1 in the

noncompartmental model framework of Figures 3.4.3 and 3.4.4. This is shown below in Figure 11.2.1.
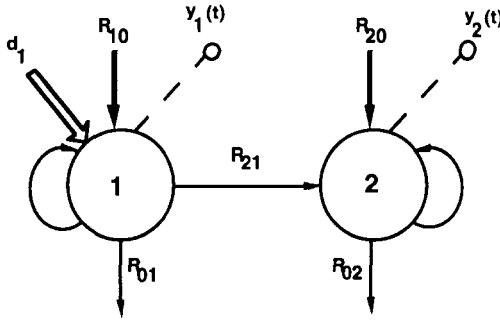
Figure 11.2.1. The noncompartmental representation of the general precursor-product model for the tracee and tracer experiment are superimposed for convenience. A bolus input in the amount of d_1 is injected into the precursor accessible pool at time zero. Sample measurements are $y_1(t)$ and $y_2(t)$ which are either specific activity or tracer to tracee ratios in the two accessible pools. The exchange with the remainder of the system, and inputs and losses from this part of the system, are combined with the recirculation-exchange arrows; this is consistent with the noncompartmental models discussed in Chapter 3. See text for additional explanation.

This figure differs from Figures 3.4.3 and 3.4.4 in that there is a uni-directional movement of material between the two accessible pools. In addition, as indicated in Figure 11.1.1, it is important to remember in this setting that there may be several intermediary steps between pools 1 and 2, i.e. unlike the situation in §11.3 and §11.4, pool 1 need not necessarily be the immediate precursor of pool 2.

What information can be obtained from the one input-two output study? From (3.4.24) since $R_{12} = 0$,

$$\frac{d}{\int_0^\infty y_1(t)dt} = R_{a_1} = R_{10} = R_{01} + R_{21} \qquad (11.2.1)$$

Additionally, from (C.34) and remembering from (3.4.3) that $R_{01} = C_1 v_{01}$, $R_{21} = C_1 v_{21}$, and $R_{02} = C_2 v_{02}$, one has

$$\frac{\int_0^\infty y_2(t)dt}{\int_0^\infty y_1(t)dt} = \frac{R_{21}}{R_{02}} \qquad (11.2.2)$$

Equation (11.2.1) gives the rate of appearance of material into accessible pool 1. Since $R_{02} = R_{20} + R_{21}$ is the total flux of material through pool

2, (11.2.2) gives the fraction of this flux originating from pool 1. This is the parameter which is usually desired from the analysis.

An additional assumption that is sometimes made is that pool 1 is the only precursor of pool 2, i.e. no de novo material can enter pool 2 except from pool 1. This situation is schematized in Figure 11.2.2 where the absence of de novo input into pool two indicates $R_{20} = 0$.

In this situation, $R_{21} = R_{02}$, and from (11.2.2),

$$\int_0^\infty y_1(t)dt = \int_0^\infty y_2(t)dt \qquad (11.2.3)$$

The equality of these two integrals can thus be used to determine if pool 1 is the sole precursor to pool 2.
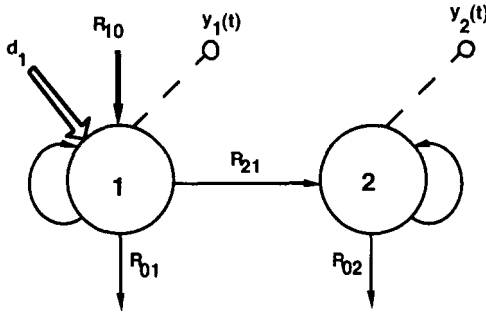
Figure 11.2.2. The model shown in Figure 11.2.1 where it is assumed that pool 1 is the only precursor of pool 2.

11.3   ESTIMATING THE FRACTIONAL SYNTHETIC RATE: THE DERIVATIVE APPROACH

The above formulas have been derived from the formulas of noncompartmental analysis. Another analytic approach that is more closely related to compartmental analysis is available to estimate the **fractional synthetic rate** defined as the rate of incorporation of a precursor into a product per unit time of product mass. A number of techniques have been developed to estimate this parameter from tracer data [Zak et al., 1979]. In this section, a method developed from the so-called derivative approach will be discussed. More details of the method and examples

are given in Foster et al. [1993]. In the next section, a method based on the so-called integral approach will be discussed.

The usual formula to estimate this parameter is given

$$\text{FSR} = \frac{\text{initial rate of change in product tracer to tracee ratio}}{\text{initial precursor tracer to tracee ratio}}$$

(11.3.1)

For the radioactive tracer, the formula is given in terms of specific activity. For the stable isotope tracer, often in this formula, tracer to tracee ratio is replaced by enrichment. As seen in Foster el al. [1993], this is not correct, and can lead to errors in the parameter estimate.

In what follows, the assumptions necessary to derive this formula will be explicitly given, and then the formula will be derived. The particular form of the precursor-product model is given for the tracee and tracer system respectively in Figure 11.3.1.

Notice that this system differs from that shown in Figure 11.1.1; the difference is that the conversion is direct in Figure 11.3.1.

In order to derive (11.3.1), the following assumptions must be made:

1. The tracee system remains in a steady state during the experiment.

2. The accessible precursor pool 1 and the accessible product pool 2 are each described by a single compartment which may interact with a complex network of other compartments.

3. The accessible precursor pool 1 is the immediate precursor to the accessible product pool 2.

4. There is no recirculation of material from the product system back to the precursor system.

Clearly this model is a hybrid noncompartmental and compartmental model. While it is not necessary to postulate a multicompartmental structure for the "remainder of the system" of the precursor or product systems, the accessible pool precursor compartment must immediately precede the accessible pool product compartment. This is clearly different from the models shown in §11.2 where the interconversion between pools 1 and 2 could have any number of intermediary steps.

For the system under study, the mass balance equation is

$$\frac{dm_2(t)}{dt} = k_{21}m_1(t) - k_{02}m_2(t) + f(t)$$

(11.3.2)

where $m_i(t)$ is the tracer mass in compartments 1 and 2. In this expression, $f(t)$ is a term which describes the interactions of compartment 2 with the "remainder" of the product system.
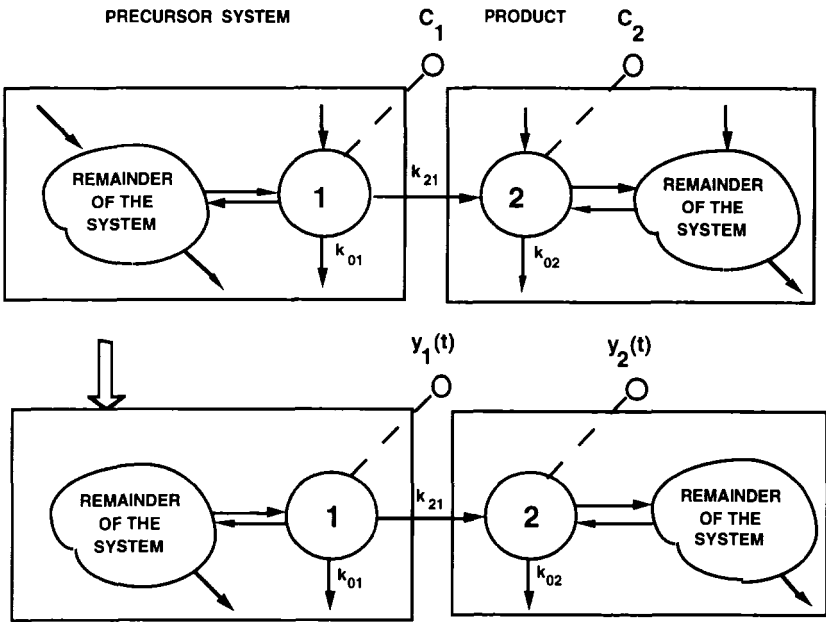
Figure 11.3.1. The precursor-product model for the tracee (top panel) and tracer (bottom panel) assumed in the derivation of the derivative formula. The rate constant quantitating the fraction of precursor converted to product is k_{21} (time^{-1}). The rate constant quantitating the fraction of product lost from pools 1 and 2 are k_{01} (time^{-1}) and k_{02} (time^{-1}) respectively. The tracer system is shown in the bottom panel. Tracer masses at time t are $m_1(t)$ and $m_2(t)$ respectively.

There are two situations to consider. First, assume there is no tracer in the product system at time zero. Then $m_2(0) = f(0) = 0$, and (11.3.2) can be rewritten

$$\frac{dm_2(0)}{dt} = k_{21}m_1(0) \qquad (11.3.3)$$

Writing

$$\dot{m}_2(t) = \frac{dm_2(t)}{dt} \qquad (11.3.4)$$

one can rewrite (11.3.3)

$$k_{21} = \frac{\dot{m}_2(0)}{m_1(0)} \qquad (11.3.5)$$

Notice it is the presence of $m_1(0)$ in the denominator for the expression for k_{21} which requires a protocol calling either for a bolus or primed infusion of tracer directly into pool 1, so that $m_1(0) \neq 0$.

Multiplying (11.3.5) by the ratio of tracee masses $\frac{M_1}{M_2}$, one obtains

$$\text{FSR} = k_{21}\frac{M_1}{M_2} = \frac{\dot{m}_2(0)/M_2}{m_1(0)/M_1} = \frac{\dot{z}_2(0)}{z_1(0)} \qquad (11.3.6)$$

Besides this formula for the FSR, there is a convenient relationship that is worth pointing out. If pool 1 is the sole precursor to pool 2, i.e. $k_{21}M_1$ equals the production rate of pool 2, and if the only loss from the product system is via k_{02}, then the FSR equals the fractional clearance rate FCR of the product. The reason is that in this situation, $k_{21}M_1 = k_{02}M_2$, and k_{02} is the FCR of the product system. This situation is illustrated in Figure 11.3.2.
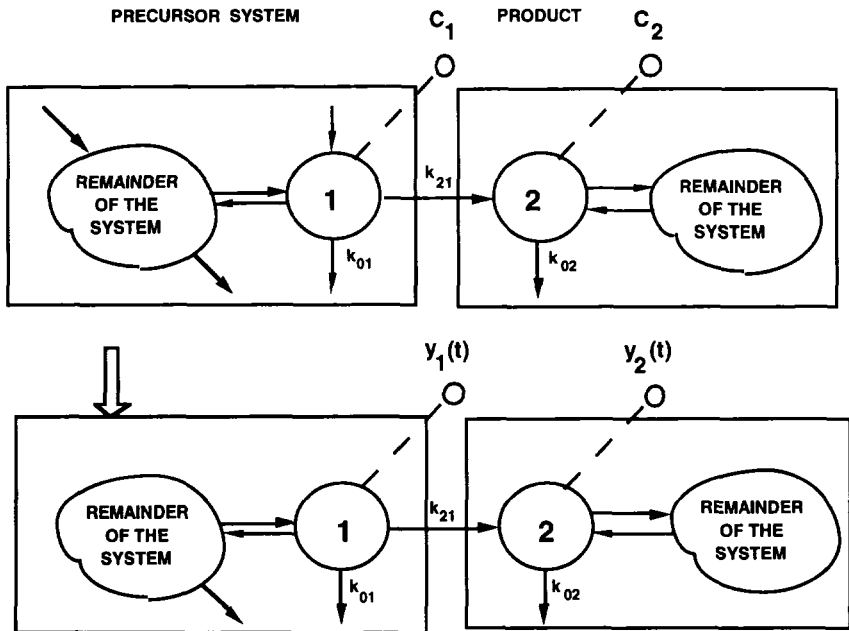
Figure 11.3.2. The model shown in Figure 11.3.1 where it is assumed that pool 1 is the only precursor to pool 2, and the only loss of the product is from pool 2.

Thus

$$\text{FSR} = \frac{k_{21} M_1}{M_2} = k_{02} = \text{FCR} \qquad (11.3.7)$$

There is another situation to consider, and this is the case when the precursor is the only precursor to the product, and the product system consists of a single pool. This is illustrated in Figure 11.3.3. In this case, $f(t)$ in (11.3.2) is zero.
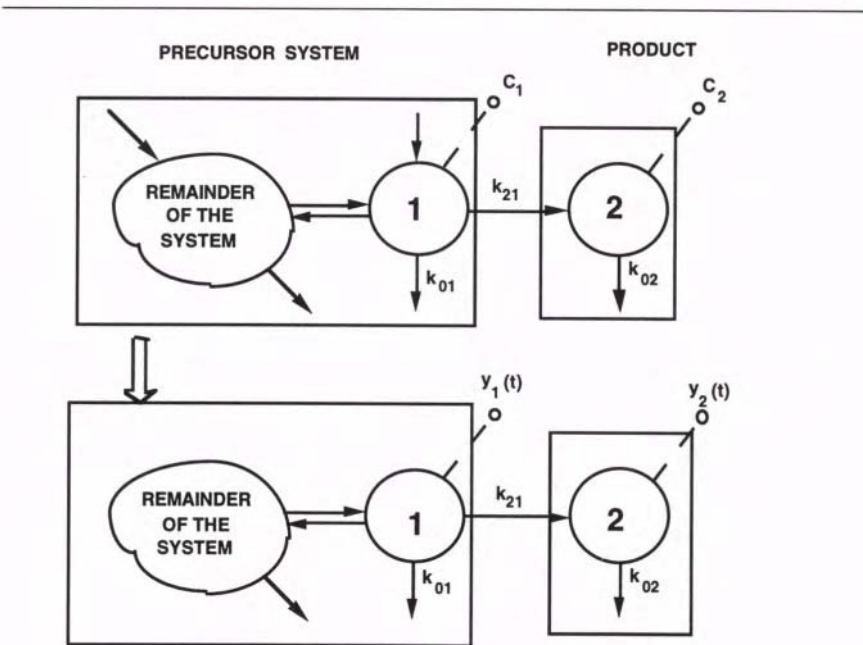
Figure 11.3.3.   The model shown in Figure 11.3.2 where it is assumed that the product system consists of a single pool.

Since $f(t) = 0$, (11.3.2) becomes

$$\frac{dm_2(t)}{dt} = k_{21} m_1(t) - k_{02} m_2(t) \qquad (11.3.8)$$

From the steady state equation for the tracee, $k_{21} M_1 = k_{02} M_2$, and one has

$$k_{21} = \frac{k_{02} M_2}{M_1} \qquad (11.3.9)$$

Substituting (11.3.9) into (11.3.8),

$$\frac{dm_2(t)}{dt} = k_{02} M_2 \frac{m_1(t)}{M_1} - k_{02} m_2(t) \qquad (11.3.10)$$

By dividing both sides of (11.3.10) by M_2, one has

$$\frac{dz_2(t)}{dt} = k_{02}(z_1(t) - z_2(t)) \qquad (11.3.11)$$

Then

$$k_{02} = \frac{\dot{z}_2(t)}{z_1(t) - z_2(t)} = \text{FCR} = \text{FSR} \qquad (11.3.12)$$

since (11.3.8) holds. This expressions permits one to evaluate the FSR at any point in time, not just at time zero.

In summary, for the model shown in Figure 11.3.2, (11.3.6) holds, but it requires that $m_1(0) \neq 0$. Thus the experimental input must either be a bolus or a primed infusion. In addition, if pool 1 is the only precursor to pool 2, and the only loss of product is from pool 2, then $\text{FSR} = \text{FCR}$. On the other hand, if the above holds and, in addition, the product system is a single pool system, then the FSR is given by (11.3.12), and there is no restriction on the tracer input.

Example

To illustrate the application of (11.3.6), consider the data given in Figure 11.3.4. These data, which were collected over a 120 minute period following a primed constant infusion, are expressed in terms of %tracer-tracee ratio; in this simulated study, the product system is a single pool system with a FCR equal to 0.1 min^{-1}. For the precursor, the true zero time value calculated from the priming dose is 10%.

To estimate the FSR using (11.3.6), must must estimate $z_1(0)$, the initial tracer-tracee ratio in the precursor pool, and $\dot{z}_2(0)$. As noted previously, $z_1(0) = 0.1$. An estimate of $\dot{z}_2(0)$ can be obtained by fitting $z_2(t) = A_0 + A_1 e^{-\lambda_1 t} + A_2 e^{-\lambda_2 t}$ to the data, and evaluating the derivative of $z_2(t)$ at time zero.

$$\dot{z}_2(0) = \frac{1}{100}[(-0.63)(-0.93) - (4.37)(-0.074)] = .0091$$

Note in the above the term $\frac{1}{100}$ converts the units to tracer-tracee ratio from %tracer-tracee ratio. Using (11.3.6), the FSR become

$$\text{FSR} = \frac{\dot{z}_2(0)}{z_1(0)} = 0.0091/0.1 = 0.091$$

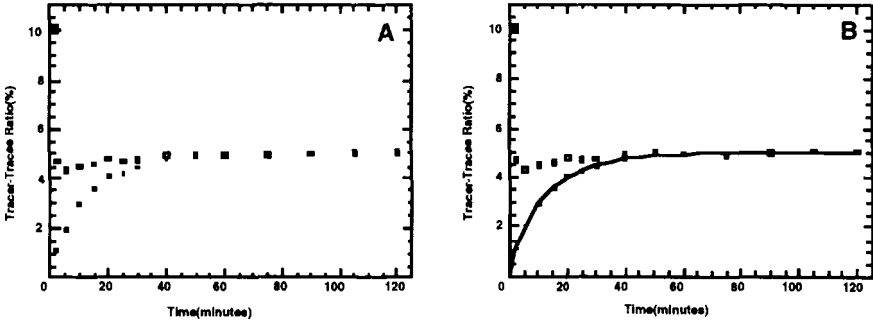| Time	Precursor	Product
2	4.69	1.13
5	4.35	2.00
10	4.47	2.92
15	4.63	3.59
20	4.80	4.09
25	4.68	4.22
30	4.73	4.45
40	4.92	4.76
50	5.02	4.93
60	4.96	4.94
75	4.96	4.93
90	5.01	5.00
105	5.07	5.06
120	5.05	5.08

Figure 11.3.4. Table of data used in the example. Panel A: Plot of the precursor (large squares) and product (small squares) expressed as %tracer-tracee ratio. A zero time value of 10% is calculated as explained in the text. Panel B: The best fit of a sum of two exponentials to the product data. The function is $z_2(t) = 5.00 - 0.63e^{-0.93t} - 4.37e^{-0.074t}$. See text for additional explanation.

This example also illustrates the need for an accurate estimate of $z_1(0)$. Using the data as shown in Figure 11.3.4, one might extrapolate to obtain a zero time value of $z_1(t)$ equal, for example, to 5%. Knowing the priming dose, a more accurate estimate of 10% can be obtained.

11.4   ESTIMATING THE FRACTIONAL SYNTHETIC RATE: THE INTEGRAL APPROACH

A second technique to estimate the FSR can be derived using the so-called integral equation approach. In this section, this method will be discussed. More details of the method and examples are given in Toffolo et al. [1993].

The form of the precursor-product model used in this section is given in Figure 11.4.1. It is important to note the following characteristics of the model which have the assumptions required for the derivation embedded in the structure.

1. The tracee system remains in a steady state during the experiment.

2. The accessible precursor pool 1 is described by a single compartment which may be embedded in a larger system the structure of which does not need to be known.
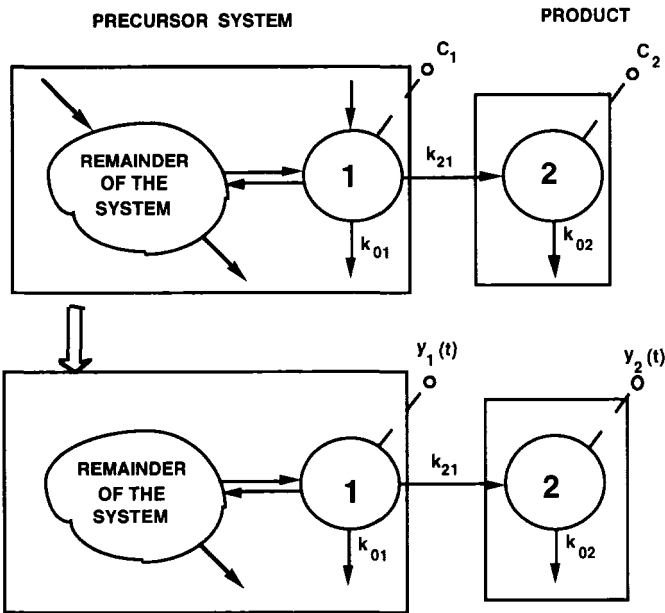
Figure 11.4.1. The precursor-product model for the tracee (top panel) and tracer (bottom panel) assumed in the derivation of the integral equation formula. The product pool 2 is represented by a single, homogeneous pool while the precursor pool 1 is embedded in the precursor system. The precursor pool 1 and product pool 2 are assumed to be accessible for measurement (denoted by the dotted line with the bullet). The rate constant quantitating the fraction of precursor converted to product is k_{21}; the rate constant quantitating the fraction of product lost from the precursor system is k_{01}. The tracer input is the open arrow. Measurements of tracee and tracer are denoted by C_i and $y_i(t)$ respectively.

3. The accessible product pool 2 is described by a single compartment only.

4. The accessible precursor pool 1 is the immediate precursor to the accessible product pool 2.

5. The accessible precursor pool is the sole precursor to the product.

6. There is no recirculation of material from the product system back to the precursor system.

As in §11.3, one has

$$\text{FCR} = k_{02} = \frac{k_{21}M_1}{M_2} = \text{FSR} \qquad (11.4.1)$$

The derivation of the FSR formula starts in the same manner as previously described by writing the mass balance equation

$$\frac{dm_2(t)}{dt} = k_{21}m_1(t) - k_{02}m_2(t) \qquad (11.4.2)$$

The difference between this situation and the mass balance equation (11.3.2) is the absence of the term $f(t)$. For two specific time points t_1 and t_2, (11.4.2) can be solved

$$\int_{t_1}^{t_2} dm_2 = \int_{t_1}^{t_2} [k_{21}m_1(t) - k_{02}m_2(t)dt \qquad (11.4.3)$$

Dividing (11.4.3) by M_2 and using (11.4.1) and the $z(t)$ notation to represent either specific activity in the radioactive case or the tracer-tracee ratio in the stable isotope case,

$$z_2(t_2) - z_2(t_1) = k_{02} \int_{t_1}^{t_2} [z_1(t) - z_2(t)]dt \qquad (11.4.4)$$

Solving this equation for k_{02} and remembering that $k_{02} = \text{FCR} = \text{FSR}$,

$$\text{FSR} = \frac{z_2(t_2) - z_2(t_1)}{\int_{t_1}^{t_2} [z_1(t) - z_2(t)]dt} = \text{FCR} \qquad (11.4.5)$$

To evaluate this expression, one must be able to measure $z_1(t)$ and $z_2(t)$ in the time interval from t_1 to t_2 to evaluate $\int_{t_1}^{t_2} [z_1(t) - z_2(t)]dt$, and measure $z_2(t_2)$ and $z_2(t_1)$. This can sometimes be difficult, and so simplification are sought.

One such simplification arises from the assumption that during the experiment the loss of tracer (but not necessarily tracee) is small. This

means $k_{02}m_2(t) \approx 0$ in (11.2.4), so the mass balance equation (11.4.2) becomes

$$\frac{dm_2(t)}{dt} = k_{21}m_1(t) \tag{11.4.6}$$

Solving this equation

$$m_2(t_2) - m_2(t_1) = \int_{t_1}^{t_2} k_{21}m_1(t)dt \tag{11.4.7}$$

whence

$$k_{21} = \frac{m_2(t_2) - m_2(t_1)}{\int_{t_1}^{t_2} m_1(t)dt} \tag{11.4.8}$$

From the definition of the FSR, one can then derive

$$\text{FSR} = \frac{z_2(t_2) - z_2(t_1)}{\int_{t_1}^{t_2} z_1(t)dt} \tag{11.4.9}$$

While this equation is simpler than (11.4.5), one is still left with the problem of evaluating the integral in the denominator. The most common way to do this is to assume one can measure $z_1(t_1)$ and $z_1(t_2)$, and assume between these points $z_1(t)$ is a straight line. In this case

$$\int_{t_1}^{t_2} z_1(t)dt = \frac{1}{2}(z_1(t_2) + z_1(t_1))(t_2 - t_1) \tag{11.4.10}$$

Thus from (11.4.9), the FSR can be calculated from

$$\text{FSR} = \frac{z_2(t_2) - z_2(t_1)}{\frac{1}{2}(z_1(t_2) + z_1(t_1))(t_2 - t_1)} \tag{11.4.11}$$

The formula can be further simplified by assuming $t_1 = 0$ and $z_2(0) = 0$ in which case (11.4.11) can be written

$$\text{FSR} = \frac{z_2(t_2)}{\frac{1}{2}(z_1(t_2) + z_1(0))(t_2)} \tag{11.4.12}$$

Another simplification as pointed out by Zak et al. [1993] involves assuming the precursor pool $z_1(t)$ in (11.4.9) is constant between t_1 and t_2. Suppose in this interval $z_1(t) = z_1$. Then from (11.4.5)

$$\text{FSR} = \frac{z_2(t_2) - z_2(t_1)}{z_1(t_2 - t_1)} \tag{11.4.13}$$

Example

Using the data from Figure 11.3.4 with $t_1 = 15$ and $t_2 = 25$,

$$\text{FSR} = \frac{0.0422 - 0.0359}{\frac{1}{2}(0.0468 + 0.0463)(25 - 15)} = 0.014$$

Again using the data from Figure 11.3.4 with $t_2 = 15$,

$$\text{FSR} = \frac{0.0359}{\frac{1}{2}15(0.1 + 0.0463)} = 0.033$$

Finally, using the data from Figure 11.3.4 where $t_1 = 50$ and $t_2 = 60$, one can calculate using (11.4.13)

$$\text{FSR} = \frac{0.0494 - 0.0493}{0.05(60 - 50)} = 0.0002$$

while if one chose $t_1 = 10$ and $t_2 = 25$,

$$\text{FSR} = \frac{0.0422 - 0.0292}{0.046(25 - 10)} = 0.019$$

Clearly the selection of time points is crucial, and in neither case does the FSR come close to the true FSR of 0.1.

11.5   ZILVERSMIT'S RULE

Zilversmit et al. [1960] published a relationship between a precursor and a product that became known as Zilversmit's rule. Although often viewed in a noncompartmental setting, to discuss the rule *per se* it is more convenient to use compartmental models, and to extend the notion of specific activity to the tracer-tracee ratio $z(t)$.

To state and derive the rule, one must assume both the precursor and product are kinetically homogeneous pools, i.e. compartments, that the precursor is the sole precursor to the product, and that the precursor transfers material directly to the product (that is, there are no intermediary steps as can be the case with the two accessible pool noncompartmental model). Then Zilversmit's rule states that, if tracer material is injected as a bolus into the precursor pool, the precursor tracer-tracee ratio intersects the product tracer-tracee ratio at the peak. This rule is often invoked in tracer studies when one is trying to identify the source of a product. However, it is a valid rule only under a very specific set of circumstances.

The proof of the relationship follows immediately from (11.3.10) since if t^* is the time at which $\dot{z}_2(t)$ is zero, i.e. the time at which $z_2(t)$ is

maximal, then $z_1(t^*) = z_2(t^*)$. This relationship holds only if all the assumptions related to Figure 11.3.3 are satisfied.

In the broader case, this is no longer true. Suppose one is dealing with an n-compartment system. Then, in the notation of Chapter 4, for compartment i, let $m_i(t)$ and M_i be respectively the tracer and tracee masses whence $z_i(t) = \frac{m_i(t)}{M_i}$. Assuming there is no de novo input into compartment i, from (4.3.11), one can write

$$\frac{dz_i(t)}{dt} = \frac{1}{M_i}\frac{dm_i(t)}{dt} = -z_i(t)\sum_{\substack{j=0 \\ j\neq i}}^{n} k_{ji} + \sum_{\substack{j=1 \\ j\neq i}}^{n} k_{ij}\frac{M_j}{M_i}z_j(t) \qquad (11.5.1)$$

Write

$$k_{ii} = -\sum_{\substack{j=0 \\ j\neq i}}^{n} k_{ji}$$

Let t^* be the time at which $\frac{dz_i(t)}{dt}$ equals zero; this is the time at which the tracer-tracee ratio in the *i-th* compartment is maximal. Prom (11.5.1),

$$z_i(t^*) = -\frac{\sum_{\substack{j=1 \\ j\neq i}}^{n} k_{ij}M_j z_j(t^*)}{M_i k_{ii}} \qquad (11.5.2)$$

Note in these equations that $z_j(t^*)$ is the tracer-tracee ratio of the *j*-th compartment at the time at which the tracer-tracee ratio in the *i-th* compartment is maximal.

One also has from the tracee steady state

$$-k_{ii}M_i = \sum_{\substack{j=1 \\ j\neq i}}^{n} k_{ij}M_j \qquad (11.5.3)$$

that is, the tracee flow into compartment i equals the flow out. Writing

$$\phi_j = -\frac{k_{ij}M_j}{k_{ii}M_i} \qquad (11.5.4)$$

one has from (11.5.2)

$$z_i(t^*) = \sum_{\substack{j=1 \\ j\neq i}}^{n} \phi_j z_j(t^*) \qquad \sum_{\substack{j=1 \\ j\neq i}}^{n} \phi_j = 1 \qquad (11.5.5)$$

Here ϕ_j is the fractional contribution of compartment j to the maximal tracer-tracee ratio in compartment i. That is, (11.5.5) shows that only
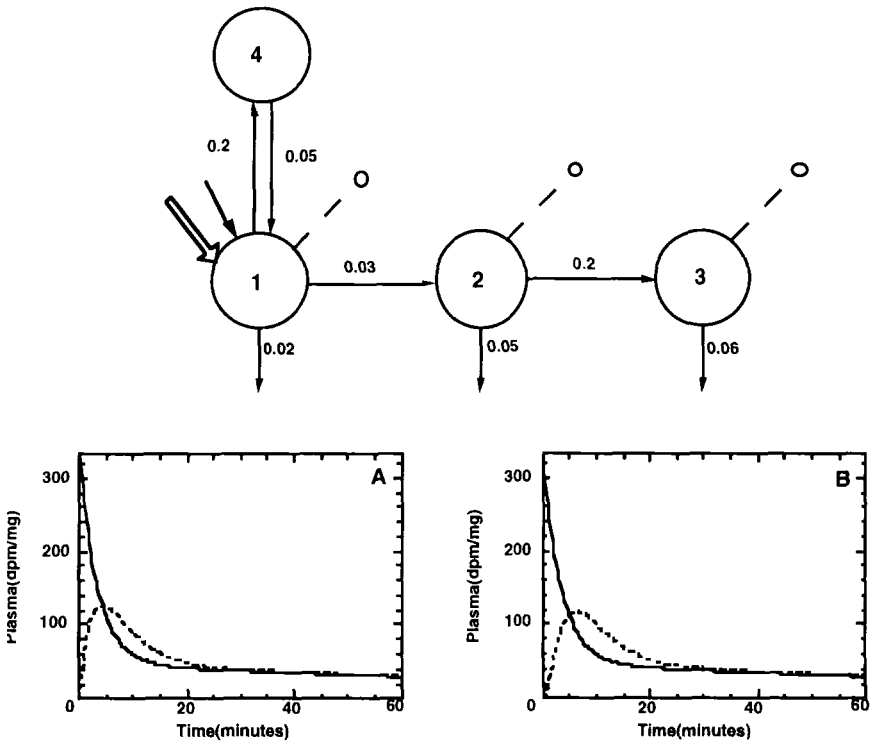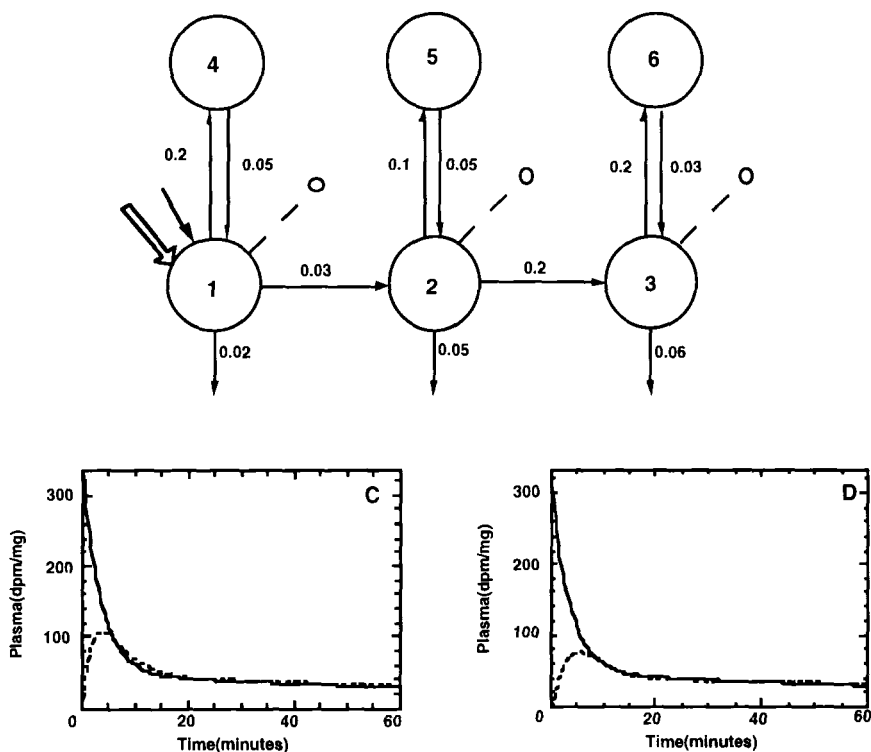
Figure 11.5.1.   Top panel. A multicompartmental model in which the precursor compartment, compartment 1, passes material directly to compartment 2 which in turn passes material directly to compartment 3. Values for the rate constants (min^{-1}) are shown. A bolus of $1 \cdot 10^{8}$dpm was injected into compartment 1. A steady state concentration of 100mg/ml was measured. Plasma samples are simulated in compartments 1, 2 and 3 where a volume of 3000ml is assumed. Data are quantitated in terms of specific activity (tracer-tracee ratio). Figures A and B show the specific activity curves for compartments 1 and 2 (Figure A) and compartments 1 and 3 (Figure B).

Figure 11.5.2. Top panel. A multicompartmental model in which the precursor compartment, compartment 1, passes material directly to compartment 2 which in turn passes material directly to compartment 3. Values for the rate constants (min^{-1}) are shown. A bolus of $1 \cdot 10^8$ dpm was injected into compartment 1. A steady state concentration of 100mg/ml was measured. Plasma samples are simulated in compartments 1, 2 and 3 where a volume of 3000ml is assumed. Data are quantitated in terms of specific activity (tracer-tracee ratio). Figures C and D show the specific activity curves for compartments 1 and 2 (Figure C) and compartments 1 and 3 (Figure D).

in the special situation when compartment j is the sole precursor of compartment i, the tracer-tracee curve intersects the product tracer-tracee curve at its maximum. Clearly it is valid only under very special circumstances.

For instance for Zilversmit's rule to be valid, the precursor pool can have any kinetics, i.e. it can be embedded in a complex system of compartments. However, the product pool must be a single compartment. That is, if the product compartment is embedded in a more complex system where material is exchanging directly, from (11.5.2) it is clear there will be two or more non-zero ϕ_j. Moreover from this equation, it is clear that the precursor must be pass material directly to the product pool. Finally, there can be situations where the precursor curve intersects the product curve at its maximal tracer-tracee ratio but other compartments can contribute material.

Figure 11.5.1 illustrates various situations of precursor-product relationships. In the figure, it is clear that the conditions to apply Zilversmit's rule apply to compartments 1 and 2, and that indeed the tracer-tracee ratio of compartment 1 intersects that of compartment 2 at its maximum. However, this is not the case when examining compartments 1 and 3. The point is that if there are any delays between the precursor and product, Zilversmit's rule does not apply.

What happens when the product pools have more complexity than a single compartment is illustrated in Figure 11.5.2

Here one sees that even though the precursor is the direct and sole precursor to the product compartment 2, because there is an exchange compartment with compartment 2 in that subsystem, Zilversmit's rule is no longer valid. The same is true for compartment 3.

While Zilversmit's rule is commonly used among many researchers, it true value is limited due to the very restrictive set of assumptions which must be made.

References

Foster D.M., Barret P.H.R., Toffolo G., Beltz W.F., Cobelli C.: Estimating the fractional synthetic rate of the plasma apolipoproteins and lipids. *J. Lipid Res., 34*:2193–2205, 1993.

Toffolo G., Foster D.M., Cobelli C.: Estimation of protein fractional synthetic rate from tracer data. *Am. J. Physiol., 264* (*Endocrinol. Metab., 27*), E128–E135, 1993.

Zak R., Martin A.F. , Blough R.: Assessment of protein turnover by use of radioactive tracers. *Physiol. Rev. 59*:407–447, 1979.

Zilversmit D.B.: The design and analysis of isotope experiments. *Am. J. Med. 29*: 832–848, 1960.

Appendix A
Relationships Among Isotopic Variables

The purpose of this Appendix is to show, following [Cobelli and Toffolo, 1990], that during an experiment involving the use of a tracer, if the relative composition of the different species in the tracer input does not change with time, then the same relative composition is maintained among tracer species in the system.

If ω^a, ω^s and ω^r are respectively the relative compositions of species ^{a}, ^{s} and ^{r} in the tracer,

$$\omega^a = \frac{d^a}{d} \qquad \omega^s = \frac{d^s}{d} \qquad \omega^r = \frac{d^r}{d} \tag{A.1}$$

then the assumed condition on the tracer can be written:

$$
\begin{aligned}
u^a(t) &= \omega^a u(t) & 0 \leq \omega^a \leq 1 \\
u^s(t) &= \omega^s u(t) & 0 \leq \omega^s \leq 1 \\
u^r(t) &= \omega^r u(t) & 0 \leq \omega^r \leq 1
\end{aligned}
\tag{A.2}
$$

where

$$\omega^a + \omega^s + \omega^r = 1 \tag{A.3}$$

To prove that the same relative composition is maintained among tracer species in the system, one must show that $m^a(t) = \omega^a m(t)$, $m^s(t) = \omega^s m(t)$, and $m^r(t) = \omega^r m(t)$

Consider first a single pool system, and write the mass balance equation for the tracer mass and its most abundant species:

$$\frac{dm(t)}{dt} = u(t) - f(t) \qquad m(0) = 0 \tag{A.4}$$

$$\frac{dm^a(t)}{dt} = u^a(t) - f^a(t) \qquad m^a(0) = 0 \tag{A.5}$$

The indistinguishability principle for species ^{a} gives

$$\frac{f^a(t)}{m^a(t)} = \frac{f^s(t)}{m^s(t)} = k(t) \tag{A.6}$$

from which

$$\frac{dm(t)}{dt} = u(t) - k(t)m(t) \qquad m(0) = 0 \tag{A.7}$$

$$\frac{dm^a(t)}{dt} = u^a(t) - k(t)m^a(t) \qquad m^a(0) = 0 \tag{A.8}$$

follows.

Multiplying (A.7) by ω^a gives

$$\frac{d(\omega^a m(t))}{dt} = \omega^a u(t) - k(t)\omega^a m(t) \qquad \omega^a m(0) = 0 \tag{A.9}$$

Equations (A.8) and (A.9) are identical since they have the same initial conditions, the same "kinetics", i.e. the same $k(t)$, and the same input $\omega^a u(t) = u^a(t)$. This means they have the same solution

$$m^a(t) = \omega^a m(t) \tag{A.10}$$

From the definition of ω^a, and using (A.10), it follows immediately that

$$\frac{m^a(t)}{m(t)} = \omega^a = \frac{u^a(t)}{u(t)} \tag{A.11}$$

The corresponding equations for the isotopic species ^{s} and ^{r} in the tracer are

$$\frac{m^s(t)}{m(t)} = \omega^s = \frac{u^s(t)}{u(t)} \qquad \frac{m^r(t)}{m(t)} = \omega^r = \frac{u^r(t)}{u(t)} \tag{A.12}$$

From (A.11) and (A.12),

$$\frac{u^a(t)}{m^a(t)} = \frac{u^s(t)}{m^s(t)} = \frac{u^r(t)}{m^r(t)} \tag{A.13}$$

follows.

While these results are valid for the single pool system, it is easy to show they are valid for a generic model provided that (A.2) is valid and that the indistinguishability principle holds for all isotopic species.

References

Cobelli C., Toffolo G.: Constant specific activity allows reconstruction of endogenous glucose concentration in non steady state. *Am. J. Physiol. 258*: E1037–E1040, 1990.

This page intentionally left blank.

Appendix B
The Use of Enrichment in the
Kinetic Formulas

Enrichment is often used in the literature to express stable isotope data. Its definition given in (2.5.9a) is similar to that of specific activity defined in (2.4.5); these formulas are given for convenience below:

$$e_1(t) = \frac{M^s + m^s(t)}{M + m(t)} - \frac{M^s}{M} \tag{B.1}$$

$$sa(t) = \frac{\nu m(t)}{M + m(t)} \tag{B.2}$$

It follows that both measure the abundance of the labelled species above the natural level which is $\frac{M^s}{M}$ for stable isotope tracers and zero for radioactive tracers. Conversely their meaning in terms of tracer and tracee variables is different since only $sa(t)$ is virtually identical to the tracer to tracee ratio $z(t)$.

It is often claimed that $e_1(t)$ is the analogue of specific activity. This has been used to justify analyzing stable isotope data quantitated in these terms by the same techniques used to interpret radioactive data quantitated in terms of specific activity. In this Appendix it will be shown why this approach is not correct.

The plateau formulas

Consider first the case where the tracer is infused at a constant rate, $u(t) = u$, and measurements are confined to the plateau portion of the data. This situation will be discussed in more detail in Chapter 3.

For the radioactive or stable isotope tracer steady state studies where the data are quantified in terms of specific activity or enrichment respectively, the most widely used formulas are

$$F = \frac{u}{sa} \tag{B.3}$$

$$F = u(\frac{e_I}{e_1} - 1) \tag{B.4}$$

from which it is clear that e_1 cannot be used an analogue for sa since the formulas for F in the radioactive and stable isotope tracer situations are different.

One can establish an equivalence between the two through the use of z. From Table 2.5.1, one has

$$\frac{e_I}{e_1} - 1 = \frac{1}{z} \tag{B.5}$$

from which the formula for F for stable isotopes can be given

$$F = \frac{u}{z} \tag{B.6}$$

Equation (B.6) gives the correct expression for F for stable isotope data quantitated in terms of $z(t)$. Since it is essentially the same as the expression for the radioactive tracer (B.3), this illustrates not only the difference between $sa(t)$ and $e_1(t)$, but how $z(t)$ accommodates the difference between the two.

The presence of e_I in (B.4) takes into account the fact that the tracer may not be pure, and $\frac{u \cdot e_I}{e_1}$ gives the total tracer plus tracee flux:

$$u \cdot \frac{e_I}{e_1} = u(\frac{1}{z} + 1) = u\frac{m(t) + M}{m(t)} = u\frac{F + f}{f} = F + f \tag{B.7}$$

Thus the "-1" term in (B.4) permits an estimate of F since $u = f$.

The time-varying tracer formulas

The previous situation deals only with data from the plateau. Suppose now one is dealing with tracer data that vary with time as was done in §2, and express F as a function of e_1. Express the tracer-tracee indistinguishability (2.2.8) in terms of e_1:

$$\frac{f(t)}{F + f(t)} = \frac{m(t)}{M + m(t)} = \frac{\frac{m(t)}{M}}{1 + \frac{m(t)}{M}} = \frac{z(t)}{1 + z(t)} = \frac{e_1(t)}{e_I} \tag{B.8}$$

where the relationship given in Table 2.5.1 has been used. From (B.8), the conservation of mass principle applied to the tracer, e.g. (2.2.17), can be written as

$$d = \int_0^\infty [F + f(t)] \frac{e_1}{e_I} dt = F \int_0^\infty \frac{e_1}{e_I} dt + \int_0^\infty f(t) \frac{e_1}{e_I} dt \qquad \text{(B.9)}$$

and thus

$$F = \frac{d - \int_0^\infty f(t) \frac{e_1(t)}{e_i} dt}{\int_0^\infty \frac{e_1(t)}{e_i} dt} \qquad \text{(B.10)}$$

whence it is clear that F cannot be recovered using this formula since $f(t)$ is not known.

The use of $z(t)$ solves all of these problems since F can be correctly recovered from (2.2.20). The use of e_1 in this equation in place of z, since $e_1(t) < z(t)$, will always overestimate F, the magnitude of which depends upon e_I and $e_1(t)$. The correct expression of F in terms of e_1 can be derived by using (B.5):

$$F = \frac{d}{\int_0^\infty z(t) dt} = \frac{d}{\int_0^\infty \frac{e_1(t)}{e_I - e_1(t)} dt} \qquad \text{(B.11)}$$

From the above, it is evident that since (B.4) is equivalent to (B.6), it assumes that the endogenous system is not perturbed by the introduction of the tracer. Only by modifying this assumption, one can use enrichment instead of z in this equation. Suppose one assumes F and M are no longer constant, but functions of time $F(t)$ and $M(t)$. In addition, assume during the experiment that $F(t) + f(t) = F$ is constant. Then from (B.9),

$$d = \int_0^\infty [F(t) + f(t)] \frac{e_1(t)}{e_I} dt = \int_0^\infty F \frac{e_1(t)}{e_I} dt \qquad \text{(B.12)}$$

whence

$$F(t) + f(t) = F = \frac{d}{\int_0^\infty \frac{e_1(t)}{e_I} dt} = \frac{d \cdot e_I}{\int_0^\infty e_1(t) dt} \qquad \text{(B.13)}$$

In this situation, i.e. if the total (tracer plus tracee) system fluxes are constant during the experiment, e_1 can be used in place of z in (B.6). One has to replace the tracer dose d with its fraction $d \cdot e_I$ associated with the stable isotope species.

Under what conditions can this happen? One experimental situation involves a manipulation which ensures that $U(t)+u(t) = U$. This means one has the ability to manipulate the endogenous flux $U(t)$ in such a way that $U(t)$ decreases to compensate for $u(t)$. Under this circumstance, the total (tracer plus tracee) system sees no perturbation, and $M(t)+m(t) = M$ and $F(t) + f(t) = F$. A similar condition can be obtained by means of a very specific experimental design in which an exogenous input of tracee, denoted $U_{ex}(t)$, is infused at a constant rate until a new steady state, denoted $M + M_{ex}$ where M and M_{ex} are the masses in the single pool system resulting from U and U_{ex}, is reached. The tracer input $u(t)$ then starts. The key is that if one decreases the exogenous tracee input $U_{ex}(t)$ by an amount equal to $u(t)$, the new exogenously induced steady state will not be perturbed by the tracer experiment. Note that the values of U and M used here may not be equal to their baseline values, i.e. the values before the exogenous infusion of tracee.

The other situation is when there is no perturbation on the tracee input, i.e. $U(t) = U = F$, but the system kinetics vary so as to maintain $F(t) + f(t)$ constant. This happens when the system has zero order kinetics, i.e. the fluxes and not the rate constants such as in the case of linear, or first order kinetics, are constant. This condition can be tested on experimental data since it implies that the total (tracer plus tracee) concentration is not perturbed by the experiment.

Appendix C
Relationships Between the Isotope Ratio and Tracer to Tracee Ratio for Multiple Tracer Experiments

Consider an experimental protocol where two different stable isotope tracers are simultaneously injected into the system. Different situations may arise. The two tracers consist of the same substance labeled with different isotopes, and are administered in two different locations. For example, ^{70}Zn can be infused intravenously and ^{67}Zn can be administered orally. The former can be used to describe the kinetics of zinc in plasma while the latter, under the assumption that once ^{67}Zn appears in plasma it has the same kinetics as ^{70}Zn, can be used to describe zinc absorption. Alternatively, two (or more) different substances can be labelled with different isotopes. For example, [l-^{13}C]leucine and [5,5,5-^{2}H]KIC can be used to study the metabolic relationship between leucine and KIC. Finally, the same isotope can be used, but at different positions in the substrate of interest. An example is [l,2-^{13}C2]AcAc and [1,2,3,4-^{13}C$_4$]βOHB

In all of these situations, samples are taken from one or more accessible pools, but in all cases, at least three isotopic species are present in each substance: the most abundant isotopic species again denoted ^{a}, species ^{s} predominating in the first tracer, and species $^{s'}$ which predominates in the second tracer. For example, for the zinc tracers, the accessible pool is plasma zinc, ^{64}Zn is the most abundant species ^{a}, and the isotopes ^{70}Zn and ^{67}Zn are species ^{s} and $^{s'}$ respectively. Similarly for the ketone body example, plasma AcAc and βOHB are the accessible pools. The most abundant species ^{a} consists of AcAc and βOHB molecules having four ^{12}C atoms in positions 1,2,3,4; in species ^{s}, ^{13}C isotopes label positions

1 and 2 while in species s' ^{13}C isotopes label all the four positions 1, 2, 3 and 4 in the AcAc and βOHB molecules.

It should be noted that species different from a, s, and s' will generally be present, e.g. one can have [1-^{13}C]AcAc or [1,2,3-^{13}C3]AcAc. To develop a means by which to analyze these data, assume first that species different from a, s, and s' are negligible; later it will be shown how one can deal with the more general situation.

The notation used in this Appendix is summarized below in Table C.1.

Table C.1. Notation for tracee and tracer variables for a two stable isotope tracer experiment.

Symbol	Definition and Units
M	tracee mass
$M^a, M^s, M^{s'}$	tracee mass of species a, s, and s'
$m(t)$	tracer mass from tracer 1 input
$m^a(t), m^s(t), m^{s'}(t)$	tracer mass of species a, s, and s' from tracer 1 input
$n(t)$	tracer mass from tracer 2 input
$n^a(t), n^s(t), n^{s'}(t)$	tracer mass of species a, s, and s' from tracer 2 input
$u(t)$	rate of tracer 1 input (mass time^{-1})
$u^a(t), u^s(t), u^{s'}(t)$	rate of tracer 1 input (mass time^{-1}) of species a, s, and s'
$w(t)$	rate of tracer 2 input (mass time^{-1})
$w^a(t), w^s(t), w^{s'}(t)$	rate of tracer 2 input (mass time^{-1}) of species a, s, and s'

The purpose of this formalism is to express the tracer to tracee ratios in the accessible pools of the system from isotope ratio measurements in the same pool. A generic expression will be derived since the rationale is the same irrespective of which specific accessible pool is considered. Using the above notation, the isotope ratios r and r' of species s and s', and the most abundant species a are defined

$$r(t) = \frac{M^s + m^s(t) + n^s(t)}{M^a + m^a(t) + n^a(t)} \tag{C.1}$$

$$r'(t) = \frac{M^{s'} + m^{s'}(t) + n^{s'}(t)}{M^a + m^a(t) + n^a(t)} \tag{C.2}$$

Write the naturally occurring isotope ratios r_N and r'_N:

$$r_N = \frac{M^s}{M^a} \tag{C.3}$$

$$r'_N = \frac{M^{s'}}{M^a} \tag{C.4}$$

The isotope ratios of tracer 1 are r_I and r'_I:

$$r_I = \frac{u^s(t)}{u^a(t)} \qquad r'_I = \frac{u^{s'}(t)}{u^a(t)} \tag{C.5}$$

Similarly the isotope ratios of tracer 2 are r_J and r'_J

$$r_J = \frac{w^s(t)}{w^a(t)} \qquad r'_J = \frac{w^{s'}(t)}{w^a(t)} \tag{C.6}$$

The ratio r'_I is small, in many cases negligible compared to r_I since species ^{s} predominates in tracer 1. Similarly, r_J is generally negligible compared with r'_J since tracer 2 consists primarily of species $^{s'}$.

Using the above notation, the tracer to tracee ratios can now be written:

$$z^1(t) = \frac{m(t)}{M} = \frac{m^a(t) + m^s(t) + m^{s'}(t)}{M^a + M^s + M^{s'}} \tag{C.7}$$

$$z^2(t) = \frac{n(t)}{M} = \frac{n^a(t) + n^s(t) + n^{s'}(t)}{M^a + M^s + M^{s'}} \tag{C.8}$$

Expressions for z^1 and z^2 as functions of r and r' can be derived following a line of reasoning similar to that of §2.5.3. To begin, the relationships among the isotopic variables written as

$$\frac{m^s(t)}{m^a(t)} = r_I \qquad \frac{m^{s'}(t)}{m^a(t)} = r'_I \tag{C.9}$$

$$\frac{n^s(t)}{n^a(t)} = r_J \qquad \frac{n^{s'}(t)}{n^a(t)} = r'_J \tag{C.10}$$

permit writing $z^1(t)$ and $z^2(t)$ in terms of the ratios $\frac{m^a(t)}{M^a}$ and $\frac{n^a(t)}{M^a}$:

$$z^1(t) = \frac{m^a(t)}{M^a} \frac{(1 + r_I + r'_I)}{(1 + r_N + r'_N)} \tag{C.11}$$

$$z^2(t) = \frac{n^a(t)}{M^a} \frac{(1 + r_J + r'_J)}{(1 + r_N + r'_N)} \tag{C.12}$$

Using equalities (C.9) and (C.10), $r(t)$ and $r'(t)$ can be expressed in terms of the same ratios:

$$r(t) = \frac{r_N + r_I \frac{m^a(t)}{M^a} + r_J \frac{n^a(t)}{M^a}}{1 + \frac{m^a(t)}{M^a} + \frac{n^a(t)}{M^a}} \tag{C.13}$$

$$r'(t) = \frac{r'_N + r'_I \frac{m^a(t)}{M^a} + r'_J \frac{n^a(t)}{M^a}}{1 + \frac{m^a(t)}{M^a} + \frac{n^a(t)}{M^a}} \tag{C.14}$$

Solving (C.13) and (C.14) for $\frac{m^a(t)}{M^a}$ and $\frac{n^a(t)}{M^a}$, and substituting into (C.11) and (C.12), one obtains

$$
z^1(t) = \frac{[r(t) - r_N][r'_J - r'(t)] - [r'(t) - r'_N][r_J - r(t)]}{[r_I - r(t)][r'_J - r'(t)] - [r'_I - r'(t)][r_J - r(t)]} \\
\cdot \frac{(1 + r_I + r'_I)}{(1 + r_N + r'_N)} \tag{C.15}
$$

$$
z^2(t) = \frac{-[r(t) - r_N][r'_I - r'(t)] + [r'(t) - r'_N][r_I - r(t)]}{[r_I - r(t)][r'_J - r'(t)] - [r'_I - r'(t)][r_J - r(t)]} \\
\cdot \frac{(1 + r_J + r'_J)}{(1 + r_N + r'_N)} \tag{C.16}
$$

The expressions for the tracer to tracee ratios z^1 and z^2 in terms of the other measurement variables, abundance and enrichment, follows directly from their definitions. For instance, extending to the multiple tracer case the definition of isotope abundance (2.5.5), the abundance a and a' of species s and s' are defined as the ratio between the mass of labelled species and the total mass:

$$a(t) = \frac{M^s + m^s(t) + n^s(t)}{M + m(t) + n(t)} = \frac{r(t)}{1 + r(t) + r'(t)} \tag{C.17}$$

$$a'(t) = \frac{M^{s'} + m^{s'}(t) + n^{s'}(t)}{M + m(t) + n(t)} = \frac{r'(t)}{1 + r(t) + r'(t)} \tag{C.18}$$

Similarly, extending the original definition (2.5.9a), the enrichment of species s and s' are respectively given:

$$e(t) = a(t) - a_N = \frac{r(t)}{1 + r(t) + r'(t)} - \frac{r_N}{1 + r_N + r'_N} \tag{C.19}$$

$$e'(t) = a'(t) - a'_N = \frac{r'(t)}{1 + r(t) + r'(t)} - \frac{r'_N}{1 + r_N + r'_N} \tag{C.20}$$

Finally, if species other than a, s and s' are present, the definitions of the isotope ratios r and r', abundance a and a', and enrichments e and e' are the same as before since they refer to species a, s and s' only. The expression of z^1 and z^2 as a function of isotopic species masses, i.e. (C.7)

and (C.8) are different since z^1 and z^2 comprise all isotopic species. If, for instance, an additional species s'' is present in the system, then

$$z^1(t) = \frac{m(t)}{M} = \frac{m^a(t) + m^s(t) + m^{s'}(t) + m^{s''}(t)}{M^a + M^s + M^{s'} + M^{s''}} \qquad \text{(C.21)}$$

$$z^2(t) = \frac{m(t)}{M} = \frac{n^a(t) + n^s(t) + n^{s'}(t) + n^{s''}(t)}{M^a + M^s + M^{s'} + M^{s''}} \qquad \text{(C.22)}$$

where $M^{s''}$, $m^{s''}$ and $n^{s''}$ denote the mass components of the additional species s'' in the tracee and first and second tracer. Expressions for z^1 and z^2 as function of r and r' can be derived following these definitions as

$$
\begin{aligned}
z^1(t) = \ & \frac{[r(t) - r_N][r'_J - r'(t)] - [r'(t) - r'_N][r_J - r(t)]}{[r_I - r(t)][r'_J - r'(t)] - [r'_I - r'(t)][r_J - r(t)]} \quad \text{(C.23)} \\[4pt]
& \cdot \frac{(1 + r_I + r'_I + r''_I)}{(1 + r_N + r'_N + r''_N)}
\end{aligned}
$$

$$
\begin{aligned}
z^2(t) = \ & \frac{-[r(t) - r_N][r'_I - r'(t)] + [r'(t) - r'_N][r_I - r(t)]}{[r_I - r(t)][r'_J - r'(t)] - [r'_I - r'(t)][r_J - r(t)]} \quad \text{(C.24)} \\[4pt]
& \cdot \frac{(1 + r_J + r'_J + r''_J)}{(1 + r_N + r'_N + r''_N)}
\end{aligned}
$$

where r''_N is the natural abundance of species s'', and r''_I and r''_J are the isotopic ratios of species s'' in tracer 1 and 2 respectively.

This page intentionally left blank.

Appendix D
Derivation of Accessible Pool and System Parameter Formulas

In this Appendix, formulas for the noncompartmental parameters given in Tables 3.2.3, 3.2.4, 3.3.3, 3.3.4, 3.4.3 and 3.4.4 are discussed. For the most common ones, either an intuitive justification or a reference will be given. For the others, a formal proof will be given; in some cases, these proofs are original. In giving the derivations, concentrations will be assumed as the measurement variable; the corresponding expressions in terms of the tracer to tracee ratio $z(t)$ easily follow.

Before beginning, the fundamental assumptions will be summarized to remind the reader:

1. The tracer system is linear and time invariant. This is a basic assumption of noncompartmental analysis, and is satisfied if the tracee system is in the steady state and the tracer is an ideal tracer.

2. The tracer experiment starts at time $t = 0$, and there is no tracer in the system prior to the experiment.

3. The system is an open system, i.e. all the tracer will leave the system at some time.

Parameters for the single accessible pool model

Volume of distribution V (Table 3.2.4)

Formulas for this volume can be derived as follows. First, when the tracer is injected as a bolus, its initial mass in the accessible pool is equal to the tracer dose. V is derived by solving the expression for the initial tracer concentration in the accessible pool $c(0)$:

$$c(0) = \frac{m(0)}{V} = \frac{d}{V} \qquad \text{(D.1)}$$

As noted previously, solving for V requires a knowledge of the amount of tracer injected, d, and a measure of $c(0)$.

For the constant infusion experiment, the tracer mass starts from an initial condition equal to zero, and then increases according to the input rate and the system kinetics. At time zero, there is no role of these system kinetics on the tracer since there is no tracer in the system, and the rate at which the tracer mass increases is equal to the input rate. Thus the rate at which the concentration increases is

$$\dot{c}(0) = \frac{u}{V} \qquad \text{(D.2)}$$

from which one can solve for V. While to calculate (D.1) requires a knowledge of d and $c(0)$, in this case, one must have an estimate of $c(t)$ near zero so that $\dot{c}(0)$ can be calculated.

For the primed, constant infusion experiment the reasoning developed for the bolus input applies, and thus V can be estimated by using (D.1).

Finally, the generic tracer input $u(t)$ can be handled using the line of reasoning developed for the constant infusion provided that $u(0) \neq 0$; (D.2) becomes

$$\dot{c}(0) = \frac{u(0)}{V} \qquad \text{(D.3)}$$

Clearance rate CR (Table 3.2.4)

Formulas for the clearance rate are derived from the conservation of mass principle applied to the tracer in the accessible pool. For the bolus injection experiment, the tracer dose equals the total tracer outflow from the accessible pool:

$$d = \int_0^\infty CR \cdot c(t) dt \qquad \text{(D.4)}$$

where the total tracer outflow has been evaluated as the integral to infinity of the time course of the tracer disappearance flux. This integral is finite because the system is an open system and hence the tracer concentration $c(t)$ decreases towards zero. Since CR is constant, it can be taken outside of the integral sign, and (D.4) can then be solved for CR.

A similar formula holds for the generic input case $u(t)$ where again total tracer input equals total tracer output:

$$\int_0^\infty u(t)dt = \int_0^\infty CR \cdot c(t)dt \tag{D.5}$$

The only assumption made here is that the total tracer dose is finite hence $\int_0^\infty u(t)dt$ is finite.

For either the constant or primed, constant infusion, when a plateau is achieved, a balance exists between tracer input and output:

$$u = CR \cdot c \tag{D.6}$$

Equation (D.6) can easily be solved for CR. In the event a plateau value c is not reached, it will have to be estimated in order to estimate CR.

Tracee mass M (Table 3.2.3)

To estimate M, the same considerations given for V apply; the only difference is that the measured variable is not the tracer concentration, i.e. the ratio between tracer mass and volume, but the ratio between tracer and tracee mass. For example, the counterpart to (D.1) becomes:

$$z(0) = \frac{m(0)}{M} = \frac{d}{M} \tag{D.7}$$

Clearly M can be determined knowing d and $z(0)$. Similar modifications hold for the constant infusion, primed, constant infusion, and generic input.

Rate of appearance R_a (Table 3.2.3)

The derivation of the formula for R_a given in Table 3.2.3 parallels that given for CR. The only difference is that the measured variable is not tracer concentration but the tracer to tracee ratio. The counterpart of (D.4) is

$$d = \int_0^\infty R_d z(t)dt = \int_o^\infty R_a z(t)dt \tag{D.8}$$

from which $R_d = R_a$ can be expressed as the quotient of d and $\int_0^\infty z(t)dt$ Similar modifications hold for the other tracer input formats.

Some remarks on the relationships among the formulas

As is evident from the previous discussion, different mathematical formulas apply for one specific parameter; which form to use depends upon the tracer input format. However, these formulas can be put into a unitary framework since the responses of a linear, time-invariant system to different input profiles are not independent, and simple relationships exist among them.

The key role is played by the impulse response $h(t)$, i.e. the tracer curve (either concentration or the tracer to tracee ratio) when a unit dose of tracer is injected at time zero. The tracer curve $y(t)$ measured after an arbitrary tracer input $u(t)$, starting at time $t = 0$, is related to $h(t)$ through the convolution integral

$$y(t) = \int_0^\infty h(\tau)u(t - \tau)d\tau \tag{D.9}$$

From (D.9), one can predict from $h(t)$ the tracer curve in the accessible pool $y(t)$ after different tracer inputs $u(t)$; these are summarized in Table D.1.

Table D.1.   Input-Output Relationships

Input	Output $(c(t)$ or $z(t))$
Unit bolus injection	$h(t)$
Bolus injection d	$d \cdot h(t)$
Unit constant infusion	$\int_0^t h(\tau)d\tau$
Constant infusion u	$u \cdot \int_0^t h(\tau)d\tau$
Primed infusion d, u	$d \cdot h(t) + u \cdot \int_0^t h(\tau)d\tau$
Generic input $u(t)$	$\int_0^\infty h(\tau)u(t - \tau)d\tau$

As an example, illustrated in Figure D.1, the tracer concentration curve in the accessible pool during a primed constant infusion results from the superposition of the tracer concentration curves measured during a bolus injection and a constant infusion experiment, the latter being proportional to the integral of the former.

The relationships given in Table D.1 can be used to link the different expressions for the parameters related to the different formats of tracer administration. Consider as an example the formulas for the clearance rate, *CR*. To derive an expression for *CR* in terms of $h(t)$, the tracer concentration curve after a unit bolus injection of tracer, one has from (D.4) (since $d = 1$)

$$CR = \frac{1}{\int_0^\infty h(t)dt} \tag{D.10}$$
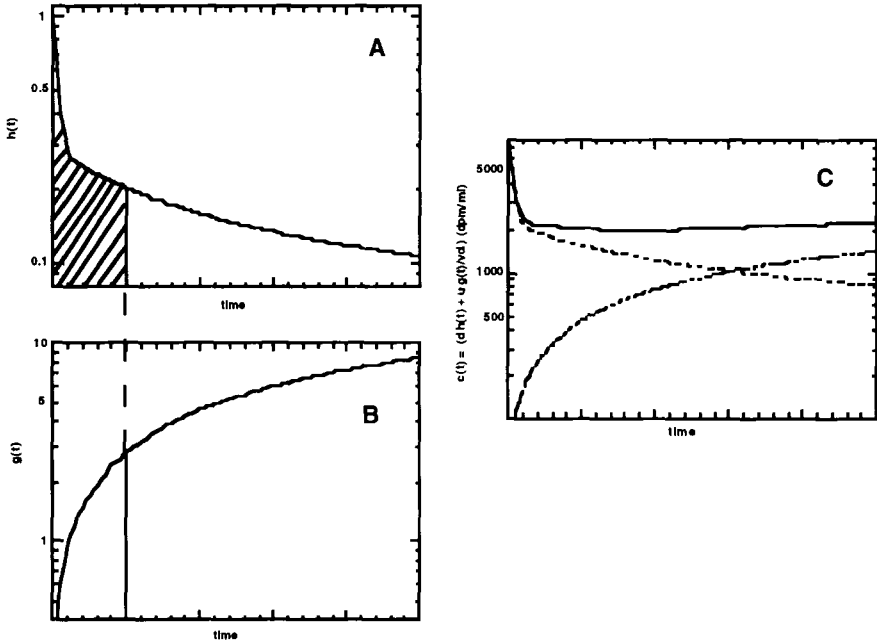
Figure D.1 A. The response of a system $h(t)$ to a unit bolus input. B. The response of the system, $g(t)$, to a unit constant infusion is the integral of $h(t)$. For a given time t_0, indicated in the Figure by the dashed line, this means $g(t_0) = \int_0^{t_0} h(\tau)d\tau$. C. The response of the system, $c(t)$, to a primed, constant infusion where the priming dose d is $2 \cdot 10^7$dpm and the constant infusion u is $440,000$dpm/min. The response $c(t)$ can be written $c(t) = (d \cdot h(t) + u \cdot g(t))/vol$ where $vol = 2600$ml is the volume of the accessible pool. The individual contribution to $c(t)$ of the bolus injection (dashed line) and infusion (dotted line) are shown.

Consider now a constant infusion of tracer. From Table D.1, the tracer concentration at time t is proportional to the integral up to time t of the impulse response. Since the plateau value c is reached at time equal to infinity, it will be proportional to the integral of $h(t)$ to infinity:

$$c = \lim_{t \to \infty} c(t) = \lim_{t \to \infty} u \int_0^t h(t)dt = u \int_0^\infty h(t)dt \qquad \text{(D.11)}$$

Equation (D.11) becomes

$$CR = \frac{1}{c/u} = \frac{u}{c} \tag{D.12}$$

When the tracer input has a generic input profile $u(t)$, the resulting tracer concentration curve $c(t)$ still permits one to calculate the integral in the denominator of (D.10). From Table D.1:

$$
\begin{aligned}
\int_0^\infty c(t)dt &= \int_0^\infty \left[\int_0^\infty h(\tau)u(t-\tau)d\tau \right] dt \tag{D.13}\\
&= \int_0^\infty h(\tau) \left[\int_0^\infty u(t-\tau)dt \right] d\tau
\end{aligned}
$$

By means of a change in the variable $w = t - \tau$, it is possible to simplify the double integrals given in (D.13)

$$
\begin{aligned}
\int_0^\infty c(t)dt &= \int_0^\infty h(\tau) \left[\int_{-\tau}^\infty u(w)dw \right] d\tau \tag{D.14}\\
&= \int_0^\infty h(\tau)d\tau \int_0^\infty u(w)dw
\end{aligned}
$$

The lower limit in the integral, $-\tau$ can be replaced by zero since the integrand is zero for all negative values of the independent variable. Finally, substituting t for τ and w in (D.14), one can write

$$\int_0^\infty h(t)dt = \frac{\int_0^\infty c(t)dt}{\int_0^\infty u(t)dt} \tag{D.15}$$

Replacing the integral of $h(t)$ in (D.10) with the right hand side of (D.15) results in an expressions for CR as a function of tracer concentration data measured after a generic tracer input.

<u>Mean Residence Time MRT^{NC} (Tables 3.3.3 and 3.3.4)</u>

The formula for the mean residence time in terms of tracer concentration data measured after a bolus injection of tracer is a very common one; its proof is not trivial but can be found, e.g. in Rescigno and Gurpide [1973]. On the other hand, expressions for MRT^{NC} following a constant, primed or generic input of tracer have not been treated extensively in the literature. Their proofs will be given below in terms of the expression of MRT^{NC} for the unit impulse response:

$$MRT^{NC} = \frac{\int_0^\infty t \cdot h(t)dt}{\int_0^\infty h(t)dt} \tag{D.16}$$

and the relationships listed in Table D.1.

Consider first the constant infusion experiment where $c(t) = u \cdot \int_0^t h(\tau) \, d\tau$. The integral in the numerator of (D.16) can be written

$$\int_0^\infty th(t)dt \; = \; \int_0^\infty \left[\int_0^t d\tau \right] h(t)dt \qquad (D.17)$$

$$= \; \int_0^\infty \int_0^t h(t)d\tau dt$$

$$= \; \int_0^\infty \int_\tau^\infty h(t)dt d\tau$$

$$= \; \int_0^\infty \left[\int_0^\infty h(t)dt - \int_0^\tau h(t)dt \right] d\tau$$

$$= \; \int_0^\infty [c - c(\tau)]d\tau$$

Finally, substituting t for τ in (D.17) one can write

$$\int_0^\infty th(t)dt = \int_0^\infty [c - c(t)]dt \qquad (D.18)$$

The integral in the denominator of (D.16) is equal to the plateau value normalized to the dose u (as given by (D.11)), and hence

$$MRT^{NC} = \frac{\frac{1}{u}\int_0^\infty [c - c(t)]dt}{\frac{1}{u}c} = \frac{\int_0^\infty [c - c(t)]dt}{c} \qquad (D.19)$$

Consider next the primed infusion experiment where $c(t) = d \cdot h(t) + u \int_0^t h(\tau)d\tau$. Defining

$$g(t) = \int_0^t h(\tau)d\tau \qquad (D.20)$$

one has

$$c(t) = d \cdot \dot{g}(t) + u \cdot g(t) \qquad (D.21)$$

Equation (D.21) is a linear, first order differential equation whose initial conditions are zero, i.e. $g(0) = 0$. The solution is given by

$$g(t) = \frac{1}{d} \int_0^t c(t - \tau)e^{-\frac{u}{d}\tau}d\tau \qquad (D.22)$$

Equation (D.22) links the tracer concentration during the primed infusion experiment $c(t)$ to the tracer concentration $g(t)$ as measured during a unit constant infusion. In this latter case, (D.19) gives the MRT^{NC} as

$$MRT^{NC} = \frac{\int_0^\infty [g - g(t)]dt}{g} \tag{D.23}$$

where g indicates the plateau value. By making use of (D.22) and of the relationship between the plateau values of concentrations, $g = \frac{1}{u}c$, MRT^{NC} can be expressed as a function of the tracer concentration during a primed constant infusion experiment:

$$MRT^{NC} = \frac{\int_0^\infty [c - \frac{u}{d}\int_0^t c(t-\tau)e^{-\frac{u}{d}\tau}d\tau]dt}{d} \tag{D.24}$$

For the proof of the expression for MRT^{NC} in terms of tracer concentration data $c(t)$ following a generic input of tracer $u(t)$, one first uses the convolution integral to calculate

$$\int_0^\infty t \cdot c(t)dt = \int_0^\infty t \left[\int_0^\infty h(\tau)u(t-\tau)d\tau\right]dt \tag{D.25}$$
$$= \int_0^\infty h(\tau)\left[\int_0^\infty tu(t-\tau)dt\right]d\tau$$

Writing $w = t - \tau$, and recalling that $u(t)$ is zero for $t < 0$, one has

$$\int_0^\infty t \cdot c(t)dt = \int_0^\infty h(\tau)\left[\int_{-\tau}^\infty (w+\tau)u(w)dw\right]d\tau$$
$$= \int_0^\infty h(\tau)\left[\int_0^\infty w \cdot u(w)dw\right]d\tau + \int_0^\infty \tau h(\tau)\left[\int_0^\infty u(w)dw\right]d\tau$$
$$= \int_0^\infty h(\tau)d\tau\int_0^\infty w \cdot u(w)dw + \int_0^\infty \tau h(\tau)d\tau \cdot \int_0^\infty u(w)dw \tag{D.26}$$

Substituting t for w and τ in the last expression above,

$$\int_0^\infty t \cdot c(t)dt = \int_0^\infty h(t)dt \cdot \int_0^\infty t \cdot u(t)dt + \int_0^\infty t \cdot h(t)dt \cdot \int_0^\infty u(t)dt \tag{D.27}$$

Equation (D.27) permits one to express the numerator of (D.16) as a function of the $c(t)$ measurements:

$$\int_0^\infty t \cdot h(t)dt = \frac{\int_0^\infty t \cdot c(t)dt}{\int_0^\infty u(t)dt} - \int_0^\infty h(t)dt \cdot \frac{\int_0^\infty t \cdot u(t)dt}{\int_0^\infty u(t)dt} \tag{D.28}$$

An expression for the denominator has already been given in (D.15). By dividing (D.28) and (D.15), then, the formula for MRT^{NC} is obtained.

Finally, in §4.3, an expression for MRT^{NC} is given for measurements taken from the plateau value and washout phase. Let T be the time at which, after a plateau has been reached, the tracer input is stopped. This input format can be viewed as the sum of two components, a constant infusion u, resulting in the plateau value c, minus a negative constant infusion having the same magnitude u but starting from time T. The tracer concentration for $t > T$, starting from the plateau value c, is:

$$c(t) = c - u \cdot g(t - T) = u[g - g(t - T)] \tag{D.29}$$

where as before $g(t)$ is the response to a unit tracer infusion, (D.20); $c = u \cdot g$ is the plateau value, and $-u \cdot g(t - T)$ is the response to the step decrease to zero of the input.

Consider now (D.23) giving MRT^{NC} as a function of $g(t)$. By multiplying the numerator and denominator by u, and using (D.29), one has

$$MRT^{NC} = \frac{\int_0^\infty u[g - g(t)]dt}{u \cdot g} = \frac{\int_0^\infty c(t + T)dt}{c} = \frac{\int_T^\infty c(t)dt}{c} \tag{D.30}$$

The formulas for the MRT^{NC} in terms of the tracer to tracee ratio $z(t)$ could be developed by following the same arguments as before since the basic ingredients, i.e. an expression parallel to (D.16) in terms of $h(t)$ and the results in Table D.1 hold when the measured variables are either tracer concentration or the tracer to tracee ratios. As an alternative, the equivalent role played by $c(t)$ and $z(t)$ in the MRT^{NC} formulas can be verified by noting that there is a proportionality constant between the two variables:

$$z(t) = \frac{c(t) \cdot V}{M} = \frac{c(t)}{C} \tag{D.31}$$

where C is the constant value of tracee concentration. Since in all MRT^{NC} formulas $c(t)$ appears in both the numerator and denominator, it can be divided by C to give $z(t)$ as exemplified below for (D.18):

$$MRT^{NC} = \frac{\int_0^\infty [c - c(t)]dt}{c} = \frac{\int_0^\infty [\frac{c - c(t)}{C}]dt}{\frac{c}{C}} = \frac{\int_0^\infty [z - z(t)]dt}{z} \tag{D.32}$$

Parameters for the two accessible pool model (Tables 3.4.3 and 3.4.4)

Formulas for the tracer fluxes v_{01} and v_{02} can be derived by solving a set of two linear equations in two unknowns:

$$d_1 = v_{01} \int_0^\infty c_1^1(t)dt + v_{02} \int_0^\infty c_2^1(t)dt \tag{D.33}$$

$$d_2 = v_{01} \int_0^\infty c_1^2(t)dt + v_{02} \int_0^\infty c_2^2(t)dt \tag{D.34}$$

Equations (D.33) and (D.34) represent the extension of (D.4) to the two accessible pool configuration, since they express the conservation of mass principle applied to tracers injected into pool 1 and 2, e.g. (D.33) equals the tracer dose injected into pool 1 to its total outflow from the accessible pools.

In order to obtain expressions for v_{12} and v_{21}, the following equations are solved:

$$v_{21} \int_0^\infty c_1^1(t)dt = (v_{02} + v_{12}) \int_0^\infty c_2^1(t)dt \tag{D.35}$$

$$v_{12} \int_0^\infty c_2^2(t)dt = (v_{01} + v_{21}) \int_0^\infty c_1^2(t)dt \tag{D.36}$$

They still express the conservation of mass principle, e.g. (D.35) refers to the tracer injected into pool 1, and expresses the balance between the total tracer fluxes entering and leaving pool 2. Once v_{01} and v_{02} are known, they can be solved in v_{21} and v_{12}.

References

Rescigno A., Gurpide E.: Estimation of average times of residence, recycle, and interconversion of blood-borne compounds using tracer methods. *J. Clin. Endocrinol. Metab. 36*:263–276, 1973.

Appendix E
Derivation of the
Exhaustive Summary

Obtain first an expression for $\frac{dm_1(t)}{dt}$ and $\frac{dm_2(t)}{dt}$ as a function of $e^{-\lambda_1 t}$ and $e^{-\lambda_2 t}$. From (5.4.3) - (5.4.6), one has for $m_1(t)$ and $m_2(t)$

$$m_1(t) = V_1 c_1(t) = V_1(A_1 e^{-\lambda_1 t} + A_2 e^{-\lambda_2 t}) \qquad (E.1)$$

$$m_2(t) = V_2 c_2(t) = V_2(-A_3 e^{-\lambda_1 t} + A_3 e^{-\lambda_2 t}) \qquad (E.2)$$

and thus their derivatives are given by

$$\frac{dm_1(t)}{dt} = V_1(-A_1 \lambda_1 e^{-\lambda_1 t} - A_2 \lambda_2 e^{-\lambda_2 t}) \qquad m_1(0) = d_1 \qquad (E.3)$$

$$\frac{dm_2(t)}{dt} = V_2(A_3 \lambda_1 e^{-\lambda_1 t} - A_3 \lambda_2 e^{-\lambda_2 t}) \qquad m_2(0) = 0 \qquad (E.4)$$

However, $\frac{dm_1(t)}{dt}$ and $\frac{dm_2(t)}{dt}$ have also been defined by (5.4.1) and (5.4.2). In each of these equations, $m_1(t)$ and $m_2(t)$ appear, and (E.1) and (E.2) give an expression for each of these as a sum of two exponentials. Substituting these sums of exponentials into (5.4.1) and (5.4.2), one obtains:

$$\begin{aligned} \frac{dm_1(t)}{dt} &= k_{11} V_1(A_1 e^{-\lambda_1 t} + A_2 e^{-\lambda_2 t}) \\ &+ k_{12} V_2(-A_3 e^{-\lambda_1 t} + A_3 e^{-\lambda_2 t}) \\ &\qquad m_1(0) = V_1(A_1 + A_2) \end{aligned} \qquad (E.5)$$

379

$$\frac{dm_2(t)}{dt} = k_{21}V_1(A_1e^{-\lambda_1 t} + A_2e^{-\lambda_2 t}) \tag{E.6}$$
$$+ k_{22}V_2(-A_3e^{-\lambda_1 t} + A_3e^{-\lambda_2})$$
$$m_2(0) = 0$$

where

$$k_{11} = -(k_{01} + k_{21}) \tag{E.7}$$
$$k_{22} = -(k_{02} + k_{12}) \tag{E.8}$$

Rewriting these equations in terms of $e^{-\lambda_1 t}$ and $e^{-\lambda_2 t}$

$$\frac{dm_1(t)}{dt} = (k_{11}V_1A_1 - k_{12}A_3V_2)e^{-\lambda_1 t} \tag{E.9}$$
$$+ (k_{11}V_1A_2 + k_{12}A_3V_2)e^{-\lambda_2 t}$$
$$m_1(0) = V_1(A_1 + A_2)$$

$$\frac{dm_2(t)}{dt} = (k_{21}A_1V_1 - k_{22}V_2A_3)e^{-\lambda_1 t} \tag{E.10}$$
$$+ (k_{21}A_2V_1 + k_{22}V_2A_3)e^{-\lambda_2 t}$$
$$m_2(0) = 0$$

(E.3) and (E.4) and (E.9) and (E.10) are both expressions for the derivative of $m_1(t)$ and $m_2(t)$ respectively, and hence must be equal. This means the four coefficients of $e^{-\lambda_1 t}$ and $e^{-\lambda_2 t}$ respectively must be equal. By equating these coefficients, one obtains the four relations among the observational parameters and the unknown model parameters given by (5.4.14)–(5.4.17). The fifth relation, (5.4.18), can be obtained by equating the initial conditions for $m_1(0)$.

Table F.1. Measurements and numbers of solutions (in brackets) for nonuniquely identifiable cases

Loss from cpt =>	1	2	3	1,2	1,3	2,3	1,2,3
Model Structure							
1		2(2)	a		a		
2	2(2);3(2)	3(2)	3(2)	2,3(2)	3(6);1,3(2)	3(6);1,3(2)	2,3(2)
3					3(3)	3(3)	
4	3(2)	3(2)	3(2)	2,3(2)	3(6);1,3(2)	3(6);1,3(2)	2,3(2)
5	2,3(2)				2,3(2)		
6	1(2);3(6)	1(2);3(6)	1(2);3(4)	2(2)	2(2);1,3(2)	1,3(2)	2,3(2)
7	2(2)	3(6);1,3(2)	3(3)	2(3)	2(3)		2,3(3)
8	2,3(2)						
9	1(2);2(3);3(3)	1(2);2(2);3(3)	a		a		
10	1(2);2(6);3(3)	1(2);2(4);3(4)	1(2);2(6);3(2)	1,2(2)	2,3(2)	1,2(2)	2,3(2)
11		2(3);3(6);1,3(2)	a		a		2,3(3)
12	1(2);2(2);2,3(2)	1(2)	1(2)		1,3(2);2,3(2)	1,3(2)	
13	2(3)				2,3(3)		
14	2(3)	1,3(2)		2,3(3)			
15	2,3(2)		1,2(2)		1,3(2);2,3(2)	1,3(2)	
16			1,2(2)		2,3(3)		
17	2,3(3)	1,3(2)					
18	2,3(3)	1,3(2)	a		a		

[a] Covered by preceding case by symmetry: reverse 2 and 3

Table F.2.   Number of solutions for each nonuniquely identifiable rate constant[b]

Model Structure	Loss from Compartments	Measured Compartments	Number of Solutions: Rate Constants With This Number
1	2	2	2: k_{02}, k_{31}
2	1	2	2: k_{01}, k_{32}
		3	2: k_{01}, k_{21}, k_{32}
	2	3	2: k_{21}, k_{02}, k_{32}
	3	3	2: k_{21}, k_{32}
	1,2	2,3	2: k_{01}, k_{02}
	1,3	3	6: k_{01}; 3: k_{21}, k_{32}, k_{03}
		1,3	2: $k_{01}, k_{21}, k_{32}, k_{03}$
	2,3	3	6: k_{02}; 3: k_{21}, k_{32}, k_{03}
		1,3	2: k_{02}, k_{32}, k_{03}
	1,2,3	2,3	2: k_{01}, k_{02}
3	1,3	3	3: k_{01}, k_{21}, k_{03}
	2,3	3	3: $k_{21}, k_{02}, k_{12}, k_{03}$
4	1	3	2: k_{01}, k_{21}, k_{32}
	2	3	2: k_{21}, k_{02}, k_{32}
	3	3	2: k_{21}, k_{32}
	1,2	2,3	2: k_{01}, k_{02}, k_{32}
	1,3	3	6: k_{01}; 3: k_{21}, k_{32}, k_{03}
		1,3	2: $k_{01}, k_{21}, k_{32}, k_{03}$
	2,3	3	6: k_{02}, k_{32}; 3: k_{21}, k_{03}
		1,3	2: k_{02}, k_{32}, k_{03}
	1,2,3	2,3	2: k_{01}, k_{02}, k_{32}
5	1	2,3	2: k_{01}, k_{12}
	1,3	2,3	2: k_{01}, k_{12}
6	1	1	2: k_{32}, k_{13}
		3	6: k_{01}, k_{21}, k_{32}; 3: k_{13}
	2	1	2: k_{02}, k_{32}, k_{13}
		3	6: k_{21}, k_{02}, k_{32}; 3: k_{13}
	3	1	2: k_{32}, k_{03}, k_{13}
		3	4: k_{21}, k_{32}; 2: k_{13}
	1,2	2	2: k_{01}, k_{02}, k_{32}
	1,3	2	2: $k_{01}, k_{32}, k_{03}, k_{13}$
		1,3	2: $k_{01}, k_{21}, k_{32}, k_{03}$
	2,3	1,3	2: k_{02}, k_{03}
	1,2,3	2,3	2: k_{01}, k_{02}

[b]Cases marked "a" in Table F.1 not included.

Table F.2 (continued).

Model Structure	Loss from Compartments	Measured Compartments	Number of Solutions: Rate Constants With This Number
6	1	1	2: k_{32}, k_{13}
		3	6: k_{01}, k_{21}, k_{32}; 3: k_{13}
	2	1	2: k_{02}, k_{32}, k_{13}
		3	6: k_{21}, k_{02}, k_{32}; 3: k_{13}
	3	1	2: k_{32}, k_{03}, k_{13}
		3	4: k_{21}, k_{32}; 2: k_{13}
	1,2	2	2: k_{01}, k_{02}, k_{32}
	1,3	2	2: $k_{01}, k_{32}, k_{03}, k_{13}$
		1,3	2: $k_{01}, k_{21}, k_{32}, k_{03}$
	2,3	1,3	2: k_{02}, k_{03}
	1,2,3	2,3	2: k_{01}, k_{02}
7	1	2	2: k_{01}, k_{32}
	2	3	6: k_{02}, k_{23}; 3: k_{21}, k_{32}
		1,3	2: k_{02}, k_{23}
	3	3	3: k_{21}, k_{32}, k_{23}
	1,2	2	3: k_{01}, k_{02}, k_{32}
	1,3	2	3: $k_{01}, k_{32}, k_{03}, k_{23}$
	1,2,3	2,3	3: $k_{01}, k_{02}, k_{03}, k_{23}$
8	1	2,3	2: k_{01}, k_{12}, k_{32}
9	1	1	2: $k_{21}, k_{31}, k_{12}, k_{13}$
		2	3: k_{01}, k_{31}, k_{12}
		3	3: k_{01}, k_{21}, k_{13}
	2	1	2: $k_{21}, k_{31}, k_{02}, k_{12}, k_{13}$
		2	2: k_{31}, k_{12}
		3	3: $k_{21}, k_{02}, k_{12}, k_{13}$
10	1	1	2: $k_{21}, k_{31}, k_{12}, k_{23}$
		2	6: k_{01}, k_{31}, k_{23}; 3: k_{12}
		3	3: k_{01}, k_{21}, k_{23}
	2	1	2: $k_{21}, k_{31}, k_{02}, k_{12}, k_{23}$
		2	4: k_{31}, k_{23}; 2: k_{12}
		3	4: $k_{21}, k_{02}, k_{12}, k_{23}$
	3	1	2: $k_{21}, k_{31}, k_{12}, k_{03}, k_{23}$
		2	6: k_{31}, k_{03}, k_{23}; 3: k_{12}
		3	2: k_{21}, k_{23}
	1,2	1,2	2: $k_{01}, k_{31}, k_{02}, k_{23}$
	1,3	2,3	2: k_{01}, k_{03}, k_{23}
	2,3	1,2	2: k_{02}, k_{03}, k_{23}
	1,2,3	2,3	2: k_{01}, k_{03}, k_{23}

[b]Cases marked "a" in Table F.1 not included.

Table F.2 (continued).

Model Structure	Loss from Compartments	Measured Compartments	Number of Solutions: Rate Constants With This Number
11	2	2	3: k_{31}, k_{32}, k_{23}
		3	6: k_{02}, k_{32}, k_{23}; 3: k_{21}
		1,3	2: k_{02}, k_{32}, k_{23}
	1,2,3	2,3	3: $k_{01}, k_{02}, k_{32}, k_{03}, k_{23}$
12	1	1	2: k_{32}, k_{13}
		2	2: k_{01}, k_{12}
		2,3	2: k_{01}, k_{12}
	2	1	2: k_{02}, k_{32}, k_{13}
	3	1	2: k_{32}, k_{03}, k_{13}
	1,3	1,3	2: $k_{01}, k_{21}, k_{12}, k_{32}, k_{03}, k_{13}$
		2,3	2: k_{01}, k_{12}
	2,3	1,3	2: k_{02}, k_{03}, k_{13}
13	1	2	3: k_{01}, k_{12}, k_{32}
	1,3	2,3	3: $k_{01}, k_{12}, k_{03}, k_{23}$
14	1	2	3: $k_{01}, k_{32}, k_{13}, k_{23}$
	2	1,3	2: k_{02}, k_{23}
	1,2	2,3	3: $k_{01}, k_{02}, k_{13}, k_{23}$
15	1	2,3	2: k_{01}, k_{12}, k_{32}
	3	1,2	2: $k_{12}, k_{32}, k_{03}, k_{13}$
	1,3	1,3	2: $k_{01}, k_{21}, k_{12}, k_{32}, k_{03}, k_{13}$
		2,3	2: k_{01}, k_{12}, k_{32}
	2,3	1,3	2: $k_{02}, k_{12}, k_{32}, k_{03}, k_{13}$
16	3	1,2	2: $k_{12}, k_{32}, k_{03}, k_{23}$
	1,3	2,3	3: $k_{01}, k_{12}, k_{32}, k_{03}, k_{23}$
17	1	2,3	3: $k_{01}, k_{12}, k_{13}, k_{23}$
	2	1,3	2: k_{02}, k_{13}, k_{23}
18	1	2,3	3: $k_{01}, k_{12}, k_{32}, k_{13}, k_{23}$
	2	1,3	2: $k_{02}, k_{12}, k_{32}, k_{13}, k_{23}$

[b]Cases marked "a" in Table F.1 not included.

Appendix G
Obtaining Initial Estimates of Exponentials

Introduction

The most commonly used functional expression to describe a set of tracer data is a sum of exponentials. As indicated in Chapter 9, once a particular sum of exponentials has been chosen, fitting this expression to a given set of data requires, as the first step, initial estimates for the exponentials and the coefficients. This appendix will focus on how to obtain these estimates.

The general formula for an exponential function $y(t)$ is given by

$$y(t) = A_0 + A_1 e^{-\lambda_1 t} + A_2 e^{-\lambda_2 t} + \cdots + A_n e^{-\lambda_n t} \qquad \text{(G.1)}$$

where the $\lambda_1, \lambda_2, \cdots \lambda_n$ are the exponentials, the $A_1, \cdots, A_n$ are the coefficients, and A_0 is a constant term. This function describes the various experimental configurations indicated in Chapter 9. For the single accessible pool noncompartmental model, when $A_0 = 0$ and the remaining A_i are positive, (G.1) describes the decay of tracer from the accessible pool following a bolus injection of tracer into that pool. When $A_0 \neq 0$ and the sum of the A_i equals zero, i.e. $A_0 + A_1 + \cdots + A_n = 0$, (G.1) describes the appearance of tracer in the accessible pool following a constant infusion of tracer into that pool. In the situation when the sum of the coefficients is not zero, (G.1) describes the tracer in the accessible pool following a primed, constant infusion of tracer. Finally, when $A_0 = 0$ and $A_1 + \cdots + A_n = 0$, (G.1) describes the appearance of tracer in a second accessible pool following its input into a first accessible pool. In this situation, (G.1) can be used in estimating the noncompartmental parameters of the two accessible pool model.

How can initial estimates for the λ_i and A_i be obtained? There are several ways based upon the fact that semi-logarithmic plot is a linearizing plot for a monoexponential decay. That is, a semi-logarithmic plot of the monoexponential $Ae^{-\lambda t}$ is a straight line whose slope is $-\lambda$ and whose intercept is $\ln(A)$. This can easily be seen by taking the natural logarithm of $Ae^{-\lambda t}$:

$$\ln(Ae^{-\lambda t}) = -\lambda t + \ln(A) \tag{G.2}$$

This observation will be used in obtaining estimates of the A_i and λ_i in (G.1) for a variety of common experimental designs.

Semi-logarithmic plots of data, i.e. plots resulting from the logarithmic transformation of a set of data, are obtained as follows. Each datum z_i is transformed into the natural logarithm of z_i, $\ln(z_i)$. If the data decay monoexponentially, $\ln(z_i)$ when plotted against t is a straight line. Using semi-logarithmic plots, the $\ln(z_i)$ are calculated automatically because the scale on the ordinate is logarithmic.

Figure G1 illustrates how (G.2) can be used to obtain an estimate for λ and A. These data are taken from Table 8.5.1. The linear plots of these data are curvilinear but, when transformed logarithmically by plotting them using a semi-logarithmic scale on the ordinate, the transformed data appear to be a straight line whose intercept with the ordinate is $\ln(A)$ and whose slope is $-\lambda$. As shown in the next section, it is easy to go from the semi-logarithmic plot to an estimate for λ and A.

The semi-logarithmic plot as a linearizing transformation succeeds only for the monoexponential decay. The semi-logarithmic plot of the monoexponential rise $(A_0 + A_1 e^{-\lambda t})$, or of data containing more the one exponential is not a linear plot. That is, with the exception of the monoexponential decay, there is no transformation of (G.1) that will result in an expression in which the λ_i are linear. However the transformation of the monoexponential will serve as the foundation to obtain the initial estimates of the exponentials.

Initial Estimates of a Single Exponential Model

Monoexponential decays: Bolus injection of tracer

Single or monoexponential decays are described by the equation:

$$y(t) = Ae^{-\lambda t} \tag{G.3}$$

The question to be addressed in this part of the Appendix is the following: given a set of data to be fitted by the single exponential decay (G.3), how are initial estimates for the nonlinear parameter λ and linear
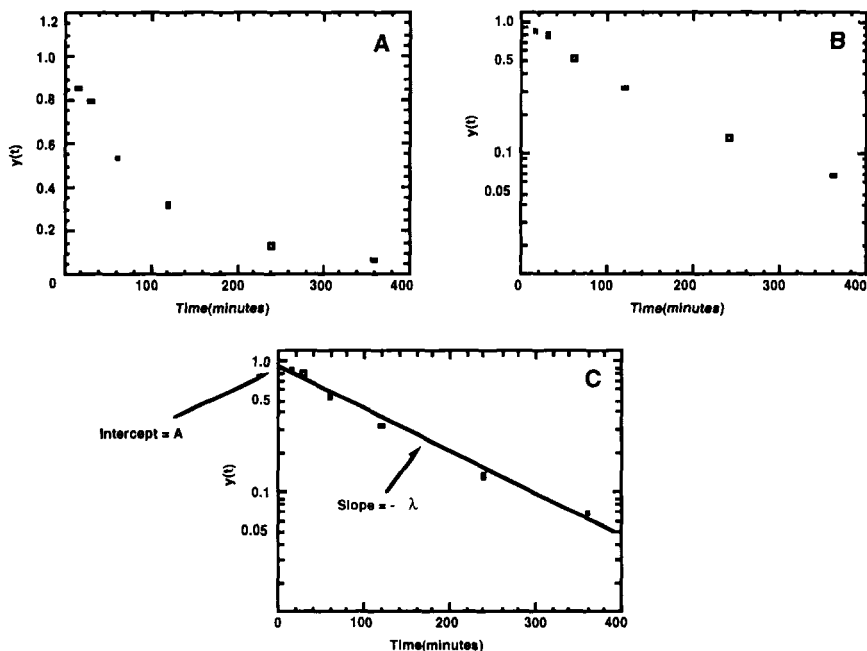
Figure G.1.   **A.** Linear plot of a set of data following a bolus injection into a single pool system **B** Semi-log plot of the same set of data. **C.** Straight line drawn through data illustrating $-\lambda$ and A.

parameter A in (G.3) obtained? Whereas the answer is not difficult in this situation, a number of fundamental ideas will be introduced which then form the basis for dealing with the multiexponential case.

To estimate A and λ in (G.3), consider the set of monoexponentially decaying data shown first in Figure G.1 and reproduced in Figure G.2. Recall the reason why the semi-logarithmic plot of a set of monoexponentially decaying data appears as a straight line is because of the transformation of $Ae^{-\lambda t}$:

$$\ln(Ae^{-\lambda t}) = -\lambda t + \ln(A) \qquad (G.4)$$

Then it is possible to use a linear regression routine and the logarithmically transformed data to estimate $-\lambda$ as the slope and A as the intercept. This would result in estimates for $-\lambda$ and (A) as indicated in Figure G.2. However, since all that is needed are approximate estimates
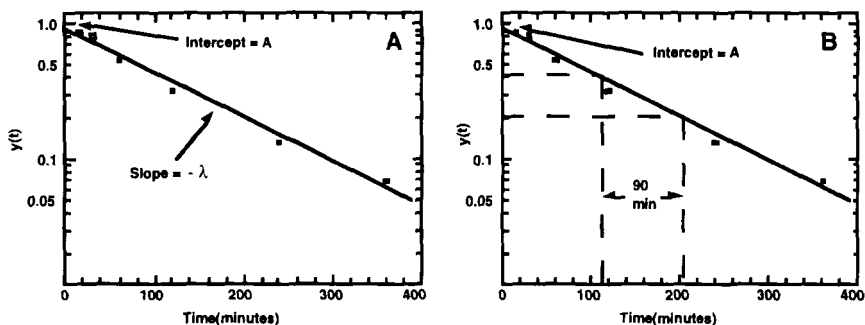
Figure G.2.   A: Data from Figure G.1 with arbitrary straight line through the data illustrating λ and $\ln(A)$. B: Two arbitrarily chosen points are used to estimate λ. See text for additional information.

of $-\lambda$ and *A,* it is not necessary to go through the formal procedure of linear regression.

A more practical way to obtain an initial estimate λ and A can be described as follows. First, draw a straight line through the data as indicated in Figure G.2A. Second, chose two arbitrary points on this line as indicated in Figure G.2B. If, for example, the two time points chosen are t_1 and t_2, the corresponding points on the line are $(\ln(y(t_1)), t_1)$ and $(\ln(y(t_2)), t_2)$. An estimate for the slope of this line, which is $-\lambda$, can be obtained from

$$\lambda = -\frac{\ln(y(t_2)) - \ln(y(t_1))}{t_2 - t_1} \qquad (G.5)$$

In Figure G.2B, the two points are $(\ln(0.4), 115)$ and $(\ln(0.2), 205)$. Applying (G.5), one can calculate

$$\lambda = -\frac{\ln(0.2) - \ln(0.4)}{205 - 115} = -\frac{-1.609 - (-0.916)}{90} = \frac{0.693}{90} \approx 0.008$$

Notice that the points chosen are points on the line, not two arbitrary data points. The reason is that the data may not lie on the line, i.e. if one were to choose two arbitrary data and substitute the appropriate values into (G.5), one may not obtain a reasonable estimate of λ because of noise in the data.

Finally, an estimate for A can be obtained as the point where the line through the data intersects the ordinate. In Figure G.2B, since the data are plotted is semi-logarithmically, A can be read immediately as approximately 1.

While the single exponential model has been dealt with here, an extension of this method will form the basis for the curve-peeling method of estimating exponentials in multiexponential functions discussed later.

The method can also be adapted to use "biological half-life" as a parameter. This variation when adapted to the multiexponential case is much quicker than curve-peeling in providing initial estimates for the exponentials.

The biological half-life of a substance in the body is defined as the length of time required for one-half of the material present in the system at a given time to leave the system irreversibly. For a tracer which decays monoexponentially, this can be discussed in terms of (G.3). For example, if the units of measure are concentration, the constant A is the amount of material injected into the system as a bolus at time zero per unit volume. Hence one half of the material is equal to $A/2$. If $t_{1/2}$ represents the half-time, that is the time it takes for one half of the material to leave the system, then in terms of (G.3),

$$\frac{A}{2} = Ae^{-\lambda t_{1/2}} \qquad (G.6)$$

Solving (G.6) for $t_{1/2}$:

$$t_{1/2} = \frac{\ln 2}{\lambda} \approx \frac{0.693}{\lambda} \qquad (G.7)$$

This equation provides the relationship between the half-time $t_{1/2}$ and the exponential λ that will be used below to estimate λ. More specifically, once $t_{1/2}$ is known,

$$\lambda = \frac{\ln 2}{t_{1/2}} \approx \frac{0.693}{t_{1/2}} \qquad (G.8)$$

Whereas (G.7) and (G.8) were derived starting from the initial amount of material in the system, A, it is important to note that it is not necessary to "start" with the zero time amount. Since $y(t) = Ae^{-\lambda t}$ is decaying monoexponentially, one can "start" at any arbitrary time t_1. The amount of material in the system at this time is $y(t_1) = Ae^{-\lambda t_1}$ One half of this material is $\frac{y(t_1)}{2} = \frac{1}{2}Ae^{-\lambda t_1}$. The time at which half of this material would be left is $t_1 + t_{1/2}$. Equation (G.7) and hence (G.8) can be obtained from solving $\frac{y(t_1)}{2} = Ae^{-\lambda(t_1+t_{1/2})}$ for $t_{1/2}$. It is this observation, i.e. that one can start from any arbitrary point on the decaying monoexponential, that makes this adaption of the curve peeling method very easy.

To illustrate how the relationship between half-times and exponentials can be used to estimate the numerical value of the exponential λ,

consider again the data given above in Figure G.2. First, chose an arbitrary point on the y-axis, say $y(t_1)$ and note the corresponding time t_1 at which the point $(y(t_1), t_1)$ lies on the line. One half of this amount is $\frac{y(t_1)}{2}$. Second, find the time t_2 on the abscissa at which the point $(\frac{y(t_1)}{2}, t_2)$ is on the line. In Figure G.2B, $y(t_1) = 0.4$ occurring at time 115, $y(t_2) = 0.2$ occurring at time 205. The difference $t_2 - t_1 = 90$ is the half-time for this particular situation, and an estimate λ can be obtained from (G.8): $\lambda \approx \frac{0.693}{90} = 0.008$.

That this method is a specific case of the first method described can be seen as follows. The two specific points chosen, when plotted on semi-logarithmic paper, are $(\ln(y(t_1)), t_1)$ and $(\ln(\frac{y(t_1)}{2}), t_2)$. From (G.5) and the above discussion, one has

$$\lambda = -\frac{\ln(\frac{y(t_1)}{2}) - \ln(y(t_1))}{t_2 - t_1} = \frac{\ln(y(t_1)) - \ln(2) - \ln(y(t_1))}{t_2 - t_1} = \frac{\ln(2)}{t_2 - t_1}$$

Because the monoexponential when plotted semi-logarithmically is a straight line, the same estimate for λ will be obtained for any starting value $y(t_1)$. This is not the case either for the monoexponential rise discussed next, or for multiexponentials. However, extensions of the method can be used in these cases.

Monoexponential rises: the constant and primed, constant infusion of a tracer

A "monoexponential rise" is described by the equation

$$y(t) = A_0 + A_1 e^{-\lambda t} \tag{G.9}$$

The reason why monoexponential rise is in quotation marks is because in the case of the constant infusion of tracer, the tracer data rise towards a plateau value actually reaching it if the infusion is carried out for a sufficiently long period of time, while in the case of the primed, constant infusion, the data can either rise or fall to the plateau depending upon the size of the priming dose.

In (G.9), the parameter A_0 is always positive. If the tracer is infused for an infinite time, this is the constant value $y(t)$ can assume; it is called the plateau value. The parameter A_1 equals $-A_0$ in the case of the constant infusion since $y(0) = A_0 + A_1 = 0$, but can be either positive or negative for the primed constant infusion depending upon the situation. Various examples are illustrated in Figure G.3.

The question to be addressed now is how to obtain an initial estimate for A_0, A_1 and λ when the data are to be described by a monoexponential
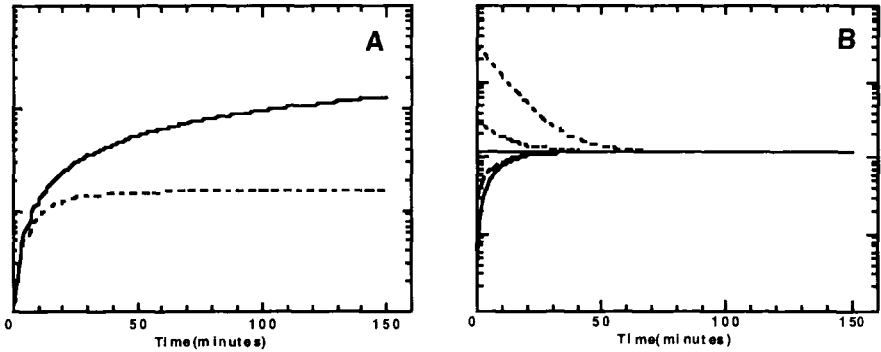
Figure G.3. A: Two examples of a monoexponential rise following a constant infusion of tracer where one reaches a plateau and the other does not. B: Different situations possible for the primed, constant infusion illustrating rises, falls, and the "ideal" situation where the primed dose results in an "immediate" plateau.

rise. Obtaining this initial estimate for λ in (G.9) is more complex that the monoexponential decay because the logarithmic transformation of (G.9) is not a linearizing transformation.

In describing how to obtain estimates for λ, it is instructive to deal separately with the constant and then the primed, constant infusion of tracer. This separation for the monoexponential case will make the extension to multiexponential functions easier.

Case 1: The constant infusion of tracer

Since A_0 and A_1 in (G.9) are equal and opposite in this situation, the monoexponential rise to a plateau in experiments where tracer is administered into the accessible pool as a constant infusion can be described by rewriting (G.9) as

$$y(t) = A - Ae^{-\lambda t} \qquad 0 \le t \le T \qquad \text{(G.10)}$$

where T is the time at which the infusion stops. Two situations can arise; in one, a plateau value is clearly reached and in the other, a plateau is not reached. Both will be considered using the data given in Table G.1 plotted in Figure G.4 in both the linear and semi-logarithmic modes. These are simulated data from two experiments in which 40, 000 dpm of tracer labeled material was infused into the plasma for 150 minutes.

Table G.1.

Time	Study 1	Study 2
3	473	519
6	915	1038
9	1127	1433
12	1549	1841
15	1840	2178
20	2229	3050
30	2817	4125
40	3111	5344
50	3223	6342
60	3399	7601
70	3241	7891
80	3128	8790
90	3169	9470
100	3337	11040
110	3546	11080
120	3281	11980
130	3223	11490
140	3543	12150
150	3624	13870
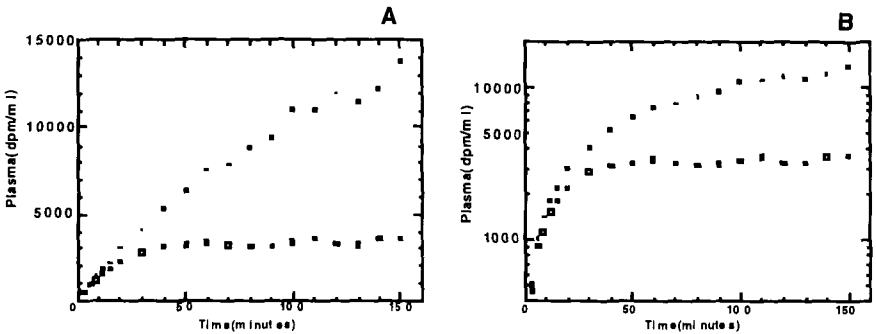
Figure G.4.   Data given in Table G.1 shown on a linear plot (panel A) and a semi-logarithmic plot (panel B). The large squares are the data from Study 1 and the small squares are the data from Study 2.

From this Figure, it should clear that, unlike the situation described for the bolus injection of tracer followed by a monoexponential decay of the data, the semi-logarithmic plots of these data are curvilinear. Thus the estimation of the exponential λ does not directly parallel the situation described for the monoexponential.

How are estimates for A and λ obtained? The following albeit tedious method will provide a reasonable estimate; this method can be seen as an adaptation of the first method used for the bolus injection.

Step 1. Obtain an estimate for A by postulating the plateau value.

Step 2. Subtract this value from each datum producing a "new" set of data.

Step 3. Multiply this set by -1 thereby producing a second "new" set of data.

Step 4. Obtain an estimate of λ using the methods described in the previous section.

This method requires an estimation of A, the plateau value, first; this is easy in the situation when a plateau is clearly reached as is the case with Study 1 but more difficult in the case when the plateau is not reached as is the case with Study 2. Subtracting A from (G.10) leaves $-Ae^{-\lambda t}$. Multiplying this by -1 converts the expression into $Ae^{-\lambda t}$, a monoexponential decay. Thus taking the data set, subtracting A from each datum, and multiplying this number will result in a set of "modified" data decaying monoexponentially according to the expression $Ae^{-\lambda t}$. The parameter λ for the monoexponential rise can then be estimated using the methods described by the monoexponential decay.

This method will be illustrated using the set of data from Study 1 given in Table G.1. An estimate of the plateau value is 3400 (see Figure G.5A), thus $A = 3400$. The results of steps 2 and 3 for this set of data are summarized in Table G.2.

Notice the values for the modified data after 50 time units vary between positive and negative values; this is because the original data are on the plateau, and are randomly distributed above and below plateau. A plot of the modified data is shown in Figure G.5B. To estimate λ, one can use the half-life method discussed for the monoexponential decay. This is also illustrated in Figure G.5B where, as can be seen, the half life is 12 minutes resulting in an estimate of λ equal to 0.06. Figure G.5C shows the prediction of the data by the function $y(t) = 3400(1 - e^{-0.06t})$

These estimates should be more than sufficient to use as a starting point for an algorithm of nonlinear weighted least squares to obtain a "best fit" of the data.
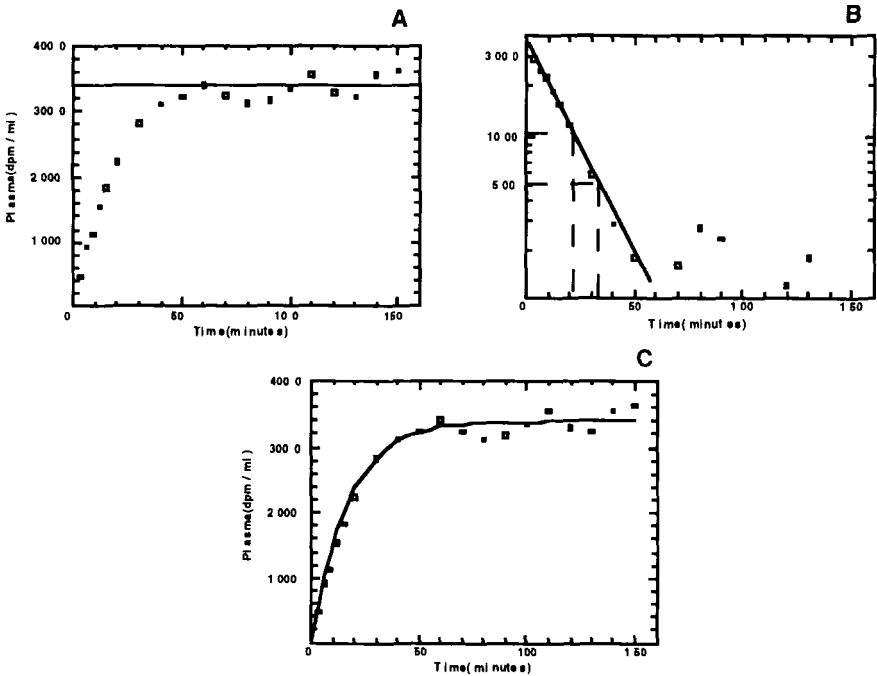
Figure G.5.   A: A plot of the data from Study 1 from Table G.1; the line through the plateau is used to estimate $A = 3400$. B: A plot of "$-(data - 3400)$" from Table G.2. A line through the monoexponential decay is used to estimate a value for λ equal to 0.06. C: A plot of $y(t) = 3400(1 - e^{-0.06t})$.

There is a second technique which can be used to obtain an estimate of λ; this can be described as follows. The slope of the monoexponential rise described by (G.10) at any time t is given by the derivative of $y(t) = A(1 - e^{-\lambda t})$:

$$\frac{dy}{dt} = A\lambda e^{-\lambda t} \tag{G.11}$$

In this equation, the product of A and λ is the coefficient of $e^{-\lambda t}$. The estimate of λ can be obtained by noting that $\frac{dy}{dt}$ evaluated at $t = 0$ is equal to $A\lambda$; i.e. the slope of the line describing the data at time zero is $A\lambda$. Once A is estimated as the plateau value and $A\lambda$ is estimated as the slope of the rise at time zero, an estimate of λ will follow immediately. This method, while not as tedious as that previously described, is very

Table G.2.

| | | Study 1 | |
Time	Data	Data-3400	−(Data-3400)
3	473	−2927	2927
6	915	−2485	2485
9	1127	−2273	2273
12	1549	−1851	1851
15	1840	−1560	1560
20	2229	−1171	1171
30	2817	−583	583
40	3111	−289	289
50	3223	−177	177
60	3399	−1	1
70	3241	−159	159
80	3128	−272	272
90	3169	−231	231
100	3337	−63	63
110	3546	146	−146
120	3281	−119	119
130	3223	−177	177
140	3543	143	−143
150	3624	224	−224

sensitive to the initial slope; this can create problems if there are few data describing the initial rise.

The question arises as to whether or not there is a counterpart to (G.8) for the constant infusion experiment, i.e. is it possible to define a $t_{1/2}$ from which λ can then be estimated? The answer is yes,

If A is the plateau value, define in this situation $t_{1/2}$ as the time it takes, starting from time zero, to reach $\frac{A}{2}$. Paralleling the bolus injection experiment, (G.10) can be written and solved for $t_{1/2}$:

$$\frac{A}{2} = A - Ae^{-\lambda t_{1/2}} \tag{G.12}$$

which, when simplified becomes

$$\frac{1}{2} = e^{-\lambda t_{1/2}} \tag{G.13}$$

Taking the logarithm of both sides of (G.13) and solving for λ, one obtains

$$\lambda = \frac{\ln 2}{t_{1/2}} \approx \frac{0.693}{t_{1/2}} \tag{G.14}$$

This equation is identical to (G.8)!

In fact, this notion can be extended in a way that will be very useful for multiexponential rises. If one draws a curve through the rise and picks an arbitrary point on the curve $(y(t_1), t_1)$, then $y(t_1) = A - Ae^{-\lambda t_1}$. Solving for the time it takes to go from that value half way to the plateau, one obtains (G.14). To see how this works, suppose the time taken to go half way to the plateau is written $t_2 = t_1 + t^*$. Since $y(t_2)$ is numerically equal to the average between A and $y(t_1)$, $y(t_2)$ can be written

$$y(t_2) = \frac{1}{2}(A + y(t_1)) = \frac{1}{2}(A + A - Ae^{-\lambda t_1}) = A - \frac{A}{2}e^{-\lambda t_1}$$

Combining this with (G.10), one has

$$y(t_2) = A - Ae^{-\lambda t_2} = A - Ae^{-\lambda(t_1 + t^*)} = A - \frac{A}{2}e^{-\lambda t_1} \qquad \text{(G.15)}$$

This equation can be solved for t^* giving $t^* = \frac{\ln(2)}{\lambda}$ from which it follows immediately that $t^* = t_{1/2}$.

To see how this is used to estimate λ for the constant infusion experiment, consider the data from Table G.1 plotted in Figure G.6. For Study 1. an estimate of λ of 0.05 is obtained; this differs from the value 0.06 obtained from the previous. In theory, both methods are correct; the difference in estimates is due to how they are implemented. For Study 2, an estimate for λ equal to 0.01 is obtained as explained in the figure legend. A plot of $y(t) = 3400 - 3400e^{-0.05t}$ and the data from Study 1, and a plot of $y(t) = 15000 - 15000e^{-0.01t}$ and the data from Study 2 are shown in Figure G7.

One can see immediately that if the plateau value can be estimated with some reasonable confidence that the estimate of λ is also reasonable, but if one has to more or less guess at a plateau value, the estimate both of the plateau and λ is not as good. However, both are sufficient as initial estimate for most computer programs to begin the optimization process.

Case 2: The primed, constant infusion

In the case of the primed, constant infusion the coefficients in (G.9) are not equal and opposite; the difference between this and the previous situation is that at time zero, $y(t) \neq 0$. Hence to obtain an initial estimate of λ, the scheme for the constant infusion must be modified. The examples to be used in developing the techniques are the data from two simulated studies given in Table G.3 (plotted in Figure G.8). In Study 1, a priming dose of $3 \cdot 10^6$ dpm followed by a constant infusion of
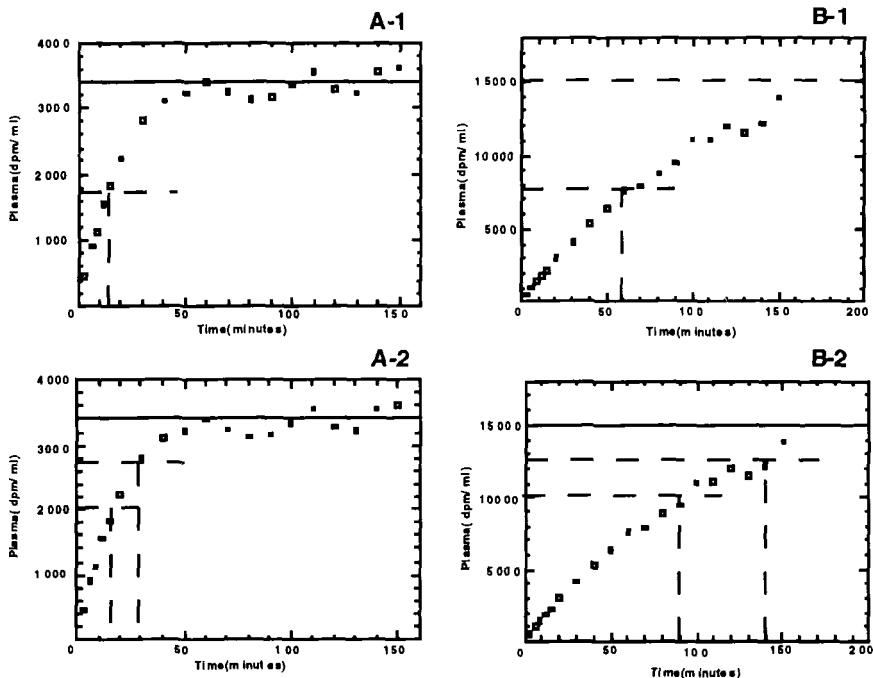
Figure G.6. Illustration of using $t_{1/2}$ to estimate λ in the constant infusion experiment. Panel A shows the data for Study 1 in Table G.1 indicating the time it takes to reach half of the plateau value of 3400 (A-1) and the time taken to go from 2000 to 2700, half way between 2000 and 3400 (A-2). In both cases, the time is approximately 14 minutes. Panel B shows the the data from Study 2 in Table G.1, and assumes a plateau value of 15000. Panel B-1 shows the time taken to go half-way to the plateau; panel B-2 shows the time taken to go from 10000 half-way to the plateau. The two times, 60 and 50 minutes, produce the same approximate estimate of 0.01 for λ.

550, 000dpm/min was given; in Study 2, the priming dose was $6 \cdot 10^7$dpm. The columns other than the two data columns will be explained later.

The equation describing data from a primed, constant infusion is

$$y(t) = A_0 + A_1 e^{-\lambda t} \qquad 0 \le t \le T \qquad (G.16)$$

where A_0 is the plateau, $A_0 + A_1$ is the intercept with the ordinate, and T is the time at which the infusion stops.
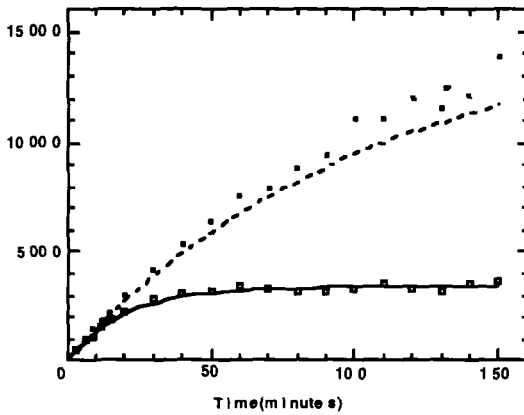
Figure G.7.   A plot of $y(t) = 3400 - 3400e^{-0.05t}$ and the data from Study 1 (big squares and solid line), and a plot of $y(t) = 15000 - 15000e^{-0.01t}$ and the data from Study 2 (small squares and dotted line).

Table G.3.

| | | Study 1 | | | Study 2 | |
t	Data	Data-3300	$-(Data$-$3300)$	Data	Data-3300
3	1298	-2002	2002	16073	12773
6	1624	-1676	1676	14932	11632
9	1850	-1450	1450	12778	9478
12	2095	-1205	1205	11483	8183
15	2199	-1101	1101	10910	7610
20	2426	-874	874	9306	6006
30	2839	-461	461	6812	3512
40	2965	-335	335	5513	2213
50	3232	-68	68	4516	1216
60	3178	-122	122	3935	635
70	3330	30	-30	3941	641
80	3223	-77	77	3773	473
90	3376	76	-76	3598	298
100	3280	-20	20	3622	322
110	3255	-45	45	3291	-9
120	3319	19	-19	3495	195
130	3323	23	-23	3345	45
140	3310	10	-10	3213	-87
150	3280	-20	20	3439	139
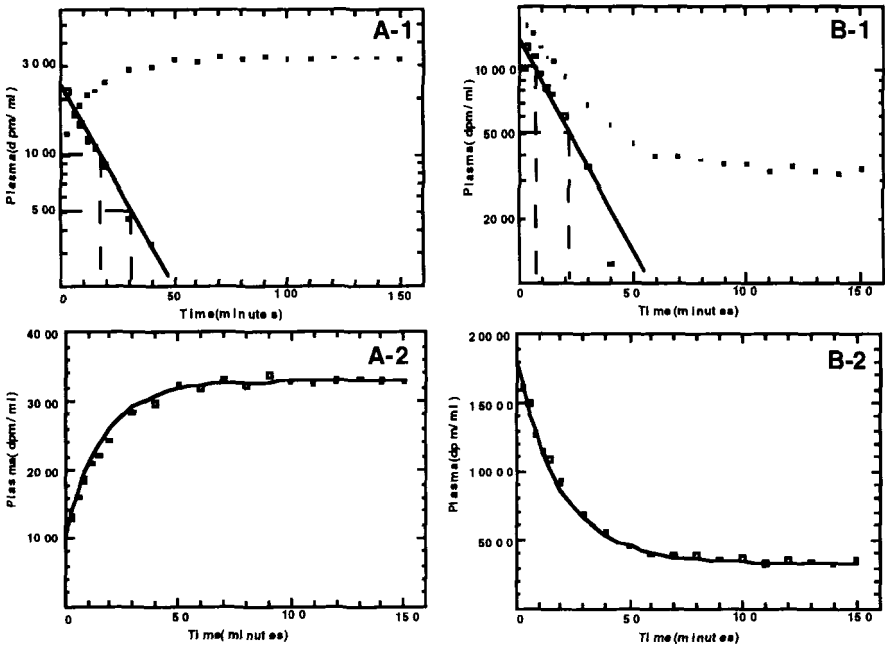
Figure G.8. A-1: The data from Study 1 from Table G.3 are plotted on a semi-logarithmic scale (small squares). A_0 is estimated from the plateau value of 3300. The intercept with the ordinate, $A_0 + A_1$, is estimated to be 1000. A plot of the modified data (large squares) reveals a monoexponential; λ is estimated to be 0.06 using the half-life method. See text for additional explanation. A-2: A plot of $y(t) = 3300 - 2300e^{-0.06t}$. B-1: The data from Study 2 from Table G.3 are plotted on a semi-logarithmic scale (small squares). A_0 is estimated from the plateau value of 3300. The intercept with the ordinate, $A_0 + A_1$ is estimated to be 18000. A plot of the modified data (large squares) reveals a monoexponential; λ is estimated to be 0.05 using the half-life method. B-2: A plot of $y(t) = 3300 + 14700e^{-0.05t}$. See text for additional explanation.

How are estimates for A_0, A_1, and λ obtained in this situation? The following modification of the first method described above for the constant infusion can be illustrated using the data in Table G.3 and Figure G.8.

Step 1. Obtain an estimate for the plateau A_0.

Step 2. Subtract this value from each datum producing a modified set of data.

At this point, there are two possible situations. If the data are rising (as is the case in Study 1 from Table G.3), then:

Step 3. Multiply this set by -1 thereby producing a second modified set of data.

Step 4. Obtain an estimate of λ using one of the methods described for the monoexponential decay.

If the data are falling (as is the case in Study 2 from Table G.3), one can proceed directly to an estimate of λ.

How does this work? Subtracting A_0 from each datum eliminates the constant term from (G.16) leaving only the expression $A_1 e^{-\lambda t}$. If this expression is negative, multiplying each modified data by -1 converts them into a second set of modified data which will appear as a monoexponential decay whose zero time value is A_1. If the expression is positive, the modified data will already appear as a monoexponential decay. These cases are illustrated in Figure G.8.

It is sufficient to estimate two parameters since the third can be derived from the constraint (9.2.23) which is derived in Appendix H:

$$A_0 + A_1 \frac{\frac{u}{d}}{\frac{u}{d} - \lambda_1} = 0 \tag{G.17}$$

The easiest way to apply this is to estimate A_0 from the plateau value and $A_0 + A_1$ from the intercept. Then from (G.17)

$$\lambda_1 = \frac{u}{d} \frac{A_0 + A_1}{A_0} \tag{G.18}$$

However, this method cannot be extended to the multiexponential case where it is necessary to estimate the λ_i from the data. Another point must be made. In the event that the plateau is reached "immediately", $y(0) = A_0$. In this case, while $A_1 = 0$, λ can still be estimated as the ratio between the constant infusion and the priming dose (see (9.2.23)).

Finally, there is a counterpart for (G.8), the half-life method, for the primed, constant infusion case. Consider the data from Studies 1 and 2 from Table G.3 redrawn in Figure G.9. Unlike the case for the constant infusion where $y(0) = 0$, for the primed, constant infusion, $y(0) = A_0 + A_1$. Panels A-1 and B-1 in Figure G.9 illustrates for both studies A_0 as the plateau value, and the intercept $A_0 + A_1$ with the ordinate.

Define t^* in this situation as the time it takes to go from $A_0 + A_1$ to $A_0 + \frac{A_1}{2}$ (see Figure G.9). Then (G.16) can be solved for t^* from the
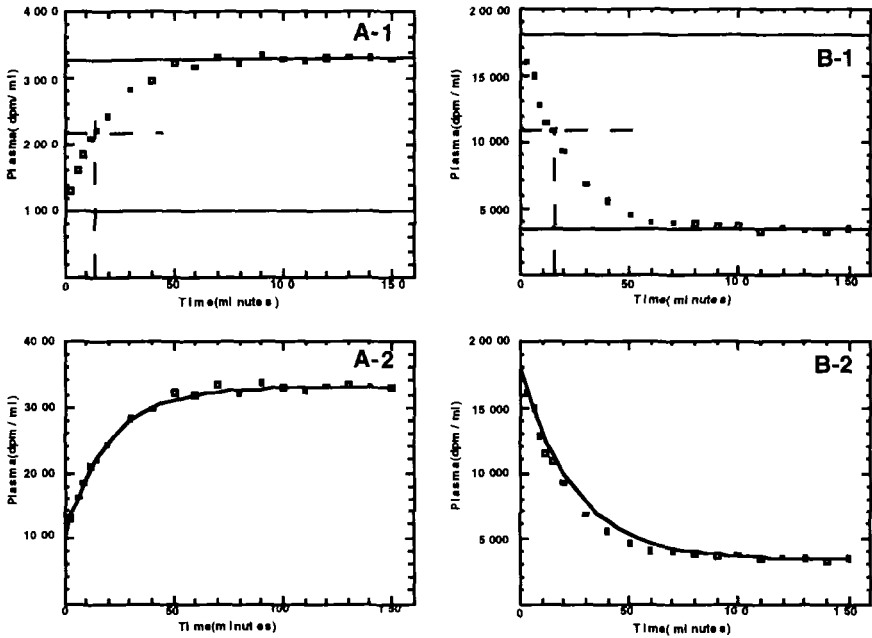
Figure G.9. A-1: Data from Study 1 from Table G.3 with two lines drawn parallel to the abscissa representing the values for A_0 and $A_0 + A_1$. The dotted lines represent the time to go from $A_0 + A_1$ to $A_0 + \frac{A_1}{2}$. This "half-time" is 15 minutes producing an estimate of 0.05 for λ. A-2: A plot of $y(t) = 3300 - 2300e^{-0.05t}$. B-1: Data from Study 2 from Table G.3 with two lines drawn parallel to the abscissa representing the values for A_0 and $A_0 + A_1$. The dotted lines represent the time to go from $A_0 + A_1$ to $A_0 + \frac{A_1}{2}$. This "half-time" is 16 minutes producing an estimate of 0.04 for λ. B-2: A plot of $y(t) = 3300 + 13700e^{-0.04t}$. See text for additional information.

following equation:

$$A_0 + \frac{A_1}{2} = A_0 + A_1 e^{-\lambda t^*} \qquad (G.19)$$

which, when simplified, becomes

$$\frac{1}{2} = e^{-\lambda t^*} \qquad (G.20)$$

The exponential λ can be estimated from $\lambda = \frac{\ln 2}{t^*} \approx \frac{0.693}{t^*}$. Since this equation is identical to (G.8), $t^* = t_{1/2}$.

As with the constant infusion, the definition can be extended. If one starts at a given point $(y(t_1), t_1)$ where $y(t_1) = A_0 + A_1 e^{-\lambda t_1}$, and defines the half-time $t_{1/2}$ as the time it takes to go from that point half-way to the plateau, one can solve the equation

$$A_0 + \frac{A_1}{2} e^{-\lambda t_1} = A_0 + A_1 e^{-\lambda(t+t_{1/2})} \qquad (G.21)$$

to obtain (G.20).

Monoexponential washout after stopping an infusion of tracer

The constant or primed, constant infusion of tracer lasts for a finite duration of time. After the infusion is stopped, the so-called washout period starts. It is called this because with no more tracer entering from outside the system, what remains will be removed by the various pathways of the particular system under study; it is being washed out. Whether the tracer is administered as a constant or primed constant infusion, the analysis of the washout phase is the same. An example of monoexponential washout is given in Figure G.10.

The equation for the rising portion of the curve is

$$y_r(t) = A_0 + A_1 e^{-\lambda t} \qquad t \leq T \qquad (G.22)$$

This equation is valid only during the infusion. That is, if the infusion starts at time zero and stops at time T, $y_r(t)$ is valid only for $0 \leq t \leq T$.

What is needed now is a functional description of the washout, i.e. for $t > T$. Below, a specific example is considered first followed by a discussion of the general case.

The rising portion of the data given in Figure G.10A are those from Study 1 given in Table G.1. These data can, as was discussed previously, be described during the infusion period by the function $y(t) = 3300 - 3300e^{-0.06t}$. That is, for any specific $\hat{t}$ between 0 and 150 minutes, a datum at that point is approximately equal to $y(\hat{t}) = 3300 - 3300e^{-0.06\hat{t}}$. In particular, when $t = 150$, i.e. when the infusion is stopped, the calculated tracer concentration in the accessible pool for Study 1 is $y(150) = 3300 - 3300e^{-0.06 \cdot 150}$. The question to be addressed now is how does this material leave the system?

As seen Figure G.10B, the washout phase appears on the semi-logarithmic plot as a straight line suggesting a monoexponential decay. In fact, the exponential λ for this decay can be estimated using the same methods for the monoexponential decay discussed earlier! The half-time method illustrated in Figure G.10 gives an estimate for λ equal to 0.06; this value is the same as those obtained during the rising portion of the curve. That
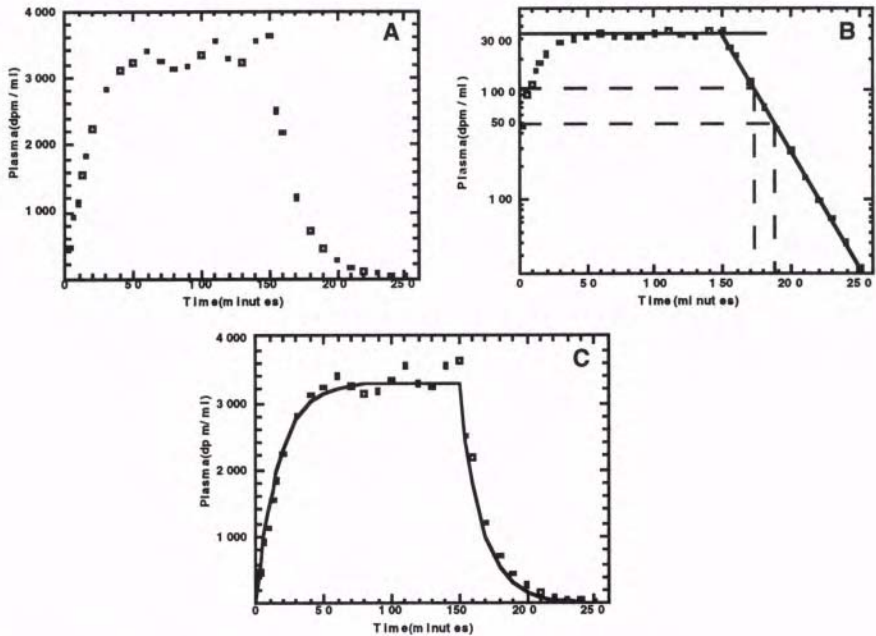
Figure G.10. A: An example of data collected from a constant infusion experiment where the infusion was stopped at 150 minutes, and data were collected during the washout phase until 250 minutes. B: The data plotted semi-logarithmically showing a line drawn for the plateau giving an estimate of $A = 3300$ and a straight line drawn through the monoexponential decay. Using the half-time method, an estimate for λ of 0.06 was obtained. C: A plot of $y_r(t) = 3300 - 3300e^{-0.06t}$ for $0 \le t \le 150$ and $y_w(t) = (3300 - 3300e^{-0.06 \cdot 150})e^{-0.06(t-150)}$ for $150 < t$. See text for explanation.

this is the case can be seen from the observation that the monoexponential model deals with a single pool system, and the exponential during a steady state experiment cannot change.

However, the decay representing the washout cannot be described by $e^{-\lambda t}$ since this implies the monoexponential decay starts at time zero. In this example, the decay starts 150 minutes into the experiment. Thus to describe the monoexponential decay which starts at 150 minutes, the time t in the exponential function is not t but $(t - 150)$. The effect of this is that when the infusion stops, i.e. when $t = 150$, $t - 150 = 0$, and the decay from 150 minutes proceeds as if there had been a bolus

injection equalling $3300 - 3300e^{-0.06 \cdot 150}$ into the system. The equation describing the washout for this example is

$$y(t) = (3300 - 3300e^{-0.06 \cdot 150})e^{-0.06(t-150)} \qquad t > 150 \qquad (G.23)$$

The result of combining the two expressions is shown in Figure G.10C. These equations are valid only for t greater than 150 minutes

What happens in the general case? The function describing the exponential rise during the constant or primed constant infusion is (G.22). Suppose in a given experiment, the infusion is stopped at time T, and data are collected during the washout phase. Then the calculated concentration of material in the system at T is:

$$y_r(T) = A_0 + A_1 e^{-\lambda T} \qquad (G.24)$$

The equation to describe the monoexponential decay of the washout is then:

$$y_w(t) = (A_0 + A_1 e^{-\lambda T})e^{-\lambda(t-T)} \qquad t > T \qquad (G.25)$$

where the subscript w indicates the washout portion of the curve. The function $y(t)$ describing all the data is thus

$$yt = y_r(t) \qquad - \le t \le T \qquad (G.26)$$
$$y_w(t) \qquad T < t$$

One can observe that in experiments where the tracer is introduced as a constant or primed, constant infusion, a rough, initial estimate of the exponential λ to describe both the rising and washout portion of the curve can be obtained from the washout phase.

Initial Estimates of a Two Exponential Model

Introduction

The equation for the general two exponential model is

$$y(t) = A_0 + A_1 e^{-\lambda_1 t} + A_2 e^{-\lambda_2 t} \qquad (G.27)$$

In this section, how to obtain initial estimates for the exponentials λ_1 and λ_2, the coefficients A_1 and A_2, and the constant term A_0 will be discussed. Biexponential decays can be used to describe tracer data in the accessible pool after a bolus injection of tracer into the accessible pool and biexponential rises can be used to describe data after a constant or primed, constant infusion of tracer into the accessible pool. For the

two accessible pool noncompartmental model, the biexponential rise and fall which represents the appearance and disappearance of tracer in the second accessible pool when the tracer was introduced into the first accessible pool will also be discussed.

For biexponential decays, the techniques given are extensions of the methods discussed in the previous section for the monoexponential model. The first method estimated the exponential from the slope of the semilogarithmic plot of the data; the extension of this is the curve peeling method. The second method was based on the notion of biological half-life. The extension of this method is called the rapid or quick curve peeling method. To describe biexponential rises, one technique described for the monoexponential carries over directly. In fact, this is the only technique that can be used with reliability. Another method which at times can be less reliable is discussed because it is less tedious. Since extensions of these methods form the basis for estimating exponentials for arbitrary multiexporiential functions, the biexponential function like the monoexponential will be discussed in some detail.

Biexponential decays: the bolus injection of a tracer

The general expression for the biexponential decay is given by (G.28):

$$y(t) = A_1 e^{-\lambda_1 t} + A_2 e^{-\lambda_2 t} \qquad \text{(G.28)}$$

where the coefficients A_1 and A_2 are positive, and λ_1 and λ_2 are the exponentials. In the following, it will be assumed that $\lambda_1 > \lambda_2$.

The difference between the monoexponential decay and the biexponential decay can be illustrated using the data given in Figure G.11. These data, which were originally used in Table 8.7.4 as Case Study 2, were collected during a study in which a bolus of tracer was injected at time 0 into an accessible pool, and serial samples taken from this pool for 150 minutes. It should be noted that in this Case Study it was seen that the data could best be described by a sum of three exponentials. To determine this, however, it was necessary to fit these data to a sum of two, three and four exponentials. These data will be used to illustrate how to obtain initial estimates for a sum of two, three and four exponentials thus providing continuity with some of the ideas presented in Chapter 8 on determining model order.

Unlike the monoexponential case, the semi-logarithmic plot of these data is not a straight line, but is curvilinear since in this case, the semilogarithmic transformation is not a linearizing plot.

However, one should not forget that all that is required are estimates for the coefficients A_i and exponentials λ_i. One wants estimates that has at least a reasonable approximation of the characteristics of the data.
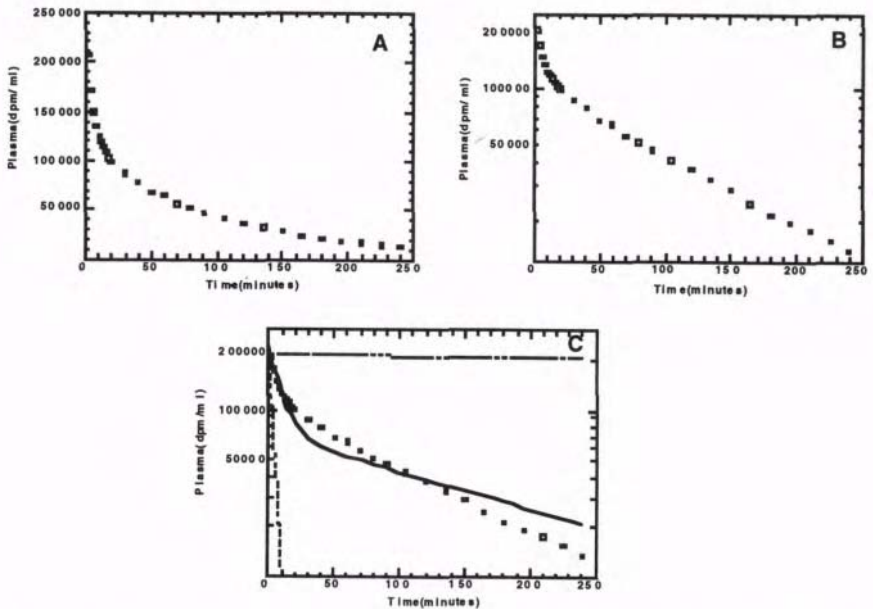
Figure G.11.   Data from an experiment are plotted on a linear scale (panel A) and semi-logarithmic scale (panel B). Panel C shows different results of estimates for the coefficients A_i and exponentials λ_i. See text for additional explanation.

Panel C in Figure G.11 illustrates this. Here one sees the middle curve cutting through the data in a reasonable fashion. This compares with the upper and lower ones. The upper one results from a set of estimates that is far too slow to represent the data while the lower one results from a set of estimates that is far too rapid. Often in these situations when the estimates are so far off, a computer program will not be able to converge to a best fit.

The two methods given below describe how to obtain initial estimate of the two coefficients and exponentials required to describe a biexponential decay. Both will rely on an analysis of the data following a semi-logarithmic transformation, and hence are easily seen as extensions of the concepts introduced for the monoexponential decay.

Curve peeling

Curve peeling is a technique to estimate the exponentials by estimating one exponential at a time. The three steps that are involved, which will be discussed in detail below, are:

- 1. estimating λ_2 and A_2;

- 2. subtracting $A_2 e^{-\lambda_2 t}$ from the data to obtain a modified data set; and

- 3. estimating A_1 and λ_1 from the modified data set.

The data given in Figure G.11 will be used to illustrate these steps. The original data and the results are the first two steps above are summarized in Table G.4 below.

Table G.4.

Time	Plasma	$Plasma - A2e^{-008\,t}$
2	206701	108288
4	171594	74743
6	148425	53112
8	134377	40577
10	123580	31268
12	119484	28638
14	113790	24386
16	109188	21203
18	103288	16699
20	99108	13894
30	87073	8410
40	78817	6202
50	68707	1675
60	64657	2779
70	56928	−193
80	51757	−972
90	47496	−1179
105	42124	−1047
120	37425	−864
135	32897	−1063
150	29102	−1017
165	24598	−2116
180	21427	−2266
195	19231	−1783
210	17596	−1041
225	15673	−857
240	13689	−972

Step 1: Estimate λ_2 and A_2

Draw a straight line through the tail portion of the data shown in Figure G.11; this is shown in Figure G.12. The idea is the following. In the case of a biexponential decay, if one exponential, say λ_1, is numerically 5 to 10 times larger than the second, λ_2, then beyond a certain time, the contribution that the term containing this exponential, $A_1 e^{-\lambda_1 t}$, makes to the decay is "lost" in the sense that $A_1 e^{-\lambda_1 t}$ is very small numerically relative to the term containing the second exponential, $A_2 e^{-\lambda_2 t}$. Mathematically, this means that beyond a certain time T, for all $t > T$, $A_2 e^{-\lambda_2 t} \gg A_1 e^{-\lambda_1 t}$. The data for $t > T$ make up what is called the tail portion of the biexponential curve. The assumption is that the tail portion of the curve is due "entirely" to $A_2 e^{-\lambda_2 t}$. Thus the slope of the line through the tail portion of the curve is $-\lambda_2$ and the intercept with the ordinate is A_2. Paralleling the monoexponential decay, the exponential λ_2 can be estimated by picking two arbitrary points on this line, $(y(t_2), t_2)$ and $(y(t_1), t_1)$, and calculating:

$$\lambda_2 = -\frac{\ln(y(t_2)) - \ln(y(t_1))}{t_2 - t_1} \tag{G.29}$$
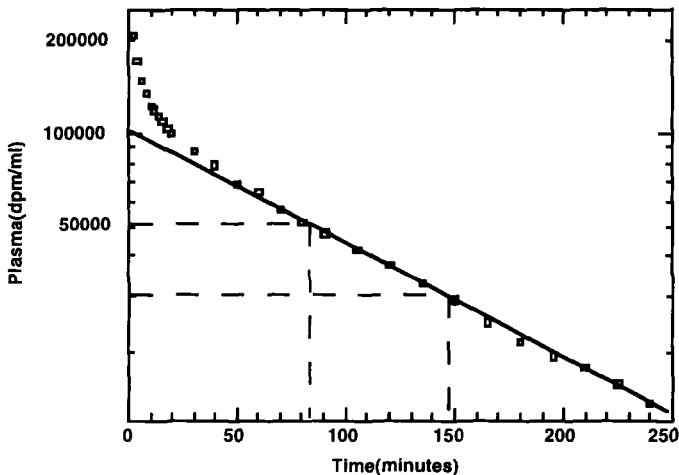
Figure G.12. The semi-logarithmic plot of the data from Figure G.11 with an arbitrary straight line drawn through the "tail" portion of the data. Two points are selected from which an estimate of λ will be obtained. See text for additional explanation.

This is the counterpart of (G.5). The two points chosen in the figure are (ln(50,000),82) and (ln(30,000), 148). Using (G.29), an estimate of 0.008 for λ_2 can be obtained. An estimate for A_2 can be obtained from the point where the line intersects the ordinate; this value at this point is 100,000.

The half-time method described for the monoexponential decay can also be used to estimate λ_2. It is clear, for example, that the time it takes to decay from 100,000 to 50,000 is 82 minutes, hence

$$\lambda_2 = \frac{0.693}{82} = 0.008 \tag{G.30}$$

The equation for the line drawn through the tail portion of the data is thus:

$$A_2 e^{-\lambda_2 t} = 100000 e^{-0.008t} \tag{G.31}$$

This first step has resulted in an estimate for one of the two exponential λ_2 and the coefficient A_2. How the estimate for the second exponential λ_1 and its coefficient A_1 is obtained reveals why the technique is called curve peeling.

Step 2: Subtract $A_2 e^{-\lambda_2 t}$ from each plasma datum in Table G.4.

The idea behind curve peeling thus is to subtract $A_2 e^{-\lambda_2 t_i}$ from each datum (z_i, t_i), i.e. to subtract from each datum the contribution from the slow exponential. For the data in the tail portion of the curve, this difference should be close to zero while in the resulting modified data, i.e. that from the beginning portion of the curve, the result should approximate a monoexponential.

This is illustrated using the data in Table G.4 where the results of subtracting $A_2 e^{-\lambda_2 t_i}$ from each datum is shown in the third column of the table. The modified data are shown in Figure G.13.

One sees that the modified data plotted semi-logarithmically in Figure G.13 is close to a straight line indicating a monoexponential decay. Because the initial decay occurs rapidly, these data have been plotted using an expanded scale; this is shown in the inset to Figure G.13.

Step 3: Estimate λ_1 and A_1

Step 1 can now be repeated using the modified data to obtain estimates of λ_1 and A_1. In the example illustrated in the Figure, using the half-time method,

$$\lambda_1 = \frac{0.693}{7.9 - 1.8} \approx 0.11 \tag{G.32}$$

and A_1 equals 110,000.

Noting that the straight line through the modified data shown in the inset to Figure G.13 intersects the ordinate approximately at 110000
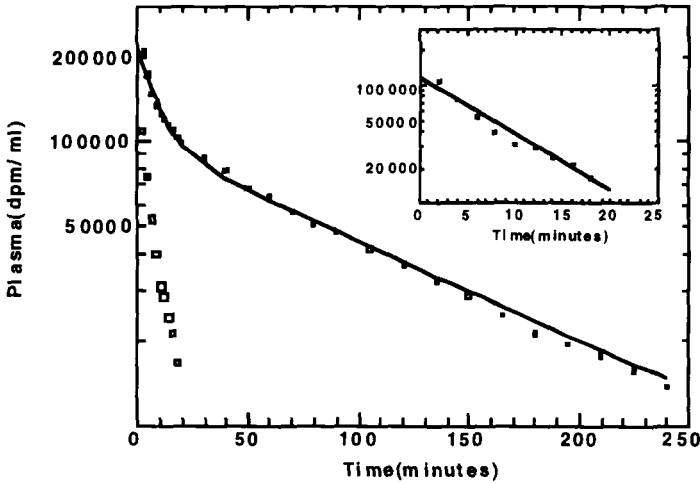
Figure G.13. Plot of the data from Table G.4 (small squares) and the modified data (large squares) obtained by subtracting $100000e^{-0.008t}$ from each datum. The inset shows the modified data to 20 minutes; an estimate of λ_1 and A_1 is obtained using the half-time method (see text). The line through the plasma data is a plot of $y(t) = 110000e^{-0.11t} + 100000e^{-0.008t}$. See text for additional explanation.

providing an estimate for A_1, one has estimates for the remaining parameters of $A_2 = 100000$, $\lambda_1 = 0.11$ and $\lambda_2 = 0.008$ are obtained. The function $y(t)$ describing the data can be written $y(t) = 110000e^{-0.11t} + 100000e^{-0.008t}$; this is shown in Figure G.13.

In Case Study 2, these were the initial estimates for the parameters of the two exponential model used for fitting this model to the data the results of which were given in Tables 8.7.5 and 8.7.6. However, one should note from the inset in Figure G.13 that the initial data may not decay monoexponentially, but biexponentially. Therefore, while the approach here can be used to estimate the parameters of the two exponential model, an analysis such as this can provide insights into whether the two or a higher order exponential model will ultimately be required.

The reader should anticipate the extension of this idea to the situation where there are more than two exponentials to estimate. Briefly, the idea of peeling the contribution of the "slow" exponential continues until only a monoexponential is left.

The "quick" curve peeling method

The traditional method of curve peeling is time consuming, especially when there are several data or more than two exponentials to be estimated. Since all that is needed is are initial estimates of λ_1 and λ_2, the question arises if there is a faster method. The answer is "yes"!

The quick method of estimating the exponentials utilizes the notion of biological half-life described previously. The relationship between the half-life and the exponential is given again below for convenience

$$\lambda = \frac{\ln 2}{t_{1/2}} \approx \frac{0.693}{t_{1/2}} \tag{G.33}$$

The application of this equation to the biexponential decay is a simple extension of the idea introduced for the monoexponential decay.

Unlike the formal curve peeling method where three steps were involved in the estimation of A_1, A_2, λ_1 and λ_2, here there are only two steps. What is avoided is the laborious step 2 above, i.e. the subtraction $A_2 e^{-\lambda_2 t}$ from the data. The price that is paid for this simplicity is that the estimates of the exponentials and coefficients may not be as accurate as those obtained in formal curve peeling, but they are usually sufficient as initial estimates for nonlinear least squares algorithms.

Step 1. Draw two lines tangent through the tail and initial decay portion of the curve.

This step can be illustrated using the data given in Table G.4 redrawn below in Figure G.14.

Step 2. Estimate λ_2, λ_1, A_1 and A_2

Using these tangent lines and the notion of biological half-life as expressed in (G.14), one can immediately estimate the exponentials.

To estimate λ_2, as illustrated in Figure G.14, using line 2, one sees the half-time calculated as the time to decay from 40000dpm/ml to 20000dpm/ml is about 85 minutes. Thus

$$\lambda_2 = \frac{\ln 2}{t_{1/2}} = \frac{\ln 2}{82} \approx \frac{0.693}{85} = 0.008 \tag{G.34}$$

The coefficient A_2 can be estimated from the intercept of the tangent line with the y-axis. This is also illustrated in Figure G.14, and is 100000.

The estimation of λ_1 is simply a repetition of the above steps only using the tangent line drawn through the rapidly decaying portion of the curve (line 1 in Figure G.14). As illustrated in the Figure, the half-time is being calculated as the time it takes to decay from 40000cpm/ml
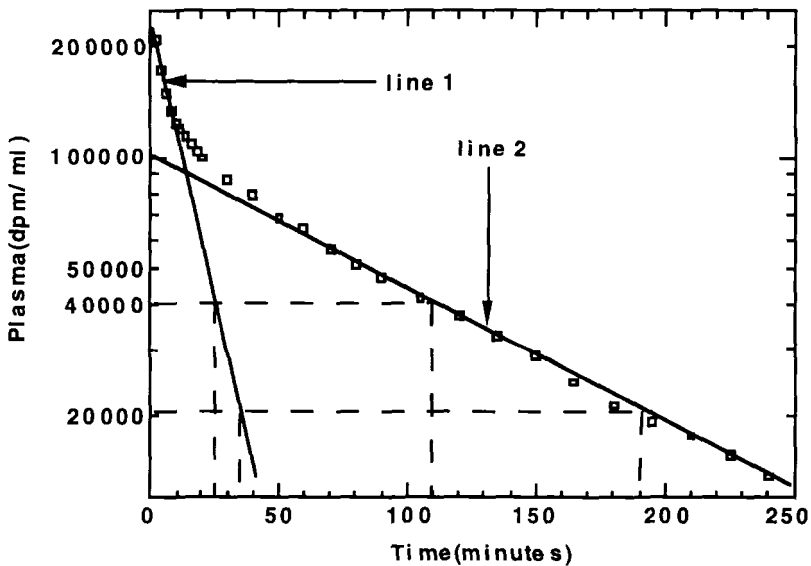
Figure G.14.   The data from Table G.4 are shown together with tangent lines through the tail portion of the curve (line 2) and the initial decay (line 1). The line through the tail portion intersects the ordinate at A_2 and that through the initial decay at $(A_1 + A_2$. See text for additional explanation.

to 40000cpm/ml along the line; this time is about 10 minutes hence

$$\lambda_1 = \frac{\ln 2}{10} \approx \frac{0.693}{10} = 0.069 \qquad (G.35)$$

Notice this estimate differs from that obtained from formal curve peeling. This is because the affect of the tail portion has not been subtracted from the data. Estimates of λ_1 obtained in this manner will usually be less than those obtained when formal curve peeling is used. Normally this will not cause problems for initial estimates for exponentials.

   An estimate for the parameter A_1 can be obtained as follows. The intercept of the tangent line representing the rapid decay provides an estimate for $A_1 + A_2$; in this case, $A_1 + A_2$ can be estimated equal to 210000. Using the estimate of 100000 for A_2 obtained above, one can estimate A_1 by subtracting A_2 from this value; A_1 is thus 100000. Thus $y(t) = 110000e^{-0.069t} + 100000e^{-0.008t}$. Figure G.15 shows the prediction

of $y(t)$ by using the results of the quick peeling method is not quite as good as the one obtained by the formal curve peeling method.
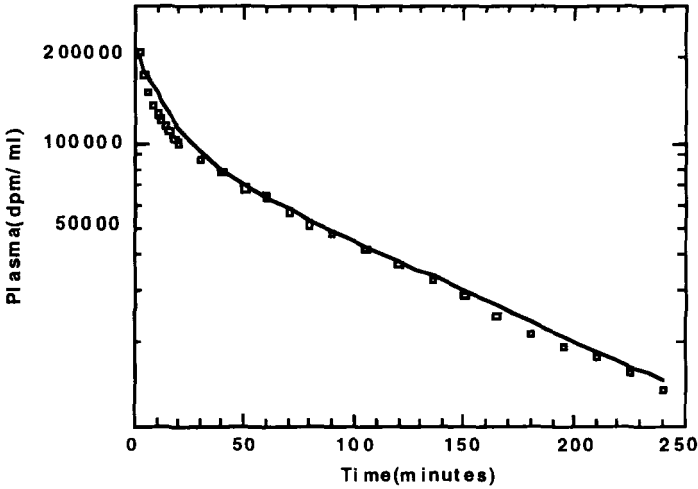
Figure G.15. Plot of $y(t) = 110000e^{-0.069t} + 100000e^{-0.008t}$ compared with the data given in Table G.4.

In summary, if $t_{1/2}^f$ and $t_{1/2}^s$ are the half times for the fast and slow exponential respectively, the general equations for the estimation of λ_2 and λ_1 using this quick method are

$$\lambda_2 \approx \frac{0.693}{t_{\frac{1}{2}}^s} \qquad (G.36)$$

$$\lambda_1 \approx \frac{0.693}{t_{\frac{1}{2}}^f} \qquad (G.37)$$

where $t_{\frac{1}{2}}^s$ and $t_{\frac{1}{2}}^f$ are the biological half-lives associated with the slow, s, and fast, f, decays respectively.

Biexponential rises: the constant and primed, constant infusion of a tracer

A "biexponential rise" is often used to describe tracer data following a constant or primed, constant infusion of tracer into the accessible pool

from which samples are obtained (where the quotation marks are used for the same reason they were for the monoexponential rise described previously). It is described by the equation

$$y(t) = A_0 + A_1 e^{-\lambda_1 t} + A_2 e^{-\lambda_2 t} \tag{G.38}$$

The plateau value A_0 is always positive, while the parameters A_1 and A_2 are can be either positive or negative depending upon the situation.

Case 1: The constant infusion

The biexponential function describing tracer data in the accessible pool following a constant infusion of tracer into a single accessible pool noncompartmental system is

$$y(t) = A_0 + A_1 e^{-\lambda_1 t} + A_2 e^{-\lambda_2 t} \qquad 0 \le t \le T \tag{G.39}$$

where $A_0 = -(A_1 + A_2)$, A_1 and A_2 are negative, and T is the time at which the infusion stops. Notice $y(0) = 0$. An example is shown below in Figure G.16.

How are estimates of λ_1 and λ_2 obtained? As described for the monoexponential case, there is only one method which will provide reliable estimates. For the biexponential case, the data must be modified before an adaption of the methods used to estimate λ_1 and λ_2 in the biexponential decay can be used. The steps involved are the following.

Step 1. Obtain an estimate of the plateau A_0.

Step 2. Subtract this value from each datum producing a modified set of data.

Step 3. Multiply each modified datum by -1 thereby producing yet another modified set of data. This set of data will decay biexponentially.

Step 4. Obtain estimates of λ_1 and λ_2 using the methods described for the biexponential decay.

In terms of (G.39), subtracting A_0 from each datum will eliminate the constant term from (G.39) leaving only $A_1 e^{-\lambda_1 t} + A_2 e^{-\lambda_2 t}$. Multiplying the modified data by -1 will convert this into $-A_1 e^{-\lambda_1 t} - A_2 e^{-\lambda_2 t}$ which is a biexponential decay whose zero time value is $-(A_1 + A_2)$. Therefore, processing the data in this manner will transform the original data from a biexponential rise into a set of data which decay biexponentially; the exponentials λ_1 and λ_2 andcoefficients A_1 and A_2 can then be estimated using the method for biexponential decays.

Is there a quicker method to estimate λ_1, λ_2 A_1 and A_2? Strictly speaking, the answer is no. The reason why is that the counterpart for (G.12), $\frac{dy}{dt}|_{t=0}$ is more complicated; the derivative of (G.39) evaluated at time zero is

$$\frac{dy}{dt}\Big|_{y=0} = -A_1 \lambda_1 - A_2 \lambda_2 \tag{G.40}$$

time	plasma
1	111
2	264
3	324
4	391
5	490
6	569
8	763
10	879
15	1210
20	1377
25	1728
30	1815
40	2238
50	2613
60	2829
90	3366
120	4015
150	4446
180	4679
210	4850
240	5214
270	5463
300	5319
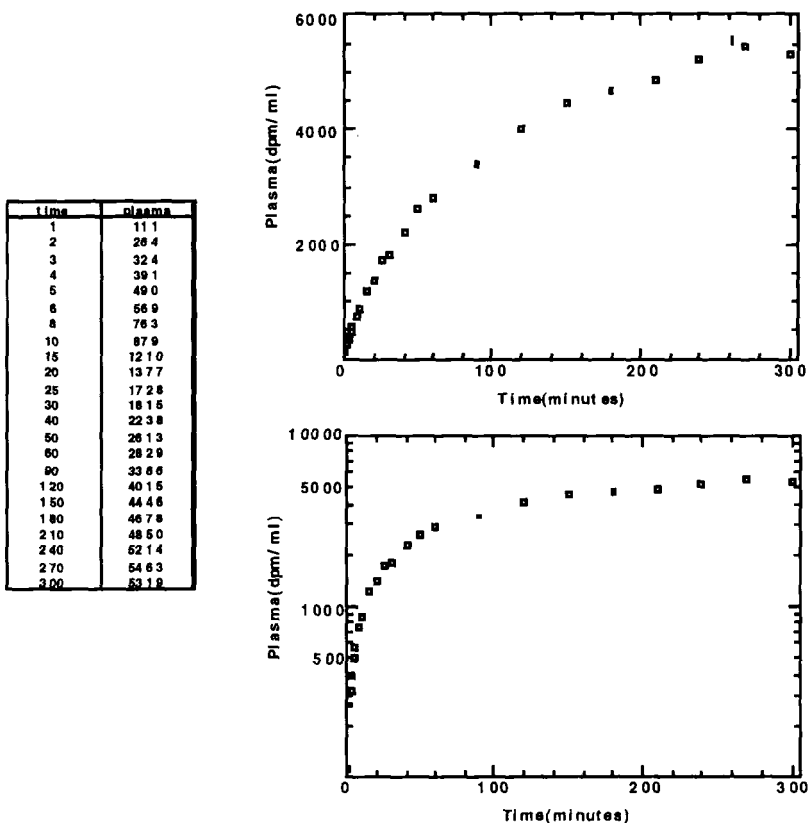
Figure G.16. An example of a biexponential rise. The data are shown in the table inset into the figure. The top and lower figures show the data plotted linearly and semi-logarithmically respectively.

While it is possible to estimate the plateau A_0, the plateau value, just as it was possible to estimate A in the monoexponential case, one cannot estimate the individual coefficients A_1 and A_2 even with estimates of λ_1 and λ_2.

It is sometimes possible to adapt the half-life method to obtain approximate estimates of λ_1 and λ_2. This adaptation, however, is sometimes unreliable. If this is the case, it is always possible to use the original method discussed above.

The "quick" method can be described using the data shown in Figure G.16, and is the counterpart for the monoexponential rise case to passing from an arbitrary point on a curve to the point half-way between that point and the plateau. As with the "quick" method for the biexponential decay, one assumes that if $\lambda_1 > \lambda_2$, then in the initial portion of the curve the term $A_1e^{-\lambda_1 t}$ will predominated while towards the plateau, later in time, the term $A_2e^{-\lambda_2 t}$ will predominated. For the initial portion of the curve, one can define a half-time by solving

$$A_0 + \frac{A_1}{2}e^{-\lambda_1 t_1} = A_0 + A_1e^{-\lambda_1(t_1 + t_{1/2})} \qquad (G.41)$$

for $t_{1/2}$. This equation can be used to derive the standard relationship between the half-time and λ_1. In this equation, the terms $\frac{A_2}{2}e^{-\lambda_2 t_1}$ and $\frac{A_2}{2}e^{-\lambda_2(t_1 + t_{1/2})}$ are assumed to be negligible. Similarly, as illustrated in the following figure, an estimate for λ_2 can be derived.

The problem with this method, as noted previously, is that although an estimate for the plateau $A_1 + A_2$ can be obtained, there is no reliable "quick" way to estimate the individual A_1 and A_2. There is a method that can sometimes work. One can draw a tangent line representing the slowly rising portion of the curve towards the plateau when the data are plotted in semi-logarithmic form. The difference where this line intersects the ordinate and the plateau can be used as an estimate for A_2. The coefficient A_1 can be estimated as the difference between the plateau value and the estimated value for A_2. This approach is illustrated in Figure G.17.

Case 2: The primed, constant infusion

If a primed, constant infusion is used, the biexponential function describing the "rise" is

$$y(t) = A_0 + A_1e^{-\lambda_1 t} + A_2e^{-\lambda_2 t} \qquad 0 \le t \le T \qquad (G.42)$$

where $A_0 \ne -(A_1 + A_2)$, A_1 and A_2 can be either positive or negative, and T is the time at which the infusion stops.

Estimating λ_1 and λ_2 in this case parallels the arguments developed for the monoexponential "rise" following the primed, constant infusion. Again, one must deal with the possibilities that the data are rising or falling. The steps to obtain reliable estimates of λ_1 and λ_2 and the coefficients are given below.

Step 1. Obtain an estimate of the plateau A_0.

Step 2. Subtract this value from each datum producing a modified set of data.
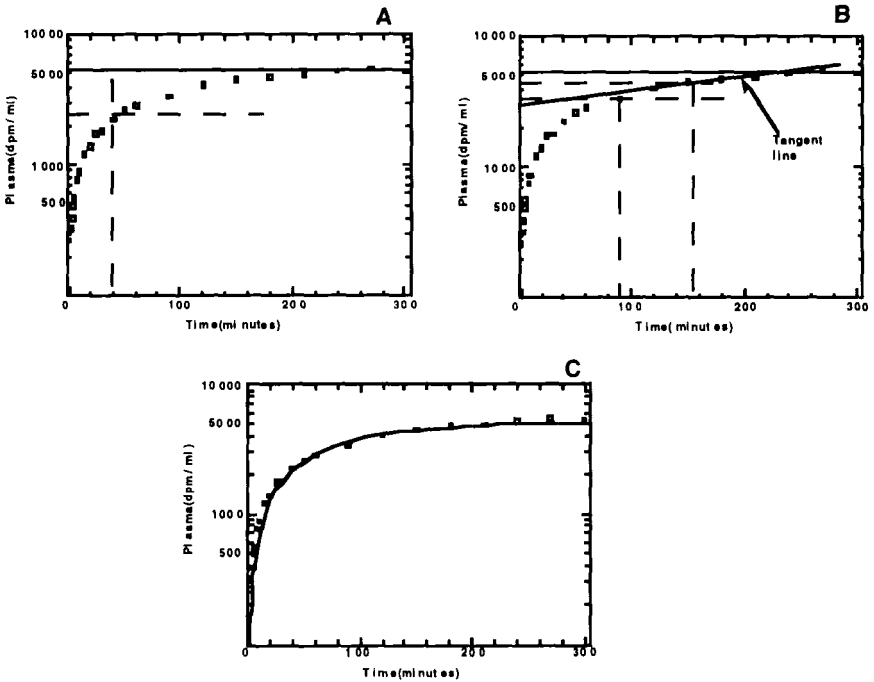
Figure G.17. Illustration of the "half-life" method to estimate λ_1 and λ_2, and A_1 and A_2 from data displaying a biexponential rise. Panel A shows an estimate of the plateau value, $-(A_1 + A_2)$, equals 5200. The time it takes to reach half of that value, 2600, is approximately 40 minutes. Using the half-time method, an estimate of 0.02 for λ_1 can be obtained. Panel B shows again the plateau value of 5200. A point of 3200 is chosen on the slowly rising portion of the curve, and, as indicated by the dashed line parallel to the abscissa on the figure, the time it takes to reach half way to the plateau (indicated by the dashed line through 4200) is approximately 65 minutes. Again, using the half time method, an estimate of 0.01 for λ_2 can be obtained. A line drawn tangent to the slowing rising portion of the curve intersects the ordinate at about 3000; this provides an estimate for $-A_2$. With an estimate of 5200 for the plateau, an estimate of -2200 can be obtained for A_1. Panel C shows a plot of $y(t) = 5200 - 2200e^{-0.02t} - 3000e^{-0.01t}$.

If the resulting data are negative which corresponds to the case when the data are rising to a plateau, the following steps must be employed.

Step 3. Multiply each modified datum by -1 thereby producing yet another modified set of data.

Step 4. Obtain estimates of A_1, A_2, λ_1 and λ_2 using the methods described for the biexponential decay.

If the data following step 2 are positive corresponding to the data falling to a plateau, estimates of A_1, A_2, λ_1 and λ_2 can be obtained without step 3.

The rationale for this strategy is the same as for the constant infusion case with the modifications discussed originally for the monoexponential rise following the primed, constant infusion applied.

The quick method described above for the constant infusion case can also be used in this case when modified as was done for the monoexponential situation. The difference is that rather than starting from a value of 0 at time 0 to estimate λ_1, one starts with the initial value of $A_0 + A_1 + A_2$. If the data are rising, one can adapt the method for the constant infusion as illustrated in Figure G.9. If the data are falling, one can estimate estimate λ_1 and λ_2 using the quick method described for biexponential decays. Finally, as discussed for the monoexponential case, one can obtain an estimate for the smaller exponential λ_2 as the quotient of the priming dose divided by the infusion rate.

Biexponential washouts

Describing biexponential washouts is a direct extension of the ideas given in for the monoexponential washout. An example is given in Figure G.18.

The discussion given for the monoexponential washout provides a means by which to describe data following a constant or primed, constant infusion. The equation which provides this description, (G.38), is given a more precise formalism below

$$y_r(t) = A_0 + A_1 e^{-\lambda_1 t} + A_2 e^{-\lambda_2 t} \qquad 0 \le t \le T \qquad \text{(G.43)}$$

where the r in $y_r(t)$ is used to denote the rising portion of the curve. This equation, which is the counterpart to (G.22) for the monoexponential case, is valid only during the infusion. That is, if the infusion starts at time zero and stops at time T, $y_r(t)$ is valid only for $0 \le t \le T$.

As before, consider first an example of how to describe a biexponential washout. The data shown Figure G.18 will be used. The rising portion are the same data as those shown in Figure G.16.

The data given in Figure G.18 can be described during the infusion period by the function $y(t) = 5200 - 2200 e^{-0.02t} - 3000 e^{-0.01t}$. That is, for any specific time $\hat{t}$ between 0 and 300 minutes, a datum at that point is approximately equal to $y(\hat{t}) = 5200 - 2200 e^{-0.02\hat{t}} - 3000 e^{-0.01\hat{t}}$. In particular, when $t = 300$, i.e. when the infusion is stopped, the calculated tracer concentration is $y(300) = 5200 - 2200 e^{-0.02 \cdot 300} - 3000 e^{-0.01 \cdot 300}$.

time	plasma	time	plasma
1	111	305	5228
2	264	310	4679
3	324	315	4361
4	391	320	4286
5	490	325	3792
6	569	330	3781
8	763	360	2842
10	879	390	2230
15	1210	420	1707
20	1377	450	1261
25	1728	480	932
30	1815		
40	2238		
50	2613		
60	2829		
90	3366		
120	4015		
150	4446		
180	4679		
210	4850		
240	5214		
270	5463		
300	5319		
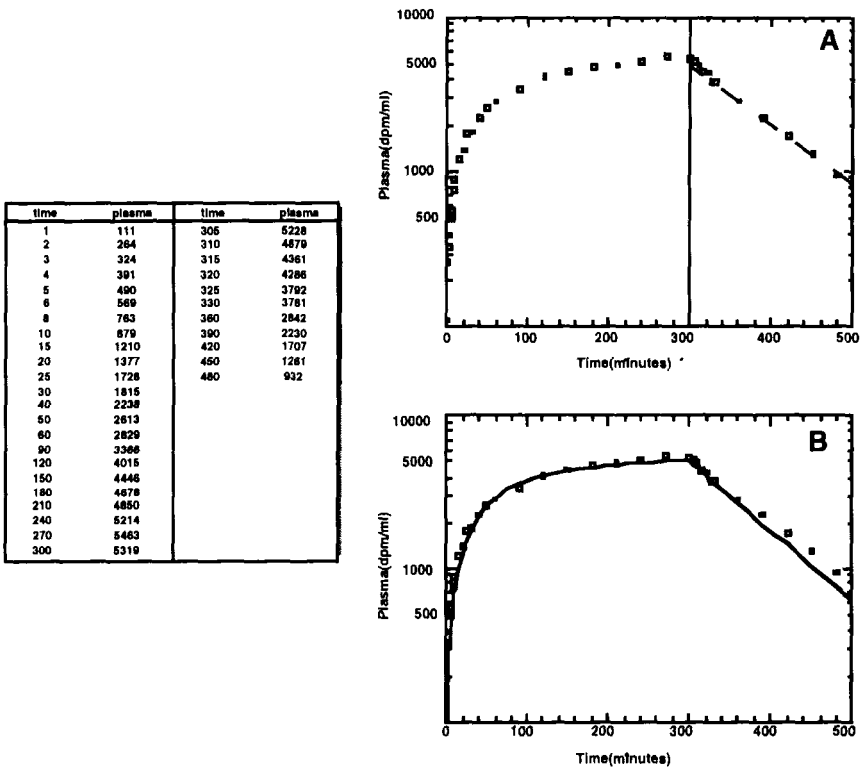
Figure G.18. An example of a biexponential rise and washout. The data are given in the tabular inset. See text for explanation.

How does this amount of material decay from the system when the infusion stops? As with the monoexponential case, one can regard this decay as equivalent to injecting a bolus of magnitude $y(300)$ at time 300. This is the "total injected"; thinking in terms of (G.28), the expression for the biexponential decay, this numerically is equal to $A_1 + A_2$ in this expression. Thus besides offsetting the time, as described for the monoexponential case, by utilizing the expression $(t - 300)$ in this example, $y(300)$ must also be subdivided into two constituent parts one of which is the coefficient of the exponential containing λ_1 and the other with λ_2. If α is the fraction associated with λ_1, then $(1 - \alpha)$ is the fraction as-

sociated with λ_2. This gives rise to the expression for the biexponential decay:

$$
\begin{aligned}
y_w(t) \; = \; & \alpha \cdot y(300)e^{-\lambda_1(t-300)} \\
& +(1-\alpha) \cdot y(300)e^{-\lambda_2(t-300)} \qquad t \geq T
\end{aligned}
\tag{G.44}
$$

In this expression, it is the constant α which partitions $y(300)$ so that $\alpha \cdot y(300)$ and $(1-\alpha) \cdot y(300)$ are the appropriate coefficients of the exponential terms which will result in a description of the data. In fitting this function to the washout, both the exponentials λ_1 and λ_2 and the linear parameter α must be estimated.

An estimate for α can be obtained as indicated in Figure 18, Panel A. Here one sees that most of the material, approximately 90%, decays following the smaller exponential. Thus an estimate of 0.1 for α can be obtained. Using the estimates for λ_1 and λ_2 obtained from the rising portion of the curve, $y_w(t)$ given in (G.44) can be written. Panel B in Figure G.18 shows a plot of

$$
\begin{aligned}
y(t) \; = \; & 5200 - 2200e^{-0.02t} - 3000e^{-0.01t} \qquad t \leq 300 \\
= \; & \alpha \cdot y(300)e^{-\lambda_1(t-300)} + (1-\alpha) \cdot y(300)e^{-\lambda_2(t-300)} \qquad t \geq T
\end{aligned}
\tag{G.45}
$$

It should be noted that one could use the decaying portion of the curve to estimate λ_1 and λ_2 respectively. This may produce slightly different estimates of λ_1 and λ_2, but this should not materially affect the estimates as used in a nonlinear regression algorithm.

What happens in the general case? The function describing the exponential "rise" during the primed constant infusion is:

$$
y_r(t) = A_0 + A_1 e^{-\lambda_1 t} + A_2 e^{-\lambda_2 t}
\tag{G.46}
$$

where the subscript r indicates the rising portion of the curve. Suppose in a given experiment, the infusion is stopped at time T, and data are collected during the washout phase. Then the calculated amount of material in the accessible pool at T is approximated by $y(t)$ evaluated at T:

$$
y_r(T) = A_0 + A_1 e^{-\lambda_1 T} + A_2 e^{-\lambda_2 t}
\tag{G.47}
$$

The equation to describe the biexponential decay of the washout is then:

$$
y_w(t) = \alpha \cdot y_r(T)e^{-\lambda_1(t-T)} + (1-\alpha) \cdot y_r(T)e^{-\lambda_2(t-T)}
\tag{G.48}
$$

where the subscript w indicates the washout portion of the curve. At time T, of course, $y_r(T) = y_w(T)$.

Biexponential rises and falls

In the two accessible pool noncompartmental model, a tracer introduced in one accessible pool that is measured in the second accessible pool will, following a bolus injection of tracer, rise and then fall. This situation is illustrated in Figure G.19.
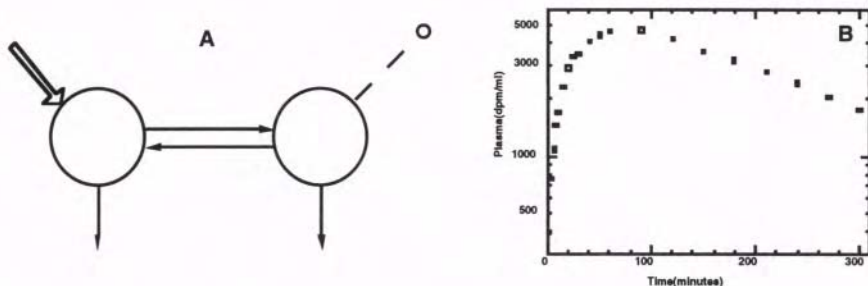
Figure G.19.   A: The two accessible pool noncompartmental model showing label being introduced in one pool and sampled from the second. B: A representative set of data collected from pool 2 following the bolus injection of a tracer into pool 1.

Notice in this Figure, there are no "recirculation-exchange" arrows associated with either accessible pool since, in the case of two exponentials, such arrows do not exist.

Data such as these which rise first and then fall can be described by a sum of two exponentials

$$y(t) = -Ae^{-\lambda_1 t} + Ae^{-\lambda_2 t} \tag{G.49}$$

where A is positive. Notice (G.49) with the additional assumption that $\lambda_1 > \lambda_2$ ensures that $y(0) = 0$ and $y(t) > 0$ for $t > 0$.

How does one obtain initial estimates for A, λ_1 and λ_2 in (G.49) for data such as those shown in Figure G.19? Two steps, as illustrated in Figure G.20, are involved.

Since the falling portion of the curve is decaying monoexponentially, one can estimate the exponential, say λ_2, associated with it. If one assumes by the time the data are decaying monoexponentially that the contribution in (G.49) from $-Ae^{-\lambda_1 t}$ is negligible, then what remains in the expression for $y(t)$ is the term $Ae^{-\lambda_2 t}$. Using the technique for monoexponential decays, one can immediately estimate A and λ_2 by

drawing a tangent line through the decaying data, and extrapolating this line to the ordinate to obtain the estimate for A.

To obtain an estimate of λ_1, one can use the quick method for the monoexponential rise described previously. These are illustrated in Figure G.20. This example illustrates the case where the tracer is injected as a bolus into one accessible pool and measured in the second accessible pool. If the tracer is infused either as a constant or primed constant infusion into one accessible pool and measured in the second, then the product will also rise and may fall depending upon the experimental
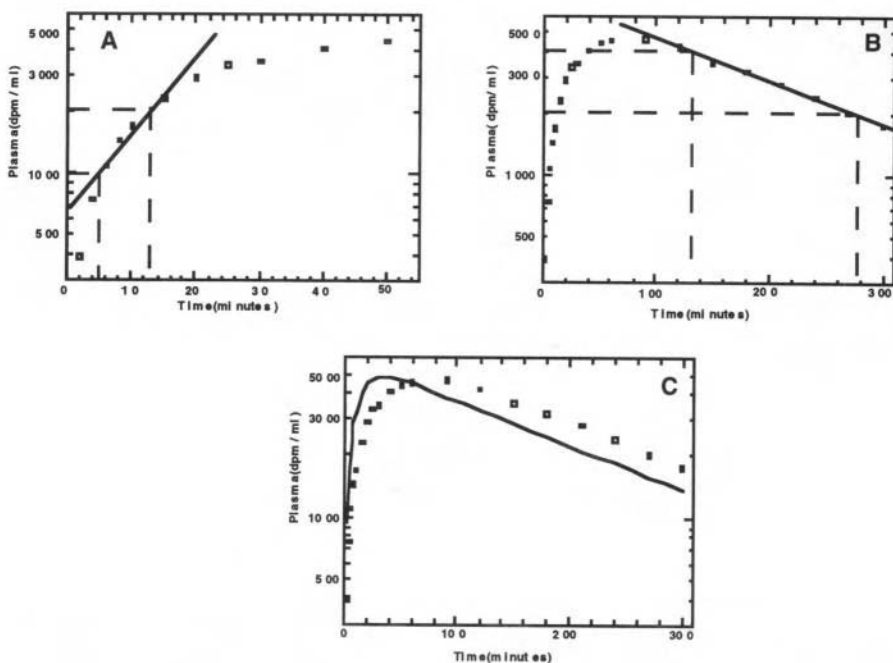
Figure G.20. A: The initial rise is plotted on an expanded scale to aid in the estimate of λ_1. A line tangent to the curve is drawn as indicated, and a half-time of the rise (as opposed to the fall in the biexponential decay situation) is 8 minutes resulting in an estimate for λ_2 of 0.09. B: A line drawn through the tail portion of the curve is used to estimate λ_1. The half-time is 130 giving an estimate of λ_1 of .005. An estimate of A can be obtained by extrapolating the tangent line to the ordinate; the estimate is 6100 (not shown). Panel C: A of the function $y(t) = 6100e^{-0.005t} - 6100e^{-0.09t}$.

protocol. A sum of two exponential can still be used to describe the data, but the discussion must be modified to take into account different experimental protocols.

Initial estimates of models with more than two exponentials

Introduction

In the previous two sections, techniques to obtain initial estimates of the exponentials for monoexponential and biexponential models were given. In this section, these techniques will be expanded to permit the investigator to obtain initial estimates for the exponentials and coefficients in multiexponential models. The example given will be for three exponential models since the ideas carry over directly to models with more than three exponentials.

Multiexponential decays: the bolus injection of tracer

The general expression for the multiexponential function describing a decay is:

$$y(t) = A_1 e^{-\lambda_1 t} + A_2 e^{-\lambda_2 t} + \cdots + A_n e^{-\lambda_n t} \tag{G.50}$$

where $y(0) = A_1 + \cdots + A_n$, $A_i > 0$ for all i, and the λ_i are exponentials to be estimated.

As with the biexponential decay, the curve peeling method will produce reliable estimates for the exponentials λ_i. Assuming the exponentials satisfy the relationship $\lambda_1 > \lambda_2 > \cdots > \lambda_n$, the steps involved are the following.

1. Estimate A_n and λ_n from the tail portion of the curve as was done with the biexponential decay.

2. Subtract $A_n e^{-\lambda_n t}$ from each datum z_i producing a modified set of data $z_i - A_n e^{-\lambda_n t_i}$. This modified set of data can be described by

$$y_1(t) = A_1 e^{-\lambda_1 t} + A_2 e^{-\lambda_2 t} + \cdots + A_{n-1} e^{-\lambda_{n-1} t} \tag{G.51}$$

3. Estimate A_{n-1} and λ_{n-1} from the modified data set.

4. Subtract $A_{n-1} e^{-\lambda_{n-1} t}$ from the modified data producing $z_i - A_n e^{-\lambda_n t_i} - A_{n-1} e^{-\lambda_{n-1} t}$.

This process continues until all coefficients and exponentials have been estimated, clearly a tedious exercise.

In what follows, three approaches will be discussed for a sum of three exponentials. The last which is an empirical method is the easiest to use in moving from three exponentials to four and more. It will also be used when estimating the rate constants $k_{i,j}$ in multicompartmental models. The three exponential model to be discussed is

$$y(t) = A_1 e^{-\lambda_1 t} + A_2 e^{-\lambda_2 t} + A_3 e^{-\lambda_3 t} \qquad (G.52)$$

For the first method, consider the data given in Figure G.13. The inset in this figure indicated that the data modified by subtracting the contribution of the tail portion of the curve from the remaining data could be biexponential rather than monoexponential. These modified data are shown in Panel A in Figure G.21 below. If one assumes $A_3 e^{-\lambda_3 t}$ describes the decay of the tail portion of the curve, then as before $A_3 = 100,000$ and $\lambda_3 = 0.008$. Rather than continuing the formal curve peeling method, one can use the quick method to estimate the coefficients A_1 and A_2 and the exponentials λ_1 and λ_2 of (G.52). This is indicated in Figure G.13 where estimates for A_1 and A_2 of 100,000 and 65,000 are obtained, and for λ_1 and λ_2 of 0.17 and 0.07 respectively.
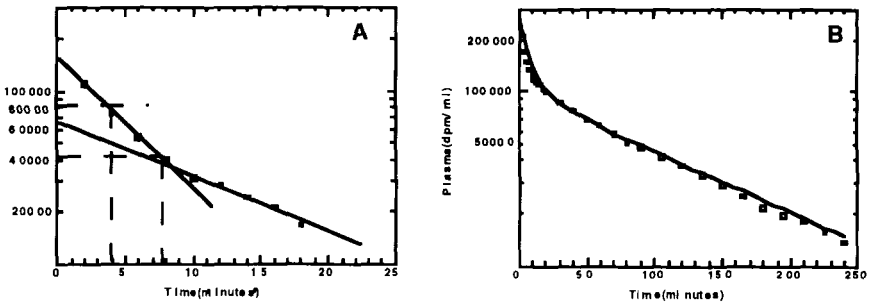
Figure G.21. A: A plot of the modified data from Figure G.13 showing how to estimate A_1, A_2, λ_1 and λ_2 of (G.52). B: A plot of $y(t) = 100000e^{-0.17t} + 65000e^{-0.07t} + 100000e^{-0.008t}$.

The method is a direct extension of the quick method used for a sum of two exponentials, but it suffers from a difficultly in estimating more than two exponentials. The reason is that in this method, the contribution of the individual exponentials is not subtracted out as it is in curve peeling. If the exponentials are ordered $\lambda_1 > \lambda_2 > \lambda_3$, then the estimate for λ_3 is the most reliable and λ_1 the least reliable. In addition, one can only

estimate the sum of the A_i and not the individual A_i as was the case with a sum of two exponentials.

Figure G.22 will be used to show how the quick method will work with a sum of three exponentials. Notice in this example the initial portion of the decay curve had to be plotted on an expanded scale in order to estimate A_1, A_2, λ_1 and λ_2 more conveniently.
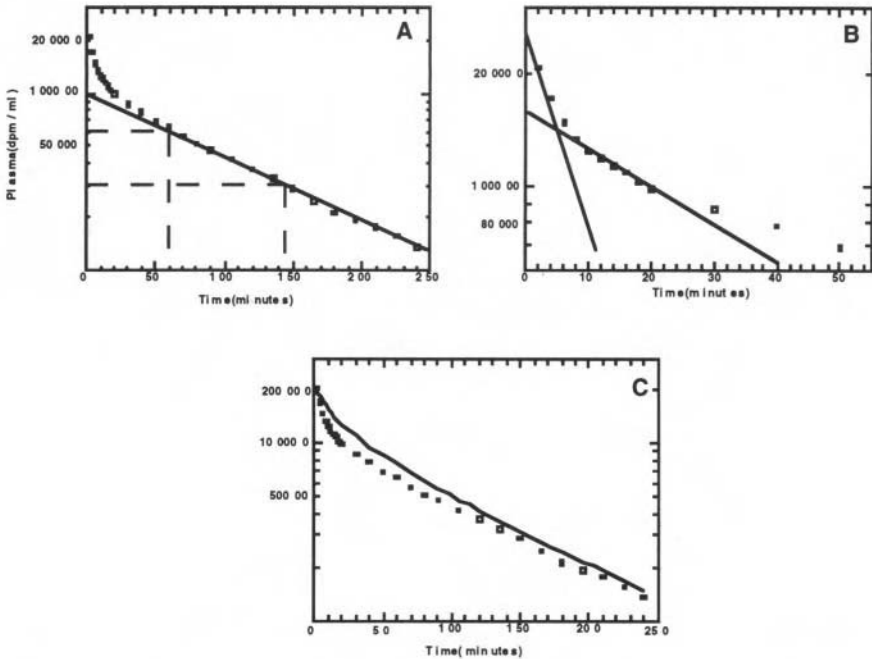
Figure G.22. A: The data given in Figure G.13 with a straight line drawn through the tail portion of the curve to estimate $A_3 = 100,000$ and $\lambda_3 = 0.008$ of (G.52). B: The initial decay of the data given in Figure G.13 plotted on an expanded scale. The quick method has been used to estimate $A_1 = 50,000$, $A_2 = 60,000$, $\lambda_1 = 0.12$ and $\lambda_2 = 0.024$. C: A plot of $y(t) = 50000e^{-0.12t} + 60000e^{-0.024t} + 100000e^{-0.008t}$.

Finally, there is a third even quicker method that can be used; it is an empirical method. As one goes through the process of determining the number of exponential required to describe set of data, suppose as in this situation the data have been fitted by a sum of two exponentials. Since Case Study 2 is being used here, initial estimates for a sum of two

exponentials were described in the previous section of this Appendix. As described in §8.7, a best fit by a sum of two exponentials is given by $y(t) = 122044e^{-0.14t} + 107211e^{-0.00877t}$. That is, $A_1 = 122044$, $A_2 = 107211$, $\lambda_1 = 0.14$ and $\lambda_2 = 0.0087$. This information can actually be used to obtain initial estimates for the three exponential model (G.52).

First, since the tail portion of the curve can be best determined in general, the initial estimate obtained for A_2 and λ_2 of the sum of two exponentials can be used to estimate A_3 and λ_3 in (G.52). Thus $A_3 = 100000$ and $\lambda_3 = 0.008$. Knowing from the sum of two exponentials that the initial decay is described by $122044e^{-0.14t}$, one can obtain initial estimates for the coefficients A_1 and A_2, and of the exponentials λ_1 and λ_2 as follows. To obtain an estimate of λ_2, simply find the average of the two exponentials best describing the biexponential decay. In this case, this is the average of 0.14 and 0.0087 which is approximately 0.07. An estimate for λ_1 can be found by doubling the most rapid exponential of the biexponential; in this case, that would equal $2 \cdot 0.14 = 0.28$. Estimates for A_1 and A_2 can be obtained by dividing the coefficient of the rapid exponential of the biexponential, and adding an additional small amount to each. In this case, that coefficient is 122,044 hence set $A_1 = A_2 = 65000$. The result of this strategy is shown in Figure G.23A.
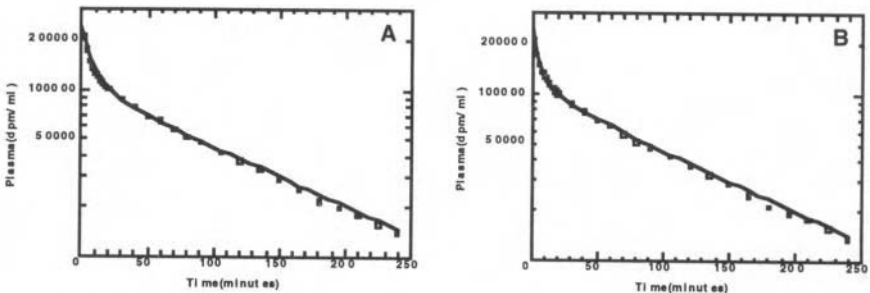
Figure G.23.   A: A plot of $y(t) = 65000e^{-0.28t} + 65000e^{-0.07t} + 100000e^{-0.008t}$. B: A plot of $y(t) = 65000e^{-0.5t} + 80000e^{-0.16t} + 20000e^{-0.025t} + 98000e^{-0.008t}$. See text for additional explanation.

It is instructive to carry this one more step to a sum of four exponentials. In §8.7, it was found that the best fit to the data by a sum of three exponentials was $y(t) = 126173e^{-0.27t} + 38783e^{-0.042t} + 98298e^{-0.0083t}$. How this information can be used to obtain initial estimates of the coef-

ficients and exponentials of a sum of four exponentials $y(t) = A_1 e^{-\lambda_1 t} + A_2 e^{-\lambda_2 t} + A_3 e^{-\lambda_3 t} + A_4 e^{-\lambda_4 t}$ is an extension of what was done in passing from two to three exponentials. First, since the tail portion of the curve is the most reliable to estimate, one can let $A_4 = 98000$ and $\lambda_4 = 0.008$. A_3 can be estimated as half the value of the coefficient of the second term of the sum of three exponentials; as noted, this value is close to 40,000 so $A_3 = 40,000$. An estimate for λ_3 can be obtained as the average between the middle and slowest exponential of the sum of three exponentials; in this case, these values are 0.042 and 0.0083 so $\lambda_3 = 0.025$. Repeating this process, one can obtain estimates for A_2 and λ_2 equal to 80,000 and 0.16 respectively (the number 80,000 arises as the sum of approximately one half of the value for the coefficient of the rapid and middle term of the sum of three exponentials, 126,173 and 38,783 respectively). Finally, an estimate of λ_1 can be obtained, as before, by doubling 0.27 (approximately 0.5), and an estimate for A_1 can be obtained as slightly more than one half of 126,173. The results of this strategy are shown in Figure G.23B.

This strategy is usually very reliable when one is trying to determine model order. To be successful, one must go through the process of formally fitting each sum of exponentials to the data before proceeding to a model of higher order. If one wanted to proceed directly to a sum of three exponentials, some form of curve peeling would have to be used.

While in what follows, this final strategy can be applied to multiexponential rises, or rises and falls, more "formal" methods will be discussed. This method, however, will be very useful in understanding how quickly to obtain initial estimates of the rate constants k_{ij} in linear, multicompartmental models.

Multiexponential rises: the constant and primed, constant infusion

A "multiexponential rise" is often used to describe tracer data following a constant or primed, constant infusion of tracer into the accessible pool from which samples are obtained (where the quotation marks are used for the same reason they were for the monoexponential and biexponential rise described earlier). It is described by the equation

$$y(t) = A_0 + A_1 e^{-\lambda_1 t} + \cdots + A_n e^{-\lambda_n t} \qquad 0 \le t \le T \qquad \text{(G.53)}$$

where A_0 is the plateau value, the parameters A_i can be either positive or negative depending upon the situation, and T is the time at which the infusion stops.

Case 1: The constant infusion

The multiexponential function describing tracer data in the accessible pool following a constant infusion of tracer into a single accessible pool noncompartmental system is

$$y(t) = A_0 + A_1 e^{-\lambda_1 t} + \cdots + A_n e^{-\lambda_n t} \qquad 0 \leq t \leq T \qquad (G.54)$$

where $A_0 = -(A_1 + A_2 + \cdots + A_n)$, and the A_i are negative. Notice this means $y(0) = 0$.

The estimates of the λ_i are obtained using the same methods described for the biexponential rise following the constant infusion of tracer. The steps involved are the following.

Step 1. Obtain an estimate of the plateau A_0.

Step 2. Subtract this value from each datum producing a modified set of data.

Step 3. Multiply each modified datum by -1 thereby producing yet another modified set of data.

Step 4. Obtain estimates of the λ_i and A_i using the methods described for the multiexponential decay.

The rationale for this is exactly the same as that given for the mono-exponential rise. Subtracting A_0 from each datum will eliminate the constant term from (G.54) leaving only $A_1 e^{-\lambda_1 t} + \cdots + A_n e^{-\lambda_n t}$. Multiplying the modified data by -1 will convert this into $-(A_1 e^{-\lambda_1 t} + \cdots + A_n e^{-\lambda_n t})$ which is a multiexponential decay whose zero time value is A_0. Therefore, processing the data in this manner will transform the original data from a multiexponential rise into a set of data which decay multiexponentially; both sets will be characterized by the same coefficients A_i and exponentials λ_i.

It is possible use the quicker method described previously to estimate the λ_i, but as noted in this discussion, the estimates can sometimes be unreliable. Application of this technique to the data shown in Figure G.24. As with the biexponential case, the key in using this method is drawing the tangent lines to the curve, one at the beginning initial rise, and the other as the curve approaches the plateau. These are illustrated in the figure.

One can estimate A_3 as the difference between where the line L3 intersects the ordinate and the plateau value. Similarly $A_2 + A3$ can be estimated as the point where L2 intersects the ordinate from which an estimate for A_2 can be obtained. Since the plateau value equals A_0 and $A_0 = -(A_1 + A_2 + A_3)$, and estimate for A_1 can be obtained.

As noted previously, if a best fit of these data by a two exponential model had been obtained, then paralleling the strategy discussed for
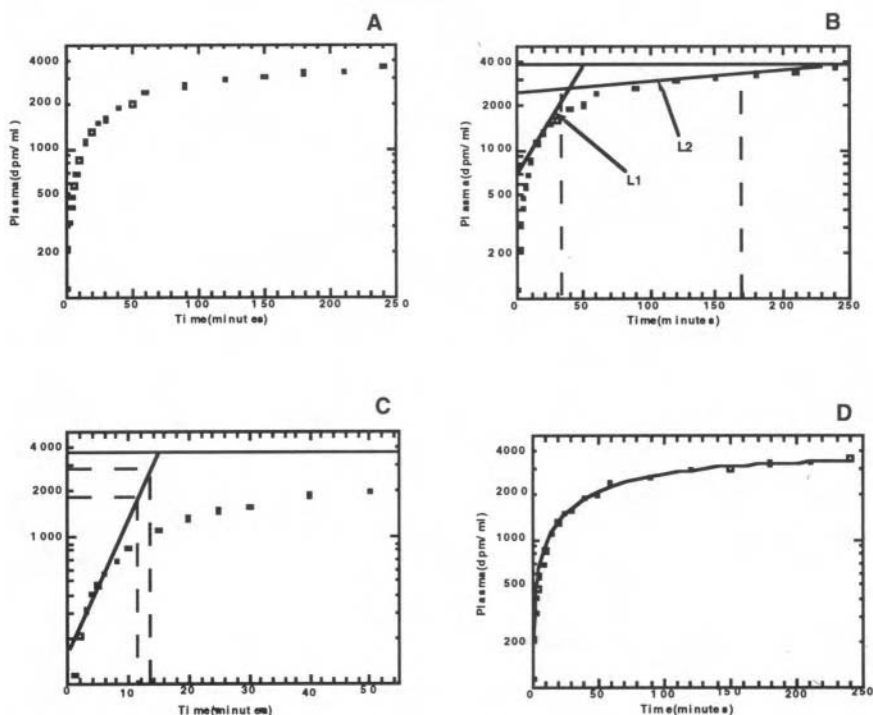
Figure G.24. A: A set of data rising to a plateau following a constant infusion of a tracer. B: Two arbitrary lines L_2 and L_3 are drawn describing the approach of the "tail" to the plateau and a mid-slope (lines are indicated by $L2$ and $L3$ with arrows point the lines respectively. Half times of 35 and 170 minutes produce estimates for λ_2 and λ_3 of 0.02 and 0.004 respectively as indicated on the figure. C: The scale is expanded to aid in estimating λ_1. A line describing the initial rise indicates a half-time of just over 2 minutes producing an estimate for λ_1 of 0.34. C: A plot of $y(t) = 3900 - 500e^{-0.34t} - 2200e^{-0.02t} - 1200e^{-0.004t}$ superimposed upon the data. The plateau value was estimated from the data. Estimates for the A_i were obtained by extending the method used for the biexponential rise (see text for additional explanation).

the multiexponential decay, one could proceed to estimate the initial parameters for the three exponential model.

Case 2: The primed, constant infusion of tracer

If a primed, constant infusion is used, the multiexponential function describing the "rise" is

$$y(t) = A_0 + -A_1 e^{-\lambda_1 t} + A_2 e^{-\lambda_2 t} + \cdots + A_n e^{-\lambda_n t} \qquad 0 \le t \le T \quad \text{(G.55)}$$

where $A_0 \neq -(A_1 + \cdots + A_n)$, the A_i can be positive or negative, and T is the time at which the infusion stops.

As before, the only way to obtain reliable estimates of the λ_i is the following:

Step 1. Obtain an estimate of the plateau A_0.

Step 2. Subtract this value from each datum producing a modified set of data.

If the resulting data are negative which corresponds to the case when the data are rising to a plateau, the following steps must be employed.

Step 3. Multiply each modified datum by –1 thereby producing yet another modified set of data.

Step 4. Obtain estimates of λ_i using the methods described previously. If the data following step 2 are positive corresponding to the data falling to the plateau, estimates of λ_i can be obtained directly using the methods described for the multiexponential decay.

The quick method described above for the constant infusion case can also be used here. However, this method is usually successful only if one is using an interactive computer program to test the estimates for the λ_i and coefficients A_i.

Multiexponential washouts

The multiexponential washout is a direct extension of the biexponential washout case. Paralleling this situation, the equation which provides a description of the rising portion of the curve is

$$y_r(t) = A_0 + A_1 e^{-\lambda_1 t} + \cdots + A_n e^{-\lambda_n t} \qquad t \leq T \qquad \text{(G.56)}$$

where the r in $y_r(t)$ is used to denote the rising portion of the curve. The calculated amount of material in the accessible pool at T is approximated by $y(t)$ evaluated at T:

$$y_r(T) = A_0 + A_1 e^{-\lambda_1 T} + \cdots + A_n e^{-\lambda_n T} \qquad \text{(G.57)}$$

The equation to describe the multiexponential decay of the washout is then:

$$y_w(t) = y_r(T)(\alpha_1 \cdot e^{-\lambda_1(t-T)} + \cdots + \alpha_n e^{-\lambda_n(t-T)}) \qquad \text{(G.58)}$$

where

$$\alpha_1 + \cdots + \alpha_n = 1$$

In this case, the $n - 1$ new parameters $\alpha_1, \cdots, \alpha_{n-1}$ which assign the coefficients to each exponential term must also be estimated from the

data. As with the biexponential case, the exponentials can be estimated either from the rising or decaying portion of the curve.

Multiexponential rises and falls

The two accessible pool noncompartmental model discussed in the biexponential case for the situation when the tracer is introduced as a bolus into one accessible pool and measurements are taken in the second accessible pool has a counterpart in the multiexponential case when the system is more complex than only two accessible pools. This situation is illustrated in Figure G.25.
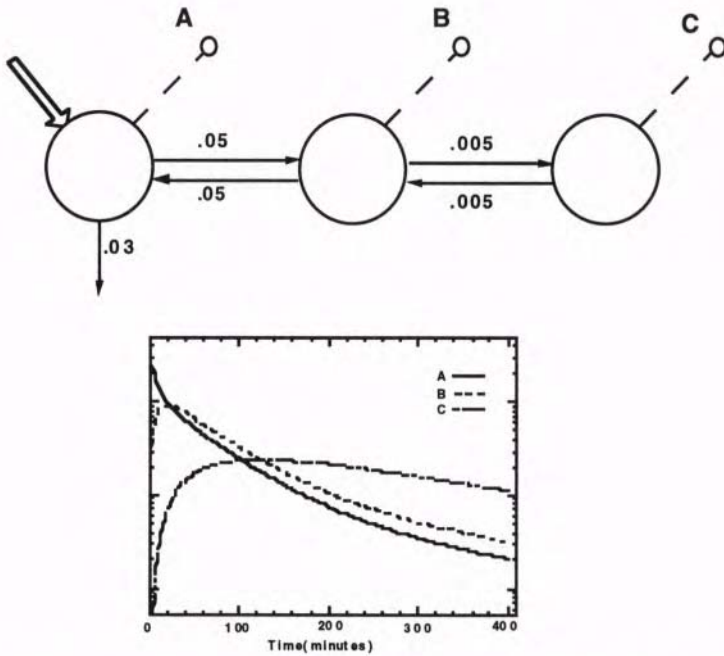
Figure G.25. Examples of tracer curves in a second accessible pool when the tracer is introduced as a bolus into the first accessible pool. The three compartment model used to generate the curves is shown in the upper panel. Curve A shows the decay following the bolus injection into the first accessible pool. Curves B and C show two different situations that can occur in the second accessible pool when more than two exponentials are involved. See text for additional explanation.

Data such as those shown in curves B and C which rise first and then fall can be described by the equation

$$y(t) = A_1 e^{-\lambda_1 t} + \cdots + A_n e^{-\lambda_n t} \qquad (G.59)$$

where some of the A_i are positive and others are negative. Notice that $y(0) = 0$, i.e. the sum of the A_i is zero. Equation (G.59) is the counterpart of (G.49). Notice, however, that in G.49) there was only one coefficient, A, while in this case, there are n coefficients A_i about which little is known except they sum to zero.

Estimates for the λ_i can be obtained by extending the method described earlier. Estimates for the coefficients A_i are best obtained using an interactive computer program, and starting by using a biexponential to describe the data, and proceeding adapting the philosophy of the last method described for the multiexponential decay. The reason why this strategy is best is because one does not immediately know if, for the three exponential model, two exponentials are required to describe the rise or the fall; this is the point of the two situations illustrated in Figure G.25 where in curve C two exponentials are required for the rise while in curve B two are required to describe the decay.

Appendix H
Relationships Among the
Parameters of Multiexponential Models

While a sum of exponential function

$$y(t) = A_1 e^{-\lambda_1 t} + \cdots + A_n e^{-\lambda_n t} \tag{H.1}$$

is able to describe the response of a linear, time invariant system to a bolus injection, the generic response to other canonical inputs such as the constant infusion or the primed constant infusion is

$$y(t) = A_0 + A_1 e^{-\lambda_1 t} + \cdots + A_n e^{-\lambda_n t} \tag{H.2}$$

However, constraints exist among the coefficients A_i depending upon which input is applied. These constraints can be derived by using the concept of the impulse response of the system $h(t)$ already introduced in Appendix C. The function $h(t)$ represents the tracer curve (either tracer concentration or tracer to tracee ratio) when a unit dose of tracer is injected into the system at time zero. For linear, time invariant systems, $h(t)$ is a sum of exponentials, and denoting by H_i the amplitudes, one has

$$h(t) = H_1 e^{-\lambda_1 t} + \cdots + H_n e^{-\lambda_n t} \tag{H.3}$$

The constant infusion protocol

When (H.2) is used to describe data following a constant infusion of tracer, the relationship among the coefficients A_i is

$$A_0 + A_1 + \cdots + A_n = 0 \tag{H.4}$$

which insures $y(0) = 0$. It can be formally derived by considering that the response $y(t)$ to a constant infusion u of tracer is proportional to the integral of $h(t)$ (see Table C.1):

$$y(t) = u[\frac{H_1}{\lambda_1}(1 - e^{-\lambda_1 t}) + \cdots + \frac{H_n}{\lambda_n}(1 - e^{-\lambda_n t})] \qquad \text{(H.5)}$$

or equivalently

$$y(t) = u[\frac{H_1}{\lambda_1} + \cdots + \frac{H_n}{\lambda_n} - \frac{H_1}{\lambda_1}e^{-\lambda_1 t} - \cdots - \frac{H_n}{\lambda_n}e^{-\lambda_n t}] \qquad \text{(H.6)}$$

By letting

$$A_0 = \frac{H_1}{\lambda_1} + \cdots + \frac{H_n}{\lambda_n} \qquad \text{(H.7)}$$

$$A_1 = \frac{H_1}{\lambda_1} \qquad \cdots \qquad A_n = \frac{H_n}{\lambda_n}$$

equation (H.2) is obtained for $y(t)$, and condition (H.4) follows.

The primed constant infusion protocol

The link between the exponential model parameters in this case is

$$A_0 + A_1(\frac{\frac{u}{d}}{\frac{u}{d} - \lambda_1}) + \cdots + A_n(\frac{\frac{u}{d}}{\frac{u}{d} - \lambda_n}) = 0 \qquad \text{(H.8)}$$

This relationship can be derived by expressing the response to a primed constant infusion as the sum of the responses to the bolus injection (proportional to $h(t)$) and to the constant infusion (proportional to the integral of $h(t)$):

$$y(t) = d[H_1 e^{-\lambda_1 t} + \cdots + H_n e^{-\lambda_n t}] + u[\frac{H_1}{\lambda_1}(1 - e^{-\lambda_1 t}) \qquad \text{(H.9)}$$
$$+ \cdots + \frac{H_n}{\lambda_n}(1 - e^{-\lambda_n t})$$

where d is the tracer dose injected as a bolus at time zero and u is the rate at which the tracer is infused. By letting

$$A_0 = u(\frac{H_1}{\lambda_1} + \cdots + \frac{H_n}{\lambda_n}) \qquad \text{(H.10)}$$

$$A_1 = H_1(d - \frac{u}{\lambda_1}) \qquad \cdots \qquad A_n = H_n(d - \frac{u}{\lambda_n})$$

equation (H.9) can be written as in (H.2), and condition (H.8) follows.

The washout phase

Relationships exist among the coefficients describing the rising $y_r(t)$ and washout phase $y_w(t)$. Write these as

$$y_r(t) = A_0 + A_1 e^{-\lambda_1 t} + \cdots + A_n e^{-\lambda_n t} \qquad t \le T \qquad \text{(H.11)}$$

$$y_w(t) = B_1 e^{-\lambda_1 t} + \cdots + B_n e^{-\lambda_n t} \qquad t > T \qquad \text{(H.12)}$$

Suppose, as indicated in (H.11) and (H.12), that the tracer is administered as a constant infusion u up to time T. Condition (H.4) holds among the coefficients A_i. In addition, if the plateau is reached before the infusion is stopped, then

$$A_1 = -B_1 \qquad \cdots \qquad A_n = -B_n \qquad \text{(H.13)}$$

If this condition is not met, then the following relationships hold:

$$B_1 = A_1(e^{-\lambda_1 T} - 1) \quad \cdots \quad B_n = A_n(e^{-\lambda_n T} - 1) \qquad \text{(H.14)}$$

In order to derive (H.14), interpret $y_w(t)$ as the response to an input consisting of a constant infusion u minus a negative constant infusion having the same magnitude but starting from time T as was done in Appendix C. Then

$$
\begin{aligned}
y_w(t) &= [A_0 + A_1 e^{-\lambda_1 t} + \cdots + A_n e^{-\lambda_n t}] \qquad &\text{(H.15)}\\
&\quad - [A_0 + A_1 e^{-\lambda_1 (t-T)} + \cdots + A_n e^{-\lambda_n (t-T)}]\\
&= e^{-\lambda_1 (t-T)}[A_1(e^{-\lambda_1 T}\\
&\quad - 1)] + \cdots + e^{-\lambda_n (t-T)}[A_n(e^{-\lambda_n T} - 1)]
\end{aligned}
$$

Equation (H.15) described the washout phase, and it is expressed in the general form (H.12) using (H.13). If the plateau value is reached by time T, then $e^{-\lambda_i T} \approx 0$. Thus under these conditions (H.14) reduces to (H.14). In any event, these equalities guarantee the continuity of exponential function describing the data at time T, i.e. $y_r(T) = y_w(T)$

Equation (H.14) needs to be explicitly considered when data from both the rising portion and washout phase are simultaneously analyzed. However, if only data from the washout phase are considered, (H.12) can be used with no constraints among the coefficients $B_1, \cdots, B_n$, and MRT^{NC} can be estimated from (8.2.34).

This page intentionally left blank.

Appendix I
Calculation of Model Output
Partial Derivatives

As described in §10.2, for parameter estimation the problem is how to evaluate $\frac{\partial y(\mathbf{p},t)}{\partial \mathbf{p}}$ for a given value of the parameter vector $\mathbf{p}$ for the various sampling times t_i. The most common technique is based upon the approximation of the derivative with the finite difference formula; that is, for the generic element $\frac{\partial y(\mathbf{p},t)}{\partial p_i}$

$$\frac{\partial y(\mathbf{p}, t)}{\partial p_i} = \frac{y(p_1, \cdots, p_i + h, \cdots, p_p, t) - y(p_1, \cdots, p_i, \cdots, p_p, t)}{h} \tag{I.1}$$

where h is a very small number. Often to improve the accuracy of the approximation, the central difference formula is used:

$$\frac{\partial y(\mathbf{p}, t)}{\partial p_i} = \frac{y(p_1, \cdots, p_i + h, \cdots, p_p, t) - y(p_1, \cdots, p_i - h, \cdots, p_p, t)}{2h}$$
$$\tag{I.2}$$

Another technique for evaluating the required partial derivatives is to calculate the so-called sensitivity equations.

Given the model

$$\dot{\mathbf{m}}(\mathbf{p}, t) = \mathbf{K}(\mathbf{p})\mathbf{m}(\mathbf{p},t) + \mathbf{u}(t) \qquad \mathbf{m}(0) = 0 \tag{I.3}$$

$$y(\mathbf{p}, t) = \mathbf{C}(\mathbf{p})\mathbf{m}(\mathbf{p},t) \tag{I.4}$$

one notes that the partial derivative of $y(\mathbf{p}, t)$ with respect to the parameter vector p can be written

$$\frac{\partial y(\mathbf{p}, t)}{\partial \mathbf{p}} = \mathbf{C}(\mathbf{p})\frac{\partial \mathbf{m}(\mathbf{p}, t)}{\partial \mathbf{p}} + \frac{\partial \mathbf{C}(\mathbf{p})}{\partial \mathbf{p}}\mathbf{m}(\mathbf{p},t) \tag{I.5}$$

437

Moreover,

$$\frac{\partial \dot{\mathbf{m}}(\mathbf{p}, t)}{\partial \mathbf{p}} = \frac{\partial \dot{\mathbf{m}}(\mathbf{p}, t)}{\partial \mathbf{p}} = \mathbf{K}(\mathbf{p}) \frac{\partial \mathbf{m}(\mathbf{p}, t)}{\partial \mathbf{p}} + \frac{\partial \mathbf{K}(\mathbf{p})}{\partial \mathbf{p}} \mathbf{m}(\mathbf{p}, t) \qquad (I.6)$$

Thus at a given value of the parameter vector $\mathbf{p}$, if one solves for $\mathbf{m}$ as given by (I.3), then from (I.6) one has $\mathbf{m}(\mathbf{p},t)$ and $\frac{\partial \mathbf{m}((\mathbf{p},t)}{\partial \mathbf{p}}$, and thus $y(\mathbf{p}, t)$ and $\frac{\partial y(\mathbf{p},t)}{\partial \mathbf{p}}$ from (I.4) and (I.5) respectively.

In general for an n compartment model with P parameters, there is a need to solve $n + P \cdot n$ differential equations. In most cases, however, this number is usually less as often many of the derivatives are equal to zero.

Example

To illustrate the sensitivity approach, consider the two compartment model shown in Figure 10.2.1 where a bolus input dose d_1 is assumed. The equations describing this model are

$$\frac{dm_1(t)}{dt} = -k_{21}m_1(t) + k_{12}m_2(t) \qquad m_1(0) = d_1 \qquad (I.7)$$

$$\frac{dm_2(t)}{dt} = k_{21}m_1(t) - (k_{02} + k_{12})m_2(t) \qquad m_2(0) = 0 \qquad (I.8)$$

$$y(t) = \frac{m_1(t)}{V_1} \qquad (I.9)$$

The equations of (I.4) are given for the example by

$$\frac{\partial \dot{m}_1(t)}{\partial k_{21}} = -k_{21}\frac{\partial m_1(t)}{\partial k_{21}} + k_{12}\frac{\partial m_2(t)}{\partial k_{21}} - m_1(t) \qquad (I.10)$$

$$\frac{\partial \dot{m}_1(t)}{\partial k_{12}} = -k_{21}\frac{\partial m_1(t)}{\partial k_{12}} + k_{12}\frac{\partial m_2(t)}{\partial k_{12}} + m_2(t) \qquad (I.11)$$

$$\frac{\partial \dot{m}_1(t)}{\partial k_{02}} = -k_{21}\frac{\partial m_1(t)}{\partial k_{02}} + k_{12}\frac{\partial m_2(t)}{\partial k_{02}} \qquad (I.12)$$

$$\frac{\partial \dot{m}_2(t)}{\partial k_{21}} = k_{21}\frac{\partial m_1(t)}{\partial k_{21}} - (k_{02} + k_{12})\frac{\partial m_2(t)}{\partial k_{21}} + m_1(t) \qquad (I.13)$$

$$\frac{\partial \dot{m}_2(t)}{\partial k_{12}} = k_{21}\frac{\partial m_1(t)}{\partial k_{12}} - (k_{02} + k_{12})\frac{\partial m_2(t)}{\partial k_{12}} - m_2(t) \qquad (I.14)$$

$$\frac{\partial \dot{m}_1(t)}{\partial k_{02}} = k_{21}\frac{\partial m_1(t)}{\partial k_{02}} - (k_{02} + k_{12})\frac{\partial m_2(t)}{\partial k_{02}} - m_2(t) \qquad (I.15)$$

In the above equations, all initial conditions are equal to zero.
Equation (I.5) becomes

$$\frac{\partial y(t)}{\partial k_{21}} = \frac{1}{V_1}\frac{\partial m_1(t)}{\partial k_{21}} \tag{I.16}$$

$$\frac{\partial y(t)}{\partial k_{12}} = \frac{1}{V_1}\frac{\partial m_1(t)}{\partial k_{12}} \tag{I.17}$$

$$\frac{\partial y(t)}{\partial k_{02}} = \frac{1}{V_1}\frac{\partial m_1(t)}{\partial k_{02}} \tag{I.18}$$

$$\frac{\partial y(t)}{\partial V_1} = -\frac{1}{V_1^2}m_1(t) \tag{I.19}$$

The need to solve the two sets of equations (I.7)–(I.8) and (I.10)–(I.19) in series is clear since the sensitivity system (I.10)–(I.19) requires as "forcing functions" thefunctions m_1 and m_2. That is, to solve (I.10–I.19), one needs to know m_1 and m_2 which is precisely what the solution to (I.7)–(I.8) provides.

This page intentionally left blank.

Appendix J
Initial Estimates of the Rate Constants of Multicompartmental Models

Introduction

Obtaining the initial estimates of the rate constants of multicompartmental models will rely heavily on knowing how to obtain the initial estimates of the exponentials and coefficients of the multiexponential models discussed in Appendix G. In addition to initial estimates of the rate constants, it is also necessary, depending upon the measurement variable(s), to obtain initial estimates for the volume or mass of the accessible pool(s). In this appendix, how to obtain initial estimates for the linear compartmental model from a knowledge of the exponential model of corresponding order will be illustrated.

The single compartment model

The single compartment model is shown in Figure J.1. What is known is the input, i.e. the amount of the bolus injection, the rate of infusion, or the priming dose and rate of infusion. What is to be estimated from the data is k_{01} and either the volume V or mass M. Hence initial estimates for these parameters are needed. For the single pool model, an estimate for k_{01} is λ_1 in $y(t) = A_0 + A_1 e^{-\lambda_1 t}$ where $y(t)$ is the generic expression for the monoexponential model. To obtain an estimate for V or M depends upon how the tracer is administered.
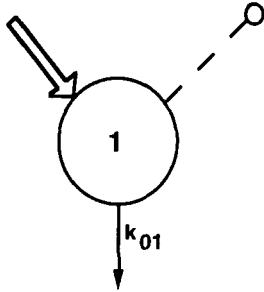
Figure J.1.   The single compartment model. See text for additional explanation.

Bolus injections

To discuss the bolus injection, use the data given in Table 8.5.1 given below for convenience in Figure J.2. These were data collected after a
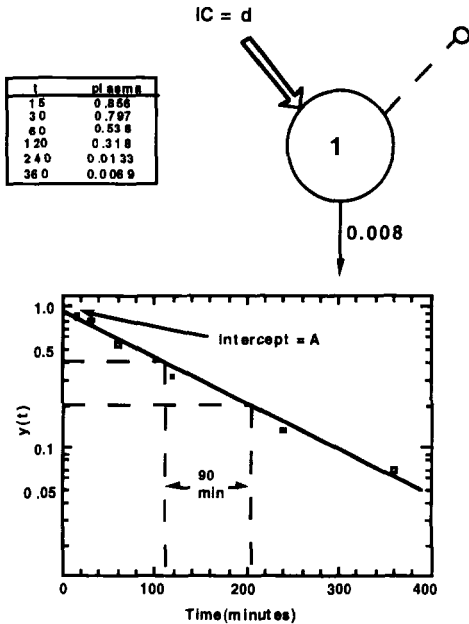
Figure J.2.   The data from Table 8.5.1 and Figure G.2 indicating how to obtain initial estimates for $A = 1$ and $\lambda = 0.008$. The single compartmental model is shown indicating the initial estimate for the initial condition is 1 and for k_{01} is 0.008.

bolus injection of dose d. These data were also discussed in Figure G.2 where it was seen that initial estimates for A and λ in the monoexponential model $y(t) = Ae^{-\lambda t}$ of 1 and 0.008 respectively were obtained. For convenience, Figure G.1C is reproduced in Figure J.2 indicating how A and λ were estimated.

The value A is the extrapolated value of the data to time zero. If the data are measured in concentration units in which case V needs to be estimated, then $y(0) = A = \frac{d}{V}$ in which case an initial estimate for V equals $\frac{d}{A}$, in this case 1. If the data are measured in the tracer-tracee ratio, then $y(0) = A = \frac{d}{M}$ in which case an initial estimate for M equals $\frac{d}{A}$.

Thus for the bolus injection into the single compartment model, initial estimates for the rate constant k_{01} and either V or M are immediate using the monoexponential model.

Constant and primed constant infusions

For the constant or primed, constant infusion into the single pool system, the monoexponential model is either $y(t) = A - Ae^{-\lambda_1 t}$ or $y(t) = A_0 + A_1 e^{-\lambda_1 t}$. As with the bolus case, an initial estimate for k_{01} equals the initial estimate for λ. Again, what is required is an initial estimate for V or M.

For the constant infusion case, recalling from Appendix H that $A = \frac{u}{\lambda M}$ or $A = \frac{u}{\lambda V}$ where, in both cases, u is the infusion rate depending upon whether the data are collected in terms of tracer-tracee ratio or concentration, an initial estimate for M can be obtained from $M = \frac{u}{\lambda A}$ or V from $V = \frac{u}{\lambda A}$.

For the primed constant infusion where the priming dose is d, $y(0) = A_0 + A_1$ estimates the zero time value for the data, and the same equations as those given for the bolus can be used to obtain initial estimates for V or M: $V = \frac{d}{(A_0 + A_1)}$ or $M = \frac{d}{(A_0 + A_1)}$

Thus there is an easy comparison between the monoexponential model and the parameters of the single compartment model. Knowing how to obtain the initial estimates for the monoexponential model will let one immediately obtain the required estimates for the compartmental model. The situation is more complex, however, for compartmental models with two or more compartments.

The two compartment model

The general two compartment model for the single input-single output experiment is shown in Figure J.3A. The parameters to estimate are V or

M, and the rate constants $k_{2,1}, k_{1,2}, k_{0,1}$ and k_{02}. However, as discussed in §5.4, this model is not identifiable. Figures J.3B and J.3C show two extreme situations which are commonly used by many investigators and which are identifiable. In this section of the appendix, how to obtain the estimates for M and V, and the rate constants of these two models will be discussed.
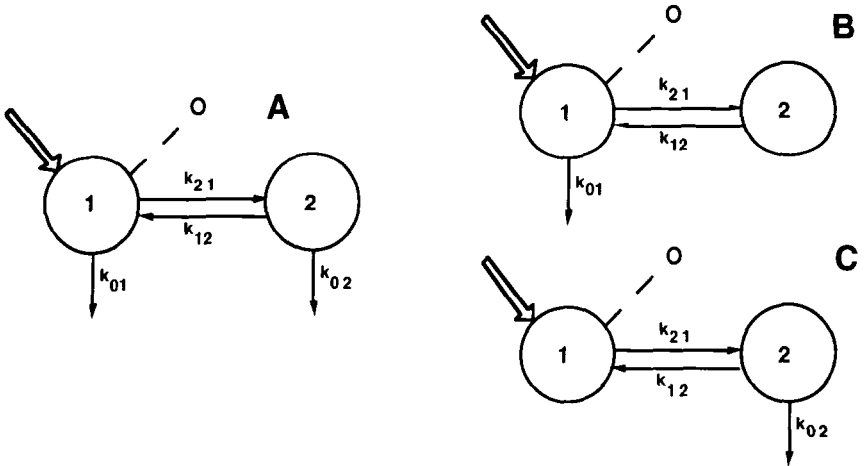
Figure J.3.   The two compartment model. See text for additional explanation.

Bolus injections

Data decaying biexponentially following a bolus injection of tracer means that the data can be explained by a two compartment model as well as the two exponential model. In Appendix G, how to obtain initial estimates for the coefficients and exponentials in the biexponential model

$$y(t) = A_1 e^{-\lambda_1 t} + A_2 e^{-\lambda_2 t} \tag{J.1}$$

was discussed. The question is: how can one use this information to obtain initial estimates for V or M, and the rate constants k_{21}, k_{12} and k_{01} in, for example, model B shown in Figure J.3? One can use the information in §5.4 to answer the question.

Suppose one has used a strategy discussed in Appendix G to obtain initial estimates for A_1, A_2, λ_1 and λ_2. Knowing the dose d of the tracer, an estimate for V or M can be obtained. For example from (5.4.18),

and initial estimate for V is

$$V = \frac{d}{y(0)} = \frac{d}{A_1 + A_2} \tag{J.2}$$

In addition, from (5.4.14) and (5.4.17),

$$k_{11} = -(k_{21} + k_{01}) = -\frac{A_1\lambda_1 + A_2\lambda_2}{A_1 + A_2} \tag{J.3}$$

$$k_{22} = -k_{12} = -\frac{A_2\lambda_1 + A_1\lambda_2}{A_1 + A_2} \tag{J.4}$$

Notice in (J.4) that because $k_{02} = 0$, $k_{22} = k_{12}$. Finally, for the configuration given in Figure J.3B, k_{01} equals the FCR:

$$k_{01} = \frac{A_1 + A_2}{\int_0^\infty y(t)dt} = \frac{A_1 + A_2}{\frac{A_1}{\lambda_1} + \frac{A_2}{\lambda_2}} \tag{J.5}$$

With this information, one can now easily estimate the rate constants. Using the data of Case Study 2 given in Table 8.7.4, the quick method to estimate the coefficients and exponentials of the two exponential model are given in Figure G.15; these are $A_1 = 110000, A_2 = 100000, \lambda_1 = 0.069$ and $\lambda_2 = 0.008$. Knowing that the initial dose of radioactivity was $4.5 \cdot 10^8$dpm, one can obtain the following initial estimates for the parameters of the two compartment model shown in panel B of Figure J.3:

$$V = \frac{4.5 \cdot 10^8}{A_1 + A_1} = \frac{4.5 \cdot 10^8}{210000} = 2143 \tag{J.6}$$

$$k_{01} = \frac{210000}{\frac{110000}{0.069} + \frac{100000}{0.008}} = 0.015 \tag{J.7}$$

$$k_{12} = \frac{100000 \cdot 0.069 + 110000 \cdot 0.008}{210000} = 0.037 \tag{J.8}$$

$$k_{21} = -k_{11} - k_{01} = 0.04 - 0.015 = 0.025 \tag{J.9}$$

A plot of the results of the two compartment model shown in Figure J.3B using these initial estimates is shown below in Figure J.4.

Suppose now that one wanted to examine the model shown in Figure J.3C. In this case, $k_{01} = 0$ and $k_{02} \neq 0$. While one can use the information on the coefficients A_1, A_2, λ_1 and λ_2 as was done in deriving (J.3)–(J.5), there is another approach that is useful to illustrate. First, one notes that (J.2) can be used to estimate V in either case.

From §5.4, it is clear that there are many possible choices of values for the rate constants k_{21}, k_{12}, k_{01} and k_{02} of model A in Figure J.3
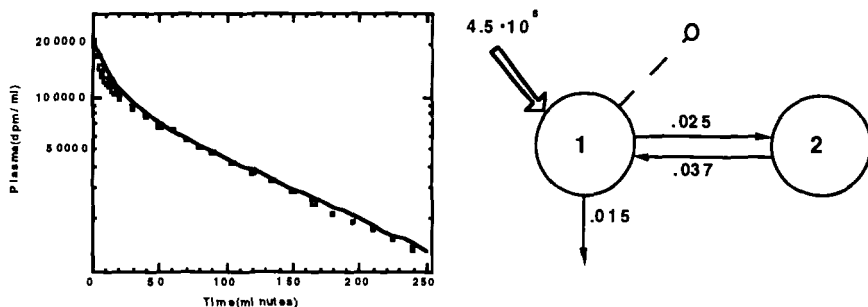
Figure J.4. A plot of the result of the two compartment model shown in Figure J.3B compared to the data of Case Study 2 given in Table 8.7.4 using the initial estimates calculated in (J.5)–(J.8).

which will give the same result as those given in Figures J.4. Given one particular set of values such as those given in Figure J.4, one can take advantage of the fact that, for each different set of values, k_{11}, k_{22} and $k_{12}k_{21}$ are preserved. This can be derived easily from the information given in §5.4.

One can therefore use the initial set of values given in Figure J.4 to calculate initial estimates of the rate constants in Figure J.3C.

First, in Figure J.4, one sees $k_{11} = -(0.025 + 0.015) = -0.04$. Therefore for the model shown in Figure J.3C, since $k_{01} = 0$, $k_{21} = 0.04$. Next for the rate constants in Figure J.3C, $k_{12}k_{21} = 0.025 \cdot 0.037 = 0.000925$. Since this number must be preserved between models B and C in Figure J.3, and since one knows for model C that $k_{21} = 0.04$, one can calculate for model C, $k_{12} = \frac{0.000925}{0.04} = 0.023$. Finally, from Figure J.4, $k_{22} = -k_{12} = -0.037$. For model C, $k_{22} = -(k_{12} + k_{02})$ whence $k_{02} = 0.037 - 0.023 = 0.014$. Thus the initial estimates for the rate constants and volume V for model C in Figure J.3 are $V = 2143$, $k_{21} = 0.040$, $k_{12} = 0.023$, and $k_{02} = 0.014$. The results are shown in Figure J.5. As expected, the plots in Figures J.4 and J.5 are essentially identical.

Before leaving this section, there is another case that needs to be considered. Up to now, it has been assumed that the tracer material is kinetically homogeneous, i.e. the accessible pool is a single compartment. It is sometimes the case that the accessible pool is kinetically heterogeneous. For example, tracer labeled plasma low density lipopro-
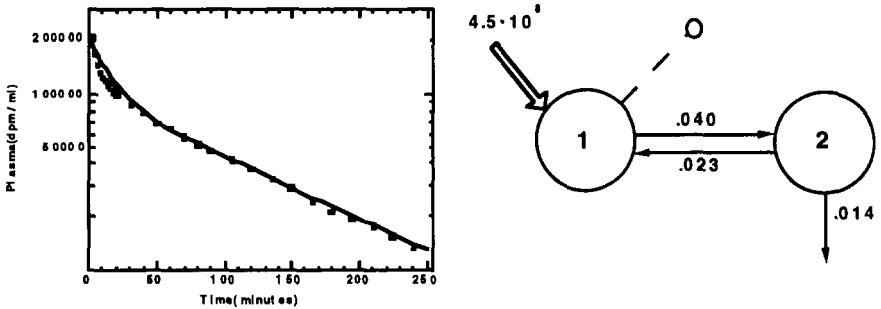
Figure J.5.   A plot of the result of the two compartment model shown in Figure J.3C compared to the data of Case Study 2 given in Table 8.7.4 using the initial estimates calculated as described in the text.

teins consist of at least two distinct plasma pools; it is the sum of the tracer in these pools that form the plasma sample. How can this situation be dealt with?

For a biexponentially decaying set of data, the appropriate two compartment model in this situation is shown in Figure J.6.
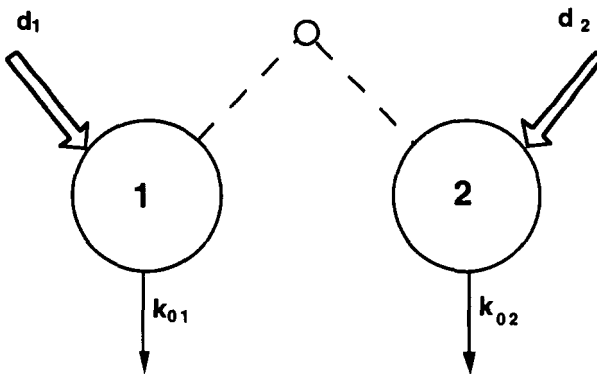
Figure J.6.   The two compartment model with heterogeneity. See text for additional explanation.

In this model, the sample is the sum of the tracer amounts in the two compartments. If the tracer samples are quantitated in units of concentration, assuming $V_1 = V_2 = V$, then the measurement equation is $\frac{m_1(t)+m_2(t)}{V}$. If the tracer samples are quantitated in units of tracer-tracee ratio, then the measurement equation is $\frac{m_1(t)+m_2(t)}{M}$ where $M = M_1+M_2$.

What is known is the total dose of tracer d together with initial estimates of the coefficients A_1 and A_2, and exponentials λ_1 and λ_2 of the two exponential model $y(t) = A_1e^{-\lambda_1 t} + A_2e^{-\lambda_2 t}$ as discussed in Appendix G. What is unknown is how the tracer is distributed between the two plasma compartments, i.e. what are d_1 and d_2 in Figure J.6, the volume V or mass M, and the rate constants k_{01} and k_{02}.

Estimates for V or M can be obtained as was done previously. For example, an estimate of V can be obtained from $\frac{d}{y(0)} = \frac{d}{A_1+A_2}$. Since there is a direct connection between the exponentials and the rate constants that parallels the single exponential case, that is, $k_{01} = \lambda_1$ and $k_{02} = \lambda_2$, initial estimates of k_{01} and k_{02} equal the initial estimates of λ_1 and λ_2.. It remains to estimate d_1 and d_2. This can be obtained by realizing $\frac{A_1}{A_1+A_2}$ and $\frac{A_2}{A_1+A_2}$ are the fractions of material at time zero in the two compartments. Thus initial estimates for d_1 and d_2 can be obtained from $d \cdot \frac{A_1}{A_1+A_2}$ and $d \cdot \frac{A_2}{A_1+A_2}$ respectively. The interested reader can try this model using the data from Table 8.7.4.

It should also be noted that for the two exponential model, the model shown in Figure J.6 is the only situation where there is a direct connection between the exponentials in the two exponential model and the rate constants in the compartmental model. As clearly seen in the two other examples and as discussed in detail in §5.4, in all other cases the rate constants are functions of the coefficients and exponentials.

Constant and primed constant infusions

For the constant or primed, constant infusion into the a two compartment system where the accessible pool is a single, homogeneous compartment, the biexponential model is either

$$y(t) = A_0 + A_1e^{-\lambda_1 t} + A_2e^{-\lambda_2 t} \qquad A_0 + A_1 + A_2 = 0 \qquad \text{(J.10)}$$

for the constant infusion case or

$$y(t) = A_0 + A_1e^{-\lambda_1 t} + A_2e^{-\lambda_2 t} \qquad A_0 + A_1 + A_2 \neq 0 \qquad \text{(J.11)}$$

for the primed, constant infusion.

In what follows, it will be assumed that estimates for A_0, A_1, A_2, λ_1 and λ_2 have been obtained as described in Appendix G for the biexponential rising situation. It will also be assumed that the infusion rate u is known for the constant infusion, and that the priming dose d and infusion rate u is known for the primed, constant infusion experiment.

The required volume V or mass M can be estimated from $\frac{u}{\dot{y}(0)}$ where $\dot{y}(0) = -A_1\lambda_1 - A_2\lambda_2$. For the primed constant infusion, the required volume V or mass M can be estimated from $\frac{d}{y(0)}$.

Clearly for the single input, single output experiment, the model shown in Figure J.3A is not identifiable. As before, therefore, consider the situation of model B shown in Figure J.3. The problem is how to estimate the rate constants k_{01}, k_{21}, and k_{12} knowing the coefficients A_i and exponentials λ_i.

The constant infusion

For the constant infusion, consider as an example the data given in Figure G.16. Using the quick method to estimate the the coefficients A_1 and A_2, and the exponentials λ_1 and λ_2 of (J.10), one obtained as an initial estimate

$$y(t) = 5200 - 2200e^{-0.02t} - 3000e^{-0.01t} \tag{J.12}$$

Thus $A_0 = 5200, A_1 = -2200, A_2 = -3000, \lambda_1 = 0.02$ and $\lambda_2 = 0.01$. How can this information be used to estimate the rate constants k_{21}, k_{12} and k_{01} of model B in Figure J.3?

First, the volume can be estimated from $\frac{u}{y'(0)} = \frac{u}{-A_1\lambda_1 - A_2\lambda_2} = \frac{400000}{70} \approx 5700$.

Next, it is known as stated previously that k_{01} equals the FCR. The clearance rate can be estimated as $\frac{u}{c} = \frac{u}{A_0} = \frac{u}{5200}$, For this case, the initial estimate for the clearance rate CR is 77ml/min. The FCR is the ratio of the clearance rate and volume; for this example, this ratio is $\frac{77}{5700} = 0.013$. This provides an estimate for k_{01}.

To estimate k_{21} and k_{12}, one can derive from the constant infusion response (J.12) the biexponential response to a bolus injection. Denoting this by $y^*(t)$ and using (H.7)

$$y^*(t) = (2200 \cdot 0.02)e^{-0.02t} + (3000 \cdot 0.01)e^{-0.01t} = 44e^{-0.02t} + 30e^{-0.01t} \tag{J.13}$$

Thus one can use (J.3) and (J.4) to estimate k_{11} and k_{12}. The results are

$$k_{11} = -\frac{44 \cdot 0.02 + 30 \cdot 0.01}{44 + 30} = -0.016 \tag{J.14}$$

$$k_{12} = \frac{30 \cdot 0.02 + 44 \cdot 0.01}{44 + 30} = 0.014 \qquad \text{(J.15)}$$

Knowing k_{01} is estimated at 0.013, k_{21} can be estimated $k_{21} = -k_{11} - k_{01} = 0.003$. The results are summarized in Figure J.7
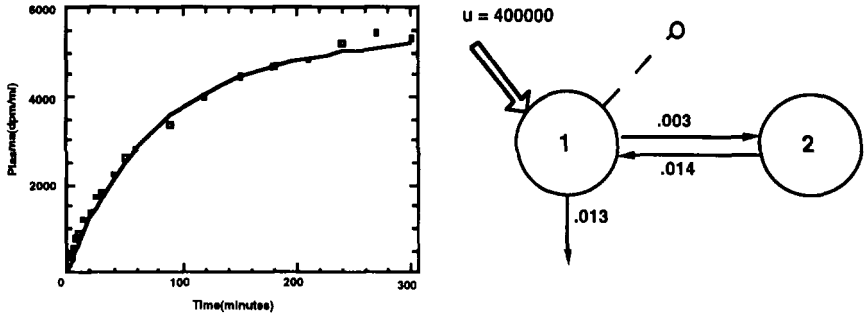
Figure J.7. A plot of the result of the two compartment model shown in Figure J.3B compared to the data Figure G.16 using the initial estimates calculated as described in the text.

It should be pointed out that an estimate for the FCR could be obtained from (J.13) as $\frac{44+30}{\frac{44}{0.02} + \frac{30}{0.01}}$ which is the normalized area under (J.13).

At this point, the interested reader can use the strategy discussed for the biexponential decay to estimate the initial rate constants for model C of Figure J.3 since the strategy discussed there is independent of the method of introducing the tracer.

The primed constant infusion

To estimate the rate constants for model B or model C of Figure J.3 for the primed constant infusion parallels that for the constant infusion. If (J.ll) is used to describe the data, and if the coefficients and exponentials A_0, A_1, A_2, λ_1 and λ_2 have been estimated as described in Appendix H, the one can proceed as follows. It is assumed that the priming dose d and the infusion rate u is known.

Estimates of M or V can be obtained from $\frac{d}{y(0)}$ where $y(t)$ is given by (J.11) with the estimated coefficients and exponentials. To estimate k_{21}, k_{12} and k_{01}, one can derive from the primed constant infusion response (J.11) the biexponential decay response to a bolus injection by using the relationship derived from (J.1).

Models with more than two compartments

When dealing with more than two compartments, there are, especially for the mammillary and catenary models, known relationships between the coefficients and exponentials of the exponential model, and the rate constants of the multicompartmental model. These are usually complex and tedious to apply, especially when the only goal is sufficiently good estimates of the rate constants to proceed with the estimation process, e.g. weighted linear regression.

This part of the appendix will discuss some strategies which permit one to increase the model order, i.e. number of compartments, using an interactive computer program and a knowledge of the parameter values providing the best fit of the model of lower order, e.g. passing from a two to a three compartment model. The data from Case Study 2 will be used only since the philosophy is independent of how the tracer is introduced into the system.

For the first part of the discussion, the results from analyzing a two compartment model applied to the data will be discussed in terms of passing to the three compartment catenary and mammillary model shown in Figure J.8 as Models D and E respectively. The results for the two compartment model are shown for reference purposes.

In passing from the two to three compartment model, suppose that the predictions of the two compartment model underestimate the initial decay, overestimate the final decay, and overestimate the FCR. This is because only two exponentials are available to describe a three exponential process. Thus when a third compartment gets added to the model, one wants to have one which exchanges more rapidly with the accessible pool, and one that exchanges more slowly either with that pool (catenary model D) or with the accessible pool (mammillary model E).

The following is not meant to be a precise set of instructions to obtain initial estimates of the parameters, but a heuristic one that under normal conditions will produce initial estimates that are sufficient to proceed with the fitting process.

Since the fractional catabolic rate is a function of the area under the decay curve, the best estimate for the two compartment model can be taken as an slight overestimate for the three compartment model. In the example here, k_{01} shown in Figure J.8 equals 0.017; thus an initial estimate for k_{01} in either model D or E can be 0.015. Also, since the two compartment model usually underestimates the initial decay, the best estimate for the volume V should be increased 10% to 20% depending upon how big the underestimate is. In this example, the best estimate is 1970ml; since the fit of the two compartment model is not
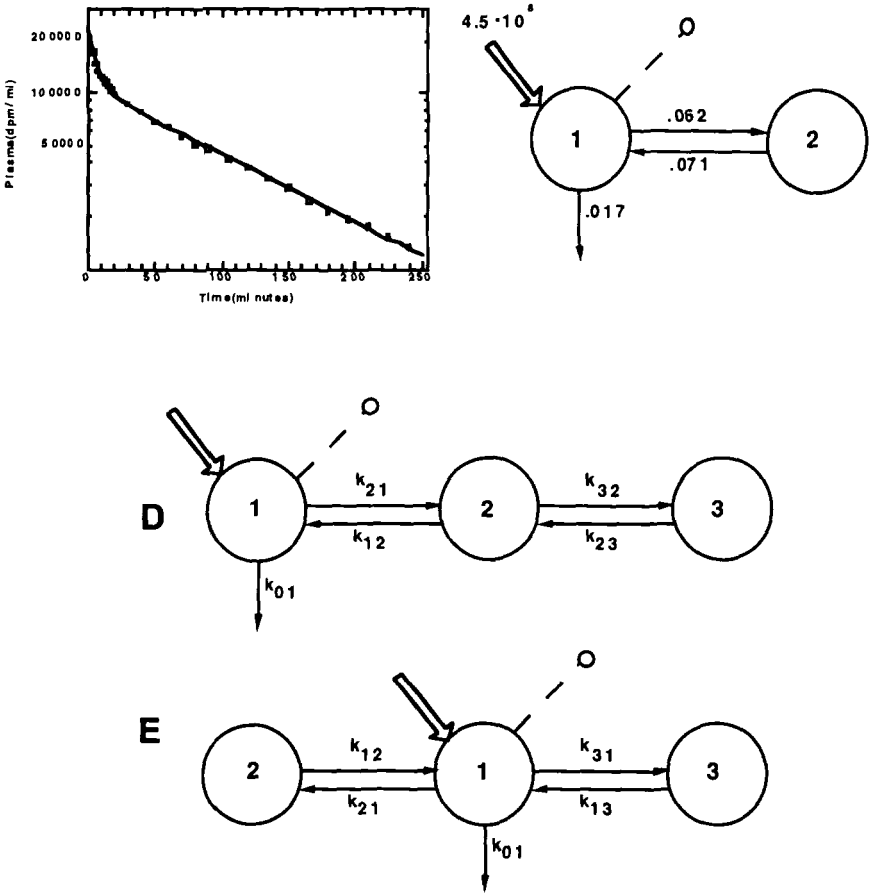
Figure J.8. A plot of the best fit of the two compartment model shown in Figure J.3B compared to the data of Case Study 2 given in Table 8.7.4 using the initial estimates calculated in (J.5)–(J.8). The rate constants are shown on the figure; the best estimate for the volume V is 1970ml. Models D and E are the three compartment catenary and mammillary models discussed in the text.

too bad, increasing this by about 10% to 2200ml is reasonable. A more accurate estimate for the FCR (k_{01}) and the volume can be obtained by fitting a sum of three exponentials to the data, and using the formulas in Table 3.4.3.

It remains to estimate the remaining k_{ij}. Here one can take advantage of relationships among the parameters of the two pool model derived in Chapter 5. In particular, k_{ii} and $k_{12}k_{21}$ are invariant meaning the estimates from the two compartment model can be used for the three compartment models. How can this be done?

For the two compartment model in this example , $k_{11} = 0.079$, $k_{22} = 0.071$ and $k_{21}k_{12} = .0044$. For model D the strategy is easy. First, if $k_{01} = 0.015$, then since $k_{11} = k_{01} + k_{21}$, an estimate for k_{21} is 0.064. Knowing $k_{21}k_{12} = 0.0044$, an estimate for k_{12} is 0.069. Since $k_{22} = 0.071$, an estimate for k_{32} is 0.002. It remains to estimate k_{23}. Since no a priori information is available, one has to guess. A value of $k_{23} = k_{32}$ can be used. If this is not sufficient, one can usually tell from the first simulation if k_{23} needs to be increased or decreased. Normally this strategy provides sufficiently close estimates to proceed with optimization. The results of this strategy for model D is shown in Figure J.9.

For model E the strategy cannot be directly applied. The reason is that in moving from the two to the three compartment catenary model, it is easy to preserve k_{22}. In the mammillary three compartment model,
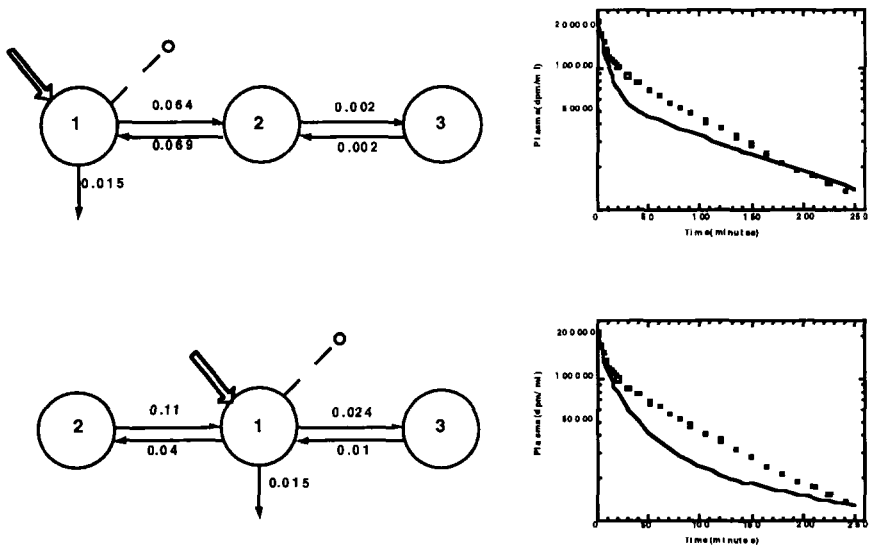
Figure J.9. Results of the estimates for the rate constants for models D and E compared to the data. See text for additional explanation.

model E, compartments 1 and 2 have the same structural relationship as the two compartment model shown in Figure J.8.

In determining k_{21} and k_{12}, knowing $k_{01} = 0.015$, one must divide $k_{11} - k_{01} = 0.079 - 0.015 = 0.064$ between k_{21} and k_{31} For example, if $k_{21} = 0.04$, then $k_{31} = 0.024$. For this case, k_{22} and $k_{12}k_{21}$ cannot both be preserved. Thus to estimate k_{12}, one can use either. If one chooses to preserve the produce, then an estimate for k_{12} equal to 0.11 is obtained. Finally, to estimate k_{13}, there is no a priori information available. One can usually let $k_{13} = k_{31}$, or a number smaller. Although not done in this example, it is also possible to obtain some additional help by noting $k_{11}V_1^{2comp} = k_{11}V_1^{3comp}$. $k_{11}V_1^{2comp}$ is known from the two compartment model; if V_1 is reduced for the three compartment model, an estimate for k_{11}^{3comp} can be obtained. In the example here, suppose $k_{13} = 0.01$. The results of this strategy for model E is given in Figure J.9.

One can easily see that the model predictions compared to the data are not too close, but in general as is the case here, they are close enough so that a computer program with a weighted least squares algorithm can proceed. If one is working with an interactive program, one can always adjust by hand these first guesses to improve the fit. But, as stated above, usually all that is needed is a sufficiently good approximation that the computer program can proceed with the estimation process.

Finally, it is clear that this approach is independent of how the tracer is introduced. All that is needed is the parameter values for the two compartment model.

Index